

2

TECHNICAL REPORT GL-87-14

SEISMIC STABILITY EVALUATION OF FOLSOM DAM AND RESERVOIR PROJECT

Report 8

MORMON ISLAND AUXILIARY DAM - PHASE II

by

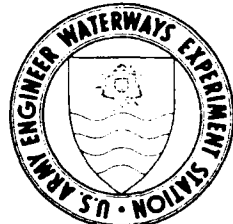
R. E. Wahl, Stanley G. Crawford, M. E. Hynes
Gregory D. Comes, Donald E. Yule

Geotechnical Laboratory

DEPARTMENT OF THE ARMY

Waterways Experiment Station, Corps of Engineers
3909 Halls Ferry Road, Vicksburg, Mississippi 39180-6199

AD-A257 485



S DTIC
ELECTE
NOV 17 1992
E D

August 1992

Report 8 of a Series

Approved For Public Release: Distribution Is Unlimited

92-29632



41280

411412

Prepared for US Army Engineer District, Sacramento
Sacramento, California 95814



US Army Corps
of Engineers



Destroy this report when no longer needed. Do not return
it to the originator.

The findings in this report are not to be construed as an official
Department of the Army position unless so designated
by other authorized documents.

The contents of this report are not to be used for
advertising, publication, or promotional purposes.
Citation of trade names does not constitute an
official endorsement or approval of the use of
such commercial products.

REPORT DOCUMENTATION PAGE

Form Approved
OMB No. 0704-0188

Public reporting burden for this collection of information is estimated to average 1 hour per response, including the time for reviewing instructions, searching existing data sources, gathering and maintaining the data needed, and completing and reviewing the collection of information. Send comments regarding this burden estimate or any other aspect of this collection of information, including suggestions for reducing this burden, to Washington Headquarters Services, Directorate for Information Operations and Reports, 1215 Jefferson Davis Highway, Suite 1204, Arlington, VA 22202-4302, and to the Office of Management and Budget, Paperwork Reduction Project (0704-0188), Washington, DC 20503

1. AGENCY USE ONLY (Leave blank)		2. REPORT DATE August 1992	3. REPORT TYPE AND DATES COVERED Report 8 of a Series	
4. TITLE AND SUBTITLE Seismic Stability Evaluation of Folsom Dam and Reservoir Project; Report 8: Mormon Island Auxiliary Dam - Phase II			5. FUNDING NUMBERS	
6. AUTHOR(S) R. E. Wahl, Stanley G. Crawford, M. E. Hynes, Gregory D. Comes, Donald E. Yule				
7. PERFORMING ORGANIZATION NAME(S) AND ADDRESS(ES) USAE Waterways Experiment Station Geotechnical Laboratory 3909 Halls Ferry Road Vicksburg, MS 39180-6199			8. PERFORMING ORGANIZATION REPORT NUMBER Technical Report GL-87-14	
9. SPONSORING/MONITORING AGENCY NAME(S) AND ADDRESS(ES) US Army Engineer District, Sacramento Sacramento, CA 95814			10. SPONSORING/MONITORING AGENCY REPORT NUMBER	
11. SUPPLEMENTARY NOTES Available from National Technical Information Service, 5285 Port Royal Road, Springfield, VA 22161.				
12a. DISTRIBUTION/AVAILABILITY STATEMENT Approved for public release; distribution unlimited.			12b. DISTRIBUTION CODE	
13. ABSTRACT (Maximum 200 words) The man-made water retaining structures at the Folsom Dam and Reservoir Project, located on the American River about 20 miles upstream of the City of Sacramento, California, have been evaluated for their seismic safety in the event of a Magnitude 6.5 earthquake occurring on the East Branch of the Bear Mountains Fault Zone at a distance of about 15 km. This report documents the Phase II study of Mormon Island Auxiliary Dam, one of the zoned embankment dams at the Folsom Dam and Reservoir Project. The evaluation process involved extensive review of construction records, field and laboratory investigations, and analytical studies. It has been determined that the portion of Mormon Island Auxiliary Dam founded on rock or undisturbed alluvium will perform satisfactorily. Evaluation of the remaining portion of the dam, founded on dredge tailings, is documented in Report 4 of this series.				
14. SUBJECT TERMS Dam safety Earthquakes and hydraulic structures Folsom Dam (CA)			15. NUMBER OF PAGES 409	
			16. PRICE CODE	
17. SECURITY CLASSIFICATION OF REPORT UNCLASSIFIED	18. SECURITY CLASSIFICATION OF THIS PAGE UNCLASSIFIED	19. SECURITY CLASSIFICATION OF ABSTRACT	20. LIMITATION OF ABSTRACT	

PREFACE

The US Army Engineer Waterways Experiment Station (WES) was authorized to conduct this study by the US Army Engineer District, Sacramento (SPK), by Intra-Army Order for Reimbursable Services Nos. SPKED-F-82-2, SPKED-F-82-11, SPKED-F-82-34, SPKED-F-83-15, SPKED-F-83-17, SPKED-F-84-14, and SPKED-D-85-12. This report is Report 8 in a series of reports which document the seismic stability evaluations of the man-made water retaining structures of the Folsom Dam and Reservoir Project, located on the American River in California. This current printing reflects editorial changes to the October 1988 printing of this report. The Reports in this series are as follows:

- Report 1: Summary
- Report 2: Interface Zone
- Report 3: Concrete Gravity Dam
- Report 4: Mormon Island Auxiliary Dam - Phase I
- Report 5: Dike 5
- Report 6: Right and Left Wing Dams
- Report 7: Upstream Retaining Wall
- Report 8: Mormon Island Auxiliary Dam - Phase II

The work on these reports is a joint endeavor between SPK and WES. Messrs. John W. White and John S. Nickell, of Civil Design Section 'A', Civil Design Branch, Engineering Division at SPK were the overall SPK project coordinators. Messrs. Gil Avila and Matthew G. Allen, of the Soil Design Section, Geotechnical Branch, Engineering Division at SPK, made critical geotechnical contributions to field and laboratory investigations. Support was also provided by the South Pacific Division Laboratory. The WES Principal Investigator and Research Team Leader was Dr. Mary Ellen Hynes, of the Earthquake Engineering and Geophysics Division (EEGD), Geotechnical Laboratory (GL), WES. Primary Engineers on the WES team for the portion of the study documented in this report were Mr. Ronald E. Wahl, Mr. Gregory D. Comes, and Mr. Donald E. Yule of EEGD; and Mr. Stanley G. Crawforth on temporary assignment to WES from the SPK. Geophysical support was provided by Messrs. Jose Llopis and Thomas B. Kean II, both of EEGD. Additional engineering support was provided by Messrs. Richard S. Olsen and Michael K. Sharp, both of EEGD, and Ms. Wipawi Vanadit-Ellis of the Soil Mechanics Division, GL, WES. Key contributions also were made by Dr. Leslie F. Harder, Jr., of Sacramento, California.

Professors H. Bolton Seed, Anil K. Chopra, and Bruce A. Bolt of the University of California, Berkeley; Professor Clarence R. Allen of the California Institute of Technology; and Professor Ralph B. Peck, Professor Emeritus of the University of Illinois, Urbana, served as Technical Specialists and provided valuable guidance during the course of the investigation.

Overall direction at WES was provided by Dr. A. G. Franklin, Chief, EEGD, and Dr. W. F. Marcuson III, Director, GL.

At the time of publication of this report, Director of WES was Dr. Robert W. Whalin. Commander and Deputy Director was COL Leonard G. Hassell, EN.

Accession For	
NTIS CRA&I	<input checked="" type="checkbox"/>
DTIC TAB	<input type="checkbox"/>
Unannounced	<input type="checkbox"/>
Justification	
By	
Distribution/	
Availability Codes	
Dist	Avail and/or Special
A-1	

DTIC Q7 4

CONTENTS

	<u>Page</u>
PREFACE.....	1
LIST OF TABLES.....	6
LIST OF FIGURES.....	6
CONVERSION FACTORS, NON-SI TO SI (METRIC) UNITS OF MEASUREMENT.....	11
PART I: INTRODUCTION.....	12
General.....	12
Project History.....	13
Hydrology and Pool Levels.....	13
Description of Mormon Island Auxiliary Dam.....	14
Site Geology.....	15
Dredging Deposition Process.....	16
Seismic Hazard Assessment.....	16
Seismological and geological investigations.....	16
Selection of design ground motions.....	19
PART II: REVIEW OF CONSTRUCTION RECORDS.....	22
General.....	22
Exploration and Sampling During Original Design and Initial Construction.....	22
Foundation Preparation at Mormon Island Auxiliary Dam.....	23
Laboratory Tests During Original Design and Initial Construction.....	25
Embankment Materials.....	27
PART III: FIELD INVESTIGATIONS.....	28
General.....	28
Geophysical Tests.....	29
Surface refraction seismic.....	29
Crosshole tests.....	30
Downhole tests.....	32
Interpreted p-wave zones.....	32
Interpreted s-wave zones.....	33
Test pits.....	34
Becker Penetration Tests.....	36
General.....	36
Data reduction procedures.....	36
Results of $(N_1)_{60}$ data	38
Statistical analysis of $(N_1)_{60}$ data	42
Becker gradations.....	43
Summary of field investigations.....	45
PART IV: ESTIMATES OF CYCLIC STRENGTH.....	47
General.....	47
Estimates of Cyclic Strength from In-Situ Tests.....	47
Empirical procedure to estimate cyclic strength.....	47
Cyclic strength estimate for shell gravels, Zones 1 and 2....	48
Cyclic strength estimate for dredged foundation gravels.....	49

	<u>Page</u>
Cyclic strength estimate for undredged foundation gravel.....	49
Cyclic strength estimates for Zone 3 filter and Zone 4 core materials.....	50
Relative Cyclic Strength Behavior of Embankment Gravels.....	50
PART V: FINITE ELEMENT AND STABILITY ANALYSES OF DAM SECTION FOUNDED ON ROCK.....	53
General.....	53
Static Finite Element Analysis.....	53
General.....	53
Section idealization and finite element input data.....	53
Results of static analysis.....	55
Dynamic Finite Element Analysis.....	57
General.....	57
Description of FLUSH.....	57
FLUSH inputs.....	57
Dynamic response results.....	60
Evaluation of Liquefaction Potential.....	61
General.....	61
Safety factors against liquefaction in embankment shell.....	62
Residual excess pore pressures.....	62
Liquefaction potential evaluation of central impervious core and transition zone.....	63
Summary.....	63
Stability Analysis.....	63
General.....	63
Post-earthquake stability analysis.....	64
Permanent Displacement Analysis.....	65
Computation of yield accelerations.....	65
Makdisi-Seed method.....	66
Sarma-Ambrayseys method.....	68
PART VI: FINITE ELEMENT AND STABILITY ANALYSES OF DAM SECTION FOUNDED ON UNDREDGED ALLUVIUM.....	70
General.....	70
Selection and idealization of representative cross section for finite element analysis.....	70
Selection and idealization of representative cross section for post-earthquake stability analysis.....	70
Static Analysis.....	71
Finite element inputs.....	71
Results of static analysis.....	72
Dynamic Finite Element Analysis.....	73
General.....	73
FLUSH inputs.....	74
Results of dynamic response calculations.....	75
Evaluation of Liquefaction Potential.....	76
General.....	76
Safety factors against liquefaction.....	77
Residual excess pore pressures.....	77
Post-Earthquake Stability Analysis.....	78

	<u>Page</u>
Permanent Displacement Analysis.....	79
General.....	79
Yield accelerations.....	80
Makdisi-Seed method.....	80
Sarma-Ambrayseys method.....	81
Summary of permanent displacement computations.....	82
PART VII: SUMMARY AND CONCLUSIONS.....	83
REFERENCES.....	87
TABLES 1-14	
FIGURES 1-102	
APPENDIX A: CONVERSION OF BECKER BLOWCOUNTS INTO EQUIVALENT STANDARD PENETRATION TEST BLOWCOUNTS FOR PHASE II FIELD INVESTIGATIONS.....	A1
APPENDIX B: DATA ACQUIRED FROM BECKER HAMMER DRILL PENETRATION TESTS FOR PHASE II FIELD INVESTIGATIONS.....	B1

LIST OF TABLES

<u>No.</u>		<u>Page</u>
1	Estimated Seismic Characteristics of Capable Faults.....	90
2	Adopted Design Shear Strengths from Construction Records.....	91
3	Placement Specifications for Embankment Materials.....	91
4	Hyperbolic Parameters Input to FEADAM for Static Analysis of Mormon Island Auxiliary Dam.....	92
5	Unit Weights and K_2 Parameter Used for Embankment and Foundation Materials Input to FLUSH.....	93
6	Unit Weights and Shear Strength Parameters Used in Post-Earthquake Stability Calculations.....	93
7	Summary of Makdisi-Seed Calculations for Set of Potential Slip Surfaces Confined to Upstream Shell for Idealized Section for Portion of Mormon Island Auxiliary Dam Founded on Rock.....	94
8	Summary of Makdisi-Seed Calculations for Set of Potential Slip Surfaces Exiting Downstream of Center Line for Idealized Section for Portion of Mormon Island Auxiliary Dam Founded on Rock.....	95
9	Summary of Sarma-Ambrayseys Calculations for Set of Potential Slip Surfaces Confined to Upstream Shell for Idealized Section for Portion of Mormon Island Auxiliary Dam Founded on Rock.....	96
10	Summary of Sarma-Ambrayseys Calculations for Set of Potential Slip Surfaces Emerging Downstream of Center Line for Idealized Section for Portion of Mormon Island Auxiliary Dam Founded on Rock.....	97
11	Summary of Makdisi-Seed Calculations for Set of Potential Slip Surfaces Exiting Downstream of the Center Line for Idealized Section for Portion of Mormon Island Auxiliary Dam Founded on Undredged Alluvium.....	98
12	Summary of Makdisi-Seed Calculations for Set of Potential Slip Surfaces Exiting Downstream of Center Line for Idealized Section for Portion of Mormon Island Auxiliary Dam Founded on Undredged Alluvium.....	99
13	Summary of Sarma-Ambrayseys Calculations for Set of Potential Slip Surfaces Confined to Shell for Idealized Section for Portion of Mormon Island Auxiliary Dam Founded on Undredged Alluvium.....	100
14	Summary of Sarma-Ambrayseys Calculations for Set of Potential Slip Surfaces Emerging Downstream of Center Line for Idealized Section for Portion of Mormon Island Auxiliary Dam Founded on Undredged Alluvium.....	101

LIST OF FIGURES

<u>No.</u>		<u>Page</u>
1	Location of Folsom Dam and Reservoir Project.....	103
2	Plan of man-made retaining structures at Folsom Dam Project.....	105
3	Plan and axial section of Mormon Island Auxiliary Dam.....	107
4	Typical embankment sections, Mormon Island Auxiliary Dam.....	109
5	Geologic map, parts of the Folsom and Auburn quadrangles.....	111

LIST OF FIGURES (Continued)

<u>No.</u>		<u>Page</u>
6	Bucyrus type of dredge, with close-connected buckets, shaking screens, belt conveyor, and spuds.....	112
7	Regional geologic map.....	113
8	Indentification of study area.....	114
9	Regional geology in vicinity of Folsom Dam and Reservoir Project.....	115
10	Regional lineament map of the Folsom area.....	116
11	Epicenter map of the Western United States.....	117
12	Seismicity map of Northern California.....	118
13	Acceleration histories used in the analysis.....	119
14	Response spectra of Records A and B.....	120
15	View of Mormon Island Auxiliary Dam foundation preparation, looking southwest from left abutment to right abutment (FOL-476, 4/10/51).....	121
16	Foundation preparation for portion of Mormon Island Auxiliary Dam founded on rock, looking southwest from sta 421+00 to right abutment (FOL-490, 4/11/51).....	121
17	Core trench excavation through undisturbed alluvium, looking southwest from sta 440+00 to right abutment (FOL-544, 6/25/51).....	122
18	Core trench excavation in alluvium, looking northeast from sta 440+00 to left abutment (FOL-538, 6/26/51).....	122
19	Completed core trench excavation, looking southwest from left abutment to right abutment (FOL-619, 9/26/51).....	123
20	Placement of zone materials in core trench, looking southwest from sta 458+00 to right abutment (FOL-633, 10/30/51).....	123
21	Placement of Zone 1 upstream shell, looking southwest from sta 421+50 to right abutment (FOL-528).....	124
22	Location of Phase II field investigation explorations at Mormon Island Auxiliary Dam.....	125
23	Typical section of downstream toe between sta 439 and 446 showing undredged foundation geometry.....	126
24	Time-distance plot for refraction line R-1.....	127
25	Crosshole P-wave velocity test results.....	128
26	Crosshole S-wave velocity test results.....	129
27	Average P-wave velocities from two downhole tests.....	130
28	Downhole S-wave velocity test results.....	131
29	Composite of P-wave velocity tests.....	132
30	P-wave velocity interpretation for downstream undredged area.....	133
31	Composite of S-wave velocity tests.....	134
32	S-wave velocity interpretation for downstream undredged area.....	135
33	Gradations of undredged alluvium underlying clay layer obtained from preconstruction test shaft 4F-10.....	136
34	Gradation of embankment gravels observed in Phase I test shaft excavations.....	137
35	Photo of AP-1000 drill rig used for Becker Hammer soundings at Mormon Island Auxiliary.....	138
36	Photo of open and closed drill bits used in Becker Penetration Tests.....	138

LIST OF FIGURES (Continued)

<u>No.</u>		<u>Page</u>
37	Schematic of energy and overburden corrections to convert Becker blowcounts into equivalent Standard Penetration Test (N_1) ₆₀ values	139
38	C_n curves used in the study of Mormon Island Dam.....	140
39	Formula used to compute equivalent level ground vertical effective stress.....	141
40	Confining stress versus depth for soil column through down- stream slope and dredged tailings.....	142
41	Cross section along downstream toe showing (N_1) ₆₀ results	143
42	Cross section at midslope of the embankment showing (N_1) ₆₀ results.....	145
43	Transverse cross section through sta 450+00 showing (N_1) ₆₀ results.....	147
44	Histogram of (N_1) ₆₀ for embankment gravels	149
45	Histogram of (N_1) ₆₀ for undredged foundation gravels	150
46a	Zone of (N_1) ₆₀ for dredged foundation gravels at Mormon Island Auxiliary Dam estimated from Phase I Becker Hammer soundings and computed vertical effective stresses from static finite element analysis of dredged foundation section documented in Report 4.....	151
46b	Zones of (N_1) ₆₀ for dredged foundation gravels at Mormon Island Auxiliary Dam estimated from Phase II Becker Hammer soundings..	151
47	Comparison of Becker sample and ring density gradations in embankment gravels.....	152
48	Comparison of Becker sample and ring density gradations in dredged foundation.....	153
49	Relationships between stress ratio causing liquefaction and (N_1) ₆₀ values for silty sands from M = 7.5 earthquakes (from Seed, et al. 1984a).....	154
50	Schematic representation of procedure for calculating the appropriate cyclic strength for elements in idealized embankment section.....	155
51	K_σ adjustment factor	156
52	K_α adjustment factor	156
53	Relationship between FS_L and R_u	157
54	Idealized embankment section of Mormon Island Auxiliary Dam founded on rock and developed from cross section of dam at sta 426+00.....	158
55	Finite element mesh used for idealized rock section.....	159
56	Unbalanced hydrostatic pressures acting across the core of the dam.....	160
57	Contours of vertical effective stress computed by FEADAM.....	161
58	Contours of horizontal effective stress computed by FEADAM.....	162
59	Contours of shear stresses on horizontal planes computed by FEADAM.....	163
60	Contours of α	164
61	Contours of effective mean normal pressure computed from FEADAM stresses.....	165
62	Low strain amplitude shear wave velocity distribution in rock section.....	166

LIST OF FIGURES (Continued)

<u>No.</u>		<u>Page</u>
63	Contours of low amplitude shear modulus, G_{max} , input to FLUSH.....	167
64	Modulus degradation and damping curves used in FLUSH analysis....	168
65	Dynamic shear stresses induced by Accelerogram A in FLUSH analysis.....	169
66	Maximum accelerations and fundamental periods computed with FLUSH for selected nodal points.....	170
67	Effective shear strains in percent, computed by FLUSH using Accelerogram A for rock section.....	171
68	Response spectra for Accelerogram A compared with low strain amplitude and design earthquake strain level fundamental periods.....	172
69	Contours of safety factor against liquefaction for section of Mormon Island Dam founded on rock.....	173
70	Contours of excess pore pressure ratio R_u in percent for section of Mormon Island Dam founded on rock.....	174
71	Safety factor against sliding and critical circle in post-earthquake stability analysis.....	175
72	Yield accelerations for critical slip circles confined to the upstream shell.....	176
73	Yield accelerations for critical slip circles exiting downstream of the center line.....	177
74	Yield acceleration versus depth for rock section.....	178
75	Normal charts for computing displacements using the Makdisi-Seed technique.....	179
76	Permanent displacements computed for the idealized section founded on rock by the Makdisi-Seed method.....	180
77	Sliding block analysis -- computed permanent displacements for Accelerograms A and B.....	181
78	Permanent displacements computed for the idealized section founded on rock by the Sarma-Ambrayseys method.....	182
79	Idealized cross section used for finite element analysis, sta 446+00, representing section of Mormon Island Dam where shells are founded on alluvium.....	183
80	Idealized cross section used for stability analysis, sta 442+00, representing section of Mormon Island Dam where shells are founded on alluvium.....	184
81	Finite element mesh used for section of Mormon Island Dam where shells are founded on undredged alluvium.....	185
82	Unbalanced hydrostatic pressures acting against impervious core dam for undredged section.....	186
83	Contours of vertical effective stress.....	187
84	Contours of horizontal effective stress.....	188
85	Contours of shear stress acting on horizontal planes.....	189
86	Contours of α	190
87	Contours of effective mean normal pressure.....	191
88	Shear wave velocity distribution.....	192
89	Low strain amplitude shear modulus G_{max} distribution.....	193
90	Dynamic shear stresses induced in the embankment and undredged foundation by Accelerogram B.....	194

LIST OF FIGURES (Concluded)

<u>No.</u>		<u>Page</u>
91	Peak acceleration computed by FLUSH for selected nodal points and fundamental period for low strain amplitude and strain amplitude levels induced by the motions of the design earthquake.....	195
92	Strain levels induced by Accelerogram B.....	196
93	Response spectra of Accelerogram B compared with the low strain amplitude and design earthquake strain level fundamental period of the embankment.....	197
94	Contours of the safety factor against liquefaction, FS_L	198
95	Contours of excess pore pressure ratio R_u in percent superimposed on the cross section used in the finite element analysis.....	199
96	Contours of R_u superimposed on idealized cross section used in stability analysis.....	200
97	Safety factor against sliding and critical circle from post-earthquake stability analysis of undredged section.....	201
98	Yield accelerations for critical slip circles confined to the upstream shell of undredged foundation cross section.....	202
99	Yield accelerations for critical slip circles exiting downstream of the center line of undredged foundation cross section.....	203
100	Yield acceleration versus tangent elevation for undredged foundation cross section.....	204
101	Permanent displacements computed for the idealized section founded on undredged alluvium by the Makdisi-Seed technique....	205
102	Permanent displacements computed for the idealized section founded on undredged alluvium by the Sarma-Ambrayseys technique.....	206

CONVERSION FACTORS, NON-SI TO SI (METRIC)
UNITS OF MEASUREMENT

Non-SI units of measurement used in this report can be converted to SI (metric) units as follows:

<u>Multiply</u>	<u>By</u>	<u>To Obtain</u>
acre-feet	1,233.489	cubic metres
feet	0.3048	metres
miles (US statue)	1.609347	kilometres
pounds (mass) per cubic foot	16.01846	kilograms per cubic metre
pounds (force) per square foot	47.88026	pascals
square miles	2.589998	square kilometres
tons (force) per square foot	95.76052	kilopascals

SEISMIC STABILITY EVALUATION OF FOLSOM DAM AND RESERVOIR PROJECT

Mormon Island Auxiliary Dam - Phase II

PART I: INTRODUCTION

General

1. This report is one of a series of reports that document the investigations and results of a seismic stability evaluation of the man-made water retaining structures at the Folsom Dam and Reservoir Project, located on the American River in Sacramento, Placer, and El Dorado Counties, California, about 20 airline miles* northeast of the City of Sacramento. This seismic safety evaluation was performed as a cooperative effort between the US Army Engineer Waterways Experiment Station (WES) and the US Army Engineer District, Sacramento (SPK). Professors H. Bolton Seed, Anil K. Chopra, and Bruce A. Bolt of the University of California, Berkeley, Professor Clarence R. Allen of the California Institute of Technology, and Professor Ralph B. Peck, Professor Emeritus of the University of Illinois, Urbana, served as Technical Specialists for the study. This report documents Phase II of the seismic stability studies of Mormon Island Auxiliary Dam, a zoned embankment dam at the Folsom project. A location map and plan of the project are shown in Figures 1 and 2.

2. Mormon Island Auxiliary Dam may be divided into three segments according to foundation conditions: the core is founded on rock along the entire length of the dam, but the shells are founded either on rock, undisturbed alluvium, or very loose dredged tailings. The Phase II investigations consisted of a review of construction records, field investigations, and analytical studies of the portions of the dam with shells founded on rock or on undisturbed alluvium to estimate the response of the embankment and its foundation to earthquake shaking, to determine the susceptibility of the embankment and foundation soils to liquefaction, and to evaluate the stability of the slopes during and immediately after the design event.

* A table of factors for converting non-SI units of measurement to SI (metric) units is presented on page 6.

3. It has been concluded from the Phase II studies that the segments of Mormon Island Dam with shells founded on rock or on undredged alluvium will be stable both during and after the design earthquake event, hence, remedial measures in these sections are not required. From the Phase I study, documented in Report 4 of this series, it was found that the portion of the dam with shells founded on dredged tailings will not be stable during and after the earthquake. Remedial measures were recommended over this length of the dam.

Project History

4. The Folsom Dam and Reservoir Project was designed and built by the Corps of Engineers in the period 1948 to 1956, as authorized by the Flood Control Act of 1944 and the American River Basin Development Act of 1949. Upon completion of the project in May 1956, ownership of the Folsom Dam and Reservoir was transferred to the US Bureau of Reclamation for operation and maintenance. As an integral part of the Central Valley Project, the Folsom Project provides water supplies for irrigation, domestic, municipal, industrial, and power production purposes as well as flood protection for the Sacramento Metropolitan area and extensive water related recreational facilities. Releases from the Folsom Reservoir are also used to provide water quality control for project diversions from the Sacramento-San Joaquin Delta, to maintain fish-runs in the American River below the dam, and to help maintain navigation along the lower reaches of the Sacramento River.

Hydrology and Pool Levels

5. Folsom Lake impounds the runoff from 1,875 square miles of rugged mountainous terrain. The reservoir has a storage capacity of 1 million acre-ft at gross pool and is contained by approximately 4.8 miles of man-made water retaining structures that have a crest elevation of 480.5 ft above sea level. At gross pool, el 466,* there is 14.5 ft of freeboard. This pool level was selected for the safety evaluation based on a review of current operational procedures and hydrologic records (obtained for a 29-year period, from 1956 to 1984) for the reservoir which shows that the pool reaches

* In this report, elevations are in ft NGVD.

el 466 about 10 percent of the time during the month of June and considerably less than 10 percent of the time during the other months of the year. Under normal operating conditions, the pool is not allowed to exceed el 466. Hydrologic records show that emergency situations which would cause the pool to exceed el 466 are rare events.

Description of Mormon Island Auxiliary Dam

6. Mormon Island Auxiliary Dam was constructed in the Blue Ravine, an ancient channel of the American River, that is about 1 mile wide at the dam site. For about 1,650 ft of its width, the Blue Ravine is filled with auriferous, gravelly alluvium of Pleistocene age. The maximum thickness of the channel gravels is approximately 65 ft. The gravels have been dredged for their gold content in the deepest portion of the channel, and the tailings were placed back into the partially water-filled channel. The replacement process tended to deposit the tailings in a very loose condition with finer materials near the base of the channel and coarser materials near the top. The remaining undisturbed alluvium is crudely stratified and slightly cemented.

7. Mormon Island Auxiliary Dam is a zoned embankment dam 4,820 ft long and 165 ft high from core trench to crest at maximum section. The shells are constructed of gravel dredged tailings from the Blue Ravine. The narrow, central impervious core is a well compacted clayey mixture founded directly on rock over the entire length of the dam to provide a positive seepage cutoff. Two transition zones, each 12-ft wide, flank both the upstream and downstream sides of the core. The transition zones in contact with the core are composed of well compacted decomposed granite which classifies as a silty sand according to the Unified Soils Classification System (USCS). The second transition zones are constructed of the -2 in. fraction of the dredged tailings. A plan and typical sections of the dam are shown in Figures 3 and 4.

8. From the right end of the dam, sta 412+00, to approximate sta 439+00 and from sta 456+50 to the left end of the dam, sta 460+75, all zones are founded on rock. Between sta 439 and sta 441+50, the downstream shells are founded on undredged alluvium and the upstream shells are founded on rock. The foundation report indicates that between sta 441+50 and sta 456+50, the undisturbed and dredged alluvium was excavated to obtain slopes of 1V:2H to

found the core and most of the filter zones on rock, but the shells are founded on alluvium. The dredged portion of the alluvium begins approximately at sta 446 and continues approximately to sta 455. The slopes of the dam vary according to the foundation conditions, with the flattest slopes in the vicinity of the dredged tailings and the steepest slopes in the segments founded on rock. The downstream slopes of the dam vary between 1V:2H and 1V:3.5H, and the upstream slopes vary between 1V:2H and 1V:4.5H.

Site Geology

9. At the time of construction, the geology and engineering geology concerns at the site were carefully detailed in the foundation report by US Army Engineer District, Sacramento (1953). This foundation report from construction records and a later paper by Kiersch and Treasher (1955) are the sources for the summary of site geology provided in this section.

10. The Folsom Dam and Reservoir Project is located in the low westernmost foothills of the Sierra Nevada in central California, at the confluence of the North and South Forks of the American River. Relief ranges from a maximum of 1,242 ft near Flagstaff Hill located between the upper arms of the reservoir to 150 ft near the town of Folsom just downstream of the Concrete Gravity Dam. The North and South Forks entered the confluence in mature valleys up to 3 miles wide, but further downcutting resulted in a V-shaped inner valley 30 to 185 ft deep. Below the confluence, the inner canyon was flanked by a gently sloping mature valley approximately 1.5 miles wide bounded on the west and southeast by a series of low hills. The upper arms of the reservoir, the North and South Forks, are bounded on the north and east by low foothills.

11. A late Pliocene-Pleistocene course of the American River flowed through the Blue Ravine and joined the present American River channel downstream of the town of Folsom. The Blue Ravine was filled with late Pliocene-Pleistocene gravels, but, with subsequent downcutting and headward erosion, the Blue Ravine was eventually isolated and drainage was diverted to the present American River Channel.

12. The important formations at the dam site are: a quartz diorite granite which forms the foundation at the Concrete Gravity Dam, Wing Dams, and Saddle Dikes 1 through 7; metamorphic rocks of the Amador Group which form the foundation at Mormon Island Auxiliary Dam and Saddle Dike 8; the Mehrten

Formation, a deposit of cobbles and gravels in a somewhat cemented clay matrix which caps the low hills that separate the saddle dikes and is part of the foundation at Dike 5; and the alluvium that fills the Blue Ravine at Mormon Island Auxiliary Dam.

13. Weathered granitic or metamorphic rock is present throughout the area. Figure 5 shows a geologic map of the project area. The Concrete Gravity Dam, the Wing Dams, and Dikes 1 through 7 are founded on the weathered quartz diorite granite. Between Dikes 7 and 8 there is a change in the bedrock. Dike 8 and Mormon Island Auxiliary Dam are underlain by metamorphic rock of the Amador Group. The Amador Group consists of predominantly schists with numerous dioritic and diabasic dikes.

Dredging Deposition Process

14. The dredging process and the procedures used in the Folsom area were documented by Aubury (1905). In the dredging process, the alluvium was excavated below the water level of the dredge pond with a chain of closely connected buckets that had a capacity of approximately 5 to 13 ft³ per bucket. Figure 6 is a drawing of a Bucyrus type of dredge typically used in the Folsom area. The excavated material was typically sorted on a shaking screen with holes 3/8 in. in size. The plus--3/8-in. material was deposited by a conveyor belt to the edges of the dredge pond in windrows. After sluicing and processing the minus--3/8-in. material on the gold-saving tables (where mercury was used for amalgamation), the dredge crew then dumped the fine tailings back into the dredged pond. The coarse tailings slopes around the edge of the pond were generally marginally stable to unstable, and slope failures occurred often, mixing slide debris with the finer tailings in the pond. The gold-bearing gravels in the Folsom area were characteristically described as "a very clean wash," which meant that there was little or no clay present.

Seismic Hazard Assessment

Seismological and geological investigations

15. Detailed geological and seismological investigations in the immediate vicinity of Folsom Reservoir were performed by Tierra Engineering, Inc.

to assess the potential for earthquakes in the vicinity, to estimate the magnitudes these earthquakes might have, and to assess the potential for ground rupture at any of the water-retaining structures (see Tierra Engineering Consultants, Inc. 1983 for comprehensive report). The 12-mile wide by 35-mile long study area centered on the Folsom Reservoir was extensively investigated using techniques such as areal imagery analysis, ground reconnaissance, geologic mapping, and detailed fault capability assessment. In addition, studies by others relevant to the geology and seismicity of the area around Folsom were also compiled. These additional literature sources include numerous geologic and seismologic studies published through the years, beginning with the "Gold Folios" published by the US Geological Survey in the 1890's, the engineering geology investigations for New Melones and the proposed Marysville and Auburn Dams, studies performed for the Rancho Seco Nuclear Power Plant as well as unpublished student theses and county planning studies. As described in this section, the East Branch of the Bear Mountains fault zone is the seismic source of concern.

16. Figure 7 shows a generalized geologic map of north central California and identifies the location of the 12-mile by 35-mile study area. Figure 8 shows a close-up of the study area as it surrounds the Folsom Project. Figure 9 shows the regional geology and highlights the basement rocks in the study zone. The western edge of the study zone contains Quaternary and Tertiary deposits of the Great Valley. The central and eastern portions of the study zone contain primarily metamorphic rock with granitic, gabbroic, and ultramafic intrusives.

17. Figure 9 also shows the major faults in the area. In the investigation of faults, shears, and lineaments, five features within the study area were selected for more detailed study. These were (a) the West Branch of the Bear Mountains fault zone, (b) the Bass Lake fault, (c) the Linda Creek lineament, (d) the Mormon Island fault, and (e) the Scott Road lineament. The East Branch of the Bear Mountains fault zone is located near the boundary of the study area. The characteristics of this fault zone were fully examined and reported in the above-mentioned references. This fault zone was not investigated further as part of this study by Tierra Engineering Consultants, Inc. Characteristics of this fault zone are discussed later in this section. The five features that were selected for further study are identified on the regional lineament map in Figure 10. On the basis of review of available

data, geologic mapping, and imagery analysis, it was determined that the Bass Lake fault is more than 168 million years old and shows no evidence of movement in recent geologic time. Consequently, the fault is not considered capable. Based on the seismological studies for Auburn Dam, it was also determined that the Linda Creek lineament does not represent a capable fault (by Corps criteria). The Scott Road lineament was determined to be of erosional origin and is not considered to be a fault. The remaining two faults, the West Branch of the Bear Mountains fault zone and the Mormon Island fault, required additional studies.

18. The detailed lineament analyses, geomorphic analyses, geologic mapping and trenching at selected locations indicated that the West Branch of the Bear Mountains fault zone is overlain by undisplaced soils more than 60 to 70 thousand years old. There were no geomorphic indications of Holocene faulting along the zone; it was concluded that the West Branch of the Bear Mountains fault zone is not a capable fault. Studies of the Mormon Island fault showed that the lineament zone associated with the fault dies out before reaching Mormon Island Auxiliary Dam. A review of the dam construction reports and trenching of the Mormon Island fault south of Mormon Island Auxiliary Dam revealed no evidence of faulting of quaternary alluvium in this ancestral channel of the American River. Based on the observation of undisplaced colluvium and weathering profiles more than 65,000 years old that overlie the sheared bedrock as well as the lack of geomorphic indicators of Holocene faulting in this zone, it was concluded that neither the Mormon Island fault is a capable fault nor does it pass through the foundation of Mormon Island Auxiliary Dam (Tierra Engineering Consultants, Inc. 1983).

19. Tectonic studies of the Folsom Project show it is located in the Sierran block. Within the Sierran block there is a very low level of seismicity. The more seismically active areas are located along the eastern and southern edges of the block. Figure 11 shows epicentral locations for the western United States. On this map, the Sierra Nevada and Great Basin areas are identified. Tectonic studies of the Sierran block indicate an extensional stress regime which suggests that a major stress buildup and release sequence associated with large earthquakes is unlikely in the central or northern Sierran block.

20. Figure 12 shows epicentral locations in north central California from data accumulated between 1910 and 1981. As indicated in the previous

discussion, a low level of seismicity can be observed in the vicinity of the Folsom Dam and Reservoir Project. The nearest highly active areas are the Calaveras Hayward-San Andreas System located 70 to 100 miles to the west of the study area and the Genoa Jack Valley zone located more than 70 miles to the east. Table 1 summarizes the characteristics of the capable fault zones near the Folsom Dam and Reservoir Project. Although these 2 highly active zones are capable of generating maximum earthquake magnitudes in excess of Local Magnitude $M_L = 7$, the ground motions generated by such earthquakes would be significantly attenuated by the time the motions arrived at the Folsom Reservoir.

21. The closest capable fault is the East Branch of the Bear Mountains fault zone which has been found to be capable of generating a maximum magnitude $M_L = 6.5$ earthquake. The return period for this maximum earthquake is estimated to exceed 400 years (Tierra Engineering, Inc. 1983). The tectonic and seismicity studies also indicated that it is unlikely that Folsom Lake can induce major macroseismicity. Faults that underlie the water retaining structures at the Folsom Dam and Reservoir Project were found to be noncapable, so seismic fault displacement in the foundations of the water retaining structures is judged to be highly unlikely.

22. Determination that the East Branch of the Bear Mountains fault zone is a capable fault came from the Auburn Dam earthquake evaluation studies in which it was concluded that this fault was capable of generating a maximum magnitude earthquake of 6 to 6.5. The minimum distance between the East Branch of the Bear Mountains fault zone and Mormon Island Auxiliary Dam is 8 miles, and the minimum distance between this fault zone and the Concrete Gravity Dam is 9.5 miles. The focal depth of the earthquake is estimated to be 6 miles. This hypothetical maximum magnitude earthquake would cause more severe shaking at the project than earthquakes originating from other known potential sources.

Selection of design ground motions

23. The seismological and geological investigations summarized in the Tierra report were provided to Professor Bruce A. Bolt and Professor H. B. Seed to determine appropriate ground motions for the seismic safety evaluation of the Folsom Dam and Reservoir Project. The fault zone of concern is the East Branch of the Bear Mountains fault zone located at a distance of about 15 km from the site. This fault zone has an extensional tectonic setting and

a seismic source mechanism that is normal dip-slip. The slip rate from historic geomorphic and geological evidence is very small, less than 10^{-3} cm per year with the most recent known displacement occurring between 10,000 and 500,000 years ago in the late Pleistocene period.

24. Based on their studies of the horizontal ground accelerations recorded on an array of accelerometers normal to the Imperial Valley fault during the Imperial Valley earthquake of 1979, as well as recent studies of a large body of additional strong ground motion recordings, Bolt and Seed (1983) recommend the following design ground motions:

Peak horizontal ground acceleration = 0.35 g

Peak horizontal ground velocity = 20 cm/sec

Bracketed Duration (≥ 0.05 g) = 16 sec

Because of the presence of granitic plutons at the site, it is expected that the earthquake accelerations might be relatively rich in high frequencies. Bolt and Seed (1983) provided two accelerograms that are representative of the design ground motions expected at the site as a result of a maximum magnitude M_L equal to 6.5 occurring on the East Branch of the Bear Mountains fault zone. The accelerograms are designated as follows (Bolt and Seed 1983):

M6.5 - 15K - 83A. This accelerogram is representative of the 84-percentile level of ground motions that could be expected to occur at a rock outcrop as a result of a Magnitude 6-1/2 earthquake occurring 15 kms from the site. It has the following characteristics:

Peak acceleration = 0.35g

Peak velocity = 25 cm/sec

Duration = 16 sec

M6.5 - 15K - 83B. This accelerogram is also representative of the 84-percentile level of ground motions that could be expected to occur at a rock outcrop as a result of a Magnitude 6-1/2 earthquake occurring 15 kms from the site. It has the following characteristics:

Peak acceleration = 0.35g

Peak velocity ▪ 19.5 cm/sec

Duration ▪ 15 sec

Figure 13 shows plots of acceleration as a function of time for the two design accelerograms and Figure 14 shows response spectra of the motions for damping ratios of 0, 2, 5, 10, and 20 percent damping.

PART II: REVIEW OF CONSTRUCTION RECORDS

General

25. Detailed construction records were kept to document the initial site reconnaissance, selection of borrow areas, foundation preparation, and construction sequence for the dam. Pertinent information from these construction records is summarized in this chapter. This information provides (a) key background data used in development of an idealized section for analysis, (b) detailed descriptions of foundation and embankment materials and the geometry of excavated areas, important to the planning of field investigations and interpretation of results, and (c) initial values for material properties of foundation and embankment materials.

Exploration and Sampling During Original Design and Initial Construction

26. Mormon Island Auxiliary Dam may be divided into three different segments according to foundation conditions--an approximately 900-ft-long segment (sta 446 to sta 455) that has shells founded on dredged alluvium, an approximately 700-ft-long segment (sta 439+50 to sta 446, and sta 455 to sta 456+50) that has shells founded on undisturbed alluvium, and the remaining length of the dam (sta 412 to sta 439+00, and sta 456+50 to sta 460+75) is founded on weathered bedrock. The undisturbed alluvial deposit consists generally of sands and gravels overlain by silty and clayey soils. In the dredged alluvium, the coarser tailings are distributed throughout the thickness of the deposit (but are somewhat more concentrated in the top portion) and the finer tailings (approximately the minus 3/8-in. fraction) are found mainly in the lower portion of the deposit. The boring logs from the exploration and sampling efforts prior to construction are summarized in Figure 3. The undredged portion of the alluvial foundation was explored by 1 churn drill hole, 4 6-in.-diam rotary core drill holes, and 3 test pits from which undisturbed and disturbed samples were obtained. The dredged portion of the foundation was explored by 4 churn drill holes in which an effort was made to obtain 5-in.-diam undisturbed push tube samples. Undisturbed sampling of the gravels was generally unsuccessful due to the large particle sizes. The

weathered schist foundation was investigated with 6-in.-diam rotary core drill holes and test pits from which undisturbed samples were obtained.

Foundation Preparation at Mormon Island Auxiliary Dam

27. At Mormon Island Auxiliary Dam, the Blue Ravine is about 1 mile wide. The foundation rock consists of nonuniformly weathered metamorphic rock with isolated, relatively fresh blocks surrounded by highly weathered material to a considerable depth. From the right abutment, sta 412+00 to sta 439, a 1- to 16-ft thickness of overburden was removed to found the core and shells of the dam on blocky, moderately hard schist bedrock. Stripping depths averaged 4 ft (range 1 to 10 ft) from sta 412+00 to sta 439+00 and 8 ft (16-ft maximum) from sta 439+00 to sta 441+50.

28. From sta 439 to sta 458+00, the channel was filled with auriferous gravelly alluvium of Pleistocene age. The maximum thickness of the channel gravels is approximately 65 ft. The gravels have been dredged for their gold content in the deepest portion of the channel, from sta 446+10 to sta 455+00, and the tailings were placed back into the partially water-filled channel. The replacement process tended to deposit the tailings in a very loose condition with finer materials (minus 3/8-in. size) near the base of the channel and coarser materials (plus 3/8-in. size) near the top. The remaining undisturbed alluvium is crudely stratified and, in some areas, slightly cemented.

29. The undisturbed and dredged alluvium and any other overburden present was excavated along the entire length of the core to found the core on the blocky, somewhat weathered schist. The remaining foundation was stripped to found the shells on suitable materials. During stripping and core trench excavation of the undisturbed gravels, it was observed that some portions were somewhat cemented, whereas others were soft and somewhat plastic. Consequently, several feet of undisturbed gravels were stripped from the foundation area. It was decided that an average of 18 ft of overburden and undisturbed alluvium would have to be excavated between sta 439 and sta 446+10 since this material was a relatively loose clayey and silty material and unsuitable as a foundation for the embankment shells. A minimum of 12 ft was excavated near sta 445+25, and a maximum of 24 ft was excavated near sta 446+00. This material was left in place immediately downstream of the embankment toe. The undisturbed channel gravels were excavated to have a slope of 1V:2H along the

sides of the core trench. The average thickness of undisturbed alluvium left in place between sta 439 and sta 446+10 was approximately 20 ft.

30. The construction records (US Army Engineer District, Sacramento 1953) indicate that the dredged tailing piles (located from sta 446+10 to sta 455+00) were leveled off at approximately el 390 ft to receive embankment material, and the slope of this material was 1V:2H along the sides of the core trench.* Kiersch and Treasher (1955) reported that the dredged channel gravels were cut back on a gentle slope of 1V:5H due to an unstable condition caused by an abundance of clay lenses.**

31. Kiersch and Treasher (1955) also reported that the core trench slopes were compacted by passes of a Caterpillar tractor before placing earthfill. This field practice was not mentioned in the construction records, which describe placement of cobbles and gravel on the core trench slopes to collect incoming drainage and divert it away from the core trench as the core material was being placed and compacted. The construction record did state that, away from the core trench, the pervious fill was compacted by such equipment as moved across the fill during construction operations.† Both references stated that exposure of the top of the schist bedrock revealed numerous springs, and a large quantity of water was seeping into the core trench, and had to be pumped out for construction to continue.

32. From sta 455+00 to sta 456+10, an average of 8 ft of undisturbed channel gravel was stripped prior to placement of embankment fill. Finer alluvium (sand, silt, and clay) exposed from sta 456+10 to sta 458+00 was considered to be unsuitable as a foundation for the embankment and was removed to expose schist bedrock. Approximately, 18 ft of material was excavated near sta 456+10, and 4 to 6 ft of material was excavated near sta 458+00.

* Data obtained from the Becker Hammer field investigations presented in Part III of this report detected the presence of dredge tailings beneath the embankment slopes as high as el 420.

** The Becker Hammer field investigation results presented in Part III of this report and additional results presented in Report 4 of this series are generally consistent with the construction record description of stripping and excavation in this area and do not confirm the excavated slopes and abundant presence of clay lenses reported by Kiersch and Treasher (1955).

† The Becker Hammer field investigation results presented in Part III and Report 4 of this series indicate there is some increase in energy- and overburden-corrected blowcounts in the dredged foundation gravels beneath the slopes compared with the dredged gravels downstream of the toe of the dam.

Approximately, 3 ft of overburden was stripped from the foundation from sta 458+00 to sta 460+75 to expose the hard, blocky schist bedrock.

33. To drain the area for construction, the water that normally flowed through the Blue Ravine channel was diverted so that most of the water drained into the South Fork. There was a need for water from the Blue Ravine in the downstream area to serve dredge ponds, domestic, and irrigation purposes. To provide water downstream, a bypass tunnel was constructed through the left abutment of Mormon Island Auxiliary Dam. The 6 x 6-1/2 ft tunnel was approximately 1,300 ft long. The metamorphic rock encountered during tunneling was extensively weathered, blocky with numerous clayey seams, and required timbering for support, except for a 311-ft-long section near the middle of the tunnel. The rock in this unsupported section of the tunnel was typically hard, blocky schist. The bypass tunnel was plugged once construction was completed. After some placement of earthfill, the foundation rock was grouted.

Laboratory Tests During Original Design and Initial Construction

34. The laboratory test results reported in this section were used in the original design of the dam. The design and initial construction data were used to assist in characterizing the site and formatting an idealized section for the seismic safety evaluation. These design values for material properties were used as initial estimates for comparison with material property values determined in the field and laboratory investigations reported in Parts III and IV and Report 4. Index tests on the materials obtained from the dredged and undisturbed alluvium during this preconstruction period indicated the materials are a mixture of gravel, sands, and silty and clayey fines. Specific gravities ranged from 2.72 to 3.03. An average specific gravity of 2.82 was adopted for both the dredged and undredged alluvial materials and for both the +No. 4 and -No. 4 (sieve) particle sizes. Specific gravity of the bedrock ranged from 2.77 to 2.89 and averaged 2.84.

35. The in situ dry density of the dredged tailings was estimated to vary from 83 to 117 pcf. The average was estimated to be 108.5 pcf with an average in situ water content of 23.8 percent in the finer dredge tailings which were estimated to extend from approximately 10 ft below ground surface to bedrock (based on examination of push-tube samples), a maximum distance of 55 ft. The adopted (for initial design purposes) dry density of the coarser

dredged tailings located from 0 to 10 ft below the ground surface was 125.0 pcf.* This is the same density that was adopted during design for the dredge tailing gravel fill that was compacted to the embankment shells.*

36. In situ dry density of the undredged alluvial foundation varied from 80.0 to 117.5 pcf. The average dry density was estimated to be 100.0 pcf with an in situ moisture content of approximately 19.7 percent. For the coarser undisturbed alluvium, the in situ dry density varied from 108.0 to 133.7 pcf with a weighted average of 122.6 pcf and an average moisture content of 11.1 percent. In situ measurements of the density of the weathered bedrock varied from a dry density of 101.6- to 118.7-pcf with an average of 107.5 pcf. The in situ moisture content of the weathered bedrock averaged 18.6 percent.

37. Permeability tests were run on block samples of the undisturbed alluvium and ranged from 0.07×10^{-4} to 40×10^{-4} cm/sec in the vertical direction. In the horizontal direction permeability ranged from 0.02×10^{-4} to 10×10^{-4} cm/sec. Permeability tests were not run on the dredge tailings.

38. The shear strength of the undredged and dredged alluvium was determined from consolidated-drained direct shear tests on remolded specimens of -No. 4 fraction and large-scale (12-in. diam) consolidated-undrained triaxial tests on remolded samples. The results of these shear tests are summarized in Table 2.** In addition to the laboratory work, the shear strength of the dredged tailings was estimated by assuming that the tailing slopes that existed in the field prior to dam construction had a safety factor of 1. The average value of $\tan \phi$ required to hold the section in equilibrium was determined. The back-calculated friction angles ranged from about 24 deg to 26 deg. A value of ϕ' equals to 24 deg ($\tan \phi$ equals to 0.45) was adopted for design. Shear tests were not performed on the weathered and decomposed schist.

* Test pit results presented in Report 4 indicate that the average in situ dry density of the dredge tailings in the upper 7 ft of the foundation downstream of the toe of the dam was 117.5 pcf, and in the downstream shell of the embankment the dry density averaged 137.7 pcf.

** These results were not corrected for membrane compliance effects since membrane compliance had not yet been recognized as a problem at the time the tests were performed.

Embankment Materials

39. The Mormon Island Auxiliary Dam cross section consists of 4 zones. Zone 1 is constructed of dredged gravels and forms the upstream and downstream shells. These gravels came from Borrow Area 5, the Blue Ravine itself. Zone 2 is a 12-ft-wide transition zone constructed upstream and downstream between the central zones and embankment shell. Zone 2 consists of the -2 in. fraction of the dredge tailings and was also obtained from Borrow Area 5. Zone 3 consists of impervious decomposed granite from Borrow Area 1. Zone 4 consists of impervious material (clayey sand) from Borrow Area 6. Zone 3 was added due to the fact that insufficient clayey material was available in Borrow Area 6 to construct Zone 4 as wide as originally planned. The specifications for placement of these zones are summarized in Table 3. The locations of the borrow areas are shown in Figure 2.

40. Figures 15 through 21 are photos from construction records which show key features of foundation preparation and construction procedures. Figure 15 was taken on 10 April 1951 and shows the foundation preparation in progress. The view is taken from the left abutment, facing the right abutment. The dredged tailing windrows are shown in the foreground, and the cleared bedrock schist foundation is shown in the background. Figure 16 is taken from sta 421+00 facing the right abutment and shows the cleared bedrock schist foundation for this portion of the dam. Figure 17 is taken from sta 440+00 looking toward the right abutment and shows core trench excavation as it approached the dredged section. Figure 18 is taken from sta 440+00 facing the left abutment and shows core trench excavation through the undredged portion of the alluvium. Figure 19 was taken on 26 September 1951 and is taken from the left abutment facing the right abutment. This photo shows the completed core trench excavation. Figure 20 was taken at sta 458+00 facing the right abutment and shows placement of Zones 2, 3, and 4 materials in the excavated core trench. Figure 21 was taken at sta 421+50 facing the right abutment and shows compacted Zone 1 material in the upstream shell.

PART III: FIELD INVESTIGATIONS

General

41. Field investigations were conducted at Mormon Island Dam in the embankment and foundation materials to obtain information about the cyclic strength and other input parameters used in the seismic stability analysis. The field investigations were performed in two phases. In both phases the field testing was confined to the downstream side of the center line. The information gathered is assumed to be representative of the materials on the upstream side of the center line.

42. The Phase I field investigations consisted of Standard Penetration Testing (SPT), disturbed and undisturbed soil sampling, geophysical investigations, test pits and shafts (to obtain disturbed samples and determine in-situ densities), and Becker Hammer Testing. The Phase I field investigation focused on the segment of the dam where the shells were founded on dredged tailings. Only surface geophysical measurements were made on the undredged foundation during this field investigation. Detailed descriptions of each of the components of the Phase I field investigations are included in Report 4 of this series.

43. The Phase II field investigation was performed to supplement the field data acquired from the earlier investigation. The program consisted of geophysical testing, excavation of test pits, and Becker Penetration Testing. These tests provided data which were useful in characterizing and idealizing the site and in determining key material properties such as shear wave velocities and cyclic strengths of the embankment and foundation soils. The investigation provided data from the undredged foundation and added to the data bases of the embankment shells and dredged foundation gravels developed in the Phase I investigation. A discussion of each component of the Phase II investigation is described in the following sections of this part.

44. A layout of the field investigation program is shown in Figure 22. This plan view shows the locations of each of the various tests performed during the program. The drawing shows the location and areal extent of the various foundation conditions present at Mormon Island Auxiliary Dam. The pool level during the time the Phase II work was conducted varied between el 433.3 and el 444.5. One of the goals of the Phase II field investigation was to

acquire information about the undredged alluvium. Information obtained from construction documents and specifications was used to derive a typical cross-section of the embankment and foundation geometry in the undredged foundation segment of the dam. This cross section is shown in Figure 23 and was useful in interpreting the data acquired in the field investigation. This sketch shows that prior to construction the undisturbed alluvium consisted of two distinct layers. The upper layer was a fairly soft clayey gravel with a varying thickness which averaged approximately 11 ft. This was underlain by a dense gravelly alluvium containing less fine content which extended to bed-rock. Engineers involved with the design of the embankment decided that the soft clayey gravel layer was an unsuitable foundation material. This layer was removed and the shells were founded directly on the firmer, denser, and stronger undredged alluvium. The clayey gravel layer was excavated only under the shells and was left in place immediately upstream and downstream of the toes of the dam. Due to this excavation, the clayey gravel material was considered to have no significant effect on the dynamic response and stability of the embankment. Nonetheless, the clay layer was encountered in many of the field tests which were performed in the downstream toe area of the undredged segment of the dam and affected the manner in which these tests were interpreted.

Geophysical Tests

45. The geophysical investigation conducted as part of the Phase II field investigation consisted of surface refraction seismic, crosshole, and downhole tests (Kean 1988). The objective of this program was to determine the in situ variation of compression wave (p-wave) and shear wave (s-wave) velocities with depth for the foundation materials of the undredged area. The p-wave and s-wave velocity variations with depth for the embankment and dredged foundation materials were determined from a similar testing program performed during Phase I and documented in Report 4 of this series.

Surface refraction seismic

46. In the surface p-wave seismic refraction technique, a seismic signal is generated at the surface by the impact of a hammer striking a steel plate. The signal is then detected by an array of geophones placed on the ground surface and extending in a straight line away from the source of the

seismic disturbance. All signals are then recorded on a twelve channel seismograph. The data are interpreted to determine the p-wave velocities of the soil and rock materials at the site and the depths to interfaces between materials with contrasting velocities. Seismic disturbances are initiated at each end of the line to detect the dip of the refracting surfaces and to ascertain the true seismic velocities of subsurface zones. It is not possible to detect a velocity inversion, a low velocity layer underlying a high velocity layer, with the seismic refraction test. The data acquired from this test are useful for detecting saturated zones and the depth to rock. These velocities and interface depths were considered with other tests in developing a recommended p-wave velocity profile of the undredged alluvium downstream of the toe of the dam.

47. One seismic refraction test, R1, was conducted during the Phase II field investigation. As shown in Figure 22, this line was located in the undredged area about 100 ft downstream of the toe. The line was 75 ft long. The test data are displayed in the time-distance plot shown in Figure 24. Three p-wave velocity zones were interpreted. The first had a velocity of 1,070 fps and extended to a depth of approximately 1.0 to 1.5 ft. The second zone had a velocity of 1,760 fps and extended to depths ranging between 10.5 and 14.0 ft where it was underlain by the third zone which had a velocity of 4,330 fps and extended to an unknown depth.

48. An overburden shear-wave seismic refraction test, 16 ft long, was performed to measure the shear-wave velocities of the near surface soils. The test was run in the same location as seismic line R1. This test indicated that the shear-wave velocities in the top foot are 210 fps. This is underlain by a layer in which has a shear-wave velocity of 700 fps. Due to the short length of the line the results are applicable only to the top four or five feet of the foundation deposit.

Crosshole tests

49. The cross hole tests were performed to determine both p-wave and s-wave velocities. Only one set of crosshole tests was performed during Phase II. The tests were conducted in two borings, each 45 ft deep, spaced 10 ft apart. The borings were located about 100 ft downstream of the toe of the dam, near sta 441+00 in the undredged segment of the dam as shown in Figure 22. The holes were drilled using a rotary drill and then cased with 4-in.-diam polyvinylchloride (PVC) pipe. The annular space between the sides

of the hole and the pipe was filled with a grout mixture which, when set up, has the approximate consistency of soil. Due to logistical difficulties, only one of the boreholes was surveyed for its deviation from the vertical. Since the drift in this boring was minimal, the drift of the unsurveyed hole was assumed to be negligible in the data reduction calculations. Unfortunately, the materials encountered in the subsurface during drilling were not logged. Consequently, narrative descriptions of the subsurface in the immediate vicinity of the crosshole borings were not available to help guide the interpretation. There was also no record of the observation of water levels in the borings at the time the drilling was performed.

50. Crosshole s-wave velocity tests were conducted with a downhole vibrator inserted at a given depth into the source borehole. The vibrator was then swept through a range of frequencies (50 to 500 Hz) to find the frequency which propagated best through the soil and transmitted the highest amplitude signal to the receiver geophone lowered to the same depth in the receiver hole. The p-wave cross-hole tests were performed in a similar manner except that exploding bridge-wire detonators were used as the source in place of the vibrator. The measurements for both p-wave and s-wave velocity tests were performed at 2.5-ft-depth intervals.

51. The results of the crosshole p-wave velocity tests are shown in Figure 25. The measured velocities range from 1,390 fps near the ground surface to 11,260 fps near the bottom of the hole. The plot shows that the general trend is for the velocities to increase with depth; however one inversion was encountered at a depth of 12.5 ft where a layer with a 5,000-fps velocity was underlain by one with a 4,000-fps velocity. These observations were used to determine an idealized p-wave profile for the undredged soils in this area.

52. The results of the crosshole s-wave velocity tests are shown in Figure 26. As with the p-wave velocities, the s-wave velocities generally increase with depth. They range from 680 fps near the ground surface to 2,120 fps at a depth of 47.5 ft near the bottom of the holes. A slight inversion was encountered at a depth of 32.5 ft where a velocity of 1,620 fps was overlain by a layer with a velocity of 1,890 fps. These velocities and interface depths were considered with other tests in developing a recommended s-wave velocity profile of the undredged alluvium downstream of the toe of the dam.

Downhole tests

53. Downhole p- and s-wave tests were performed in the same borings used for crosshole testing. The downhole tests provide supplemental data for checking the results of the crosshole tests. Downhole seismic tests were performed by placing the source of the seismic disturbance at ground surface midway between the two boreholes. P-waves are generated by striking a steel plate with a sledge hammer. The resulting seismic signal is then detected using a triaxial geophone array located within the borehole at the depth tested. The s-waves are generated by alternately striking the ends of a wooden plank. The s-wave arrival is determined by noting the time where the two seismic signals reverse direction and become out of phase. Both types of tests were conducted at 2.5-ft-depth intervals.

54. The downhole p-wave test results are shown in Figure 27. The velocities in this figure represent the average velocities of the results obtained from the tests performed in each of the two borings. The figure shows that four p-wave velocity zones were detected with velocities ranging from 1,100 fps near the ground surface to 7,150 fps at depths near the bottom of the hole. As with the crosshole tests, the downhole results show that the velocities increase with depth. The results of these tests were also considered in developing an idealized p-wave velocity profile for the undredged area.

55. The downhole s-wave velocity test results are shown in Figure 28. The s-wave downhole tests were only performed in one of the boreholes, hence the results are presented in the form of the standard time versus slant distance plot. Four s-wave velocity zones were detected. The range of velocities of these four zones is from 500- to 2,200 fps. The results of these tests were also considered in developing an idealized s-wave velocity profile for the undredged area.

Interpreted p-wave zones

56. The data acquired from the surface refraction, crosshole, and downhole tests were assembled into the composite shown in Figure 29. A recommended final interpretation of the p-wave zones was arrived at through study of the composite and by consideration of the strengths and weakness of each of the tests. A comparison of the test results shown on the composite indicates that the refraction line was not long enough to detect the higher velocities (greater than 7,000 fps) detected by the downhole and crosshole tests at

depths of about 25 ft. Other than that, the composite shows that the velocity profiles obtained from each of the three tests are basically in good agreement.

57. The recommended interpreted p-wave velocity zones for the downstream toe area are shown in Figure 30. Two velocity zones of 1,070 and 1,700 fps are associated with the clayey gravel layer (see Figure 23) which was left in place upstream and downstream of the toes of the dam but removed beneath the embankment shells. The water table was estimated to occur at a depth of about 10 ft where the velocity was about 5,200 fps. This interpreted water table roughly coincides with the top of the undredged gravel alluvium underlying the clayey layer. Between the depths of 10 and 25 ft, the undredged alluvium is estimated to be saturated or nearly saturated as evidenced by the velocity zones of 4,400 and 5,200 fps. It was interpreted that weathered rock occurred at a depth of about 25 ft where the velocities ranged from 7,240 to 11,260 fps.

Interpreted s-wave zones

58. The s-wave velocity zones were interpreted in a manner similar to the p-wave velocity zone interpretation. The s-wave composite showing the seismic refraction, downhole, and crosshole results is shown in Figure 31. From study of the composite, the recommended interpreted s-wave velocity zones shown in Figure 32 were determined. This plot shows that two zones having velocities of 210 and 700 fps were associated with the clayey layer which extended from the ground surface to a depth of about 10 ft. The underlying layer in the depth interval 10 to 22.5 ft has a velocity of 1,000 fps and is associated with the undredged gravel alluvium. At depths greater than 22.5 ft, the shear wave velocities were interpreted to indicate rock as opposed to the 25-ft depth to the rock-alluvium interface indicated by the p-waves. The velocity of rock increases with depth and ranges from 1,560 to 2,150 fps at the lower limit of the depth of investigated profile, about 50 ft.

59. The interpreted shear-wave velocity profile was used to estimate the K_2 value of the various strata in the undredged alluvium. K_2 is a unitless measure of shear modulus that is essentially independent of confining pressure and is computed using the following equation:

$$K_2 = \frac{G}{1,000 \times \sigma'_m{}^{1/2}} \quad (1)$$

where

G = shear modulus, psf

σ'_m = mean normal pressure, psf

At low levels of shear strain, G and K_2 can be estimated from shear wave velocity measurements as follows:

$$G = V_s^2 \times \rho \quad (2)$$

$$K_2 = \frac{V_s^2 \times \rho}{1,000 \times \sigma'_m{}^{1/2}} \quad (3)$$

where ρ is mass density. Any consistent set of units can be used in Equation 2, but in Equation 3 the units must be in feet, pounds, and seconds. From the interpreted profile of Figure 31, it was estimated that K_2 for the clayey gravel layer was 110, and K_2 for the undredged alluvium was 130. These values fall within the range of K_2 values reported for gravelly materials by Seed et al. (1984). These K_2 values were later used to determine stress-dependent low strain shear moduli in the dynamic finite element analysis.

Test pits

60. Two test pits, RD-1 and RD-2, were excavated during the Phase II field investigation to acquire data regarding the gradation and densities of the undredged alluvium. The location of the test pits is shown in plan in Figure 22. RD-1 and RD-2 were located near sta 440 and sta 442, respectively, approximately 100-ft downstream of the toe of the dam. Each was excavated to a depth of 13 ft as shown in the cross section of Figure 23. Unfortunately, most if not all of the 24 samples retrieved from the test pits were located in the layer of clayey material. The average dry density of the sampled material was 134.7 pcf. The average fines content (percent passing the No. 200 sieve) of the samples was 40 percent; the average liquid limit was 40 percent; the

plasticity index of the fines was 22 percent. As expected, the indices from all samples retrieved plotted well above the A-line on the plasticity chart indicating a clayey material.

61. The best data on the gradations of the undredged alluvium beneath the clay layer were obtained from a test shaft, 4F-40, excavated during the preconstruction exploration program. This shaft was approximately excavated at sta 444+00, upstream of the dam center line, in a location now covered by the upstream shell. The location of 4F-10 is shown in Figure 22. The location of this test shaft and the profile of materials sampled are also shown in Figure 3. Four samples were excavated at depths below the 11-ft thick clay layer. Figure 33 shows the observed range of gradations of the excavated samples. The plot shows that D_{50} was about 30 mm, the fines content was less than 10 percent, and the fines were nonplastic. The samples classified as GW according to the USCS. Dry densities of 133.7 and 129.4 pcf were measured in this test shaft at el 353 and el 350. The size of the samples used for the gradation tests and the technique used to measure the in situ densities in test shaft 4F-40 are unknown.

62. In situ densities and gradations for the dredged foundation gravels and the embankment shell gravels were obtained from test pits excavated during the Phase I study. Details about the data and sampling procedures are given in Report 4 of this series. The locations of the test pits from the Phase I studies are shown in Figure 22. Samples retrieved from the test pit located on the downstream face of the dam at midslope (19 ft deep) indicated that embankment gravels in the shell have relative densities of about 70 percent. The range of gradations of the samples is shown in Figure 34. The fines are somewhat plastic and have an average plasticity index of 11 percent and a liquid limit of 28 percent. The fines content was about 5 percent. Samples retrieved from the test pits (7 ft deep) excavated along the downstream toe of the dam indicated that the dredged foundation gravels have a relative density of about 35 percent. Samples recovered from the test pits and shafts were used to reconstruct specimens for laboratory testing.

Becker Penetration Tests

General

63. Becker Hammer penetration tests were conducted in the downstream embankment shell, the undredged alluvium, and the dredged foundation material. The data collected were used to develop stratigraphy for site characterization and to estimate the cyclic strength of the soils at the site. Twenty-six pairs of open and closed bit Becker soundings were performed at each of the locations shown in Figure 22. Becker blowcounts N_B were obtained from each of the closed bit soundings at 1-ft depth intervals. Index properties, soil classification data, and N_B were collected from each of the open bit soundings.

64. The drilling was performed by Layne-Western, Inc. in September of 1986. Two Becker AP-1000 drill rigs were employed to accomplish the drilling. Soundings BH-1 through BH-24 were performed using rig No. 404, and BH-24 and BH-25 were performed with rig No. 403 (see Appendix A). A photo of this type of drill rig is shown in Figure 35. For the closed-bit soundings, an 8 tooth crowd-out bit with a 6-5/8-in. OD and a 4-1/4-in. ID (plugged at the end) was used with a 6-5/8-in. OD casing. The open-bit soundings were made with a Felcon bit which is a 3-web crowd-in bit for 6-5/8-in. casing but has an enlarged diameter near the bit (7-1/4-in. OD) and an inner casing ID of 3-7/8 in. Each sample spanned a 2-ft depth interval. Blowcounts were taken at 1-ft intervals. A photo of these bits is shown in Figure 36.

Data reduction procedures

65. Only penetration data from the closed bit soundings were used in the liquefaction and stratigraphy evaluation of the soils at the site. The Becker Hammer blowcounts N_B were corrected to equivalent SPT N_{60} (energy corrected) and $(N_1)_{60}$ (overburden corrected) blowcounts. A schematic of this process is presented in Figure 37.

66. The energy corrections were made by Dr. Les Harder using techniques which he developed in his research of the Becker Hammer Drill. His report is included in Appendix A. The conversion of the field Becker blowcounts into equivalent SPT blowcounts depends on combustion conditions (throttle and supercharger settings, temperature and altitude) of the diesel powered drill rig and the type of equipment used (type of bit, size of casing, and drill

rig). Hammer energy readings were collected with the blowcount so that $(N_1)_{60}$ values could be estimated.

67. The overburden correction to convert equivalent SPT N_{60} into $(N_1)_{60}$ was made using the following formula:

$$(N_1)_{60} = C_n \times N_{60} \quad (4)$$

where

$(N_1)_{60}$ = SPT blowcount at energy level of 60 percent and overburden pressure of 1 tsf

C_n = overburden correction factor which is dependent upon vertical effective stress

N_{60} = SPT blowcount at energy level of 60 percent of theoretical maximum

68. The C_n curves used in this study are shown in Figure 38. The figure shows curves recommended by Seed (1983) to be used for sands with loose ($D_r = 40$ to 60 percent) to medium-dense ($D_r = 60$ to 80 percent) relative densities. The third curve is for gravels and is an extrapolation based on the relationships between mean grain size C_n and confining pressure from data reported by Marcuson and Bieganousky (1977). A discussion of the rationale for this extrapolation is included in Harder's report in Appendix A. In this study, the gravel curve was used for blowcounts in the embankment gravels and in the dredged alluvium. The medium-dense sand curve was used to determine C_n for blowcounts in the undredged alluvium. At a given vertical stress, the use of the gravel curve will result in a smaller correction than will use of the sand curve which in turn results in a higher value for $(N_1)_{60}$.

69. To determine the overburden corrected blowcount, the effective vertical confining stress must be computed for each location where a blowcount is measured. For each location, an adjustment is made to the vertical effective stress computed in a two-dimensional, nonlinear static finite element analysis to account for the fact that the overburden correction (C_n) charts were developed for level ground conditions rather than sloping ground. The vertical effective stresses computed in the finite element analysis are presented later in this report. The formulas employed for computing the vertical effective stress used to determine the overburden correction factor C_n are derived and shown in Figure 39. The figure shows that the mean confining stress

corresponding to the vertical effective stress in sloping ground is larger than in level ground for the same depth below the surface. It is assumed that blowcounts in a given soil deposit increase as the mean confining stress increases.

70. To determine an equivalent vertical effective stress for selection of C_n , the following formula was used:

$$\sigma'_{v1} = 1.67 \times \sigma'_{ms} \quad (5)$$

where

σ'_{v1} = equivalent level ground vertical effective stress used to determine C_n

σ'_{ms} = effective mean stress under sloping ground determined in the static finite element analysis

Equation 5 was derived by equating the expressions for mean normal pressure for plane strain and level ground conditions and solving for the level ground vertical stress as shown in Figure 39. Equation 5 was developed using a Poisson's ratio of 0.3 and a K_o of 0.4.

71. Figure 40 shows the effective vertical and mean normal stresses from the finite element analysis and the equivalent vertical effective stress computed from Equation 5 for a column of soil through the downstream slope of Mormon Island Auxiliary Dam. The equivalent level ground vertical effective stress σ'_{v1} is higher than the sloping ground vertical effective stress at all depths. As shown in Figure 38, the use of σ'_{v1} will result in a more severe C_n correction factor than if C_n were determined from the finite element vertical stresses for blowcounts at depths where the vertical effective stress is greater than 1 tsf. The reverse is true at depths where the vertical effective stress is less than 1 tsf.

Results of $(N_1)_{60}$ data

72. Values of $(N_1)_{60}$ were computed using the procedure outlined above from the N_B values obtained from the 26 closed bit soundings performed during the Phase II studies. The results of these computations are shown in the cross sections shown in Figures 41 through 43 and also in Appendix B. Figures 41 through 43 show plots of $(N_1)_{60}$ versus depth superimposed on three geologic cross sections at the site. The cross sections are along the downstream toe, along the downstream midslope, and transverse to the dam's axis at

sta 450. These cross-sectional plots were useful for refining the locations of boundaries between embankment and foundation materials and also for determining the average value and variation of penetration resistance for both the dredged and undredged alluvium and the embankment shell gravels.

73. Figure 41 shows the $(N_1)_{60}$ results for Becker soundings BH-1 through BH-14 superimposed on the geologic cross section running parallel to the dam axis about 100 ft downstream of the toe. The cross section can be divided into two parts. The undredged section of the channel is located approximately between sta 436+00 and sta 444+50 and the dredged section is located between sta 444+50 and sta 456+00. The undredged foundation was explored with soundings BH-1 through BH-6. The clay layer, unexcavated downstream of the toe, was encountered in the top several feet of each of these borings. Its thickness varies from 8 to 20 ft and it is characterized by $(N_1)_{60}$ values which are typically less than 5 blows/ft. As discussed previously, the clay layer is underlain by the undredged gravel alluvium upon which the embankment shells are founded. As shown by soundings BH-1 through BH-6 in Figure 41, the $(N_1)_{60}$ values of the undredged foundation alluvium are typically well in excess of 30 blows/ft and show a trend of increasing steadily with depth.

74. Figure 41 shows the results for Becker soundings BH-7 through BH-14 along the toe, between sta 445+00 and sta 455+50. Soundings BH-7 through BH-13 were performed in the tailings. The tailings are characterized by $(N_1)_{60}$ values which are typically less than 10 blows/ft. Variations in $(N_1)_{60}$ in each of these soundings is slight and there is no obvious trend in $(N_1)_{60}$ with depth. Blowcounts less than 10 were also encountered in the upper 10 ft of BH-14. A study of the preconstruction photos and the Mormon Island Dam foundation report (US Army Engineer District, Sacramento 1953) indicates that these low penetration resistances can be attributed to a clayey overburden and slope wash material rather than the tailings. This material is similar to the material encountered in the near surface clay layer in BH-1 through BH-6 in the undredged area. Undredged alluvium was detected beneath the tailings and overburden in BH-13 and BH-14 at depths of 42 and 10 ft, respectively, as evidenced by marked increases in $(N_1)_{60}$. Below these depths, the $(N_1)_{60}$ values show a tendency to increase with depth in much the same manner as those observed in the undredged alluvium encountered in BH-1 through BH-6.

75. Figure 42 shows a geologic cross section through the downstream midslope of the embankment between sta 444+50 and sta 456+00. Soundings BH-15 through BH-21 were located at the midslope of the embankment (el 420) to obtain information pertaining to the embankment shells and their underlying foundation materials. The interpreted location of the contact between the embankment gravels and their underlying foundation is approximately el 375 as shown by the dashed line on this figure. Above this contact the embankment gravels are typically characterized by $(N_1)_{60}$ values which are typically between 15 and 30 blows/ft. All blowcounts in the embankment were made in the Zone 1 shell gravels. The soundings show that there is a very noticeable amount of variation in the $(N_1)_{60}$ values in the embankment materials. Additionally these soundings show that there is no apparent increase in $(N_1)_{60}$ with depth.

76. Dredged foundation gravels were encountered beneath the embankment gravels in BH-16 through BH-20 as shown in Figure 42. The foundation gravels are characterized by a lower penetration resistance than the overlying embankment gravels. This decrease is not great at these locations. The $(N_1)_{60}$ values in the dredged foundation are typically between 10 and 25 blows/ft and show significantly less variation than those in the overlying embankment gravels. The $(N_1)_{60}$ values under the embankment shells appear to be slightly higher than those taken on the downstream toe in soundings BH-7 through BH-12 as was shown in Figure 41. This increase in $(N_1)_{60}$ is probably caused by a combination of effects including compaction by construction activities, densification under the embankment loads, and aging. A similar increase in blowcounts was observed at Comanche Dam (Seed 1985).

77. Undredged alluvium was encountered beneath the embankment shell gravels in BH-21 and BH-15. These soundings show that $(N_1)_{60}$ is higher in the undredged alluvium than in the embankment and that $(N_1)_{60}$ has a tendency to increase with depth. The increase in foundation blowcounts is marked in BH-21. These soundings show that the penetration resistance is more variable in the undredged alluvial foundation than in the dredged foundation encountered by BH-16 through BH-20. The contact between the embankment gravel and the undredged alluvium is at el 355 in BH-21 which is about 20 ft lower than the contact interpreted from the other soundings in Figure 42. The lower foundation contact on BH-21 reflects the removal of the clay layer between

sta 439 and sta 446 where the shells are founded directly on the undredged gravel alluvium.

78. Figure 43 shows the transverse cross-section of the dam at sta 450. The $(N_1)_{60}$ profiles from BH-10, 18, 22, 23, 24, 25, and 26 are superimposed on this cross-section. At sta 450 the shells are founded on the dredged tailings. These soundings were performed to acquire information on the gravels in the shells and in the dredged foundation. The contact between the shell and the dredged foundation gravels is shown by the dashed line in Figure 43. The figure shows that the penetration resistance of the embankment gravels was measured above the dashed line of soundings BH-25, 26, and 18. All blowcounts in the embankment were made in the Zone 1 shell gravels. As noted before, the $(N_1)_{60}$ profiles over the depth range of the embankment gravels in these soundings show a significant amount of variation. Typically, $(N_1)_{60}$ lies between 15 and 30 blows/ft though there are several exceptions. In BH-25, the $(N_1)_{60}$ profile shows that embankment gravels were encountered through nearly the entire depth of this sounding. The tailings were encountered beneath the embankment gravels in BH-18 and BH-26. As noted before, the $(N_1)_{60}$ values of the tailings are noticeably lower than those in overlying embankment and show only slight variation. Soundings BH-22, 23, 24, and 10 encountered the dredge tailings throughout the depth of the profile. The $(N_1)_{60}$ profiles of these soundings show the typical characteristics for the tailings. The data from BH-22, BH-23, and BH-24, performed on the slope of the embankment, indicate that tailings were incorporated into the embankment in this area. This agrees with a detail shown in Figure 4 for the typical cross section between sta 446 and sta 454 which shows the presence of tailings in the embankment. Also, the embankment gravel-dredged foundation contact line interpreted from the penetration resistance has a slope of approximately 2H:1V which agrees with the slopes excavated for the core trench which is shown on the same cross-section in Figure 4.

79. Figure 43 shows that the values of $(N_1)_{60}$ taken in the tailings in BH-10, 24, 23, 22, 18, and 26 increase slightly with depth. Additionally, $(N_1)_{60}$ values in the dredged foundation of BH-18 and BH-26, where the tailings are under the weight of the embankment, are somewhat greater than the blowcounts taken in BH-22, 23, 24, and 10 where the tailings are not loaded by the weight of the embankment.

Statistical analysis of $(N_1)_{60}$ data

80. In order to gain a better understanding of the data acquired from the Becker Hammer Penetration Tests performed during Phase II, a statistical analysis was performed. A statistical analysis was performed on the energy corrected-overburden corrected blowcounts $(N_1)_{60}$ acquired from the embankment gravels, the dredged foundation gravels, and the undredged alluvium. For each material, the average and standard deviation of $(N_1)_{60}$ was computed. A histogram of $(N_1)_{60}$ was developed showing the distributions of $(N_1)_{60}$ for all observations. The average $(N_1)_{60}$ values were used to determine the cyclic strengths for each material as will be discussed later in the report. All blowcounts taken at depths of 5 ft or less were excluded from the analysis to avoid excessive extrapolation of C_n values at low vertical effective stresses from Figure 38. Additionally, blowcounts taken in both the dredged and undredged foundation zones near rock were also excluded. This is because the presence of the relatively rigid rock surface artificially raises the blowcounts of materials when the penetrometer is located within three or four diameters of the rock surface.

81. The average value of $(N_1)_{60}$ for the Zone 1 embankment gravels was computed to be 24.8 blows/ft. The standard deviation was 8.8 blows/ft. These were computed from a population sample of 516 blowcounts from BH-15 through BH-21 and BH-25. A histogram showing the sample distribution is shown in Figure 44. The histogram shows the data fit a normal distribution fairly well except for the fairly large number of blowcounts above 42 blows/ft. Most of these high values were obtained in BH-26 which is located just downstream of the core. It is hypothesized that there was more compaction in this part of the shell due to a larger volume of construction equipment traffic than in other parts of the shell. However, as mentioned previously, BH-25 and BH-26 were performed using a different drill rig (No. 403) than was used for BH-1 through BH-24 (No. 404). If the $(N_1)_{60}$ values from BH-25 and BH-26 are excluded from the analysis, the average value for $(N_1)_{60}$ is 24.2 blows/ft which is only 0.6 blows/ft less than the case where all data are included. The overall results obtained agree fairly well with the average $(N_1)_{60}$ observed from one closed-bit and one open-bit soundings during the Phase I study where the average value for $(N_1)_{60}$ was determined to be about 23. The results also agree with the analyses performed on the same data by Harder in

Appendix A. Harder's analyses indicate that the mean value of $(N_1)_{60}$ will be within the range of 22 and 25 blows/ft.

82. The undredged foundation gravels had an average $(N_1)_{60}$ of 46.9 blows/ft. A standard deviation of 20.8 blows/ft was computed for this material. These computations were based on a sample population of 182 blowcounts. A histogram of the sample distribution for the undredged foundation is shown in Figure 45.

83. It was observed that the $(N_1)_{60}$ values of the dredged foundation gravels under the shells were higher than the values obtained in the dredged materials downstream of the toe of the dam. This trend was also observed in the Phase I Becker soundings. Due to this trend, zones of characteristic $(N_1)_{60}$ values were estimated. In the Phase I studies, the blowcount values were distributed throughout the dredged foundation guided by the vertical effective stress contours determined in the static analysis of the dredged foundation section documented in Report 4. The interpreted $(N_1)_{60}$ zones from Phase I are shown in Figure 46a. This figure shows that the average $(N_1)_{60}$ in these zones varies from a minimum of 6.5 blows/ft in the free field to a maximum of 20 blows/ft under the embankment shells. Much more data were obtained in the Phase II studies to establish these zones. Blowcount zones interpreted from the Phase II Becker tests are shown in Figure 46b. The larger Phase II data base shows three $(N_1)_{60}$ zones which have values of 7.1 in the free field, 13.7 beneath the toe of the slope, and 16.9 near the core trench. The boundaries between the zones coincide with vertical effective stress contours of 5 and 9 ksf. A comparison of the data in Figures 46a and 46b shows that the Phase II $(N_1)_{60}$ values of the dredged alluvium under the shells are slightly less than those interpreted from the Phase I data. In general, the Phase I and Phase II interpreted $(N_1)_{60}$ zones are quite similar and do not show any major differences that would alter the stability decision for this portion of the dam.

Becker gradations

84. Disturbed samples and blowcounts were obtained from the open-bit Becker hammer test at each location shown in Figure 22. Gradation tests and index tests were made from the recovered samples. The Becker samples spanned 2-ft-depth intervals. As will be discussed later, the cyclic strength of a soil deposit depends on the fines content (the percentage passing the No. 200

sieve) in addition to the $(N_1)_{60}$ value. Hence, the fines content was the desired information sought from samples recovered from the open-bit soundings.

85. The ability of the Becker Hammer drill to accurately sample the in situ gradations of the foundation and embankment gravels was tested by comparing the gradations of the Becker samples with those from ring density samples from nearby test pits.

86. During the Phase I study, an 18-ft-deep test shaft was excavated at midslope in the downstream shell approximately halfway between BH-20 and BH-21. Grain size distribution ranges of the test pit samples and the Becker samples from the upper 18 ft of BH-20 are shown in Figure 47. The Becker range includes the gradation of 7 samples and the test pit range includes the gradation of 16 samples. A comparison of the ranges indicates that the Becker gradations are finer than the test pit gradations. The average Becker fines content is 15 percent and the test pit fines content is less than 5 percent which represents a ratio which is larger than 3:1.

87. A similar comparison of the gradation ranges of Becker and test pit samples was made in the dredged gravel alluvium. The ranges for each are shown in Figure 48. The Becker gradations were obtained from four samples in the upper 6 ft of soundings BH-9 and BH-10, and the ring density samples were obtained from eight samples in the upper 6 ft of a test pit excavated during the Phase I studies. Both soundings BH-9 and BH-10 and the test pit are located near sta 450 downstream of the toe of the dam. Again, a comparison of the two ranges shows that the Becker samples are finer than the ring density samples. At midrange the fines content is 13 percent for the Becker samples and less than 5 percent for the test pit samples which represents a ratio which is larger than 2:1.

88. Ideally, the Becker gradations should not be significantly different from the test pit gradations which in turn should reflect the in situ gradation of the zones sampled. The data shown in Figures 47 and 48 indicate that the Becker open-bit samples will bias the sampled gradation of the embankment and dredged foundation gravels by retrieving samples which are finer than the in situ gradation. The fines content (percent passing the No. 200 sieve) for the gradations studied appears to be overestimated by at least 3:1. A number of possible reasons might explain these differences. For example, the coarsest portion is scalped due to the 3-7/8-in. ID of the open bit. Scalping definitely occurred since maximum particle sizes of 6 in. are

known to exist in the in situ gradations. The air circulation system might cause the fines content to be oversampled by vacuuming in fine particles from outside the volume which the penetrometer occupies as it is advanced through the subsurface. Particle crushing may also bias the sampled gradations.

89. The fines content is a necessary parameter for determining the cyclic strength of a deposit. To account for the overestimation of fines content when sampling with the Becker open bit, the fines content used for determining the cyclic strength was determined by adjusting the fines content of the Becker sample by a factor of two. The corrected fines content for each Becker sounding is indicated in the plots in Appendix B. Typically, after adjustment, the fines content of the embankment gravels, and both the dredged and undredged alluvium, was between 5 and 10 percent. The fines content adopted for use in the analysis was 5 percent.

Summary of field investigations

90. The Phase II field investigations were performed to acquire data on the embankment gravels and dredged and undredged foundation alluvium. This data supplemented the information obtained during the Phase I field investigation performed in 1983. The Phase II investigations included geophysical testing and Becker Hammer drilling.

91. In the geophysical program, seismic refraction, crosshole, and downhole seismic tests were conducted to determine the p- and s-wave velocities of the undredged alluvium between sta 439 and sta 446. From the p-wave data, it was estimated that the undredged alluvium was saturated or nearly saturated at the time of testing. The shear-wave velocity data indicated that K_2 of the undredged alluvium is about 130. K_2 for the embankment gravels and dredged alluvium were determined in the Phase I investigation to have values of 120 and 25, respectively. The values given for K_2 are maximums since they were determined from low strain amplitude shear wave velocity measurements.

92. Open and closed bit Becker Penetration tests were performed at 26 locations to provide data on the gravels in the shell, and in the dredged and undredged alluvium. The penetration tests provided data which proved to be useful in evaluating the site stratigraphy (i.e., identified and located the boundaries between materials of different types), and also determined the penetration resistances of the soils in the three zones of interest. From analysis of the data, the mean energy and overburden-corrected blowcounts

$(N_1)_{60}$ for the Zone 1 embankment gravel and the undredged alluvium were 24.8 and 48 blows/ft. In the dredged alluvium, $(N_1)_{60}$ values were higher under the embankment shells than in the free field. The dredged foundation was divided into $(N_1)_{60}$ zones with values which varied from 7.1 blows/ft in the free field to 16.9 blows/ft under the embankment shells. The $(N_1)_{60}$ values of the Zone 1 embankment gravels and of the dredged foundation gravels are similar to those obtained in the same zones during the Phase I field investigation. Becker tests were not conducted in the undredged alluvium during the Phase I studies.

93. The Becker Hammer open-bit soundings produced samples which over-estimated the fines content of the in situ gradations of the materials of interest by a factor of at least three. In the analysis, the fines content of the Becker samples was divided by a factor of 2 to account for this. After adjustment, the fines content of the embankment gravels and the dredged and undredged alluvium were all typically between 5 and 10 percent. A fines content of 5 percent, a somewhat conservative value, was adopted for purposes of estimating cyclic strength.

94. The data acquired in the field investigations were used to determine the material properties and cyclic strengths of the soils and to aid in developing idealized cross sections used in the finite element analysis. The use of this data for these purposes is discussed in subsequent parts of this report.

PART IV: ESTIMATES OF CYCLIC STRENGTH

General

95. The cyclic strength and pore pressure generation characteristics of the shell and foundation gravels (dredged and undredged) were estimated using a combination of in situ and laboratory test results. This chapter contains descriptions of the procedures used for estimating the cyclic strength from the in situ Becker Hammer test soundings. A comprehensive laboratory investigation was performed to determine the relative strength and pore pressure behavior of gravels subjected to cyclic loads. These tests were designed to determine the relative changes in cyclic strength with confining stress (K_v) and consolidation stress anisotropy (K_a). The results of these tests are reported herein. A detailed discussion of the laboratory program is included in Report 4 of this series. Tests performed on undisturbed specimens of compacted decomposed granite and index tests of all materials are reported in US Army Engineer Laboratory, South Pacific Division (1986).

Estimates of Cyclic Strength from In-Situ Tests

Empirical procedure to estimate cyclic strength

96. The cyclic strengths of the shell and dredged and undredged foundation gravels were determined using Seed's empirical procedure (Seed, Idriss, and Arango 1983, and Seed et al. 1984a). The chart used for determining cyclic strength based on Seed's work is shown in Figure 49. This chart relates measured $(N_1)_{60}$ values to estimated cyclic stress ratios at a number of sites which have been subjected to earthquake shaking from an $M_s = 7.5$ seismic event. The lines on the chart distinguish safe combinations of $(N_1)_{60}$ and cyclic stress ratios from unsafe combinations based on whether or not surface evidence of liquefaction was observed in the field. This chart is interpreted to relate $(N_1)_{60}$ to the cyclic stress ratio required to generate 100 percent residual excess pore pressure. Figure 49 provides data for clean and silty sands with different fines contents and expresses the cyclic stress ratio causing liquefaction for a confining pressure of about 1 tsf and level ground conditions and for earthquakes with $M_s = 7.5$, as a function of the

N_1 -value of a soil corrected to a 60 percent energy level, $(N_1)_{60}$. Seed's work (Seed, Idriss, and Arango 1983, and Seed et al. 1984a) shows that, for $M_s = 6.5$ events, the cyclic loading resistance is 20 percent higher for any value of $(N_1)_{60}$ than for $M_s = 7.5$ earthquakes.

Cyclic strength estimate for shell gravels, Zones 1 and 2

97. The representative $(N_1)_{60}$ values used to enter the cyclic strength chart shown in Figure 49 were determined from the field investigations discussed in Part III of this report. The representative $(N_1)_{60}$ value for the shell gravels was 25 blows/ft which is the average $(N_1)_{60}$ for all blowcounts in the shell from Becker closed-bit soundings during the Phase II investigations. As discussed earlier, the fines content of the embankment gravel was taken to be 5 percent. Thus, entering the chart at an $(N_1)_{60}$ of 25 blows/ft and using the curve for 5 percent or less fines content yields a cyclic stress ratio of 0.29 for a Magnitude 7.5 event. This value was increased by 20 percent to account for the lower Magnitude 6.5 event. This resulted in a cyclic stress ratio of 0.35 required to generate 100 percent excess pore pressure in 8 equivalent cycles (representative for an $M = 6.5$ event) under level ground at a vertical effective stress of 1 tsf. This cyclic stress ratio is equal to the value used in Report 4 for the shell gravels in the finite element and post-earthquake stability analysis performed on the section of Mormon Island Auxiliary Dam where the shells are founded on the dredged foundation gravels.

98. Due to the similarity of the Zone 2 transition gravel to the Zone 1 shell gravel in terms of gradation, fines content, plasticity, and method of placement, it was concluded that the Zone 2 gravel could reasonably be assumed to have the same cyclic strength as the Zone 1 embankment shell. Zone 2 is treated as part of Zone 1 in the rest of the analysis. The cyclic strength value of 0.35 for the Zones 1 and 2 embankment was appropriately corrected to allow for overburden pressures greater than 1 tsf and to allow for the anisotropic confining stresses occurring under sloping ground conditions. These corrections are based on laboratory test results. Figure 50 is a schematic description for determining the cyclic strengths for any element in the idealized embankment cross section used in the analysis.

Cyclic strength estimates
for dredged foundation gravels

99. The cyclic strengths of the dredged alluvium underlying the shells between sta 446+00 and sta 456+00 were determined using the results of the Becker soundings discussed in Part III and shown in Figure 46b. Different cyclic stress ratios were determined for each of the three $(N_1)_{60}$ zones in both the upstream and downstream dredged alluvium. The cyclic stress ratios were determined using Seed's correlations in Figure 49 for a fines content of 5 percent and the magnitude adjustment factor of 1.2. Based on the Phase II data, the cyclic stress ratio in the free field zone, where $(N_1)_{60}$ was 7.1 blows/ft, was determined to be 0.09. The cyclic stress ratios determined for the two zones under the shell, where the $(N_1)_{60}$ values were 13.7 and 16.9 blows/ft, were 0.18 and 0.22, respectively.

100. In Report 4, Phase I, the cyclic stress ratios of the dredged foundation were determined from the $(N_1)_{60}$ distribution shown in Figure 46a. During Phase I, less was known about the dredged gravels, and a fines content of 8 percent was assumed. For $(N_1)_{60}$ values between 6.5 and 20 blows/ft the estimated cyclic stress ratios ranged from 0.12 to 0.30. This range of cyclic stress ratios was used in the analysis of the dredged foundation section documented in Report 4.

101. The cyclic stress ratios determined for the dredged foundation from the larger Phase II data base are similar to, though slightly lower than, the values used in the Phase I analysis. Hence, the conclusion in Report 4 predicting that liquefaction will occur in the dredged foundation gravels and the recommendation for remedial measures are reinforced by the data gathered in the Phase II studies.

Cyclic strength estimate of
undredged foundation gravel

102. The cyclic strength of the undredged alluvium underlying the shells between sta 439 and sta 446 was determined using the data acquired from the Becker Hammer Drill soundings. The mean $(N_1)_{60}$ of the tailings was 48 blows/ft. Using the cyclic strength chart in Figure 49 it can be seen that for 48 blows/ft the cyclic strength of the undredged alluvium is beyond the range of available data. Thus, due to the high penetration resistance the cyclic strength of the undredged alluvium is extremely high. Therefore, the

undredged foundation gravels are not considered susceptible to liquefaction or high pore pressure buildup due to earthquake shaking.

Cyclic strength of Zone 3
filter and Zone 4 core materials

103. The cyclic strength of the compacted decomposed granite filter (Zone 3) was determined in Report 4 from data acquired in the Phase I field investigations. The results of this analysis are summarized here. Based on the sieve analysis of disturbed and undisturbed samples, the fines content of the compacted decomposed granite averages between 10 and 25 percent. At depths greater than 30 ft (where the material is saturated) the $(N_1)_{60}$ values are well in excess of 30 blows/ft. Therefore, from Seed's correlations in Figure 49 and based on the high Standard Penetration Test blowcounts and high fines content, the compacted decomposed granite in Zone 3 is not considered susceptible to liquefaction and high pore pressure buildup during the design earthquake.

104. The clayey material comprising the impervious core (Zone 4) was judged to be not susceptible to liquefaction. This was due to the plasticity of the fines, the high fines content, the method of material placement, and the high degree of compaction used in placing this material.

Relative Cyclic Strength Behavior
of Embankment Gravels

105. A series of cyclic triaxial shear tests was performed in the laboratory to measure the effects of confining pressure and stress anisotropy on the embankment gravels and the dredged foundation materials. The relationship between residual excess pore pressure and safety factor against liquefaction was also determined from analysis of the laboratory data. The undredged alluvium was not tested in the laboratory. A detailed discussion of the analysis of the laboratory data is included in Report 4 and will not be reproduced here. In this report, the embankment gravel is the only relevant material since analysis of the section of the dam founded on the dredged alluvium has already been completed in Report 4 and since the undredged alluvium is not considered susceptible to liquefaction or high pore pressure buildup.

106. The procedure for computing the cyclic strength for a location in the embankment deposit is outlined in Figure 50. The cyclic strength of a soil depends on the states of stress existing in the soil prior to the

earthquake, i.e., the static stresses. The cyclic stress ratios (τ_c/σ'_v) determined from Seed's charts using the Becker Penetration Test results for the embankment and foundation gravels apply only to level ground conditions where a vertical effective stress of 1 tsf exists. Therefore, adjustments must be made to the chart cyclic stress ratio to take into account sloping ground conditions and locations where the vertical effective stress is not equal to 1 tsf. The adjusted cyclic stress ratio is calculated with a knowledge of the states of stress using the following equation:

$$\left(\frac{\tau_c}{\sigma'_v}\right)_{(\alpha \neq 0, \sigma'_v \neq 1 \text{ tsf})} = K_\sigma \times K_\alpha \times \left(\frac{\tau_c}{\sigma'_v}\right)_{(\alpha = 0, \sigma'_v = 1 \text{ tsf})} \quad (6)$$

For the embankment gravel where the chart cyclic stress ratio equals 0.35, Equation 6 can be rewritten as follows:

$$\left(\frac{\tau_c}{\sigma'_v}\right)_{(\alpha \neq 0, \sigma'_v \neq 1 \text{ tsf})} = K_\sigma \times K_\alpha \times 0.35 \quad (7)$$

The cyclic strength can be determined by multiplying the adjusted stress ratio in Equation 6 by the vertical effective stress.

107. In Equation 6, K_σ is an adjustment factor which accounts for the nonlinear increase in cyclic strength with increasing confining stress. A chart of K_σ for the embankment gravels is shown in Figure 51. This chart shows K_σ is a function of the vertical effective stress. K_σ is < 1 for vertical stresses < 1 tsf and is > 1 for vertical stresses > 1 tsf.

108. In Equation 6, the adjustment factor K_α accounts for the increase in cyclic strength due to the presence of shear stresses on horizontal planes. Non-zero shear stress on horizontal planes is characteristic of sloping ground conditions. A chart of K_α for the embankment gravels is shown in Figure 52. K_α is a function of α , which is the ratio between shear stress at any point on a horizontal plane and the vertical effective stress at that point. K_α has a value of one for level ground conditions where α is equal to zero. The chart shows that K_α increases with

increasing α ; however α is limited by the shear strength of the soil deposit in question. K_α is equal to 1.0 for level ground conditions where α is equal to zero.

109. The static stresses required for determining the adjustment factors K_σ and K_α were computed by static finite element analysis. The static analyses of the segments of Mormon Island Auxiliary Dam where the shells are founded on rock and undredged alluvium are reported in the following chapters of this report.

110. Pore pressures induced in the embankment gravels are estimated using a relationship between safety factor against liquefaction and the pore pressure ratio R_u which was developed from laboratory test data for the Mormon Island shell and dredged foundation gravels. The safety factor against liquefaction is defined as the ratio of cyclic strength to dynamic shear stress. R_u , the excess pore pressure ratio, is the ratio of residual excess pore pressure to normal effective consolidation stress on the failure plane. A plot showing the relationship between FS_L and R_u is shown in Figure 53. As values of FS_L increase, the corresponding values of R_u decrease. This relationship was determined from laboratory data. Values of $FS_L < 1.0$ are interpreted as the development of $R_u = 100$ percent during the earthquake rather than toward the end of the earthquake.

111. The adjustment factors, K_α and K_σ , are used later to determine the cyclic strengths in the embankment for the seismic stability analysis. The dynamic stresses computed in the dynamic response computations are then compared with the cyclic strengths to obtain the FS_L for each element in the embankment shell. An excess pore pressure field is then computed for the embankment shell by translating FS_L into R_u for each element in the mesh. Post-earthquake stability and permanent displacement calculations are then made using the excess pore pressures in the shell.

PART V: FINITE ELEMENT AND STABILITY ANALYSES OF
DAM SECTION FOUNDED ON ROCK

General

112. A finite element analysis and evaluations of liquefaction potential and seismic stability were performed on a cross section representative of the portion of Mormon Island Auxiliary Dam with shells founded directly on rock. These foundation conditions occur in the segments of the dam located approximately between sta 412+00 and sta 439+00 and between sta 456+50 and sta 461+75. In this stretch, the section at sta 426 was estimated to best represent the average static stress conditions and dynamic response of the portion of the dam founded on rock. This section of the report includes discussions of the static and dynamic finite element analyses, a post-earthquake stability evaluation, and a permanent displacement analysis of this section.

Static Finite Element Analysis

General

113. The computer program FEADAM85 developed by Duncan et al. (1984) was used to calculate the initial effective stresses in the foundation and shells of the dam. This program is a two-dimensional, plane strain, finite element solution which calculates static stresses, strains, and displacements in earth and rockfill dams and their foundations. The program uses a hyperbolic constitutive model developed by Duncan et al. (1980) to estimate the nonlinear, stress history dependent, stress-strain behavior of the soils. The hyperbolic constitutive model requires 9 parameters. The program performs incremental calculations to simulate the addition of layers of fill placed during construction of an embankment. A description of the constitutive model, procedures for evaluating the parameters, and a data base of typical parameter values are given by Duncan et al. (1980).

Section idealization and
finite element input data

114. A typical cross section of the portion of the embankment dam founded on rock is shown in Figure 4. For the idealized cross section, the crest (el 480) is roughly 60 ft above the level bedrock elevation (el 420). A

sketch of the idealized cross section developed for the analyses is shown in Figure 54.

115. Table 4 contains a summary of the hyperbolic parameters used in FEADAM84 to model the stress strain behavior of each material in the cross section. The values for the parameters listed in this table were determined from consideration of several sources of information which include drained and undrained triaxial shear tests, comparison with soils having similar characteristics in a data base of over 150 soils, and geophysical test results.

116. The finite element mesh used in the analysis is shown in Figure 55. This mesh contains 104 elements and has 126 nodal points. The mesh was designed by giving consideration to the zoning of material in the dam cross section and using criteria given by Lysmer for dynamic finite element meshes which take into account the shear wave velocities of the soil zones (Lysmer et al. 1973). Since the same mesh was used in the dynamic response analysis, it represents a compromise between the needs of the dynamic and the static finite element computations. Element heights were varied throughout the mesh to meet the Lysmer criteria described in the next section. The resulting mesh had a maximum element height of 10 ft and element aspect ratios of < 2 .

117. Five different material types were used in the finite element analysis. Table 4 lists the material properties of each of these five soil types. These five types of embankment materials are (a) submerged gravel shells, (b) moist gravel shells, (c) central impervious core, (d) submerged transition zone, and (e) dry transition zone. The submerged materials were assigned the same material properties as their nonsubmerged counterparts except that buoyant rather than total unit weights were used in the stress calculations. The gravel filter, Zone 2, in Figure 4 was assumed to have the same material properties as the gravel shells in Zone 1.

118. FEADAM84 simulated the construction process by building the idealized cross section in seven lifts. Each lift was one element high. The phreatic line used in the analysis is shown in both Figure 54 and Figure 55. In the analysis it was assumed that the entire differential head imposed by the reservoir was lost across the Zone 4 impervious core material and that no head was lost in the pervious gravels which comprise the upstream shells. This situation imposes unbalanced hydrostatic pressures on the upstream face of the core, as depicted in the sketch in Figure 56. The unbalanced pressure

distribution acting on the upstream side of the impervious core was simulated in FEADAM84 by an equivalent system of forces applied to the nodes on the upstream face of the core and acting in the downstream direction. These forces were applied after the dam was "numerically" constructed. The states of stress occurring in the embankment and foundation under these conditions were then computed with FEADAM84. The results of these computations represent the pre-earthquake stresses in the embankment.

Results of the static analysis

119. The results of the static analysis computed with FEADAM84 are presented in the form of stress contours superimposed on the embankment cross-section. Figure 57 through 61 are contour plots of vertical effective stress, horizontal effective stress, static shear stress on horizontal planes, α ratio, and mean normal effective stress, respectively.

120. Figure 57 shows that the vertical effective stresses in the submerged upstream shell are less than those at corresponding locations in the downstream shell. Figure 57 shows that some arching across the relatively narrow central impervious core is present. The plot shows stress concentrations in the shells just upstream and downstream of the impervious core. Figure 57 shows that the effect is greater at depth. Some arching was expected since the gravel shells are somewhat stiffer than the transition zone and the central impervious core.

121. Figure 58 shows that the contours of horizontal effective stress generally follow the surface geometry of the embankment, with the exception that the stresses in the impervious core are slightly lower than at corresponding depths in the shells just upstream and downstream of the transition zone. This effect is more pronounced at higher elevations. The lower lateral stresses in the central portion of the cross section are typically due to displacement of both the upstream and downstream shell down and away from the center line. This spreading effect tends to reduce the lateral stresses.

122. Contours of static shear stresses on horizontal planes are shown in Figure 59. Due to the sign convention of the program and coordinate systems used, the shear stresses on the downstream side of the center line have the opposite sign of those on the upstream side. Near the surface of both the upstream and downstream slopes, the contours run parallel to the slopes. In the embankment shells, the magnitudes of the shear stresses on the downstream

side are generally slightly higher than the values for the corresponding points on the upstream side.

123. Figure 60 shows contours of α values. The α values shown in this figure are the ratios of initial static shear stress acting on horizontal planes to vertical effective stress. The contours show that the magnitude of α ranges from a value of zero near the center line to maximum of 0.4 near both the upstream and downstream slopes. The contours show that the magnitude of α in the downstream shell has approximately the same values as those at corresponding points in the upstream shell.

124. The effective mean normal pressure was computed for each element in the mesh from the FEADAM84 results. The effective mean normal stress was computed using the following equation formulated from elastic theory for plane strain conditions:

$$\sigma'_m = (\sigma'_x + \sigma'_y)(1 + \mu) \times 0.333 \quad (8)$$

where

- σ'_m = effective mean normal pressure
- σ'_x = horizontal effective stress
- σ'_y = vertical effective stress
- μ = Poisson's ratio

Each of the parameters on the right hand side of the equation was evaluated using FEADAM84 for each element in the mesh. The resulting contours of effective mean normal pressure are displayed in Figure 61. As with the vertical effective and horizontal effective stresses, the effective mean normal pressure contours generally follow the geometric shape of the embankment. Due to submergence, the effective mean normal pressures are lower in the upstream shell than for corresponding points in the downstream shell. The contours also suggest a slight indication of arching across the central impervious core due to the stiffness contrast between the shells and the impervious core.

125. These static stress results are used in subsequent portions of the seismic stability study. They are used to estimate overburden correction factors for interpretation of the equivalent SPT blowcounts from Becker Hammer soundings, extrapolation of in situ measurements to other portions of the cross section (such as geophysical results and blowcounts results), and to

determine the appropriate cyclic strength for each portion of the embankment, since cyclic strength varies with vertical effective stress and α .

Dynamic Finite Element Analysis of Representative Embankment Section Founded on Rock

General

126. A two-dimensional dynamic finite element analysis was performed with the computer program FLUSH (Lysmer et al. 1973) to calculate the dynamic response of the idealized cross section to the specified motions. The objectives of this analysis were to determine dynamic shear stresses, maximum accelerations at selected points in the cross section, earthquake-induced strain levels, and the fundamental period of the idealized cross section at both low strain levels and higher earthquake-induced strain levels.

Description of FLUSH

127. FLUSH is a finite element computer program developed at the University of California Berkeley by Lysmer et al. (1973). The program solves the equations of motion using the complex response technique assuming constant effective stress conditions. Nonlinear soil behavior is approximated with an equivalent linear constitutive model which relates shear modulus and damping ratio to the dynamic strain level developed in the material. In this approach FLUSH solves the wave equation in the frequency domain and uses an iterative procedure to determine the appropriate modulus and damping values to be compatible with the developed level of strain. FLUSH assumes plane strain conditions. As a two-dimensional, total stress, equivalent linear solution, FLUSH does not account for possible pore water pressure generation and dissipation during the earthquake. Each element in the mesh is assigned properties of unit weight, shear modulus, and strain-dependent modulus degradation and damping ratio curves. FLUSH input parameters for the various zones in the cross section are described in the next section.

FLUSH inputs

128. The same mesh from the static analysis was used in the dynamic analysis. From the static finite element solution the vertical effective, horizontal effective, initial static shear, and effective mean normal stresses were computed at the centroid of each element. In the dynamic analysis the dynamic shear stress history is calculated at the centroid of each element. The same mesh is used in both the static and dynamic finite element analyses

so that the centroid locations of the computed stresses from each match exactly. This makes the data processing and postprocessing calculations much simpler.

129. The elements were designed to ensure that motions in the frequency range of interest propagated through the mesh without being filtered by the mesh. Using the criteria of Lysmer et al. (1973) the maximum element height was determined with Equation 9:

$$h_{\max} = \frac{1}{5} \times V_e \times \frac{1}{f_c} \quad (9)$$

where

h_{\max} - maximum element height

V_e - lowest shear wave velocity compatible with earthquake strain levels in zone of interest

f_c - highest frequency in the range of interest

The low strain amplitude shear wave velocity distribution of the cross section determined from geophysical testing is shown in Figure 62. In the upper portion of the embankment the low strain amplitude shear wave velocity is about 800 fps. It was estimated that the earthquake would induce strain levels in the embankment which would degrade the velocity to fifty percent of its low strain value. The value of h_{\max} in the upper section was calculated with Equation 9 as follows:

$$h_{\max} = \frac{1}{5} \times \frac{800}{2} \times \frac{1}{10} = 8 \text{ ft}$$

According to Lysmer's criteria, the height of any element in the upper zone should not exceed 8 ft. A similar calculation was performed at the lower elevations of the embankment which indicated that the element heights should not exceed 11 ft. In the final mesh all elements had heights between 6 and 10 ft with the taller elements being located at lower elevations in the embankment.

130. The key material properties input to FLUSH were the unit weight and low strain amplitude shear modulus for each element and the strain dependent modulus degradation and damping curves for each material type in the

cross section. The unit weights used in the FLUSH analysis for each of the cross section's six material types are listed in Table 5.

131. The distribution of low strain amplitude shear moduli G_{\max} shown in Figure 63, was determined from the measured shear wave velocities, computed mean effective confining stresses, and estimated K_2 values. The shear wave velocity distribution shown in Figure 62 was determined with Equation 10:

$$V_s = \left[1,000 \times \frac{K_2}{\rho} \times (\sigma'_m)^{1/2} \right]^{1/2} \quad (10)$$

where

V_s = low strain amplitude shear-wave velocity (fps)

K_2 = shear modulus constant for a given material type (unitless)

σ'_m = effective mean normal pressure in psf

ρ = total mass density (slugs)

Table 5 lists the K_2 values for each of the five materials in the cross section. The appropriate value of G_{\max} for each element in the FLUSH mesh was determined from the shear wave velocity at the centroid of each element and Equation 11:

$$G_{\max} = V_s^2 \times \rho \quad (11)$$

The contours of low strain amplitude shear modulus are shown in Figure 63.

132. The strain dependent modulus degradation and damping curves used in the FLUSH computations are shown in Figure 64. The gravel degradation curve in the figure was the average curve for gravels based on a range of data published by Seed et al. (1984b) and was used for the embankment gravels in the shell. This curve is consistent with the laboratory test observations documented in Report 4. The degradation curve used for the transition zone and the central impervious core was the average curve for sand from Seed and Idriss (1970). The damping curve for sand from Seed and Idriss (1970) was used for all materials in the cross section.

133. The finite element mesh of the idealized cross section was excited by both Accelerograms A and B shown in Figure 13. These ground motions were

input to FLUSH at nodal points on the rigid base of the finite element mesh. The dynamic response results for each accelerogram were compared. The results from the accelerogram causing the strongest response in the section were used in the postprocessing.

Dynamic response results

134. FLUSH computes the dynamic response of each element and nodal point in the finite element mesh to the input accelerogram. From these calculations, the maximum earthquake-induced horizontal cyclic shear stress computed for each element over the entire duration of shaking was determined. The maximum value was multiplied by 0.65 to determine the average cyclic shear stress imposed by this earthquake. Contours of the average earthquake-induced dynamic shear stress using the Record A accelerogram are shown in Figure 65. Since a similar computation with Record B resulted in lower dynamic shear stresses than those caused by Record A, the Record B results were not considered further in the dynamic response of this section. The contour plots show that the dynamic shear stresses were highest in the downstream transition zone where they reached a value of about 2,000 psf and were lowest near the surface of the embankment where a value of 400 psf was computed. Safety factors against liquefaction in the embankment shell are calculated using the dynamic shear stresses in the plot.

135. FLUSH also computes the acceleration histories for each nodal point in the finite element mesh. The peak accelerations from the histories at selected nodal points are shown in Figure 66. These were computed with the Record A accelerogram. From this figure it is apparent that significant amplification of the input ground motion occurs since the peak accelerations are greater than 0.35 g throughout the embankment. At the crest, the peak acceleration is 0.91 g which represents an amplification ratio of 0.91:0.35 which is equal to 2.60.

136. The effective strain levels induced by Record A are shown in Figure 67. Representative effective strain levels for the upstream and downstream shells and the impervious core are approximately 0.1 percent for each zone. From the modulus degradation curves of Figure 64, at this strain level the shear moduli for elements in these zones have degraded to about 25 percent of their maximum value. This level of degradation is consistent with that estimated in the mesh design and corresponds to a cut off frequency of 10 Hz.

137. The lengthening of the embankment fundamental period during earthquake shaking is another measure of strain softening in the embankment materials. FLUSH was used to compute the fundamental period of the embankment just prior to the earthquake and at the strain levels induced by the design earthquake. The periods determined with FLUSH for these two strain levels are indicated in Figure 66. The pre-earthquake or low strain amplitude fundamental period was estimated by scaling the Record B accelerogram to 0.0005 g to ensure that modulus degradation was slight. The computed low strain amplitude period was 0.171 sec. The fundamental period of the embankment at the strain levels induced by Record A when scaled to 0.35 g was 0.366 sec. A comparison of these two values shows that the period lengthens by a factor of about 2 during the earthquake shaking. The pre-earthquake period and the effective period during the earthquake are compared with the response spectra for Accelerogram A in Figure 68. This comparison shows that the effective earthquake period closely matches the peaks in the response spectra. This indicates that Accelerogram A is rich in frequencies which lie between the low strain amplitude and effective fundamental periods of this cross section.

Evaluation of Liquefaction Potential

General

138. The cyclic strengths estimated from the in situ Becker Hammer tests and laboratory studies were compared with the average earthquake-induced shear stresses to compute safety factors against liquefaction throughout the upstream submerged embankment shell (Zones 1 and 2). A relationship between safety factor against liquefaction and residual excess pore pressure was developed in Part IV from laboratory data and was used to estimate the residual excess pore pressure field in the shell and foundation as a result of the earthquake shaking. These computations and their results are described in this chapter. The residual excess pore pressure fields predicted for the embankment shell in this chapter are later used to compute the post earthquake stability. As discussed in Part IV, the Zone 3 compacted decomposed granite transition and the Zone 4 compacted clayey core are not considered susceptible to liquefaction and no significant excess pore pressures are expected to occur in these zones as a result of earthquake shaking.

Safety factors against
liquefaction in embankment shell

139. As described in Part IV, the available cyclic strength (expressed as a cyclic stress ratio) of the embankment shells is 0.35. This value was obtained from Seed's field performance correlations, an $(N_1)_{60}$ of 25 and a fines content of 5 percent. This cyclic shear strength ratio is defined as the cyclic shear stress ratio required to develop 100 percent residual excess pore pressure in eight equivalent cycles at a confining stress of 1 tsf for a Magnitude 6.5 event. The cyclic strength ratios for each element were determined with the appropriate values of vertical effective stress, α , K_v , K_h , and the cyclic strength ratio value of 0.35. Figure 50, presented previously, illustrates the procedure for computing the cyclic strength of an element. The K_v and K_h curves used in the procedure were presented earlier and are shown in Figures 51 and 52, respectively. The safety factor against liquefaction is computed as the ratio of the available cyclic shear strength to the average earthquake-induced cyclic shear stress.

140. Contours of safety factors against liquefaction for the upstream shell of the cross section are shown in Figure 69. The safety factors range from 1.3 to 1.7. Generally, the lower safety factors occur at relatively shallow depths beneath the slope.

Residual excess pore pressures

141. Figure 53 was used to associate residual excess pore pressures with the computed safety factors against liquefaction. The residual excess pore pressures are expressed in terms of the pore pressure ratio R_u , defined as the ratio of residual excess pore water pressure to vertical effective stress. Contours of R_u in the upstream shell are plotted on the cross section shown in Figure 70.

142. The contours show that the maximum predicted R_u in the shell is about 35 percent. This pore pressure zone is located about 10 ft below the slope approximately midway between the crest and the upstream heel of the dam. Throughout the upstream shell, the R_u value is typically 25 percent. Figure 70 also shows that the contours are generally oriented parallel to the slope of the dam. The upstream slope represents a contour of R_u equal to zero because this surface is treated as a drainage boundary where no excess pore pressures will exist. The residual excess pore pressures in the shell were used to compute the safety factor against sliding in an effective stress

post-earthquake stability calculation discussed in a subsequent section of this chapter.

Liquefaction potential
evaluation of central imper-
vious core and transition zone

143. Due to the plasticity of the fines, the high fines content, the method of material placement, and the high degree of compaction of Zone 4, this material is not considered to be susceptible to liquefaction and no significant pore pressures are expected to develop in the core. The Zone 3 decomposed granite filter is also well compacted, has a high fines content (typically 20 to 25 percent), and has high $(N_1)_{60}$ values. It was determined that safety factors against liquefaction in these materials would be much greater than 1.0 and no significant excess pore pressures are expected to develop.

Summary of dynamic
response calculations

144. The safety factors against liquefaction in the upstream shell were computed by comparing the cyclic strengths of these gravels with the dynamic stresses induced by the earthquake. The safety factors obtained ranged from 1.3 to 1.7. The computed safety factors against liquefaction were then associated with corresponding residual excess pore pressures to determine the post-earthquake R_u field. The maximum excess pore pressure ratio in the field is expected to be 35 percent and a significant portion of the field expected is to reach 25 percent.

Stability Analysis of Embankment Section
Founded on Rock

General

145. The computer program UTEXAS2 was used to evaluate post-earthquake slope stability of the idealized cross section. UTEXAS2 was written and developed by Dr. Stephen Wright at the University of Texas, Austin. It was improved for Corps of Engineers use under the auspices of the Computer Applications of Geotechnical Engineering (CAGE) and Geotechnical Aspects of the Computer-Aided Structural Engineering (G-CASE) programs of WES (Edris and Wright 1987). UTEXAS2 uses Spencer's method to compute the factor of safety against sliding. Two approaches were used to evaluate the stability of the

slope. In the first, the safety factor against sliding was calculated with the assumption that the excess pore pressure fields shown in Figure 70 existed in the shells. In the second approach, a permanent deformation analysis was performed to estimate the amount of Newmark-type movement which might occur along potential failure surfaces in the embankment. The permanent displacement analysis was also performed using the excess pore pressure fields shown in Figure 70.

Post-Earthquake Stability Analysis

146. The post-earthquake safety factor against sliding was calculated in an effective stress analysis using the residual excess pore pressure fields shown in Figure 70. In this type of analysis, it is assumed that these pore pressures will be developed during the earthquake and they will be present in the shell immediately after the shaking stops. The shear strength parameters and unit weights used for each zone in the embankment are listed in Table 6. The friction angle tangents of the transition zone (Zone 3) and the impervious core (Zone 4) were reduced by 20 percent to account for any minor strength loss or pore pressure buildup which might occur as a result of the earthquake.

147. Only upstream circles were investigated in the stability analysis. The investigation involved a thorough search to find the critical circle. The circle judged to be most critical is that which had the lowest safety factor and involved the greatest amount of material in the failure mass. The critical circle for this analysis is shown in Figure 71. The failure surface of this circle passes through the zone of highest pore pressure where R_u is 35 percent. Though this circle is contained within the upstream shell, it involves a significant amount of material. The post-earthquake safety factor against sliding computed for this circle was 1.29. The safety factor against sliding for this same circle before the earthquake shaking was 1.85. The excess pore pressure field used in the analysis reduces the safety factor against sliding for the critical circle by about 30 percent. It was concluded that the upstream and downstream slopes of this portion of the dam will be stable immediately following the design earthquake.

Permanent Displacement Analysis

148. A permanent displacement analysis was performed to estimate the amount of displacement which might accumulate along potential failure surfaces during the earthquake. These deformations are determined from yield accelerations and dynamic response accelerations at various embankment levels in a sliding block analysis. The yield acceleration is the pseudo-static acceleration applied at the center of gravity of a sliding mass which will reduce the safety factor against sliding to one. Two methods were used to estimate permanent deformations, namely the Makdisi-Seed and the Sarma-Ambrayseys approaches. The yield accelerations were computed using the excess pore pressures in the upstream shells shown in Figure 70. The use of the excess pore pressure field in the analysis is based on the assumption that the pore pressures in the shell will build up to their maximum values during the onset of shaking and will be maintained throughout the duration of shaking. Displacements were computed for potential sliding masses which were completely contained in the upstream shell and also for deeper sliding masses which exited the embankment downstream of the dam centerline.

Computation of yield accelerations

149. The yield acceleration for various elevations in the embankment were calculated with the seismic coefficient option in UTEXAS2. The critical yield accelerations were determined for failure circles tangent to elevations of 468, 456, 444, 432, and 420 ft which correspond to dimensionless depth ratios y/h of 20, 40, 60, 80, and 100 percent, respectively. Critical yield accelerations were computed at these elevation levels for potential sliding masses contained in the upstream shell and for the deeper sliding masses emerging downstream of the centerline.

150. Figure 72 shows the critical yield accelerations and the slip surfaces for sliding masses which are contained completely within the upstream shell. The circles tangent to el 444, el 432, and el 420 have yield accelerations which range between 0.06 g and 0.11 g and pass through the R_u contour of 35 percent which is the zone with the highest amount of residual excess pore pressure. The circles tangent to el 456 and el 468 have yield accelerations of 0.18 g and 0.39 g, respectively. The slip surfaces of these circles are largely located above the elevations where the high pore pressure zones

occur and large portions of their arc length are located above the phreatic line.

151. Figure 73 shows the yield accelerations for potential slip circles which emerge from the embankment downstream of the dam center line. These yield accelerations range between 0.20 g and 0.57 g and are higher than those at corresponding elevations from the previous case. Requiring the slip circles to emerge in the downstream slope forces the circles to be deeper in the embankment and, therefore, to largely avoid the high pore pressure zones in the shell. The yield accelerations computed for the upstream shell circles and the deeper circles are compared in Figure 74.

The Makdisi-Seed method

152. The Makdisi-Seed technique (1979) was used to estimate the amount of Newmark-type sliding that might occur along potential slip surfaces in the embankment. The Makdisi-Seed technique was developed for dams founded on rock and is based on the analysis of many dynamic finite element solutions. Permanent displacements are estimated from charts and a knowledge of the embankment crest acceleration, fundamental period at earthquake-induced strain levels, and yield accelerations.

153. Permanent displacements were determined for the failure masses identified in the yield acceleration analyses. These circles were tangent to el 468, el 456, el 444, el 432, and el 420 which correspond to y/h values of 20, 40, 60, 80, and 100 percent, respectively. The charts used in the analysis are shown in Figure 75. Figure 75a shows a range of normalized maximum accelerations, k_{\max}/\ddot{u}_{\max} , versus normalized depth, y/h . In this study the average curve was used to determine the variation of the maximum acceleration ratio, k_{\max}/\ddot{u}_{\max} , with depth. At each of the depths investigated, the earthquake-induced acceleration of the sliding mass k_{\max} was determined by multiplying the maximum acceleration ratio obtained from the chart by the peak crest acceleration, \ddot{u}_{\max} . The peak crest acceleration is 0.91 g as shown in Figure 66. This was determined from the FLUSH dynamic response computations using Accelerogram A. The permanent displacements for each slip circle investigated were determined from Figure 75b. This chart displays the variation of displacement U (divided by k_{\max} , the acceleration of gravity g and fundamental period T_0) versus yield acceleration k_y (normalized by k_{\max}). The ratio k_y/k_{\max} was computed for each sliding mass and the chart was entered on the abscissa at that point. The corresponding displacement term was obtained

from the ordinate axis using the curve for Magnitude 6.5 events. The displacement, U in ft, was calculated by multiplying the chart displacement term by k_{\max} , g in ft/sec², and T_0 in seconds. This displacement in turn was multiplied by a factor α of 1.3 which accounts for the direction of the resultant shearing resistance force which comes from the solution to the equation of motion for a sliding block on a plane (see Hynes-Griffin and Franklin 1984). The term α was computed from Equation 12 (Hynes-Griffin and Franklin 1984):

$$\alpha = \frac{\cos(\beta - \theta - \phi)}{\cos \phi} \quad (12)$$

where

β = direction of the resultant shear force and displacement, and the inclination of the plane

θ = direction of the acceleration, measured from the horizontal

ϕ = friction angle between the block and the plane

The term β was assigned a value of 25 deg based on the average direction of the resultant shearing resistance of critical circles from the UTEXAS2 calculation; θ was set to zero since the applied accelerations are horizontal; and ϕ was set to 43 deg which is the effective friction angle of the embankment gravels. The fundamental period of the embankment used in this calculation is 0.171 sec, from Figure 66. Permanent displacements were determined for each of the potential failure masses shown in Figures 73 and 74.

154. The Makdisi-Seed computations are summarized in Tables 7 and 8. Table 7 shows the results for the set of failure masses in the upstream slope, and Table 8 shows the results for the set which emerges downstream of the dam center line. The displacements computed for each set are also presented in Figure 76. The computed maximum displacement in the shell set of potential failure masses was about 1.09 ft for slip surfaces tangent to el 456. The computed maximum displacement in the deeper circle was about 0.41 ft, also at el 456. In all cases, at corresponding tangent elevations, the displacements for the shell circle are greater than those for the deeper circle exiting downstream of the center line. Thus, the Makdisi-Seed computations for both sets of potential upstream slip circles indicate that the Newmark-type displacements may be approximately 1 ft or less.

Sarma-Ambrayseys method

155. The Sarma-Ambrayseys technique was the second method used to compute the permanent displacements along potential slip surfaces. This technique uses the results of a Newmark sliding block analysis, yield accelerations, and the dynamic response analysis for estimating displacements (Hynes-Griffin 1979). The yield accelerations used in this analysis are the same as those used in the Makdisi-Seed method. The yield accelerations k_y are given in Figures 72 through 73 for upstream shell circles and the deeper circles crossing the center line.

156. Figure 77 shows Newmark sliding block displacements computed for various values of N/A for Accelerograms A and B. The term N/A is the ratio of yield acceleration, k_y , to acceleration of the sliding mass, k_{max} . The curves for each accelerogram were obtained by computing the displacements for various values of N/A by numerical integration of the relative equations of motion. The displacement curves are computed for a magnification factor of one (i.e. assuming rigid body behavior for the embankment). In this analysis, the curve for Accelerogram A was used since it gives higher displacements for all values of N/A .

157. Displacements were computed for the same slip surface locations in the embankment as for the Makdisi-Seed method for both upstream shell circles and the deeper circles. The displacements were computed in the following way. The maximum earthquake-induced acceleration of the sliding mass A was set equal to k_{max} determined in the Makdisi-Seed method. The yield accelerations N are equal to k_y . The ratio of N/A was then computed. Figure 77 was entered from the abscissa at approximate values of N/A and displacements for a magnification factor of one were determined using the curve for Accelerogram A. The magnification ratio was calculated by dividing A (or k_{max}) by 0.35 g which is the peak base ground motion acceleration. The chart displacements were multiplied by the magnification factor and by α to determine the field permanent displacements along the surfaces investigated. A value of 1.3 was computed for α as discussed in the previous section. Tables 9 and 10 summarize the calculations in tabular form for both the upstream shell and deeper circles. The displacements for both cases are plotted in Figure 78. The displacements computed for the upstream shell circles are somewhat greater than those computed for the deeper circles at corresponding tangent elevations. The Sarma-Ambrayseys method indicates that the maximum potential

displacement is about 0.8 ft and will occur in the upstream shell for a slip circle tangent to el 432. The displacements are in good agreement with those of Makdisi-Seed method discussed earlier where the computed maximum displacement in the shell was about 1 ft.

PART VI: FINITE ELEMENT AND STABILITY ANALYSES OF DAM SECTION
FOUNDED ON UNDREDGED ALLUVIUM

General

158. Finite element analyses and stability evaluations were performed for a cross section representative of the portion of the embankment dam with shells founded on undredged alluvium. As with the idealized section representing sections where the embankment is founded wholly on rock discussed in Part V, the study of this section included static and dynamic finite element analyses, a post-earthquake slope stability analysis, and a permanent displacement analysis.

Selection and idealization
of representative cross
section for finite element analysis

159. Between sta 439 and sta 446, the upstream and downstream shells of the embankment dam are founded on undredged alluvium. A typical cross-sectional view of Mormon Island Auxiliary Dam in this segment is shown in Figure 4. The undredged alluvium beneath the shells consists of slightly cemented sands and gravels. Its thickness varies from 0 ft under the upstream shells near sta 439 to about 20 ft near sta 446. In this 700-ft segment of the dam, the upstream slopes vary from 1V:4.5H near sta 446, which is closest to the dredge tailings, to 1V:2H near sta 439. The downstream slopes vary from 1V:3.5H near sta 446 to 1V:2H near sta 439. The idealized cross section selected for the finite element analysis was based on conditions at sta 446 where the undredged alluvium underlying the shells is thickest. A cross-sectional view of the idealized section used in the finite element analyses is shown in Figure 79. The crest of the idealized section was 130 ft above the elevation of the rock.

Selection and idealization of
representative cross-section
for post-earthquake stability analysis

160. The post-earthquake stability analyses were based on conditions at sta 442+00 where the slopes are steeper. A sketch of this section is shown in Figure 80. As for the segment founded on rock, the post-earthquake stability analysis was performed using excess pore pressure fields determined from the finite element analyses and liquefaction potential evaluation. Since the

cross sections of the finite element and slope stability sections are different, the pore pressure fields computed from the finite element analysis were adjusted to accommodate the steeper slopes present at sta 442.

Static Analysis

Finite element inputs

161. FEADAM84 was used to calculate the pre-earthquake static stresses existing in the embankment. As shown in Figure 79, six different material types were incorporated in the idealized section:

- a. Moist embankment gravels in downstream shell.
- b. Submerged embankment gravels in upstream shell.
- c. Moist transition zone (decomposed granite).
- d. Submerged transition zone (decomposed granite).
- e. Central impervious core.
- f. Undredged alluvium in the foundation underlying the shells.

Table 4 contains a summary of the hyperbolic parameters used in FEADAM84 to model the stress strain behavior of each of the materials in the cross section. Submerged unit weights were used for all materials located beneath the phreatic line even though these materials were assigned the same hyperbolic parameters as their nonsubmerged counterparts.

162. The finite element mesh developed for the idealized cross section for sta 446 is shown in Figure 81. This mesh has a total of 332 nodes and 297 elements. This mesh was designed by giving consideration to the distribution of materials in the cross section, the distribution of shear wave velocities in the cross section, and Lysmer's criteria for finite element meshes. Element heights varied throughout the mesh with a maximum of 13 ft. The maximum aspect ratio of any element did not exceed a value of 2.7.

163. The dam and its foundation were numerically constructed by FEADAM84 in 13 incremental lifts. Each lift was one element high. As with the analysis of the section founded on the rock, it was assumed that the entire differential head due to the reservoir was lost across the impervious core. The resulting unbalanced hydrostatic pressures acting across the core are shown in Figure 82. These pressures were simulated by FEADAM84 as an equivalent system of concentrated forces applied to the nodal points on the upstream and downstream faces of the impervious core after placement of the

final construction lift. The resulting states of stress computed with FEADAM84 are discussed in the next section.

Results of static analysis

164. The results of the FEADAM84 static stress analysis are presented on the contour plots of vertical effective stress, horizontal effective stress, shear stress acting on horizontal planes, α ratio, and effective mean normal pressure shown in Figures 83 through 87, respectively. The vertical effective stress contour plot is shown in Figure 83. Generally, the contours indicate that the vertical effective stresses on the upstream side are lower than those on the downstream side, as expected due to the effect of submergence. Stress concentrations immediately upstream and downstream of the central core indicate that some arching is present, caused by the contrast in stiffness between the stiffer embankment gravels and the central core. The contours also indicate that the maximum vertical effective stress is slightly in excess of 12,000 psf.

165. Figure 84 shows the contour plot of horizontal effective stress. Generally, these contours follow the surface geometry of the embankment. As with the vertical effective stresses, due to submergence, the computed horizontal effective stresses were lower on the upstream side than they were for corresponding points on the downstream side of the embankment. The 1,000-psf contour shows that the horizontal effective stress was lower near the central impervious core than at corresponding depths below the embankment surfaces just upstream and downstream of the core. This was the result of a spreading effect whereby nodal points on the upstream and downstream sides of the embankment tended to move down and away from the center line, resulting in lower horizontal effective stresses near the center line of the embankment. These contours show that this effect decreased at greater depths within the embankment. The highest computed horizontal effective stress in the cross section was approximately 6,000 psf.

166. A contour plot of the initial static shear stresses acting on horizontal planes is shown in Figure 85. The plot reflects the sign convention of the program and selected reference frame of the mesh--the computed shear stresses were negative on the downstream side of the center line and positive on the upstream side of the center line. The contour of zero shear stress was slightly downstream of the center line due to the submergence of the upstream shell and the asymmetry of the cross section. Again, due to submergence, the

computed shear stresses on the upstream side were smaller in magnitude than those at corresponding downstream locations. The largest computed shear stress in the cross section occurred in the downstream undredged foundation and had a magnitude of 1,500 psf. The largest computed shear stress on the upstream side was located in the core trench and foundation and had a magnitude of 1,200 psf.

167. The α ratio contour plot for the undredged foundation section is shown in Figure 86. In the context of the static stresses, α was defined as the absolute value of the ratio of initial static shear stress acting on horizontal planes to the normal vertical effective stress. The α contours ranged from 0 to 0.3 in magnitude. The highest α contours generally ran parallel to and were located near the upstream and downstream slopes. The α contours decreased in magnitude and became more vertically oriented deeper in the embankment.

168. The effective mean normal pressure contour plot is presented in Figure 87. The values for effective mean normal pressure were computed from the effective normal stresses and Poisson's ratio output by FEADAM84 and Equation 8, given in Part V of this report. Due to submergence, the computed effective mean normal pressures in the upstream portion of the section were lower than those at corresponding points in the downstream portion of the section. The contours generally ran parallel to the surface geometry of the embankment. Some arching across the impervious core was evidenced by the stress concentrations in the embankment gravels just upstream and downstream of the central impervious core and transition zone. The highest computed effective mean normal pressure was about 8,000 psf. The 8,000-psf contour was located in the core trench and undredged foundation just downstream of the central impervious core.

Dynamic Finite Element Analysis

General

169. A two-dimensional dynamic response analysis using the computer program FLUSH was performed on the idealized cross section of sta 446. This analysis is similar to that performed for the section of Mormon Island Auxiliary Dam founded on rock reported in Part V. As for the rock foundation section, the primary objectives of the dynamic response analysis were to

determine the earthquake-induced shear stresses, maximum accelerations at selected points, strain levels induced by the earthquake, and the fundamental period of the idealized cross section at both low and earthquake-induced strain amplitudes.

FLUSH inputs

170. The finite element mesh used in the static analysis was also used for the FLUSH analysis. The use of the same mesh expedited both the preprocessing and postprocessing of the finite element data. The maximum heights of the elements in the mesh were computed using Lysmer's criteria which resulted in elements whose heights varied from 10 to 13 ft. The cutoff frequency used in the analysis of the section was 8 Hz.

171. As stated previously, the key material properties input to FLUSH are total unit weight and low strain amplitude shear modulus G_{max} for each element and the strain dependent moduli and damping curves for each material type in the section. The total unit weights for each material type in this section are given in Table 5.

172. The shear wave distribution shown in Figure 88 determined the G_{max} distribution shown in Figure 89. The shear wave velocity for each element was computed with Equation 10. The values of K_2 used in Equation 10 for each material are listed in Table 5. The effective mean normal pressures determined from the static analysis were used in Equation 10 to determine the shear wave velocity of each element. The value of G_{max} for each element was computed using Equation 11. The contour plot of G_{max} in Figure 89 shows that the embankment gravels, transition zone, and undredged foundation are stiffer than the materials found in the central impervious core. Since the modulus of each material is directly proportional to the square root of the effective mean normal pressure, the contours show that G_{max} increases with depth in the embankment. The G_{max} values on the upstream side are somewhat smaller than the values on the downstream side due to submergence effects. The largest G_{max} is 12,000 ksf and occurs in the downstream core trench and undredged foundation.

173. The strain-dependent modulus degradation and damping curves used in the FLUSH computation are shown in Figure 64. The average gravel modulus degradation curve was used for the embankment gravels and the undredged foundation underlying the shells. The average sand modulus degradation curve was

used for the central impervious core and the decomposed granite transition zone flanking the core. The sand damping curve was used for all materials.

174. The finite element mesh of the idealized cross-section was excited by both Accelerograms A and B shown in Figure 13. Baserock ground motions were input to FLUSH through a free field calculation using transmitting boundaries. Baserock motions in the free field were determined using SHAKE, a one-dimensional wave propagation code. The results of the two dynamic response calculations were compared, and the results from the accelerogram causing the strongest response in the section were used in the postprocessing.

Results of dynamic response calculations

175. The dynamic response calculations for the undredged foundation section were performed with FLUSH using both Accelerograms A and B. Comparison of the stresses induced by the two accelerograms showed that Accelerogram B yielded higher stresses than Accelerogram A. Therefore, only the dynamic response calculations of Accelerogram B are discussed in this section. The effective average dynamic shear stresses over the duration of shaking induced by Accelerogram B are shown on the contour plot of Figure 90. The stresses shown represent 65 percent of the peak cyclic shear stress developed during shaking. The contours generally follow the slope geometry of the embankment and increase in value at locations deeper in the embankment. The plot shows some stress concentration in the transition zone. The dynamic stresses upstream of the center line are somewhat smaller than those on the downstream side.

176. Peak accelerations resulting from the dynamic response of the undredged foundation section to Accelerogram B are presented in Figure 91. Examination of this data indicates that there was amplification of the input ground motion at several nodal points in the mesh since the computed peak accelerations exceeded 0.35 g. The amplifications were greatest at locations near the surface of the embankment. The computed accelerations on the downstream side of the embankment were slightly greater than those at corresponding locations on the upstream side. The computed peak crest acceleration was 0.67 g which indicates that the peak input acceleration of 0.35 g was amplified by a factor of 1.91.

177. Figure 92 shows the approximate cyclic shear strain levels reached in various zones of the embankment due to Accelerogram B. Of particular

interest in this study were the strain levels reached in the upstream embankment shells where the effective strains ($0.65 \times$ peak cyclic shear strains) reached a level of approximately 2×10^{-1} percent. According to the modulus degradation curve for gravels shown in Figure 64, the shear modulus will degrade to about 18 percent of its maximum value at a strain level of 2×10^{-1} percent. Also of interest were the strain levels reached in the undredged alluvium. These strain levels were somewhat less than those in the shells and were computed with FLUSH to be about $7 \times 10^{(-2)}$ percent. At this shear strain level, the modulus will degrade to about 30 percent of its maximum value.

178. The lengthening of the fundamental period of the embankment during earthquake shaking is another indication of strain softening. The low strain amplitude or the pre-earthquake fundamental period was determined with FLUSH by scaling Accelerogram B to 0.0005 g to ensure that the induced strains were kept on the order of $10^{(-4)}$ percent so that the modulus degradation in the embankment was negligible. The computed pre-earthquake fundamental period was 0.30 sec. The fundamental period at the design earthquake strain levels was determined with FLUSH by scaling Accelerogram B to 0.35 g. The computed value was 0.74 sec. A comparison of the two periods shows that the fundamental period lengthens during the earthquake shaking. The fundamental period is a function of the geometry and stiffness of the embankment. Since the changes in the embankment's geometry during the earthquake are negligible, the lengthening of the fundamental period can be attributed to material softening. The pre-earthquake and effective earthquake periods are compared with the response spectra for Accelerogram B in Figure 93. This figure shows that the pre-earthquake period closely matches the peak period in the response spectra plot. The period at earthquake-induced strain levels falls slightly outside of the peaks in the response spectra.

Evaluation of Liquefaction Potential

General

179. The liquefaction potential of the section of Mormon Island Auxiliary Dam founded on undredged alluvium was assessed in the same manner as that for the sections founded on rock, discussed in Part V of this report. Cyclic strengths were determined for the in situ stress conditions in each embankment

element by the procedures shown in Figure 50. Figure 51 and Figure 52 show the K_α and K_σ strength adjustment factors for the shell gravels. The safety factor against liquefaction, FS_L , was computed as the ratio of cyclic strength to dynamic shear stress. Residual excess pore pressure ratios corresponding to the computed values of FS_L were determined from the relationship shown in Figure 53.

Safety factors against liquefaction

180. The cyclic stress ratio required to generate $R_u = 100$ percent in the embankment and foundation gravels at an effective confining stress of 1 tsf, a Magnitude 6.5 earthquake, and 5 percent fines was determined from the $(N_1)_{60}$ values estimated from in situ Becker Hammer tests and Seed's cyclic strength charts based on observations of field performance. The average $(N_1)_{60}$ for the embankment materials was 25 which corresponds to a cyclic stress ratio of 0.35 for the above conditions. The average $(N_1)_{60}$ of the undredged alluvium was 48 blows/ft. Seed's chart indicates that a material with a penetration resistance this high will have a very high cyclic strength and will not be vulnerable to liquefaction. Hence, excess pore pressures are not expected in the undredged gravels underlying the upstream and downstream embankment shells. For reasons discussed earlier, residual excess pore pressures are also not expected in the compacted decomposed granite transition zone and in the central impervious core. Thus, development of residual excess pore pressures are anticipated only in the submerged upstream shell of the embankment.

181. A contour plot of safety factor against liquefaction is shown in Figure 94. The contours are all confined to the upstream shell. The computed safety factors in the upstream shell were relatively high and ranged from 1.5 near the face of the slope to 3.0 in the core trench. Safety factors were not computed for the undredged alluvium underlying the shells since the cyclic strengths are indeterminately high based on Seed's correlations. Since the safety factors against liquefaction were significantly greater than one throughout the cross section, liquefaction (100 percent pore pressure response) was not predicted to occur anywhere in this cross section.

Residual excess pore pressures

182. Residual excess pore pressures in the embankment shell for the undredged foundation section are shown in Figure 95. The contours show that R_u ranged between 10 and 20 percent. The face of the upstream slope was

interpreted to be a free draining boundary; hence, R_u was forced to have a value of zero at this boundary. The area surrounded by the 20 percent contour involved the lower portion of the upstream shell and was oriented parallel to the embankment slope. The residual excess pore pressure field shown in Figure 95 was used to analyze post-earthquake stability against sliding and permanent displacements.

Post-Earthquake Stability Analysis

183. The post-earthquake slope stability of the undredged section with the earthquake-induced residual excess pore pressure fields in the upstream shell was determined with UTEXAS2.

184. The embankment cross section and the residual excess pore pressure field used in the stability analysis are shown in Figure 96. This cross section is not the same as the one used in the finite element analysis. Figure 4 shows that the slopes in the undredged section between sta 446 and sta 439 become progressively steeper towards the right abutment. The idealized cross section developed for the stability analysis corresponds generally to sta 442, located at the approximate midpoint of the undredged length of the dam. The section at sta 442 has steeper slopes than the section at sta 446, idealized for the finite element analysis. At sta 442, the upstream shell has slopes of 3.25H:1V from the upstream toe to el 427.0, and 2.5H:1V from el 427.0 to the crest. The downstream shell has slopes of 2H:1V from the crest to el 466.0, 2.5H:1V from el 466.0 to el 427.0, and 3.25H:1V from el 427.0 to the downstream toe, as shown in Figure 96. The pore pressure contours computed for the finite element cross section with the flatter slopes (Figure 95) were adjusted to accommodate the steeper slopes of the stability cross section. This was accomplished by translating the contours in the horizontal direction toward the embankment center line. The resulting pore pressure contours are shown in Figure 96. Based on an examination of T_0 for all two-dimensional dam sections with shells founded on undredged alluvium, it was judged that the dynamic response of the steeper stability section would not be significantly different from the dynamic response computed for the idealized section of sta 446+00.

185. The shear strength parameters input to UTEXAS2 for each of the embankment zones are listed in Table 6. The parameters for the Zone 3

transition zone, the central impervious core, and the undredged alluvium, where no significant pore pressures are expected to occur, were reduced by a factor of 20 percent to account for any minor pore pressure development or strength loss which might occur during the earthquake. A circular arc search of the upstream slope was then performed to find the sliding mass with the minimum factor of safety against sliding. Only upstream circles were studied. The results of the search are shown in Figure 97. This figure shows the critical circle superimposed on the embankment cross section and the residual excess pore pressure field. The computed post-earthquake safety factor against sliding was 1.91 for a relatively shallow circle which did not involve a large volume of material. The slope stability analysis indicated that the earthquake-induced residual excess pore pressures were not high enough to threaten the stability of this section. All deeper circles investigated had safety factors against sliding which were even higher. The pre-earthquake safety factor against sliding computed for this circle without excess pore pressures in the shell was 2.26.

Permanent Displacement Analysis

General

186. A permanent displacement analysis was performed for the undredged foundation section with steeper slopes at sta 442+00. The analysis was performed in a manner similar to that for the rock section discussed in Part V of this report. Yield accelerations were computed at various levels in the cross section with UTEXAS2. Two categories of potential slip circles were studied. These were a set of fairly shallow circles which exited the embankment upstream of the center line and a set of deeper circles which exited the embankment downstream of the center line. The Makdisi-Seed and the Sarma-Ambrayseys approaches were used to estimate the permanent displacements for the potential failure masses. Since the shells are founded on the undredged alluvium, the Makdisi-Seed approach, intended for dams founded on rock, is not strictly valid. However, since the alluvium (20 ft thick) is only about 15 percent of the total embankment height (130 ft), it is judged that this approach will still yield a reasonable approximation to the amount of displacement which might be expected.

Yield accelerations

187. The yield accelerations computed for the shallow and deep sets of circles are presented in Figures 73 and 74, respectively. For each set critical yield accelerations were determined for circles tangent to elevations of 454, 428, 402, 376, and 350 ft which represent depth ratios, y/h , of 20, 40, 60, 80, and 100 percent. The shear strength parameters were the same as those used for the post-earthquake stability analysis and are listed in Table 6.

188. Figure 98 shows the critical circles and their yield accelerations superimposed on the cross section for the set of shallow circles exiting upstream of the center line. The yield accelerations for this case varied from 0.145 g to 0.231 g. The failure mass tangent to el 442 had the lowest yield acceleration. This circle was confined to the upstream shell and was located inside the R_u 20 percent contour to a great extent.

189. Figure 99 shows a similar plot for the deeper set of critical circles emerging downstream of the center line. The yield accelerations varied from 0.189 g to 0.359 g. The circle having the lowest yield acceleration was also tangent to el 402. This circle also passed through the highest pore pressure zone for much of its arc length.

190. A plot of yield acceleration versus tangent elevation is shown in Figure 100. The yield accelerations for the deep and shallow sets of circles are summarized on this plot. With one exception, the yield accelerations for the shallow circles are lower than those for the deeper circles. The yield accelerations shown on this plot were used to calculate permanent displacements for both the Makdisi-Seed and Sarma-Ambrayseys techniques.

Makdisi-Seed method

191. The Makdisi-Seed method was used to compute the potential for Newmark-type displacement of the critical circles identified in the yield acceleration analyses. The computational procedure was discussed in Part V. The displacements were computed using the charts in Figure 75 which depend upon the crest acceleration, fundamental period, and yield acceleration. For the section under study, the crest acceleration was 0.67 g, the fundamental period was 0.74 sec, and the yield accelerations were those summarized in Figure 91. The crest acceleration and fundamental period were obtained from the dynamic response of the dam to Accelerogram B computed with FLUSH.

192. The Makdisi-Seed displacement computations for the shallow and deep sets of circles are summarized in Tables 11 and 12, respectively. The

estimated potential field displacements are shown in the last column of each of the tables. The displacements for both sets of circles are plotted versus the circle tangent elevation in Figure 101. The largest potential displacement for the deeper circles exiting downstream of the center line was 0.41 ft, computed for the circle tangent to el 428 ft. For the shallower circles, the maximum displacement was 0.93 ft, computed for the circle tangent to el 454 ft. This slip surface was located in a relatively high position in the embankment, at the $y/h = 20$ percent level. Figure 101 shows that the displacements for the shallower set of circles were greater than those for the deeper set, as expected, since the yield accelerations were lower for the shallower circles than for the deeper circles. Zero displacements were computed for circles which intercept the undredged alluvium at el 350 for both sets.

Sarma-Ambroseys method

193. The Sarma-Ambroseys technique was also used to estimate Newmark-type permanent displacements for both sets of circles. The computational procedure was discussed in Part V. The estimated field permanent displacements for this approach are determined from a Newmark sliding-block analysis of the accelerogram, the variation of accelerations of failure masses at various levels in the embankment, and the yield accelerations. The sliding block analysis results are presented in Figure 77. Displacements were determined from the curve for Accelerogram A since this would result in larger displacements than the curve for Accelerogram B. The earthquake-induced acceleration of the failure masses as determined from the Makdisi-Seed chart in Figure 75 and a crest acceleration of 0.67 g, which was determined from the FLUSH dynamic response calculations with Accelerogram B. The yield accelerations used were those shown in Figure 100. A summary of the computations for the shallow and deep sets of circles is listed in Tables 13 and 14. The estimated potential field displacements are shown in the right hand columns of the tables. The displacements of each circle are plotted versus the tangent elevation in Figure 102. The plot shows that the largest displacement for the shallower set of circles was 0.21 ft, computed for the circle tangent to el 454. The largest displacement for the deeper set of circles was 0.07 ft, computed for the circle tangent to el 428. Zero displacements were computed for circles which intercept the undredged alluvium for both sets.

Summary of permanent
displacement computations

194. The permanent displacements computed with the Makdisi-Seed and Sarma-Ambrayseys techniques were less than 1 ft for all investigated circular failure masses. These displacements are not threatening to the stability and performance of the dam in the undredged foundation section. Displacements along potential failure surfaces were computed to be larger for shallow failure masses than for deeper seated masses. This was expected since the yield accelerations are greater for deeper seated circles than for shallow circles. Permanent displacements were computed only for the upstream circles. Due to the symmetrical nature of the shells and the absence of the pool and excess pore pressures in the nonsaturated downstream shells, displacements of potential downstream failure masses will be even less than those computed for the upstream side.

PART VII: SUMMARY AND CONCLUSIONS

195. This report documented the Phase II study of the seismic stability evaluation of Mormon Island Auxiliary Dam, at the Folsom Dam and Reservoir Project, located on the American River, about 20 miles northeast of the city of Sacramento, California. In the review of the site geology and the seismic hazard assessment, it was concluded that no active faults are present immediately beneath any of the man-made water retaining structures at the site. The most severe earthquake shaking was determined to come from the East Branch of the Bear Mountains fault zone, which is considered capable of producing a maximum magnitude earthquake of $M_L = 6.5$. The shortest distance between the fault zone and the Folsom Dam and Reservoir Project is 8 miles to Mormon Island Auxiliary Dam and 9.5 miles to the Concrete Gravity Dam. The design ground motions for the site are $a_{max} = 0.35$ g, $V_{max} = 20$ cm/sec, and duration (≥ 0.05 g) = 16 sec.

196. The seismic stability evaluation of Mormon Island Auxiliary Dam consisted of a review of construction records, field and laboratory investigations, static and dynamic stress analyses, liquefaction potential evaluation, and post-earthquake slope stability analyses. Mormon Island Auxiliary Dam was constructed in the Blue Ravine, an ancient channel of the American River that was partially filled with auriferous gravels. The underlying bedrock is weathered schist of the Amador Group. The review of construction records showed that the core of the dam is founded on rock along its entire 4,820-ft length, but the foundation conditions for the shells of the dam vary. The dam may be divided into three segments according to foundation conditions for the shells--a 900-ft long segment that has shells founded on dredged alluvium, a 600-ft long segment that has shells founded on undisturbed (undredged) alluvium, and the remaining length of the dam is the segment founded on weathered rock. The Phase I study documented in Report 4 focused on the segment of the dam where the shells were founded on the dredged gravels. The Phase II study documented in this report contains analyses of the segments of the dam with shells founded on undredged alluvium and directly on rock.

197. The Mormon Island Auxiliary Dam cross sections for the Phase II studies consisted of (a) Zone 1 shell gravels (fairly well-graded, sandy gravel from the Blue Ravine, with maximum particle size of about 6 in., and fines content of about 5 percent, placed in 24-in. lifts and compacted with

one complete coverage with a Caterpillar tractor, in situ $D_r \approx 65$ to 70 percent); (b) Zone 2 transition gravel (the same borrow source as Zone 1, but scalped to a maximum particle size of 2 in., placed in 12-in. lifts, and compacted in the same manner as Zone 1); (c) Zone 3 compacted decomposed granite (decomposed granite that classifies as SM by USCS, approximately 95 percent of modified effort maximum density); and (d) Zone 4 clayey core, compacted to 82 percent modified effort compacted density. The two idealized sections analyzed represented segments of the dam with shells founded on (a) undredged foundation gravels (similar in gradation to the Zone 1 embankment gravel and having a high penetration resistance with $(N_1)_{60}$ blowcounts of about 48 blows/ft); and (b) firm rock foundation.

198. The Phase I study focused on the segment of the dam with shells founded on the dredged alluvium. From this study it was concluded that extensive liquefaction is expected in the dredged gravel foundation and to some extent in the portion of the embankment in the core trench in the event of the design earthquake. Residual excess pore pressures of about 25 to 50 percent were estimated for the upstream shell. Remedial or hazard mitigating measures were recommended.

199. The Phase II field investigation was designed to augment data collected during the Phase I field investigations. In the Phase II field investigations, data were obtained for the embankment shells and the dredged and undredged alluvium. A geophysical investigation was conducted to determine the p- and s-wave velocities of the undredged alluvium. Twenty-six pairs of open- and closed-bit Becker soundings were performed to determine the penetration resistance of the embankment shell gravels and the dredged and undredged alluvium. The penetration resistances $(N_1)_{60}$ were 25 for the embankment gravels and 48 for the undredged alluvium. The penetration resistance in the dredged foundation varied with vertical effective stress and ranged from 7.2 blows/ft in the free field to 16.9 blows/ft under the embankment shells. The penetration resistances determined for the embankment gravels and the undredged alluvium in the Phase II field investigation were similar to those obtained in the Phase I field investigation. These data reinforced the conclusions from the Phase I analysis of the segment of the dam with shells founded on dredged alluvium.

200. In the Phase II studies, the seismic stability of the segments of Mormon Island Auxiliary Dam with shells founded on rock and on undredged

alluvium were evaluated. The analyses of both sections included evaluation of liquefaction potential, assessment of post-earthquake slope stability, and Newmark-type permanent displacement analyses. The field-performance based empirical liquefaction evaluation procedures developed by Professor H. B. Seed and his colleagues at the University of California, Berkeley, were used to estimate the cyclic strengths of the embankment and foundation materials from in situ tests, mainly the Becker Hammer and SPT soundings. Relative cyclic strengths and pore pressure generation behavior were determined from laboratory tests documented in Report 4. The cyclic strengths were compared with the earthquake-induced cyclic stresses computed with FLUSH to determine safety factors against liquefaction and to estimate the residual excess pore pressures developed due to shaking. Post-earthquake slope stability calculations and Newmark-type permanent displacement analyses were then performed with the earthquake-induced residual excess pore pressure field. Two types of permanent displacement analyses were employed to estimate the magnitude of displacement. These were the Makdisi-Seed and the Sarma-Ambrayseys techniques.

201. The results of the analysis of the idealized section of the dam founded on rock indicate that residual excess pore pressures developed in the upstream shell will be between 25 and 35 percent. No significant excess pore pressures are expected in Zones 3 and 4. The post-earthquake safety factor against sliding was computed to be 1.29. The permanent displacement analyses of the idealized rock foundation section indicate that Newmark-type displacements will be less than 1 ft along potential sliding surfaces confined to the upstream shell. Potential displacements will be even smaller for deeper failure surfaces which exit the dam downstream of the center line.

202. The results of the analysis of the idealized section of the dam with shells founded on undredged alluvium indicate that residual excess pore pressures developed in the upstream gravel shell will be between 10 and 20 percent. Due to its high penetration resistance, no significant residual excess pore pressures are expected to develop in the undredged alluvium beneath the shells. The post-earthquake safety factor against sliding was computed to be 1.91. As with the rock foundation section, potential Newmark-type displacements are expected to be less than 1 ft and will be even smaller for deeper circles emerging downstream of the center line. No movement is expected for potential failure surfaces that intercept the undredged alluvium.

203. Based on the above analyses it is concluded that the segments of Mormon Island Auxiliary Dam with shells founded on rock and on undredged alluvium (between sta 412 and sta 439 and sta 456+50 and sta 461+75) will perform satisfactorily during the earthquake. The magnitude of permanent displacements will be < 1 ft and will probably be confined to the upstream shell. This amount of displacement will be tolerable. No further study or remedial measures are recommended for these sections. Data collected in the dredged tailings in the Phase II field investigations support the conclusions drawn in Report 4--liquefaction is predicted in the dredged foundation, and remedial action is recommended for the portion of the dam with shells founded on dredged alluvium.

REFERENCES

- Allen, M. G. 1984. "Liquefaction Potential Investigation of Mormon Island Auxiliary Dam, Folsom Project, California," Soil Design Section US Army Engineer District, Sacramento, CA.
- Aubury, Lewis E. 1905. "Gold Dredging in California," The California State Mining Bureau, San Francisco, CA.
- Banerjee, N. G., Seed, H. B. and Chan, C. K. 1979. "Cyclic Behavior of Dense Coarse-Grained Materials in Relation to the Seismic Stability of Dams," Report No. EERC 79-13, Earthquake Engineering Research Center, University of California, Berkeley, CA.
- Bieganousky, W. A. and Marcuson, W. F. III. 1976. "Liquefaction Potential of Dams and Foundations - Report 1: Laboratory Standard Penetration Test on Reid Bedford Model and Ottawa Sands," Report S-76-2, US Army Engineer Waterways Experiment Station, Vicksburg, MS.
- Bolt, B. A. and Seed, H. B. 1983. "Accelerogram Selection Report for Folsom Dam Project, California," Contract Report DACW 05-83-Q-0205, US Army Engineer District, Sacramento, CA.
- Duncan, J. M., Byrne, P., Wong, K. S. and Mabry, P. 1980. "Strength, Stress-Strain and Bulk Modulus Parameters for Finite Element Analyses of Stresses and Movements in Soil Masses," Report No UCB/GT/80-01, Geotechnical Engineering, Department of Civil Engineering, University of California, Berkeley, CA.
- Duncan, J. M., Seed, R. B., Wong, W. S. and Ozawa, Y. 1984. "FEADAM84: A Computer Program for Finite Element Analysis of Dams," Research Report No. SU/GT/84-03. Stanford University, Stanford, CA.
- Edris, E. V. and Wright, S. G. 1987. "User's Guide: UTEXAS2 Scope-Stability Package, Vol 1," Instruction Report GL-87-1, US Army Engineer Waterways Experiment Station, Vicksburg, MS.
- Harder, L. F. 1986. "Evaluation of Becker Penetration Tests Performed at Mormon Island Auxiliary Dam in 1983," WES Contract Report, Vicksburg, MS.
- Harder, L. F. and Seed, H. B. 1986. "Determination of Penetration Resistance for Coarse-Grained Soils Using the Becker Hammer Drill," UCB/EERC Report No. 86/06, University of California, Berkeley, CA.
- Hynes-Griffin, M. E. 1979. "Dynamic Analyses of Earth Embankments for Richard B. Russell Dam and Lake Project," Final report prepared for US Army Engineer District, Savannah, GA.
- Hynes-Griffin, M. E. and Franklin, A. G. 1984. "Rationalizing the Seismic Coefficient," Miscellaneous Paper GL-84-13, US Army Engineer Waterways Experiment Station, Vicksburg, MS.
- Kean, T. B. 1988. "Geophysical Investigation of Undredged Alluvium at Mormon Island Auxiliary Dam, California," Memorandum for Record, US Army Engineer Waterways Experiment Station, Vicksburg, MS.
- Kiersch, G. A., and Treasher, R. C. 1955. "Investigations, Areal and Engineering Geology - Folsom Dam Project, Central California," Economic Geology, Vol 50, No. 3, pp 271-310.

Llopis, J. L. 1983 (Jul). "Preliminary Results of an In-Situ Seismic Investigation of Folsom Dam, California," Draft Letter Report to US Army Engineer District, Sacramento, California, from US Army Engineer Waterways Experiment Station, Vicksburg, MS.

Llopis, J. L. 1984 (Sep). "Preliminary Results of In Situ Surface Vibratory Tests of Folsom Dam, California," Letter Report to Commander, US Army Engineer District, Sacramento, California, from US Army Engineer Waterways Experiment Station, Vicksburg, MS.

Lysmer, J., Udaka, T., Tsai, C. F., and Seed, H. B. 1973. "FLUSH: A Computer Program for Approximate 3-D Analysis of Soil-Structure Interaction Problems." Report No. EERC 75-30. Earthquake Engineering Research Center, University of California, Berkeley, CA.

Marcuson, W. F., III, and Bieganousky, W. A. 1977. "SPT and Relative Density in Coarse Sands," Journal of the Geotechnical Engineering Division, ASCE, Vol 103, No. GT11, pp 1295-1309.

Newmark, N. M. 1965. "Effects of Earthquakes on Dams and Embankments," Geotechnique, Vol 15, No. 2, pp 139-160.

Sarma, S. K. 1979. "Response and Stability of Earth Dams During Strong Earthquakes." Miscellaneous Paper GL-79-13, US Army Engineer Waterways Experiment Station, Vicksburg, MS.

Schnabel, P. B., Lysmer, J., and Seed, H. B. 1972. "SHAKE, A Computer Program for Earthquake Response Analysis of Horizontally Layered Sites," Report No. EERC 72-12, Earthquake Engineering Research Center, College of Engineering, University of California, Berkeley, CA.

Seed, H. B. 1979. "19th Rankine Lecture: Considerations in the Earthquake Resistant Design of Earth and Rockfill Dams," Geotechnique, Vol 29, No. 3, pp 215-263.

_____. 1983. "Earthquake-Resistant Design of Earth Dams." Presented at the American Society of Civil Engineers Spring Convention, May 1983, Philadelphia, PA.

Seed, H. B., and Idriss, I. M., 1970. "Soil Moduli and Damping Factors for Dynamic Response Analyses." Report No. EERC 70-10. Earthquake Engineering Research Center, University of California, Berkeley, CA.

Seed, H. B., Idriss, I. M., and Arango, I. 1983. "Evaluation of Liquefaction Potential Using Field Performance Data," Journal of the Geotechnical Engineering Division, American Society of Civil Engineers, Vol 109, No. GT3, pp 458-482.

Seed, H. B. and Peacock, W. H. 1971. "Test Procedures for Measuring Soil Liquefaction Characteristics," Journal of the Soil Mechanics and Foundations Division, American Society of Civil Engineers, Vol 97, No. SM8. pp 1099-1119.

Seed, H. B., Tokimatsu, K., Harder, L. F., and Chung, R. M. 1984a. "The Influence of SPT Procedures in Soil Liquefaction Resistance Evaluations," UCB/EERC Report No. 84/15, University of California, Berkeley, CA.

Seed, H. B., Wong, R. T., Idriss, I. M., and Tokimatsu, K. 1984b. "Moduli and Damping Factors for Dynamic Analyses of Cohesionless Soils," Report No. EERC 84-14. Earthquake Engineering Research Center, University of California, Berkeley, CA.

Tierra Engineering Consultants, Inc. 1983. "Geologic and Seismologic Investigations of the Folsom, California Area," Contract Report DACW 05-82-C-0042, US Army Engineer District, Sacramento, CA.

US Army Corps of Engineers. 1985. "Earthquake Analysis and Response of Concrete Gravity Dams," Engineer Technical Letter (ETL) 1110-2-303, Washington, DC.

US Army Engineer District, Sacramento. 1953. "Foundation Report, American River, California, Mormon Island Auxiliary Dam, Folsom Project," Sacramento, CA.

US Army Engineer Laboratory, South Pacific Division. 1986. "Report of Soil Tests, Folsom Dam Laboratory Program," Sausalito, CA.

Table 1

Estimated Seismic Characteristics of Capable Faults (1)

<u>Name of Fault Zone</u>	<u>Minimum Distance To Site mile</u>	<u>Type of Faulting</u>	<u>Maximum Earthquake Magnitude (2)</u>	<u>Approximate Slip Rate (3)</u>	<u>Most Recent Displacement Known (4)</u>
San Andreas	102	Strike-slip	8	1-2 cm/year	Historic
Hayward	85	Strike-slip	7	0.5 cm/year	Historic
Calaveras	77	Strike-slip	7	0.25 cm/year	Historic
Genoa Jack Valley	70+	Normal-slip	7.25	0.01-0.02	Holocene
West Walker River	85	Normal-slip	7.25	0.01	Historic
Melones	16.5	Normal-slip	6.5	0.0006-0.0001	Pleistocene ±100,000
East Branch Bear Mountains	8.0	Normal-slip	6.5 (5)	0.0006-0.0001	Pleistocene ±100,000

(1) Capable fault, under criteria used by Tierra Engineering Consultants, Inc. in this study, is one that exhibited displacement at or near the ground surface within the past 35,000 years, recurrent movement within the past 500,000 years, exhibits creep movement, and/or exhibits aligned macro ($M \geq 3.5$) seismicity determined from instruments.

(2) Maximum earthquake estimate on rupture length of continuous strands, type of faulting, fault displacement, historic earthquakes, seismic moment, experience and judgment.

(3) Slip rates estimated from historic, geomorphic, or geologic evidence.

(4) Late Pleistocene period displacement may be as old as 500,000 years ago or as young as 10,000 years ago.

(5) Hypothetical value (acceptance based on USBR Auburn Dam studies).

Table 2
Adopted Design Shear Strengths from Construction Records

<u>Material</u>	Dry Unit Weight pcf	Moist Unit Weight pcf	Saturated Unit Weight pcf	Buoyant Unit Weight pcf	Effective Friction, tan ϕ'	Effective Cohesion c', pcf
Dredged tailings below el 369	108.5	125.5	132.2	69.8	0.45	0
Dredged tailings above el 369	125	133.0	143.8	81.4	0.84	0
Zone 1 shell	125	133.0	143.8	81.4	0.84	0
Zone 2 transition	125	133.0	143.8	81.4	0.84	0
Zone 3 filter*	(123.4)	(134.0)	(140.0)	(77.6)	(0.70)	(0)
Zone 4 core**	108.5	125.5	132.2	69.8	0.55	0

* Zone 3 was assumed to have the same strengths as Zone 4. Tabulated information is from Wing Dams for 95 percent modified effort compacted density.

** Zone 4 was compacted to 82 percent modified effort compacted density.

Table 3
Placement Specifications for Embankment Materials

<u>Zone</u>	<u>Source</u>	<u>Compaction Equipment</u>	<u>No. of Passes</u>	<u>Maximum Lift Thickness in.</u>
1 (Gravel shell)	Borrow No. 5	D-8 Caterpillar tractor	3*	24
2 (Gravel transition)	Borrow No. 5 (-2 in. fraction)	D-8 Caterpillar	3*	12
3 (Decomposed granite filter)	Borrow No. 1	Sheepsfoot roller Pneumatic-tired roller	8 4	12 18
4 (Clayey core)	Borrow No. 6	Sheepsfoot roller Pneumatic-tired roller	10 4	8 8

* One complete coverage with a D-8 Caterpillar tractor with standard width treads was specified. One complete coverage is estimated to correspond to 3 or 4 passes.

Table 4
 Hyperbolic Parameters Input to FEADAM for Static Analysis of Mormon Island Auxiliary Dam

Material Location	Effective Unit Weight pcf	Young's Modulus		Young's Modulus Exponent N	Failure Ratio R_f	Bulk Modulus K_b	Bulk Modulus Exponent M	Effective Cohesion Intercept C, ksf	Effective Friction Angle ϕ , deg	Change in ϕ Per Log Cycle Change in Confining Stress $\Delta\phi$	Static Stress Ratio K_s
		Loading K_u , ksf	Unloading K_{ur}								
Embankment gravel	$\gamma_b = 90$	1,900	1,900	0.14	0.90	1,267	0.33	0	43	0	0.50
	$\gamma_{moist} = 146$										
Impervious core	$\gamma_b = 72.4$	925	925	0.15	0.69	1,186	0.59	0	29	0	0.59
	$\gamma_b = 79.4$	1,175	1,175	0.53	0.69	979	1.43	0	37	0	0.43
Transition zone	$\gamma_{moist} = 136$										
	$\gamma_b = 84$	1,680	1,680	0.15	0.90	1,120	0.33	0	43	0	0.50
Undredged alluvium											

Table 5
Unit Weights and K_2 Parameter Used for Embankment and
 Foundation Materials Input to FLUSH

<u>Material Type</u>	<u>Unit Weight pcf</u>	<u>K_2</u>
Moist embankment gravel	139	120
Submerged embankment gravel	154	120
Zone 3 - decomposed granite (moist)	136	125
Zone 3 - decomposed granite (submerged)	142	125
Central impervious cone	136	90
Undredged alluvium	146	130

Table 6
Unit Weights and Shear Strength Parameters Used In
 Post-Earthquake Stability Calculations

<u>Material Type</u>	<u>Unit Weight pcf</u>	<u>c psf</u>	<u>ϕ' deg</u>
Embankment gravels:			
Moist	146	0	43
Submerged	152	0	43
Zone 3 - Decomposed Granite:			
Moist	136	0	31
Submerged	142	0	31
Zone 4 - Impervious core Submerged	135	0	35
Undredged alluvium Submerged	130	0	35

Note: Shear strengths (c and $\tan \phi'$) for Zone 4 and the undredged alluvium were reduced by a factor of 20 percent.

Table 7
Summary of Makdisi-Seed Calculations for Set of Potential Slip Surfaces Confined to Upstream Shell
for Idealized Section for Portion of Mormon Island Auxiliary Dam Founded on Rock

<u>y/h</u> <u>percent</u>	\ddot{U}_{max} Crest <u>g</u>	k_y <u>g</u>	$\frac{k_{max}}{\ddot{U}_{max}}$	k_{max} <u>g</u>	$\frac{k_y}{k_{max}}$	$\frac{U/k_{max} \times g \times T_o}{sec}$	$\frac{U}{ft}$	α	$\frac{U \times \alpha}{ft}$
20.00	.91	.39	.88	.80	.49	.02	.22	1.30	.28
40.00	.91	.18	.70	.64	.28	.08	.56	1.30	.73
60.00	.91	.11	.52	.47	.23	.10	.56	1.30	.72
80.00	.91	.06	.41	.37	.16	.19	.84	1.30	1.09
100.00	.91	.08	.34	.31	.26	.08	.29	1.30	.38

Note: $T_o = 0.366$ sec, $\ddot{U}_{max(crest)} = 0.91$ g, Magnitude 6.5 event.

Table 8

Summary of Makdisi-Seed Calculations for Set of Potential Slip Surfaces Exiting Downstream of Center Line for Idealized Section for Portion of Mormon Island Auxiliary Dam Founded on Rock

<u>y/h</u> <u>percent</u>	\dot{U}_{max} <u>Crest</u> <u>g</u>	k_y <u>g</u>	$\frac{k_{max}}{\dot{U}_{max}}$	k_{max} <u>g</u>	$\frac{k_y}{k_{max}}$	$\frac{U}{k_{max}} \times g \times T_o$ <u>sec</u>	$\frac{U}{ft}$	α	$U \times \alpha$ <u>ft</u>
20.00	.91	.57	.88	.80	.71	.01	.05	1.30	.07
40.00	.91	.25	.70	.64	.39	.04	.32	1.30	.41
60.00	.91	.18	.52	.47	.38	.04	.22	1.30	.29
80.00	.91	.14	.41	.37	.38	.04	.18	1.30	.23
100.00	.91	.20	.34	.31	.65	.01	.03	1.30	.04

Note: $T_o = 0.366 \text{ sec } \dot{U}_{max(crest)} = 0.91 \text{ g, Magnitude } 6.5 \text{ event.}$

Table 9

Summary of Sarma-Ambrayseys Calculations for Set of Potential Slip Surfaces Confined to Upstream Shell for Idealized Section for Portion of Mormon Island Auxiliary Dam Founded on Rock

Y/H percent	a (rock) g	A = k _{max} g	N = k _y	N/A	U cm	A/a	U × (A/a) cm	α	U × (A/a) × α cm	U × (A/a) × α ft
20.00	.35	.80	.39	.49	1.20	2.29	2.74	1.30	3.57	.12
40.00	.35	.64	.18	.28	5.20	1.83	9.51	1.30	12.36	.41
60.00	.35	.47	.11	.23	9.00	1.34	12.09	1.30	15.71	.52
80.00	.35	.37	.06	.16	17.00	1.06	17.97	1.30	23.36	.77
100.00	.35	.31	.08	.26	7.00	.89	6.20	1.30	8.06	.26

Table 10

Summary of Sarma-Ambroseys Calculations for Set of Potential Slip Surfaces Emerging Downstream of Center Line for Idealized Section for Portion of Mormon Island Auxiliary Dam Founded on Rock

Y/H percent	a (rock) g	A - k _{max} g	N - k _y	N/A	U cm	A/a	U × (A/a) cm	α	U × (A/a) × α cm	U × (A/ε) × α ft
20.00	.35	.80	.57	.71	.34	2.29	.78	1.30	1.01	.03
40.00	.35	.64	.25	.39	2.20	1.83	4.02	1.30	5.23	.17
60.00	.35	.47	.18	.38	2.10	1.34	2.82	1.30	3.67	.12
80.00	.35	.37	.14	.38	2.10	1.06	2.22	1.30	2.89	.09
100.00	.35	.31	.20	.65	.42	.89	.37	1.30	.48	.02

Table 11

Summary of Makdisi-Seed Calculations for Set of Potential Slip Surfaces Exiting Downstream of the Center Line for Idealized Section for Portion of Mormon Island Auxiliary Dam

Founded on Undredged Alluvium, Shallow Circles

<u>y/h</u> <u>percent</u>	<u>U_{max}</u> <u>Crest</u> <u>g</u>	<u>k_y</u> <u>g</u>	<u>k_{max}</u> <u>U_{max}</u>	<u>k_{max}</u> <u>g</u>	<u>k_y</u> <u>k_{max}</u>	<u>U/k_{max}</u> × <u>g</u> × <u>T₀</u> <u>sec</u>	<u>U</u> <u>ft</u>	<u>α</u>	<u>U × α</u> <u>ft</u>
20.00	.67	.22	.88	.59	.36	.05	.72	1.30	.93
40.00	.67	.21	.70	.47	.44	.03	.35	1.30	.45
60.00	.67	.15	.52	.35	.42	.04	.32	1.30	.41
80.00	.67	.19	.41	.27	.70	.01	.03	1.30	.04
100.00	.67	.23	.34	.23	1.01	.00	.00	1.30	.00

Note: T₀ = 0.74 sec, U_{max(crest)} = 7.67 g, Magnitude 6.5 event.

Table 12

Summary of Makdisi-Seed Calculations for Set of Potential Slip Surfaces Exiting Downstream of Center Line for Idealized Section for Portion of Mormon Island Auxiliary Dam
Founded on Undredged Alluvium, Deep Circles

<u>y/h</u> <u>percent</u>	$\frac{\ddot{U}_{max}}{g}$ Crest	$\frac{k_y}{g}$	$\frac{k_{max}}{\ddot{U}_{max}}$	$\frac{k_{max}}{g}$	$\frac{k_y}{k_{max}}$	$\frac{U}{k_{max}} \times g \times T_o$ sec	$\frac{U}{ft}$	α	$\frac{U \times \alpha}{ft}$
20.00	.67	.36	.88	.59	.61	.01	.15	1.30	.20
40.00	.67	.22	.70	.47	.46	.03	.31	1.30	.41
60.00	.67	.19	.52	.35	.54	.02	.16	1.30	.21
80.00	.67	.20	.41	.27	.73	.00	.03	1.30	.03
100.00	.67	.22	.34	.23	.97	.00	.00	1.30	.00

Note: $T_o = 0.74$ sec, $\ddot{U}_{max(crest)} = 0.67$ g, Magnitude 6.5 event.

Table 13

Summary of Sarma-Ambrayseys Calculations for Set of Potential Slip Surfaces Confined to Shell for Idealized Section for Portion of Mormon Island Auxiliary Dam Founded on Undredged Alluvium

Y/H percent	a (rock) g	A = k _{max} g	N = k _y	N/A	U cm	A/a	U × (A/a) cm	α	U × (A/a) × α cm	U × (A/a) × α ft
20.00	.35	.62	.22	.35	2.80	1.76	4.93	1.30	6.41	.21
40.00	.35	.49	.21	.42	1.60	1.40	2.24	1.30	2.91	.10
60.00	.35	.36	.15	.40	1.10	1.04	1.14	1.30	1.49	.05
80.00	.35	.29	.19	.67	.40	.82	.33	1.30	.43	.19
100.00	.35	.24	.23	.97	.10	.68	.07	1.30	.09	.00

Table 14

Summary of Sarma-Ambrayseys Calculations for Set of Potential Slip Surfaces Emerging Downstream of Center Line for Idealized Section for Portion of Mormon Island Auxiliary Dam Founded on Undredged Alluvium

Y/H percent	a (rock) g	A - k _{max} g	N - k _y	N/A	U cm	A/a	U x (A/a) cm	α	U x (A/a) x α cm	U x (A/a) x α ft
20.00	.35	.62	.36	.58	.70	1.76	1.23	1.30	1.60	.05
40.00	.35	.49	.22	.44	1.20	1.40	1.68	1.30	2.18	.07
60.00	.35	.36	.19	.52	.81	1.04	.84	1.30	1.10	.04
80.00	.35	.29	.20	.70	.34	.82	.28	1.30	.36	.01
100.00	.35	.24	.22	.93	.10	.68	.07	1.30	.09	.00

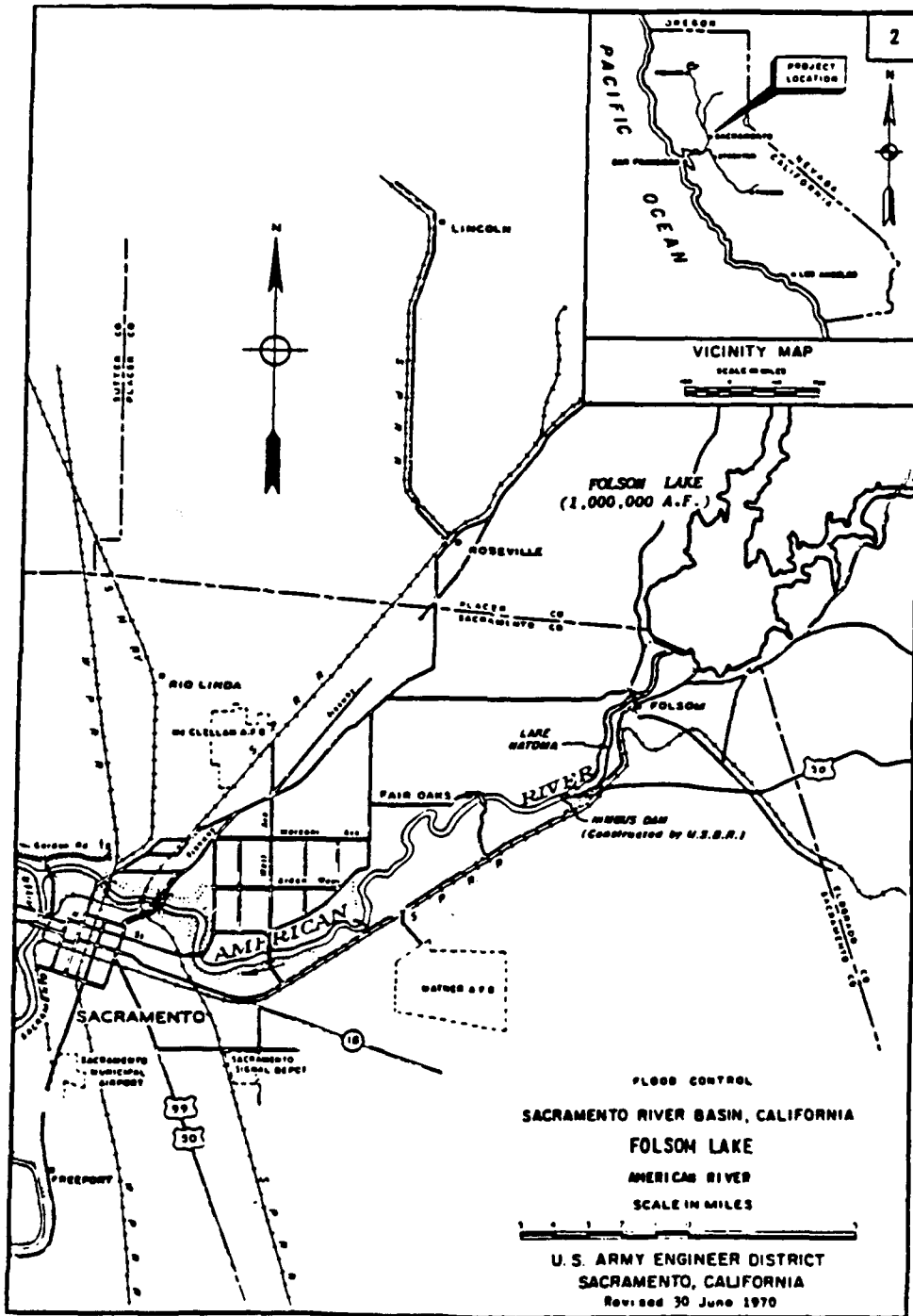


Figure 1. Location of Folsom Dam and Reservoir Project

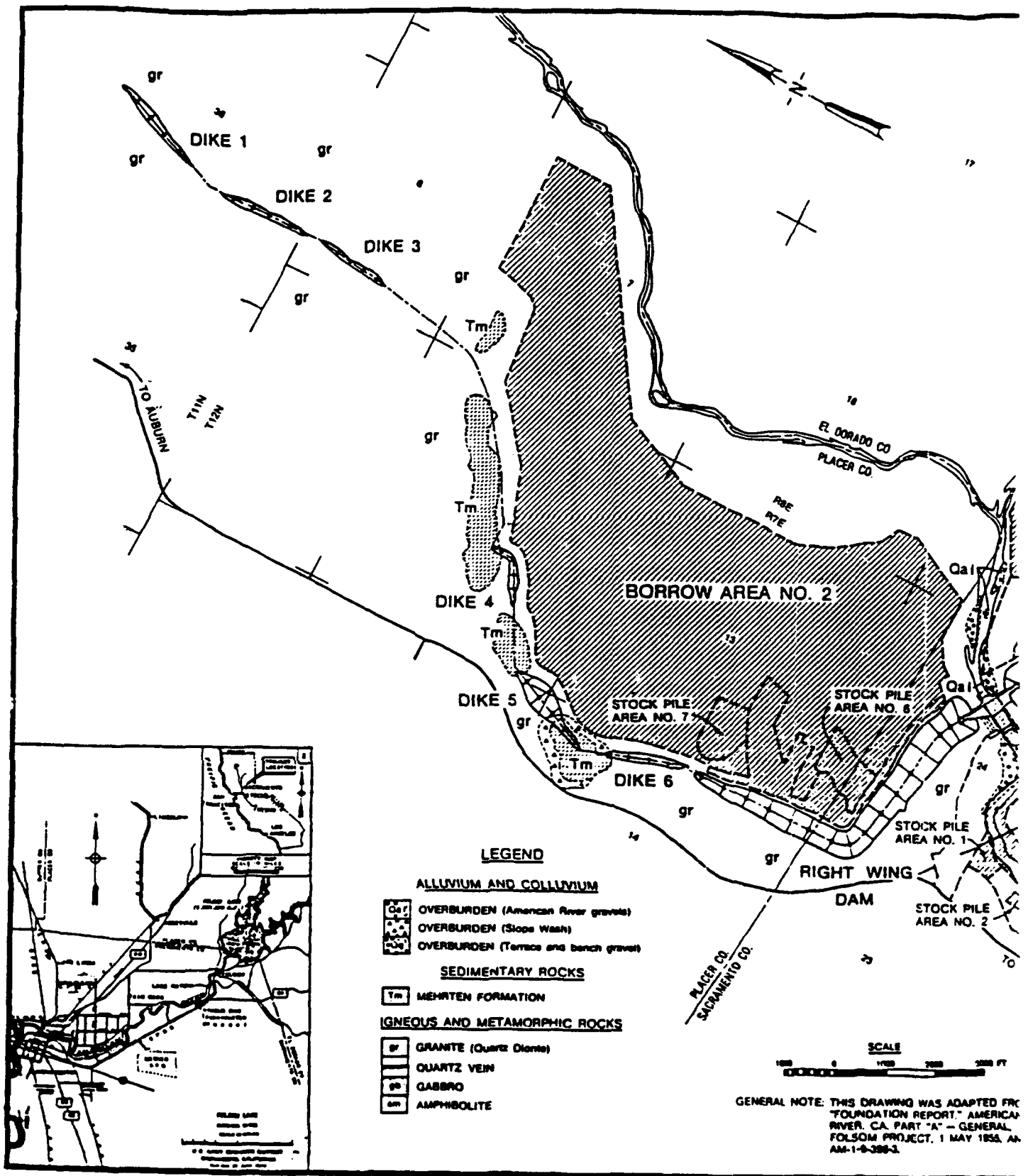
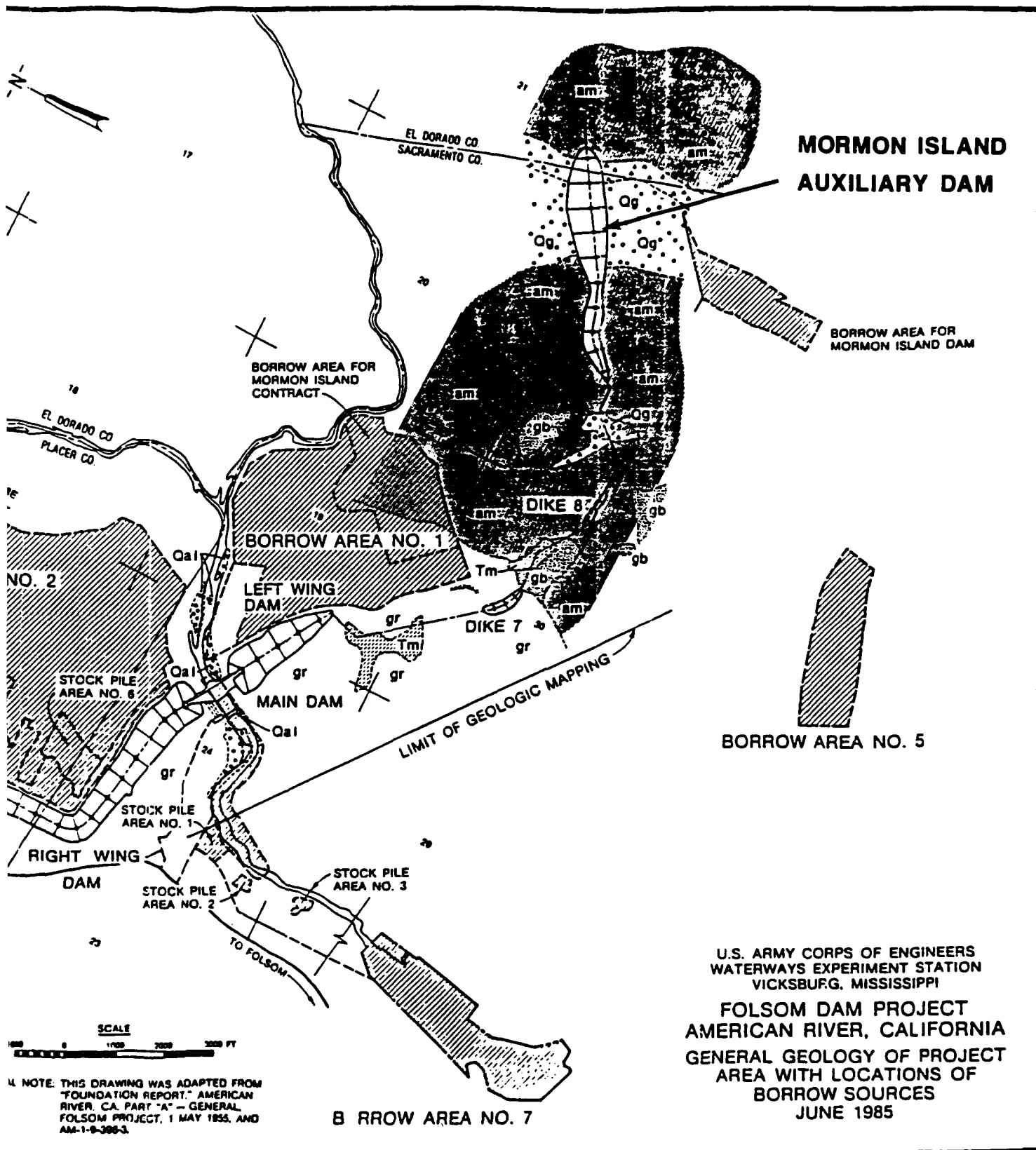


Figure 2. Plan of man-made retaining structures at the



ning structures at the Folsom Dam and Reservoir Project

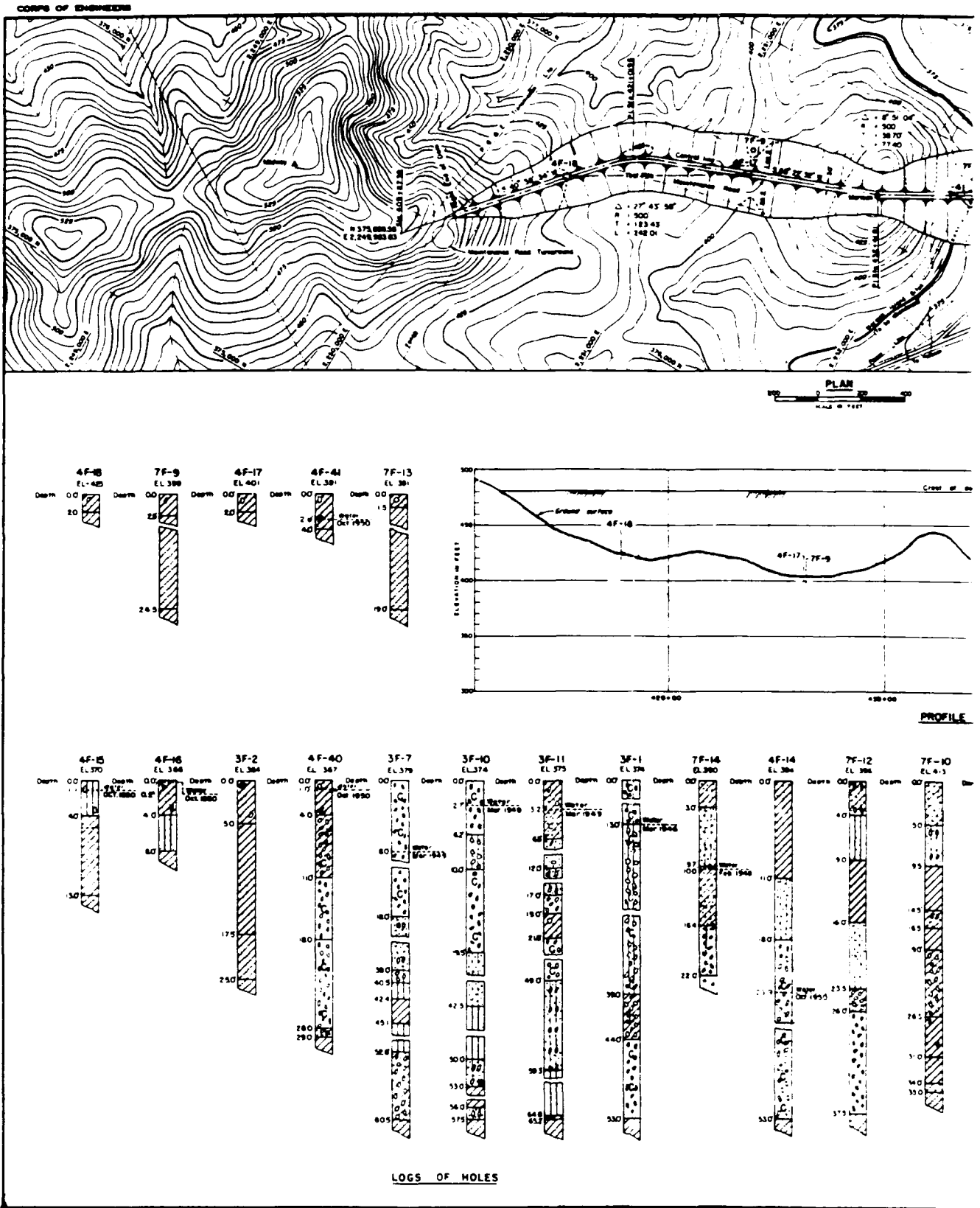
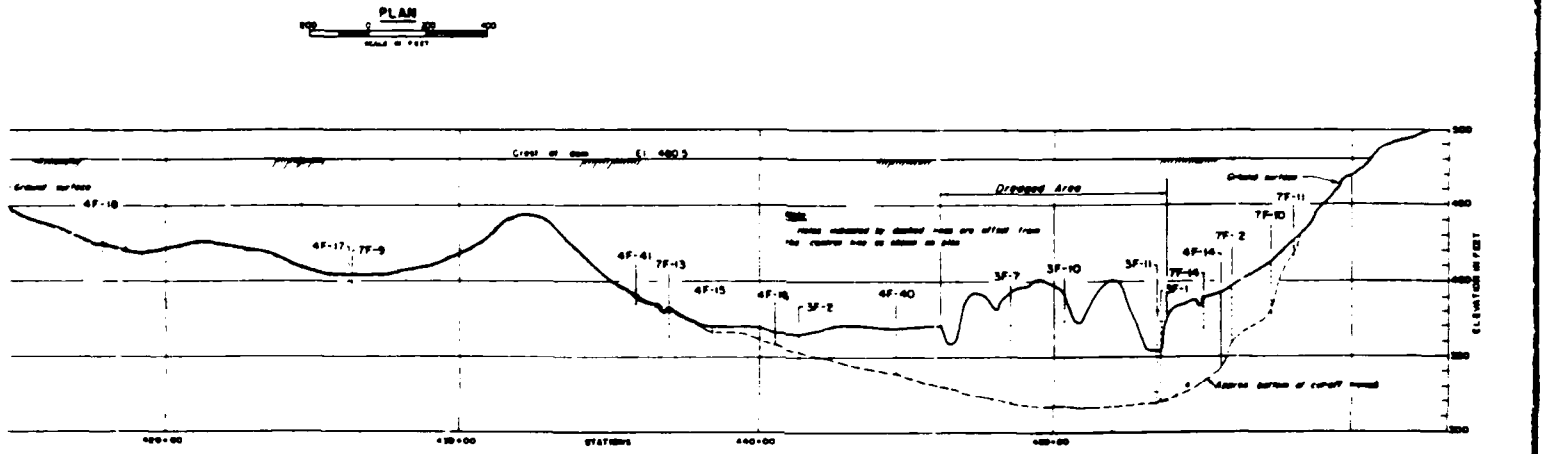
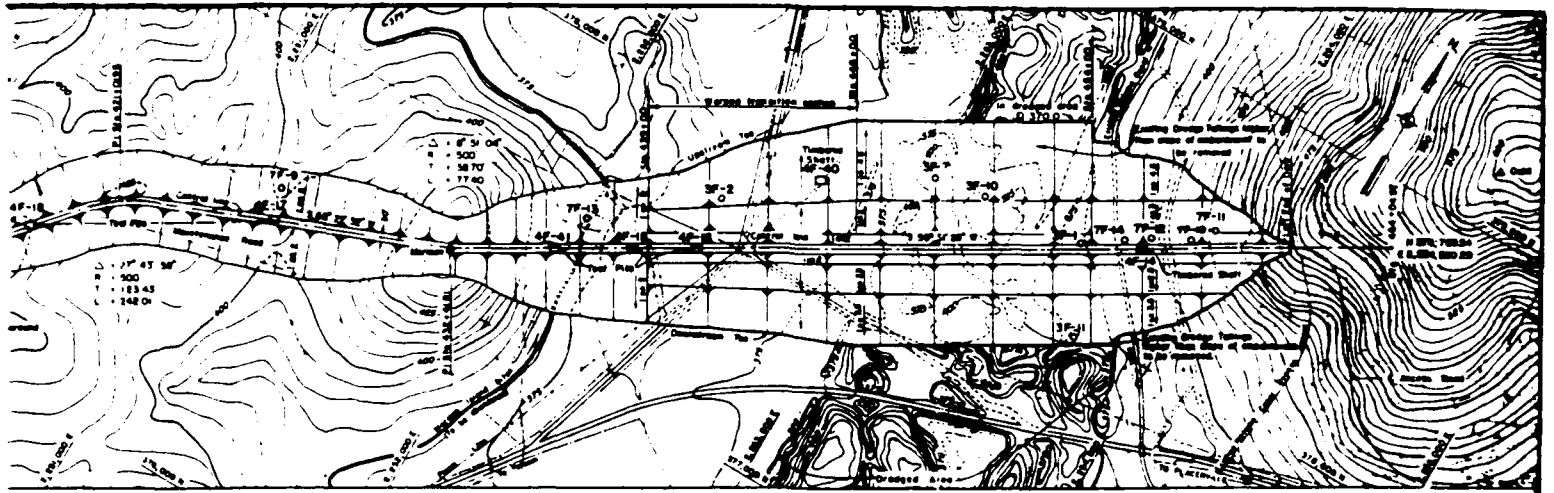
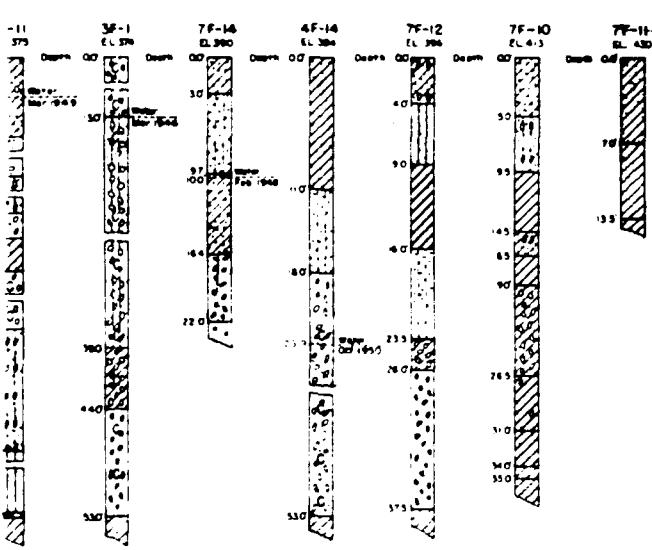


Figure 3. Plan and axial sections of Mormon Island Auxiliary



PROFILE ON CONTROL LINE



LEGEND

Gravel with gravel	Silt gravel	Gravelly sand
Sandy gravel with gravel	Silt sand	Gravelly sandy clay
Sandy gravel with gravel	Clayey gravelly silt	Sandy clay
Silt gravel	Clayey sand	Lean clay
Silt gravel	Gravelly silt	Fat clay
Gravelly sand	Sandy silt	Steady silt, medium
Gravelly clay	Cobbles	

- NOTES
- 1 Datum is Sea Level Datum of 1929
 - 2 Elevations shown on logs are ground surface elevations
 - 3 Laboratory classification shown for all materials, according to the Corps of Engineers Uniform Soils Classification, except those shown in logs of holes 3F-1, 3F-2, 7F-13 and 7F-14, which are field classifications
 - 4 Holes 3F-1 and 3F-2 were drilled with a 12" churn drill. Holes 3F-7, 3F-10 and 3F-11 were drilled with a 10" churn drill. Samples were taken with a power auger and push tube sampler, where possible
 - 5 All 4F holes are open pits or shafts
 - 6 All 7F holes were drilled with a Facing drill rig using a 7" diameter rotary core drill
 - 7 Typical embankment sections shown on Sheet No. 357/7
 - 8 Limit of contractor work areas including waste areas are shown on drawing Sheet No. 357/2
 - 9 Slopes of warped transition vary uniformly from Station 439+00 to 446+00
 - 10 The term gravel, under the classification system used for this drawing, applies to gravel sizes larger than the No. 10 sieve
 - 11 The term cobbles includes material from 3" to 16" in size and the presence of some is indicated by the letter "C" in the logs
 - 12 This drawing was taken from As-Constructed sheet no. 357/3, File No. AM-1-7-557

AMERICAN RIVER BARR DEVELOPMENT CALIFORNIA
 FOLSOM RESERVOIR PROJECT
 AMERICAN RIVER
 MORMON ISLAND AUXILIARY DAM
 FOUNDATION EXPLORATION
 PLAN, PROFILE AND LOGS OF HOLES

axial sections of Mormon Island Auxiliary Dam

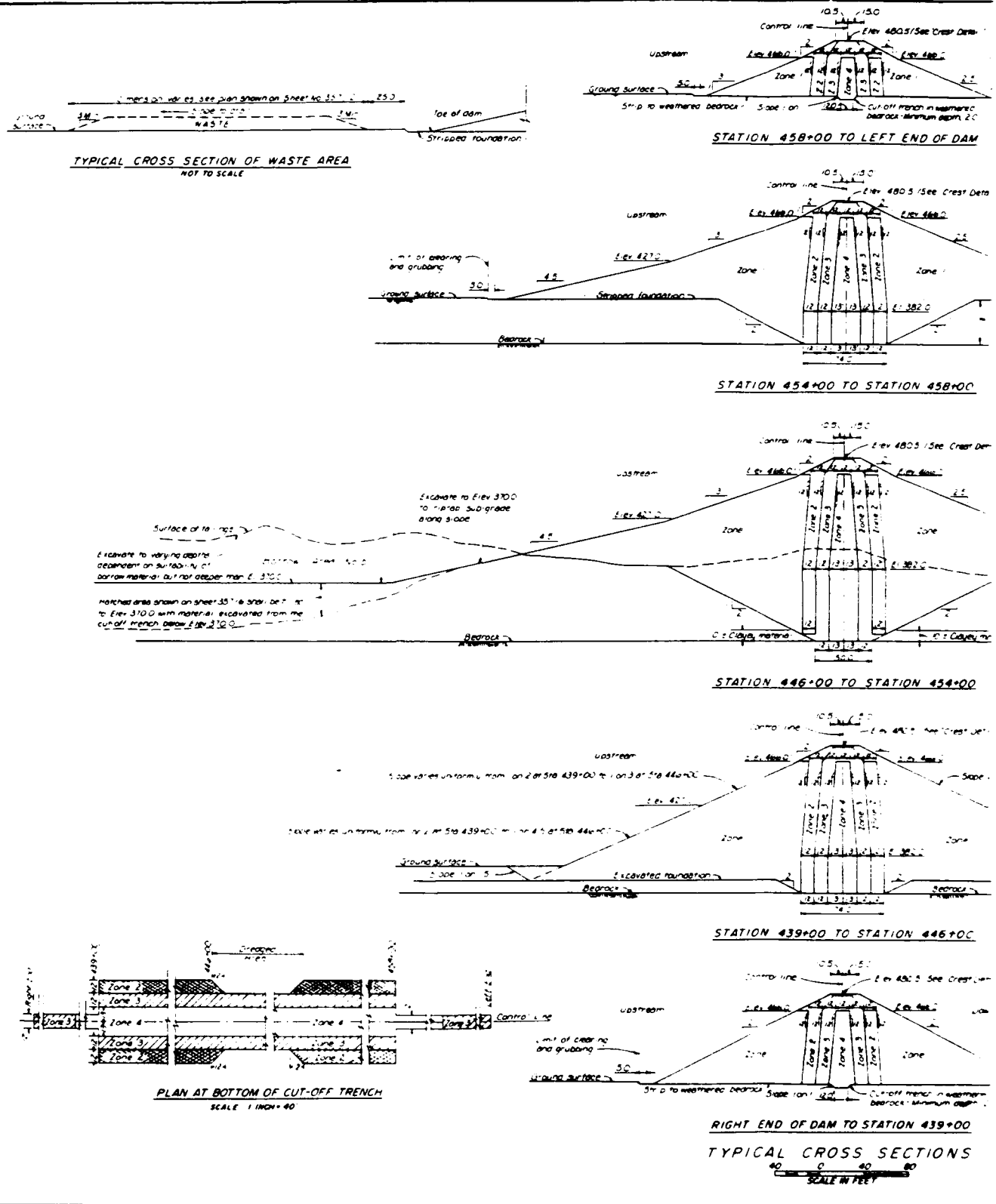
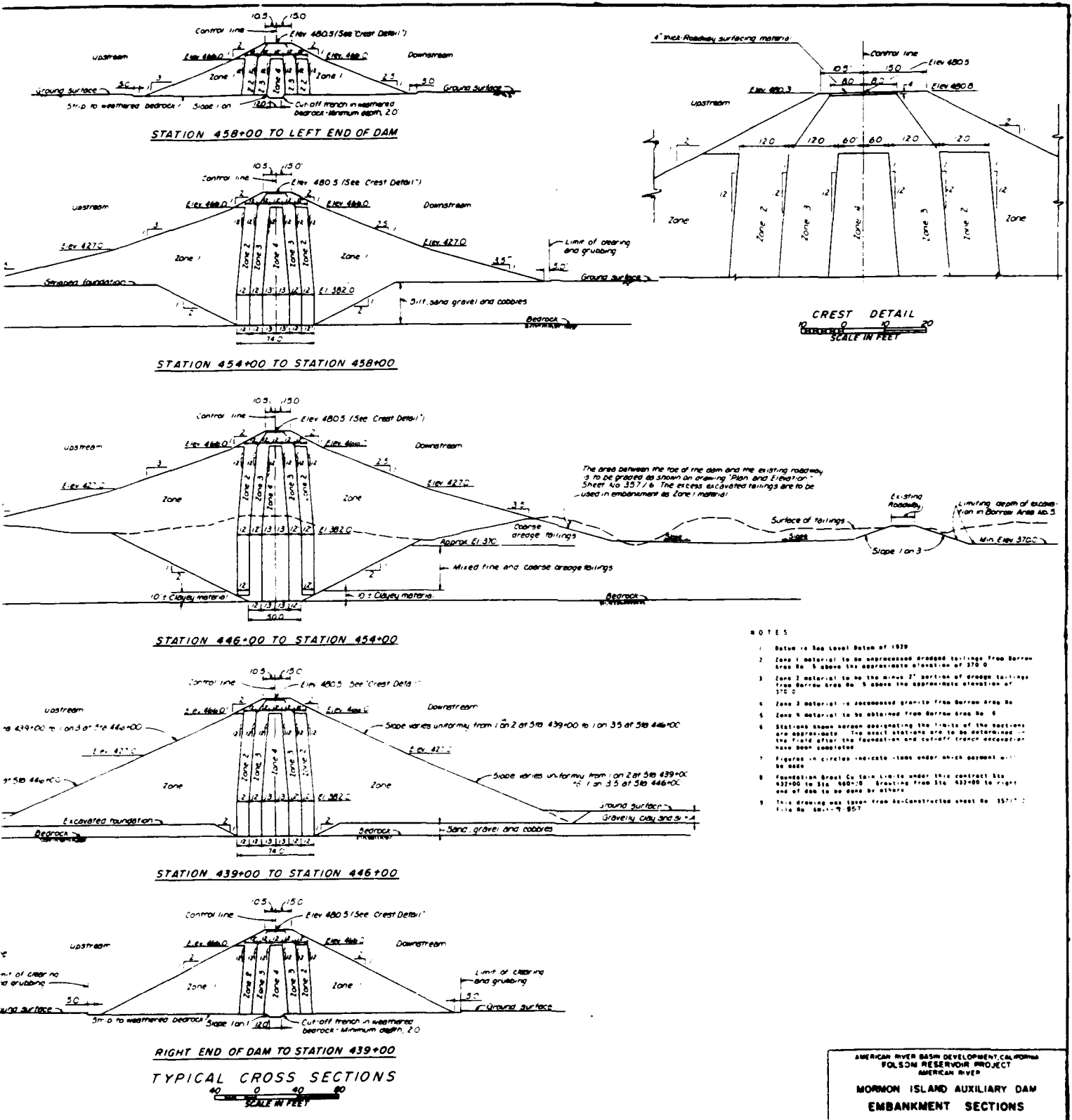


Figure 4. Typical embankment sections of Mormon



Typical embankment sections of Mormon Island Auxiliary Dam

1

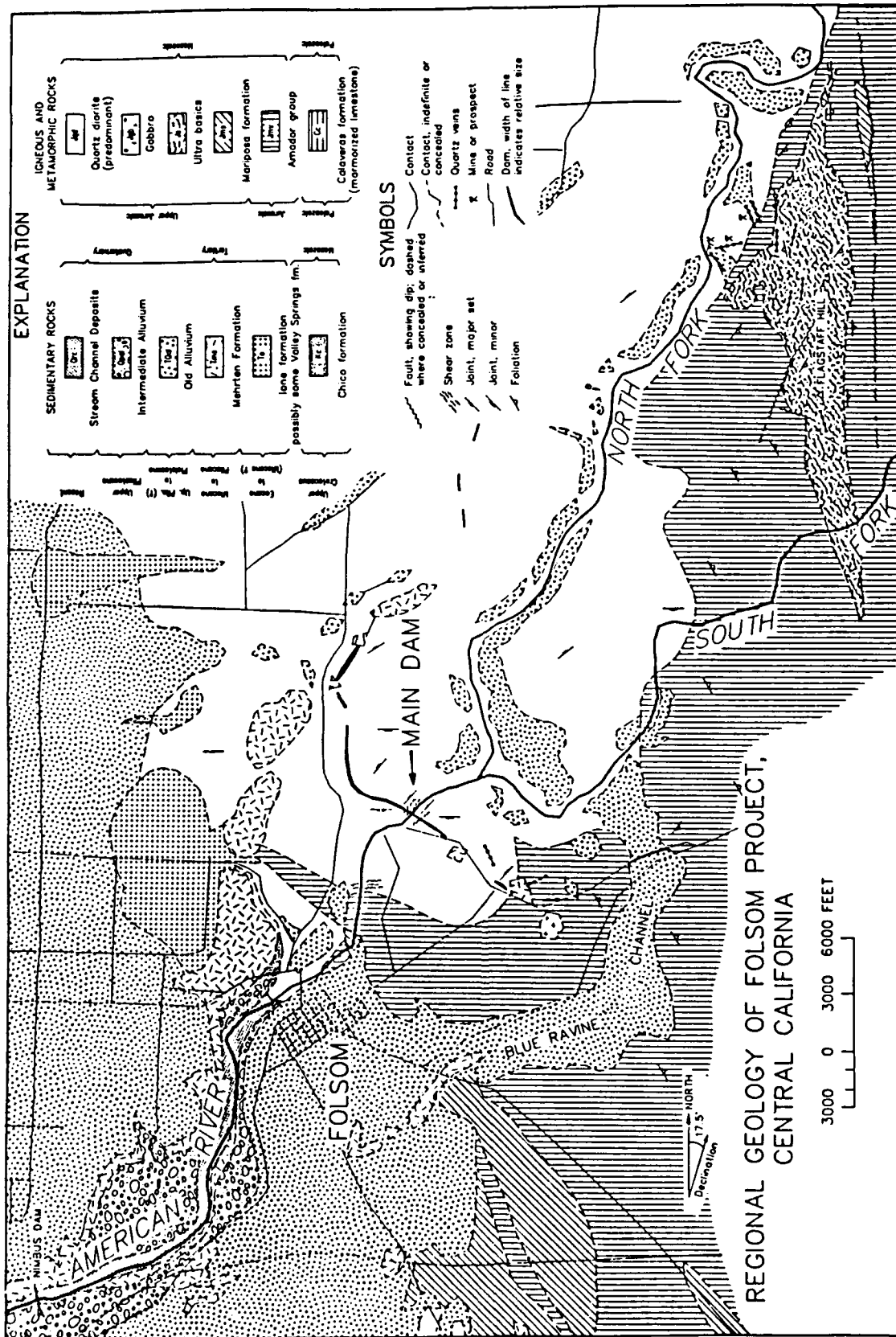


Figure 5. Geologic map, parts of the Folsom and Auburn quadrangles

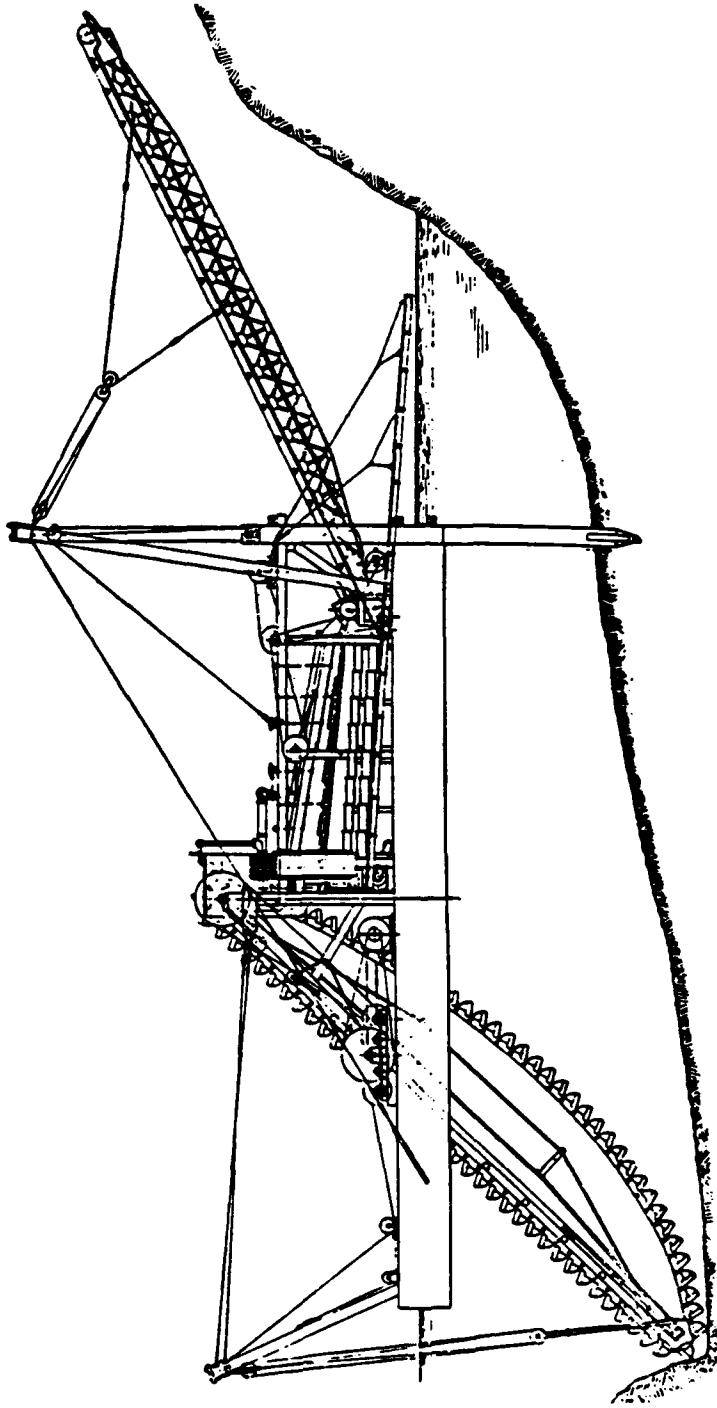


Figure 6. Bucyrus type of dredge, with close-connected buckets, shaking screens, belt conveyor, and spuds (from Aubury 1905)

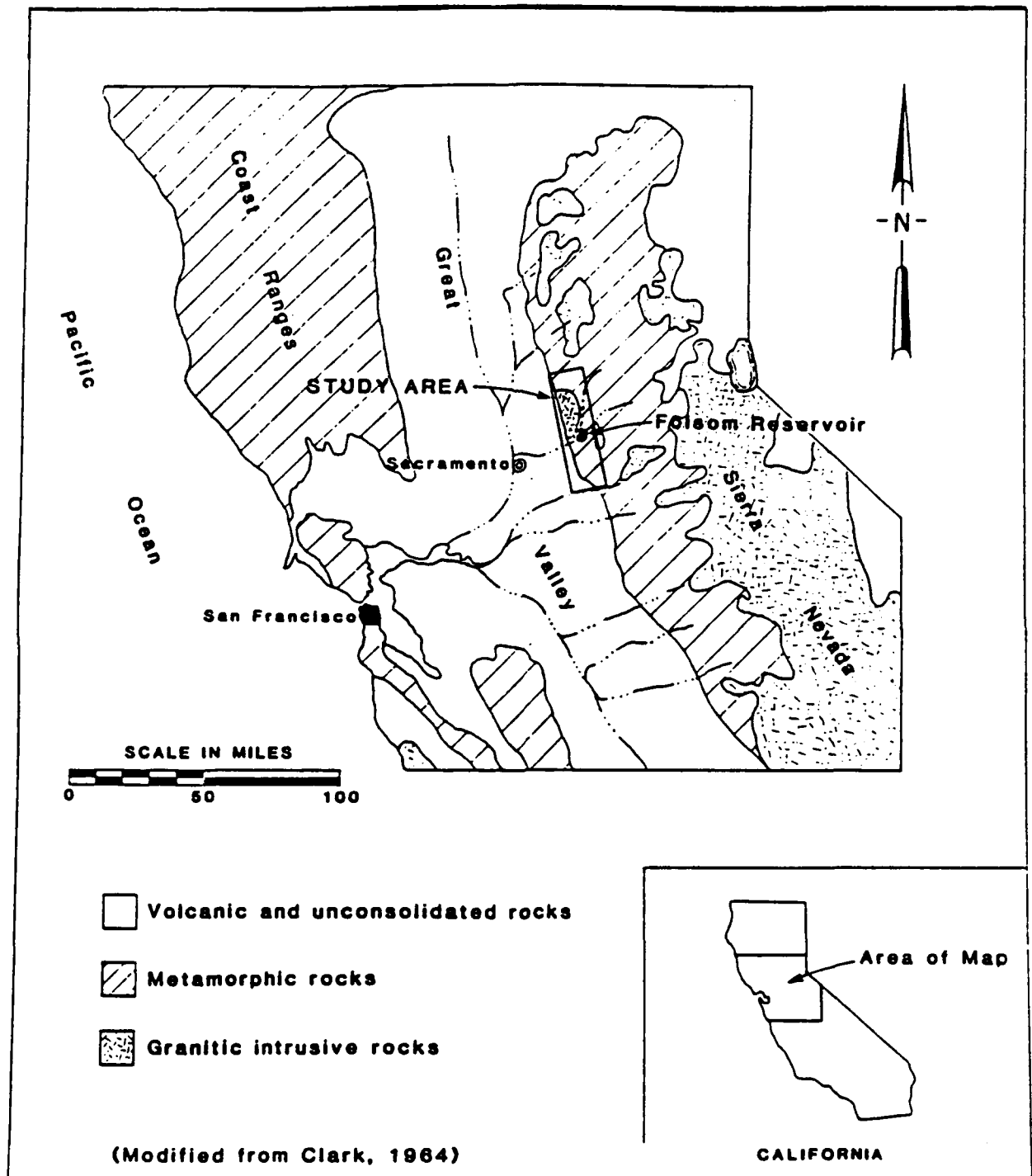


Figure 7. Regional geologic map (after Tierra Engineering Consultants, Inc. 1983)

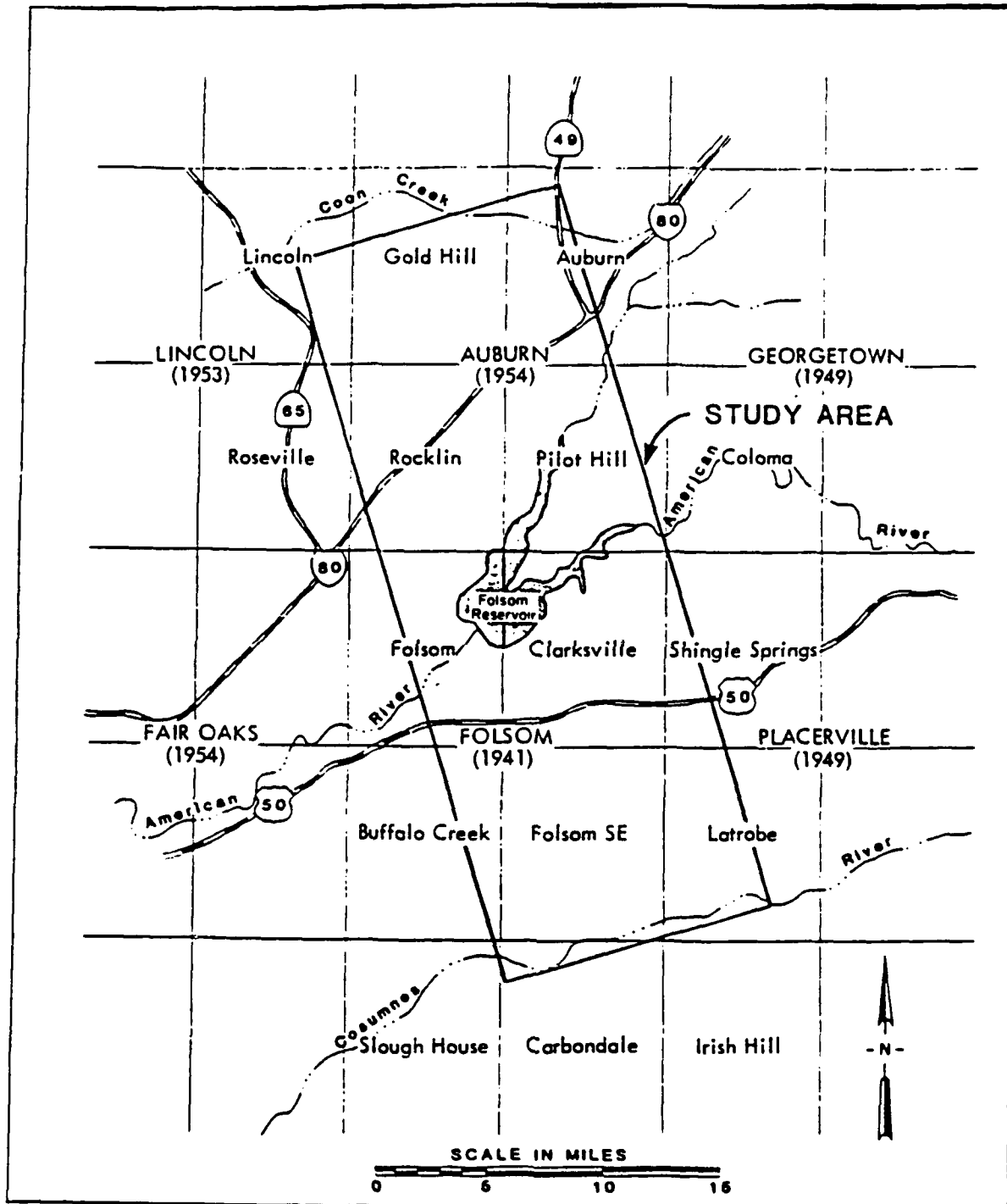


Figure 8. Identification of study area (from USGS 7.5- and 15-ft topographic maps, after Tierra Engineering Consultants, Inc. 1983)

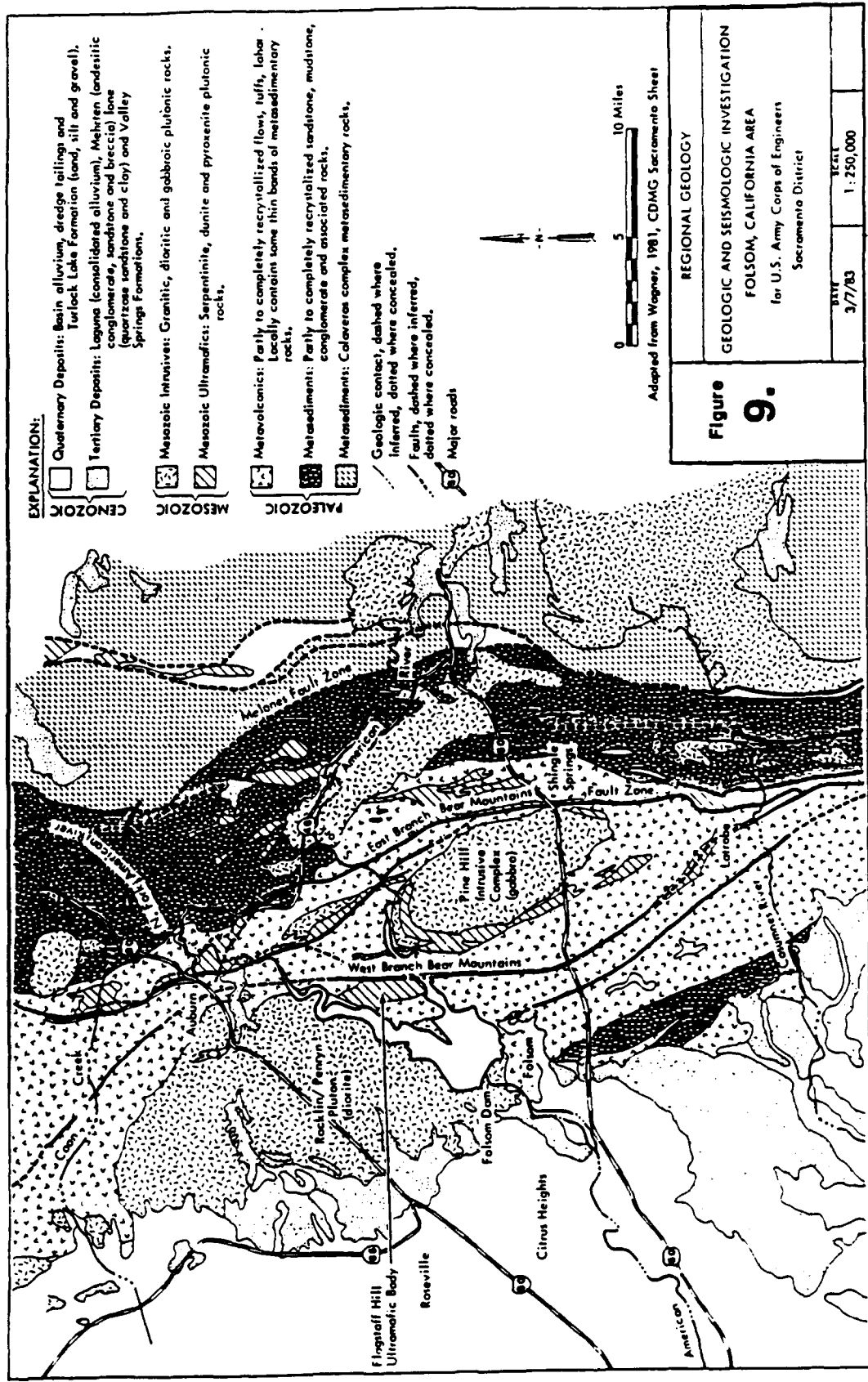


Figure 9. Regional geology in vicinity of Folsom Dam and Reservoir project (after Tierra Engineering Consultants, Inc. 1983)

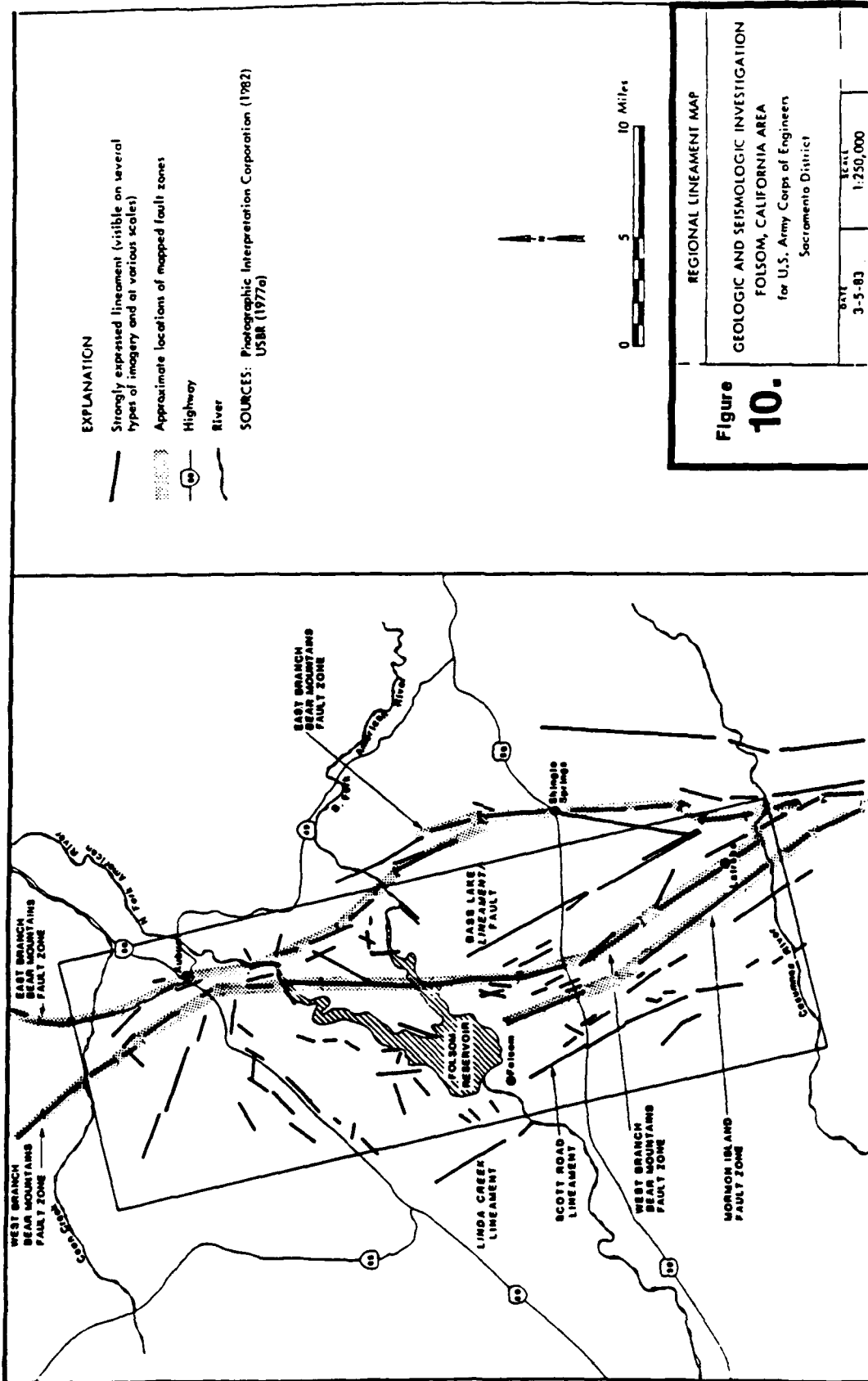
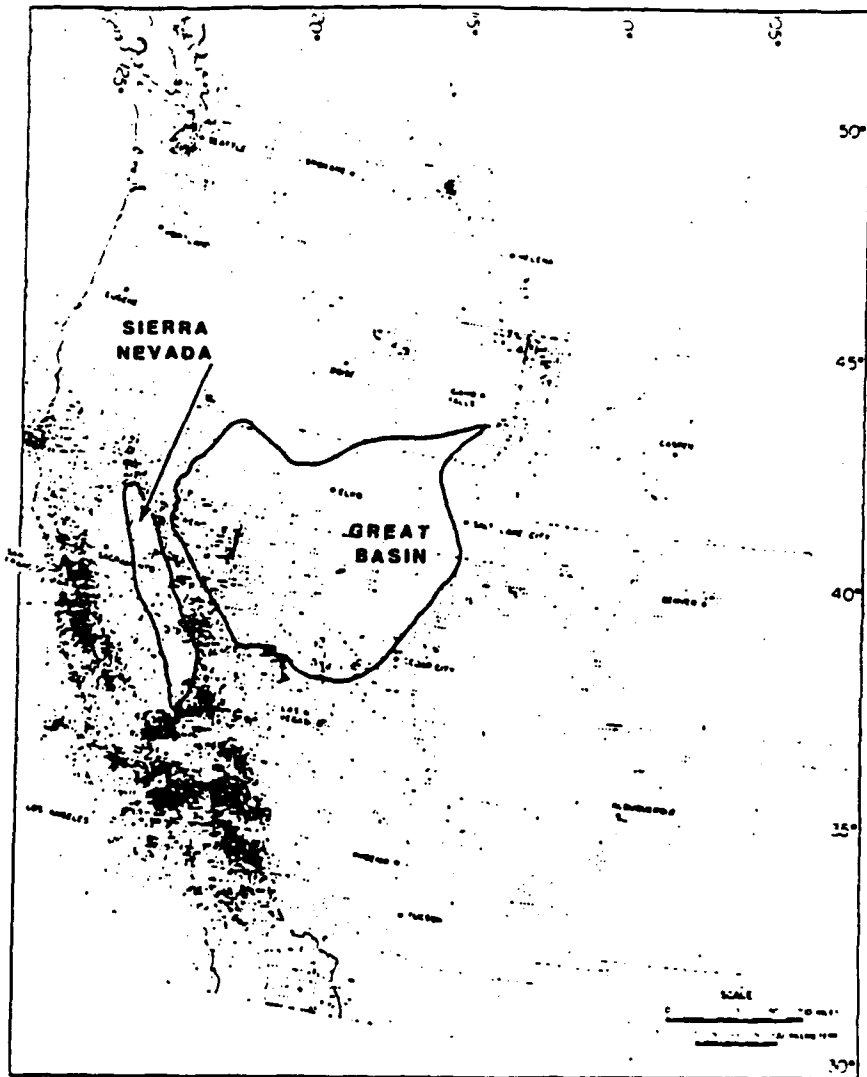


Figure 10. Regional lineament map (after Terra Engineering Consultants, Inc. 1983)



SOURCE: Adapted from Smith, 1978

Figure 11. Epicenter map of western United States (after Tierra Engineering Consultants, Inc. 1983)

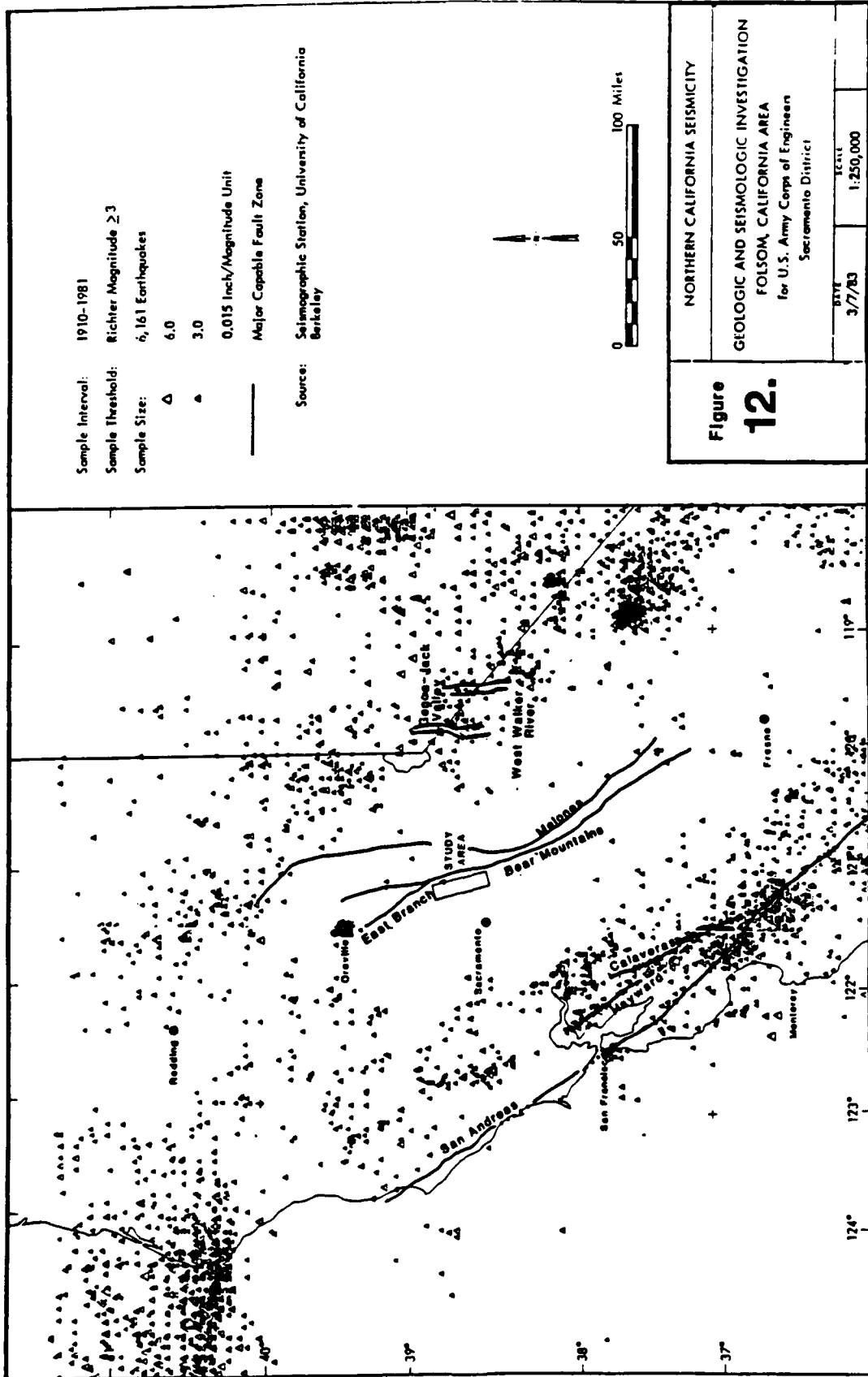
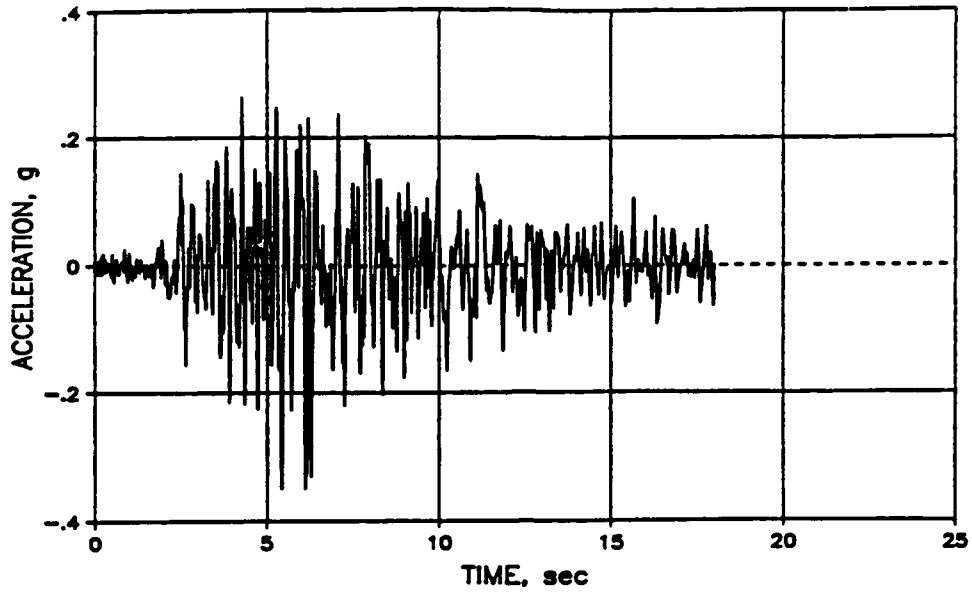


Figure 12. Seismicity map for Northern California (after Tierra Engineering Consultants, Inc. 1983)

FOLSOM DAM PROJECT
RECORD A



RECORD B

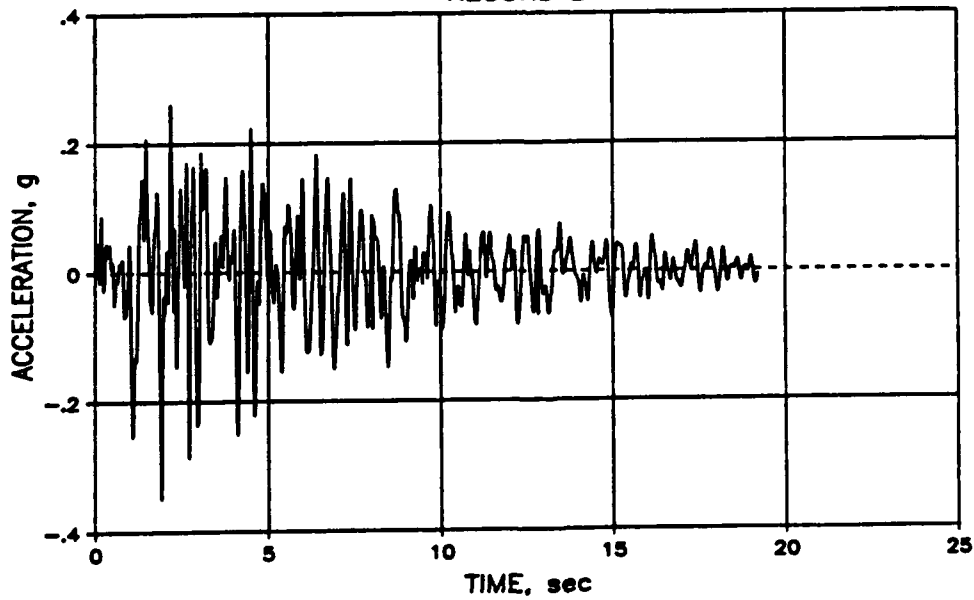


Figure 13. Acceleration histories used in the analysis

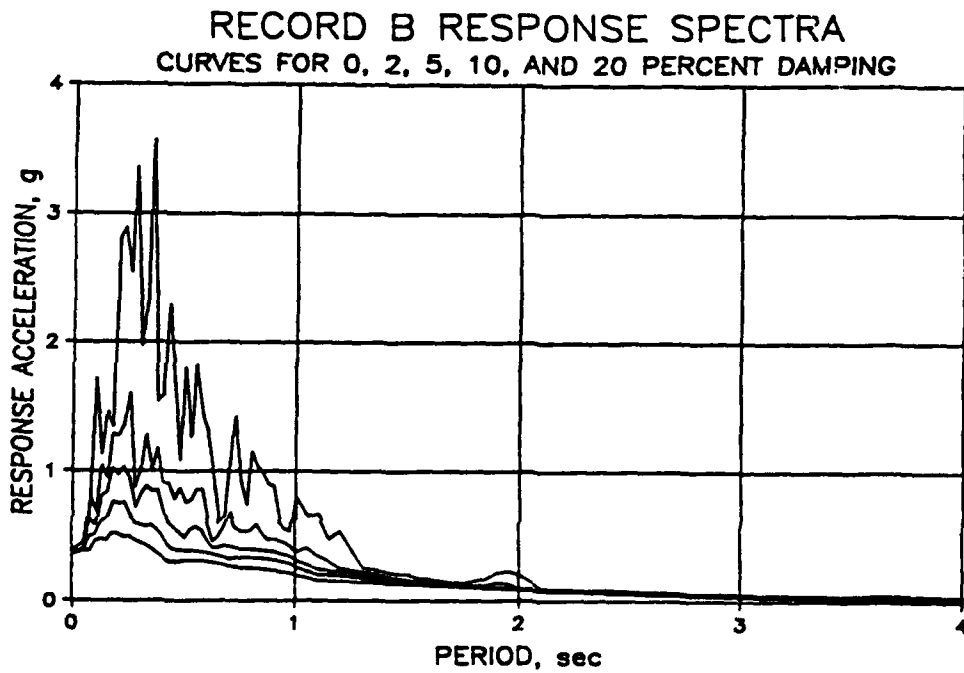
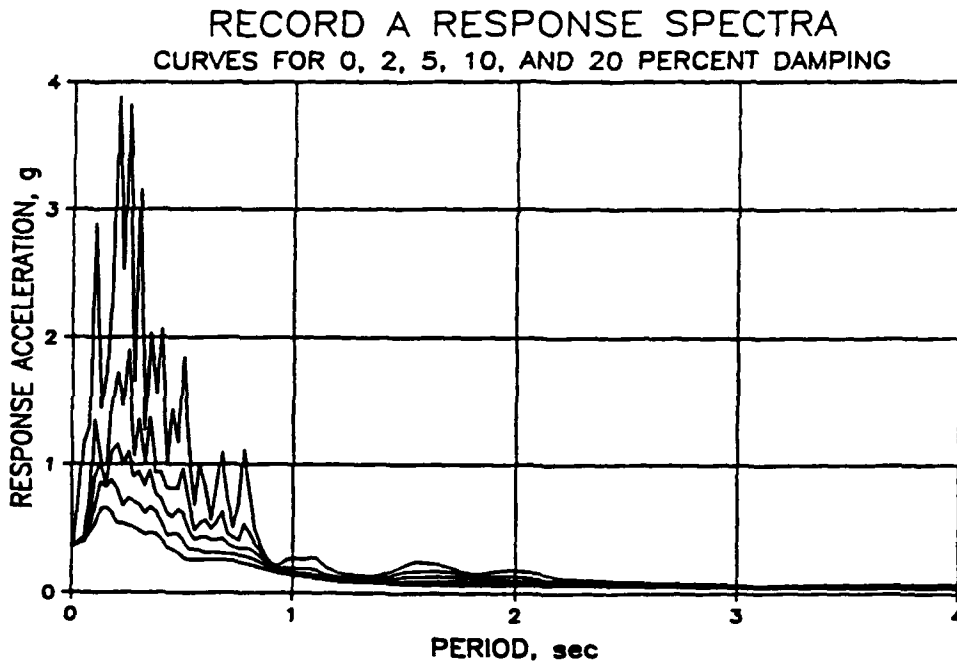


Figure 14. Response spectra of Records A and B



Figure 15. View of Mormon Island Auxiliary Dam foundation preparation, looking southwest from left abutment to right abutment (FOL-476, 4/10/51)



Figure 16. Foundation preparation for portion of Mormon Island Auxiliary Dam founded on rock, looking southwest from sta 421+00 to right abutment (FOL-490, 4/11/51)



Figure 17. Core trench excavation through undisturbed alluvium, looking southwest from sta 440+00 to right abutment (FOL-544, 6/25/51)



Figure 18. Core trench excavation in alluvium, looking northeast from sta 440+00 to left abutment (FOL-538, 6/26/51)



Figure 19. Completed core trench excavation, looking southwest from left abutment to right abutment (FOL-619, 9/26/51)



Figure 20. Placement of zone materials in core trench, looking southwest from sta 458+00 to right abutment (FOL-633, 10/30/51)



Figure 21. Placement of Zone 1 upstream shell, looking southwest from sta 421+50 to right abutment (FOL-528)

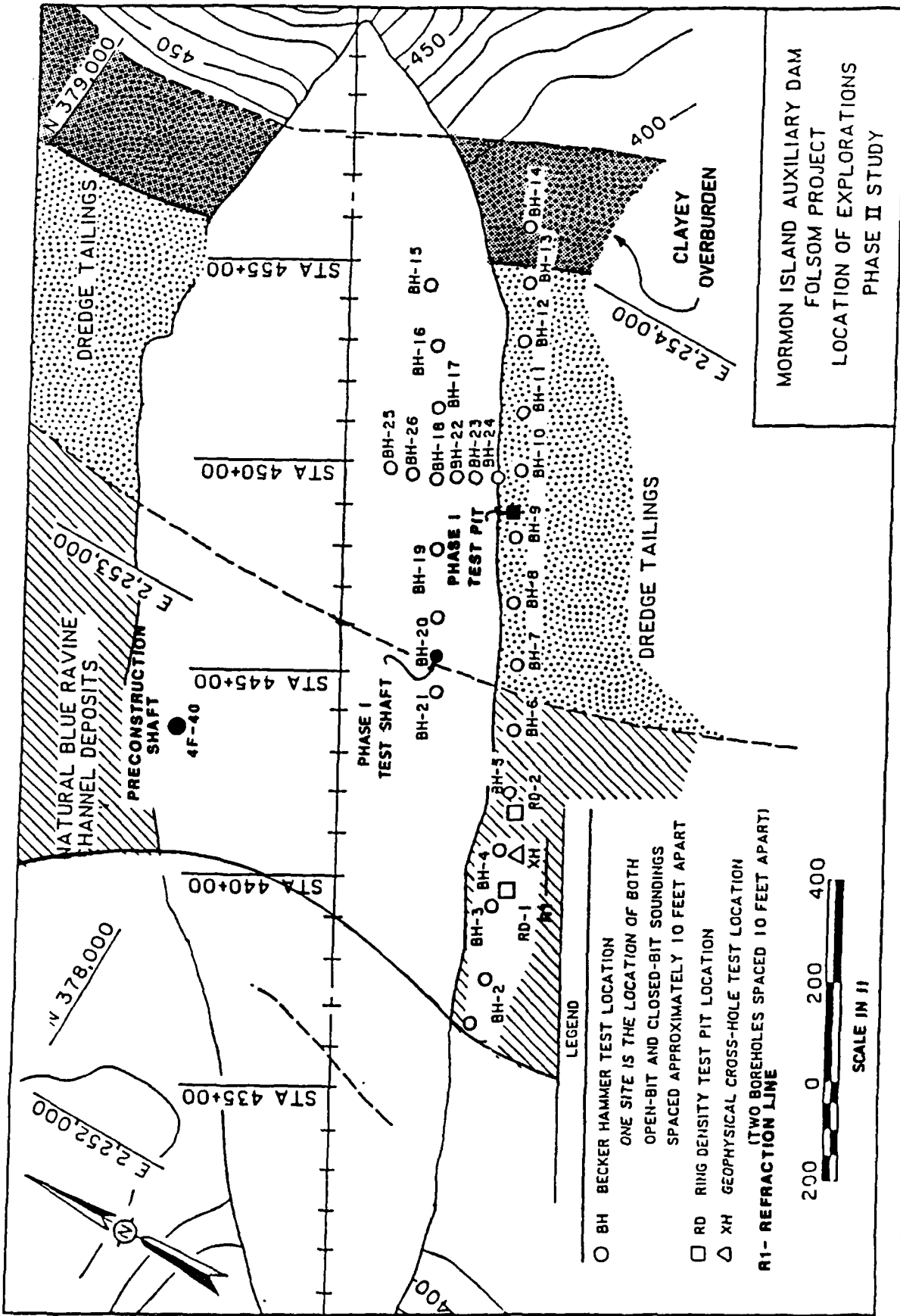
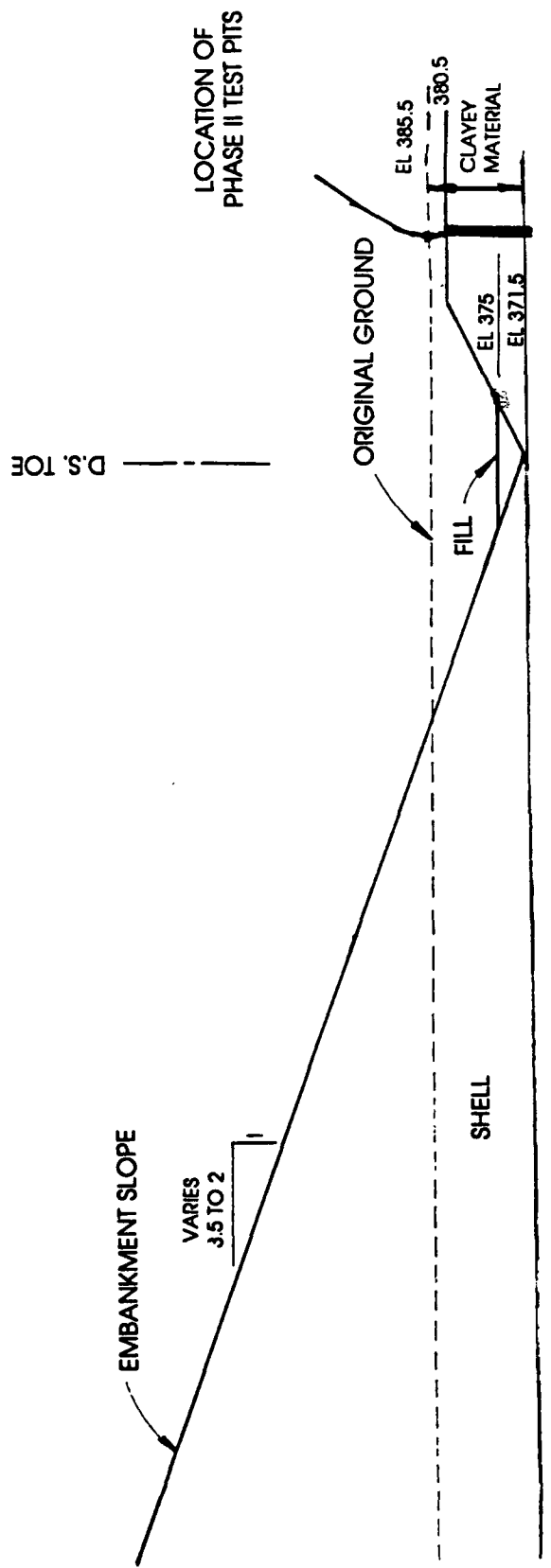
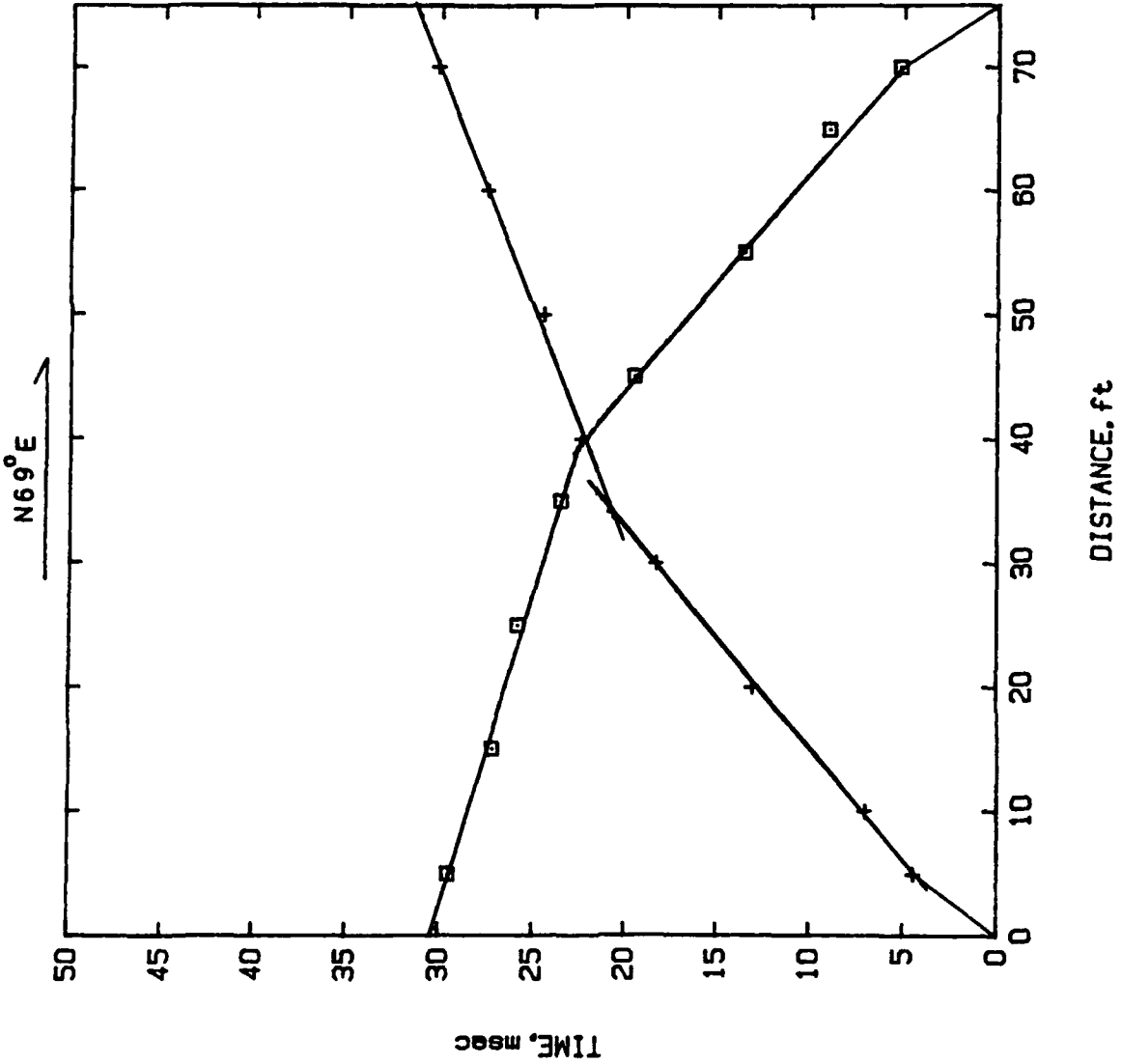


Figure 22. Location of Phase II field investigation explorations at Mormon Island Auxiliary Dam



UNDISTURBED ALLUVIAL FOUNDATION

Figure 23. Typical section of downstream toe between sta 439 and sta 446 showing undredged foundation conditions



FOR1

*** INPUT DATA ***

FORWARD REVERSE

LAYER #	VEL. FT/S	TI. MSEC	VEL. FT/S	TI. MSEC
1	1145	0.0	981	0.0
2	1777	1.6	1752	2.3
3	3817	11.8	5045	15.8

*** COMPUTED SEISMIC PROFILE ***

LAYER #	TRUE VEL. FT/S	DEPTH FOR. FT.	REV. FT.
1	1070	1.0	1.5
2	1760	10.5	14.0
3	4330		

Figure 24. Time-distance plot for refraction line R-1

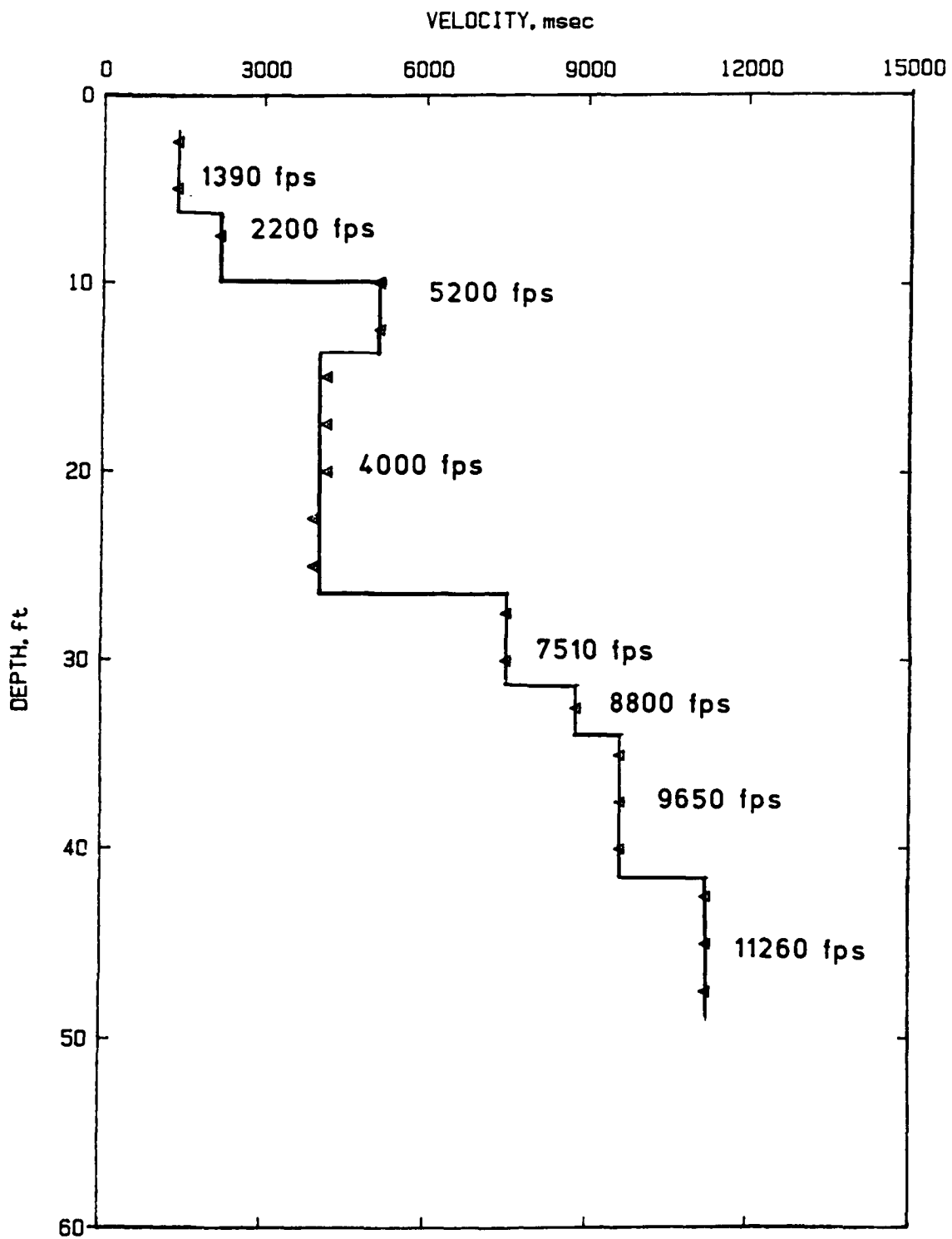


Figure 25. Crosshole P-wave velocity test results

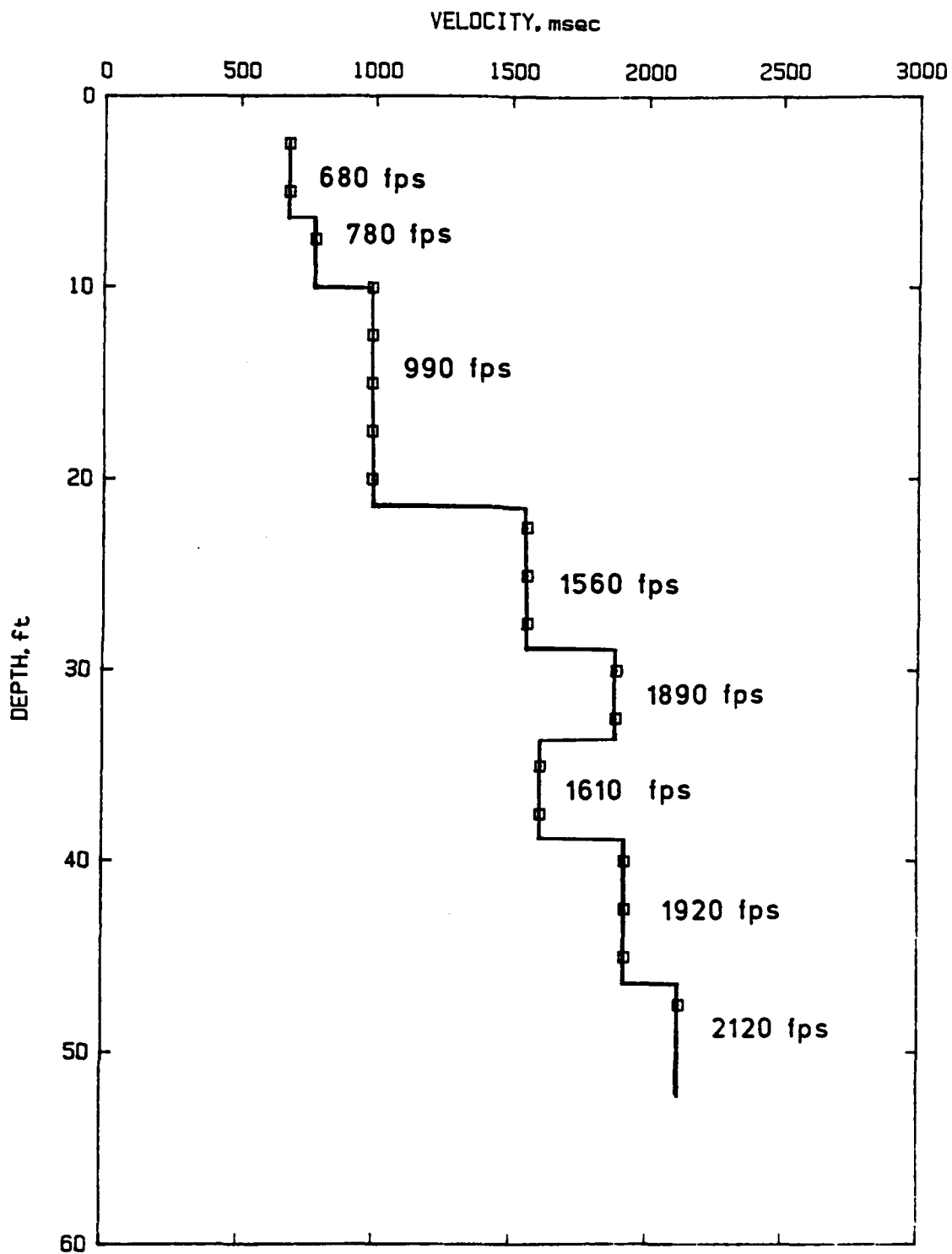


Figure 26. Crosshole S-wave velocity test results

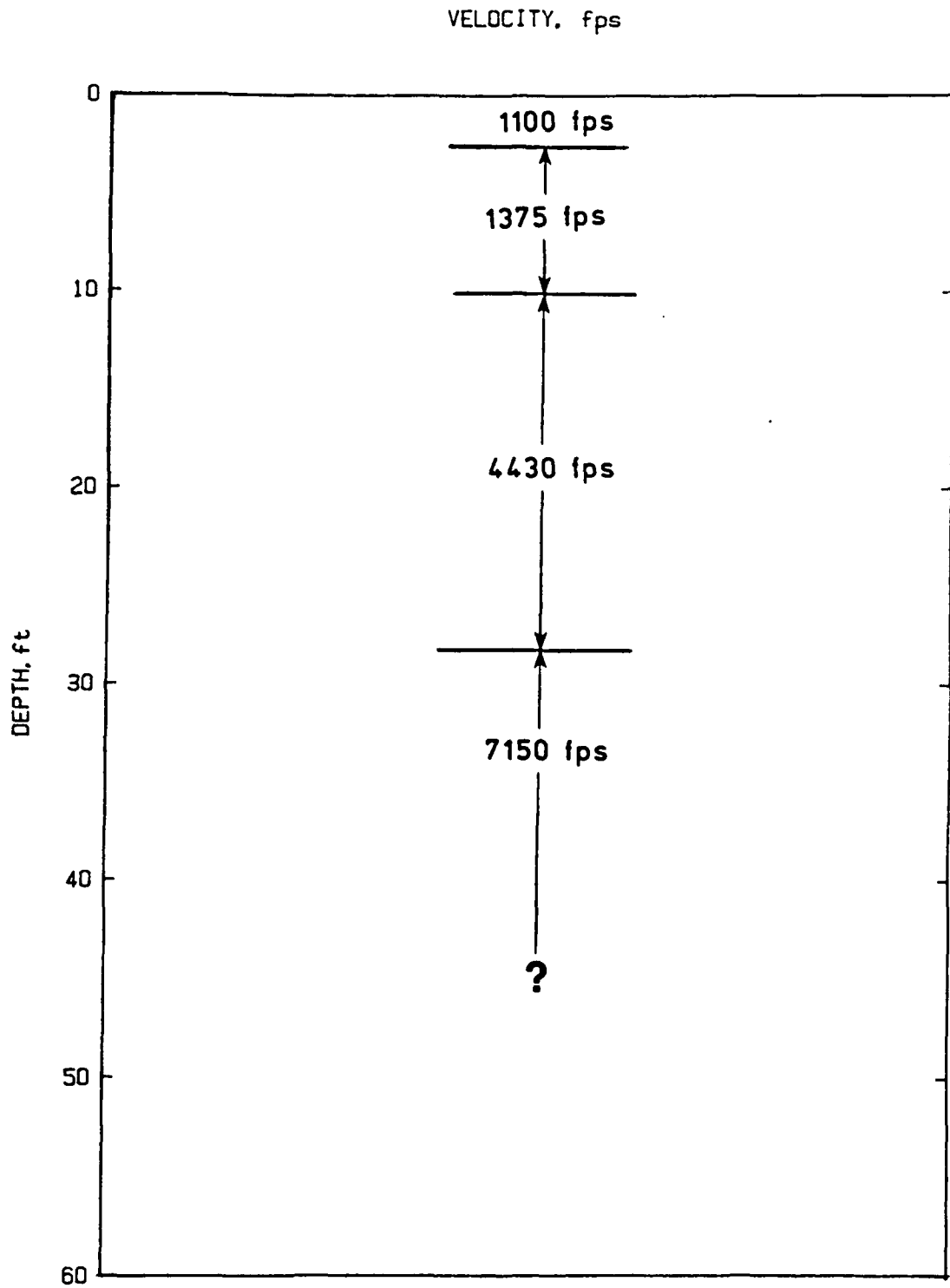


Figure 27. Average P-wave velocities from two downhole tests

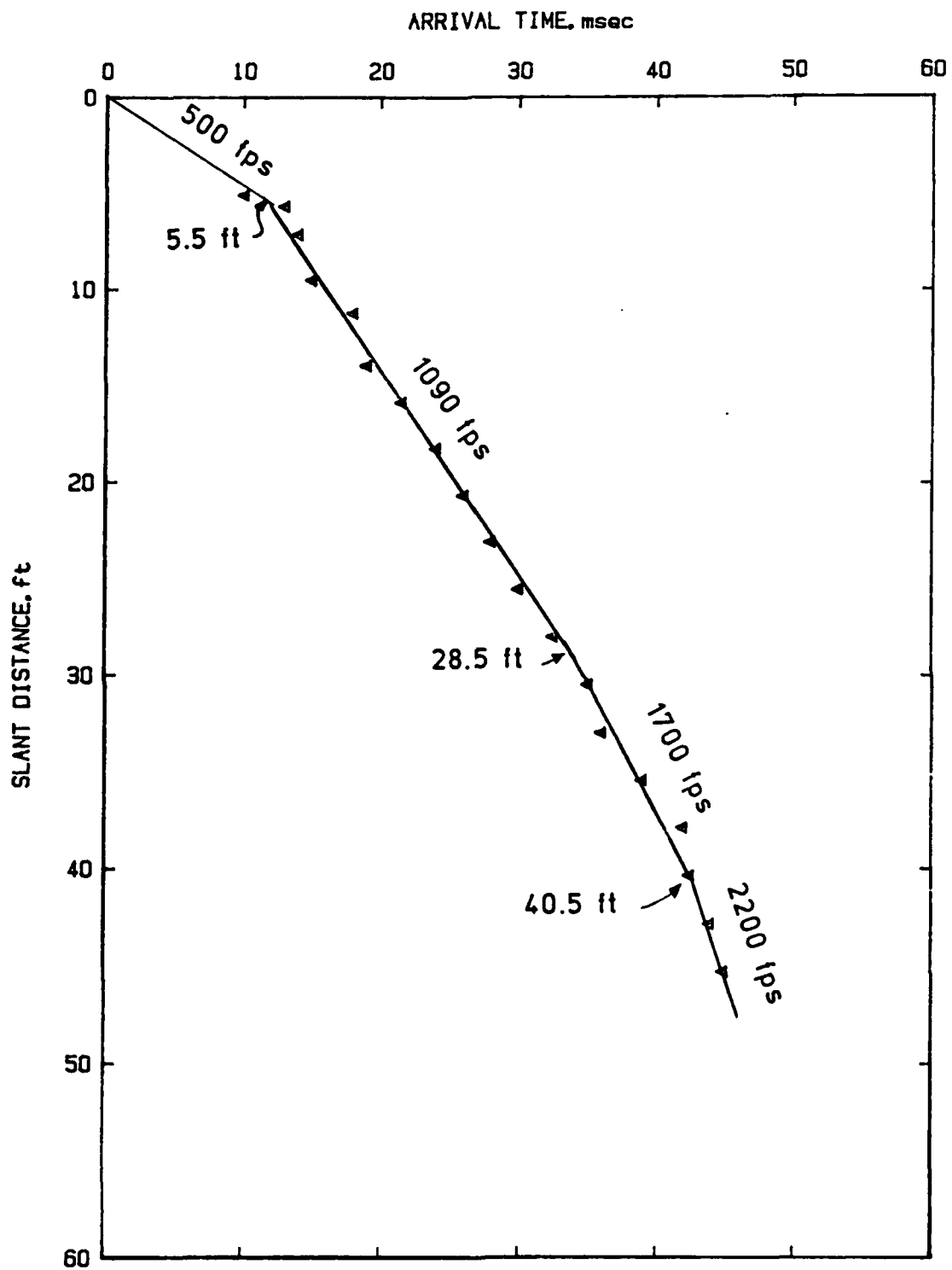


Figure 28. Downhole S-wave velocity test results

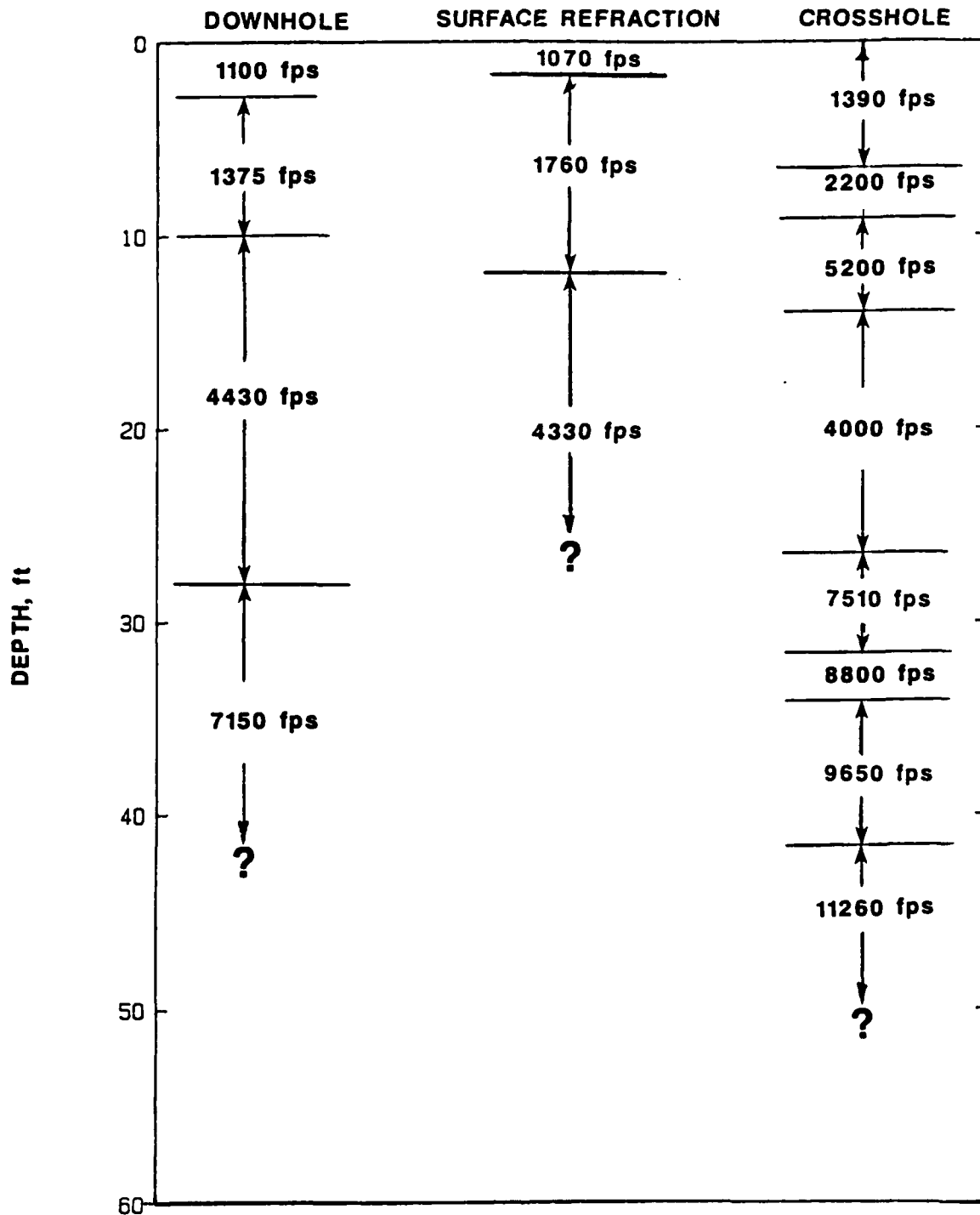


Figure 29. Composite of P-wave velocity tests

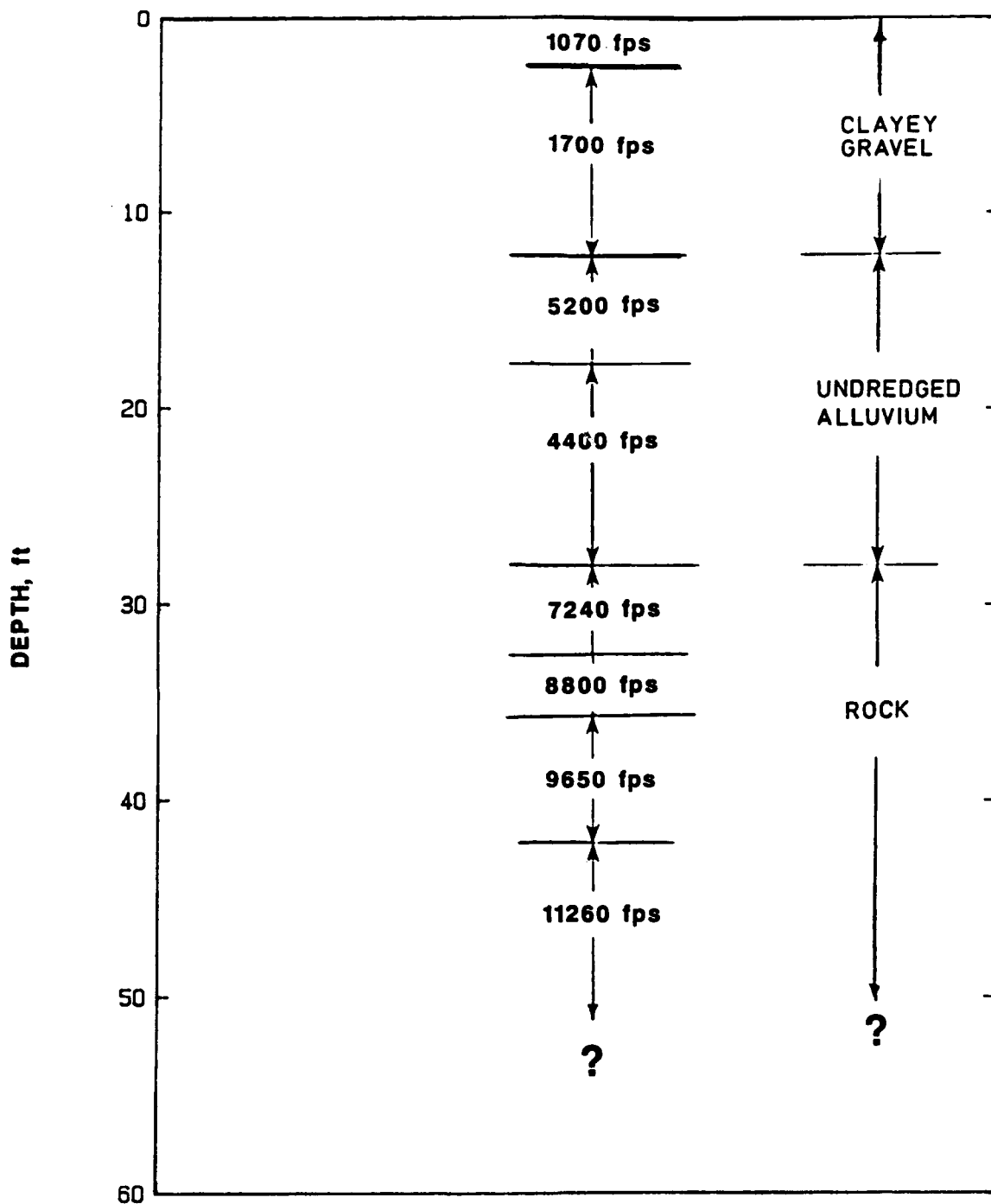


Figure 30. P-wave velocity interpretation for downstream undredged area

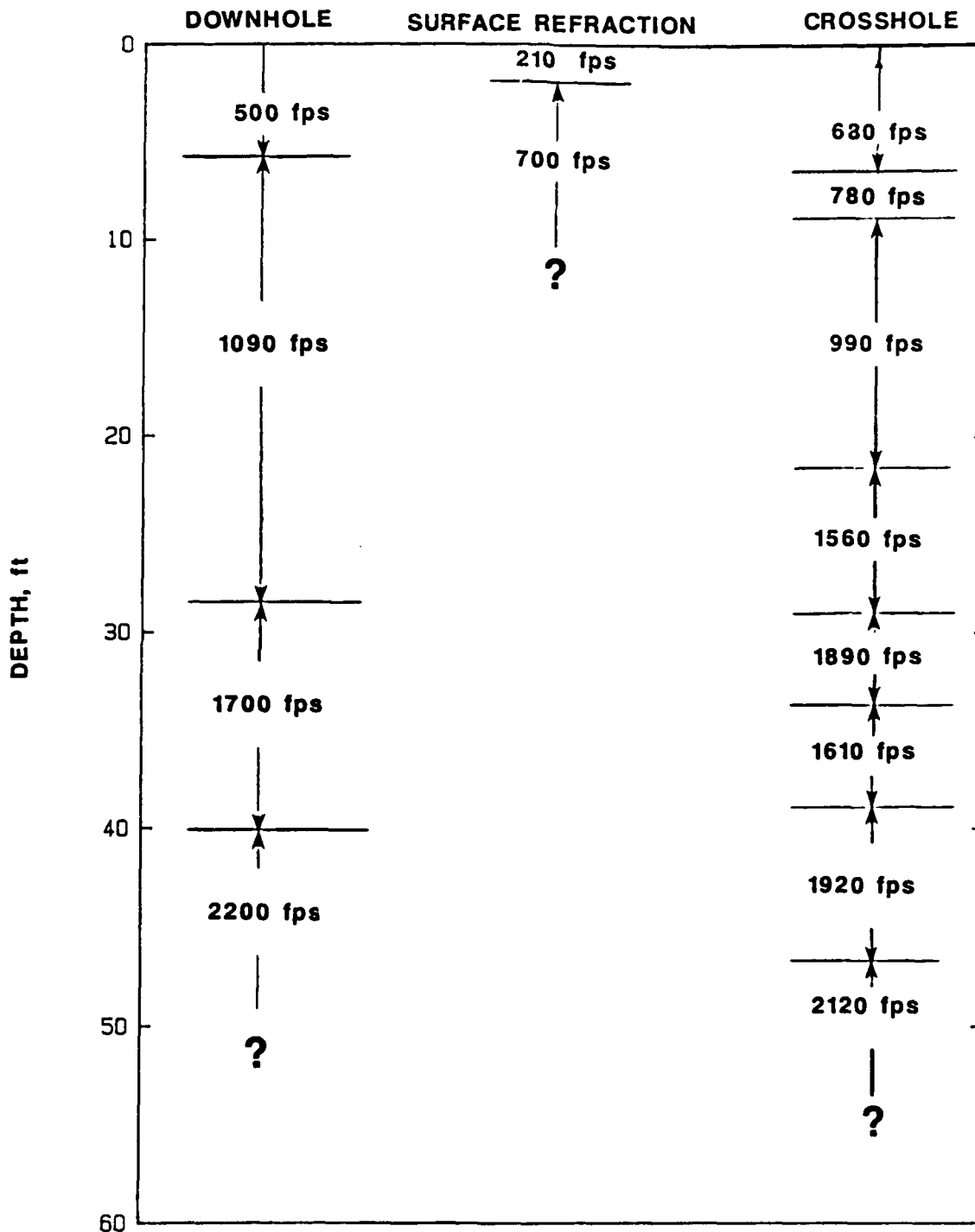


Figure 31. Composite of S-wave velocity tests

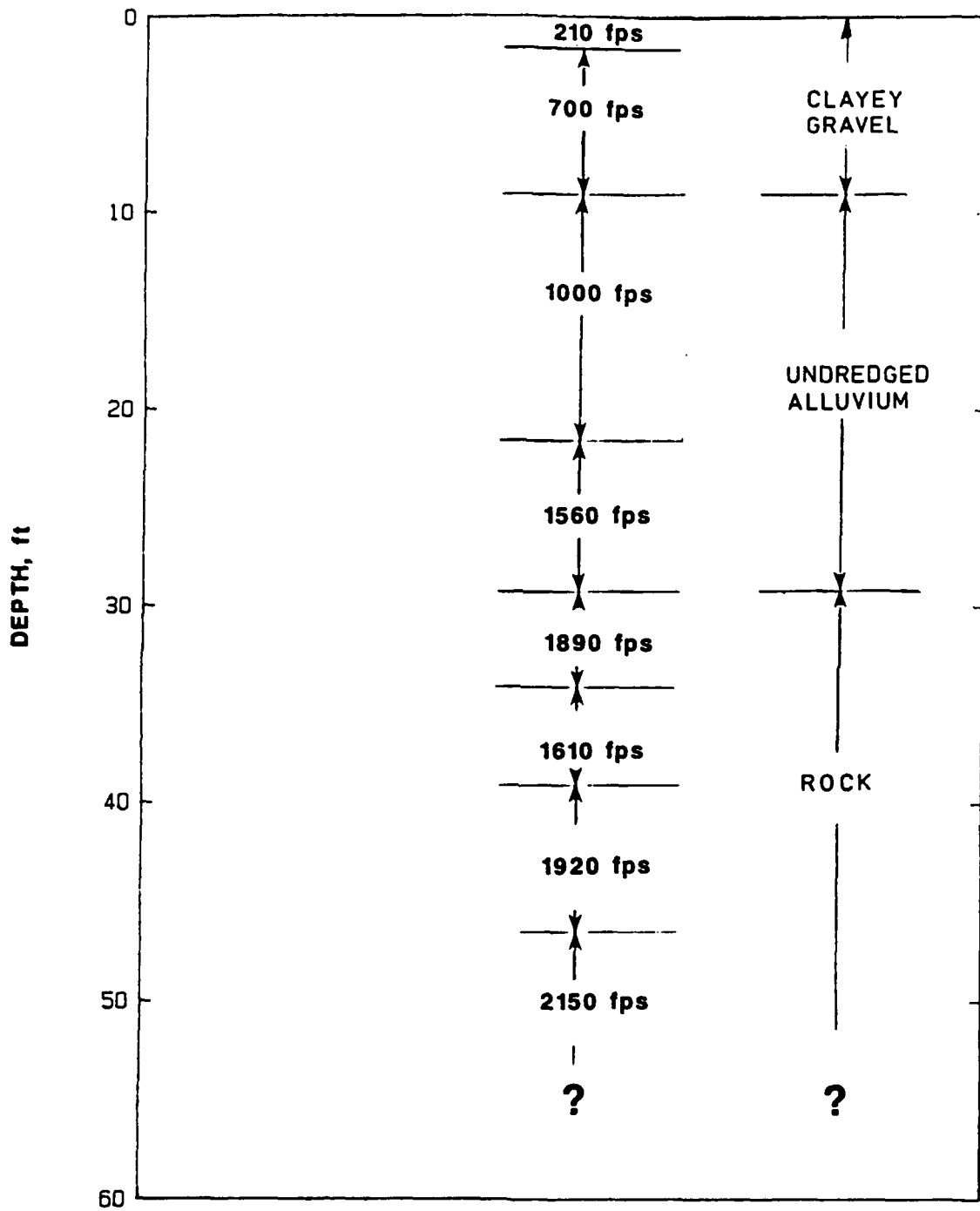


Figure 32. S-wave velocity interpretation for downstream undredged area

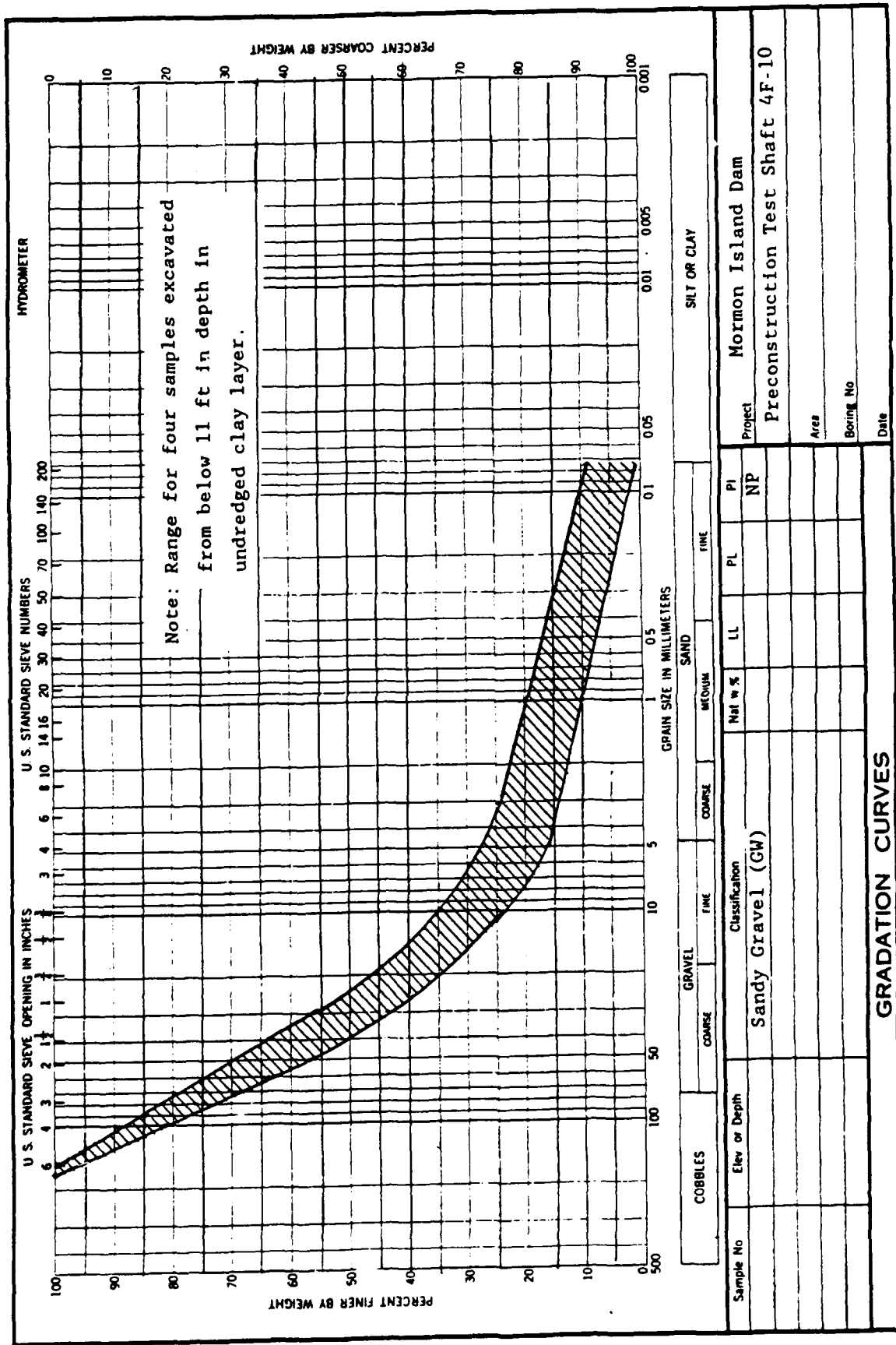


Figure 33. Gradations of undredged alluvium underlying clay layer obtained from preconstruction test shaft 4F-10

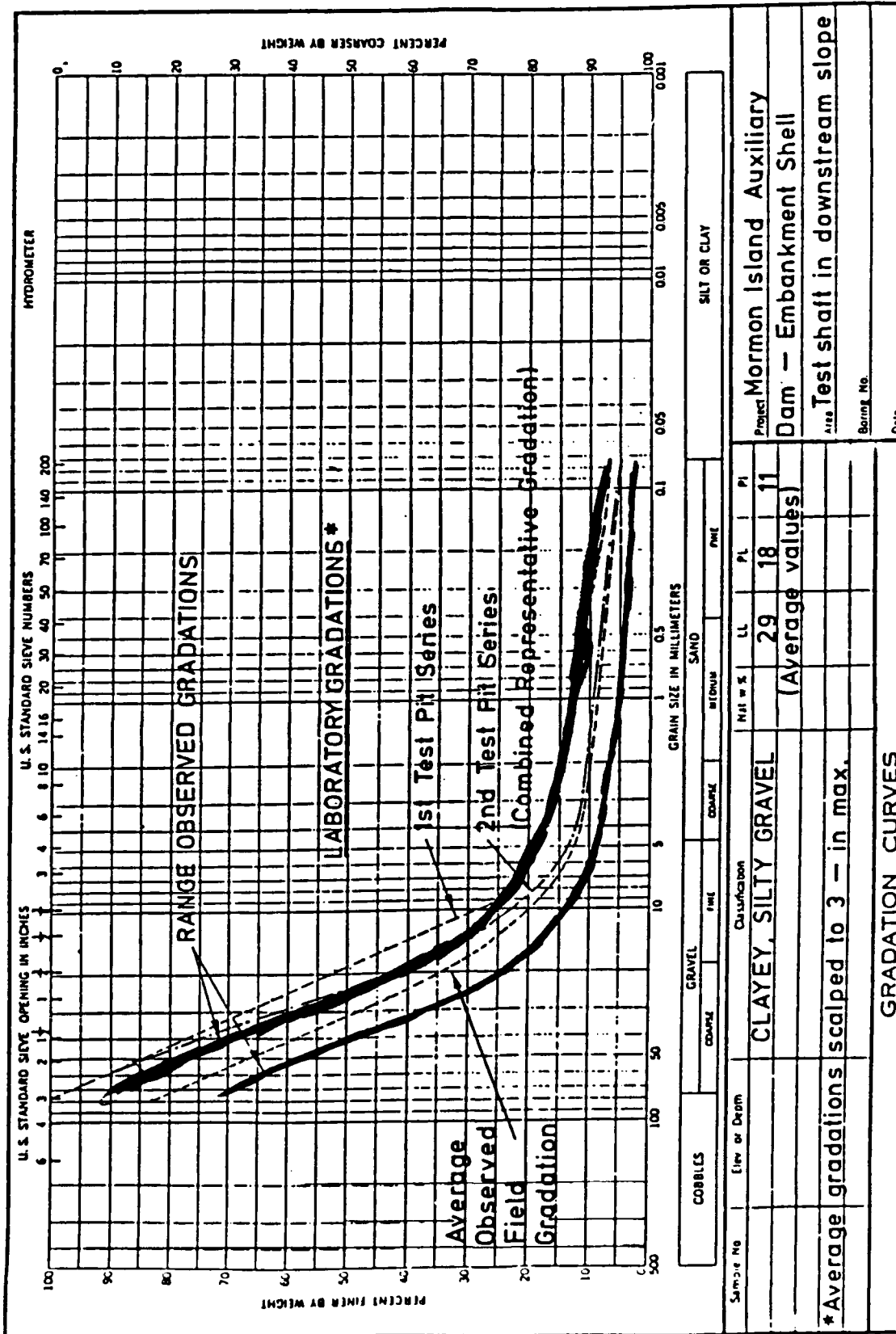


Figure 34. Gratation of embankment gravels observed in Phase I test shaft excavations



Figure 35. Photo of AP-1000 drill rig used for Becker Hammer soundings at Mormon Island Auxiliary Dam

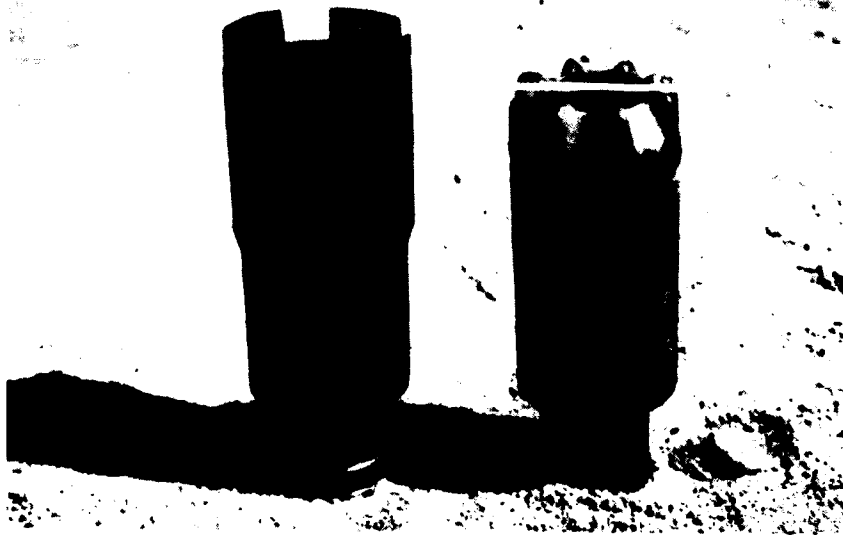


Figure 36. Photo of open and closed drill bits used in Becker Penetration Tests

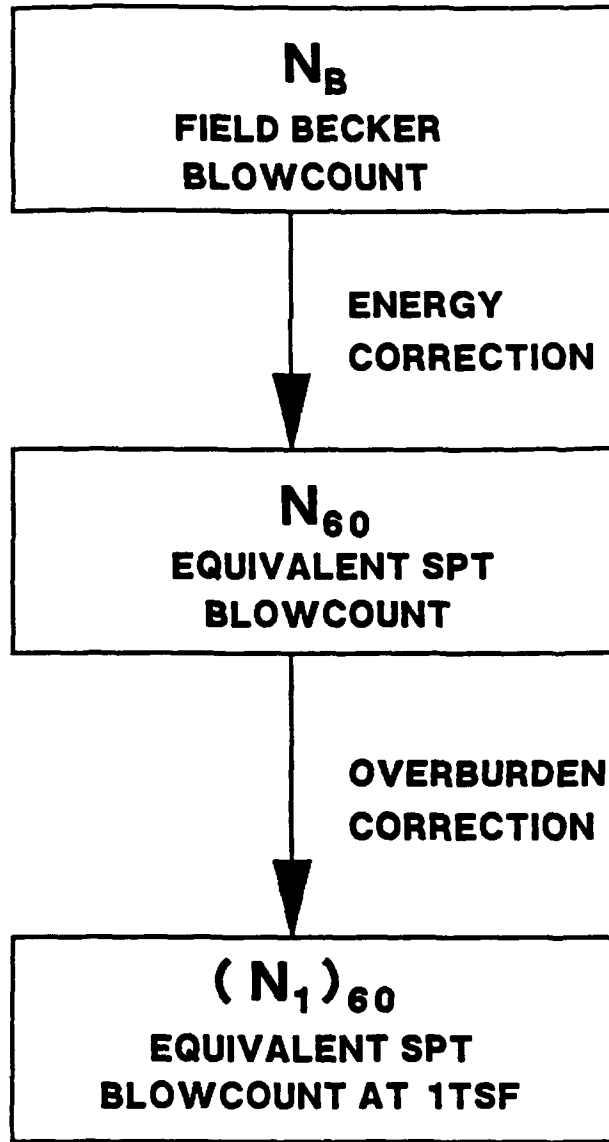


Figure 37. Schematic of energy and overburden corrections to convert Becker blowcounts into equivalent Standard Penetration Test $(N_1)_{60}$

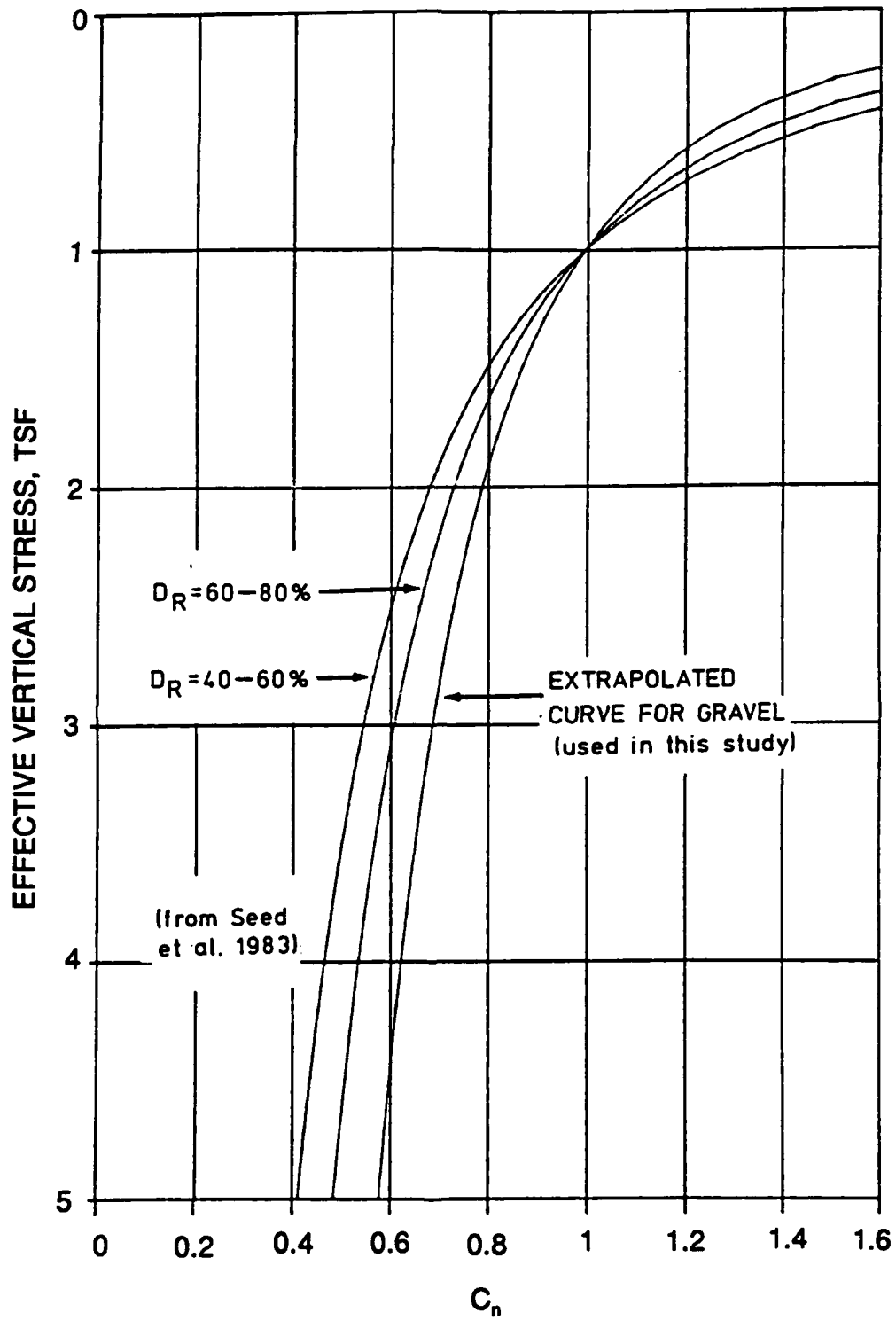
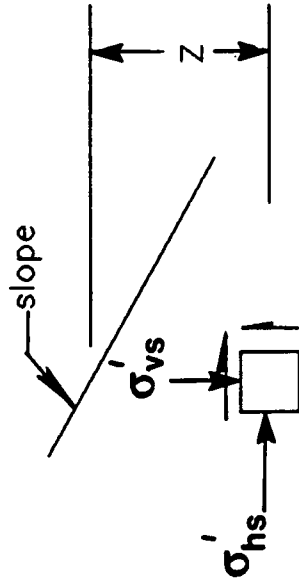
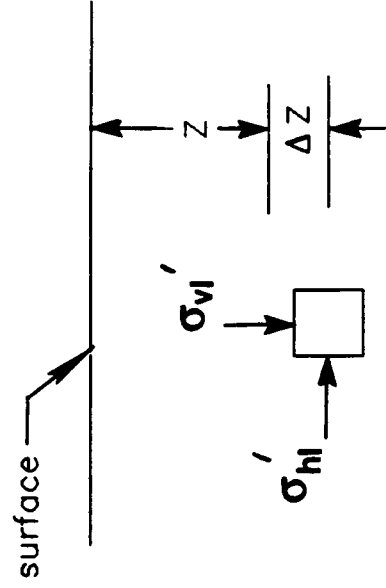


Figure 38. C_n curves used in the study of Mormon Island Dam

SLOPING GROUND



LEVEL GROUND



PLANE STRAIN

Ko CONDITIONS

$$1) \sigma'_{ms} = (\sigma'_{vs} + \sigma'_{hs})(1 + \mu) \frac{1}{3} \quad 2) \sigma'_{ml} = \frac{(\sigma'_{vl} + 2 K_o \sigma'_{vl})}{3}$$

Equating 1) and 2) with $K_o = 0.4$ and $\mu = 0.3$ yields:

$$\sigma'_{vl} = 1.67 \times \sigma'_{ms}$$

Figure 39. Formula used to compute equivalent level ground vertical effective stress

MORMON ISLAND AUXILIARY DAM
 PHASE II EXPLORATION

BH - 18

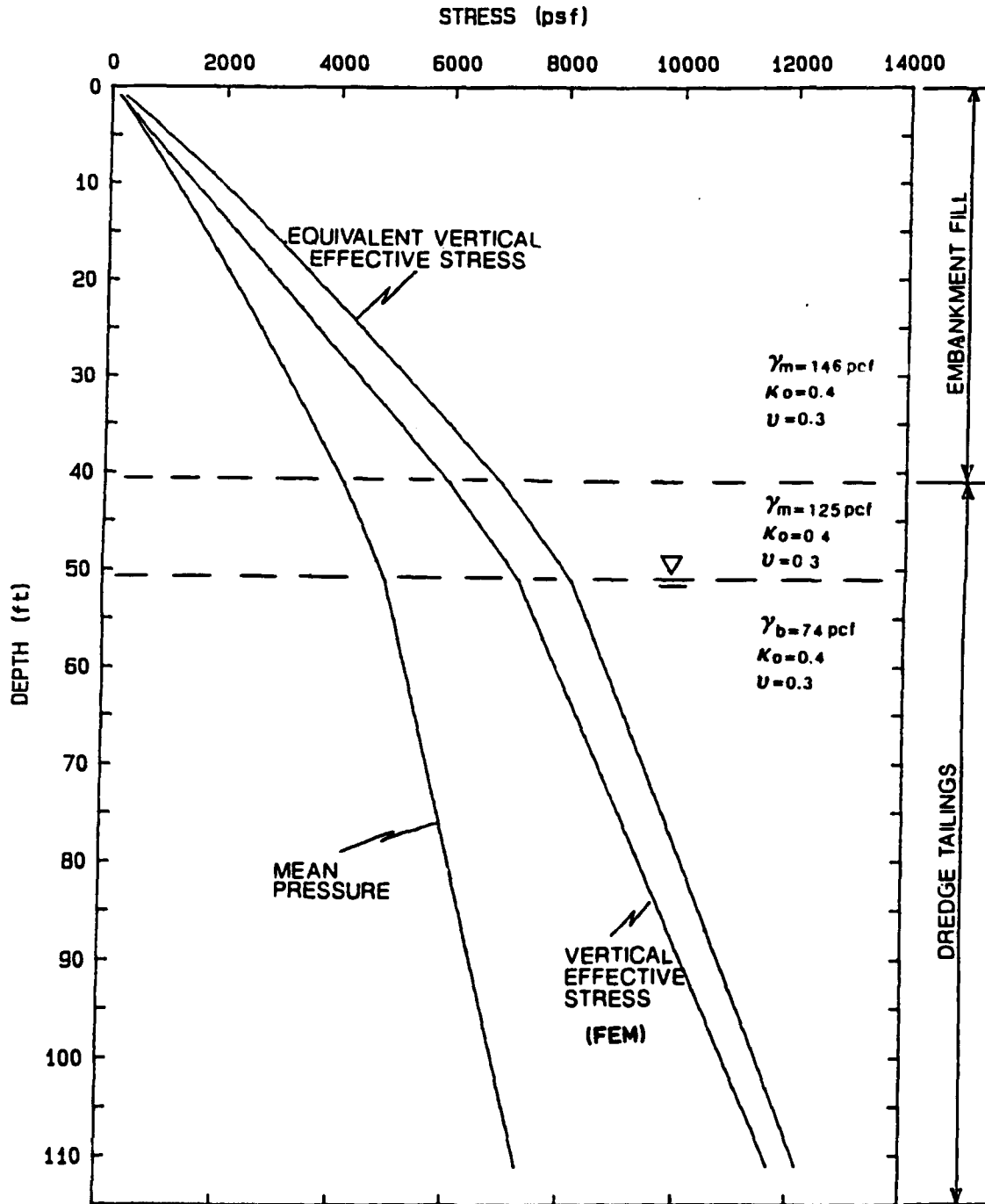
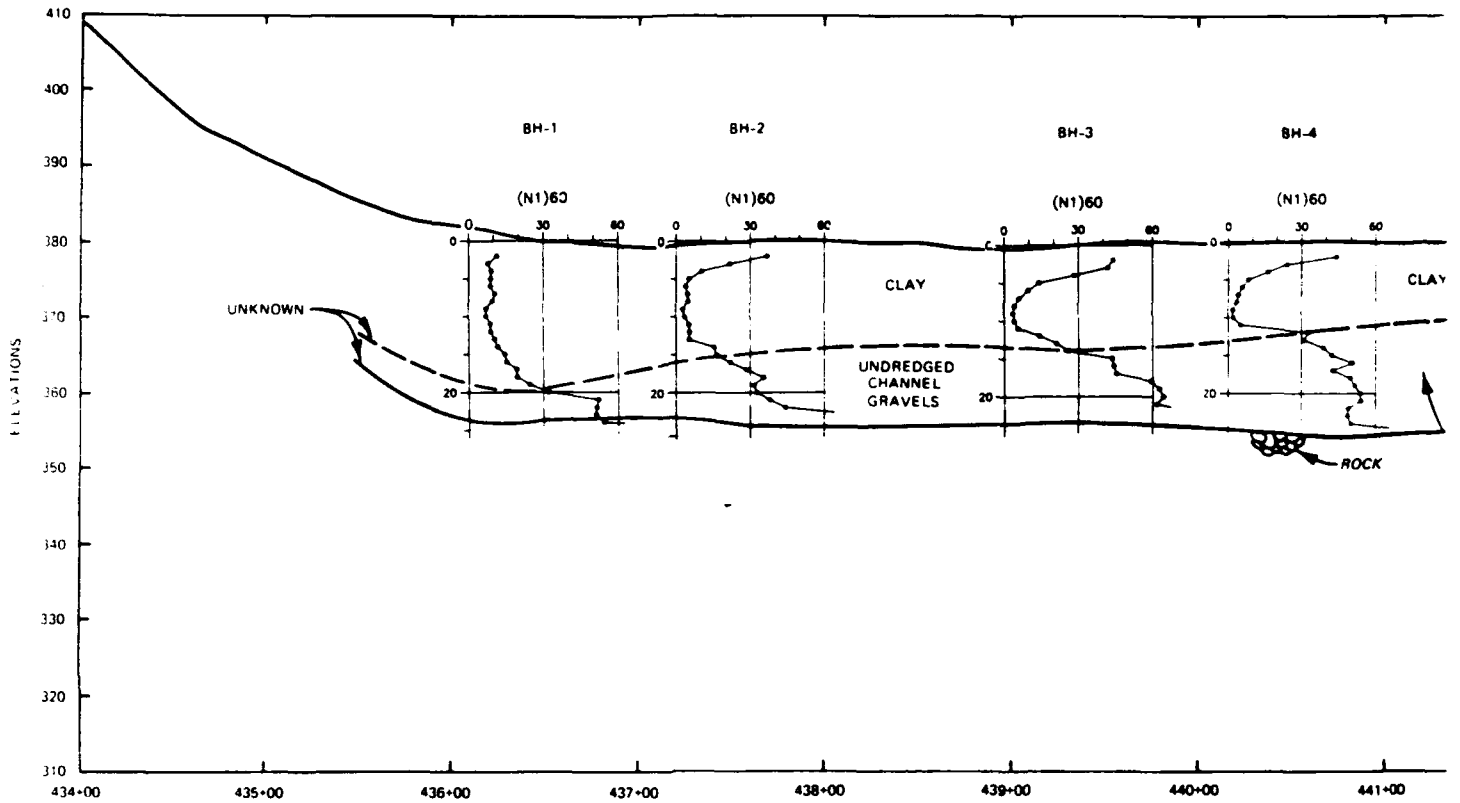


Figure 40. Confining stress versus depth for soil column through downstream slope and dredged tailings



T

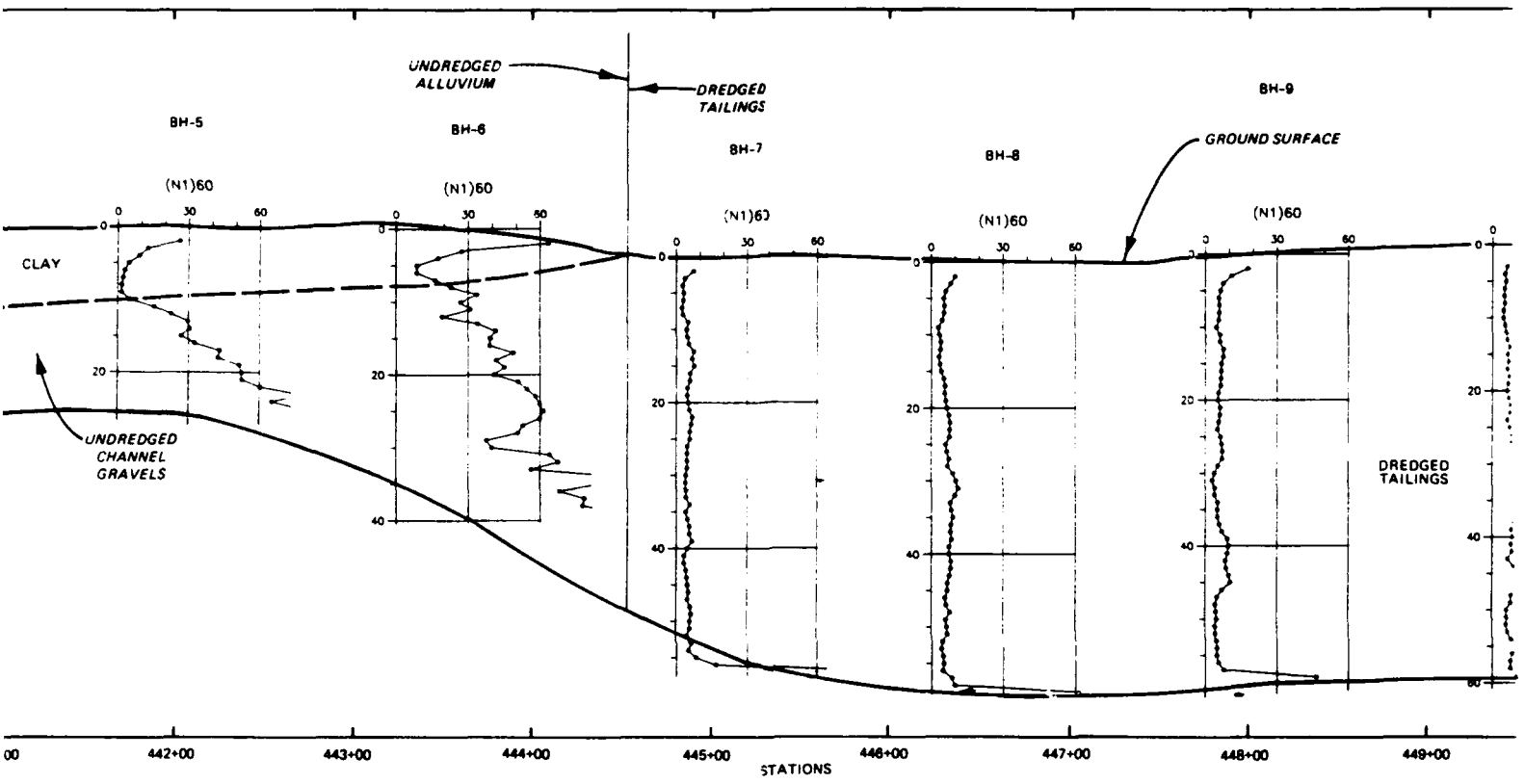
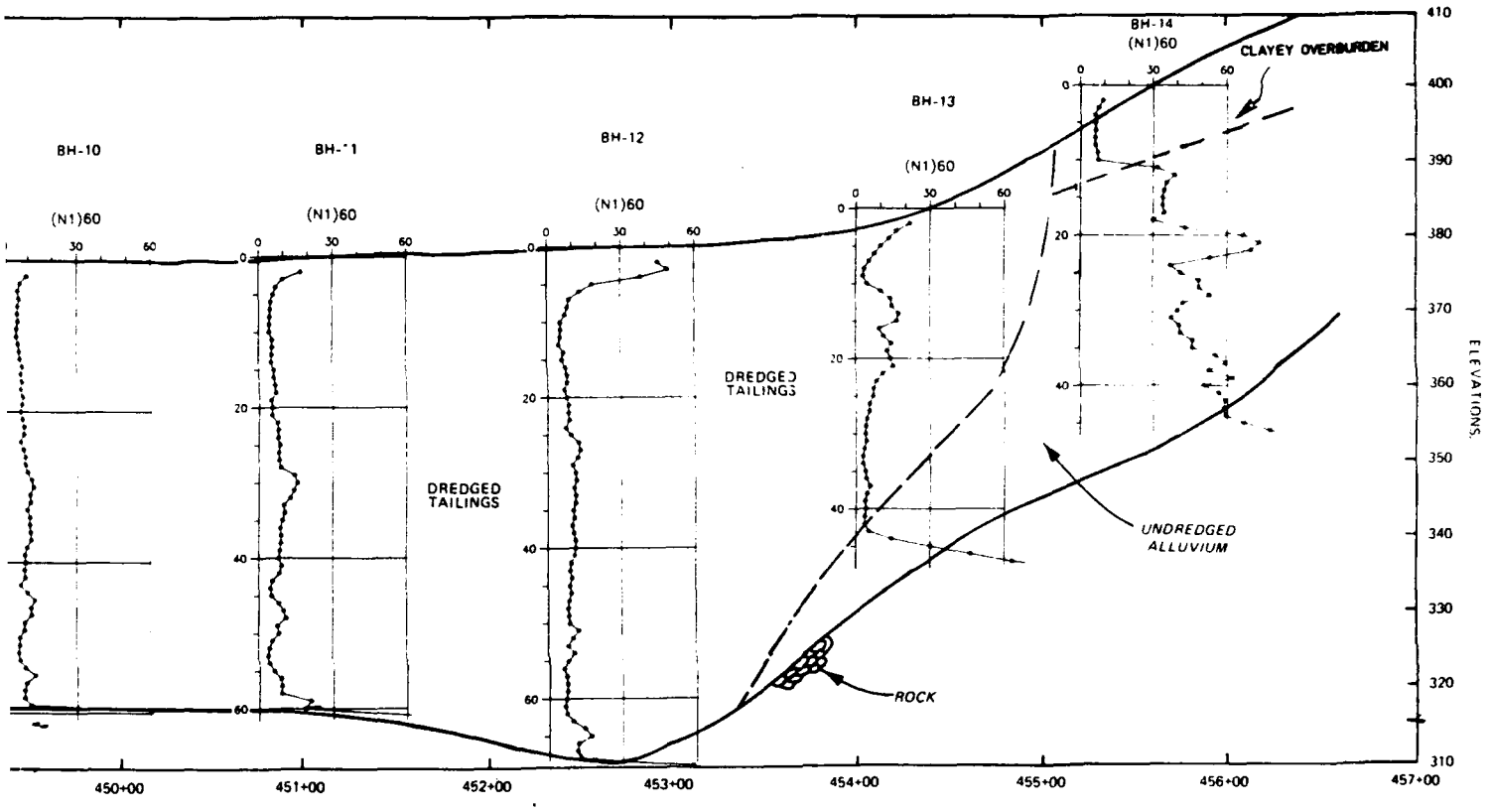
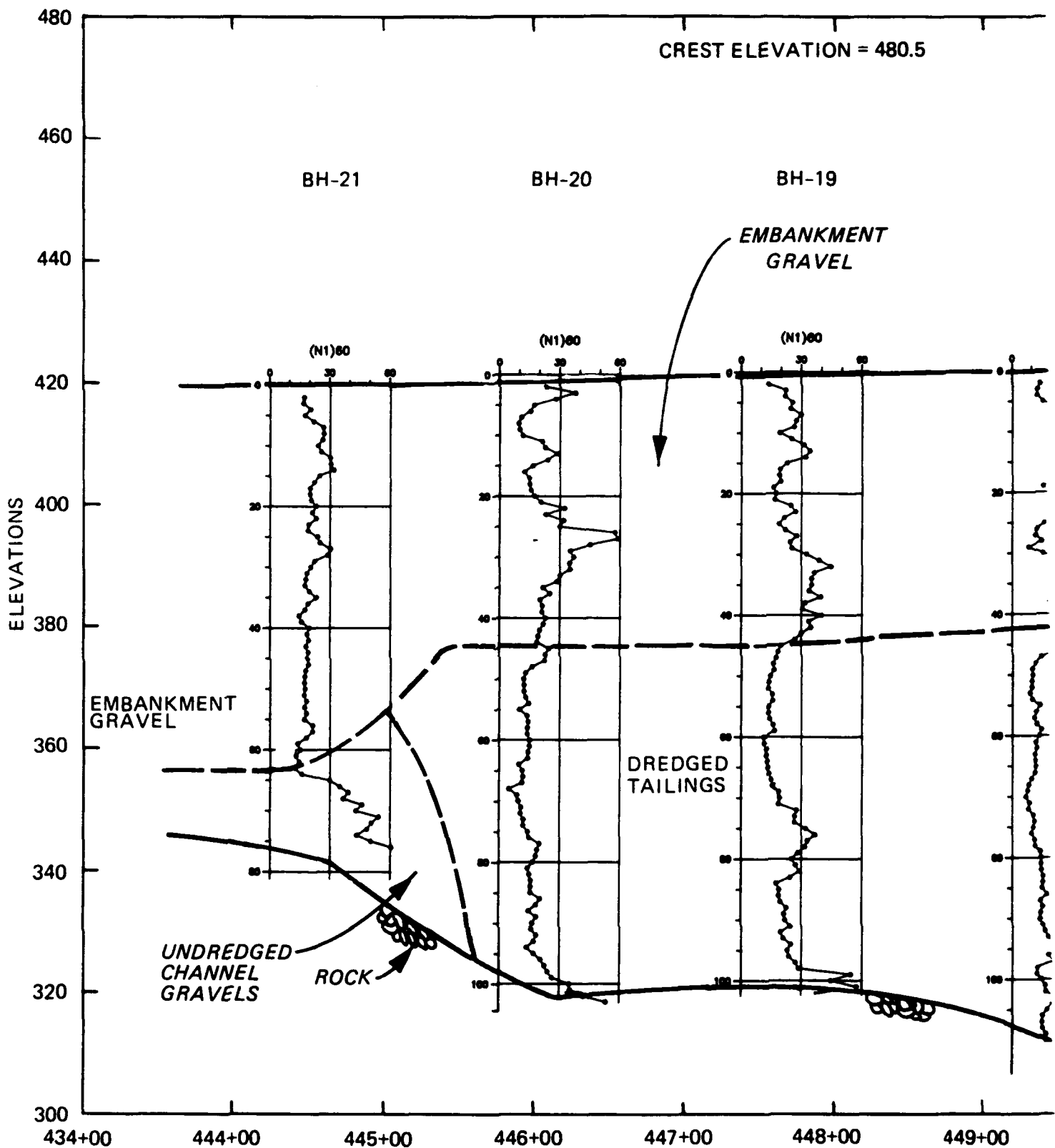


Figure 41. Cross section along downstream toe showing $(N_1)_{60}$ results

Y





Fig

H

CREST ELEVATION = 480.5

BH-19

BH-18

BH-17

BH-16

EMBANKMENT
GRAVEL

EM
G_i

(N₁)₆₀

(N₁)₆₀

(N₁)₆₀

(N₁)₆₀

DREDGED
TAILINGS

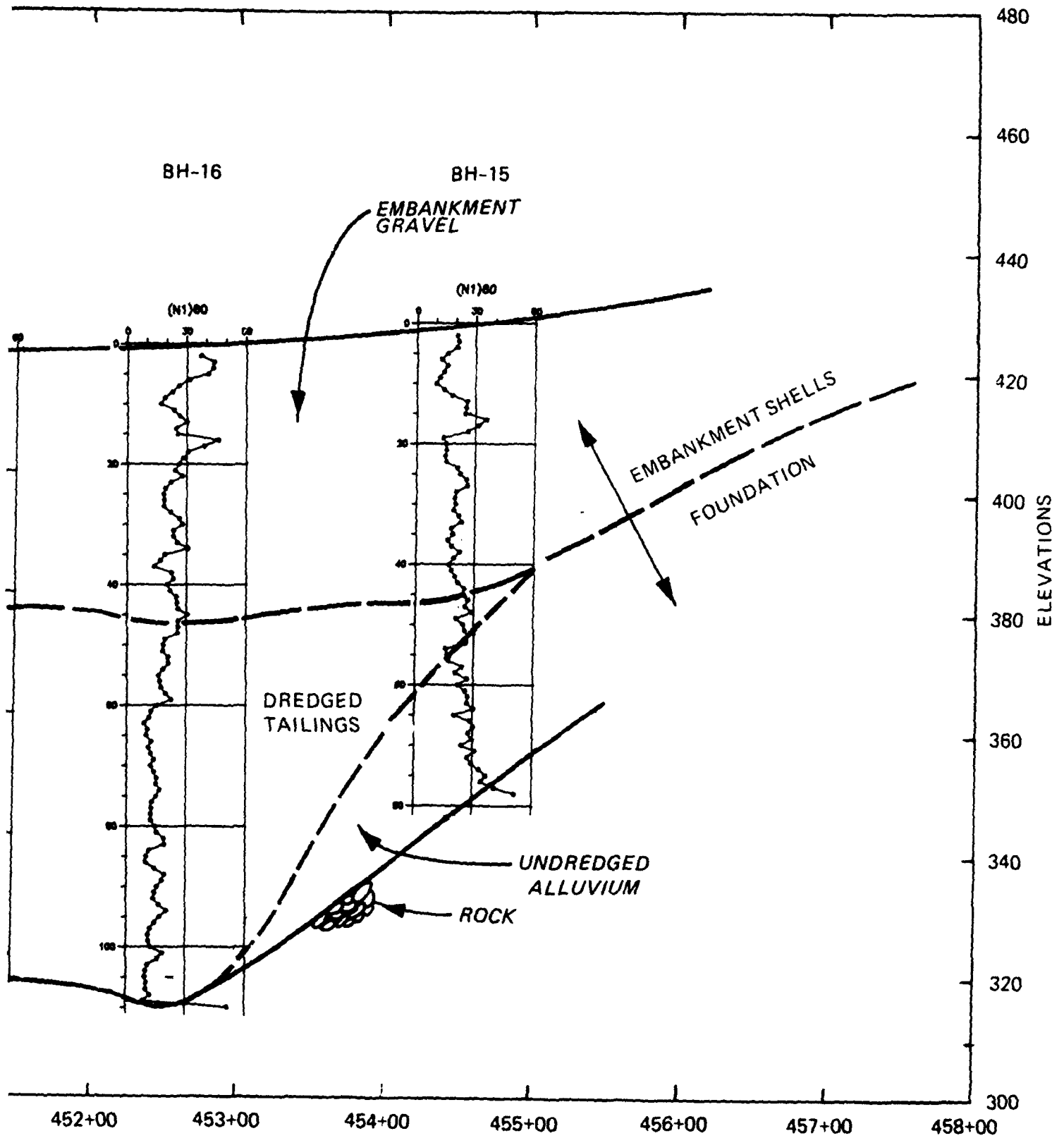
DREDGED
TAILINGS

447+00 448+00 449+00 450+00 451+00 452+00 453+00 454+00

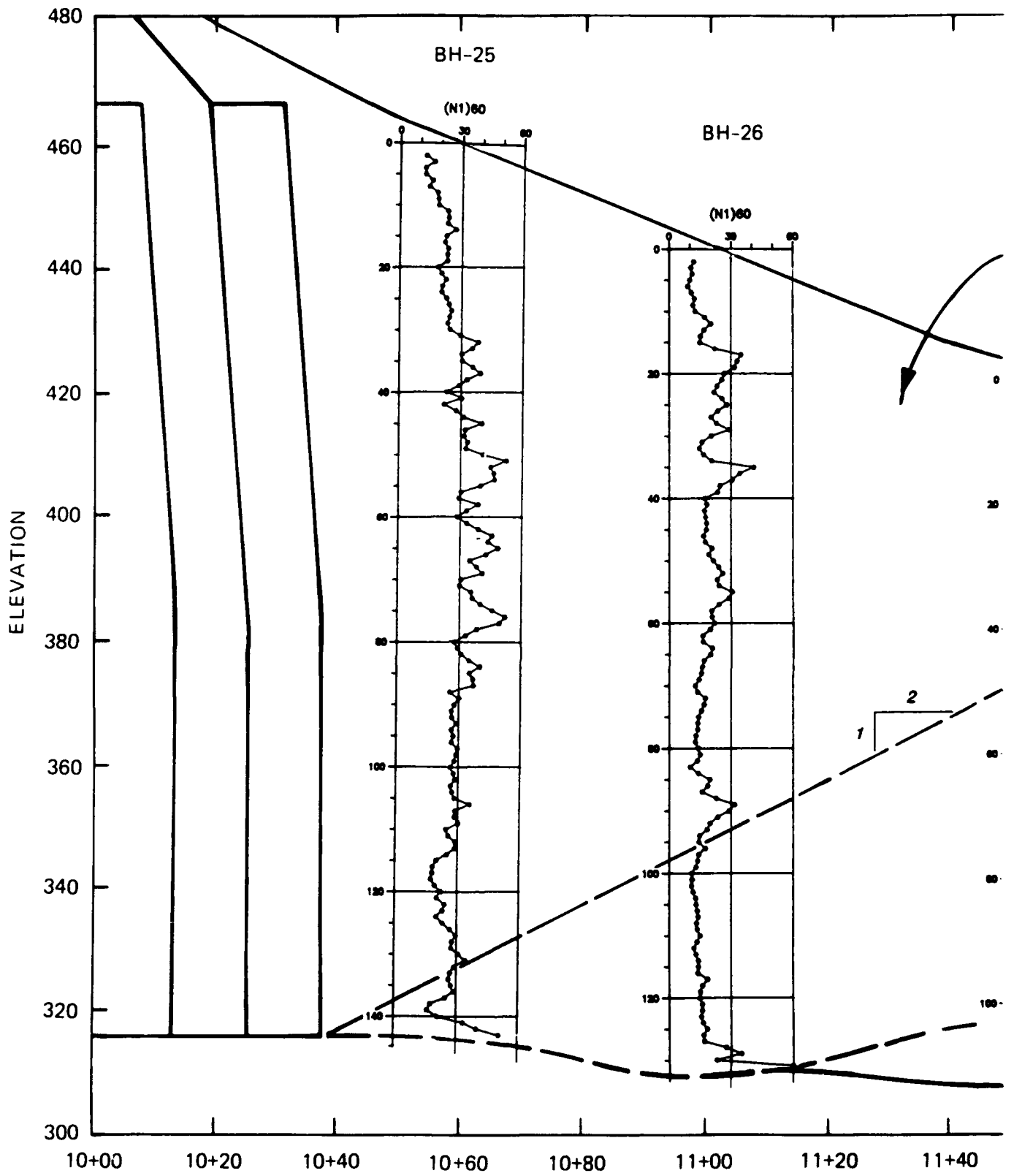
STATIONS

Figure 42. Cross section at midslope of the embankment showing (N₁)₆₀ results

b



Mid-slope of the embankment showing results



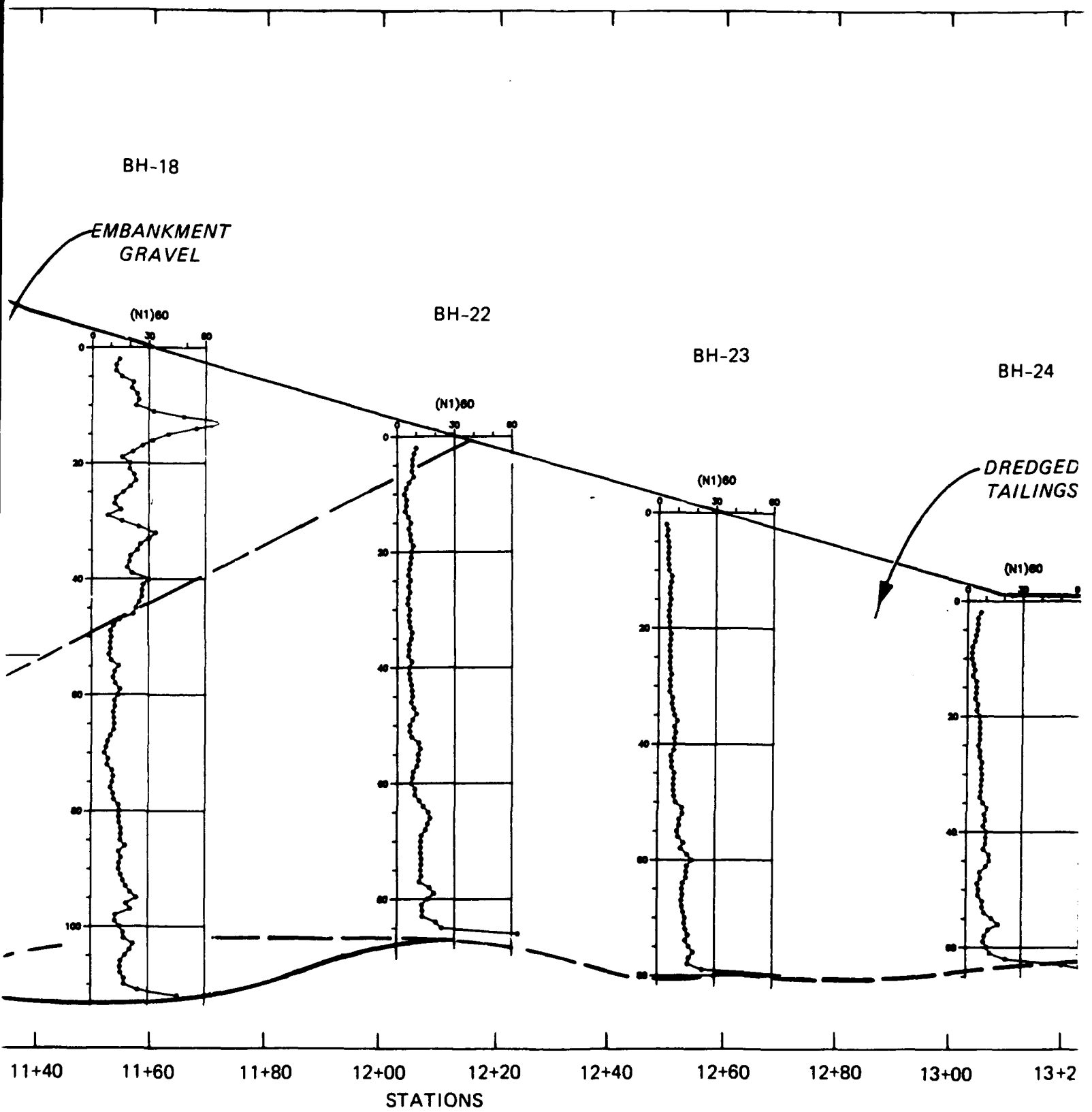
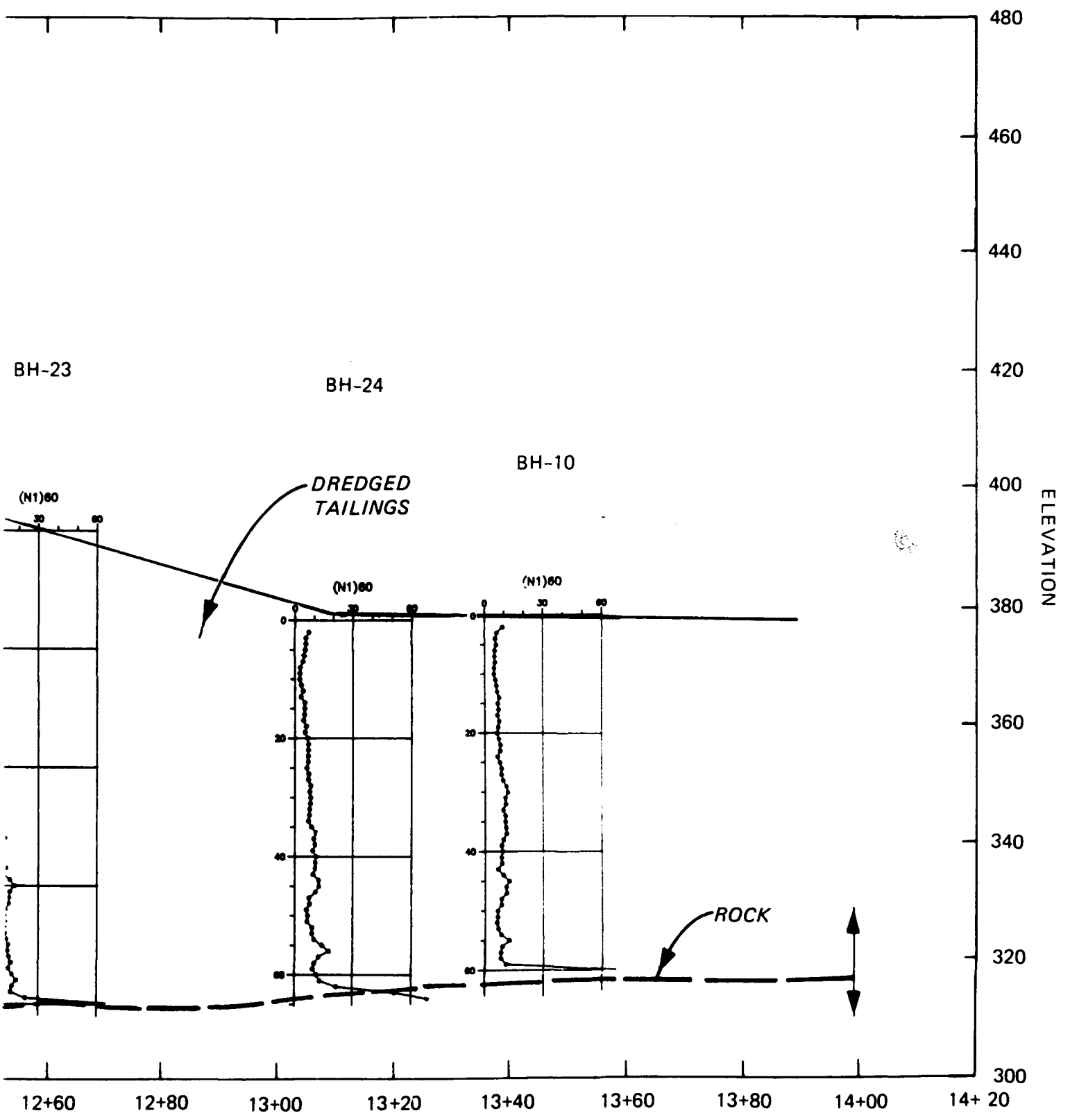
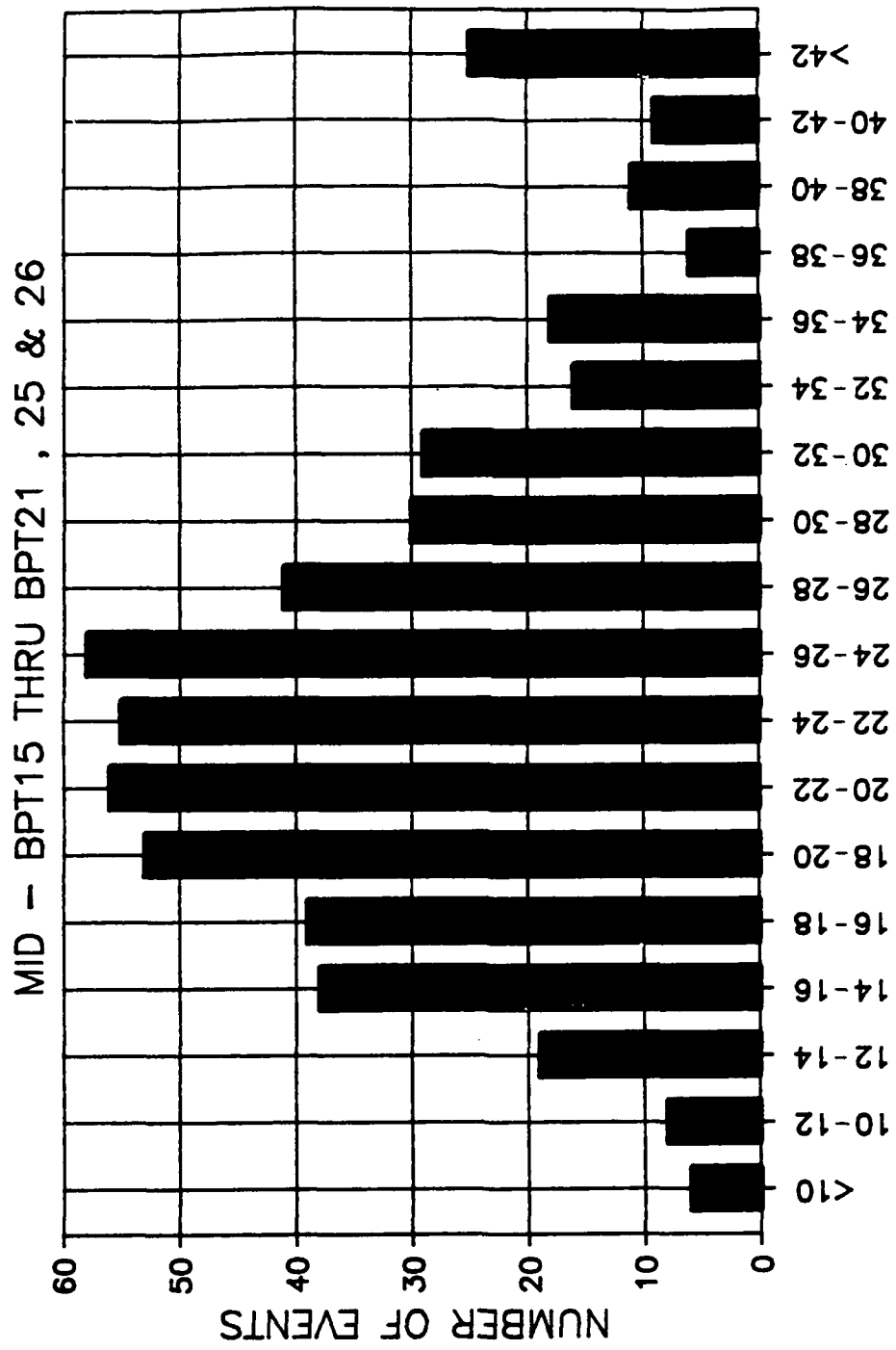


Figure 43. Transverse cross section through sta 450+00 showing $(N_1)_{60}$ results

1

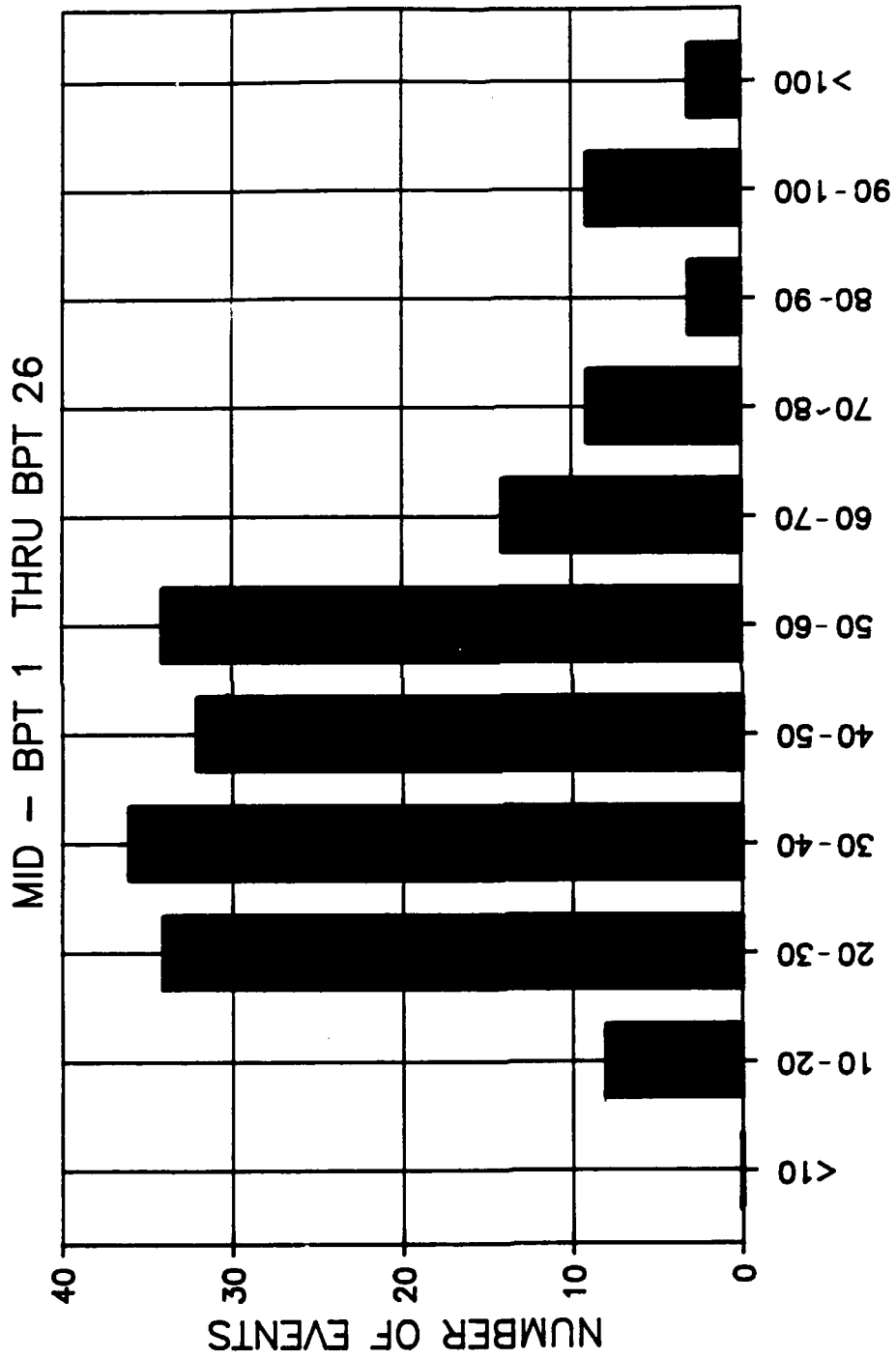


50+00



N1(60) BLOWS/FT

Figure 44. Histogram of $(N_1)_{60}$ for embankment gravels



$N_1(60)$ BLOWS/FT

Figure 45. Histogram of $(N_1)_{60}$ for undredged foundation gravels

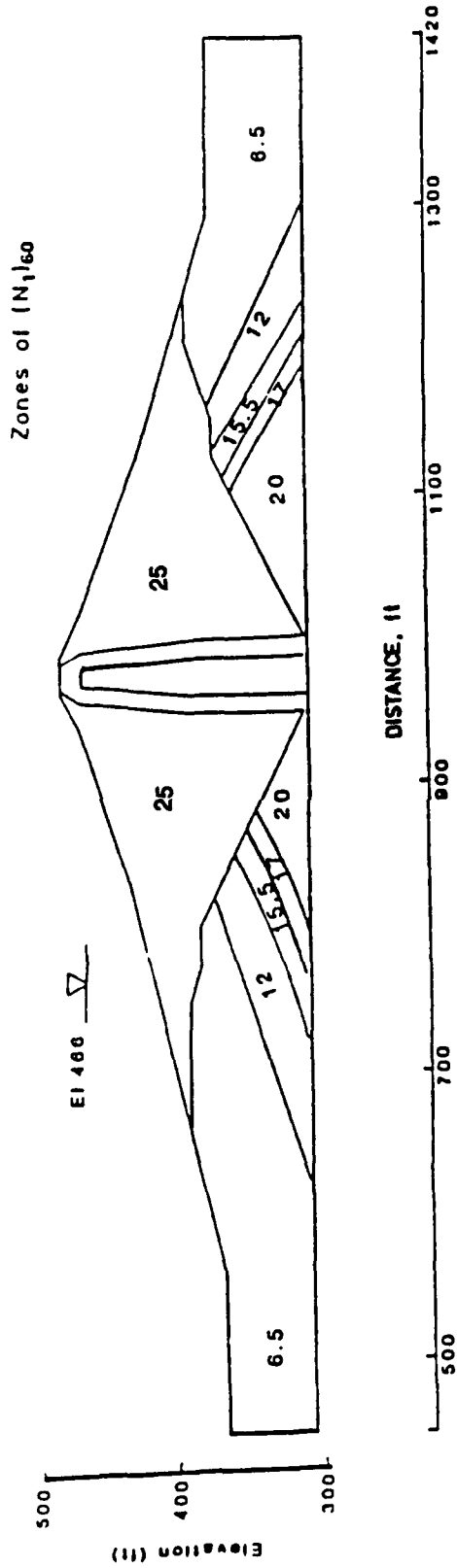


Figure 46a. Zones of $(N_1)_{60}$ for dredged foundation gravels at Mormon Island Dam estimated from Phase I Becker Hammer soundings and computed vertical effective stresses from static finite analysis of dredged foundation section documented in Report 4

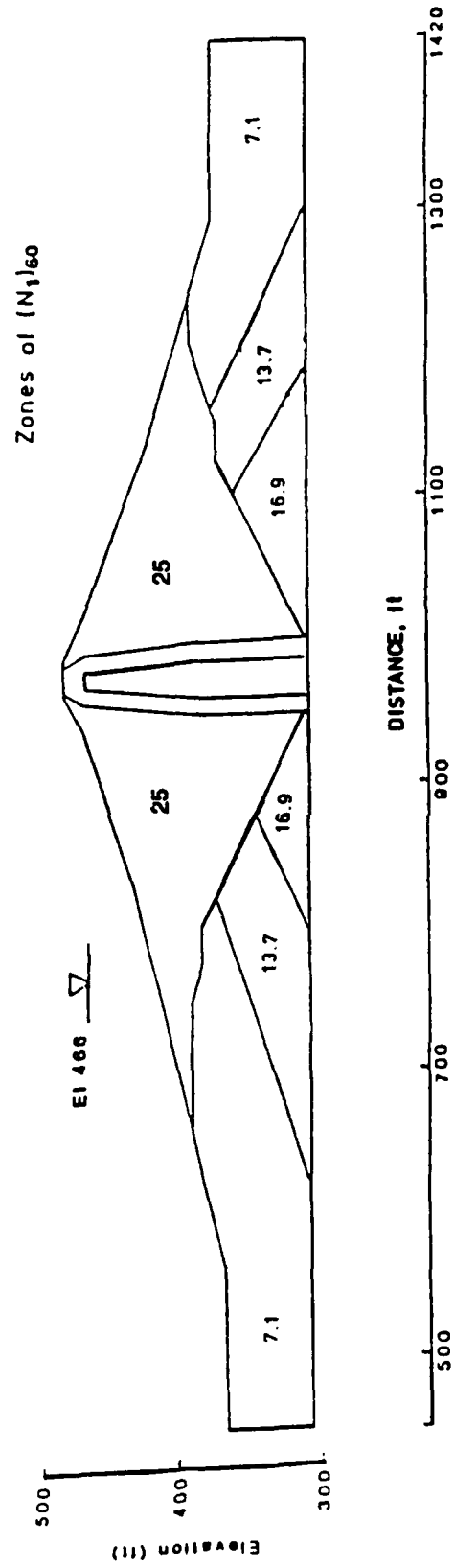


Figure 46b. Zones of $(N_1)_{60}$ for dredged foundation gravels at Mormon Island Dam estimated from Phase II Becker Hammer soundings and computed vertical effective stresses from static finite analysis of dredged foundation section documented in Report 4

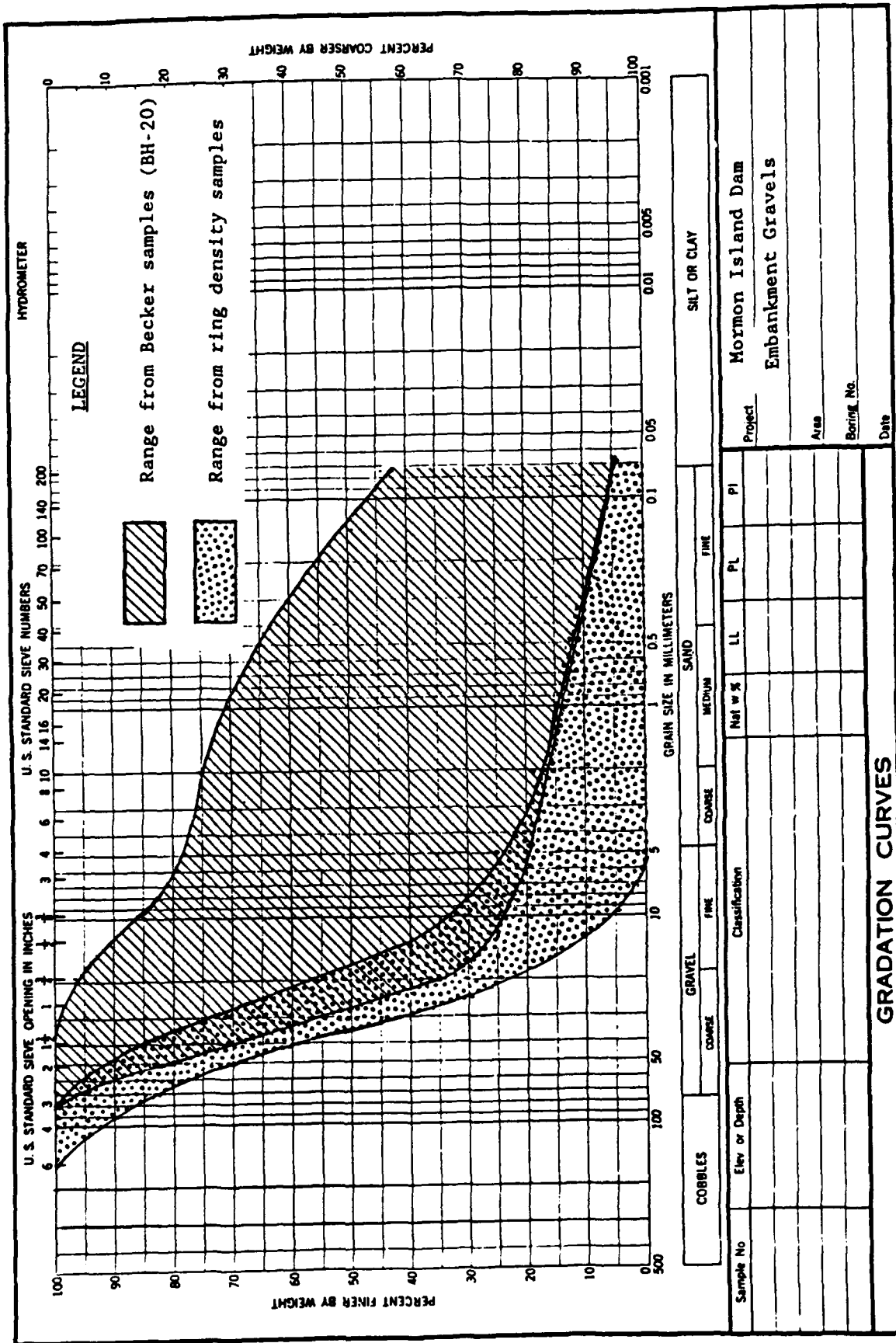


Figure 47. Comparisons of Becker sample and ring density gradations in embankment gravels

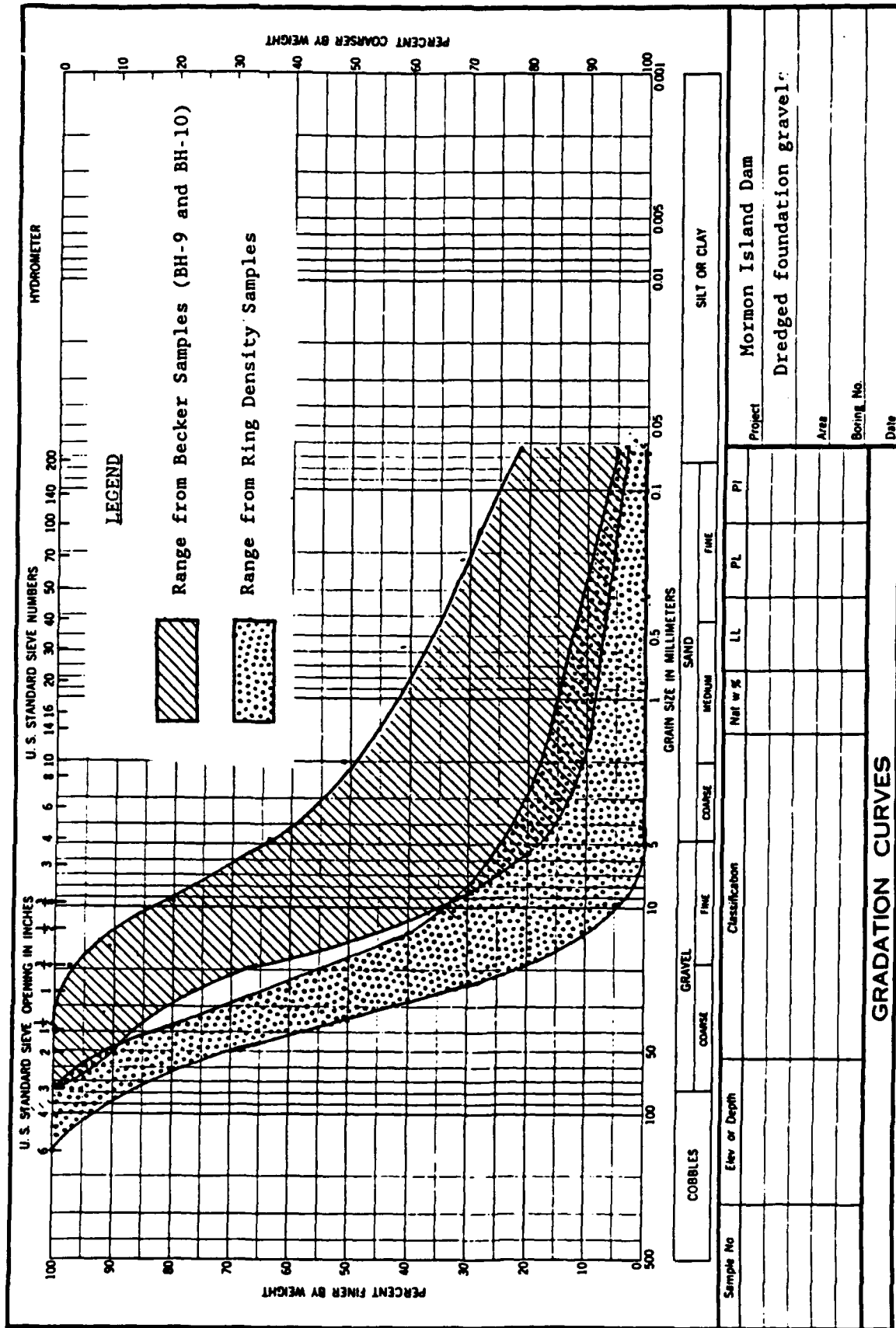


Figure 48. Comparison of Becker sample and ring density gradation in dredged foundation gravels

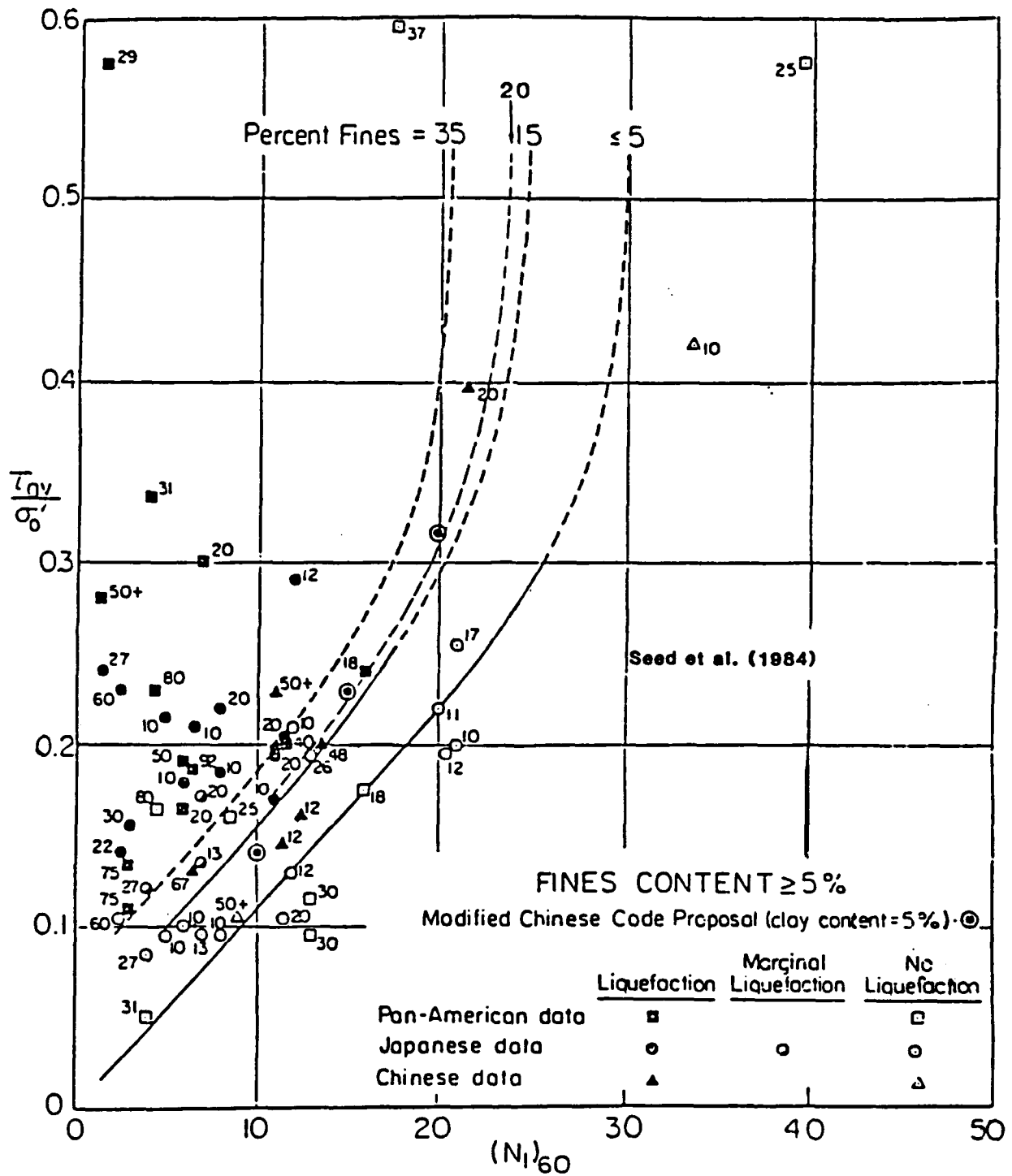
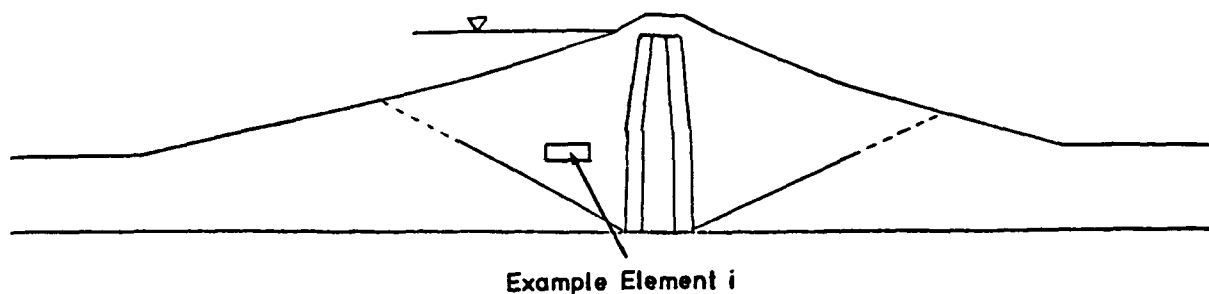


Figure 49. Relationships between stress ratio causing liquefaction and $(N_1)_{60}$ values for silty sand for $M = 7.5$ earthquakes (from Seed et al. 1984a)

Determination of Appropriate Cyclic Strength for Example Element

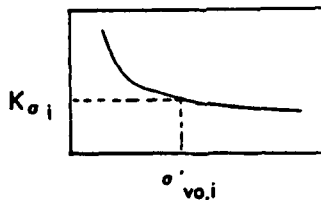


1. Analysis of Becker Penetration Test results and application of Seed's empirical procedure shows:

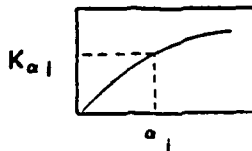
$$(N_1)_{60} \approx 25 \text{ for embankment gravel (for 5\% fines)}$$

$$\left(\frac{\tau_{CAVE}}{\sigma'_{vo}} \right) \approx 0.35 \text{ for } M_L = 6.5, \sigma'_{vo} = 1 \text{ tsf, and } \alpha = 0$$

2. Static FEM yields $\sigma'_{vo,i}$ and α_i for element i .
3. $K_{\sigma i}$ is determined from chart with $\sigma'_{vo,i}$:



4. $K_{\alpha i}$ is determined from chart with α_i :



5. Cyclic strength, τ_{ci} , for element i is:

$$\tau_{ci} = \left(\frac{\tau_{CAVE}}{\sigma'_{vo}} \right)_{\alpha=1}^{\alpha=0} \times K_{\sigma i} \times K_{\alpha i} \times \sigma'_{vo,i}$$

$$= (0.35) \times K_{\sigma i} \times K_{\alpha i} \times \sigma'_{vo,i}$$

Figure 50. Schematic representation of procedure for calculating the appropriate cyclic strength for elements in idealized embankment section

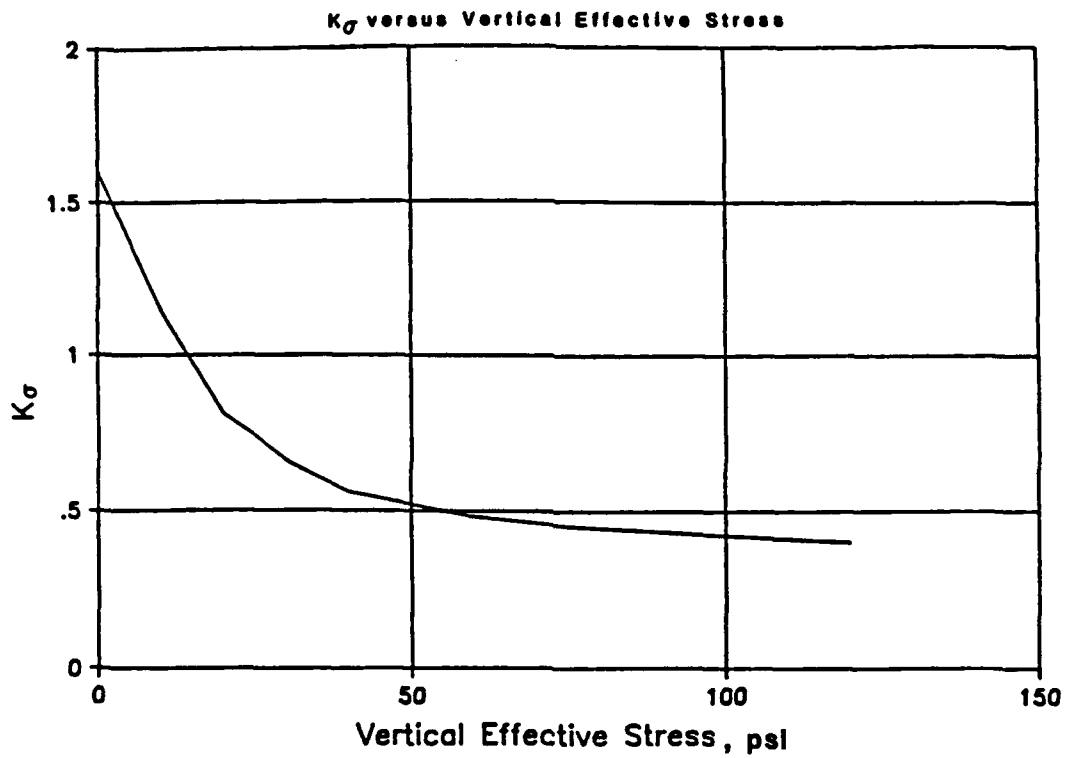


Figure 51. K_σ adjustment factor

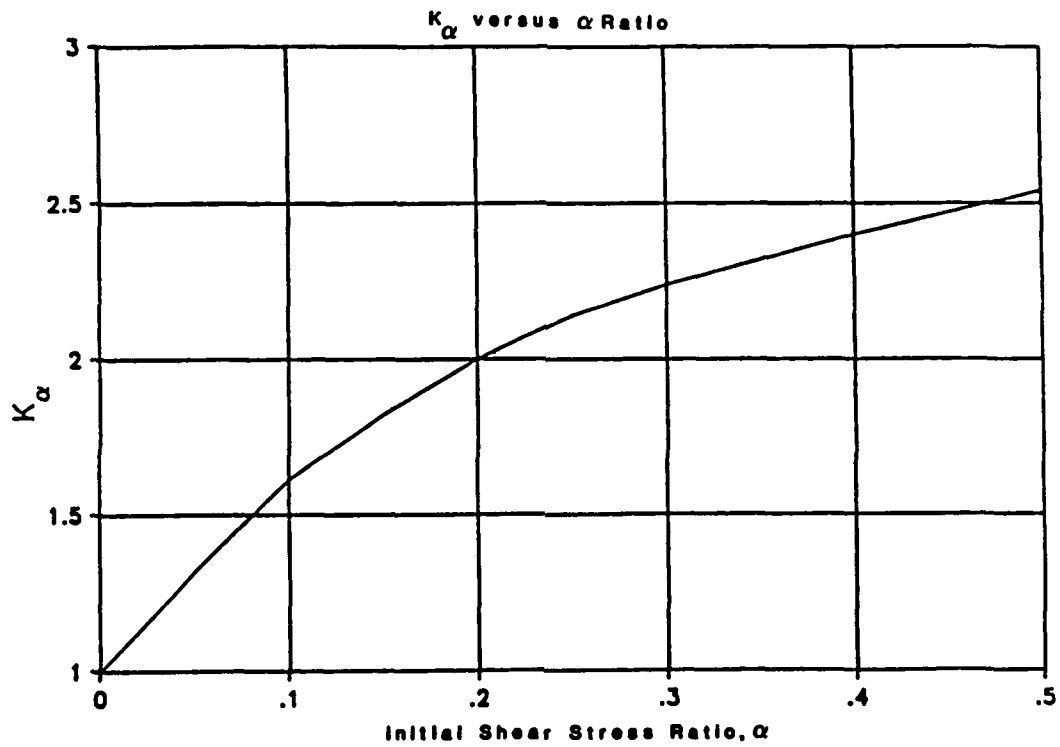


Figure 52. K_α adjustment factor

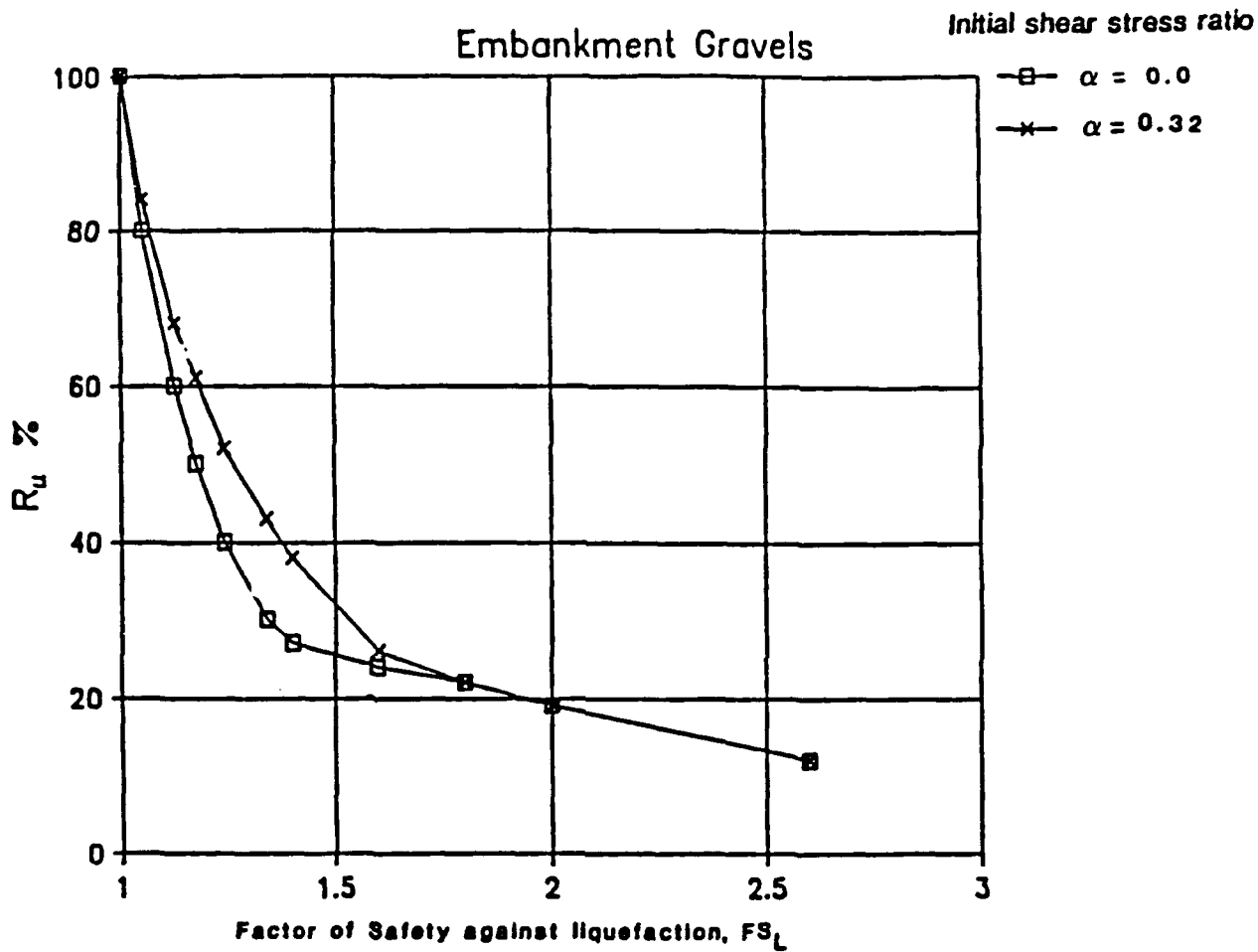


Figure 53. Relationship between FS_L and R_u

FOLSOM - MORMON ISLAND DAM STA. 426

IDEALIZED CROSS SECTION STA. 426

LEGEND:

- 1 - SUBMERGED EMBANKMENT GRAVEL
- 2 - MOIST EMBANKMENT GRAVEL
- 3 - SUBMERGED TRANSITION ZONE
- 4 - MOIST TRANSITION ZONE
- 5 - CENTRAL IMPERVIOUS CORE

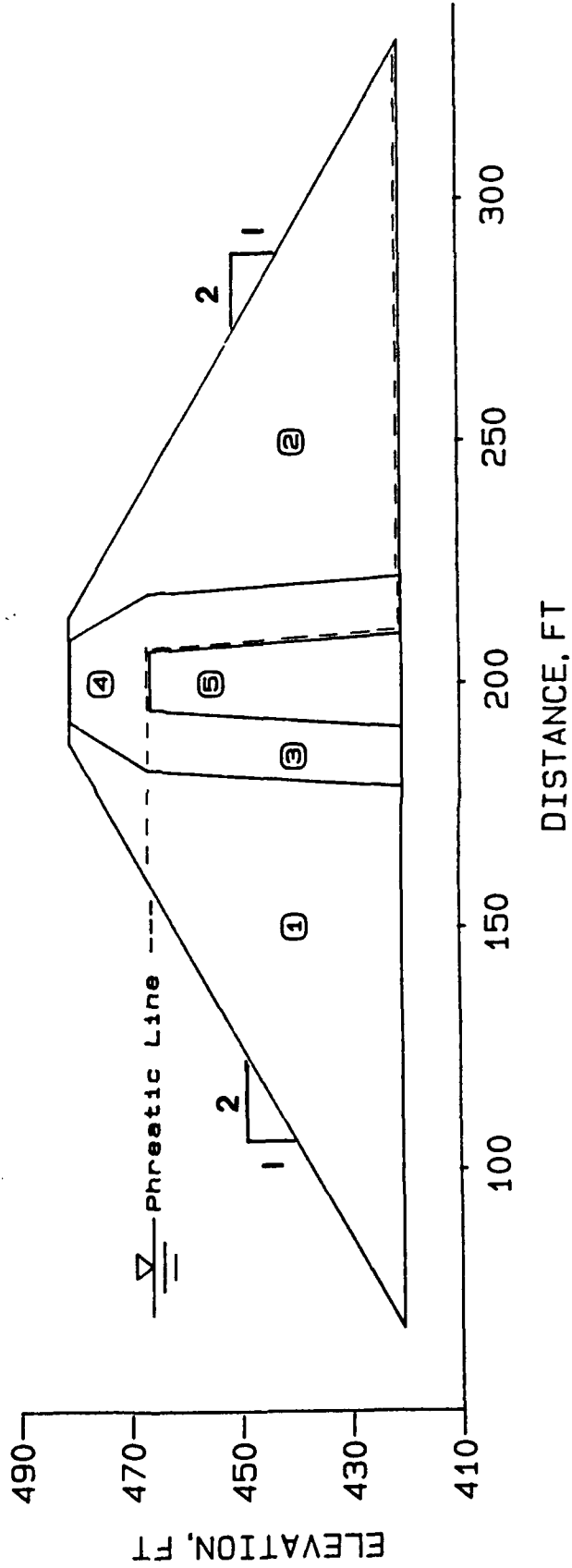


Figure 54. Idealized embankment section of Mormon Island Dam founded on rock and developed from cross section of dam at sta 426+00

FOLSOM - MORMON ISLAND DAM STA. 426
IDEALIZED CROSS SECTION STA. 426 WITH FEM MESH

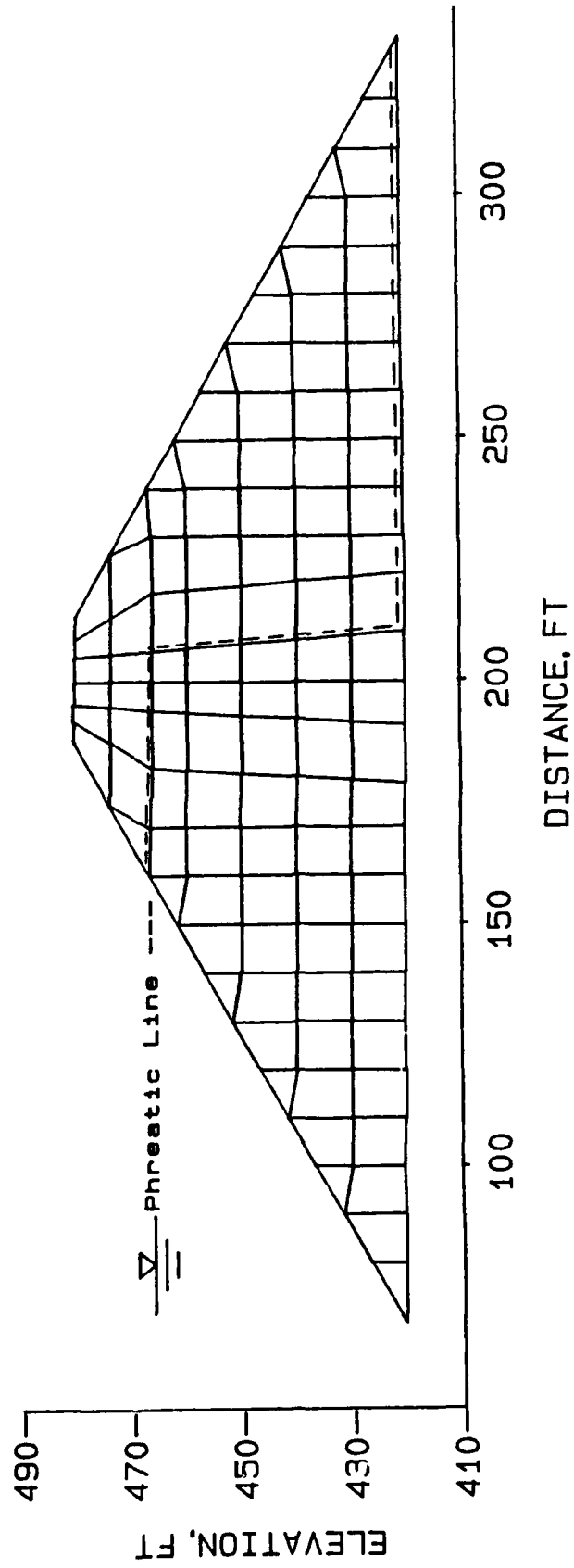


Figure 55. Finite element mesh used for idealized rock section

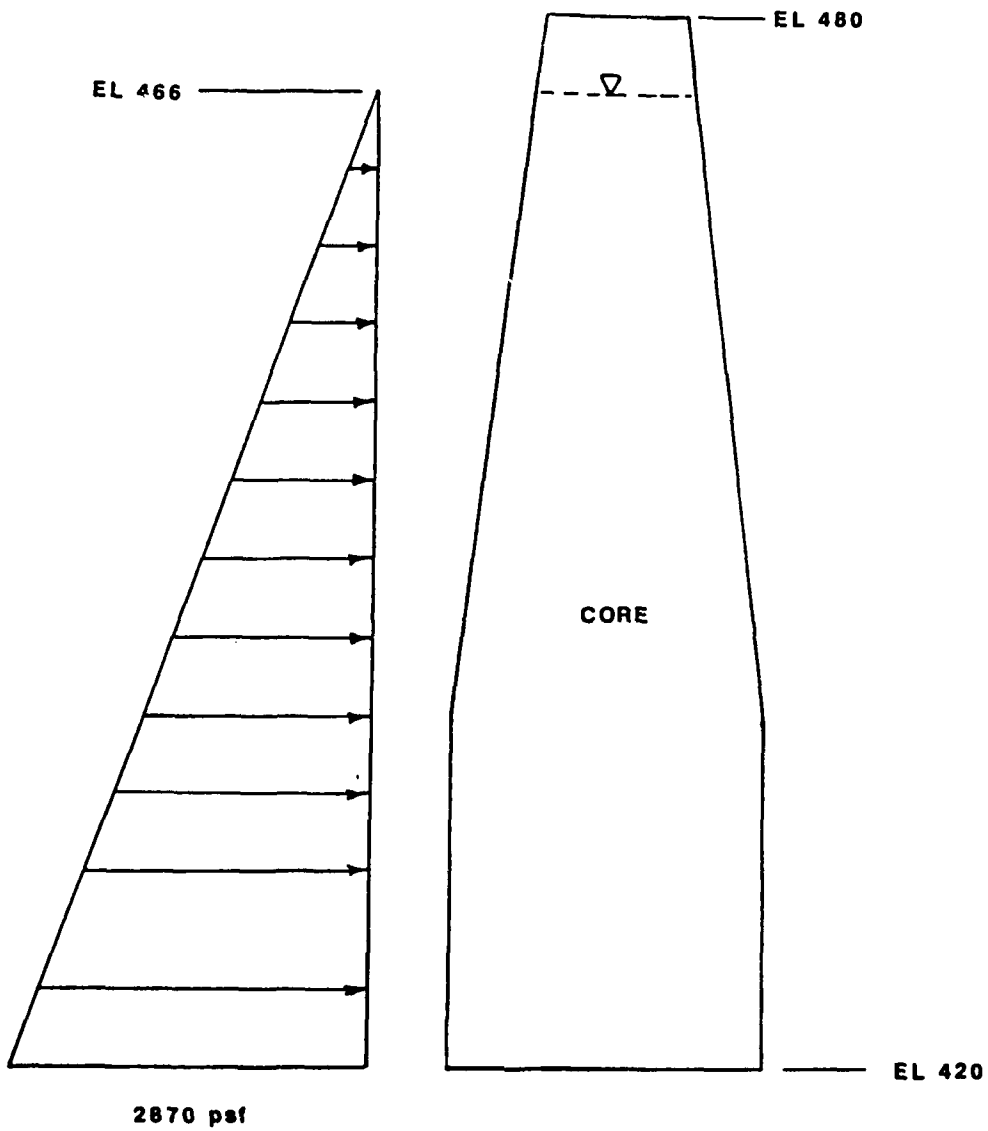


Figure 56. Unbalanced hydrostatic pressures acting across the core of the dam

FOLSOM PROJECT - MORMON ISLAND DAM

CROSS SECTION FOR ROCK FOUNDATION

STA 426+00

CONTOURS OF VERTICAL EFFECTIVE STRESS (psf)

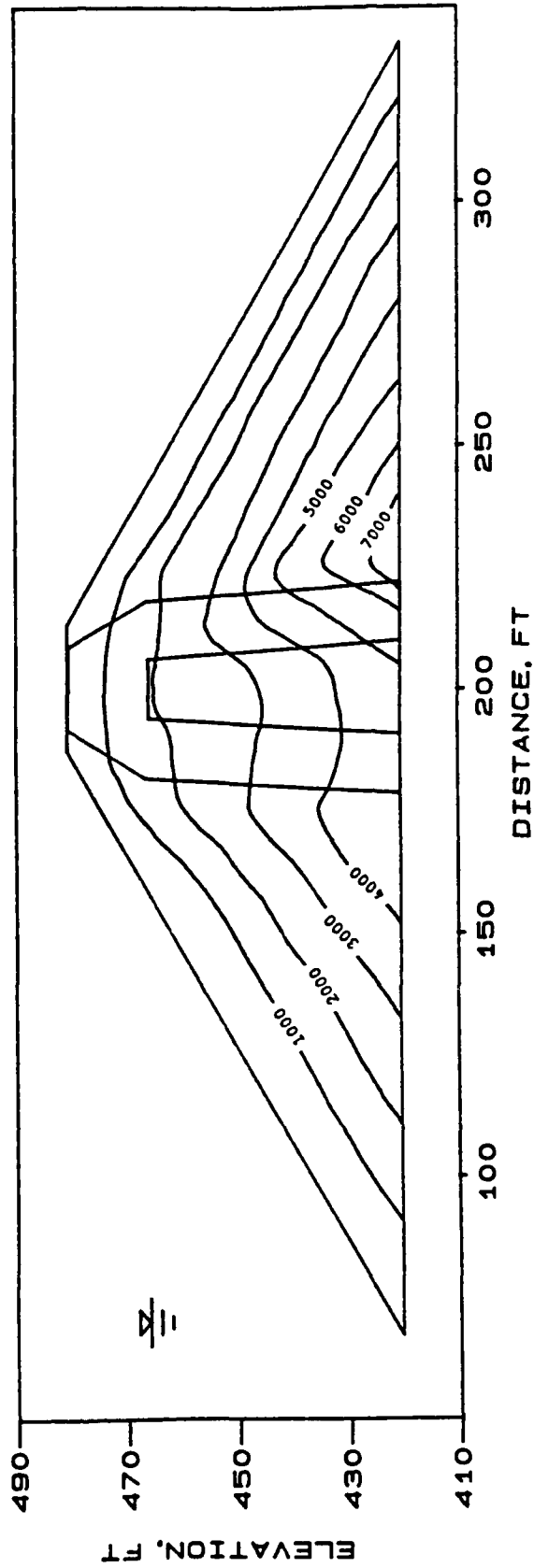


Figure 57. Contours of vertical effective stress computed by FEADAM

FOLSOM PROJECT - MORMON ISLAND DAM
CROSS SECTION FOR ROCK FOUNDATION

STA 426+00

CONTOURS OF HORIZONTAL EFFECTIVE STRESS (psf)

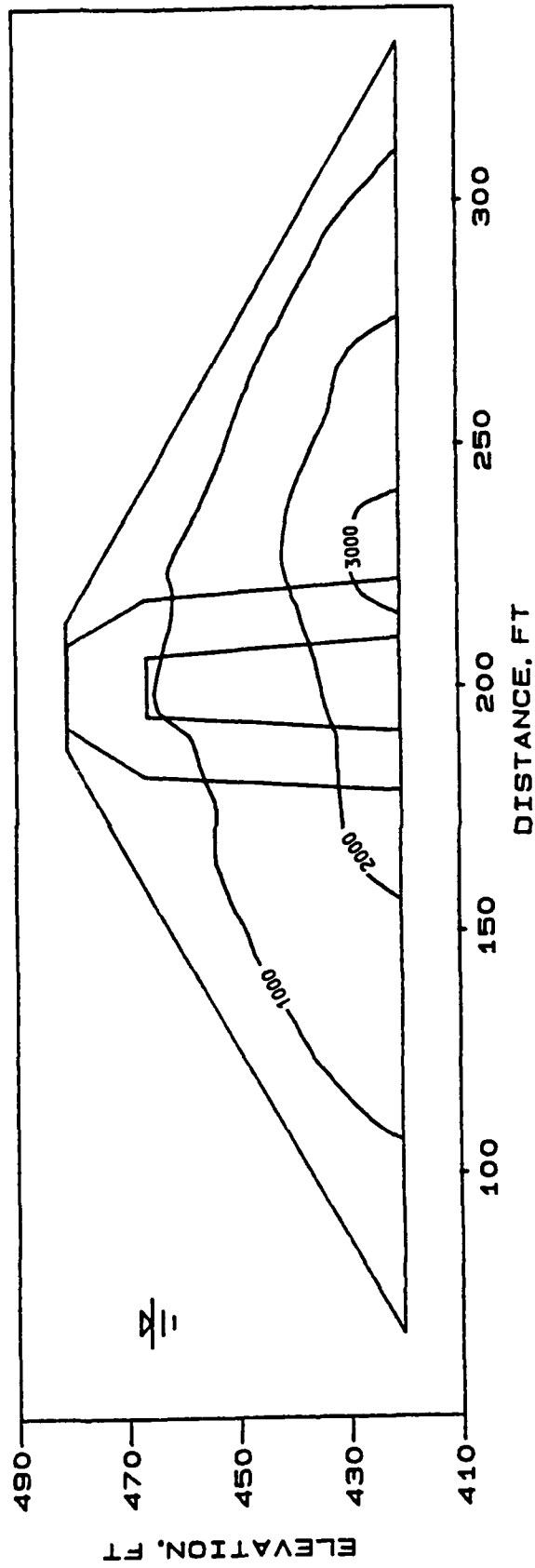


Figure 58. Contours of horizontal effective stress computed by FEADAM

FOLSOM PROJECT - MORMON ISLAND DAM

CROSS SECTION FOR ROCK FOUNDATION

STA 426+00

CONTOURS OF SHEAR STRESS ACTING ON HORIZONTAL PLANE (psf)

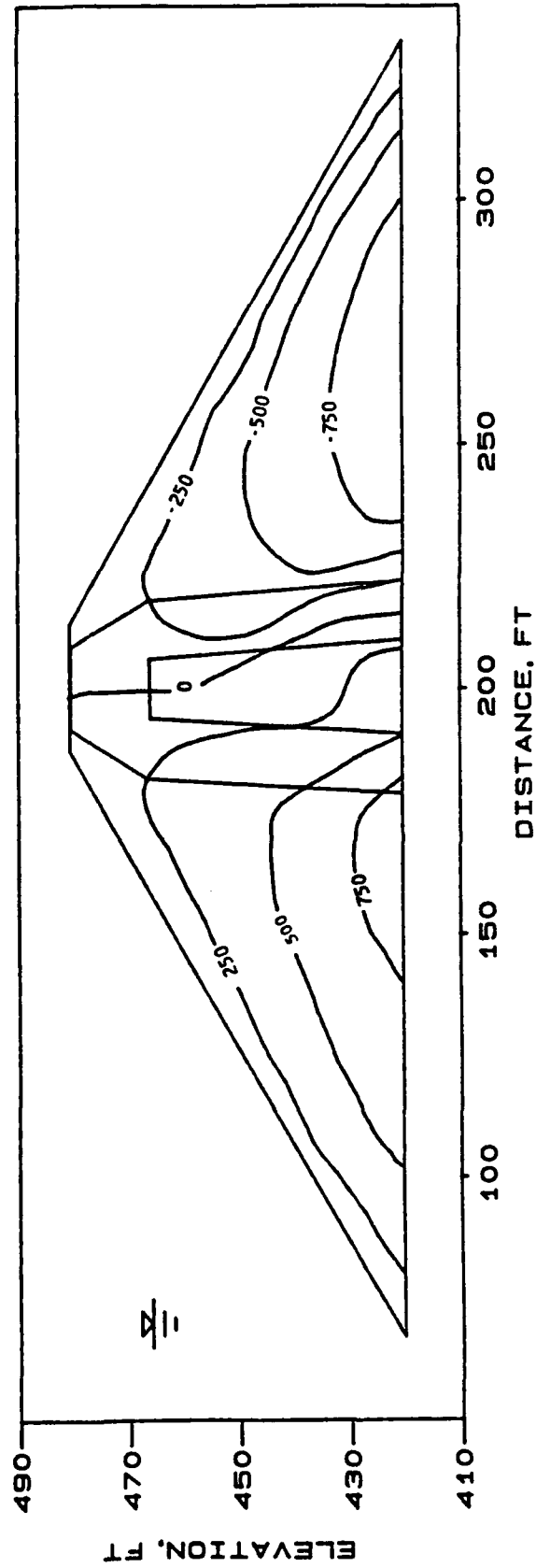


Figure 59. Contours of shear stresses on horizontal planes computed by FEADAM

FOLSOM PROJECT - MORMON ISLAND DAM

CROSS SECTION FOR ROCK FOUNDATION

STA 426+00

CONTOURS OF T_{xy}/σ_v ALPHA RATIO

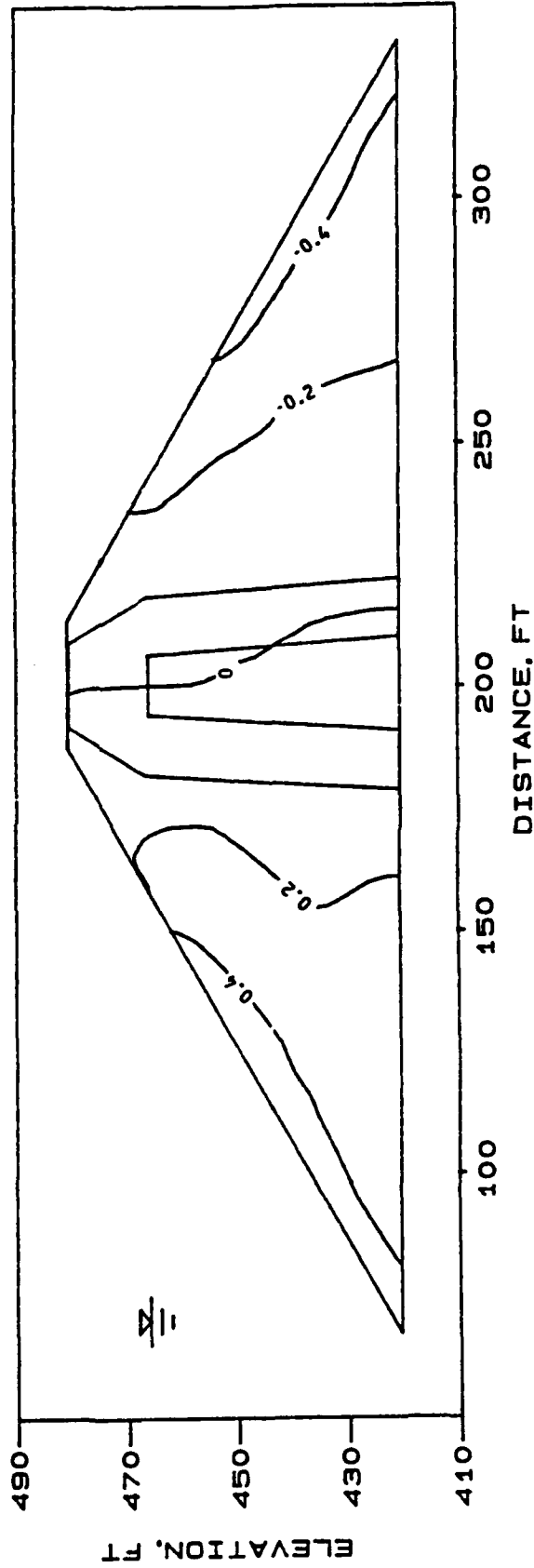


Figure 60. Contours of α

FOLSOM PROJECT - MORMON ISLAND DAM
CROSS SECTION FOR ROCK FOUNDATION

STA 426+00

CONTOURS OF MEAN NORMAL PRESSURES (psf)

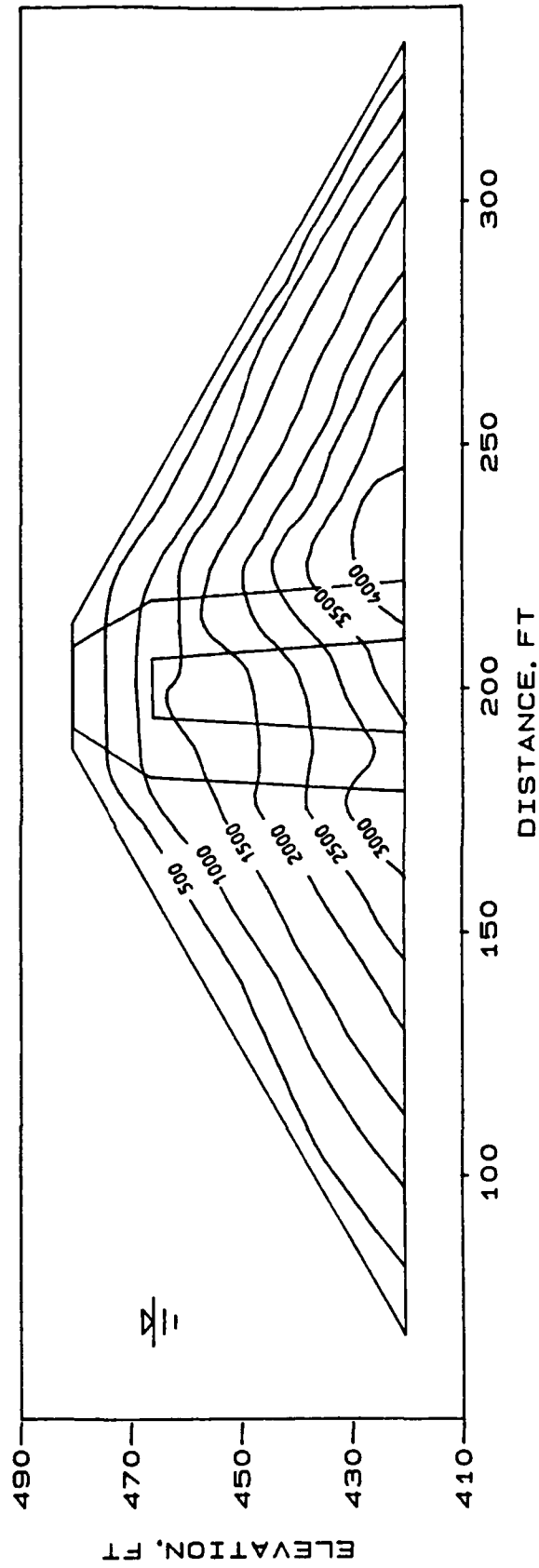


Figure 61. Contours of effective mean normal pressure computed from FEADAM stresses

FOLSOM PROJECT - MORMON ISLAND DAM

CROSS SECTION FOR ROCK FOUNDATION

STA 426+00

CONTOURS OF SHEAR WAVE VELOCITY (fps)

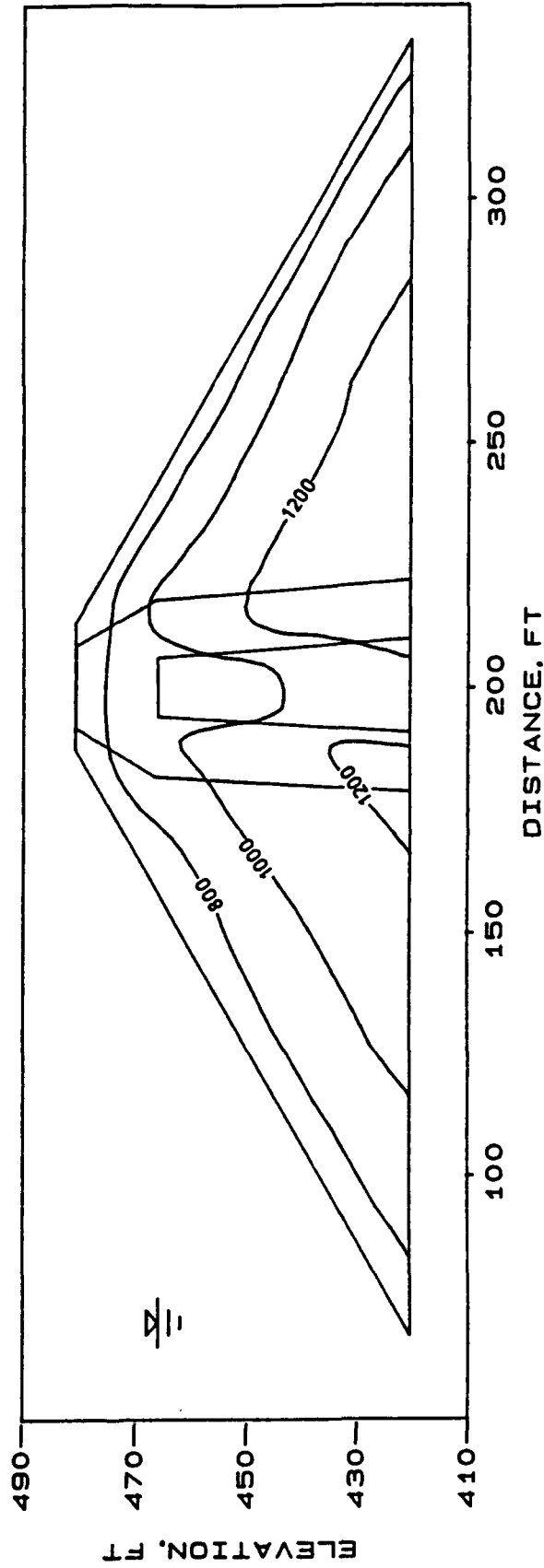


Figure 62. Low strain amplitude shear wave velocity distribution in rock section

FOLSOM PROJECT - MORMON ISLAND DAM

CROSS SECTION FOR ROCK FOUNDATION

STA 426+00

CONTOURS OF LOW STRAIN AMPLITUDE SHEAR MODULUS (ksf)

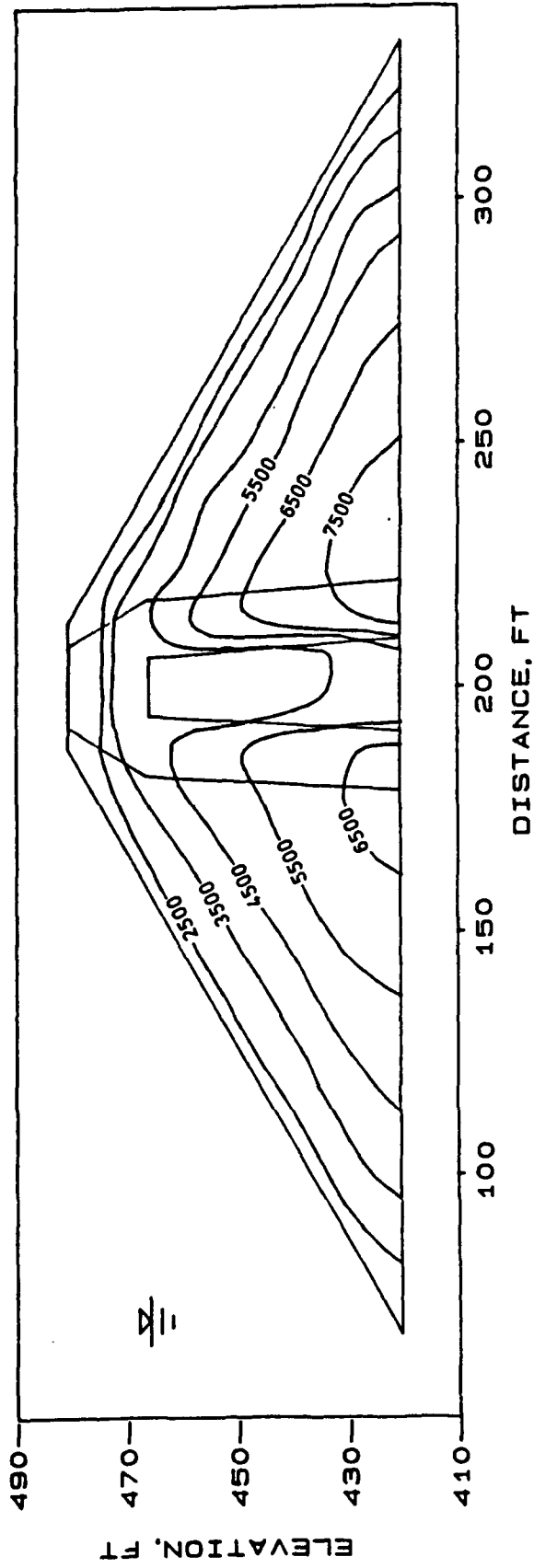
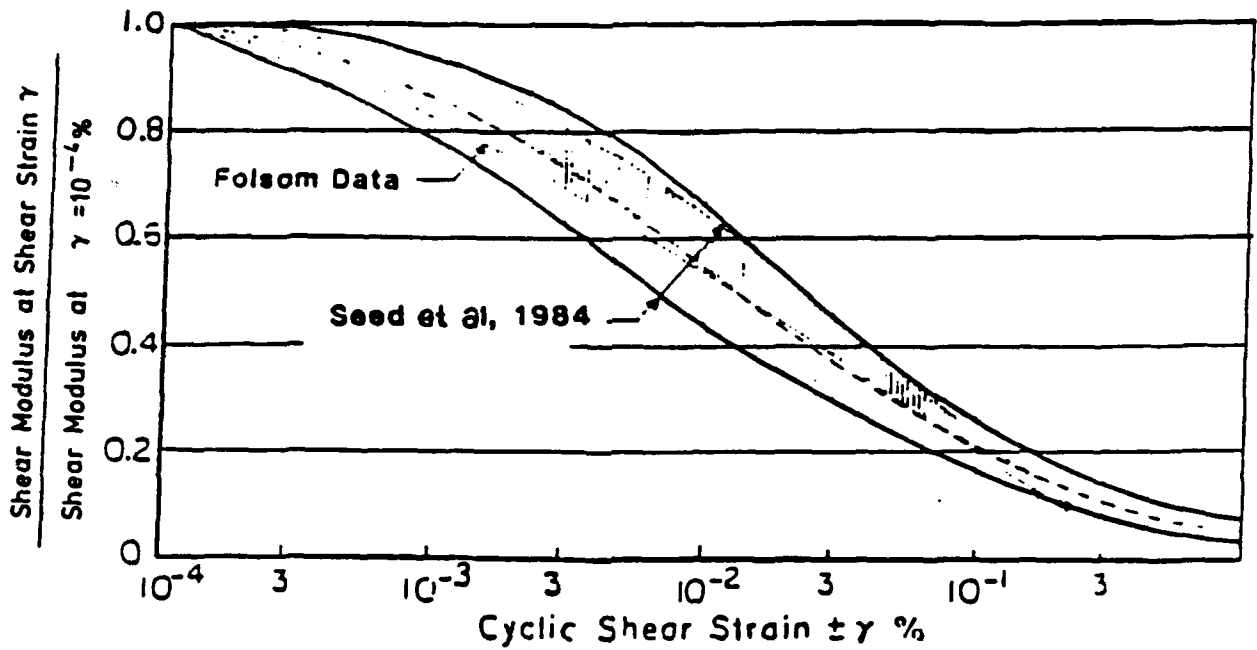
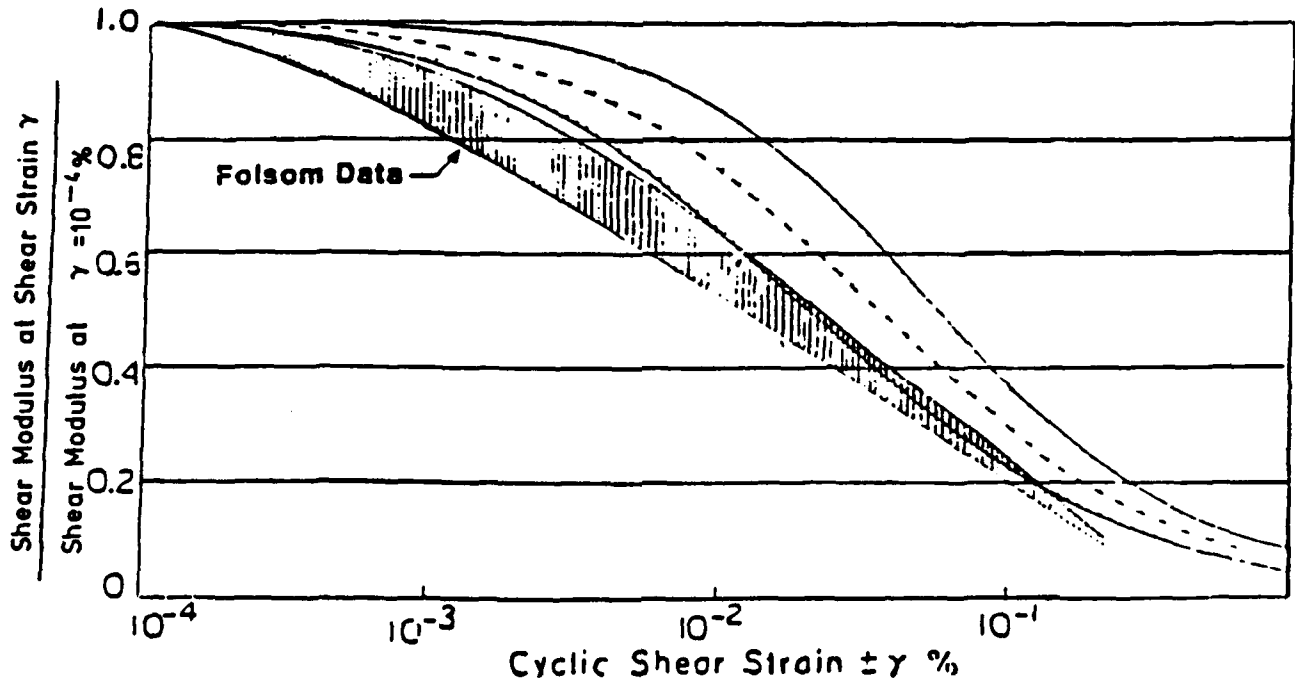


Figure 63. Contours of low amplitude shear modulus, G_{max} , input to FLUSH



a. Variation of shear modulus with cyclic shear strain for gravelly soils



b. Variation of shear modulus with cyclic shear strain for sands (after Seed and Idriss 1970)

Figure 64. Modulus degradation and damping curves used in FLUSH analysis

FOLSOM PROJECT - MORMON ISLAND DAM

CROSS SECTION FOR ROCK FOUNDATION

STA 426+00

CONTOURS OF DYNAMIC SHEAR STRESS (psf) RECORD A

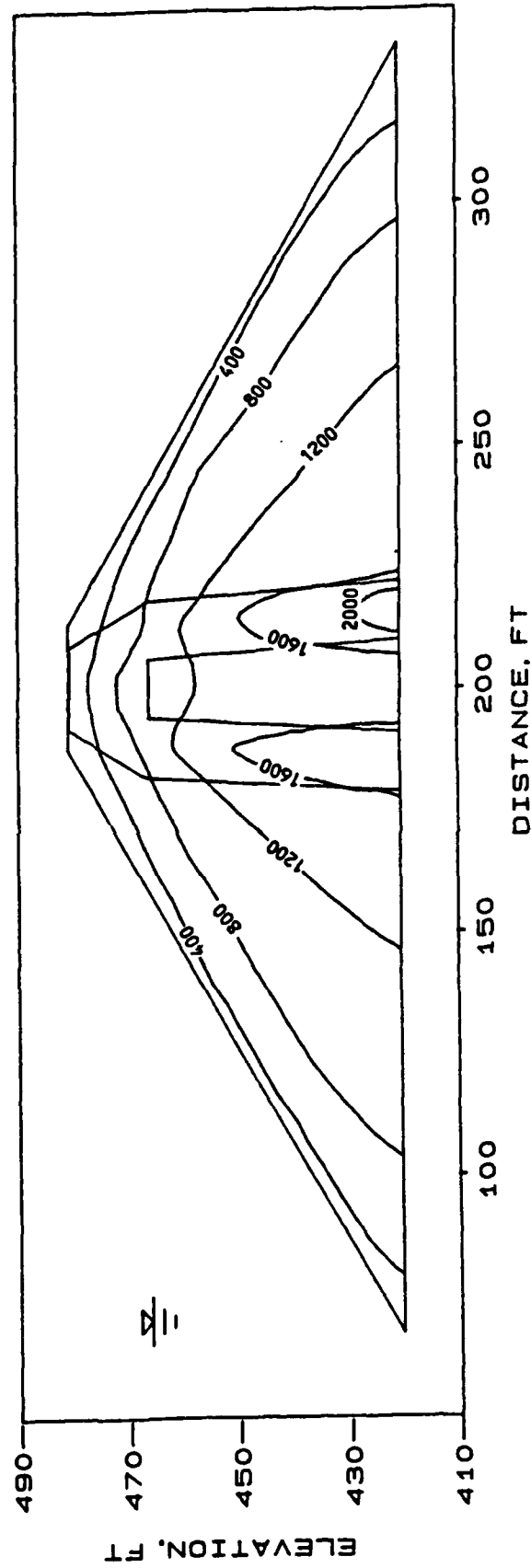


Figure 65. Dynamic shear stresses induced by Accelerogram A in FLUSH analysis

FOLSOM - MORMON ISLAND DAM STA. 426

ACCELEROGRAM A

FUNDAMENTAL PERIOD AT STRAIN LEVELS INDUCED BY RECORD A = 0.366 sec
 LOW STRAIN AMPLITUDE FUNDAMENTAL PERIOD = 0.171 sec
 ACCELERATIONS ARE IN g's

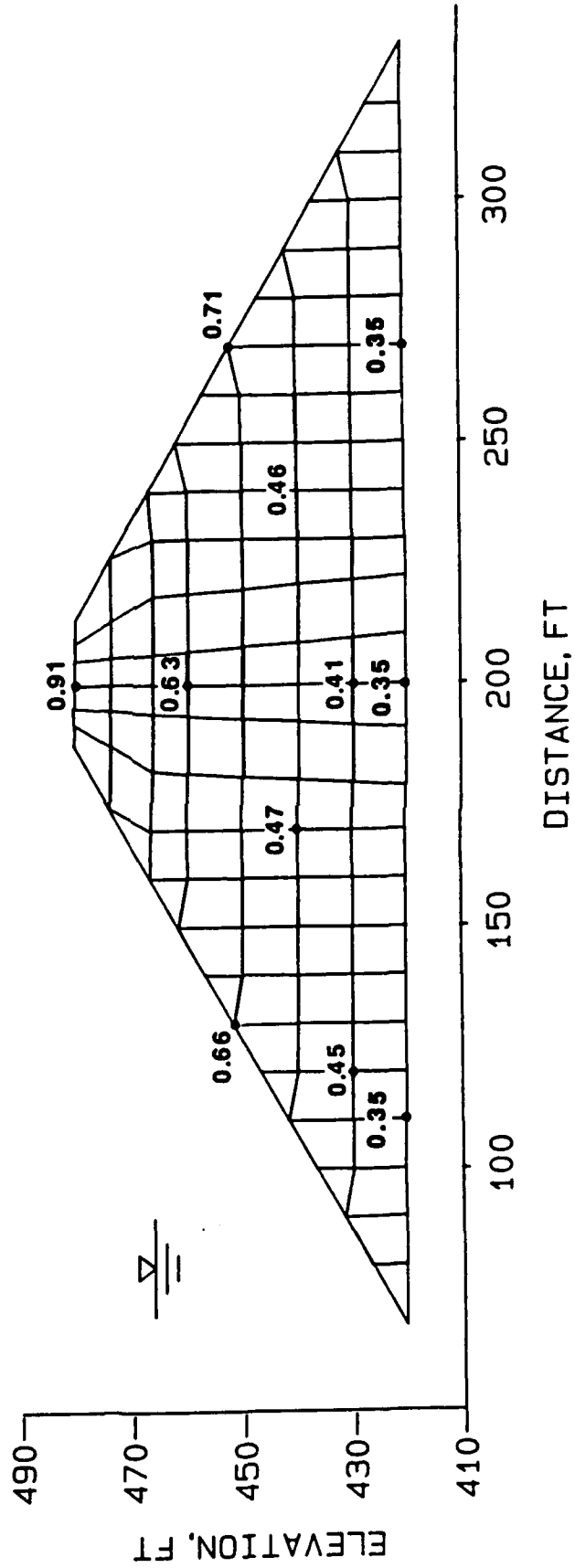


Figure 66. Maximum accelerations and fundamental periods computed by FLUSH for selected nodal points

FOLSOM - MORMON ISLAND DAM STA. 426

ACCELEROGRAM A

EFFECTIVE SHEAR STRAINS IN PERCENT

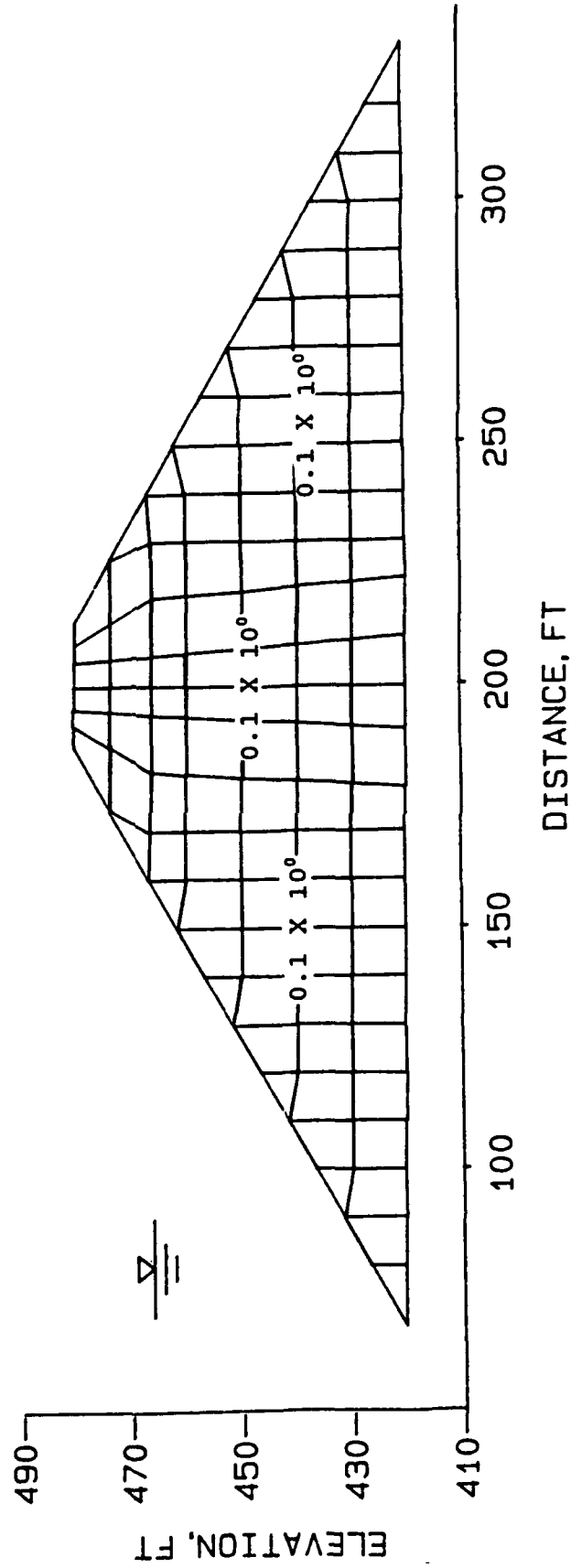


Figure 67. Effective shear strains in percent, computed by FLUSH using Accelerogram A for rock section at Mormon Island Dam

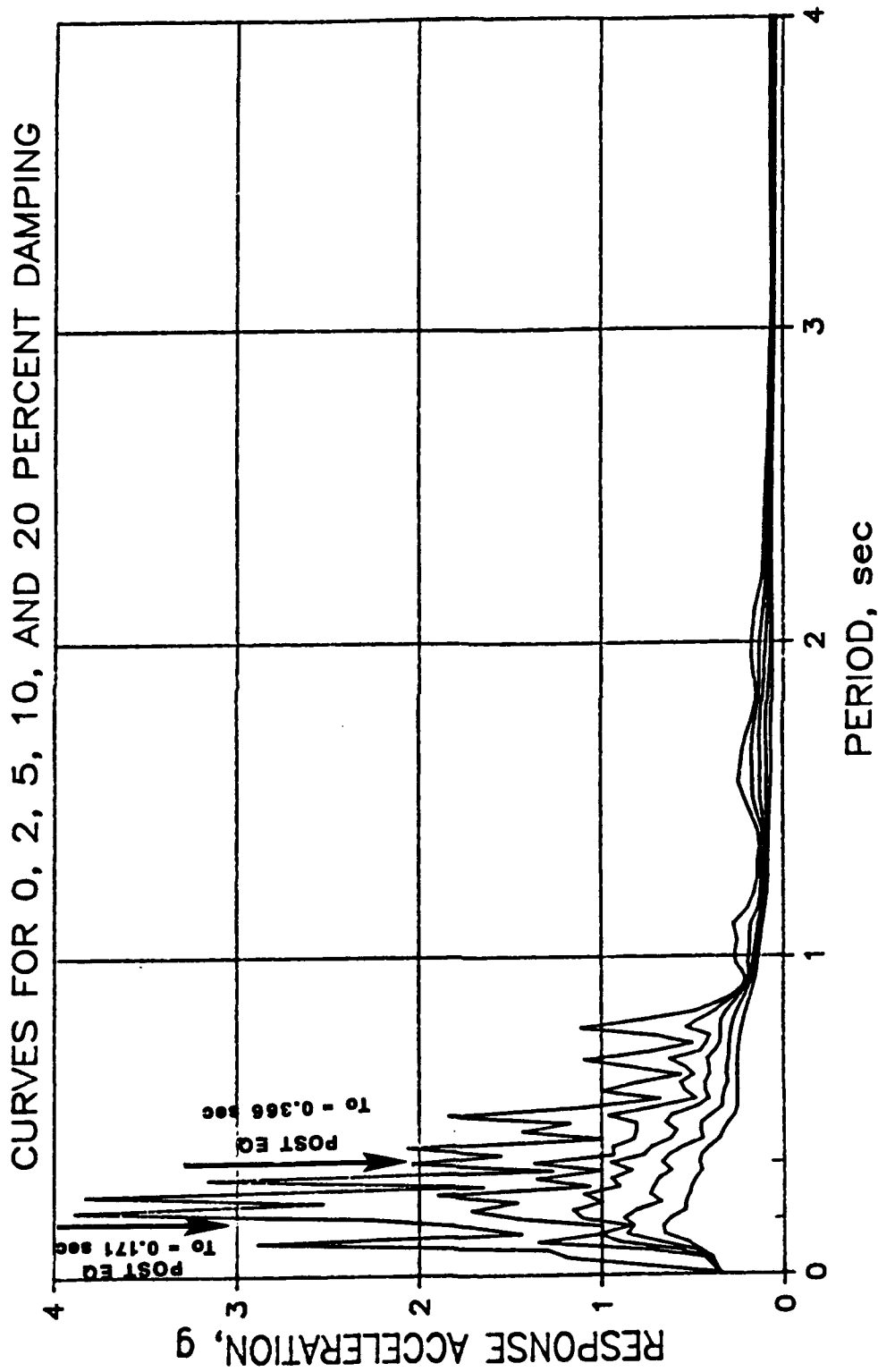


Figure 68. Response spectra for Accelerogram A compared with the low strain amplitude and design earthquake strain level fundamental periods

FOLSOM PROJECT - MORMON ISLAND DAM

CROSS SECTION FOR ROCK FOUNDATION

STA 426+00

CONTOURS OF SAFETY FACTOR AGAINST LIQUEFACTION

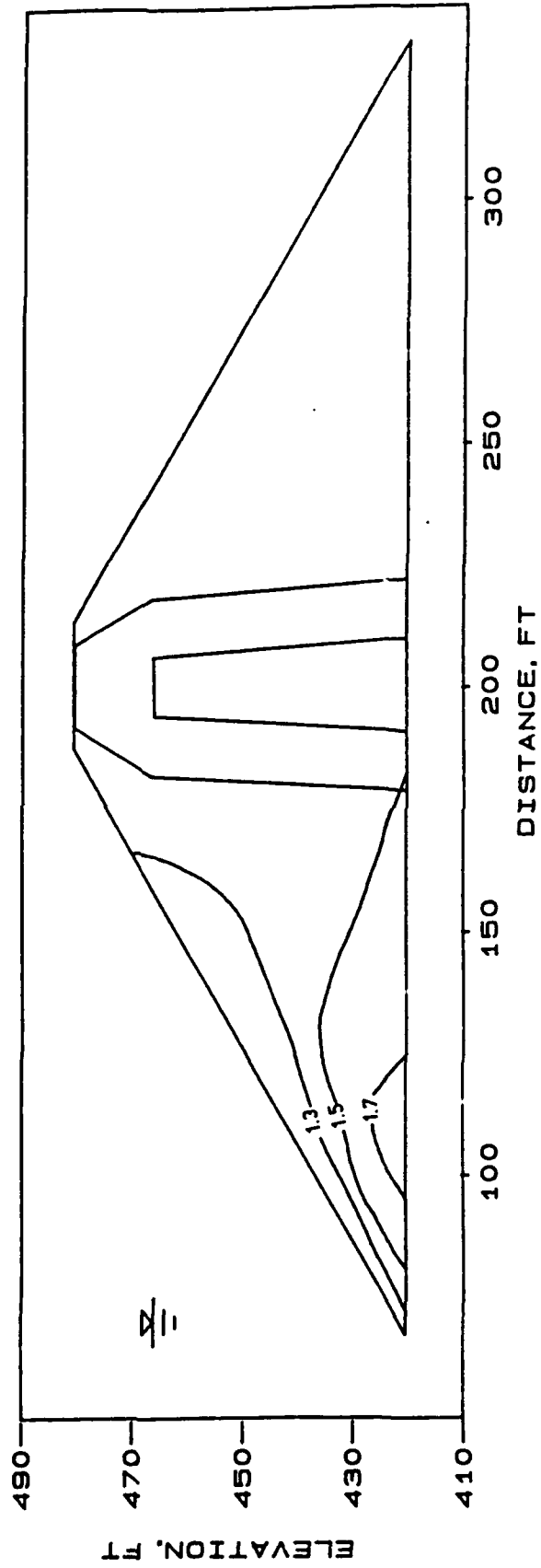


Figure 69. Contours of safety factor against liquefaction for section of Mormon Island Dam founded on rock

FOLSOM PROJECT - MORMON ISLAND DAM

CROSS SECTION FOR ROCK FOUNDATION

STA 426+00

CONTOURS OF EXCESS PORE PRESSURE RATIO R_u - $U_{\text{excess}} / \sigma_v$ PERCENT

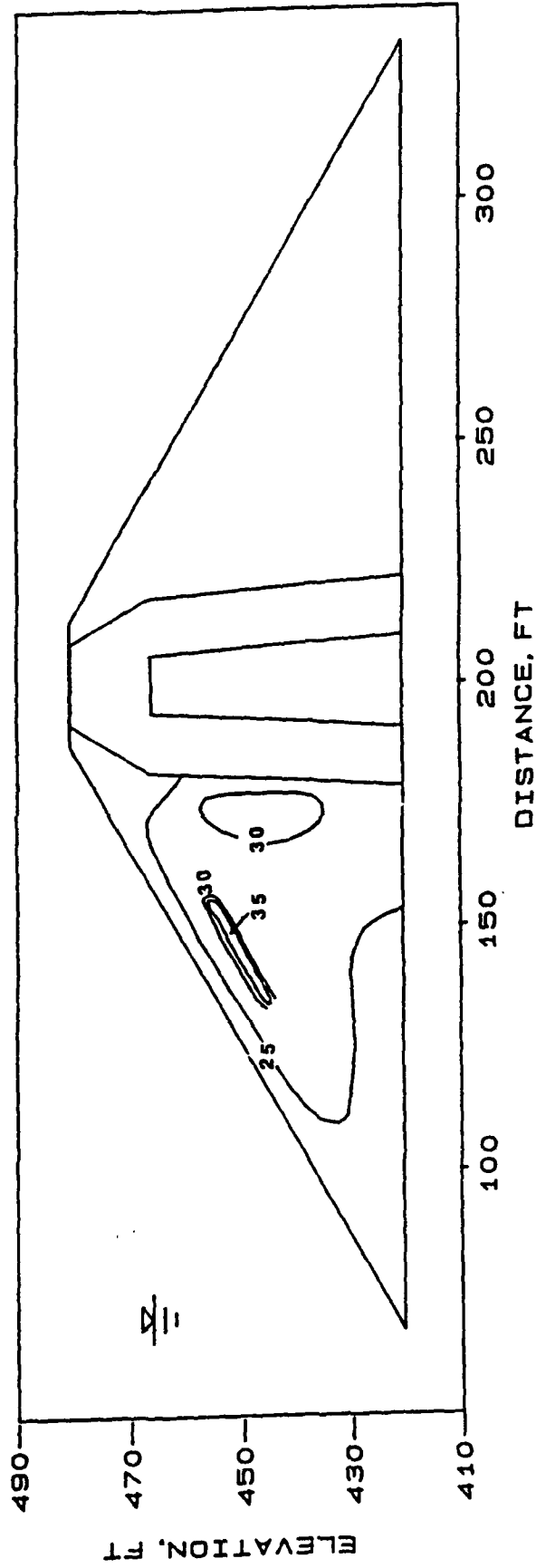


Figure 70. Contours of excess pore pressure ratio R_u in percent for section of Mormon Island Dam founded on rock

POST-EARTHQUAKE STABILITY ANALYSIS
 FOLSOM - MORMAN ISLAND DAM STA. 426+00

FACTOR OF SAFETY AGAINST SLOPE FAILURE I

PRE-EARTHQUAKE = 1.846
 POST-EARTHQUAKE = 1.286

PARAMETERS I

CRITICAL CIRCLE *****
 RADIUS CONTOURS _____

POOL EL = 488 ft
 MATERIAL CORE : C=0 -24
 SHELLS: C=0 -43
 TRANSITION: C=0 -31, 37

CONTOUR INTERVAL = 5
 RANGE = 25 - 35

(N1)60 = 25.3
 CYCLIC STRESS RATIO (1TSF) = 0.35

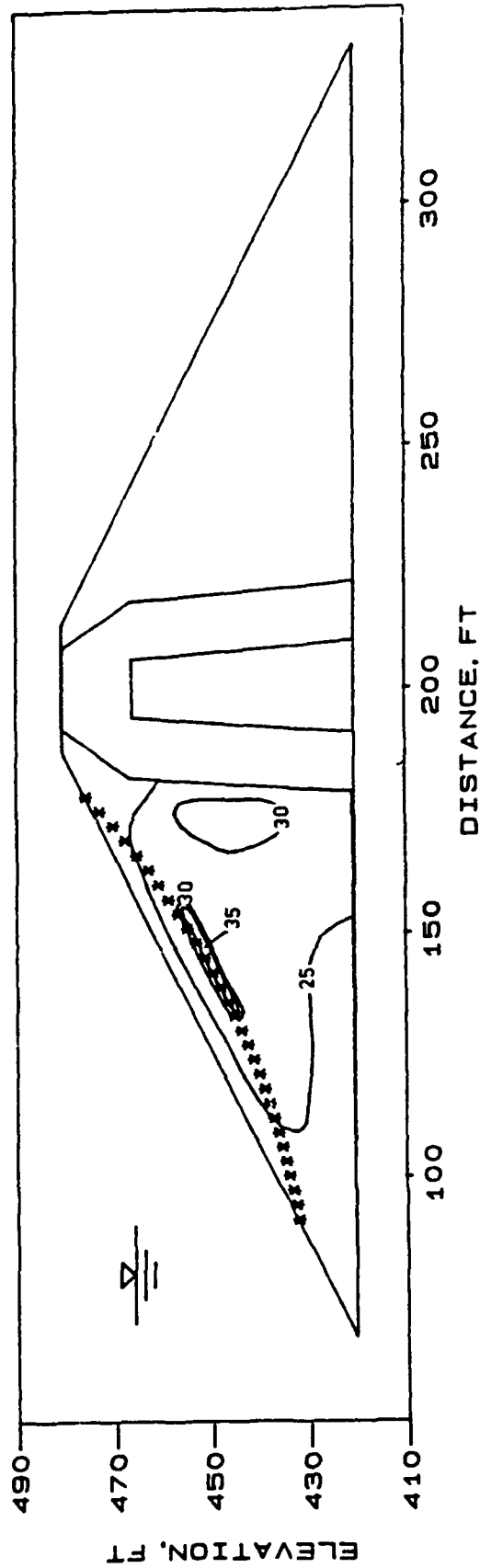


Figure 71. Safety factor against sliding and critical circle in post-earthquake stability analysis

POST-EARTHQUAKE PERMANENT DISPLACEMENT ANALYSIS

FOLSOM - MORMAN ISLAND DAM STA. 426+00 FOUNDATION: ROCK

YIELD ACCELERATION SEISMIC COEFFICIENT (KY)

CASE I FAILURE CIRCLES CONFINED TO UPSTREAM SHELL

KEY I

FAILURE CIRCLES *****
RUX CONTOURS _____

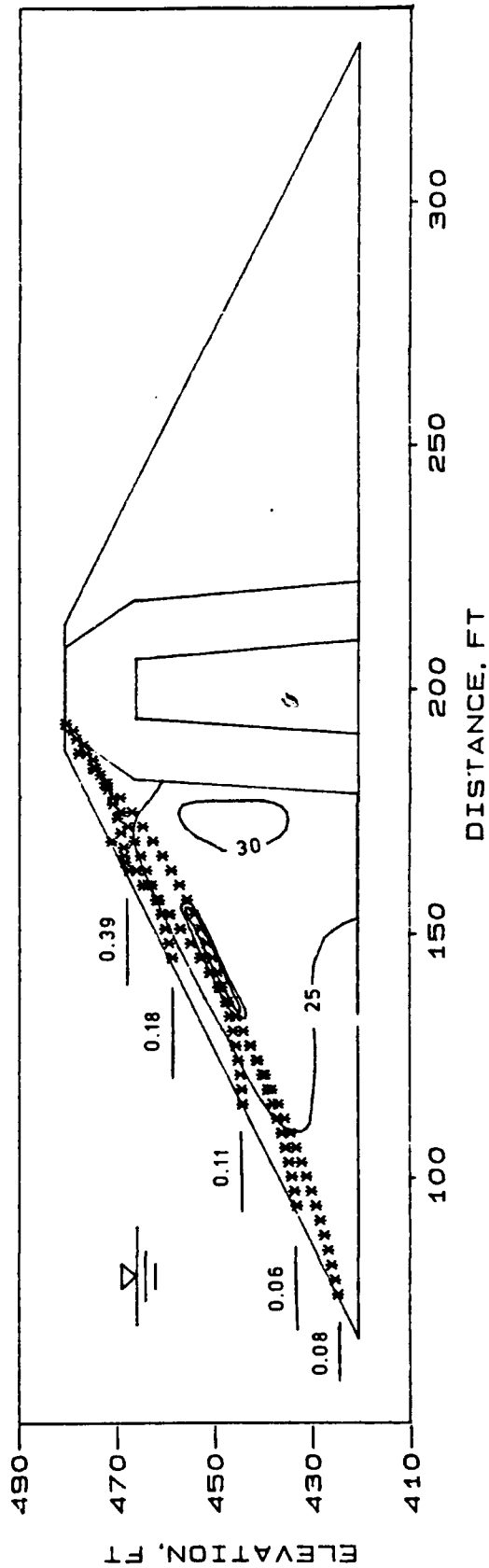


Figure 72. Yield accelerations for critical slip circles confined to the upstream shell

POST-EARTHQUAKE PERMANENT DISPLACEMENT ANALYSIS
 FOLSOM - MORMAN ISLAND DAM STA. 426+00 FOUNDATION: ROCK
 YIELD ACCELERATION SEISMIC COEFFICIENT (KY)

CASE I FAILURE CIRCLES EXITING DOWNSTREAM OF THE CENTERLINE

KEY I

FAILURE CIRCLES *****
 RUX% CONTOURS _____

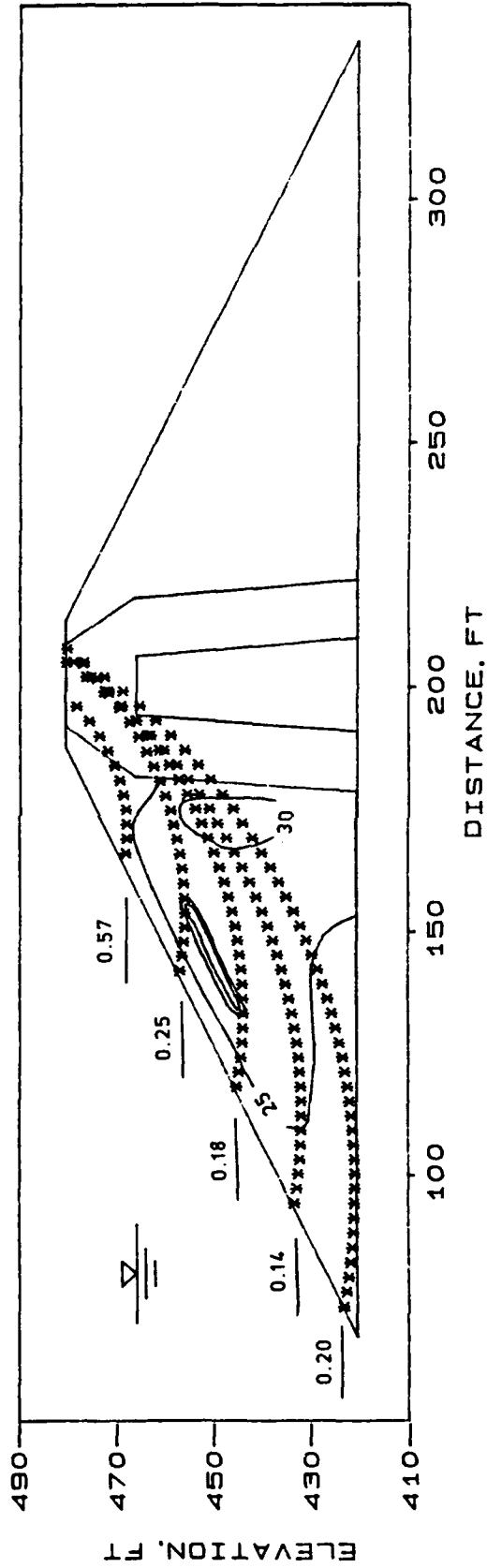


Figure 73. Yield accelerations for critical slip circles exiting downstream of the center line

MID ROCK STA 426+00

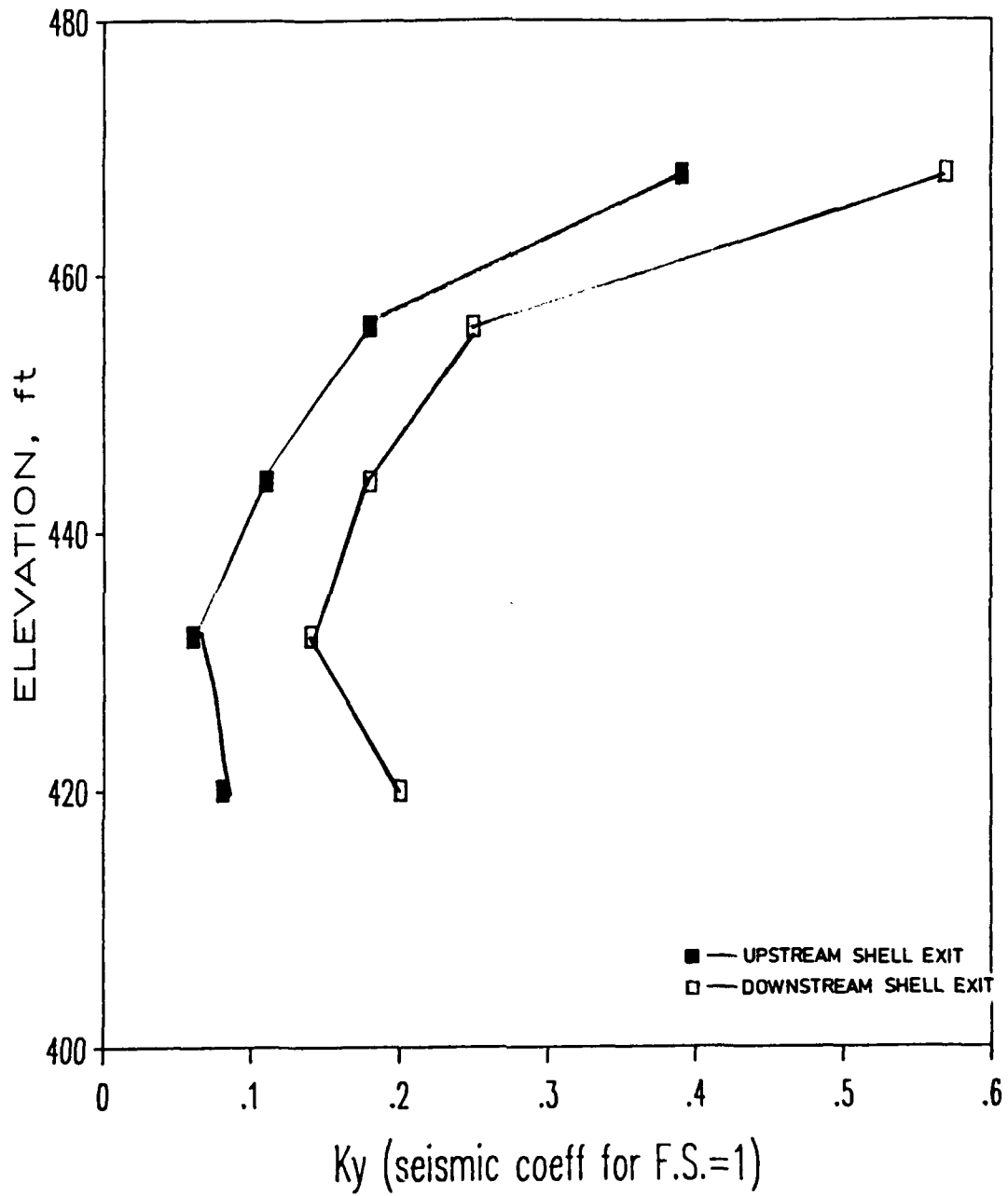
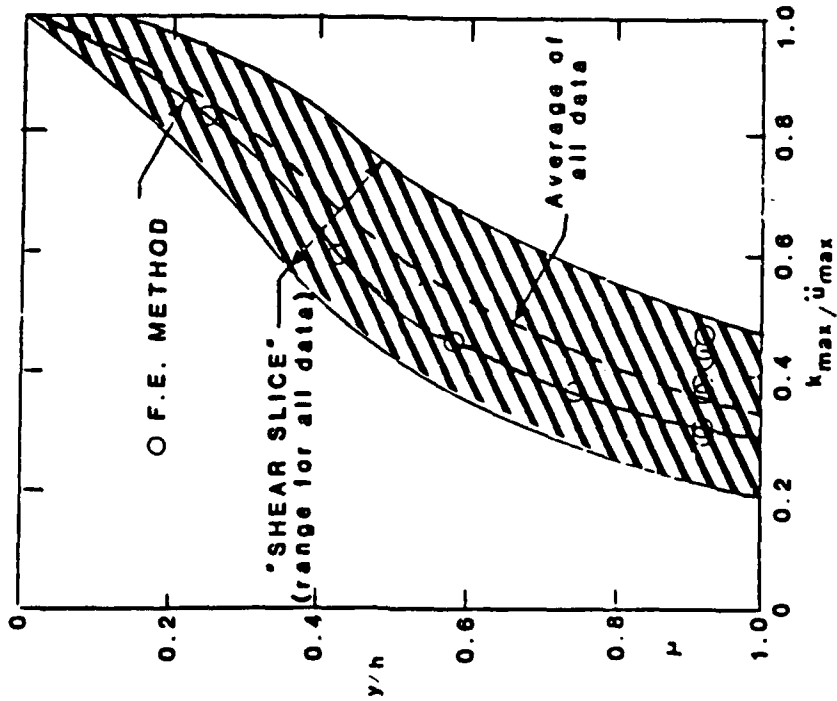
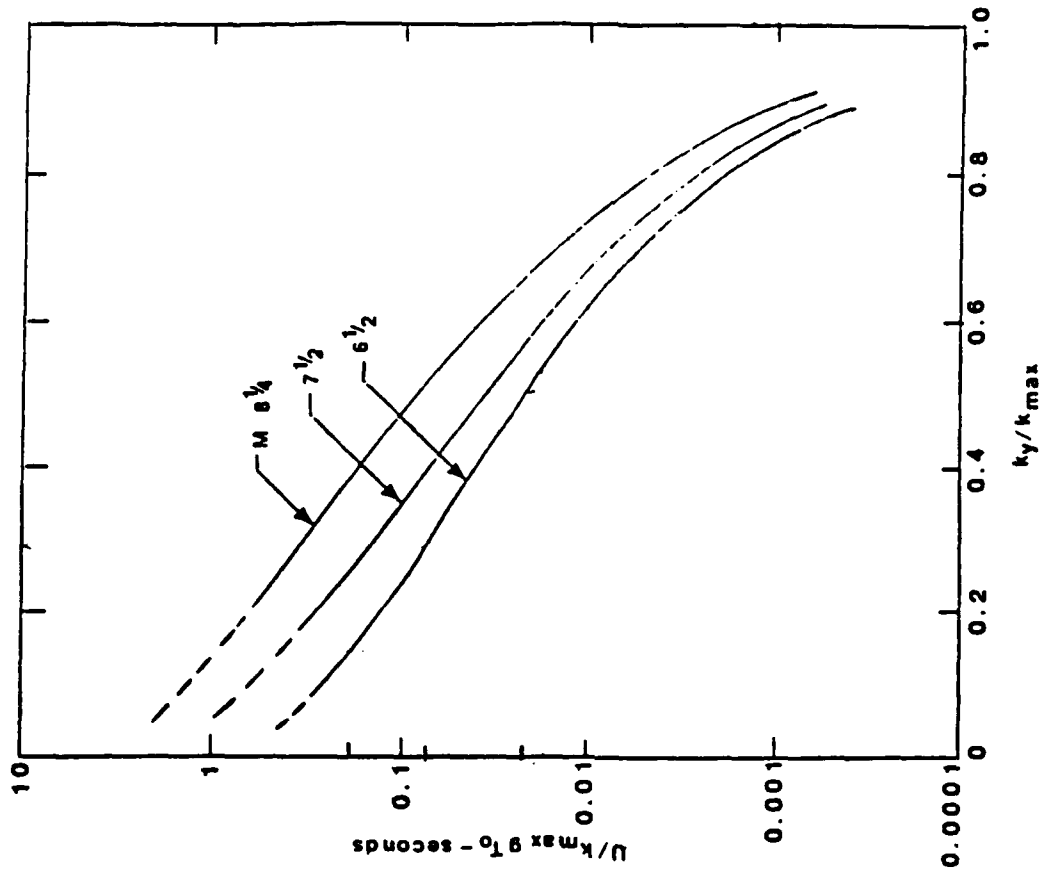


Figure 74. Yield acceleration versus depth for rock section



VARIATION OF 'MAXIMUM ACCELERATION RATIO' WITH DEPTH OF SLIDING MASS (AFTER MAKDISI-SEED, 1977)



VARIATION OF AVERAGE NORMALIZED DISPLACEMENT WITH YIELD ACCELERATION (AFTER MAKDISI-SEED, 1977)

Figure 75. Normal charts for computing displacements using the Makdisi-Seed technique

DISPLACEMENT vs. ELEVATION

MAKDISI-SEED METHOD

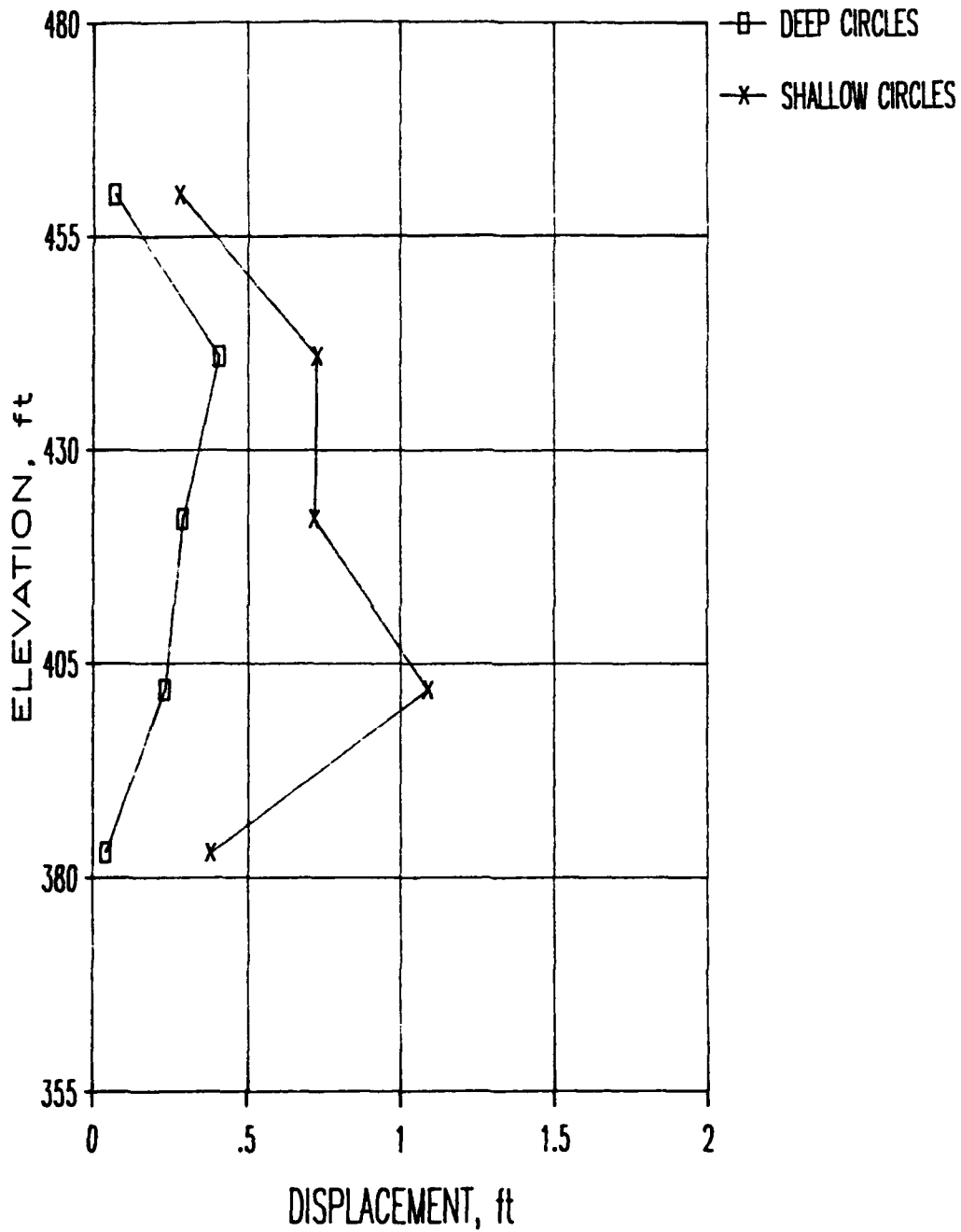
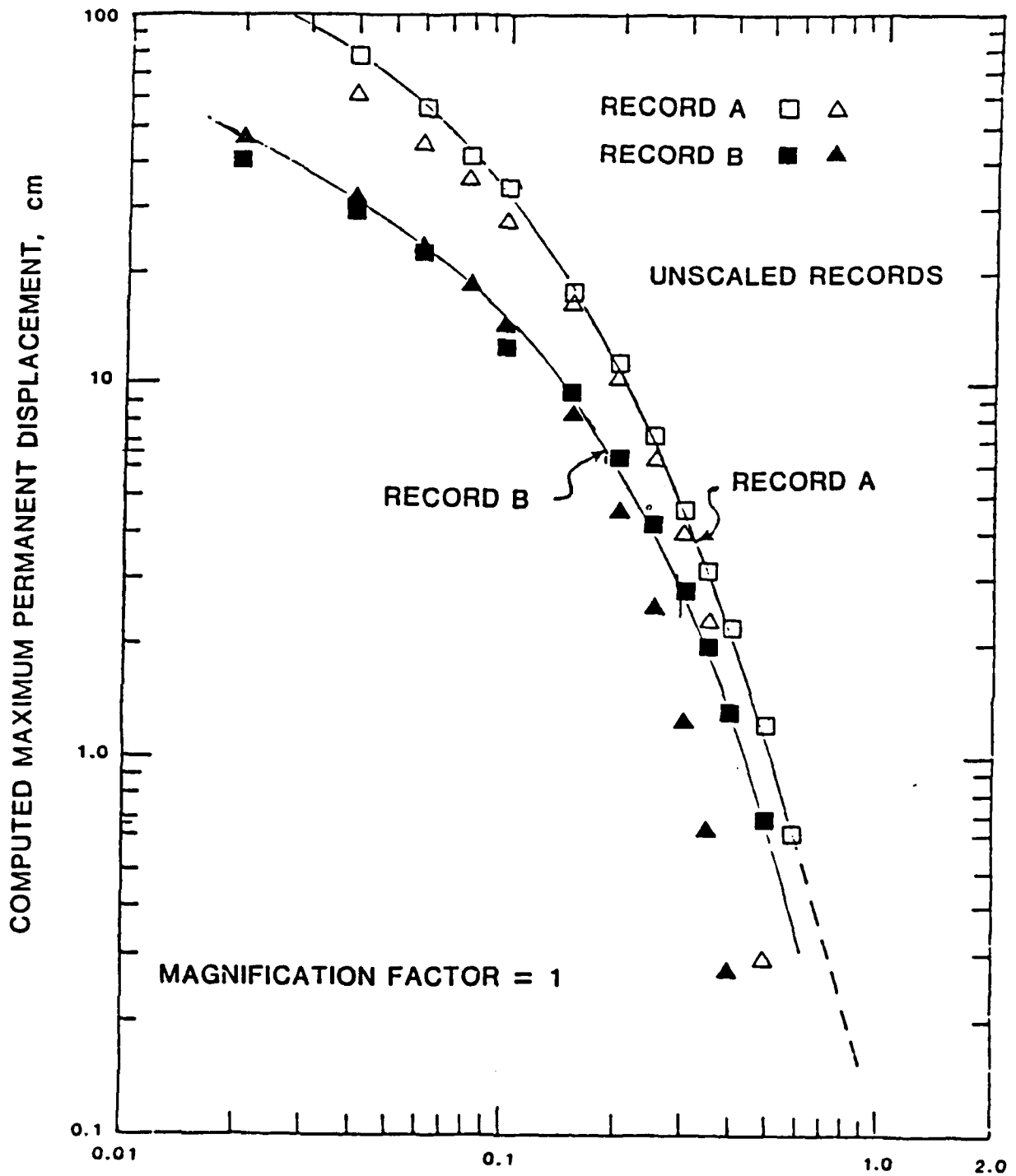


Figure 76. Permanent displacements computed for the idealized section founded on rock by the Makdisi-Seed method



$$\frac{N}{A} = \frac{\text{MAXIMUM EARTHQUAKE COEFFICIENT}}{\text{MAXIMUM EARTHQUAKE ACCELERATION}}$$

Figure 77. Sliding block analysis--computed permanent displacements for Accelerograms A and B

DISPLACEMENT vs ELEVATION

SARMA METHOD, RECORD A

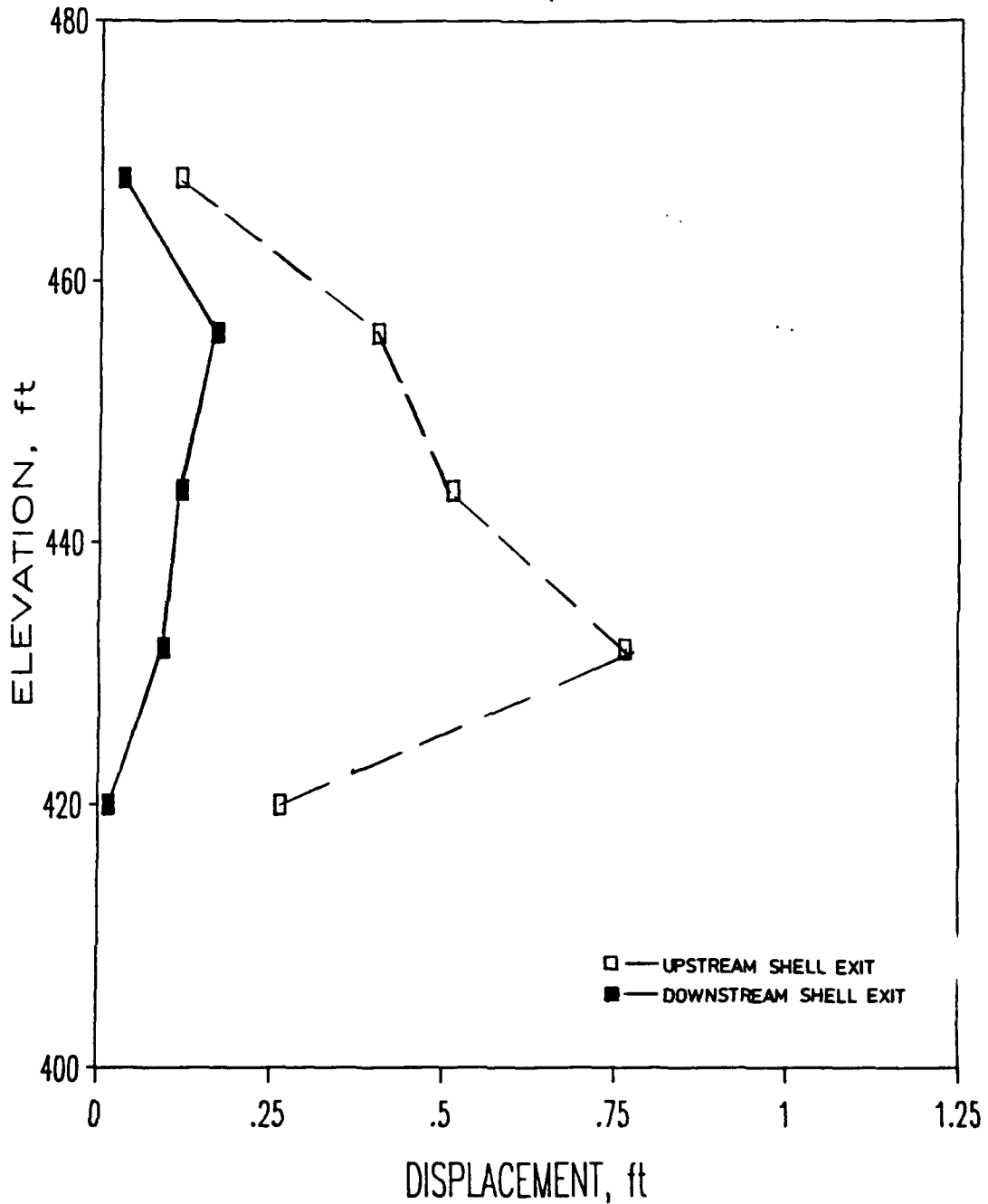


Figure 78. Permanent displacements computed for the idealized section founded on rock by the Sarma-Ambrayseys method

FOLSOM - MORMON ISLAND DAM STA. 446+00

IDEALIZED CROSS SECTION USED FOR FINITE ELEMENT ANALYSIS

LEGEND:

- 1 - MOIST GRAVEL EMBANKMENT GRAVEL
- 2 - SUBMERGED EMBANKMENT GRAVEL
- 3 - MOIST DECOMPOSED GRANITE
- 4 - SUBMERGED DECOMPOSED GRANITE
- 5 - CENTRAL IMPERVIOUS CORE
- 6 - UNDREDGED ALLUVIUM

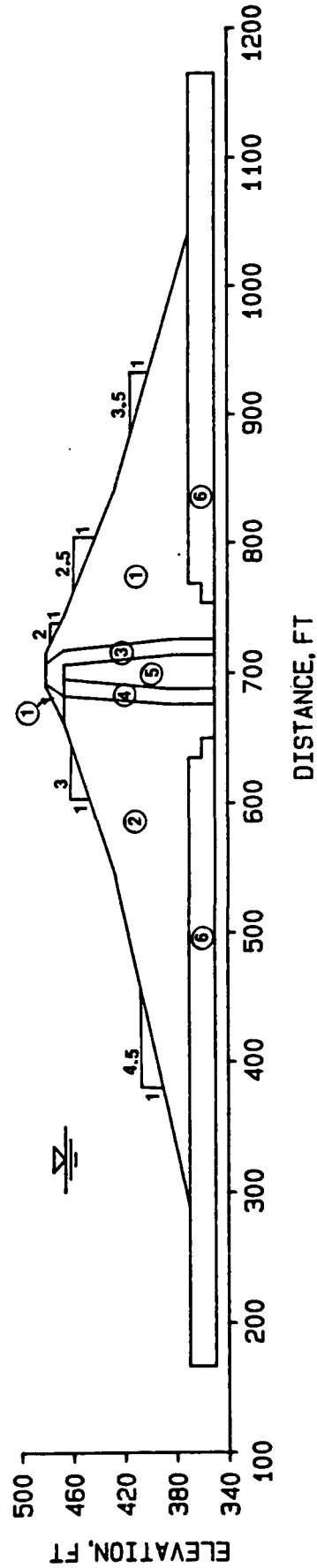


Figure 79. Idealized cross section used for finite element analysis, sta 446+00, representing section of Mormon Island Dam where shells are founded on alluvium

FOLSOM - MORMON ISLAND DAM STA. 446+00

IDEALIZED CROSS SECTION USED FOR STABILITY ANALYSIS

LEGEND:

- 1 - MOIST GRAVEL EMBANKMENT GRAVEL
- 2 - SUBMERGED EMBANKMENT GRAVEL
- 3 - MOIST DECOMPOSED GRANITE
- 4 - SUBMERGED DECOMPOSED GRANITE
- 5 - CENTRAL IMPERVIOUS CORE
- 6 - UNDRIDGED ALLUVIUM

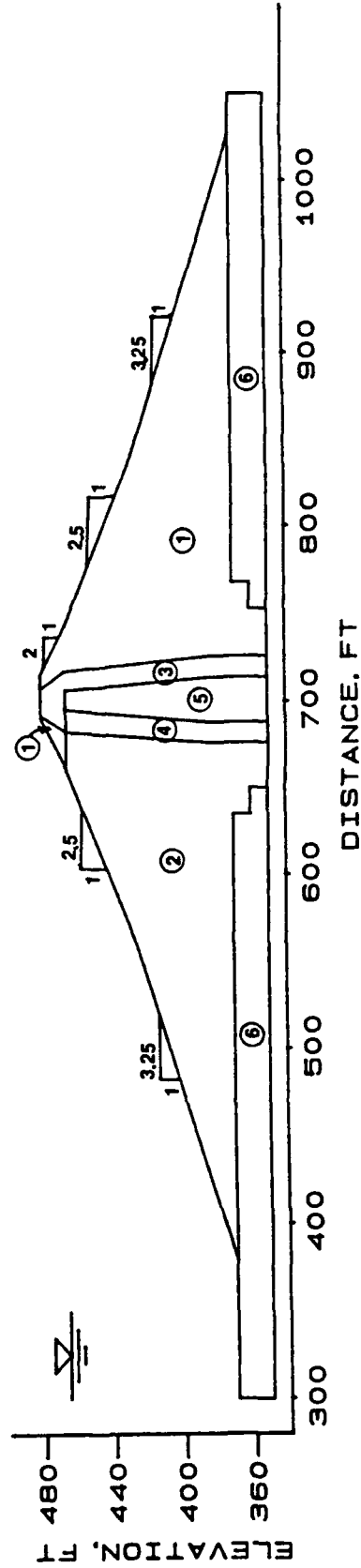


Figure 80. Idealized cross section used for stability analysis, sta 442+00, representing section of Mormon Island Dam where shells are founded on alluvium

FOLSOM - MORMON ISLAND DAM STA. 446+00
 MESH USED FOR FINITE ELEMENT ANALYSIS

NOTE:

332 NODAL POINTS
 297 ELEMENTS

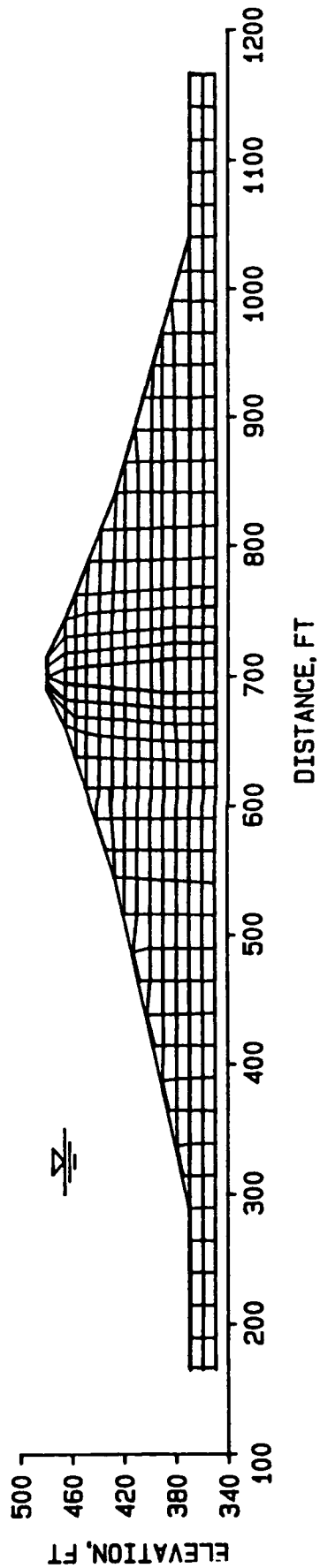


Figure 81. Finite element mesh used for section of Mormon Island Dam where the shells are founded on undredged alluvium

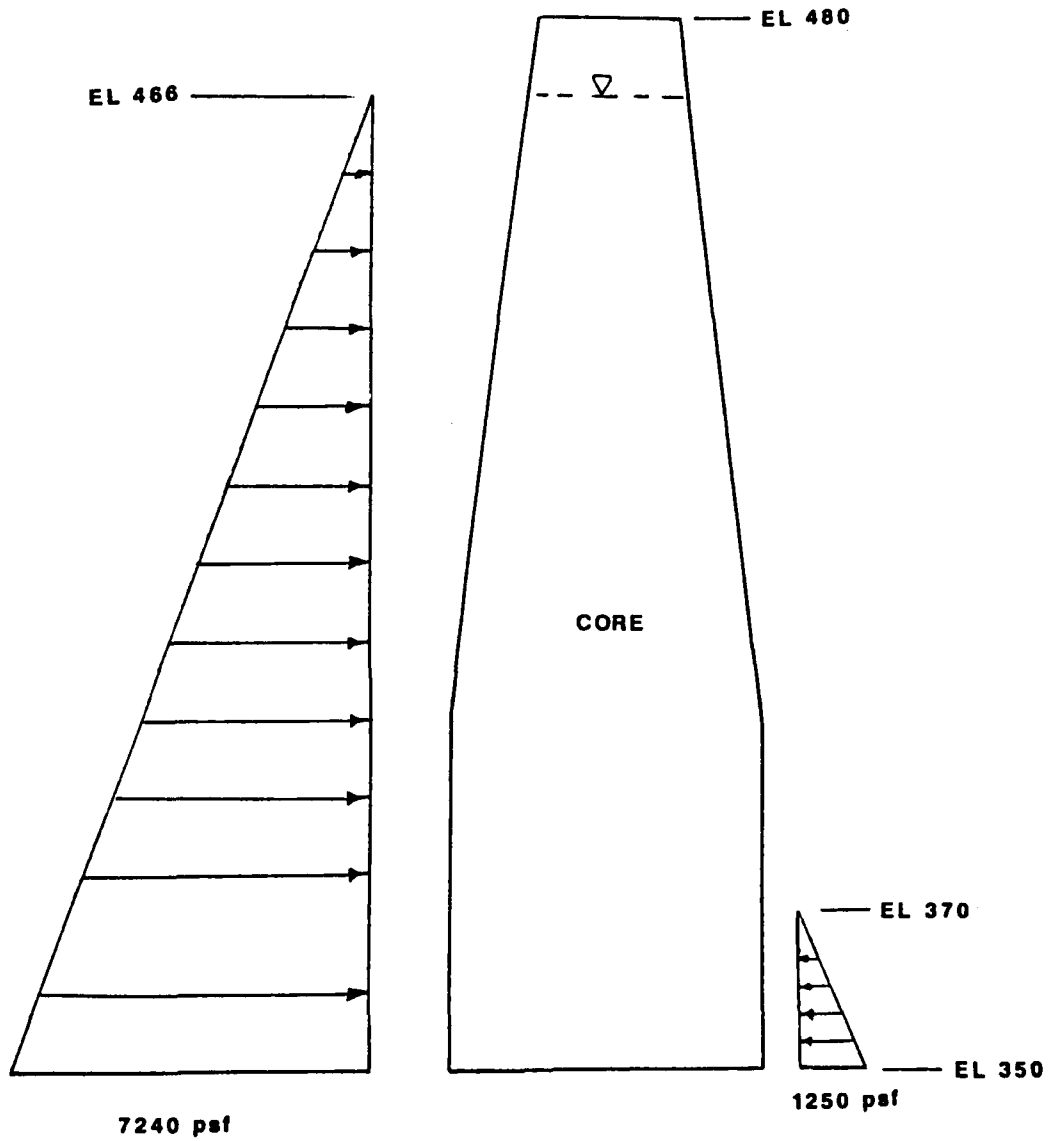


Figure 82. Unbalanced hydrostatic pressures acting against impervious core of the dam for undredged section

FOLSOM PROJECT - MORMON ISLAND DAM
CROSS SECTION FOR UNDRIDGED FOUNDATION

STA 446 + 00

CONTOURS OF VERTICAL EFFECTIVE STRESS (psf)

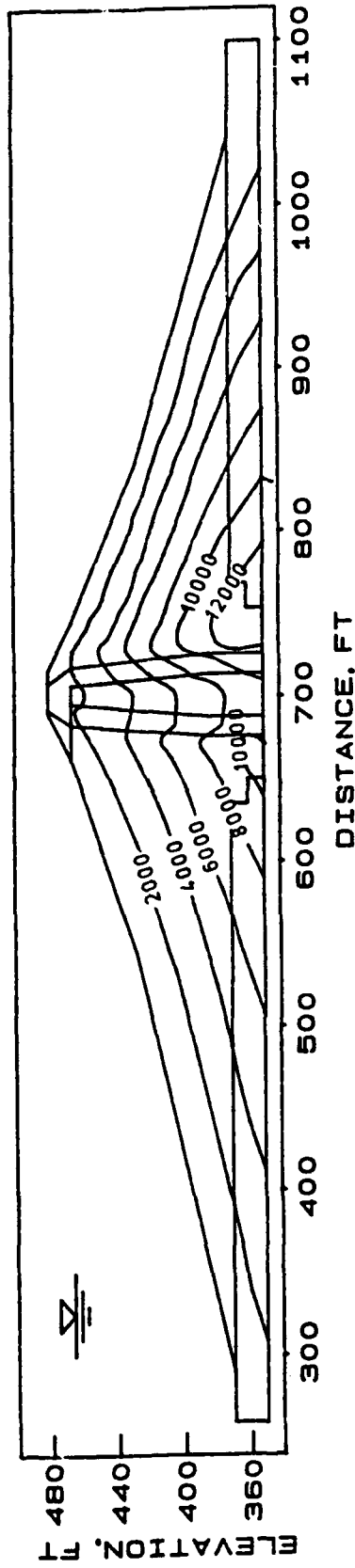


Figure 83. Contours of vertical effective stress

FOLSOM PROJECT - MORMON ISLAND DAM
CROSS SECTION FOR UNDREDGED FOUNDATION

STA 446 + 00

CONTOURS OF HORIZONTAL EFFECTIVE STRESS (psf)

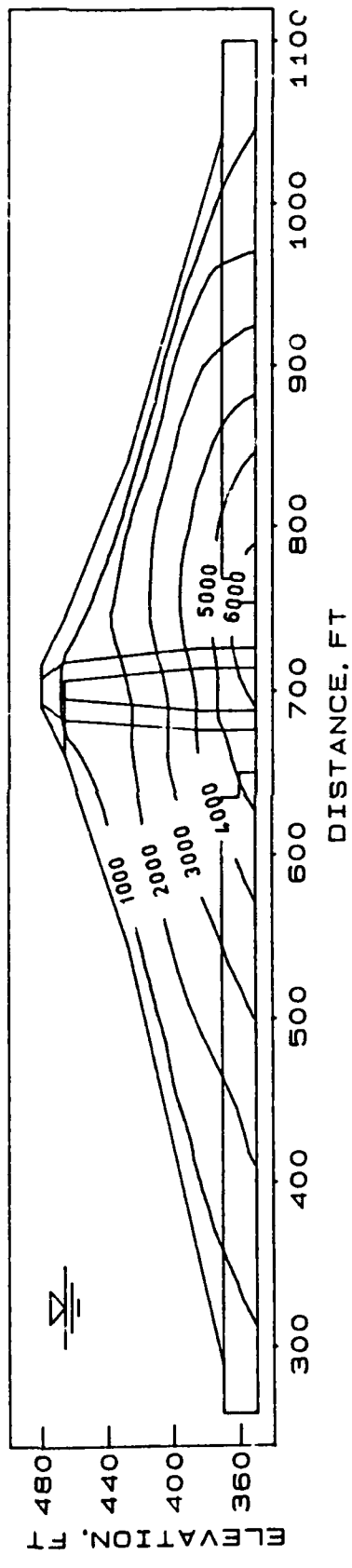


Figure 84. Contours of horizontal effective stress

FOLSOM PROJECT - MORMON ISLAND DAM
 CROSS SECTION FOR UNDRIDGED FOUNDATION

STA 446 + 00

CONTOURS OF SHEAR STRESS ACTING ON HORIZONTAL PLANE (psf)

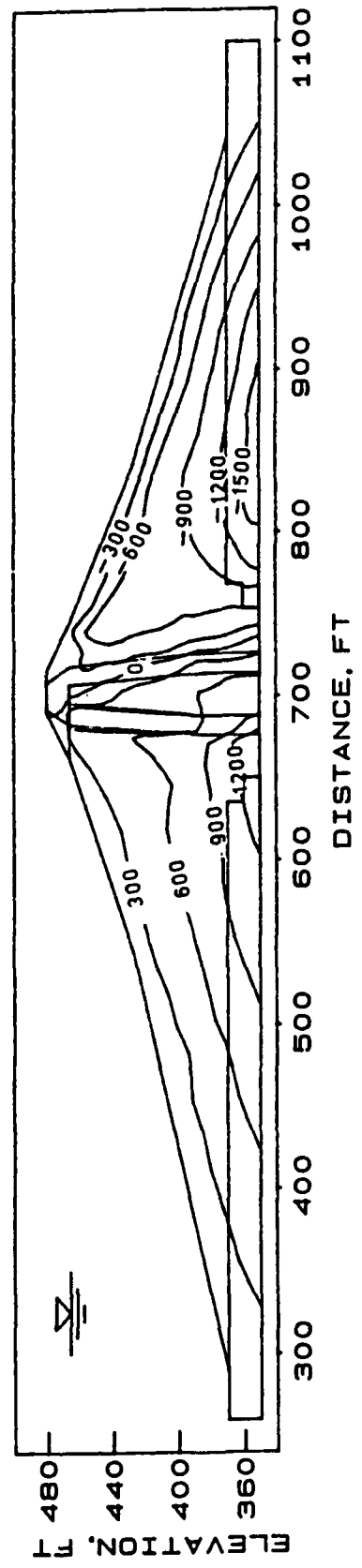


Figure 85. Contours of shear stress acting on horizontal planes

FOLSOM PROJECT - MORMON ISLAND DAM
CROSS SECTION FOR UNDRIDGED FOUNDATION

STA 446 + 00

CONTOURS OF ALPHA RATIO

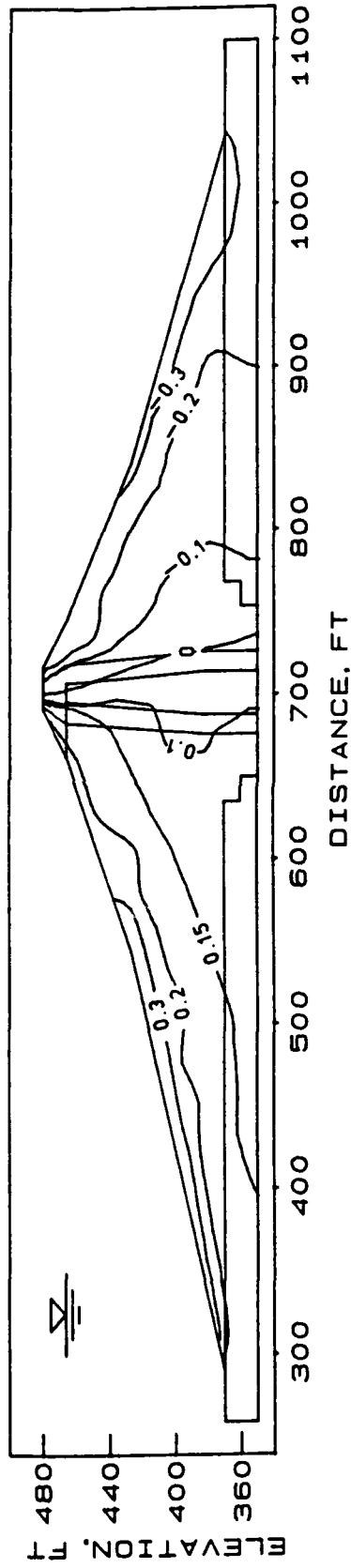


Figure 86. Contours of α

FOLSOM PROJECT - MORMON ISLAND DAM
CROSS SECTION FOR UNDRIDGED FOUNDATION

STA 446 + 00

CONTOURS OF MEAN NORMAL PRESSURE (psf)

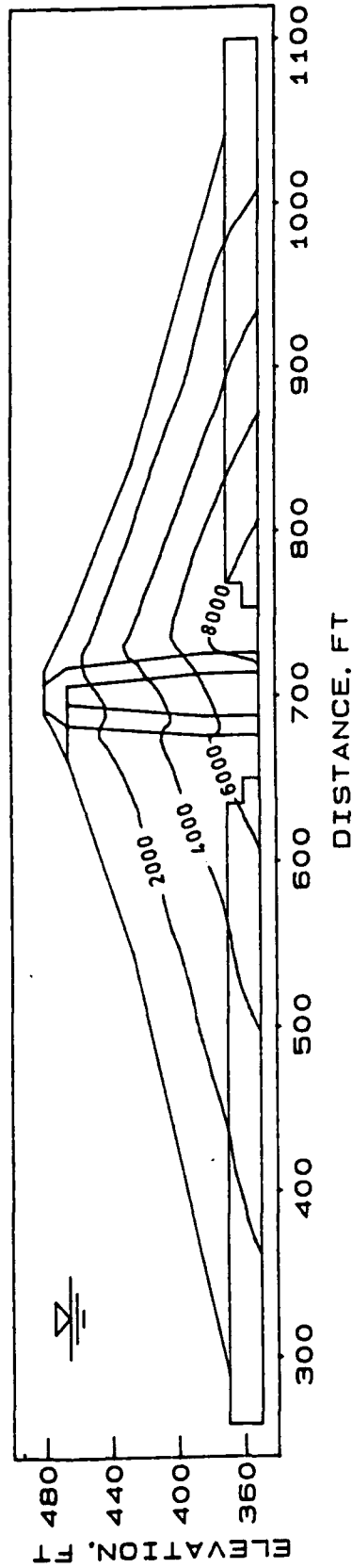


Figure 87. Contours of effective mean normal pressure

FOLSOM PROJECT - MORMON ISLAND DAM
CROSS SECTION FOR UNDREDGED FOUNDATION

STA 446 + 00

CONTOURS OF SHEAR WAVE VELOCITY (fps)

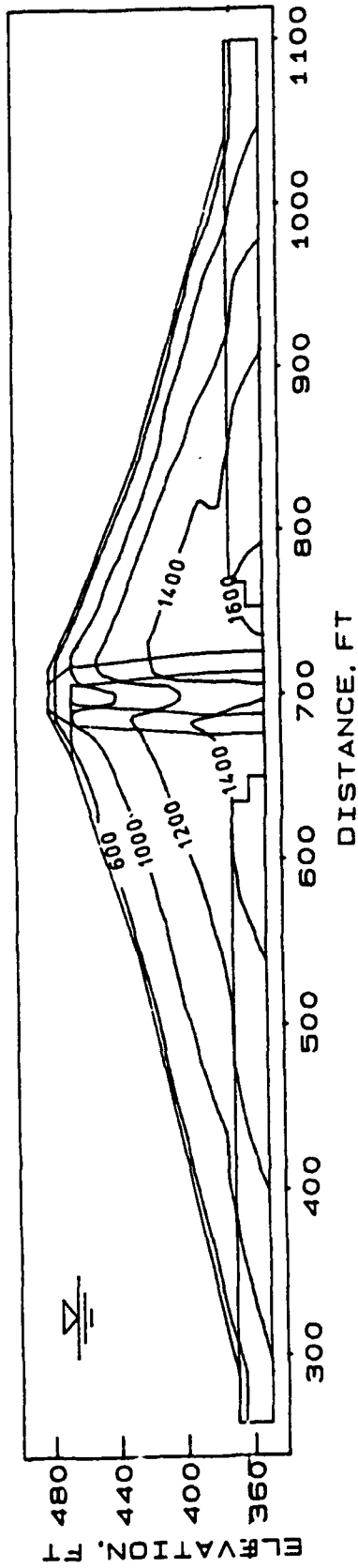


Figure 88. Shear wave velocity distribution

FOLSOM PROJECT - MORMON ISLAND DAM
 CROSS SECTION FOR UNDRIDGED FOUNDATION

STA 446 + 00

CONTOURS OF LOW STRAIN AMPLITUDE SHEAR MODULUS (ksf)

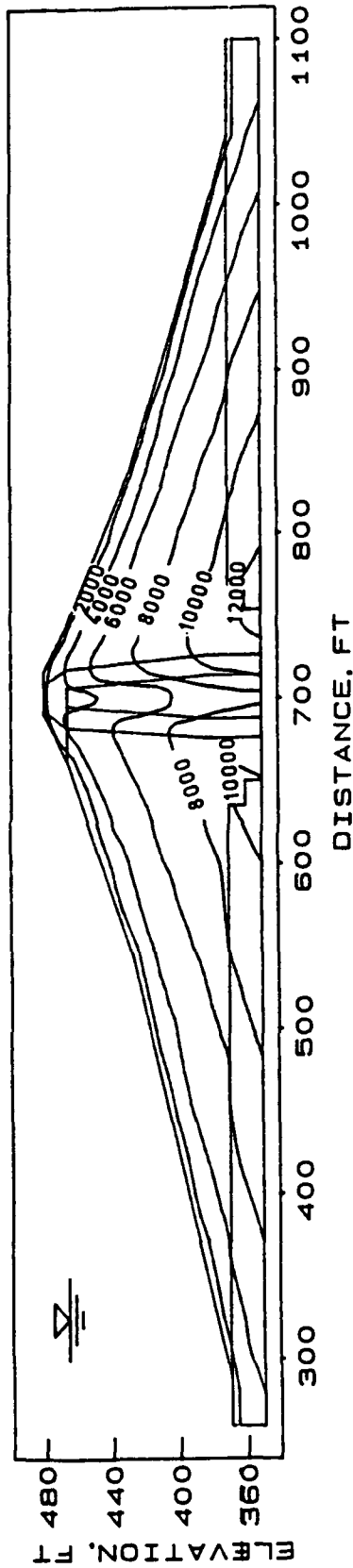


Figure 89. Low strain amplitude shear modulus G_{max} distribution

FOLSOM PROJECT - MORMON ISLAND DAM
 CROSS SECTION FOR UNDREDGED FOUNDATION

STA 446 + 00

CONTOURS OF DYNAMIC SHEAR STRESS (psf)

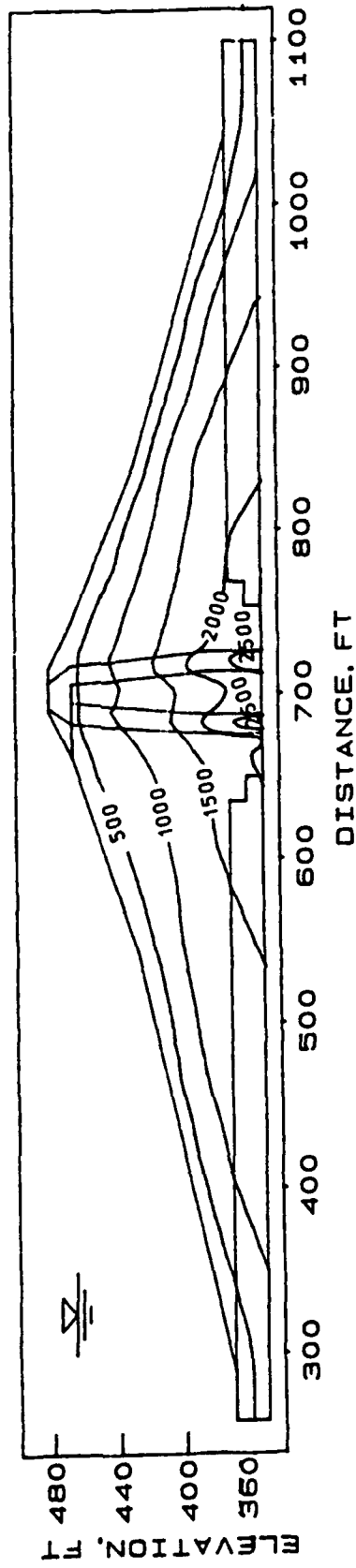


Figure 90. Dynamic shear stresses induced in the embankment and undredged foundation by Accelerogram B

FOLSOM - MORMON ISLAND DAM STA. 445+00

ACCELEROGRAM B

FUNDAMENTAL PERIOD AT STRAIN LEVELS INDUCED BY RECORD A - 0.74 sec
 LOW STRAIN AMPLITUDE FUNDAMENTAL PERIOD - 0.30 sec
 ACCELERATIONS ARE IN g's

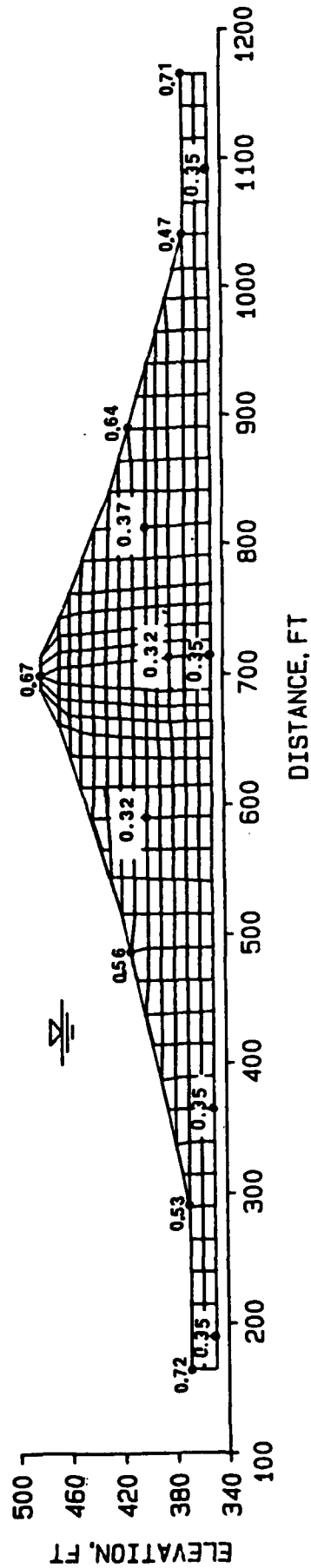


Figure 91. Peak acceleration computed by FLUSH for selected nodal points and fundamental period for low strain amplitude and strain amplitude levels induced by the motions of the design earthquake

FOLSOM - MORMON ISLAND DAM STA. 446+00

ACCELEROGRAM B

EFFECTIVE SHEAR STRAINS IN PERCENT

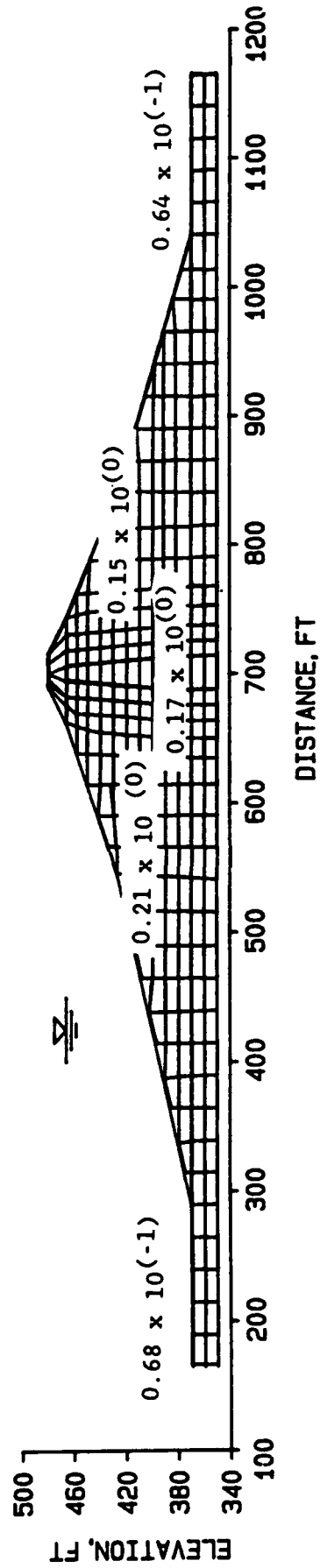


Figure 92. Strain levels induced by Accelerogram B

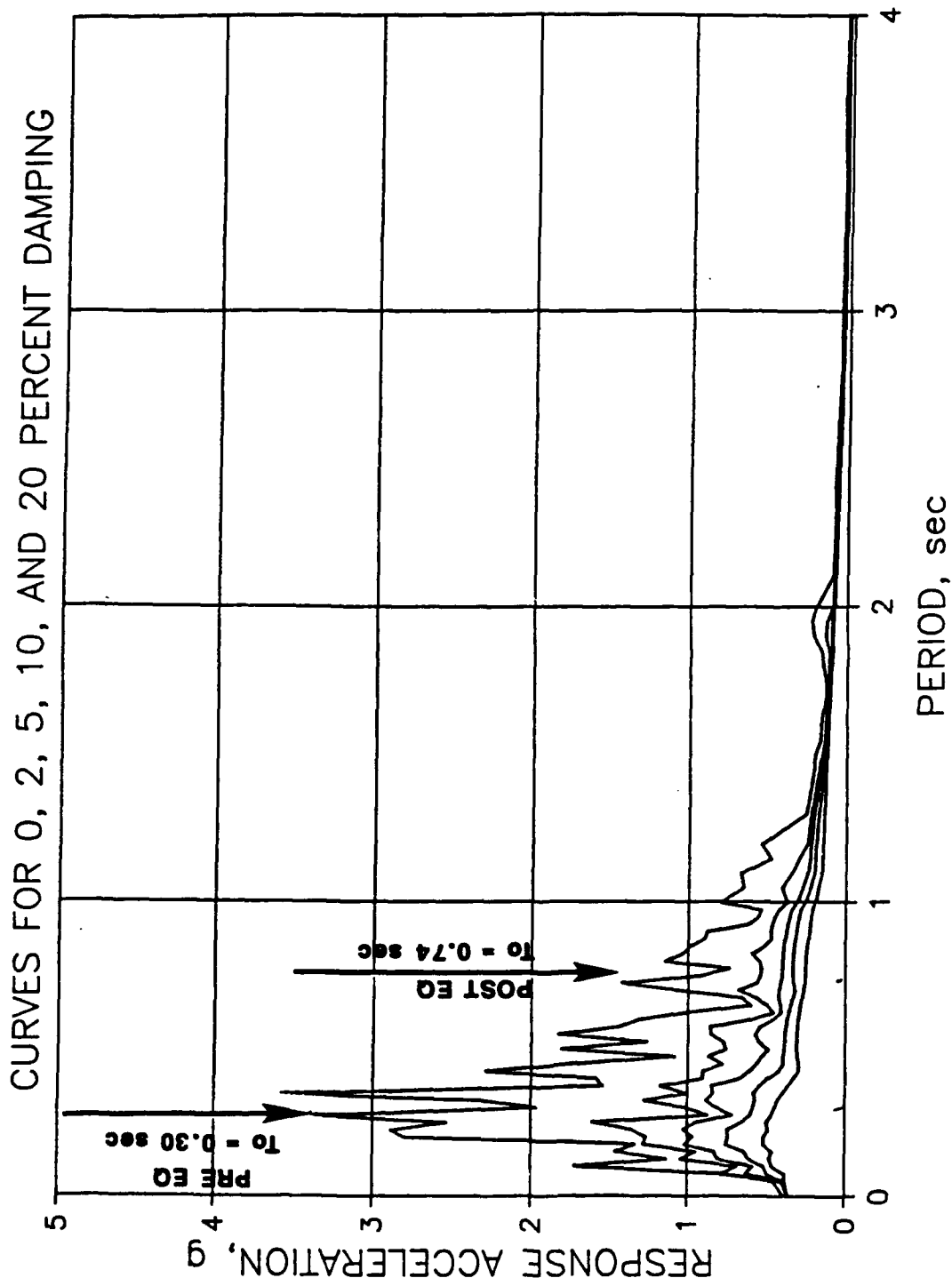


Figure 93. Response spectra of Accelerogram B compared with the low strain amplitude and design earthquake strain level fundamental periods of the embankment

FOLSOM PROJECT - MORMON ISLAND DAM

CROSS SECTION FOR UNREDGED FOUNDATION

STA 446 + 00

CONTOURS OF SAFETY FACTOR AGAINST LIQUEFACTION

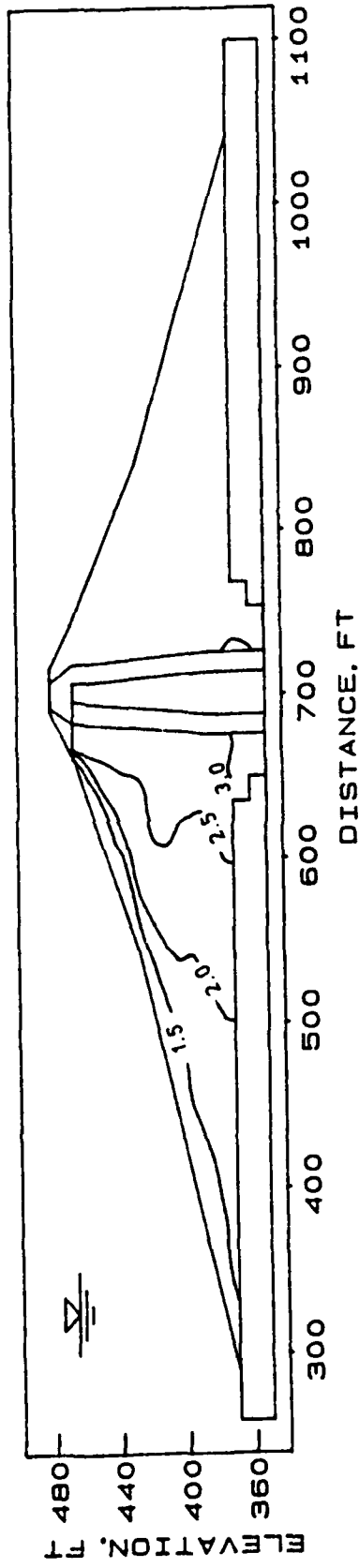


Figure 94. Contours of the safety factor against liquefaction, FS_L

FOLSOM PROJECT - MORMON ISLAND DAM

CROSS SECTION FOR UNREDGED FOUNDATION

STA 446 + 00

CONTOURS OF EXCESS PORE PRESSURE RATIO

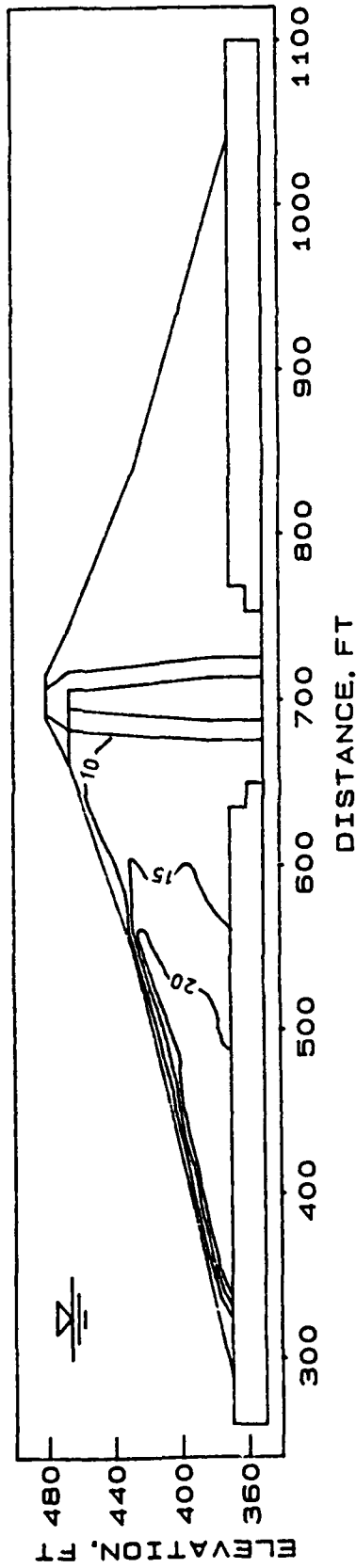


Figure 95. Contours of excess pore pressure ratio R_u in percent superimposed on the cross section used in the finite element analysis

FOLSOM PROJECT - MORMON ISLAND DAM
 CROSS SECTION FOR UNDREDGED FOUNDATION

STA 442 + 00

CONTOURS OF EXCESS PORE PRESSURE USED IN STABILITY COMPUTATIONS

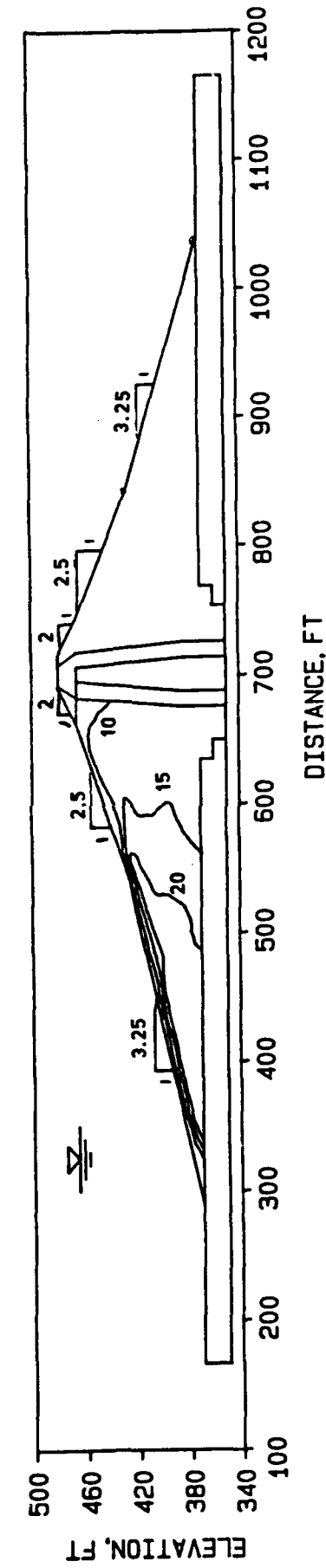


Figure 96. Contours of R_u superimposed on idealized cross section used in stability analysis

POST EARTHQUAKE STABILITY ANALYSIS

FOLSOM - MORMON ISLAND DAM STA. 442+00 FOUNDATION: UNDRIDGED GRAVELS

FACTOR OF SAFETY AGAINST SLOPE FAILURE I

PRE-EARTHQUAKE - 2.26

POST-EARTHQUAKE - 1.91

KEY I

FAILURE CIRCLE *****
 RUX CONTOURS _____

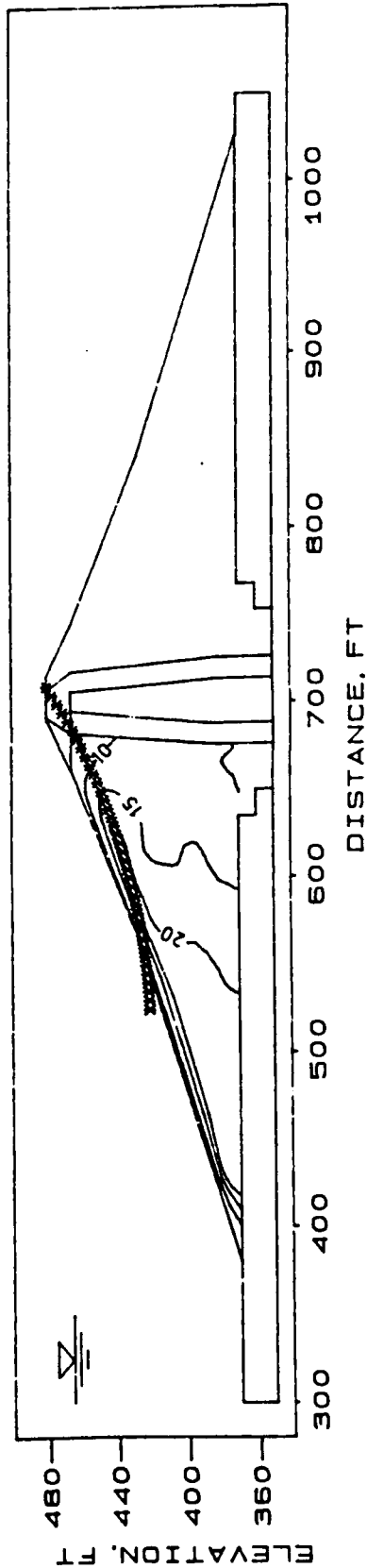


Figure 97. Safety factor against sliding and critical circle from post-earthquake stability analysis of undredged section

POST-EARTHQUAKE PERMANENT DISPLACEMENT ANALYSIS

FOLSOM - MORMON ISLAND DAM STA. 442+00 FOUNDATION: UNDREDGED GRAVELS

YIELD ACCELERATION SEISMIC COEFFICIENT (KY)

CASE I FAILURE CIRCLES CONFINED TO UPSTREAM SHELL

KEY I

FAILURE CIRCLES *****
 RUX CONTOURS _____

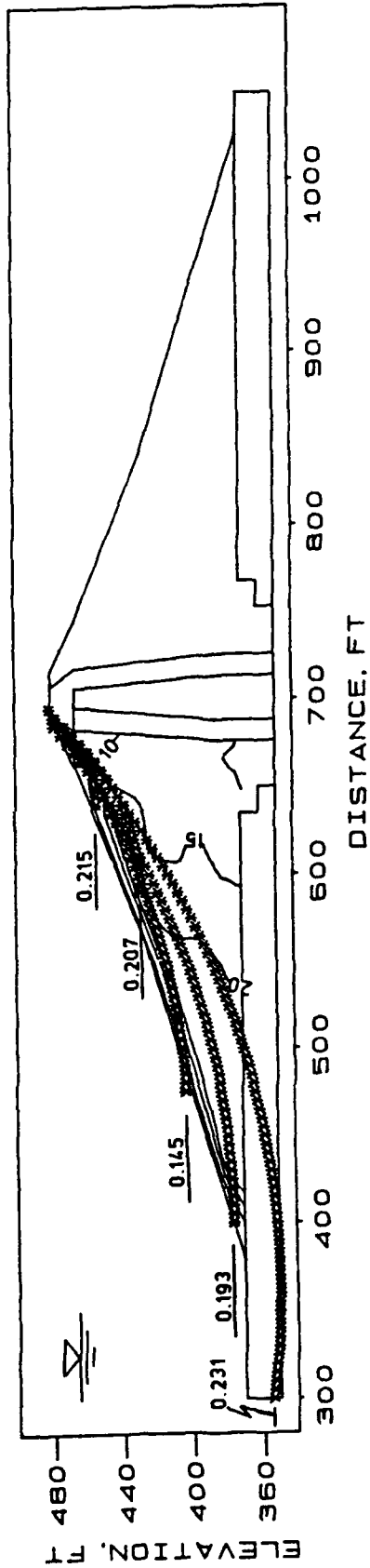


Figure 98. Yield accelerations for critical slip circles confined to the upstream shell of undredged foundation cross section

POST-EARTHQUAKE PERMANENT DISPLACEMENT ANALYSIS

FOLSOM - MORMON ISLAND DAM STA. 442+00 FOUNDATION: UNDRIDGED GRAVELS

YIELD ACCELERATION SEISMIC COEFFICIENT (KY)

CASE 1 FAILURE CIRCLES EXITING DOWNSTREAM OF THE CENTERLINE

KEY 1

FAILURE CIRCLES *****
 RUX CONTOURS _____

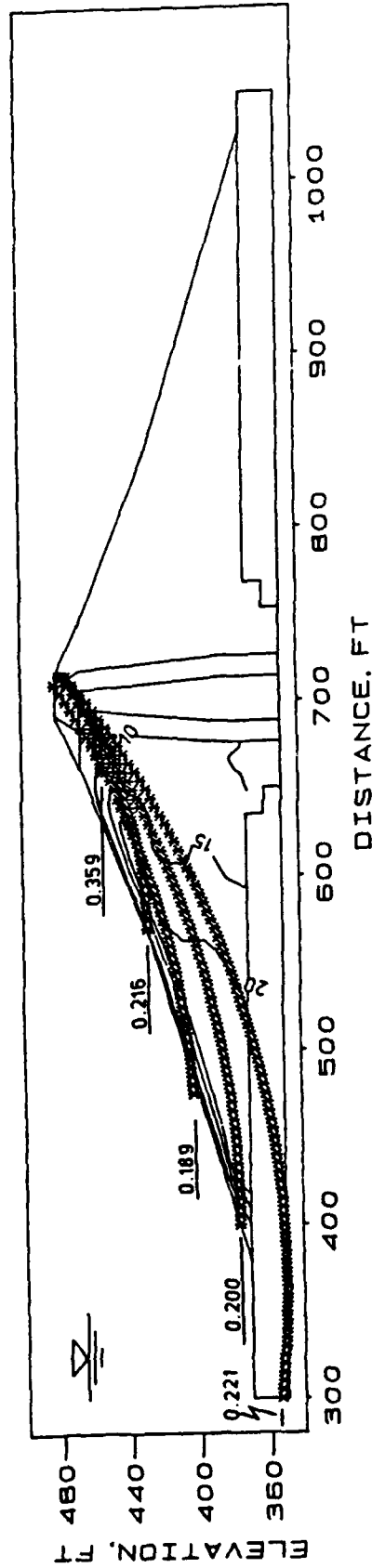


Figure 99. Yield accelerations for critical slip circles exiting downstream of the center line of undredged foundation cross section

MID UNDREDGED STA 442+00

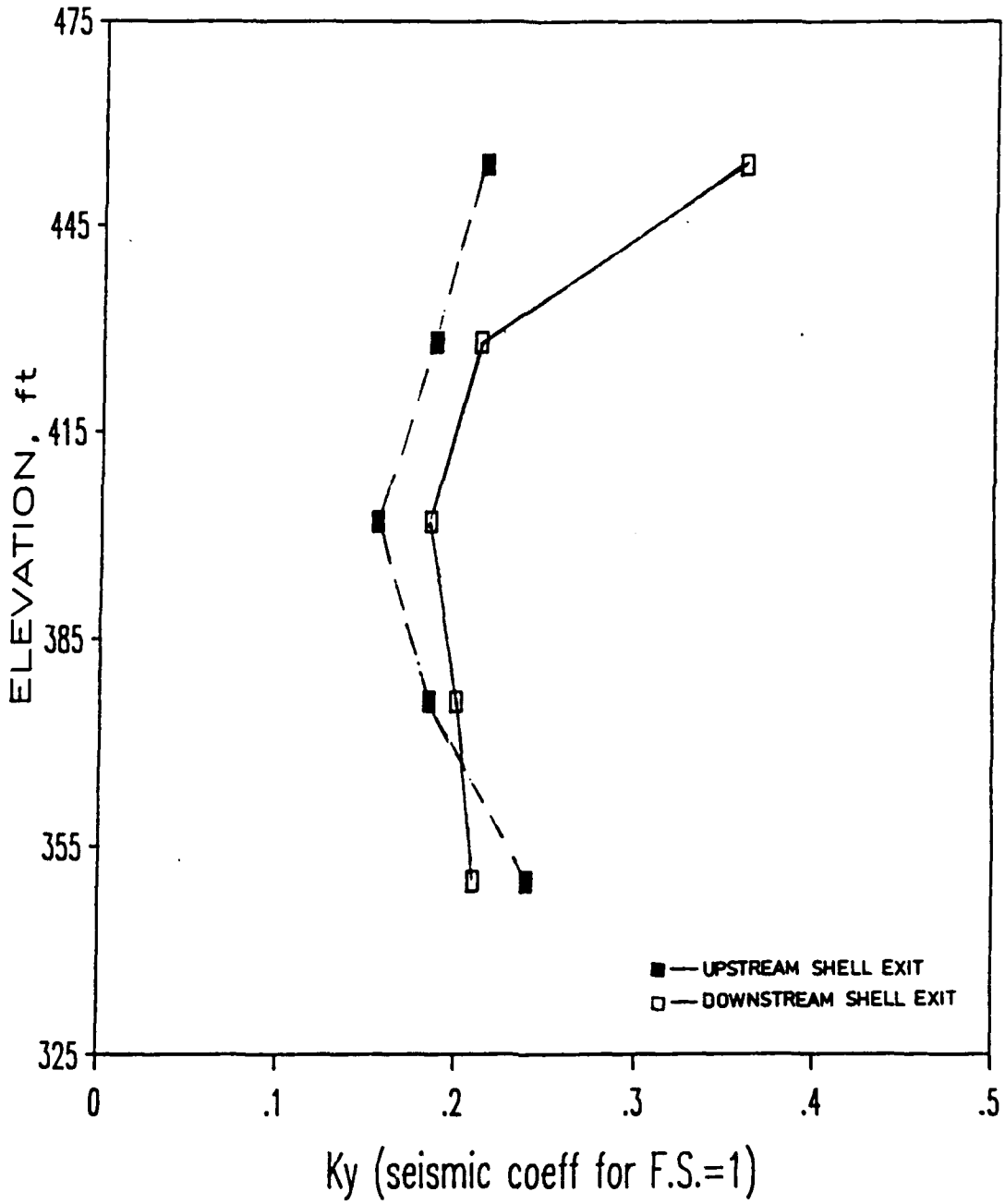


Figure 100. Yield acceleration versus tangent elevation for undredged foundation cross section

DISPLACEMENT vs ELEVATION

MAKDISI-SEED METHOD, RECORD B

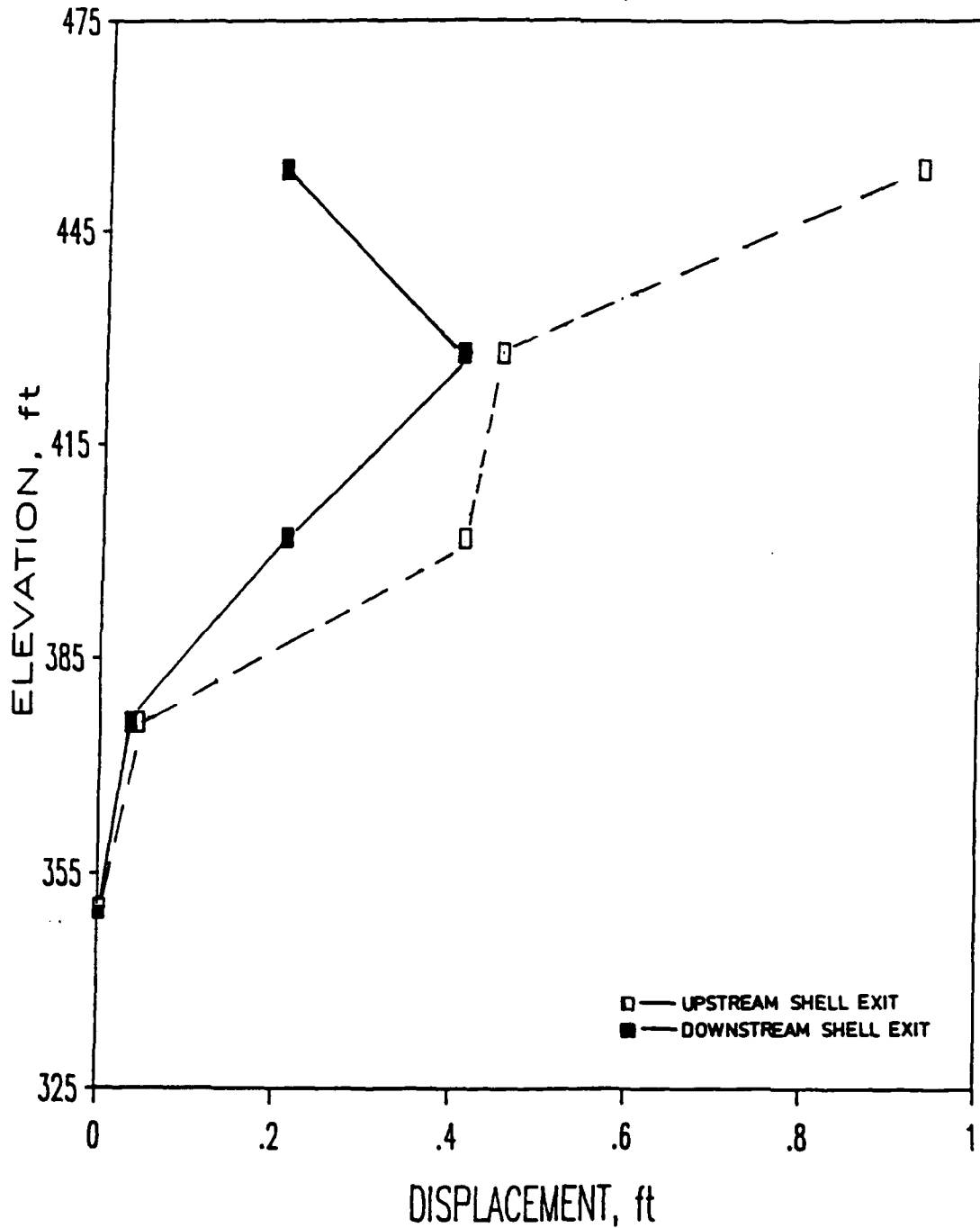


Figure 101. Permanent displacements computed for the idealized section founded on undredged alluvium by the Makdisi-Seed technique

DISPLACEMENT vs ELEVATION

SARMA METHOD, RECORD A

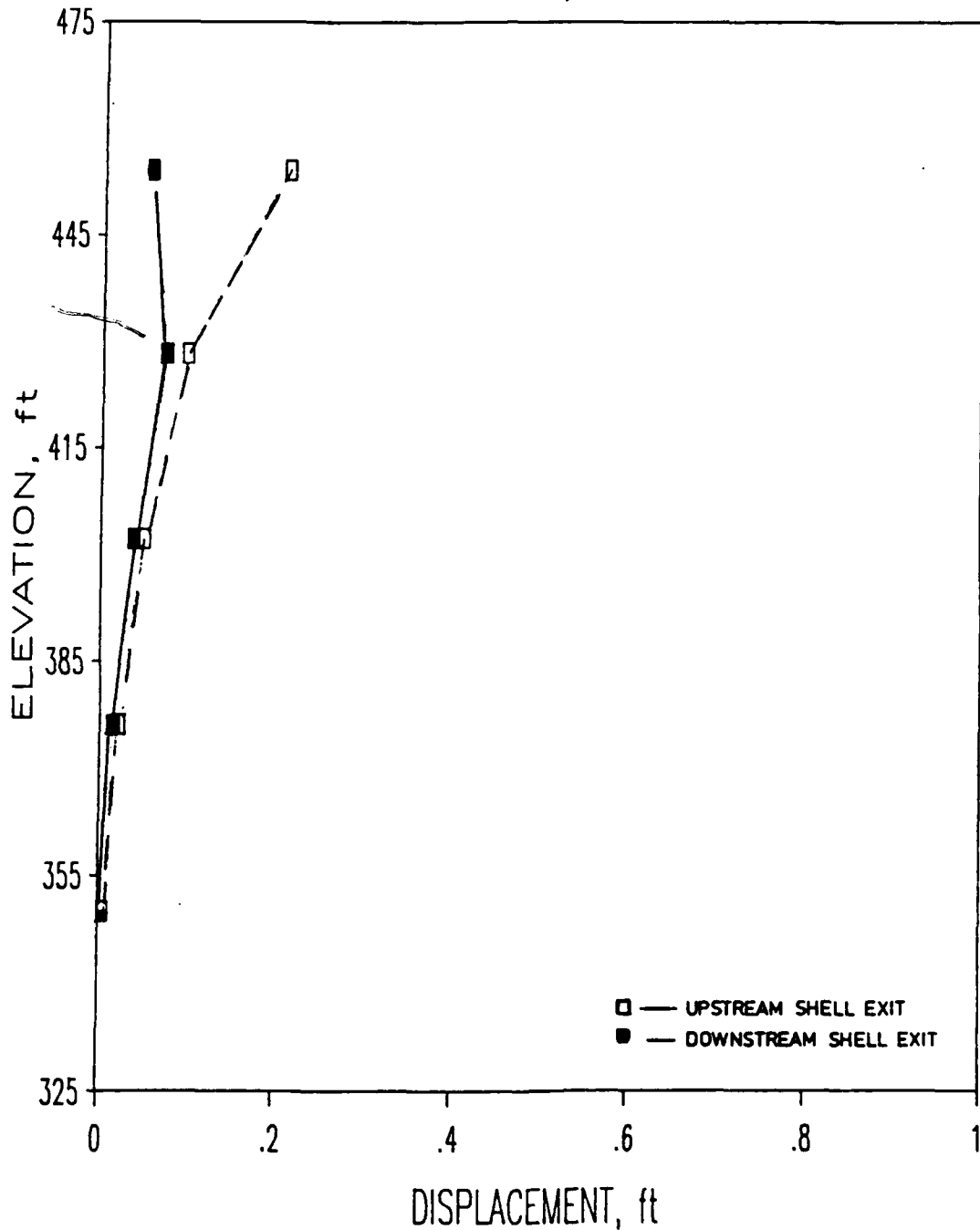


Figure 102. Permanent displacements computed for the idealized section founded on undredged alluvium by the Sarma-Ambrayseys technique

APPENDIX A
CONVERSION OF BECKER BLOWCOUNTS INTO EQUIVALENT STANDARD
PENETRATION TEST BLOWCOUNTS FOR PHASE II
FIELD INVESTIGATIONS

Contract Report by Dr. Leslie F. Harder

October, 1987

EVALUATION OF BECKER PENETRATION TESTS
PERFORMED AT MORMON ISLAND AUXILIARY DAM IN 1986

Report Prepared for:

GEOTECHNICAL LABORATORY
WATERWAYS EXPERIMENT STATION
U.S. ARMY CORPS OF ENGINEERS

by

LESLIE F. HARDER, Jr.

September 1988

Table of Contents

	<u>Page</u>
SECTION 1: INTRODUCTION	1
Background	1
Scope of Work	2
SECTION 2: DETERMINATION OF EQUIVALENT SPT BLOWCOUNTS	6
Previous Becker Explorations Performed at Mormon Island	6
1986 Mormon Island Becker Penetration Tests	14
Corrections to Becker Penetration Resistance for Combustion Energy	18
Conversion of Becker Blowcounts into Equivalent SPT Blowcounts	22
Comparisons Between 1983 and 1986 Becker Penetration Resistance	24
SECTION 3: ACCOUNTING FOR OVERBURDEN PRESSURE	29
Correction to 1 tsf Overburden Pressure	29
Effect of Sloping Ground Conditions on Overburden Correction Factor	33
SECTION 4: PRESENTATION OF RESULTS AND DETERMINATION OF CYCLIC LOADING RESISTANCE	37
Presentation of Results	37
Statistical Summary of Becker Data	65
SECTION 5: SUMMARY OF FINDINGS	78

Table of Contents (continued)

	<u>Page</u>
SECTION 6: REFERENCES	80
APPENDIX A: COMPUTATION TABLE FOR DETERMINING EQUIVALENT SPT BLOWCOUNTS FROM 1986 PLUGGED-BIT BECKER SOUNDINGS PERFORMED AT MORMON ISLAND AUXILIARY DAM	
APPENDIX B: CLASSIFICATION DATA FOR SAMPLES OBTAINED FROM 1986 OPEN-BIT BECKER SOUNDINGS PERFORMED AT MORMON ISLAND AUXILIARY DAM	

List of Figures

Title	Page
1. Schematic Diagram of Becker Sampling Operation (after Harder and Seed, 1986)	3
2. Plan View of Mormon Island Auxiliary Dam Showing Location of Becker Soundings Performed in 1983 (after U.S. Army Corps of Engineers, Sacramento Dist.)	7
3. Section View of Mormon Island Auxiliary Dam Showing Location of Becker Soundings Performed in 1983 (after U.S. Army Corps of Engineers, Sacramento Dist.)	8
4. Uncorrected Becker and Equivalent SPT Blowcounts for Soundings BH-1,2,4,5,7, and 8 (Performed in the Downstream Flat Area)	9
5. Uncorrected Becker and Equivalent SPT Blowcounts for Soundings BH-3 and BDT-1 (Performed in the Downstream Flat Area)	10
6. Uncorrected Becker and Equivalent SPT Blowcounts for Soundings BH-6 and BDT-2 (Performed in the Downstream Flat Area)	11
7. Uncorrected Becker and Equivalent SPT Blowcounts for Sounding BH-10 (Performed through Downstream Slope)	12
8. Uncorrected Becker and Equivalent SPT Blowcounts for Soundings BH-9 and BDT-3 (Performed through Downstream Slope)	13
9. Plan View of Mormon Island Auxiliary Dam Illustrating the Locations of the 1986 Becker Drilling Sites (after U. S. Army Corps of Engineers, Sacramento Dist.)	15
10. Cross Section of Mormon Island Auxiliary Dam at Station 449+90	16
11. Typical Relationship Between Becker Blowcount and Bounce Chamber Pressure (after Harder and Seed, 1986)	20
12. Idealization of How Diesel Hammer Combustion Efficiency Affects Becker Blowcounts (after Harder and Seed, 1986)	21
13. Correction Curves Adopted to Correct Becker Blowcounts to Constant Combustion Curve Adopted for Calibration (after Harder and Seed, 1986)	23
14. Correlation Between Corrected Becker and SPT Blowcount (after Harder and Seed, 1986)	25

List of Figures (continued)

Title	Page
15. Comparison of Equivalent SPT Blowcounts Determined in the 1983 and 1986 Becker Explorations Performed Along the Downstream Flat of Mormon Island Auxiliary Dam	26
16. Comparison of Equivalent SPT Blowcounts Determined in the 1983 and 1986 Becker Explorations Performed Along the Downstream Face of Mormon Island Auxiliary Dam	27
17. Relationship Between C_N Correction and Overburden Pressure for Sands with Relative Densities of 50 Percent	31
18. Relationship Between C_N Correction and Overburden Pressure for Sands with Relative Densities of 65 Percent	32
19. Equivalent SPT Blowcounts for Becker Sounding BCC 86-1 Performed in Downstream Flat of Mormon Island Auxiliary Dam	38
20. Equivalent SPT Blowcounts for Becker Sounding BCC 86-2 Performed in Downstream Flat of Mormon Island Auxiliary Dam	39
21. Equivalent SPT Blowcounts for Becker Sounding BCC 86-3 Performed in Downstream Flat of Mormon Island Auxiliary Dam	40
22. Equivalent SPT Blowcounts for Becker Sounding BCC 86-4 Performed in Downstream Flat of Mormon Island Auxiliary Dam	41
23. Equivalent SPT Blowcounts for Becker Sounding BCC 86-5 Performed in Downstream Flat of Mormon Island Auxiliary Dam	42
24. Equivalent SPT Blowcounts for Becker Sounding BCC 86-6 Performed in Downstream Flat of Mormon Island Auxiliary Dam	43
25. Equivalent SPT Blowcounts for Becker Sounding BCC 86-7 Performed in Downstream Flat of Mormon Island Auxiliary Dam	44
26. Equivalent SPT Blowcounts for Becker Sounding BCC 86-8 Performed in Downstream Flat of Mormon Island Auxiliary Dam	45
27. Equivalent SPT Blowcounts for Becker Sounding BCC 86-9 Performed in Downstream Flat of Mormon Island Auxiliary Dam	46
28. Equivalent SPT Blowcounts for Becker Sounding BCC 86-10 Performed in Downstream Flat of Mormon Island Auxiliary Dam	47
29. Equivalent SPT Blowcounts for Becker Sounding BCC 86-11 Performed in Downstream Flat of Mormon Island Auxiliary Dam	48
30. Equivalent SPT Blowcounts for Becker Sounding BCC 86-12 Performed in Downstream Flat of Mormon Island Auxiliary Dam	49

List of Figures (continued)

	Title	Page
31.	Equivalent SPT Blowcounts for Becker Sounding BCC 86-13 Performed in Downstream Flat of Mormon Island Auxiliary Dam	50
32.	Equivalent SPT Blowcounts for Becker Sounding BCC 86-14 Performed in Downstream Flat of Mormon Island Auxiliary Dam	51
33.	Equivalent SPT Blowcounts for Becker Sounding BCC 86-15 Performed on Downstream Face of Mormon Island Auxiliary Dam	52
34.	Equivalent SPT Blowcounts for Becker Sounding BCC 86-16 Performed on Downstream Face of Mormon Island Auxiliary Dam	53
35.	Equivalent SPT Blowcounts for Becker Sounding BCC 86-17 Performed on Downstream Face of Mormon Island Auxiliary Dam	54
36.	Equivalent SPT Blowcounts for Becker Sounding BCC 86-18 Performed on Downstream Face of Mormon Island Auxiliary Dam	55
37.	Equivalent SPT Blowcounts for Becker Sounding BCC 86-19 Performed on Downstream Face of Mormon Island Auxiliary Dam	56
38.	Equivalent SPT Blowcounts for Becker Sounding BCC 86-20 Performed on Downstream Face of Mormon Island Auxiliary Dam	57
39.	Equivalent SPT Blowcounts for Becker Sounding BCC 86-21 Performed on Downstream Face of Mormon Island Auxiliary Dam	58
40.	Equivalent SPT Blowcounts for Becker Sounding BCC 86-22 Performed on Downstream Face of Mormon Island Auxiliary Dam	59
41.	Equivalent SPT Blowcounts for Becker Sounding BCC 86-23 Performed on Downstream Face of Mormon Island Auxiliary Dam	60
42.	Equivalent SPT Blowcounts for Becker Sounding BCC 86-24 Performed on Downstream Face of Mormon Island Auxiliary Dam	61
43.	Equivalent SPT Blowcounts for Becker Sounding BCC 86-25 Performed on Downstream Face of Mormon Island Auxiliary Dam	62
44.	Equivalent SPT Blowcounts for Becker Sounding BCC 86-26 Performed on Downstream Face of Mormon Island Auxiliary Dam	63
45.	Range of Equivalent SPT Blowcounts Obtained from Becker Soundings Performed in Downstream Flat of Mormon Island Auxiliary Dam Between Stations 445 and 455	69

List of Figures (continued)

	Title	Page
46.	Mean and 35th Percentile Equivalent SPT Blowcounts Obtained from Becker Soundings Performed in Downstream Flat of Mormon Island Auxiliary Dam Between Stations 445 and 455	70
47.	Range of Equivalent SPT Blowcounts Obtained from Becker Soundings Performed at Midpoint of Downstream Slope of Mormon Island Auxiliary Dam Between Stations 445 and 455	75
48.	Mean and 35th Percentile Equivalent SPT Blowcounts in Embankment Shell Obtained from Becker Soundings Performed at Midpoint of Downstream Slope of Mormon Island Auxiliary Dam Between Stations 445 and 455	76
49.	Mean and 35th Percentile Equivalent SPT Blowcounts in Dredge Tailings Obtained from Becker Soundings Performed at Midpoint of Downstream Slope of Mormon Island Auxiliary Dam Between Stations 445 and 455	77

List of Tables

Title	Page
1. Locations and Maximum Depths for 1986 Plugged-Bit Becker Soundings	17
2. Determination of Overburden Pressure Corrections for Soundings Performed Through Midpoint of Downstream Slope (Soundings BCC 86-15 through BCC 86-21)	36
3. Determination of Overburden Pressure Corrections for Soundings Performed Beyond Downstream Toe	36
4. Summary of Equivalent SPT Blowcounts From Becker Soundings Along Downstream Flat of Mormon Island Auxiliary Dam - Station 445 to 455	66
5. Summary of Equivalent SPT Blowcounts From Becker Soundings Along Midpoint of Downstream Slope of Mormon Island Auxiliary Dam - Station 445 to 455	71

1. INTRODUCTION

Background

The Mormon Island Auxiliary Dam is part of the Folsom Dam and Reservoir Project and is located approximately 20 miles northeast of Sacramento, California. As part of a seismic safety evaluation of the Folsom project, the sands and gravels which make up the embankment's shells and foundation are being studied for their potential to liquefy and lose strength during earthquake shaking.

For sandy soils, evaluations of liquefaction potential usually employ the Standard Penetration Test (SPT). This test consists of driving a standard 2-inch O.D. split-spoon sampler into the bottom of a borehole for a distance of 18 inches. The SPT blowcount, or N value, is defined as the number of blows required to drive the sampler the last 12 inches. Based on the performance of sites which have sustained strong earthquake shaking, researchers have developed correlations between the cyclic loading resistance of sands and the SPT blowcount (Seed et al. 1983, Seed et al. 1985).

Unfortunately, the large gravel and cobble particles present in the embankment's shell and foundation precluded the use of the SPT at the Mormon Island Auxiliary Dam. Any SPT blowcounts obtained would have given a misleadingly high blowcount due to the 2-inch sampler simply bouncing off the large particles, or by having a large gravel particle block the opening of the sampler's shoe and resulting in the sampler being driven as a solid penetrometer. As an alternative to the SPT, a larger penetration test was selected to explore the site. This test, known as the Becker Penetration Test (BPT), is generally used

with a 6.6-inch O.D. double-walled casing and is driven into the ground with a diesel pile hammer. The Becker Penetration Test basically consists of counting the number of hammer blows required to drive the casing one foot into the ground. By counting the blows for each foot of penetration, a continuous record of penetration resistance can be obtained for an entire profile. The casing can be driven with an open bit and reverse air circulation to obtain disturbed samples (Figure 1), or with a plugged bit and driven as a solid penetrometer.

An initial exploration program was performed with a Becker Hammer drill rig at the Mormon Island Auxiliary Dam in October 1983. A total of 13 open and plugged-bit soundings were conducted on the downstream face and beyond the downstream toe of the embankment. The results of these explorations were presented in an earlier report submitted to the U. S. Army Corps of Engineers (USACE) in October 1986 (Reference 1). Subsequent to this initial investigation, a second phase of explorations was performed in September 1986. In this second phase, 52 Becker soundings were performed through the downstream slope and beyond the downstream toe of the embankment. The soundings in this second phase were performed at 26 sites with an open-bit and a plugged-bit sounding performed at each site. The purpose of this report is to evaluate the blowcounts from the 26 plugged-bit Becker soundings and to determine the equivalent SPT penetration resistances for the deposits explored.

Scope of Work

As originally proposed, the scope of work was to convert the Becker blowcounts into equivalent SPT blowcounts, and then use the correlation between SPT blowcount and liquefaction potential developed

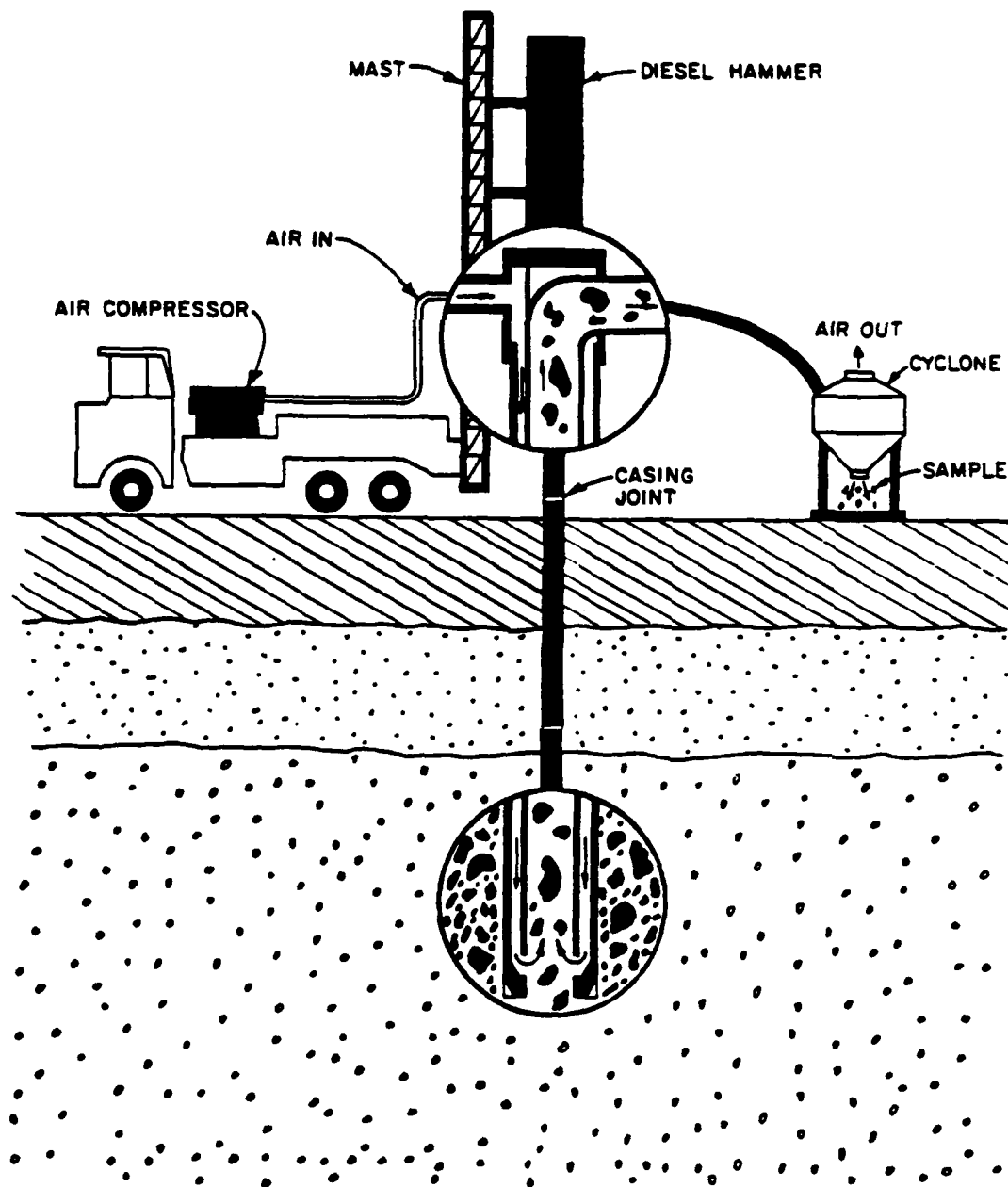


FIGURE 1: SCHEMATIC DIAGRAM OF BECKER SAMPLING OPERATION
(after Harder and Seed, 1986)

by Seed et al. (1985) to obtain an estimate of the cyclic loading resistance. The scope of the work was subsequently limited to determining the equivalent SPT blowcounts as outlined in a letter from Ron Wahl of the Waterways Experiment Station.

The conversion of Becker blowcounts into equivalent SPT blowcounts was performed using the procedures outlined by Harder and Seed (1986). Because the Becker Penetration Test is a non-standard test, there were several intermediate steps. In summary, the steps of the process are presented below:

1. Because the diesel hammer can be run at a wide variety of combustion conditions, all of the Becker Penetration Test blowcounts were corrected to blowcounts obtained with a standard set of constant combustion conditions (Section 2).
2. Using the correlation developed by Harder and Seed (1986), the corrected Becker blowcounts were converted into equivalent SPT blowcounts (Section 2).
3. Using effective stress values determined from finite element analyses, the equivalent SPT values from different depths and stress levels were normalized to those that would have been obtained in the same material under level ground conditions with an effective overburden stress of 1 tsf (Section 3).
4. Equivalent SPT blowcounts and statistical summaries of the data were presented (Section 4).
5. A summary of results is also presented (Section 5).

The sources of the basic data used in this report were the listings and plots showing uncorrected Becker data, testing depths, test locations, and classification test results obtained from Joe Koester of the Geotechnical Laboratory, Waterways Experiment Station. The stress results from finite element analyses used to normalize the equivalent SPT results to 1 tsf overburden pressure were

supplied by Ron Wahl of the Geotechnical Laboratory, Waterways Experiment Station. Additional information regarding the gradations obtained from field density test pits were obtained from Mary Ellen Hynes-Griffin.

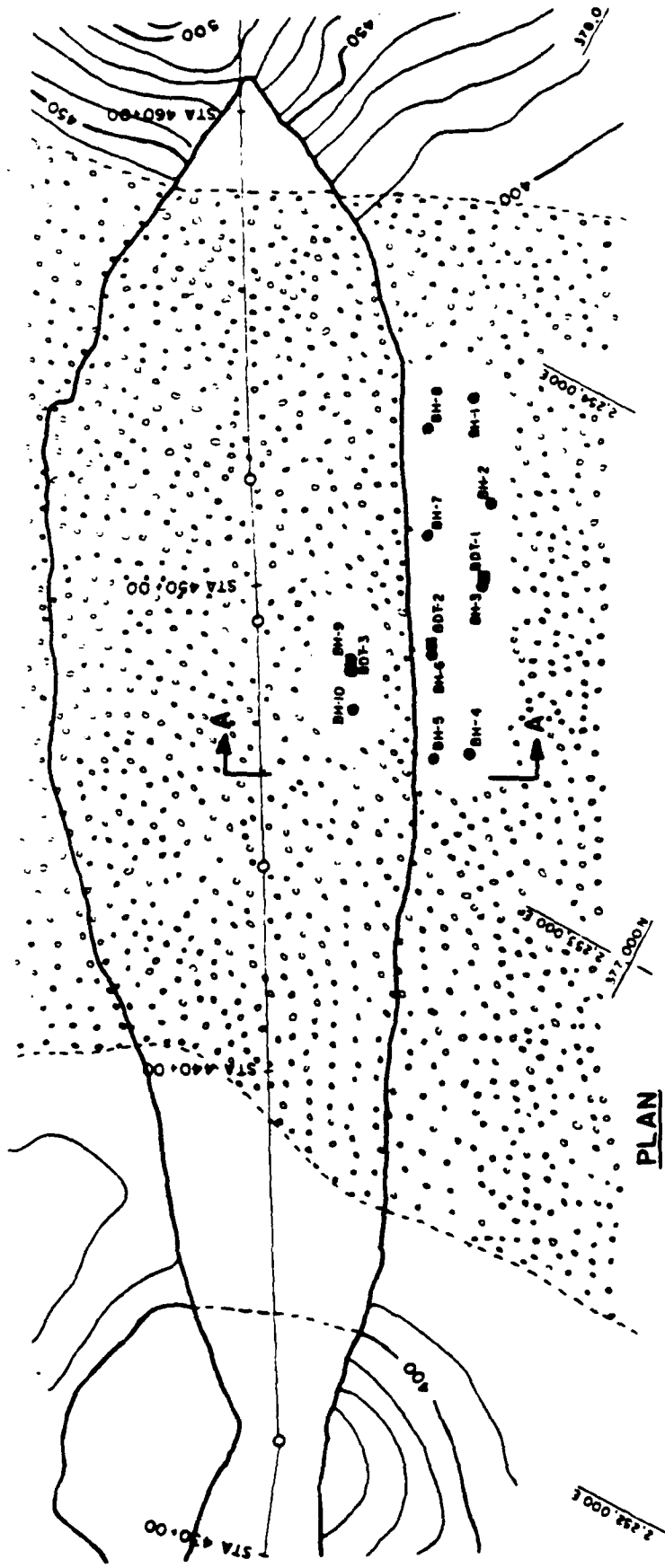
This report was prepared under Contract No. DACW 39-87-M-3246.

2. DETERMINATION OF EQUIVALENT SPT BLOWCOUNTS

Previous Becker Explorations Performed at Mormon Island

Thirteen Becker soundings were performed at the Mormon Island Auxiliary Dam during the period of October 10-21, 1983. All of the soundings were performed with 6.6-inch O.D. double-walled casing and were driven by an ICE Model 180 diesel pile hammer mounted on a Becker B-180 Drill Rig (No. 11). The drilling contractor was Becker Drills, Inc. operating out of Denver, Colorado. Ten of the soundings, designated with the prefix BH, employed an open Felcon crowd-in bit together with air-recirculation to obtain disturbed samples of penetrated soil. This open bit has a 7.3-inch O.D. and a 3.8-inch I.D. The 7.3-inch O.D. extends from the tip of the bit for a distance of about 8.5 inches before reducing down to the same outside diameter (6.6 inches) that the drill casing has. The remaining 3 soundings, given the prefix BDT, used a plugged 8-tooth crowd-out bit. This plugged bit had the same 6.6-inch O.D. as did the casing. Details and photographs of the two bit types are available in Reference 2. Figures 2 and 3 present the locations of the 1983 soundings.

The purpose of the 1983 Becker soundings was principally to determine the penetration resistance of the presumably loose dredge tailings which comprise a large portion of the foundation beneath the Mormon Island Auxiliary Dam. A second purpose was to determine the penetration resistance of the gravelly shell material which comprises a major portion of the embankment. The uncorrected Becker and equivalent SPT blowcounts for the 1983 soundings are presented in Figures 4 through 8. These figures show relatively low penetration resistance



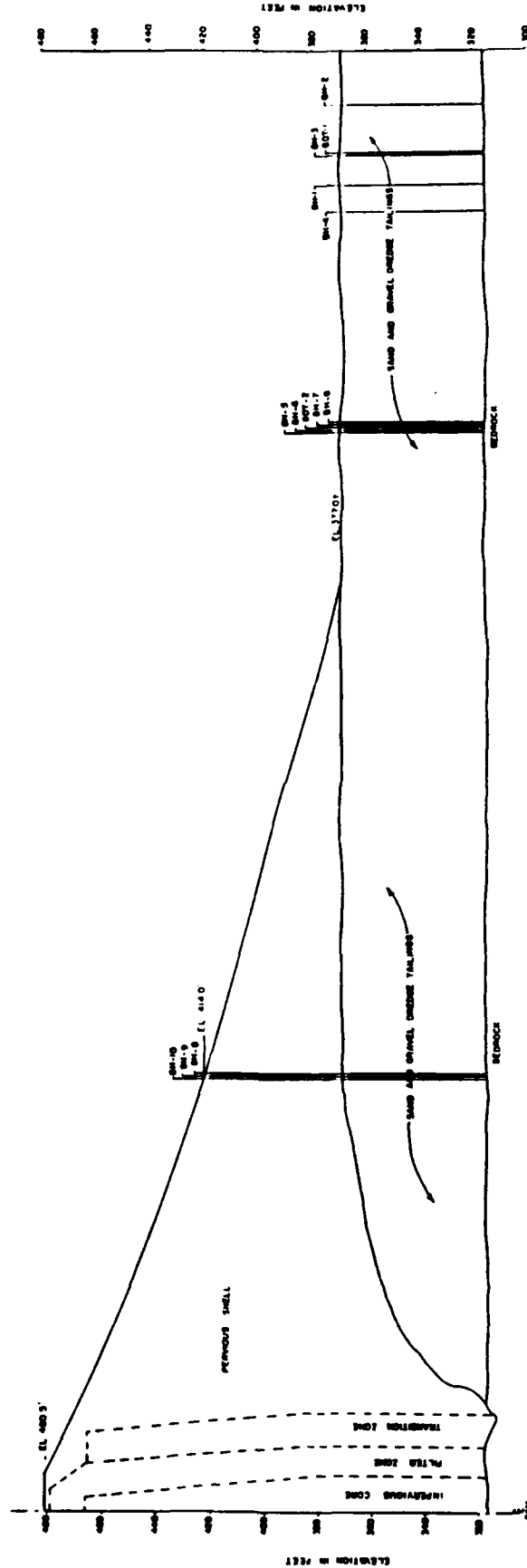
NOTES

- 1) BH PREFIX DENOTES A BECKER SOUNDING PERFORMED WITH A 7.3-INCH O.D. OPEN FELCON BIT.
- 2) BDT PREFIX DENOTES A BECKER SOUNDING PERFORMED WITH A 6.6-INCH O.D. PLUGGED 8-TOOTH BIT.
- 3) SECTION A-A SHOWN IN FIGURE 3.

PLAN



FIGURE 2: PLAN VIEW OF MORMON ISLAND AUXILIARY DAM SHOWING LOCATION OF BECKER SOUNDINGS PERFORMED IN 1983 (after U.S. Army Corps of Engineers, Sacramento District)



SECTION A-A (from Figure 2)

**FIGURE 3: SECTION VIEW OF MORMON ISLAND AUXILIARY DAM SHOWING LOCATION OF BECKER SOUNDINGS PERFORMED IN 1983
(after U.S. Army Corps of Engineers, Sacramento District)**

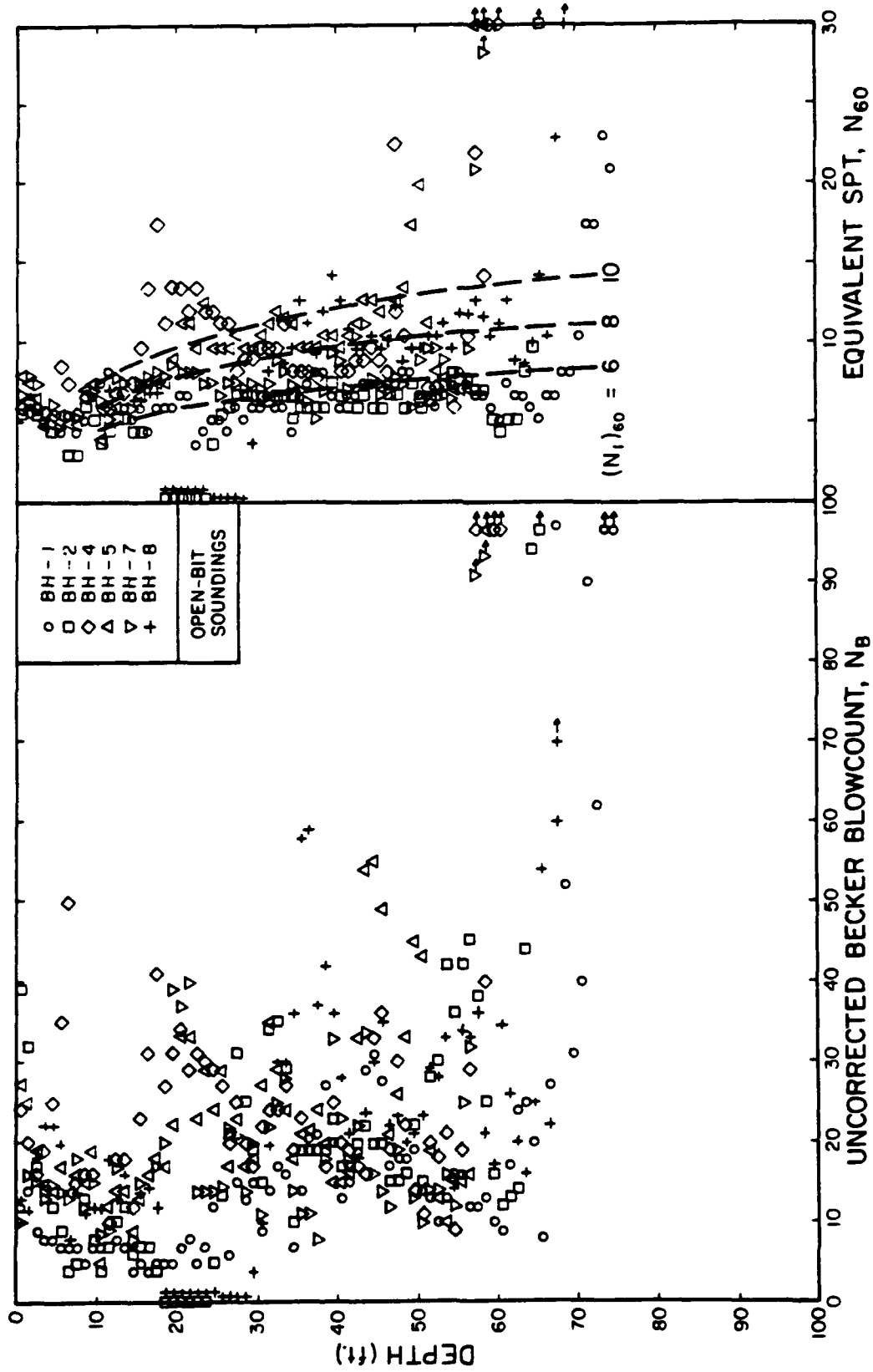


FIGURE 4: UNCORRECTED BECKER AND EQUIVALENT SPT BLOWCOUNTS FOR SOUNDINGS BH-1, 2, 4, 5, 7, AND 8
(Performed in the Downstream Flat Area)

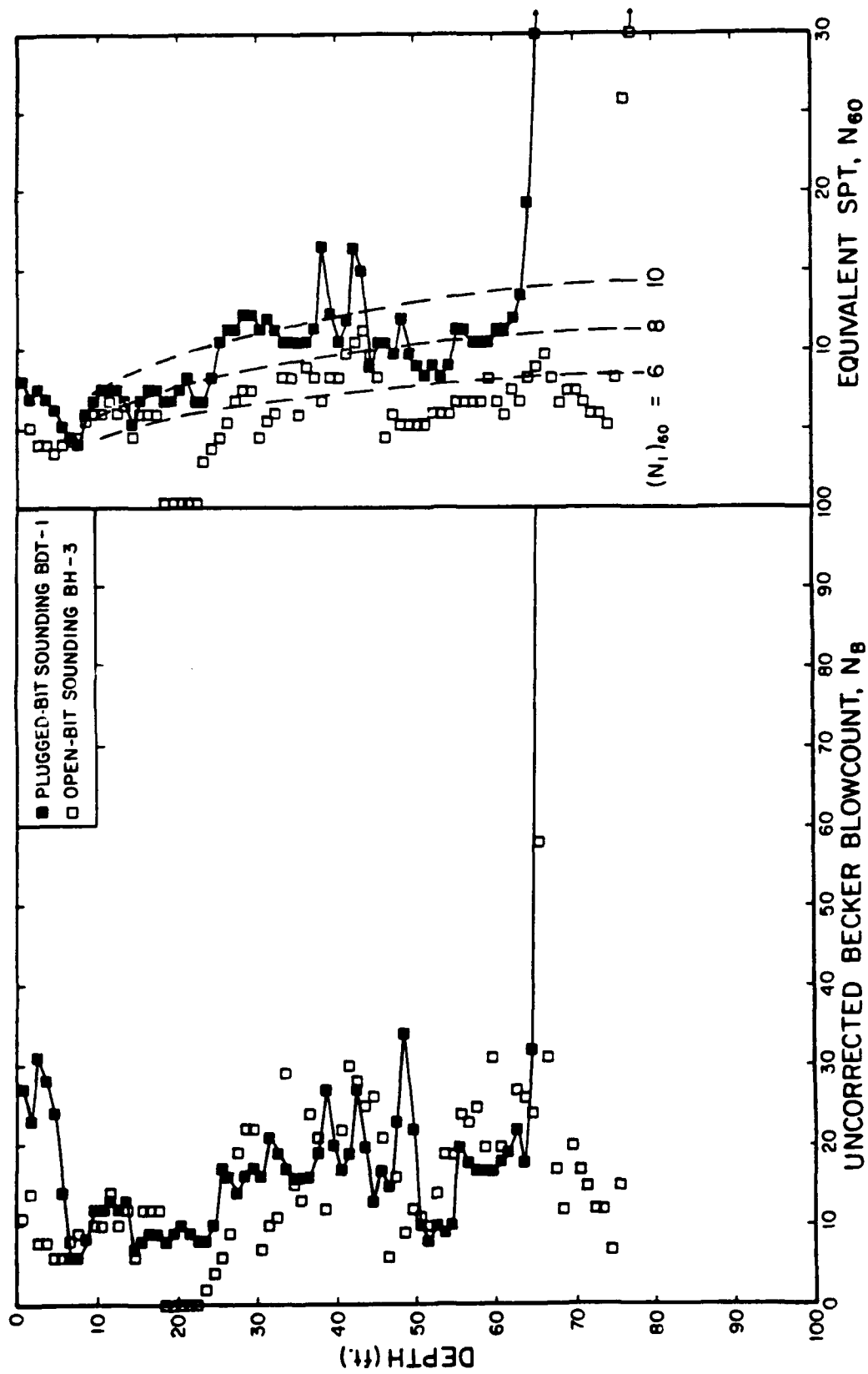


FIGURE 5: UNCORRECTED BECKER AND EQUIVALENT SPT BLOWCOUNTS FOR SOUNDINGS BH-3 and BDT-1 (Performed in the Downstream Flat Area)

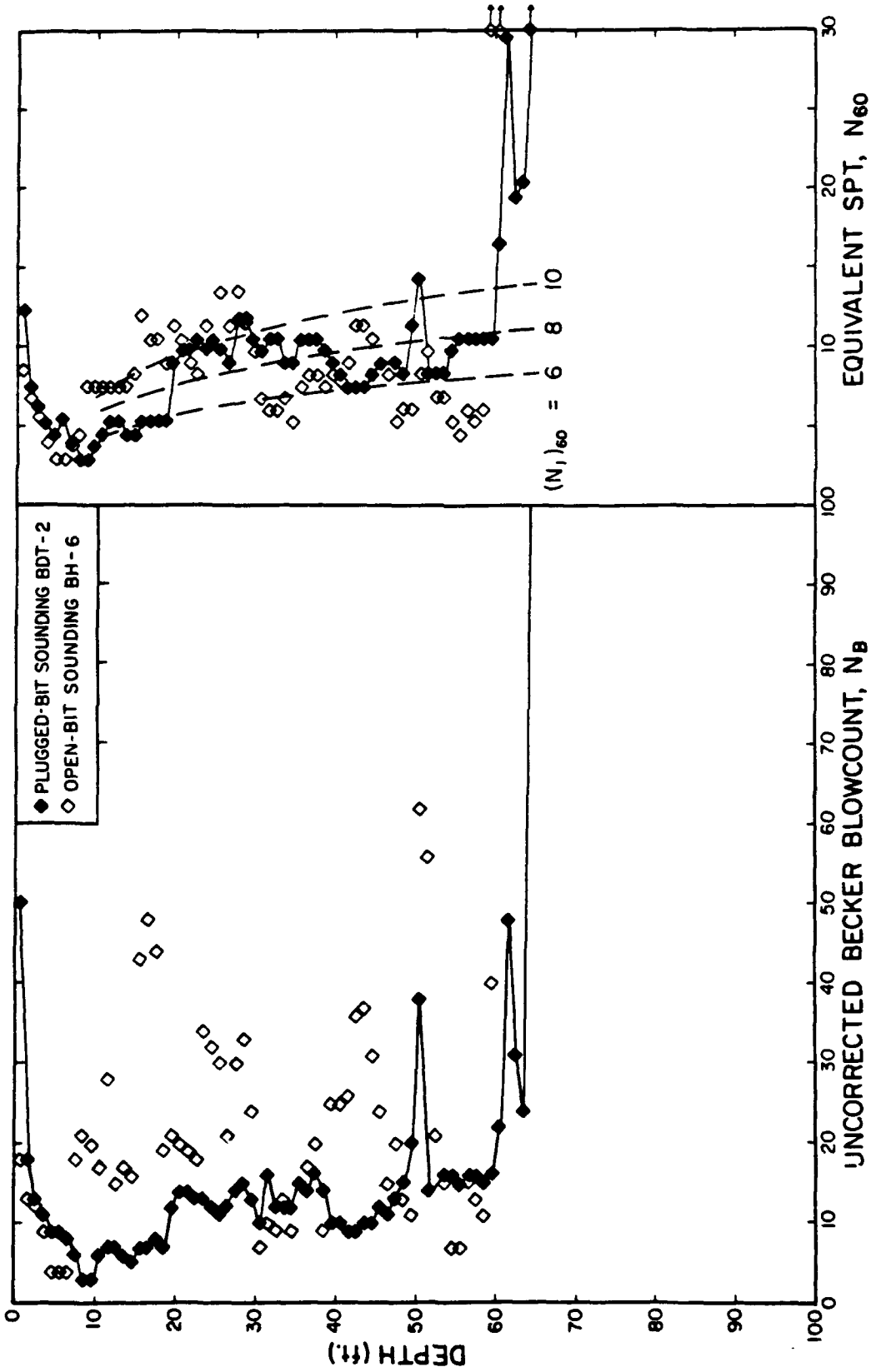


FIGURE 6: UNCORRECTED BECKER AND EQUIVALENT SPT BLOWCOUNTS FOR SOUNDINGS BH-6 and BDT-2 (Performed in the Downstream Flat Area)

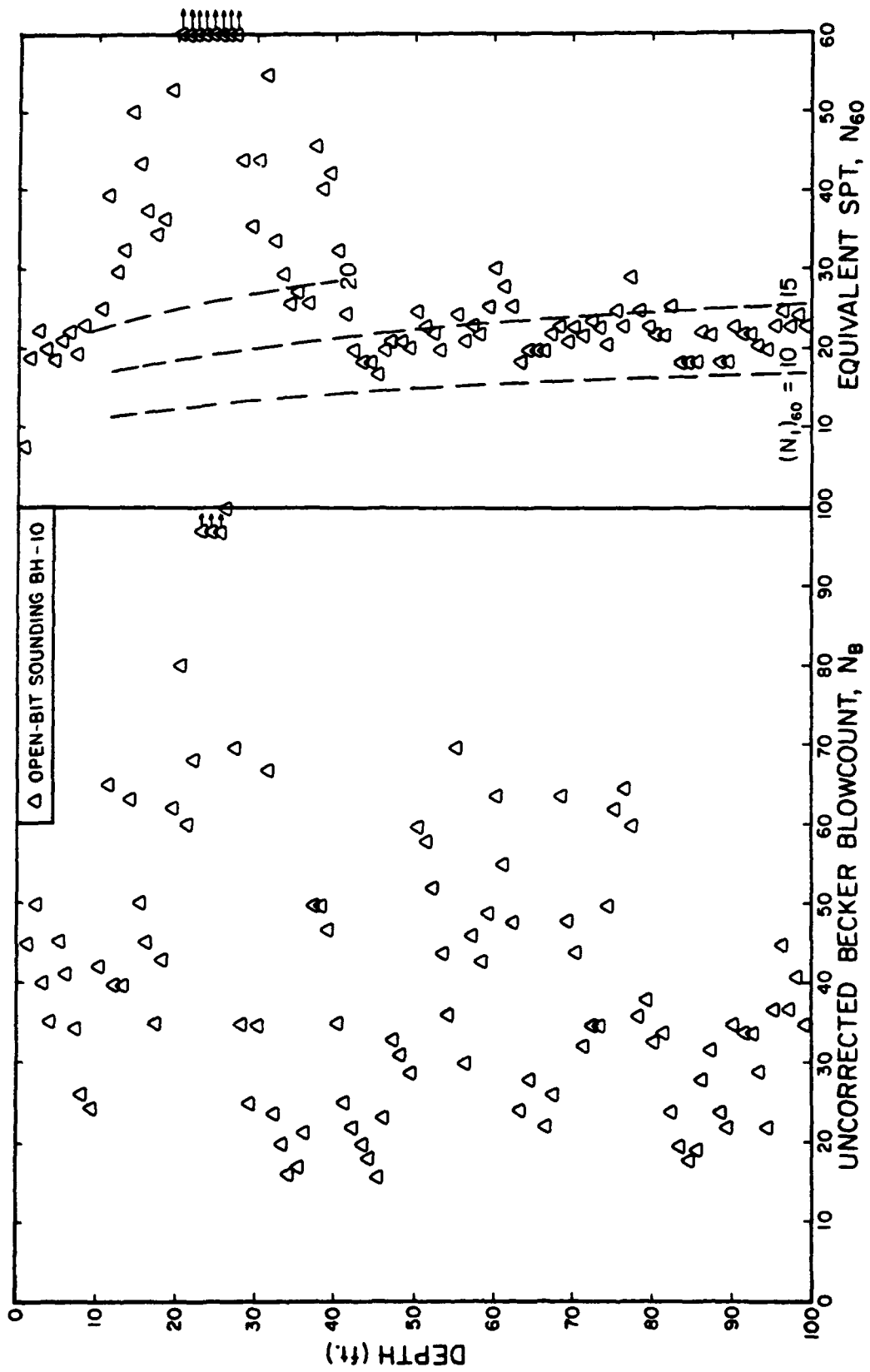


FIGURE 7: UNCORRECTED BECKER AND EQUIVALENT SPT BLOWCOUNTS FOR SOUNDING BH-10
(Performed through Downstream Slope)

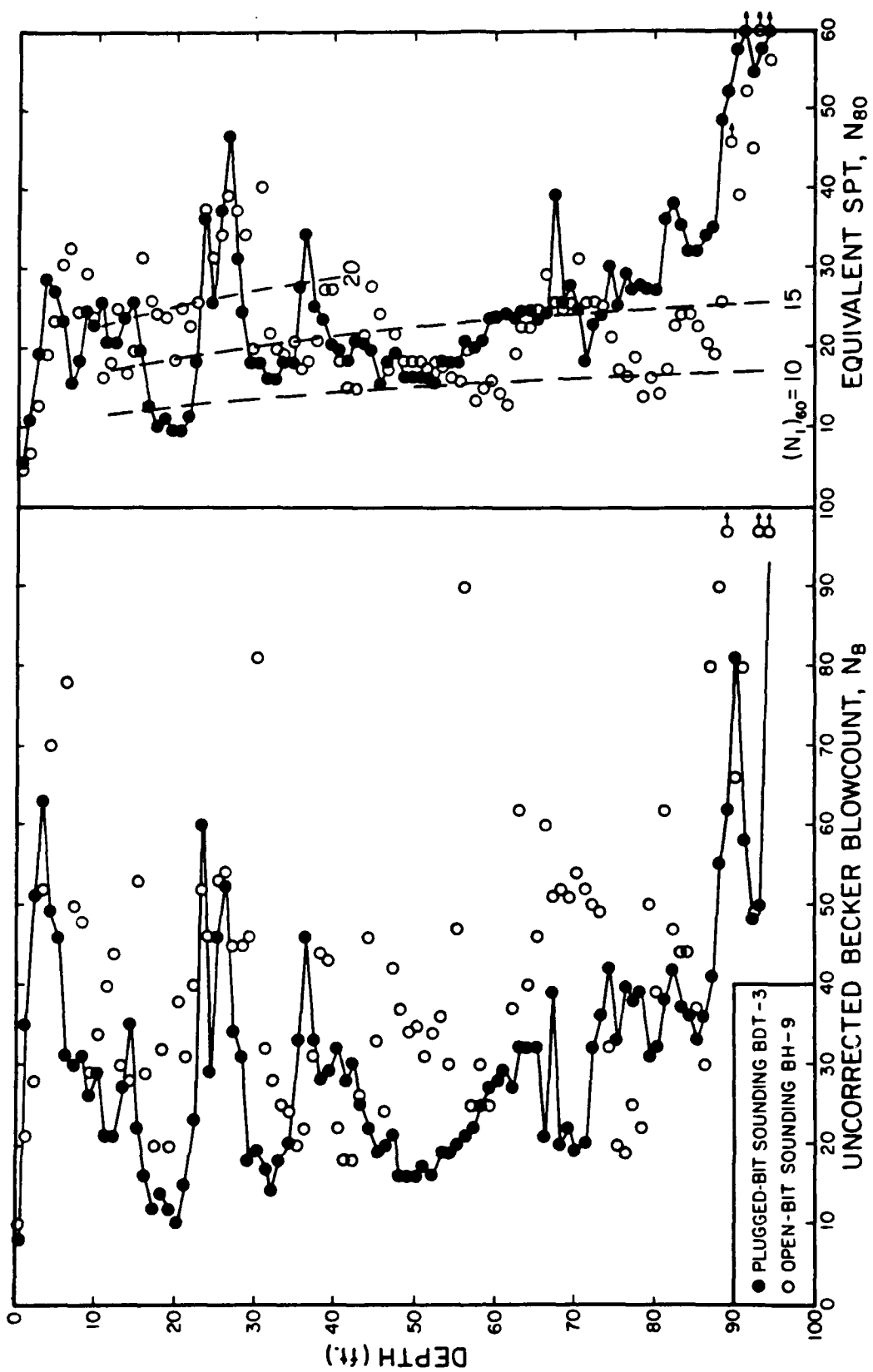


FIGURE 8: UNCORRECTED BECKER AND EQUIVALENT SPT BLOWCOUNTS FOR SOUNDINGS BH-9 AND BDT-3 (Performed through Downstream Slope)

for soundings performed in the dredge tailings along the downstream toe of the dam (see Figures 4 through 6). For soundings performed through the downstream slope of the embankment, the penetration resistance indicated a medium dense shell material and a moderately low resistance in the underlying dredge tailing foundation (see Figures 7 and 8).

1986 Mormon Island Becker Penetration Tests

In addition to dredge tailings, portions of the Mormon Island Auxiliary Dam are also founded on undisturbed Blue Ravine alluvium and slope wash. The second phase of Becker explorations was conducted in order to determine the penetration resistance of all foundation soils and to better determine the penetration resistance of the embankment shell material. Fifty-two Becker soundings were performed at the Mormon Island Auxiliary Dam in September 1986. The soundings were conducted at 26 sites where both a plugged-bit and an open-bit sounding were performed. The 1986 soundings were arranged in three rows:

1. The first row was aligned longitudinally just beyond the downstream toe (Sites 1 through 14).
2. The second row was aligned longitudinally along the midpoint of the embankment's downstream slope (Sites 15 through 21).
3. The third row was aligned transversely along the downstream slope at approximately Station 449+90 (Sites 22 through 26).

The locations of the 26 sites are illustrated in Figure 9. Figure 10 presents a partial cross-section of the dam which illustrates the locations of the 1986 soundings placed at this station. Table 1 summarizes the locations and maximum depths reached by the 1986 plugged-bit soundings.

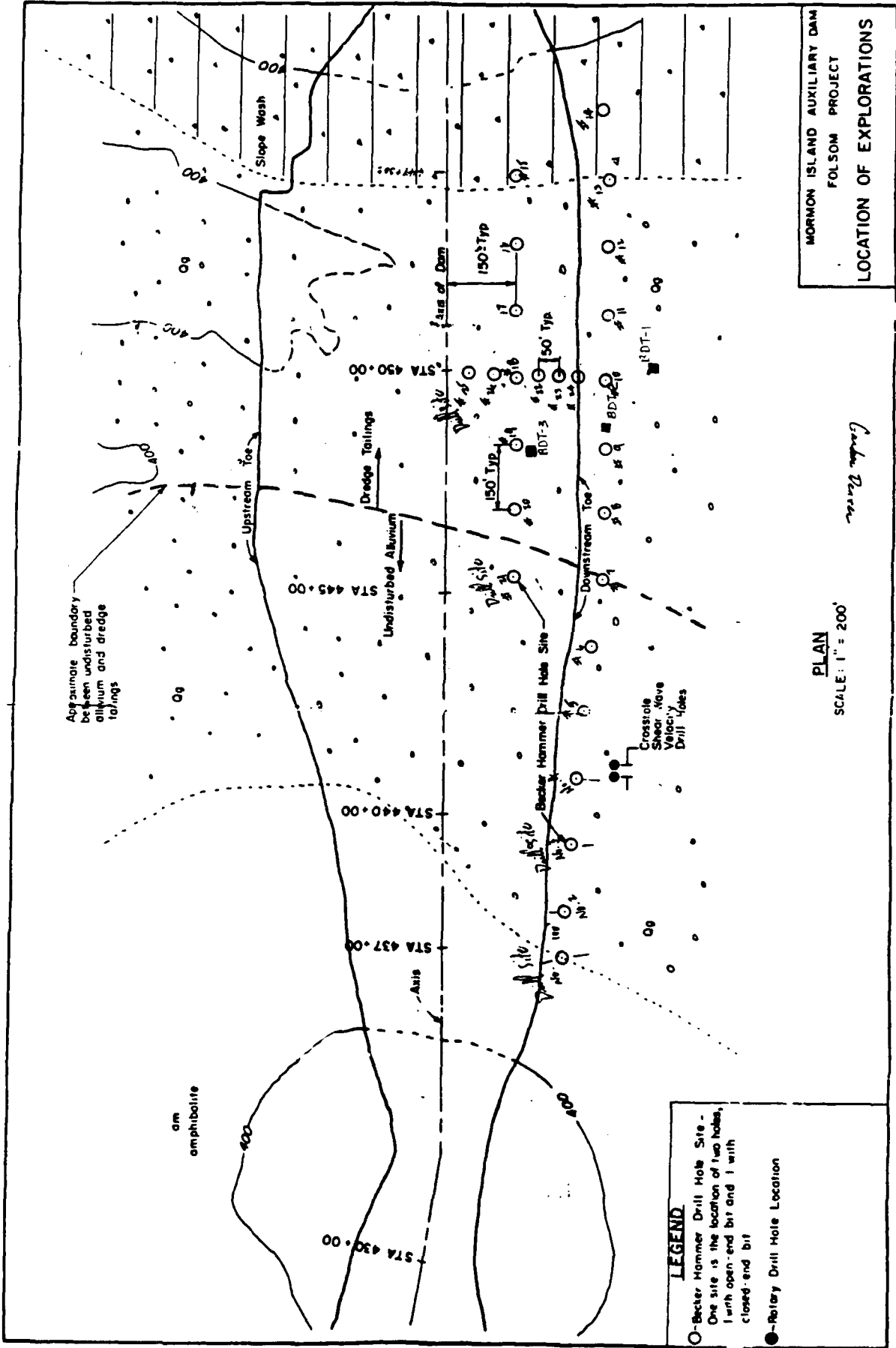
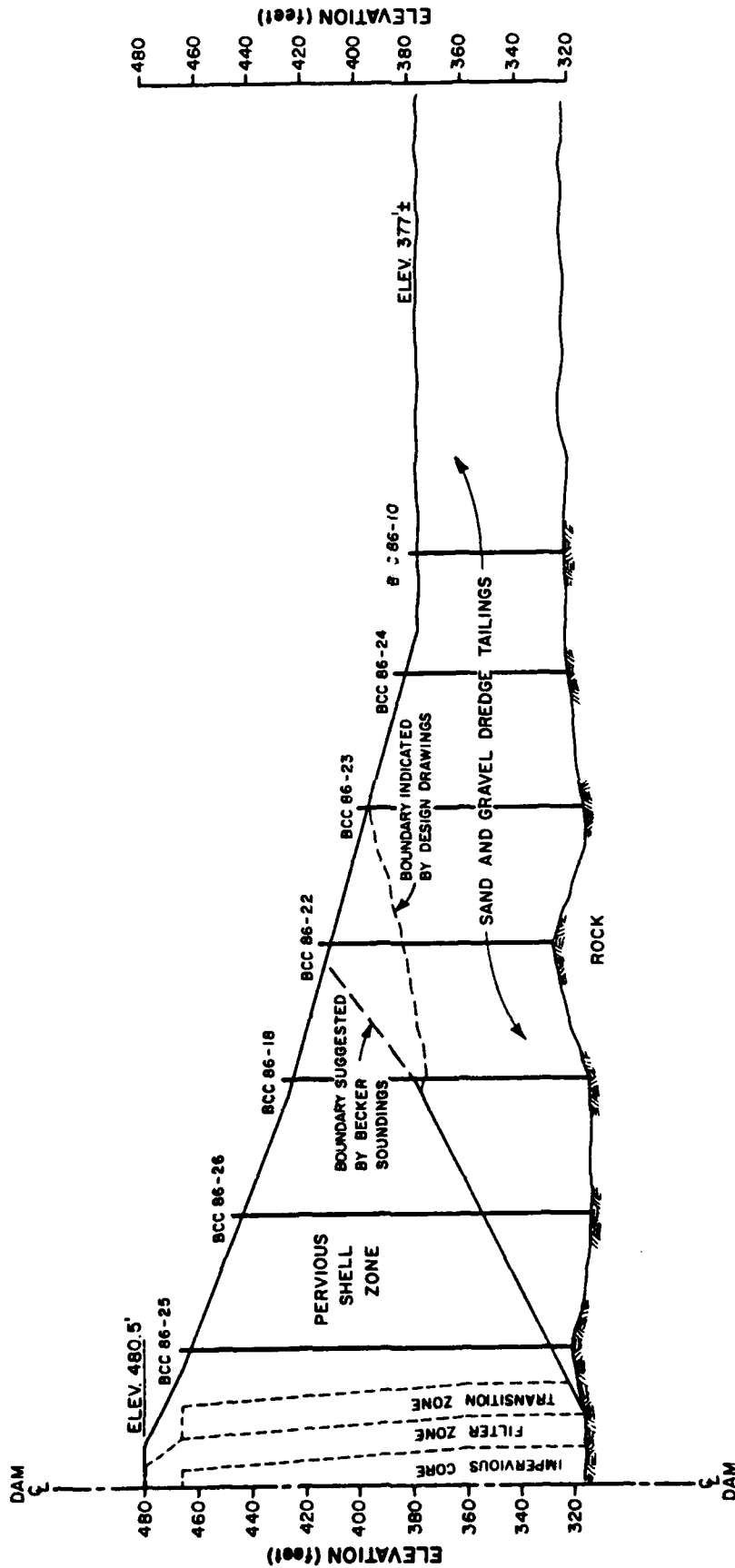


FIGURE 9: PLAN VIEW OF MORMON ISLAND AUXILIARY DAM SHOWING THE LOCATIONS OF THE 1986 BECKER DRILLING SITES (after U.S. Army Corps of Engineers, Sacramento District)



A25

FIGURE 10: CROSS SECTION OF MORMON ISLAND AUXILIARY DAM AT STATION 449+90

TABLE 1: LOCATIONS AND MAXIMUM DEPTHS FOR 1986 PLUGGED-BIT BECKER SOUNDINGS

SITE	Approximate Station (feet)	Approximate D/S Offset (feet)	Approximate Surface Elevation (feet)	Maximum Depth (feet)
1	436+75	260	382	25.
2	437+80	265	380	24.
3	439+35	280	379	22.
4	440+80	290	379	28.
5	442+35	305	380	27.
6	443+80	320	377	40.
7	445+35	345	377	57.
8	446+85	350	377	59.
9	448+30	350	377	58.
10	449+80	345	377	60.
11	451+25	350	377	61.
12	452+80	350	377	69.
13	454+30	356	377	48.
14	455+85	340	394	48.
15	454+35	150	424	78.
16	452+85	150	424	110.
17	451+35	150	424	104.
18	449+85	150	424	112.
19	448+35	150	424	101.
20	446+85	150	424	103.
21	445+35	150	424	76.
22	449+90	200	407	86.
23	449+85	250	393	80.
24	449+85	290	383	64.
25	449+95	50	461	143.
26	449+90	100	442	131.

All of the 1986 soundings were performed with 6.6-inch O.D. double-walled casing and were driven by an ICE Model 180 diesel pile hammer mounted on a Becker AP-1000 Drill Rig. Two drill rigs owned and operated by Layne-Western Co., Inc. were employed. For most of the drilling, Drill Rig No. 404 was used. However, for the four soundings performed at sites 25 and 26, Drill Rig No. 403 was used (Reference 5). Eight-tooth, crowd-out drill bits were used for both open and plugged-bit soundings.

Corrections to Becker Penetration Resistance for Combustion Energy

Constant energy conditions are not a feature of the double-acting diesel hammers used in the Becker Penetration Test. One reason for this is that the energy depends on combustion conditions; thus anything that affects combustion, such as fuel quantity, fuel quality, air mixture and pressure all have a significant effect on the energy produced. Combustion efficiency is also operator-dependent because the operator controls a variable throttle which affects how much fuel is injected for combustion. On some rigs, the operator also controls a rotary blower which adds additional air to the combustion cylinder during each stroke. This additional air is thought to better scavenge the cylinder of burnt combustion gases and has been found to produce higher energies (Reference 2).

To monitor the level of energy produced by the diesel hammer during driving, use is made of the bounce chamber pressure. For the ICE Model 180 diesel hammers used on the Becker drill rigs, the top of the hammer is closed off to allow a smaller stroke and a faster driving rate. At the top, trapped air in the compression cylinder and a connected bounce chamber acts as a spring. The amount of potential

energy within the ram at the top of its stroke can be estimated by measuring the peak pressure induced in the bounce chamber. Although calibration charts between potential energy and bounce chamber pressure are available from the manufacturer of the hammer, studies by Harder and Seed (1986) have shown that they are unable to predict the change in Becker blowcount for different levels of bounce chamber pressure.

Another reason why the energy is not a constant with the Becker Hammer Drill is that the energy developed is dependent on the blowcount of the soil being penetrated. As blowcounts decrease, the displacement of the casing increases with each stroke. With increasing casing displacement, a larger amount of energy from the expanding combustion gases is lost to the casing movement rather than being used to raise the ram for the next stroke. Thus, as blowcounts decrease, the energy developed by the hammer impact on subsequent blows also decreases. Conversely, if the blowcounts increase, then there is less casing displacement per blow and more of the combustion energy is directed upward in raising the ram for the next stroke. Figure 11 shows a curve illustrating a typical relationship between Becker blowcounts and bounce chamber pressure for constant combustion conditions (Reference 2). This curve is designated as a constant combustion rating curve and is just one member of a family of such curves that can be produced by a given drill rig and hammer.

Studies by Harder and Seed (1986) have shown that diesel hammer combustion efficiency significantly affects the Becker blowcount. Presented in Figure 12 are typical results obtained for different combustion efficiencies. In the upper plot, three combustion rating curves representing three different combustion efficiencies are shown.

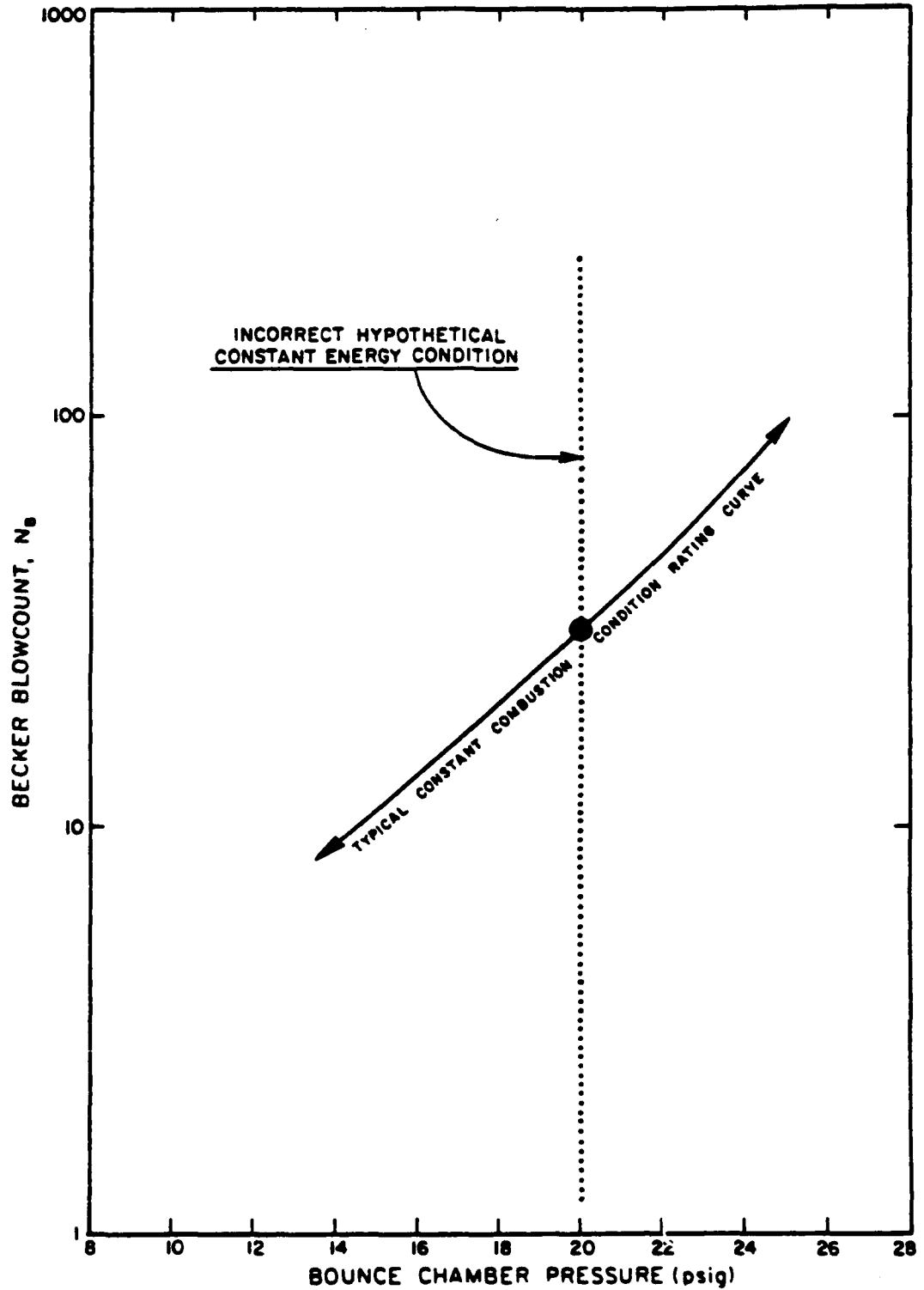


FIGURE 11: TYPICAL RELATIONSHIP BETWEEN BECKER BLOWCOUNT AND BOUNCE CHAMBER PRESSURE (after Harder and Seed, 1986)

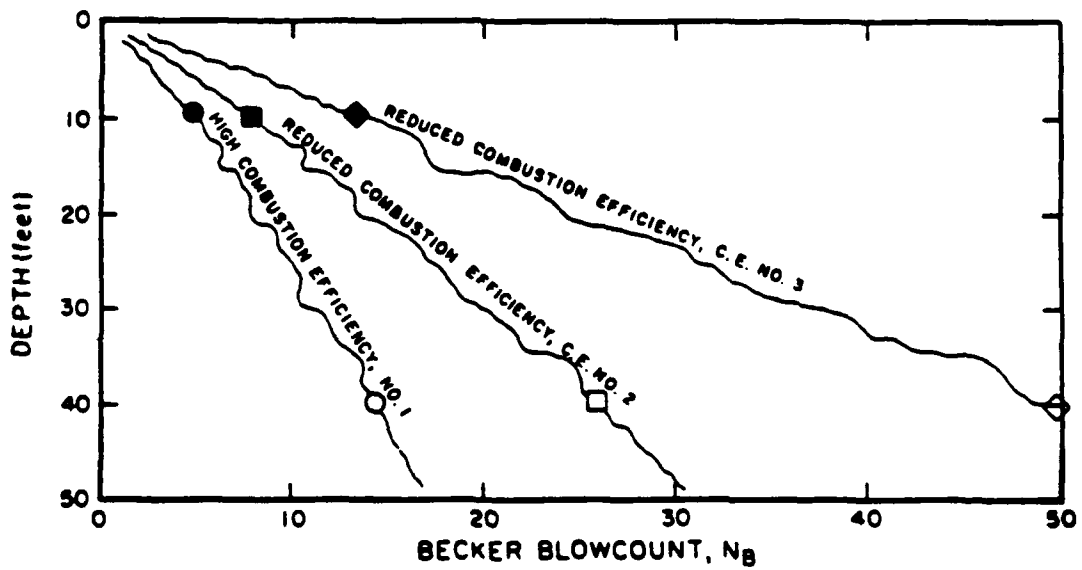
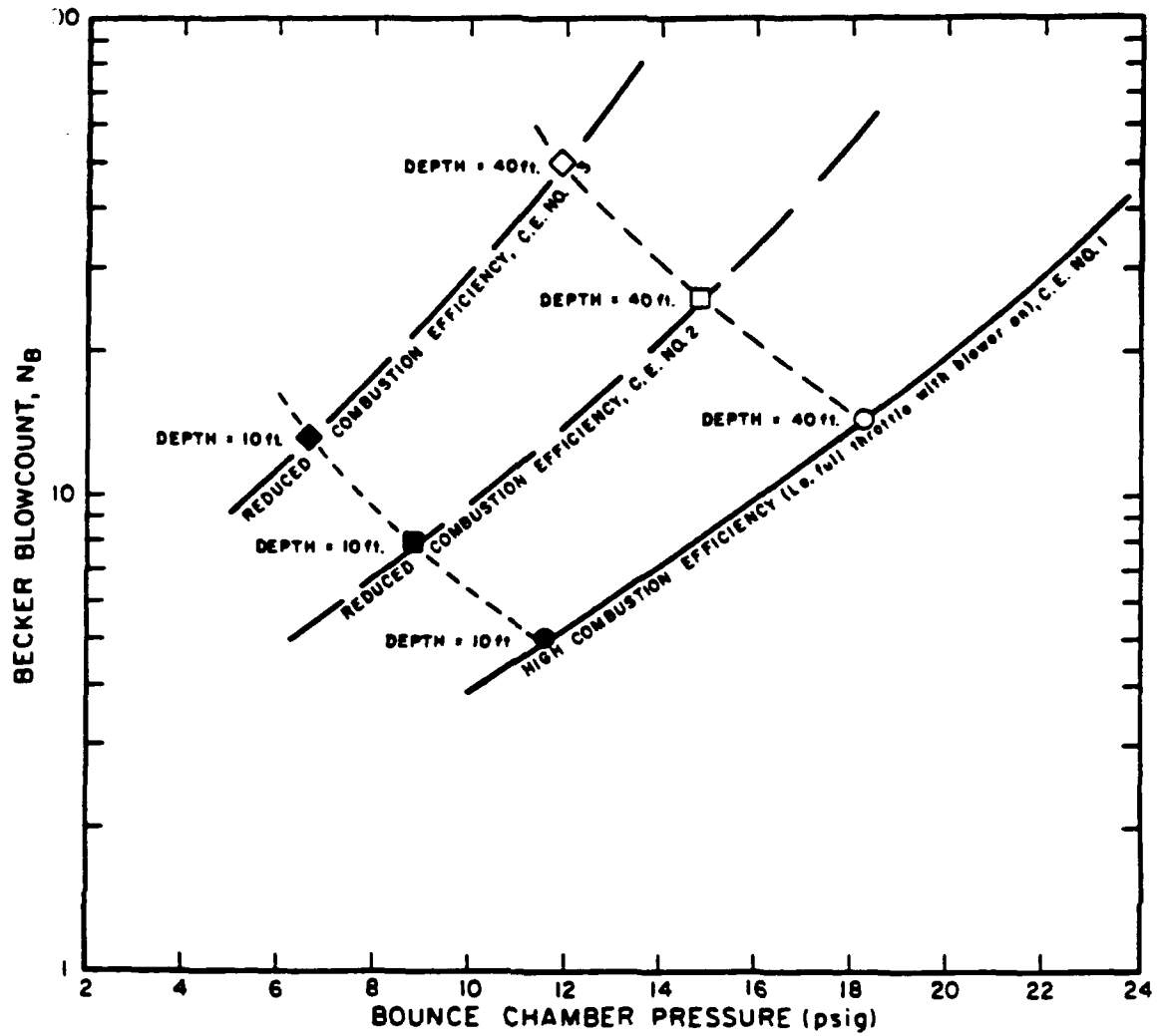


FIGURE 12: IDEALIZATION OF HOW DIESEL HAMMER COMBUSTION EFFICIENCY AFFECTS BECKER BLOWCOUNT (after Harder and Seed, 1986)

With different combustion conditions, the resulting blowcounts from tests performed in the same materials can be radically different. Consequently, tests in the same material at a depth of 40 feet can give a Becker blowcount of 14 when the hammer is operated at high combustion efficiency (throttle and blower on full), but give blowcounts of 26 and 50 at succeeding reductions of combustion energy.

To account for combustion effects, it is necessary to adopt a standard combustion efficiency and make corrections to the blowcount for different combustion conditions. For the corrections of the 1983 Mormon Island data, the curve marked in Figure 13 with the symbols AA was selected. This curve was chosen because it was the curve used by Harder and Seed (1986) to correct Becker data before correlating Becker blowcounts to SPT blowcounts. Also shown in Figure 13 are correction curves that are used to reduce measured Becker blowcounts to corrected Becker blowcounts when reduced combustion levels were employed during testing.

To use the correction curves, it is simply necessary to locate each uncorrected test result on the chart shown in Figure 13, using both the uncorrected blowcount and the bounce chamber pressure, and then follow the correction curves down to the standard rating curve AA, to obtain the corrected Becker blowcount, denoted as N_{BC} . For example, if the uncorrected blowcount was 44 and it was obtained at sea level with a bounce chamber pressure of 18 pounds per square inch-gauge (psig), then the corrected Becker blowcount would be 30 (Figure 13).

Conversion of Becker Blowcounts into Equivalent SPT Blowcounts

The correlation curve and the data used by Harder and Seed (1986) to generate the relationship between corrected Becker blowcounts and

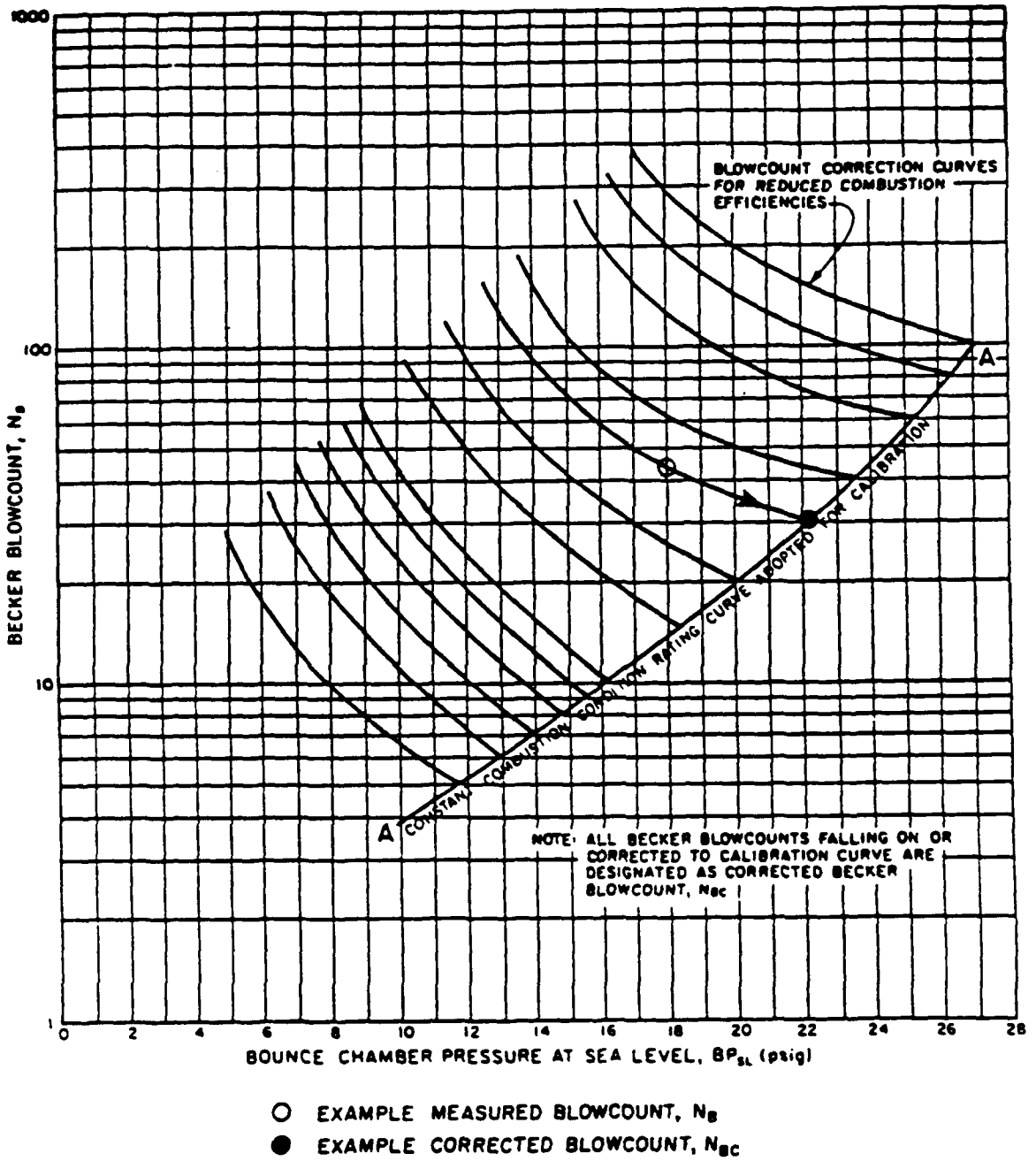


FIGURE 13: CORRECTION CURVES ADOPTED TO CORRECT BECKER BLOWCOUNTS TO CONSTANT COMBUSTION CURVE ADOPTED FOR CALIBRATION (after Harder and Seed, 1986)

equivalent SPT blowcounts are presented in Figure 14. Because open-bit soundings have been found to often give misleadingly low blowcounts due to the air recirculation process, this correlation is only intended for use with plugged-bits with 6.6-inch diameters. As detailed above, corrections for Becker hammer combustion energy are required before using this correlation. After making the energy corrections, all of the 1986 Mormon Island Becker data were converted into equivalent SPT blowcounts, denoted by the symbol N_{60} . Contained in Appendix A are copies of the work sheets used to make the corrections to the measured Becker blowcounts in order to determine equivalent SPT blowcounts.

Comparisons Between 1983 and 1986 Becker Penetration Resistance

The relationship presented in Figure 14 between corrected Becker and SPT blowcounts was developed for use with data collected with an AP-1000 drill rig. Because the 1983 Becker data was obtained using a Model B-180 drill rig, that data had to be corrected for the effect of drill rig (see References 1 and 2). Because this particular B-180 drill rig was used in the studies by Harder and Seed in developing the Becker-SPT correlation, its characteristics were well understood and there was no problem in applying a correction for the effect of a different drill rig type.

Because the 1986 soundings employed AP-1000 drill rigs, no correction for drill rig type was thought necessary. To verify this assumption, the equivalent SPT blowcounts determined in the two exploration areas were compared. Figure 15 presents a comparison between two 1983 and two 1986 soundings performed in the downstream flat area. Figure 16 presents a comparison between one 1983 and two

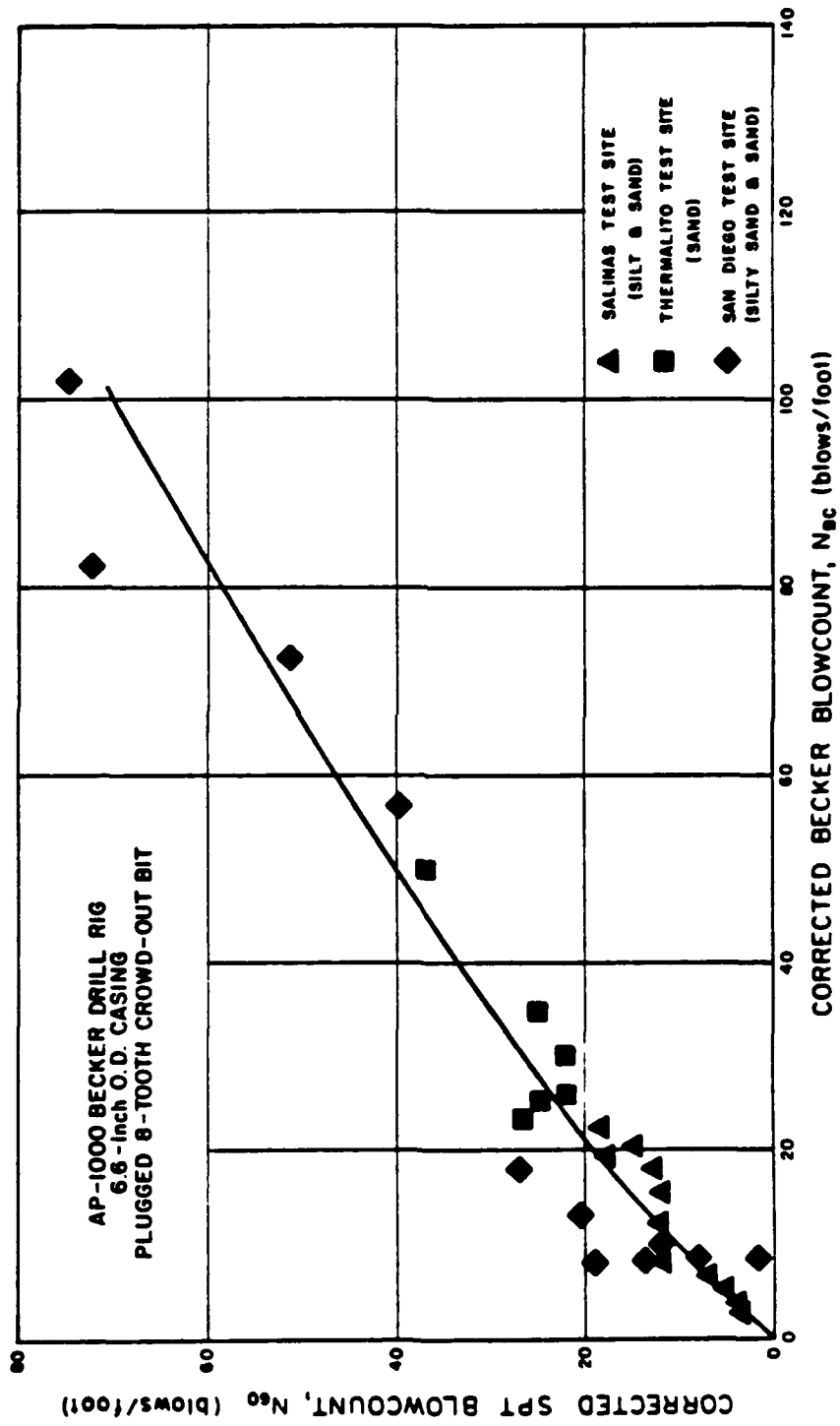


FIGURE 14: CORRELATION BETWEEN CORRECTED BECKER AND SPT BLOWCOUNT (after Harder and Seed, 1986)

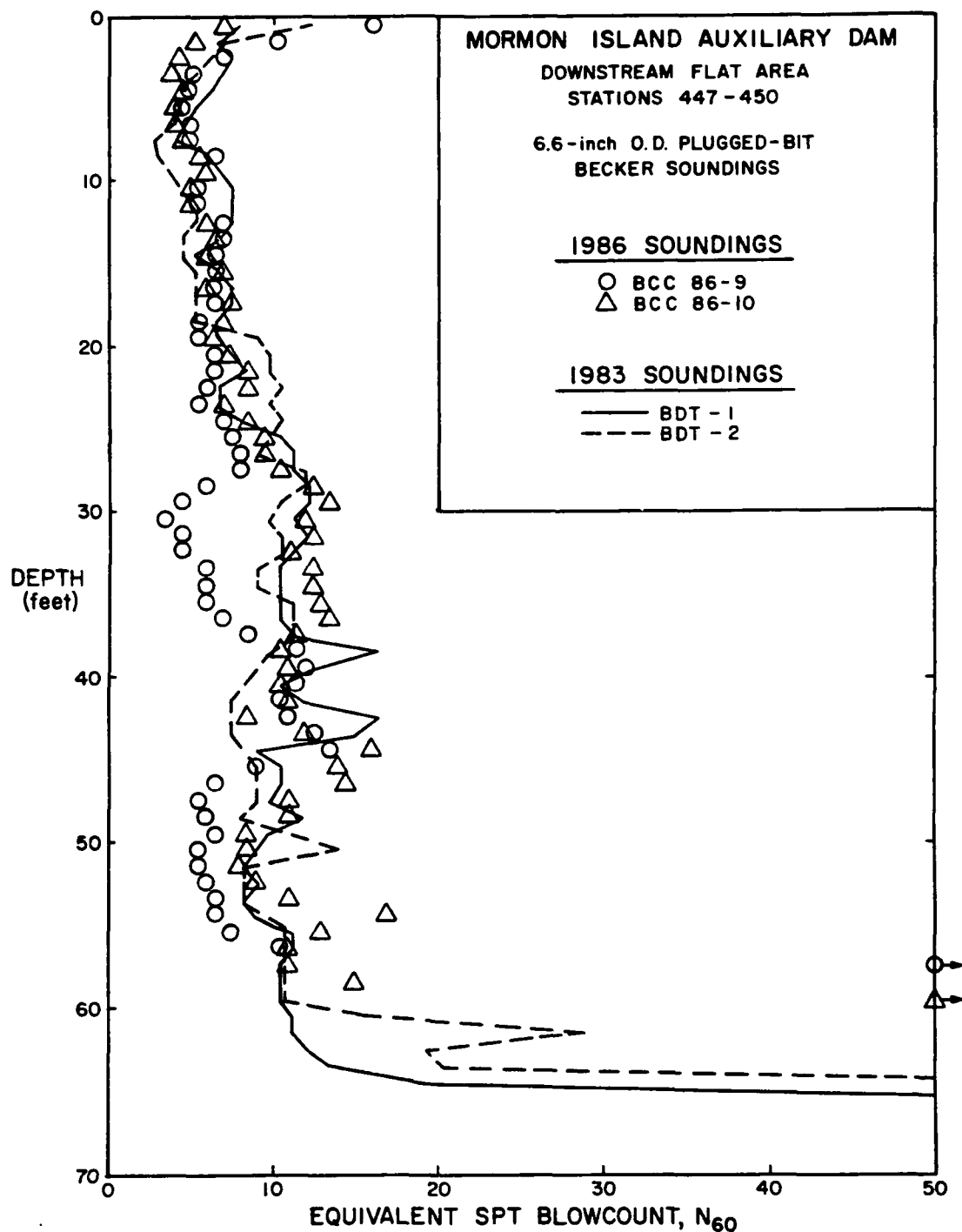


FIGURE 15: COMPARISON OF EQUIVALENT SPT BLOWCOUNTS DETERMINED IN THE 1983 AND 1986 BECKER EXPLORATIONS PERFORMED ALONG THE DOWNSTREAM FLAT OF MORMON ISLAND AUXILIARY DAM

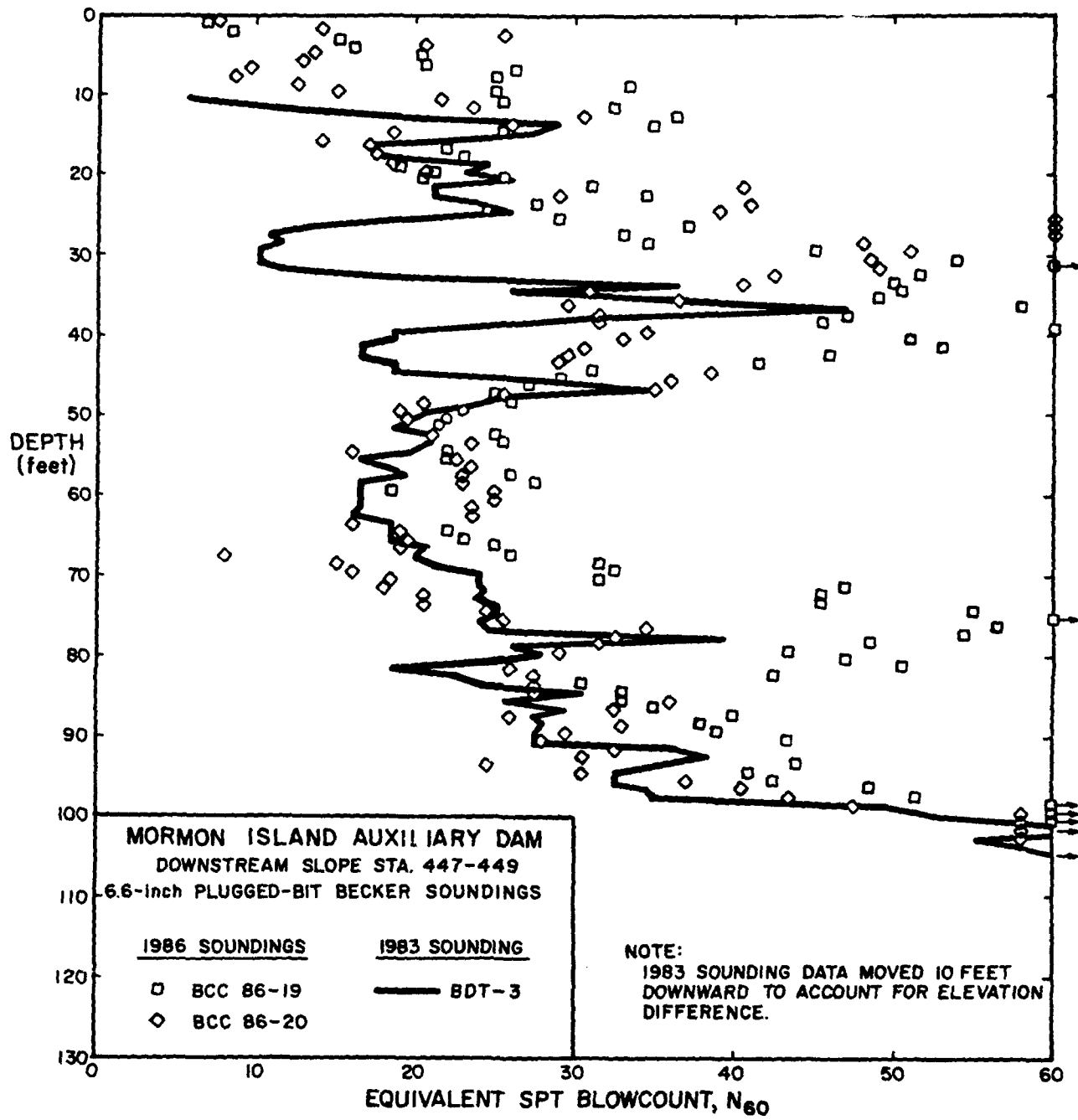


FIGURE 16: COMPARISON OF EQUIVALENT SPT BLOWCOUNTS DETERMINED IN THE 1983 AND 1986 BECKER EXPLORATIONS PERFORMED ALONG THE DOWNSTREAM FACE OF MORMON ISLAND AUXILIARY DAM

1986 soundings performed through the downstream slope (note: the 1983 data was moved 10 feet downward to account for an elevation difference). The 1986 data in these two comparisons were obtained with AP-1000 Drill Rig No. 404. These figures show generally excellent agreement between the two sets of data, thus confirming the assumption that no correction was necessary for the effect of different drill rigs for at least Drill Rig No. 404.

3. ACCOUNTING FOR OVERBURDEN PRESSURE

Correction to 1 tsf Overburden Pressure

In addition to being affected by soil properties such as relative density and cementation, penetration test results are also affected by the effective pressures confining the soil. Thus, a loose soil at great depth and confinement can have a high blowcount and a dense soil tested at shallow depth and small confinement can have a low blowcount. To account for the effect of confinement, penetration tests are usually normalized to the blowcount that would result if the soil was tested at a depth corresponding to 1 tsf of overburden pressure. This normalization is accomplished by multiplying a measured blowcount, N , by a correction factor, C_N , to obtain the normalized blowcount, N_1 (Reference 8). Because the equivalent SPT blowcounts derived from Becker blowcounts using the correlation by Harder and Seed (1986) are in terms of N_{60} values (the SPT blowcount that would be obtained with a SPT hammer delivering 60 percent of the free-fall energy of a 140-lb hammer falling 30 inches), the formula for normalizing to 1 tsf overburden pressure is as follows:

$$(N_1)_{60} = C_N * N_{60}$$

where $(N_1)_{60}$ = Normalized and corrected SPT blowcount used with correlation by Seed et al. (1985) to predict cyclic loading resistance.

N_{60} = Corrected or equivalent SPT blowcount derived from Becker Penetration Tests

C_N = Factor for correcting blowcounts to 1 tsf overburden pressure under level ground conditions

Studies have found that the C_N correction factor can vary as a function of both relative density and soil gradation. For overburden pressures greater than 1 tsf, the effect of the C_N correction is to reduce the blowcount. The studies by Marcuson and Bieganousky (1977a,b) indicate that as the soil becomes denser or the gradation becomes coarser, the magnitude of this reduction for higher overburden pressures decreases. In Figure 17 are two plots showing C_N overburden corrections indicated by Marcuson and Bieganousky's tests for four sands having a relative density of about 50 percent. A similiar pair of plots are shown in Figure 18 for tests of the same sands at a relative density of about 65 percent. The value of 50 percent was chosen because it corresponds approximately to the values determined from density tests in the Mormon Island dredge tailings (Reference 3). The value of 65 percent was chosen because it corresponds approximately to the values determined from density tests in the Mormon Island embankment shell material (Reference 3). As Figures 17 and 18 illustrate, the magnitude of the overburden correction for a particular stress level significantly decreases as the D_{50} of the sand increases from 0.2 to 2 mm.

Samples of embankment shell material and foundation soils obtained from the Becker open-bit soundings and from test pits generally indicate poorly graded to clayey gravels. The gradations measured for these soils were found to have D_{50} values generally between 2 and 40 mm. Accordingly, for the purposes of selecting appropriate C_N curves, the overall D_{50} of the Mormon Island soils sampled has been assumed to be approximately 15 mm. However, the highest D_{50} of the three sands tested by Marcuson and Bieganousky is only 2 mm.

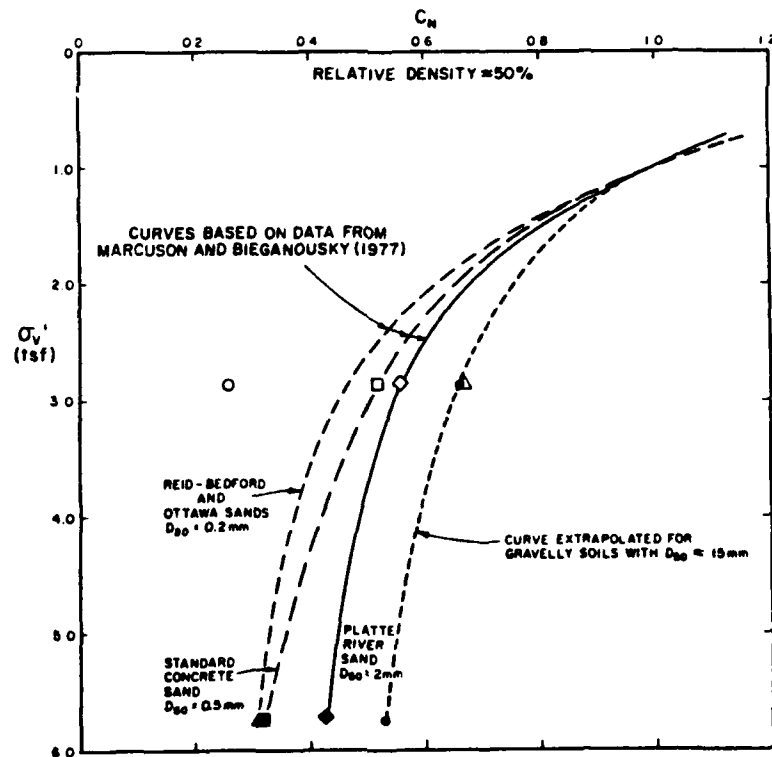
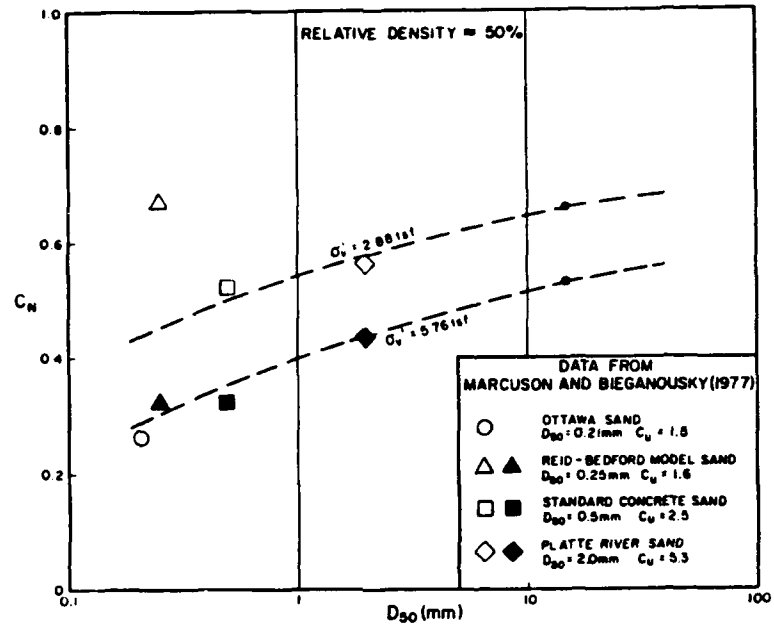


FIGURE 17: RELATIONSHIP BETWEEN C_N CORRECTION AND OVERBURDEN PRESSURE FOR SANDS WITH RELATIVE DENSITIES OF 50 PERCENT

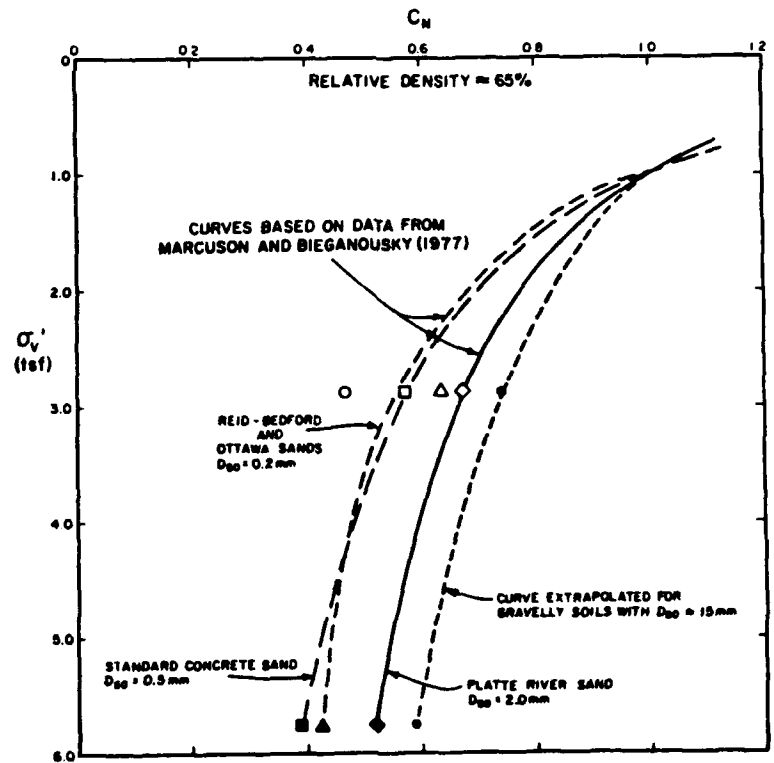
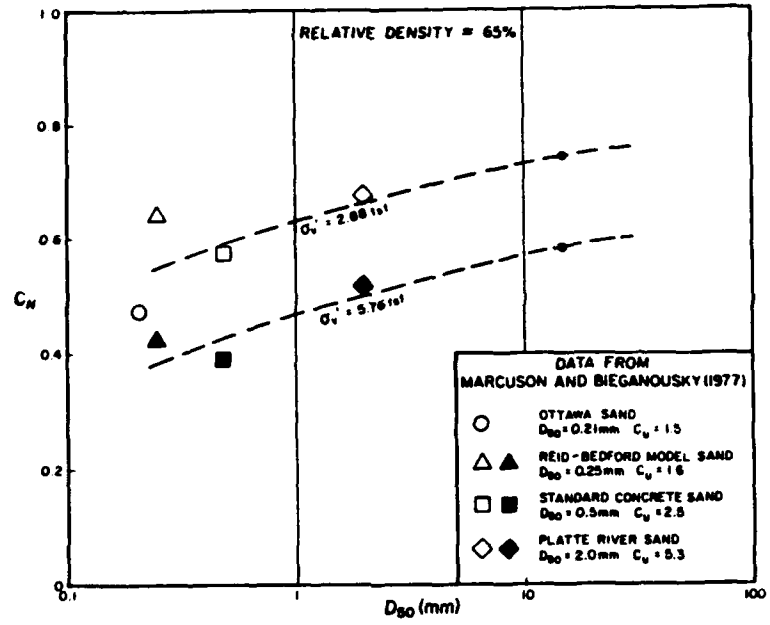


FIGURE 18: RELATIONSHIP BETWEEN C_N CORRECTION AND OVERBURDEN PRESSURE FOR SANDS WITH RELATIVE DENSITIES OF 65 PERCENT

Consequently, two new C_N curves, one each for 50 and 65 percent relative density, were developed by extrapolating the test results for the three sands. The extrapolation process is illustrated in the upper plots shown in Figures 17 and 18. The resulting C_N curves for gravels are shown as dotted lines in the lower plots in Figures 17 and 18. These extrapolated curves were used for normalizing the equivalent SPT blowcounts obtained from the 1986 Mormon Island Becker data.

Effect of Sloping Ground Conditions on Overburden Correction Factor

The C_N overburden corrections shown in Figures 17 and 18 have been developed for level ground conditions. Level ground conditions for normally-consolidated materials usually have effective mean normal stresses that are approximately equal to 60 percent of the vertical effective overburden pressure. This is equivalent to having a coefficient of lateral earth pressure at rest, K_0 , equal to 0.4. However, soils under sloping ground conditions often have higher lateral stresses due to the driving forces imparted by the weight of the slope material. This leads to mean normal stresses that may be equal to as much as 90 percent of the vertical overburden pressure. Several studies (e.g. Marcuson and Bieganousky, 1977a; Seed et al., 1975) have indicated that penetration resistance increases with increases in lateral confinement. Consequently, with increased mean confinement, a blowcount performed in soil under sloping ground conditions could be significantly greater than a blowcount conducted at the same vertical effective stress in the same soil under level ground conditions. Thus, the use of only the vertical overburden pressure with the curves in Figures 17 or 18 could lead to unconservative corrections for tests performed under sloping ground conditions.

Since the Becker tests performed at Mormon Island were located through or adjacent to sloping ground, it is necessary to account for higher mean confinement. The method adopted to correct the data was to use an equivalent level ground vertical effective pressure for use with the extrapolated C_N curves shown in Figures 17 and 18. This equivalent vertical effective pressure is set equal to 1.67 times the effective mean confinement at the depth where the penetration test was performed. In this way, the equivalent level ground vertical effective stress represents the overburden pressure that a soil element in sloping ground would have if that soil element had the same mean confinement under level ground conditions (i.e. the mean confinement is equal to 60 percent of the equivalent level ground vertical effective stress).

To determine the equivalent vertical stresses to be used with the adopted C_N curve, the results from non-linear static finite element analyses (Reference 13) were employed to calculate the mean confining pressures at the locations where Becker soundings were performed. Because the finite element stress analyses employed two-dimensional plane strain models, the mean confining pressure was calculated using the following formula:

$$\sigma'_m = (\sigma'_y + \sigma'_x) * (1. + \nu) * 0.333$$

where σ'_m = mean effective confining pressure
 σ'_y = effective vertical pressure in 2-D plane
 σ'_x = effective horizontal pressure in 2-D plane
 ν = Poisson's ratio - assumed equal to 0.3

The finite element studies were used to determine equivalent level ground overburden pressures and C_N values for all 26 of the 1986 test sites. The elements, stresses, equivalent level ground overburden pressures, and resulting C_N values for sites in the downstream flat and for sites along the midpoint of the downstream slope (Sites 15 through 21) are presented in Tables 2 and 3.

TABLE 2: DETERMINATION OF OVERBURDEN PRESSURE CORRECTIONS FOR SOUNDINGS PERFORMED THROUGH MIDPOINT OF DOWNSTREAM SLOPE (Soundings BCC 86-15 through BCC 86-21)

Element	Depth (ft)	Vertical Stress (ksf)	Horizontal Stress (ksf)	Poisson's Ratio	Mean Stress (ksf)	Equiv. Level Ground Vertical Stress (ksf)	C _N
Embankment							
330	19.5	3.350	2.957	0.3	2.733	4.555	0.80
308	33.7	5.417	3.384	0.3	3.814	6.356	0.72
274	47.5	6.586	2.854	0.3	4.091	6.818	0.70
Foundation							
274	47.5	6.586	2.854	0.3	4.091	6.818	0.62
202	69.5	8.288	3.812	0.3	5.243	8.739	0.57
155	79.3	9.216	4.336	0.3	5.873	9.788	0.55
115	89.3	9.513	4.455	0.3	6.053	10.088	0.54
73	99.4	10.534	5.047	0.3	6.752	11.253	0.53
31	110.6	11.060	5.449	0.3	7.154	11.923	0.53

TABLE 3: DETERMINATION OF OVERBURDEN PRESSURE CORRECTIONS FOR SOUNDINGS PERFORMED BEYOND DOWNSTREAM TOE

Element	Depth (ft)	Vertical Stress (ksf)	Horizontal Stress (ksf)	Poisson's Ratio	Mean Stress (ksf)	Equiv. Level Ground Vertical Stress (ksf)	C _N
250	11.1	0.857	0.728	0.3	0.687	1.145	1.29
211	19.3	1.447	1.103	0.3	1.105	1.842	1.04
164	27.2	2.094	1.464	0.3	1.542	2.570	0.90
124	33.7	2.530	1.660	0.3	1.816	3.026	0.84
83	42.3	3.239	1.909	0.3	2.231	3.718	0.78
40	56.3	4.409	2.473	0.3	2.982	4.970	0.70

Notes: 1) Stresses presented in tables above are effective stresses.
 2) Vertical and Horizontal stresses obtained from 2-D non-linear finite element analyses, Reference 13.

4. PRESENTATION OF RESULTS

Presentation of Results

Shown in Figures 19 through 44 are the equivalent SPT N_{60} blowcounts obtained from 1986 plugged-bit Becker soundings performed at Mormon Island. Also shown are dashed lines representing different levels of blowcount normalized for overburden pressure (i.e. $(N_1)_{60}$ values). For soundings performed through the embankment (Soundings BCC 86-15 through 86-26), two sets of $(N_1)_{60}$ contours are used - one set for the embankment material, one set for the foundation soils. Also shown on these plots are the soil classifications determined for samples obtained at the same depths using the open-bit Becker sounding performed at each site. The data shown in Figures 19 through 44 indicate the following trends:

1. Soundings in Blue Ravine Alluvium and Slope Wash along Downstream Flat (Soundings BCC 86-1 through BCC 86-6, and BCC 86-14) - The equivalent SPT blowcounts indicate a surficial low blowcount layer in the Blue Ravine Alluvium and slope wash material extending down to about 10 feet. Below this depth, these soils exhibited very high penetration resistance down to the rock contact. Rock was assumed to have been reached at the maximum depth of each sounding because of the extremely high penetration resistance developed.

The fines content of the low blowcount surficial material appears to be generally about 25 percent and clayey, thus leading to classifications generally of SC or GC. This soil has significantly more fines than is generally found in the loose dredge tailing deposits.

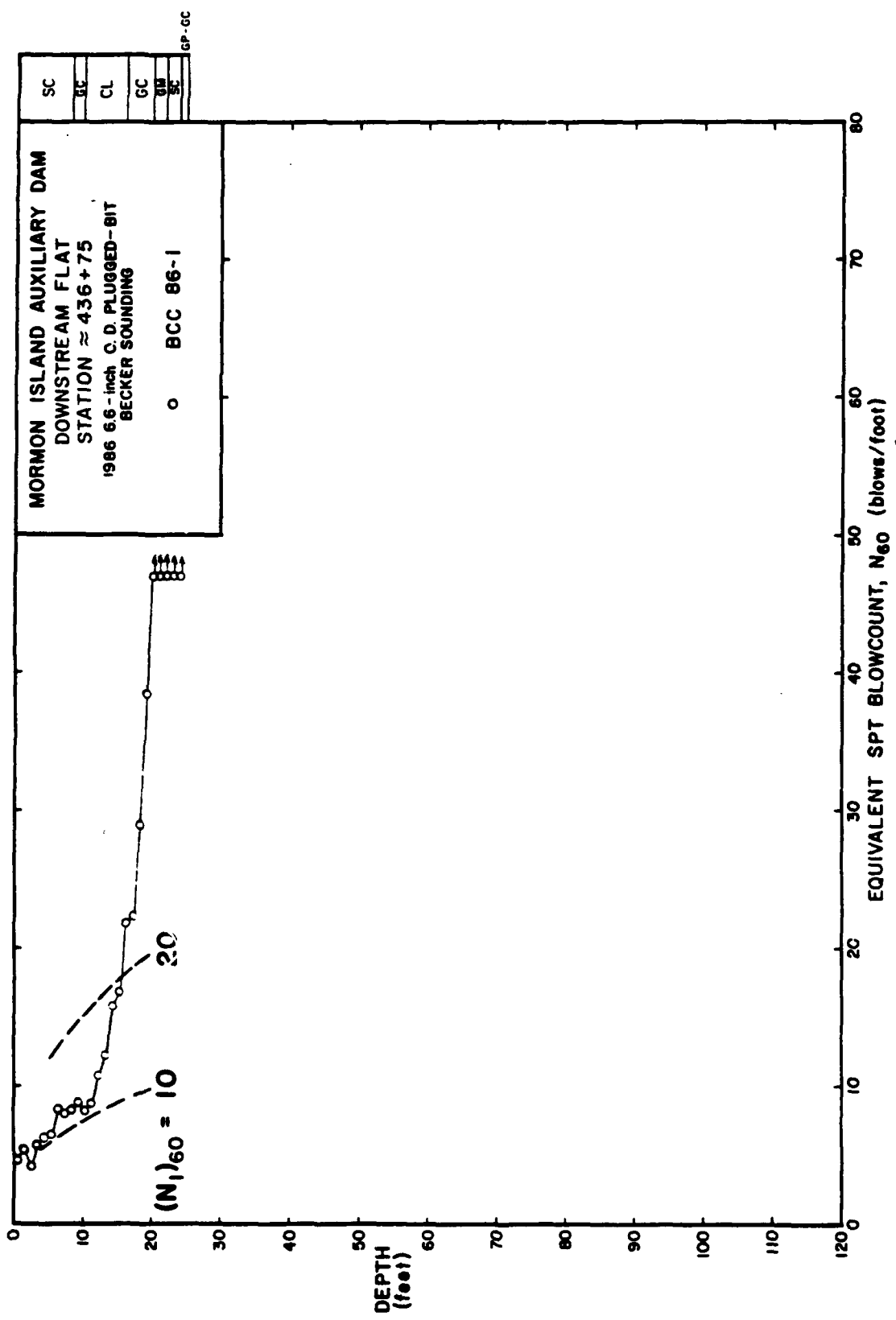


FIGURE 19: EQUIVALENT SPT BLOWCOUNTS FOR BECKER SOUNDING BCC 86-1 PERFORMED IN DOWNSTREAM FLAT OF MORMON ISLAND AUXILIARY DAM

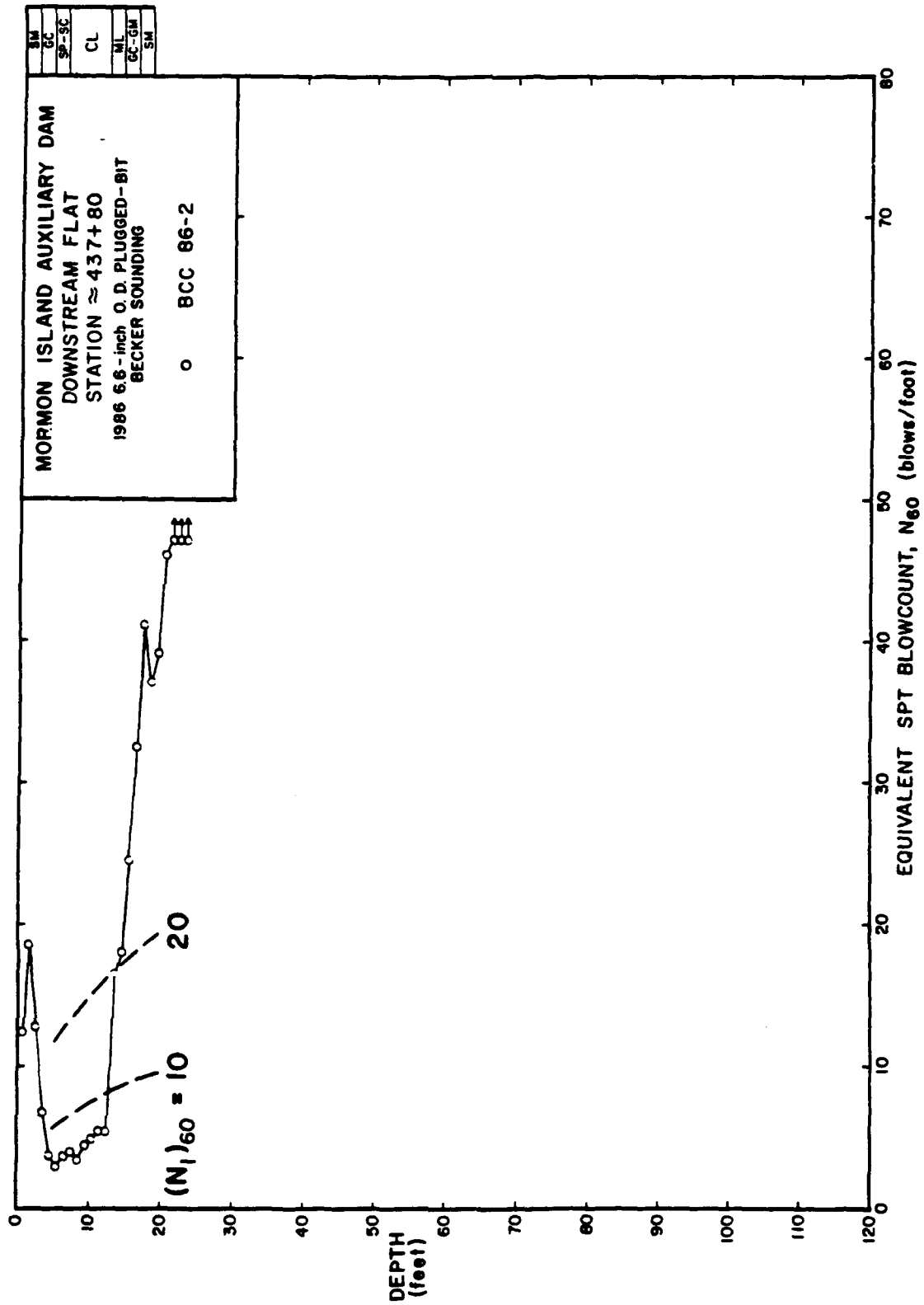


FIGURE 20: EQUIVALENT SPT BLOWCOUNTS FOR BECKER SOUNDING BCC 86-2 PERFORMED IN DOWNSTREAM FLAT OF MORMON ISLAND AUXILIARY DAM

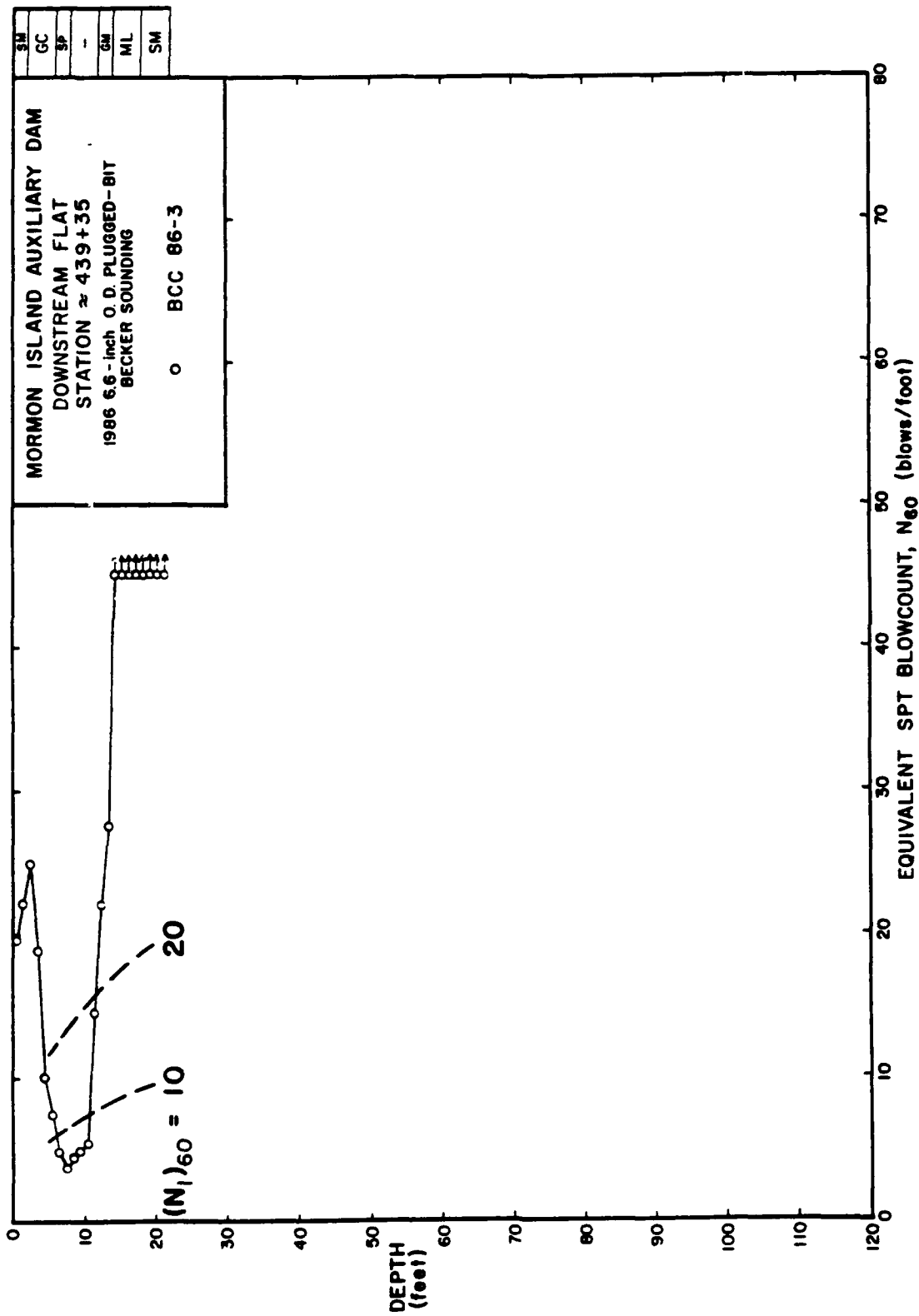


FIGURE 21: EQUIVALENT SPT BLOWCOUNTS FOR BECKER SOUNDING BCC 86-3 PERFORMED IN DOWNSTREAM FLAT OF MORMON ISLAND AUXILIARY DAM

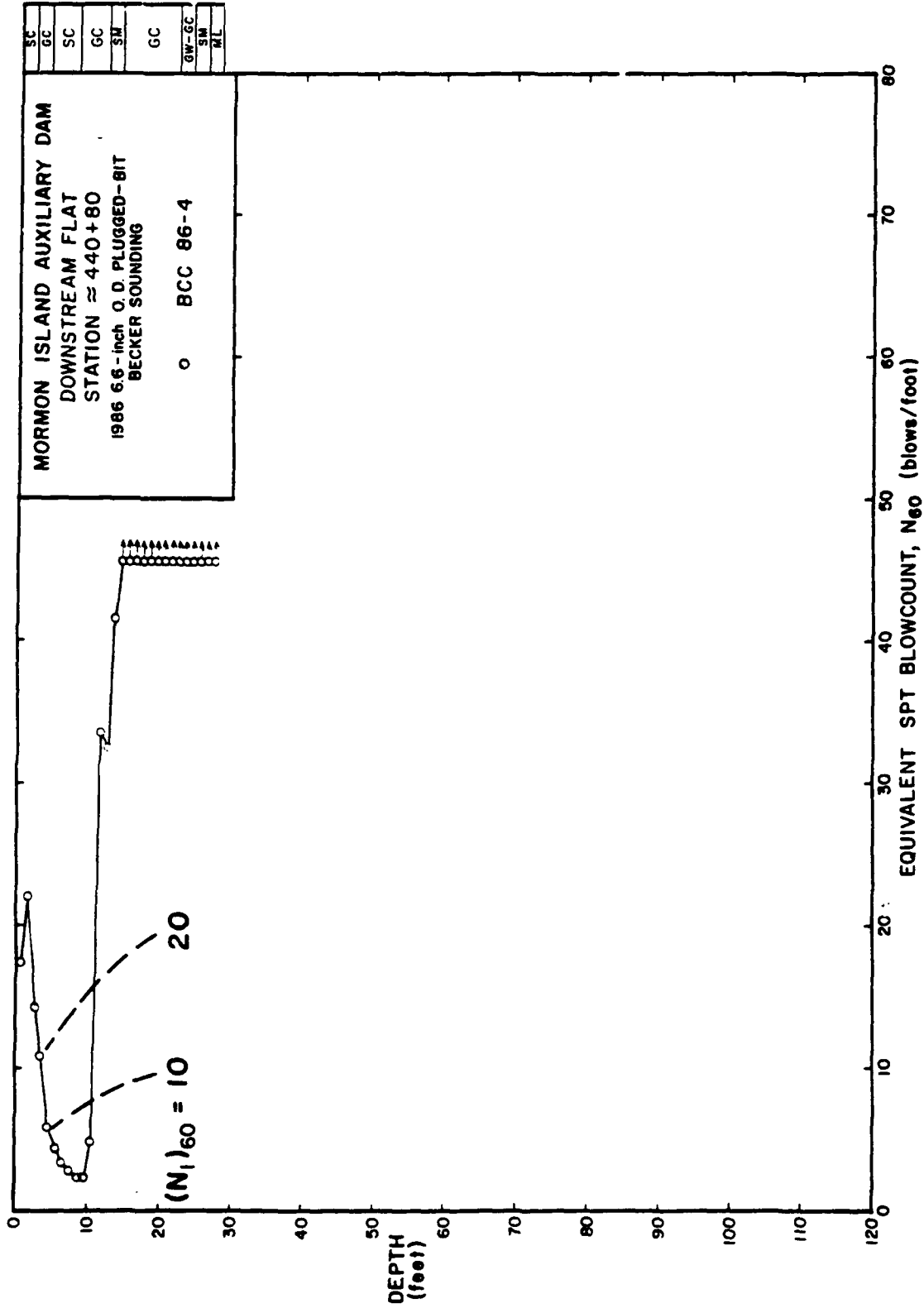


FIGURE 22: EQUIVALENT SPT BLOWCOUNTS FOR BECKER SOUNDING BCC 86-4 PERFORMED IN DOWNSTREAM FLAT OF MORMON ISLAND AUXILIARY DAM

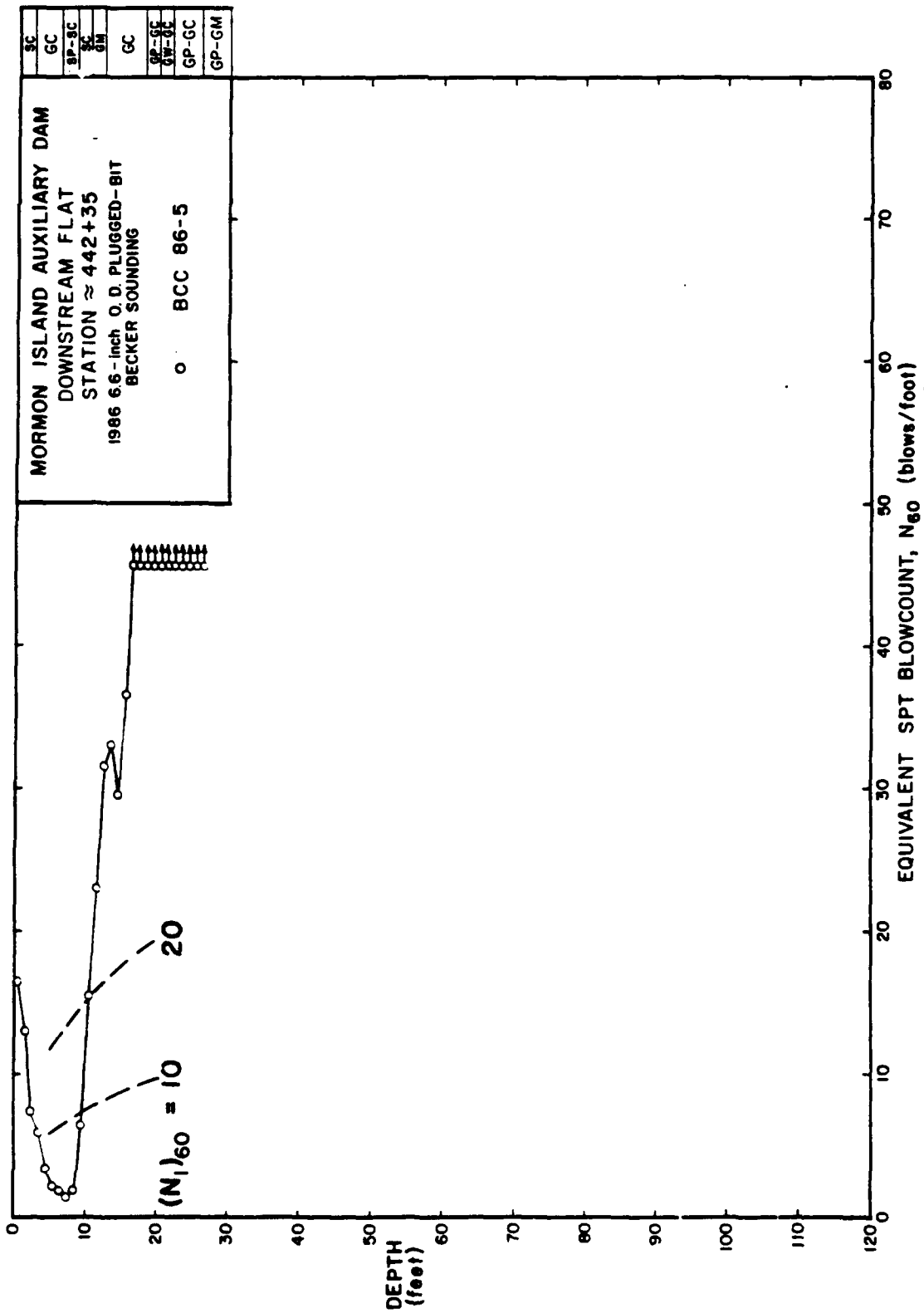


FIGURE 23: EQUIVALENT SPT BLOWCOUNTS FOR BECKER SOUNDING BCC 86-5 PERFORMED IN DOWNSTREAM FLAT OF MORMON ISLAND AUXILIARY DAM

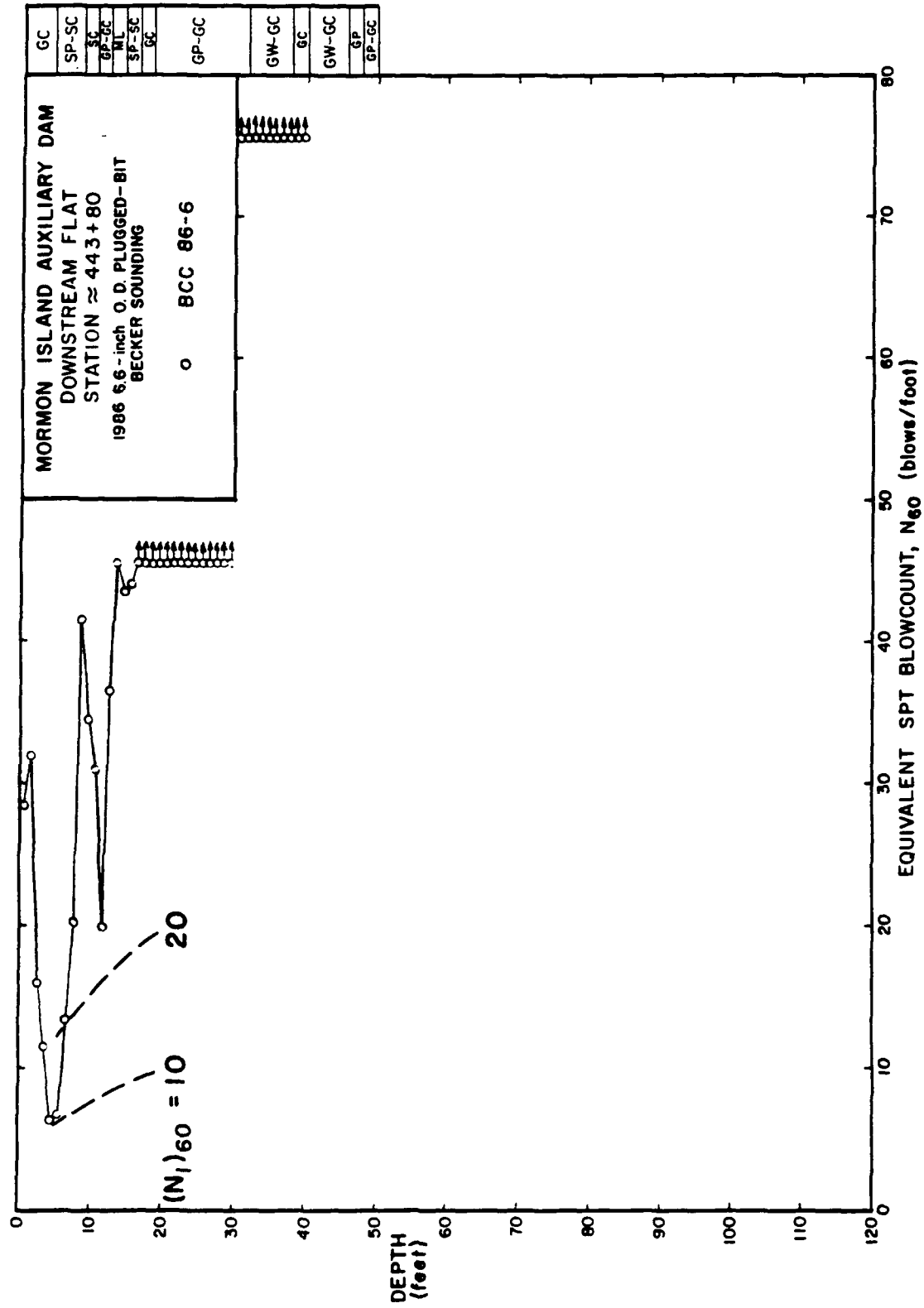


FIGURE 24: EQUIVALENT SPT BLOWCOUNTS FOR BECKER SOUNDING BCC 86-6 PERFORMED IN DOWNSTREAM FLAT OF MORMON ISLAND AUXILIARY DAM

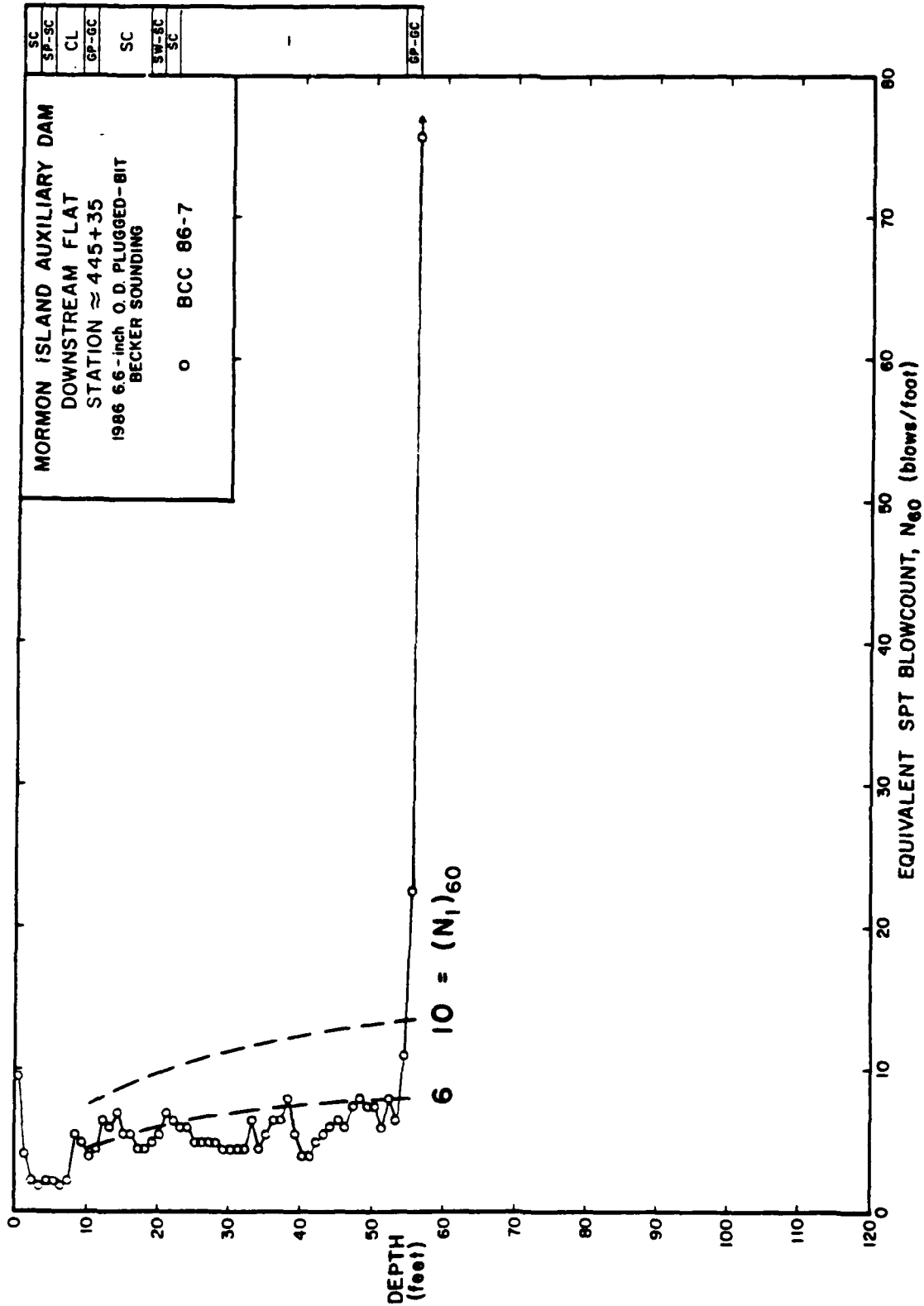


FIGURE 25: EQUIVALENT SPT BLOWCOUNTS FOR BECKER SOUNDING BCC 86-7 PERFORMED IN DOWNSTREAM FLAT OF MORMON ISLAND AUXILIARY DAM

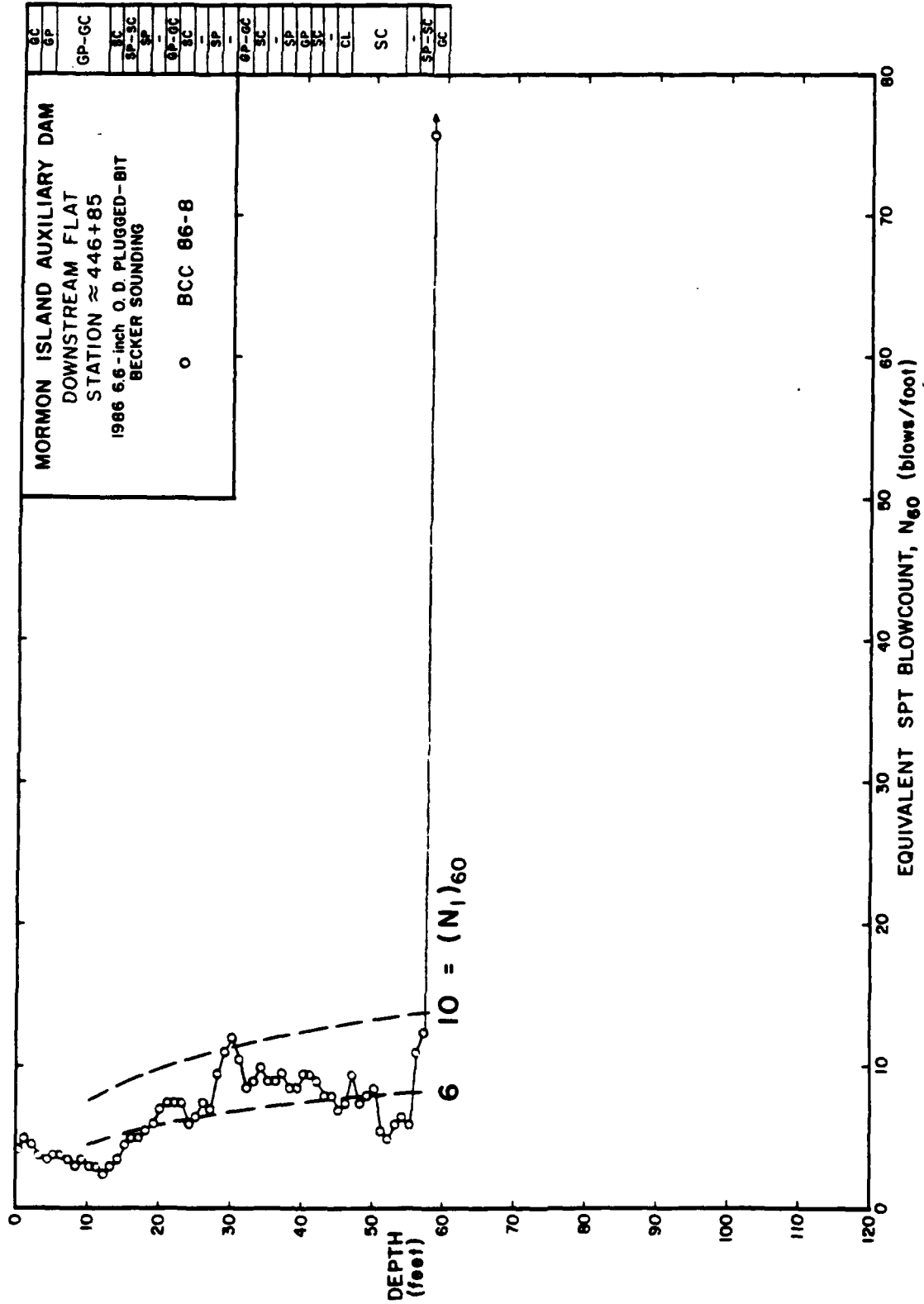


FIGURE 26: EQUIVALENT SPT BLOWCOUNTS FOR BECKER SOUNDING BCC 86-8 PERFORMED IN DOWNSTREAM FLAT OF MORMON ISLAND AUXILIARY DAM

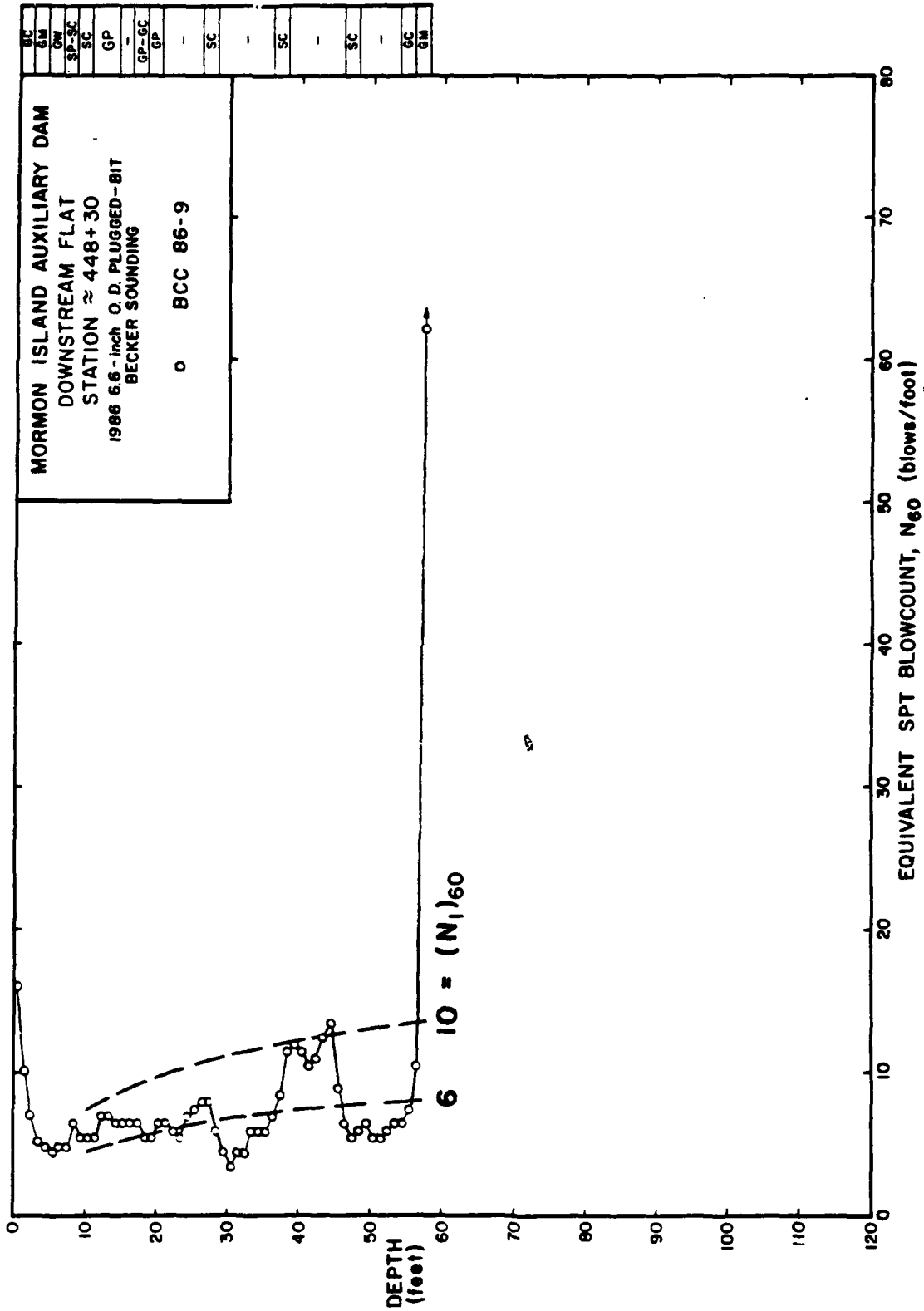


FIGURE 27: EQUIVALENT SPT BLOWCOUNTS FOR BECKER SOUNDING BCC 86-9 PERFORMED IN DOWNSTREAM FLAT OF MORMON ISLAND AUXILIARY DAM

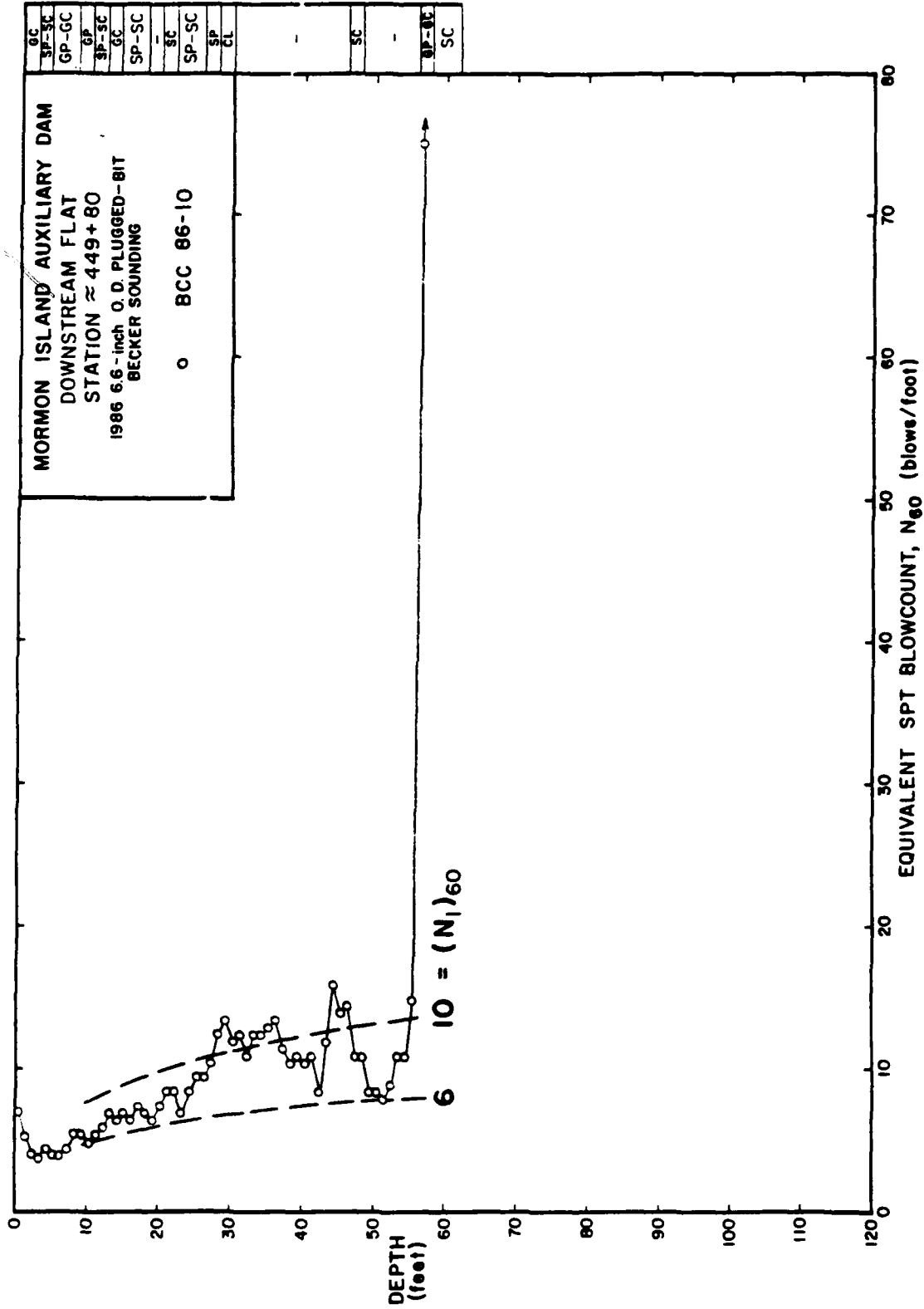


FIGURE 28: EQUIVALENT SPT BLOWCOUNTS FOR BECKER SOUNDING BCC 86-10 PERFORMED IN DOWNSTREAM FLAT OF MORMON ISLAND AUXILIARY DAM

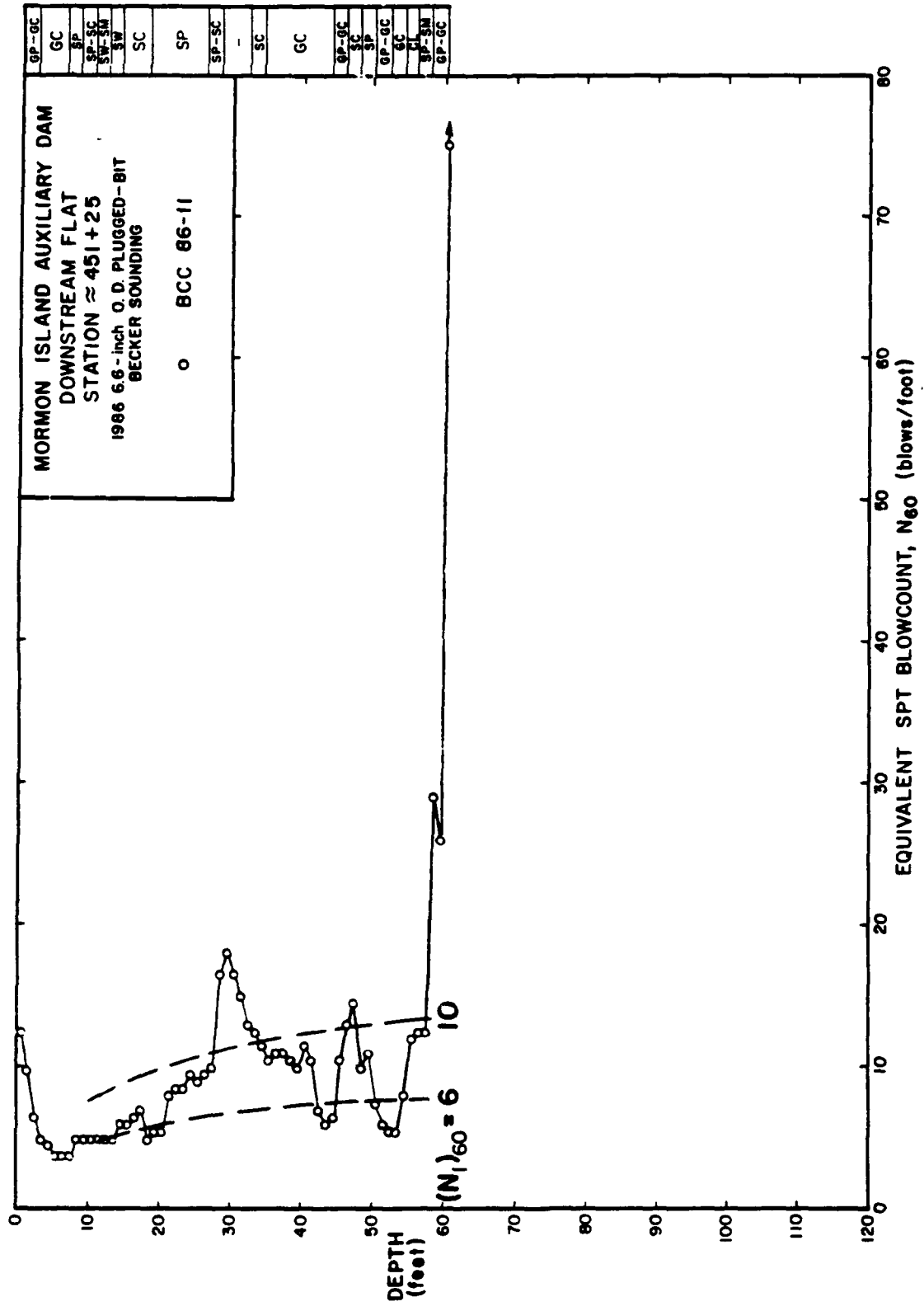


FIGURE 29: EQUIVALENT SPT BLOWCOUNTS FOR BECKER SOUNDING BCC 86-11 PERFORMED IN DOWNSTREAM FLAT OF MORMON ISLAND AUXILIARY DAM

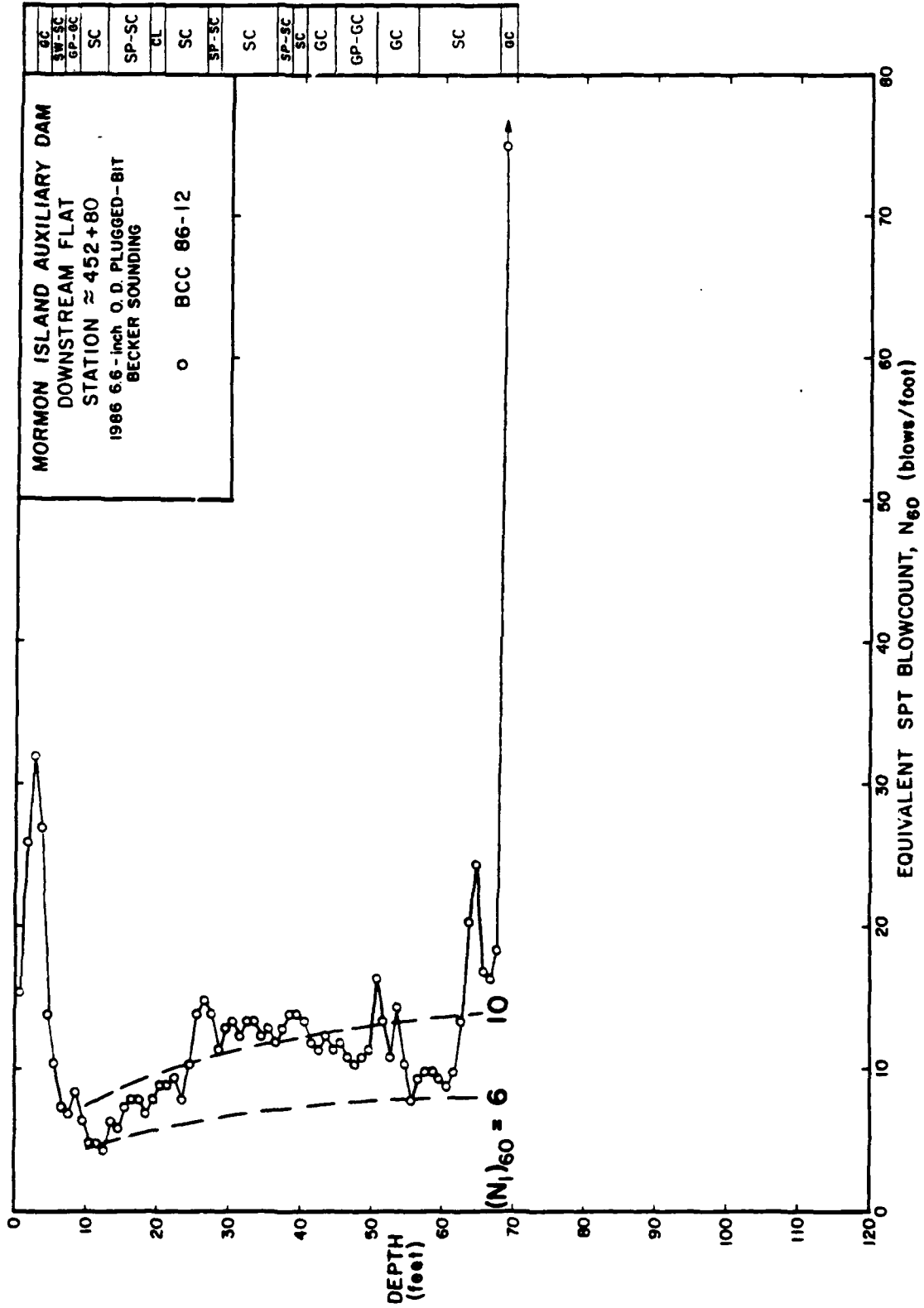


FIGURE 30: EQUIVALENT SPT BLOWCOUNTS FOR BECKER SOUNDING BCC 86-12 PERFORMED IN DOWNSTREAM FLAT OF MORMON ISLAND AUXILIARY DAM

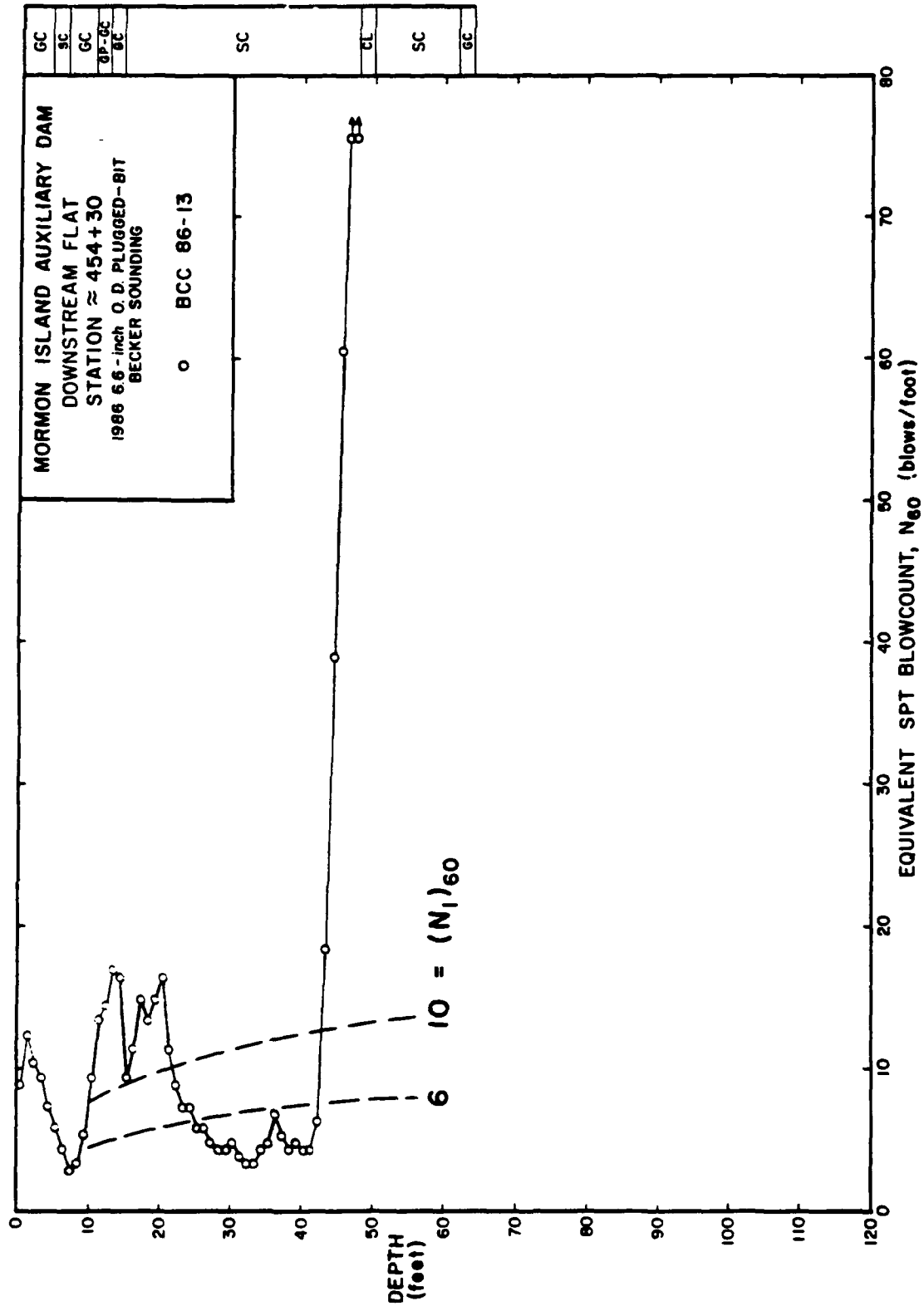


FIGURE 31: EQUIVALENT SPT BLOWCOUNTS FOR BECKER SOUNDING BCC 86-13 PERFORMED IN DOWNSTREAM FLAT OF MORMON ISLAND AUXILIARY DAM

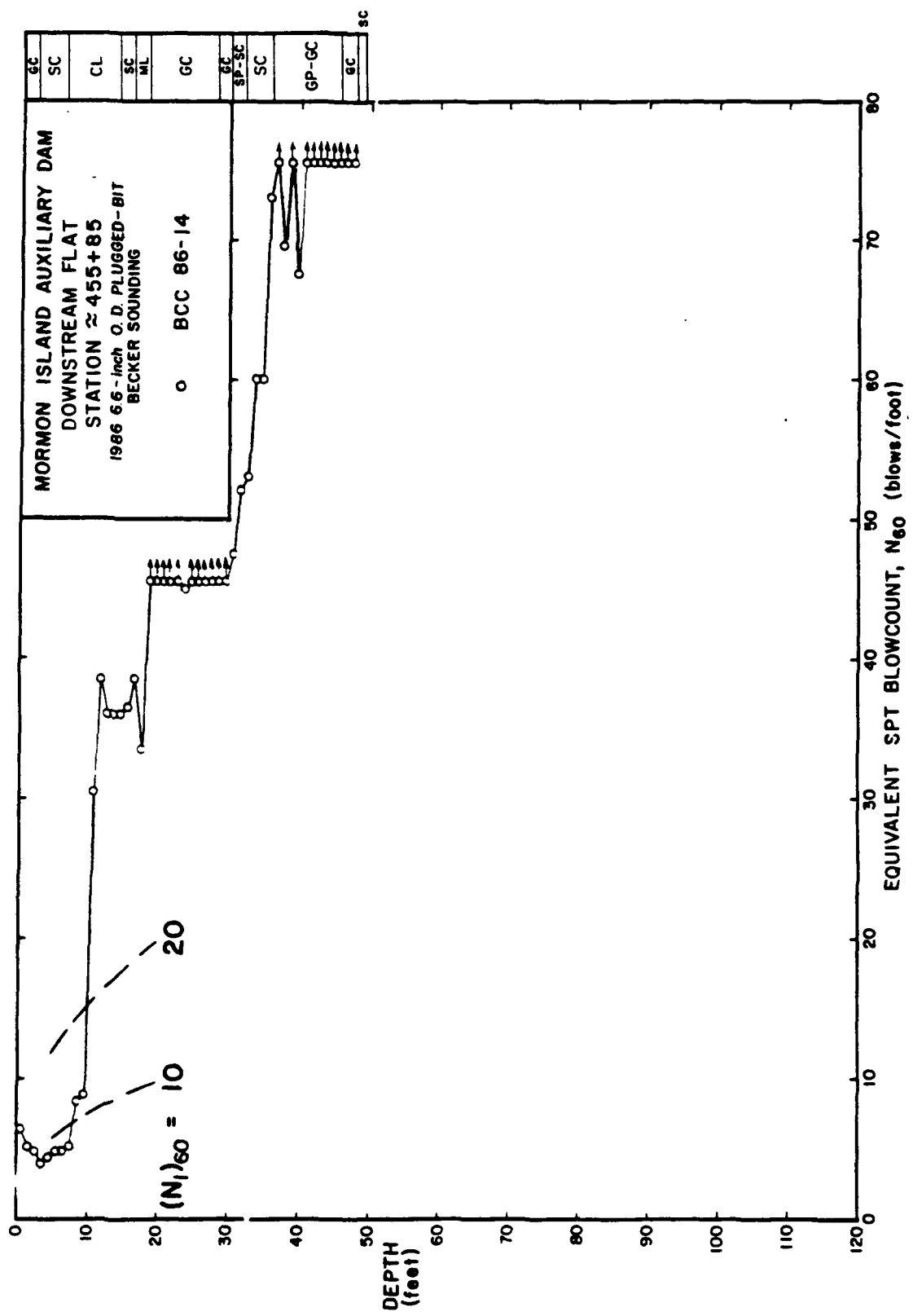


FIGURE 32: EQUIVALENT SPT BLOWCOUNTS FOR BECKER SOUNDING BCC 86-14 PERFORMED IN DOWNSTREAM FLAT OF MORMON ISLAND AUXILIARY DAM

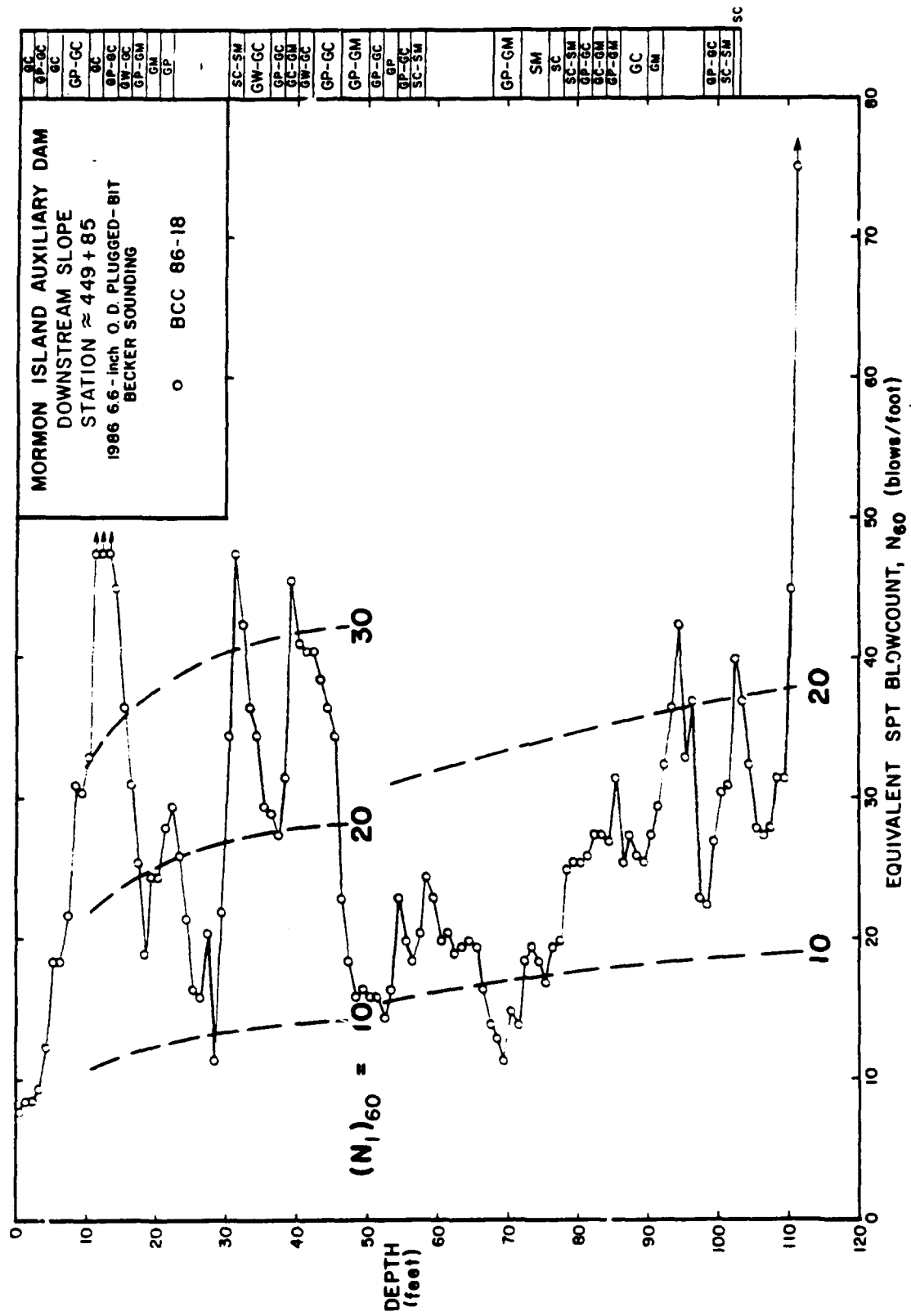


FIGURE 36: EQUIVALENT SPT BLOWCOUNTS FOR BECKER SOUNDING BCC 86-18 PERFORMED ON DOWNSTREAM FACE OF MORMON ISLAND AUXILIARY DAM

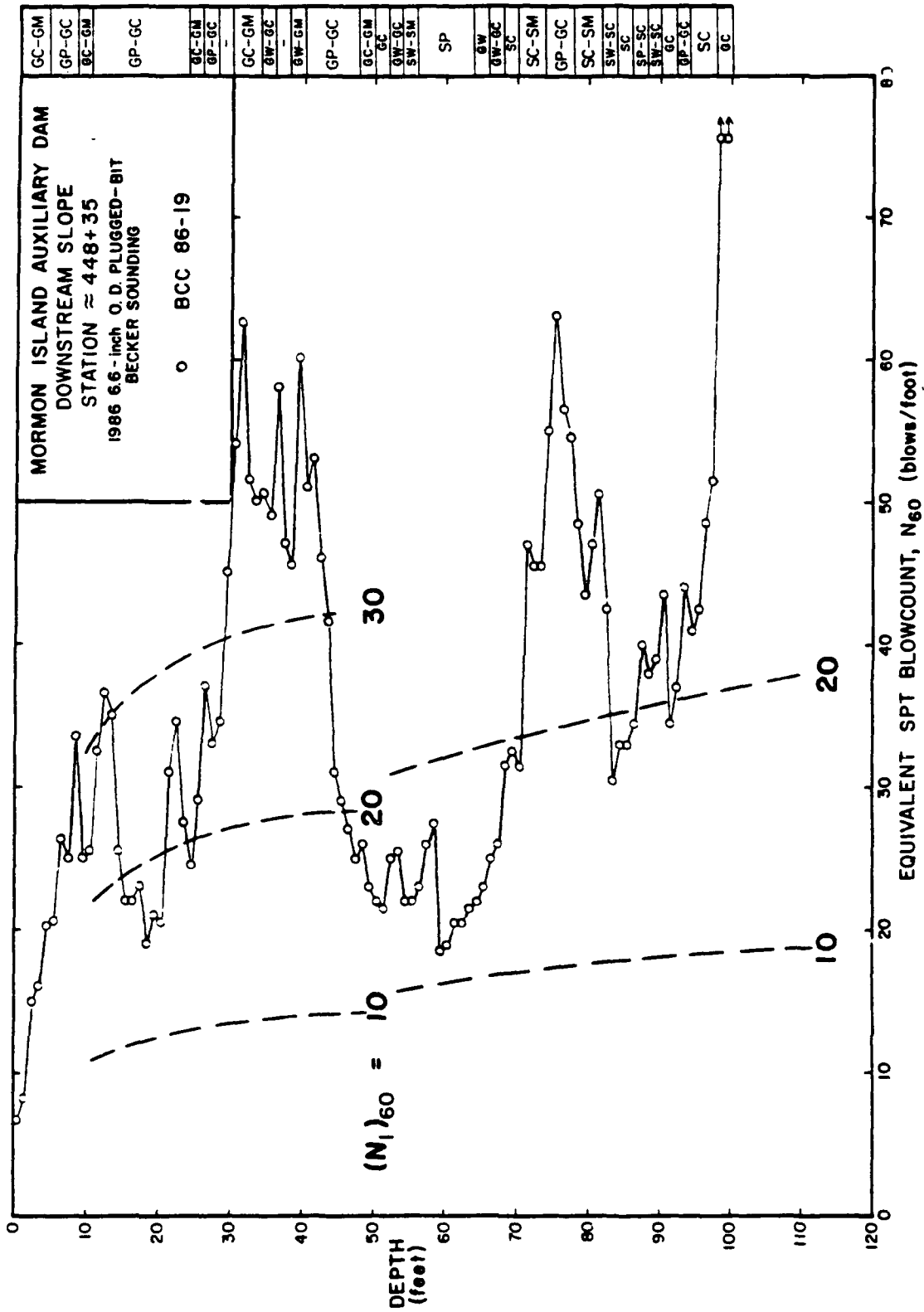


FIGURE 37: EQUIVALENT SPT BLOWCOUNTS FOR BECKER SOUNDING BCC 86-19 PERFORMED ON DOWNSTREAM FACE OF MORMON ISLAND AUXILIARY DAM

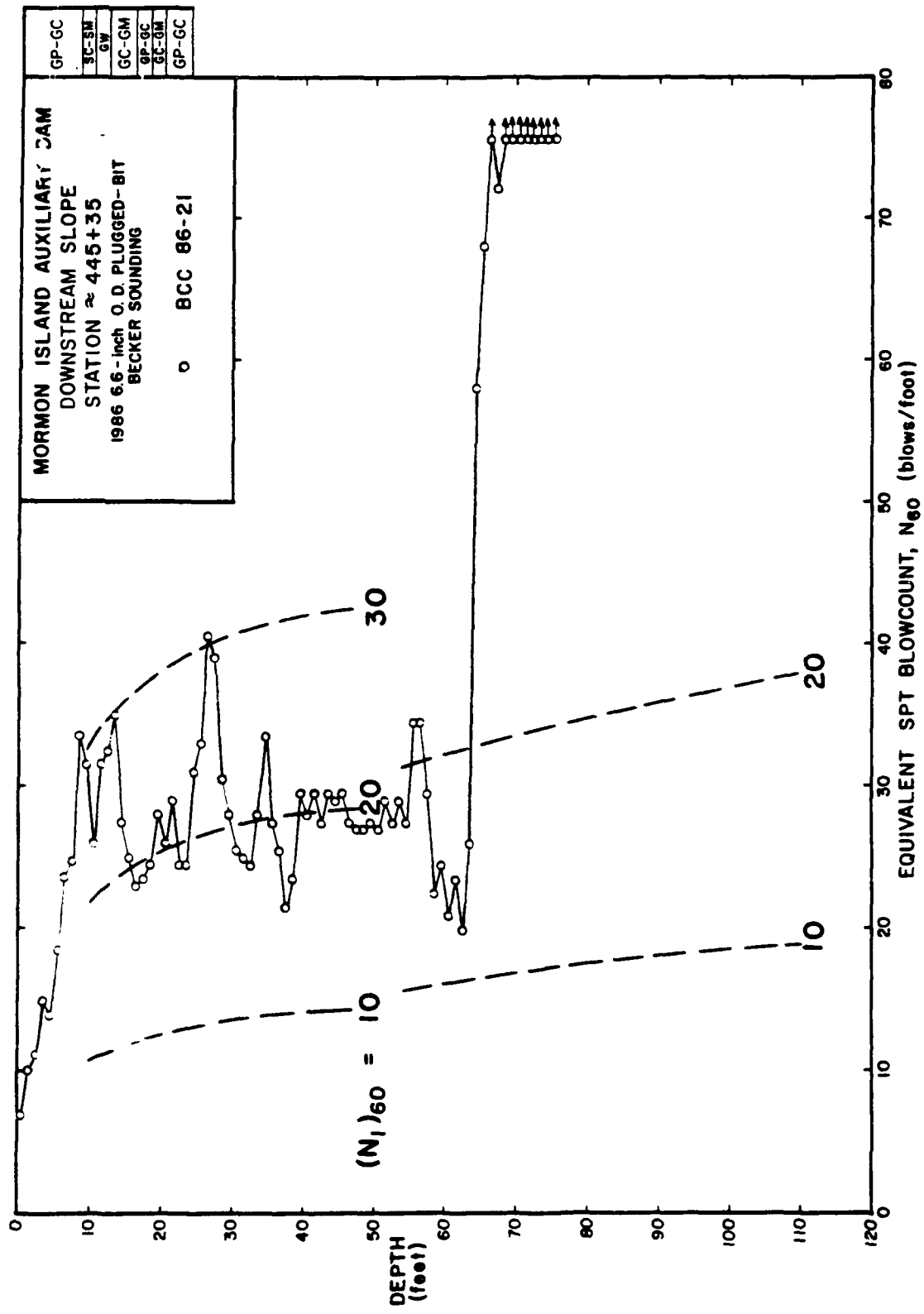


FIGURE 39: EQUIVALENT SPT BLOWCOUNTS FOR BECKER SOUNDING BCC 86-21 PERFORMED ON DOWNSTREAM FACE OF MORMON ISLAND AUXILIARY DAM

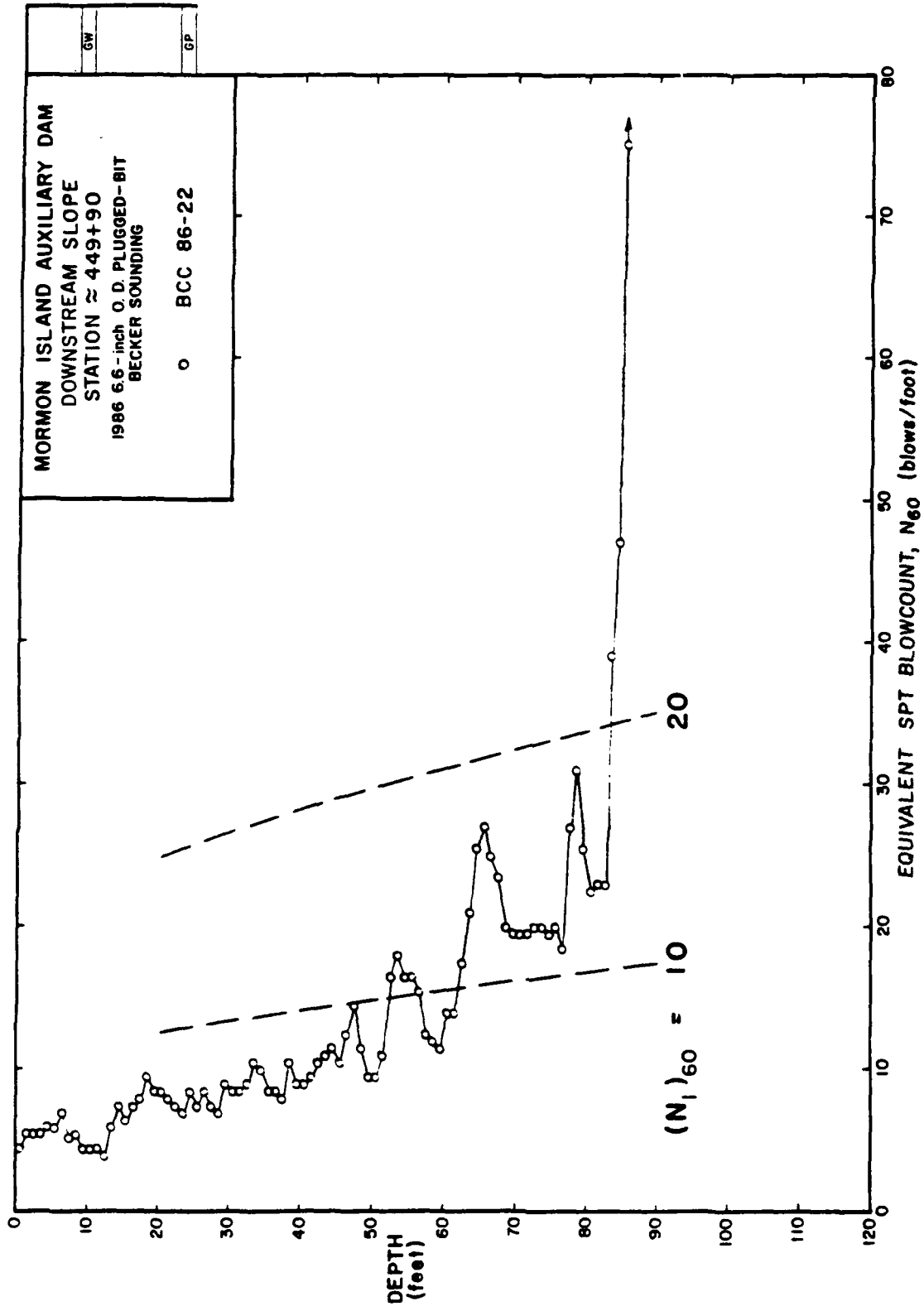


FIGURE 40: EQUIVALENT SPT BLOWCOUNTS FOR BECKER SOUNDING BCC 86-22 PERFORMED ON DOWNSTREAM FACE OF MORMON ISLAND AUXILIARY DAM

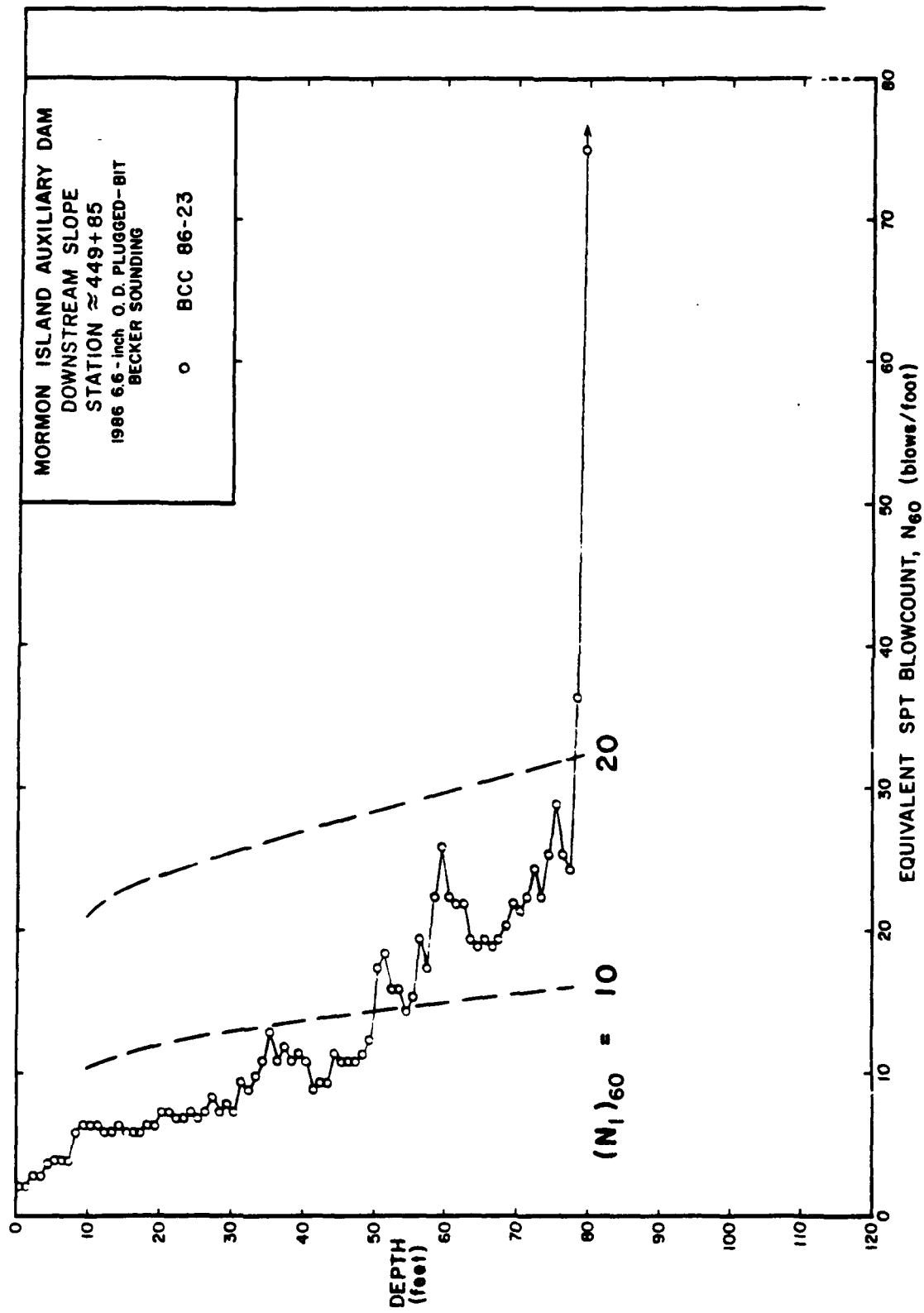


FIGURE 41: EQUIVALENT SPT BLOWCOUNTS FOR BECKER SOUNDING BCC 86-23 PERFORMED ON DOWNSTREAM FACE OF MORMON ISLAND AUXILIARY DAM

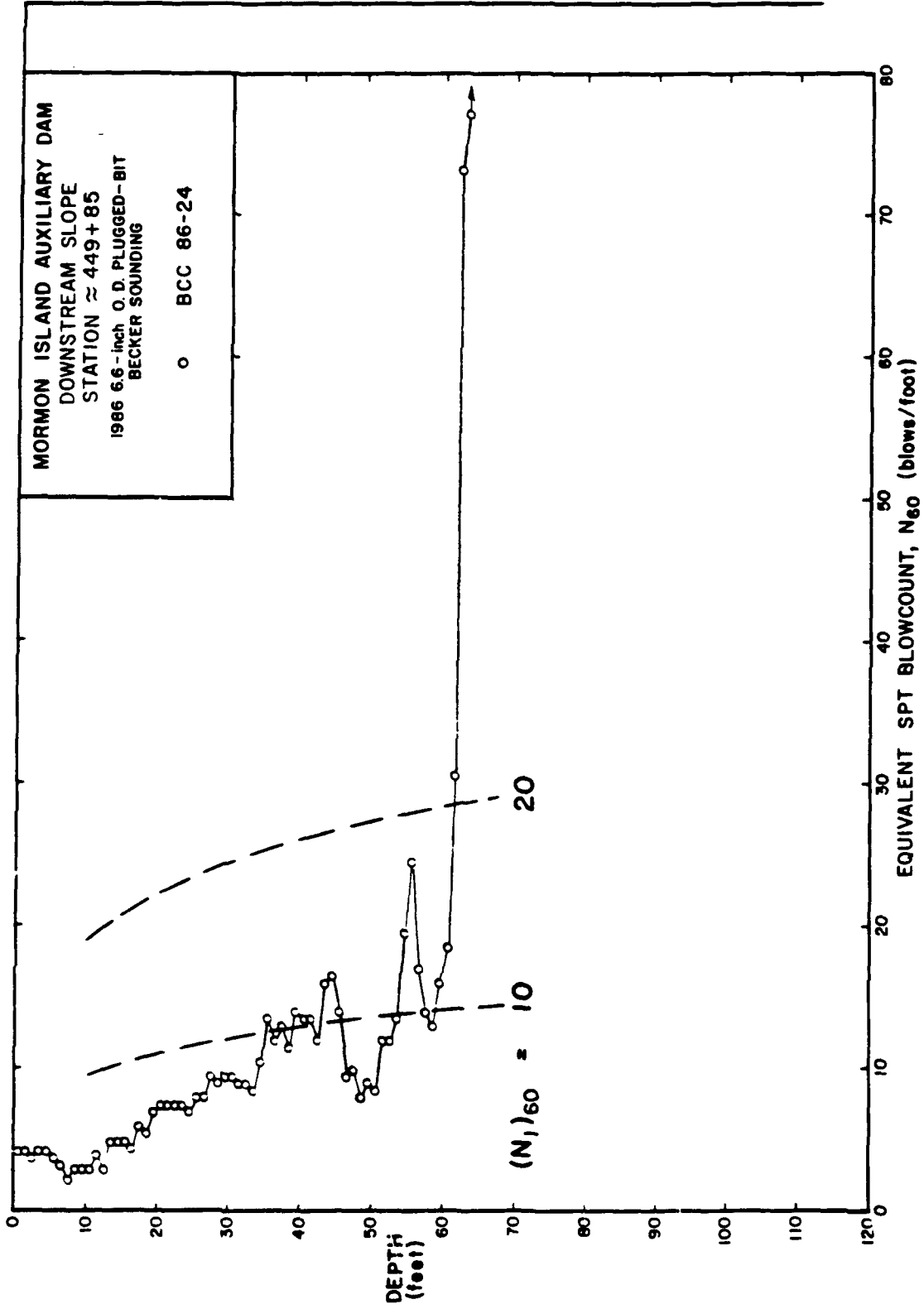


FIGURE 42: EQUIVALENT SPT BLOWCOUNTS FOR BECKER SOUNDING BCC 86-24 PERFORMED ON DOWNSTREAM FACE OF MORMON ISLAND AUXILIARY DAM

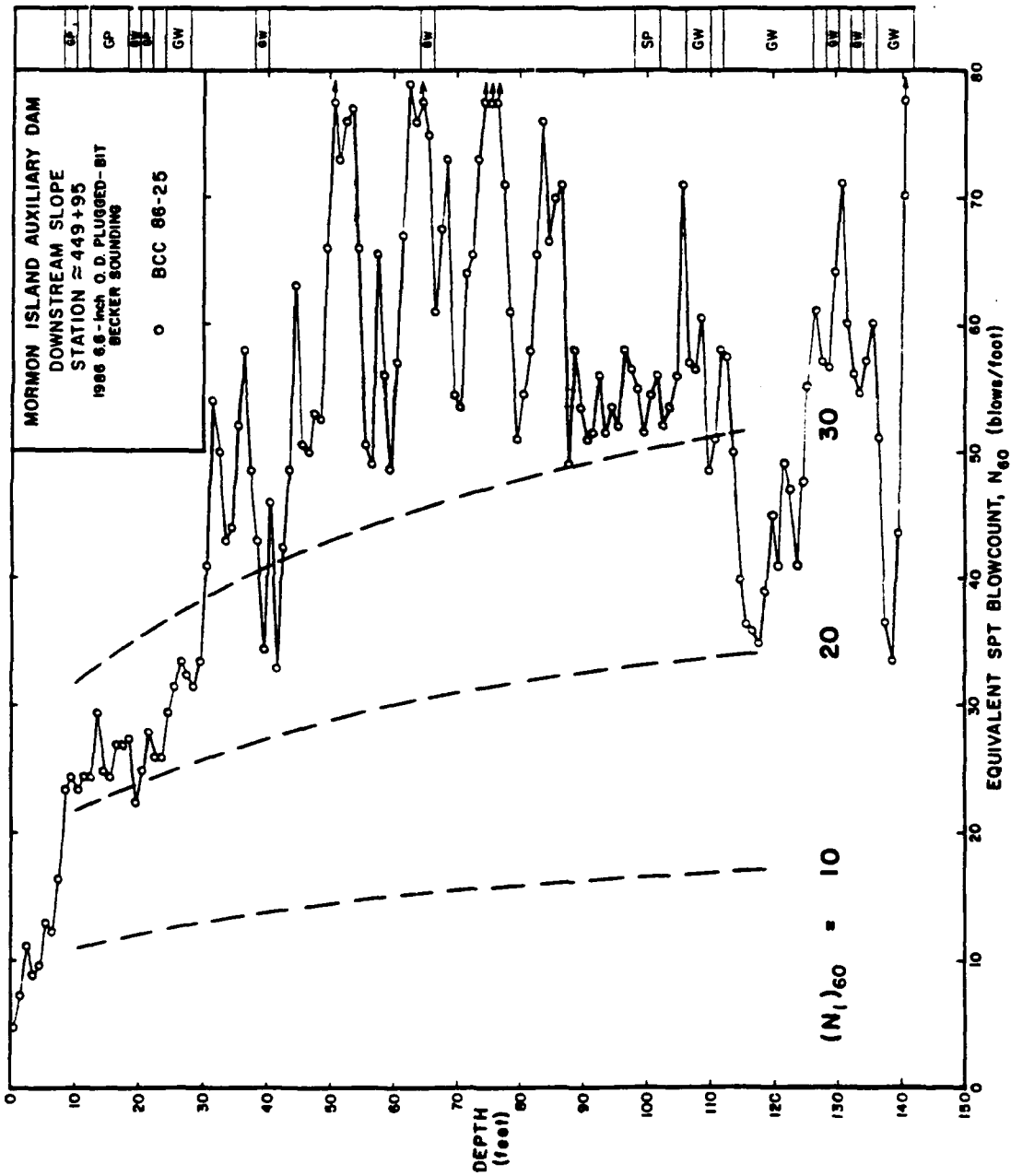


FIGURE 43: EQUIVALENT SPT BLOWCOUNTS FOR BECKER SOUNDING BCC 86-25 PERFORMED ON DOWNSTREAM FACE OF MORMON ISLAND AUXILIARY DAM

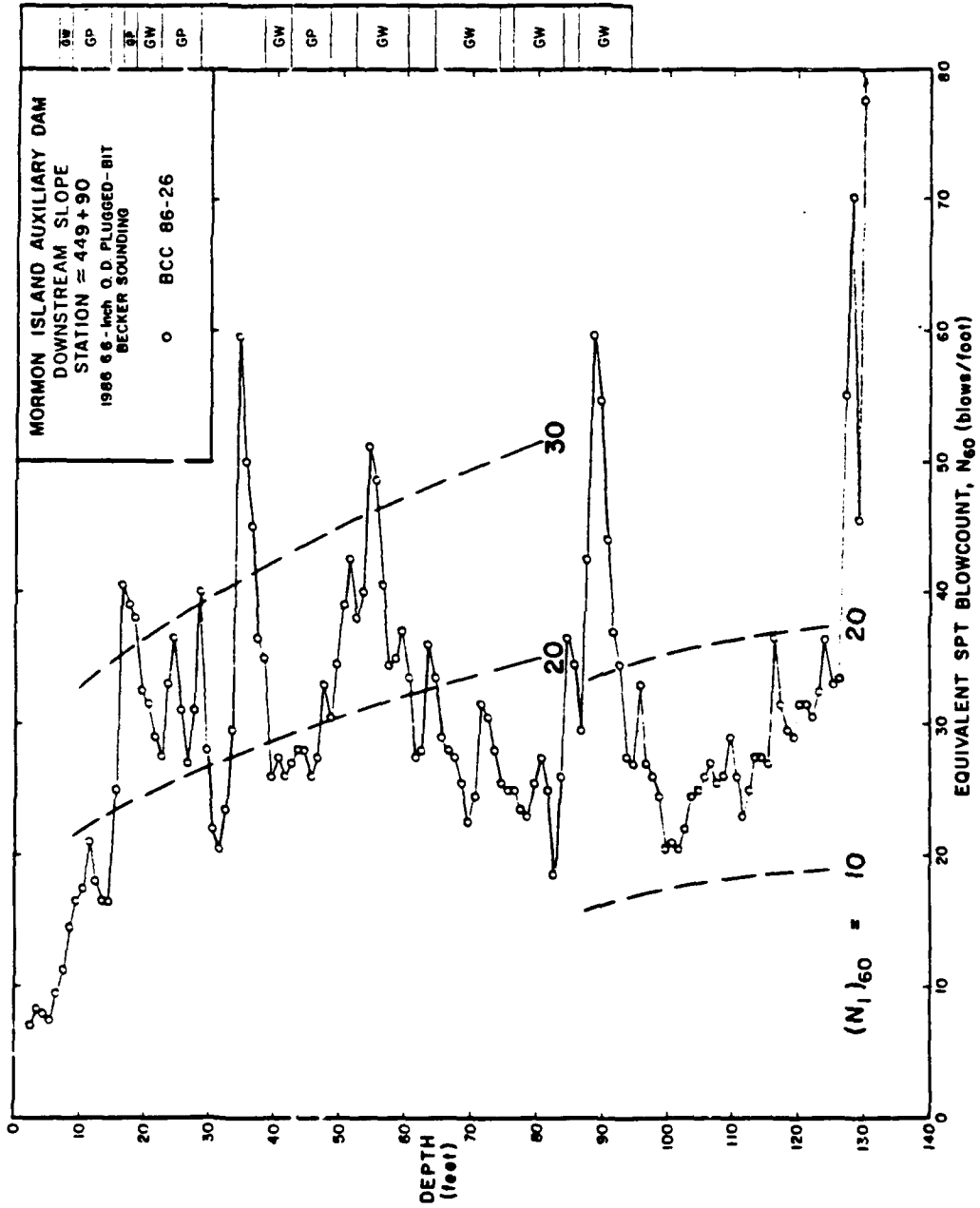


FIGURE 44: EQUIVALENT SPT BLOWCOUNTS FOR BECKER SOUNDING BCC 86-26 PERFORMED ON DOWNSTREAM FACE OF MORMON ISLAND AUXILIARY DAM

2. Soundings in Dredge Tailings along Downstream Flat (Soundings BCC 86-7 through BCC 86-13) - The 1986 data in this area basically confirms the 1983 Becker explorations which indicated a relatively loose foundation zone approximately 60 feet thick. The fines content of this material averages to about 10 percent and the Atterberg Limits results plot generally just above the "A" line or within the CL-ML zone for low liquid limits. This results in predominant classifications of either SP-SC or GP-GC. However, there are also soil samples which classify as CL, SP, SM, SC, and GC.
3. Soundings along Downstream Slope (Soundings BCC 86-15 through BCC 86-26):
 - a. The predominant soil classification of the downstream shell material is similar to that of the dredge tailings (i.e. GP-GC).
 - b. The penetration resistance of the downstream shell material is significantly stronger than that of the dredge tailings.
 - c. The samples of the dredge tailings beneath the embankment indicate exhibit somewhat lower fines contents and plasticity which leads to a higher percentage of GW, GP, SP, and GP-GM classifications.
 - d. The sounding placed through the embankment into the slope wash material (BCC 86-15) indicates no significant low blowcount zones in this area.
 - e. The sounding placed through the embankment into the Blue Ravine Alluvium (BCC 86-21) indicates a surficial low blowcount layer within the foundation. As this sounding is located near the alluvium/dredge tailings boundary, it is not immediately clear whether this limited layer represents a continuation of the material found at the downstream toe, the boundary portion of the dredge tailings, or a loose portion of the embankment.
 - f. The very low blowcounts found in the embankment intervals of Soundings BCC 86-22, BCC 86-23, and BCC 86-24 show that this material is composed of dredge tailings. Although design drawings apparently indicate that portions of the dredge tailings were incorporated into the downstream slope, the Becker data indicates that this was done to a greater degree than the drawings indicated. Figure 10 illustrates the differences in the boundary between shell and tailings material suggested by the design plans and by the Becker data.

Statistical Summary of Becker Data

In order to better summarize the Becker results for the embankment shell material and for the dredge tailings, the equivalent SPT data obtained from 1986 soundings performed between Stations 445 and 455 were analyzed. The analysis included and excluded the following data:

1. Blowcount data from 1986 soundings aligned longitudinally along the downstream toe and along the midpoint of the of the downstream toe were included.
2. Blowcount data obtained in 1983 soundings BDT-1 and BDT-2 performed along the downstream toe were also included.
3. Blowcount data from soundings BCC 86-22 through BCC 86-26 were excluded for the following reasons:
 - a. Soundings BCC 86-22 through BCC 86-24 did not penetrate embankment shell material.
 - b. Soundings BCC 86-25 and BCC 86-26 were performed with a different drill rig (No. 403) and were not performed in areas where other data could confirm reliability as was done for the other drill rig (No. 404, see Figures 15 and 16).
 - c. These soundings were all performed at about Station 450 and including their data would skew the results.
4. Blowcount data from 1983 sounding BDT-3 were also not included because of the reason cited in 3c above and because the data for the embankment shell was unusually erratic.
5. Blowcount data believed to have been obtained in foundation materials other than dredge tailings were excluded.

For soundings performed in the dredge tailings along the downstream toe between Stations 445 and 455, the data was averaged to obtain both the mean and the 35th percentile blowcount at each depth of penetration (Note: The 35th percentile is approximately equal to the mean minus 39 percent of the standard deviation). Table 4 details the

TABLE 4: SUMMARY OF EQUIVALENT SPT BLOWCOUNTS FROM BECKER SOUNDINGS ALONG DOWNSTREAM
FLAT OF MORMON ISLAND AUXILIARY DAM - STATION 445 TO 455

DEPTH (ft)	BCC 86-7		BCC 86-8		BCC 86-9		BCC 86-10		BCC 86-11		BCC 86-12		BCC 86-13		BDT-1		BDT-2		MEAN		Standard Dev.		35th Percentile	
	M ₆₀	N ₆₀	M ₆₀	N ₆₀	M ₆₀	N ₆₀	M ₆₀	N ₆₀	M ₆₀	N ₆₀	M ₆₀	N ₆₀	M ₆₀	N ₆₀	M ₆₀	N ₆₀	M ₆₀	N ₆₀	M ₆₀	N ₆₀	M ₆₀	N ₆₀	M ₆₀	N ₆₀
1	9.5	4. +	16.	7.	12.5	15.5++	9.	8.	12.5	10.4	12.5	10.4	12.5	10.4	12.5	10.4	12.5	10.4	12.5	10.4	12.5	4.0	8.9	
2	4. +	5.	10.	5.5	10.	26. ++	12.5	7.	7.5	9.7	7.5	9.7	7.5	9.7	7.5	9.7	7.5	9.7	7.5	9.7	6.0	7.1		
3	2.5+	4.5	7.	4.	6.5	32. ++	10.5	7.5	6.	8.9	6.	8.9	6.	8.9	6.	8.9	6.	8.9	6.	8.9	8.9	8.9	5.5	
4	2. +	4.	5.5	4.	5.	27. ++	9.5	7.	5.	7.7	5.	7.7	5.	7.7	5.	7.7	5.	7.7	5.	7.7	7.6	7.6	4.7	
5	2.5+	3.5	5.	4.5	4.5	14. ++	7.5	6.	4.5	5.8	4.5	5.8	4.5	5.8	4.5	5.8	4.5	5.8	4.5	5.8	3.4	4.5		
6	2.5+	4.	4.5	4.	4.	10.5++	6.	5.	4.5	5.2	4.5	5.2	4.5	5.2	4.5	5.2	4.5	5.2	4.5	5.2	2.4	4.3		
7	2. +	4.	5.	4.	4.	7.5++	4.5	4.5	4.	4.4	4.	4.4	4.	4.4	4.	4.4	4.	4.4	4.	4.4	1.4	3.9		
8	2.5+	3.5	5.	4.5	4.	7. ++	3.	4.	3.	4.1	3.	4.1	3.	4.1	3.	4.1	3.	4.1	3.	4.1	1.4	3.6		
9	5.5	3. +	6.5	5.5	5.	8.5++	3.5	6.	3.	5.2	3.	5.2	3.	5.2	3.	5.2	3.	5.2	3.	5.2	1.8	4.5		
10	5.	3.5+	5.5	5.5	5.	6.5	5.5	7. ++	4.	5.3	4.	5.3	4.	5.3	4.	5.3	4.	5.3	4.	5.3	1.1	4.9		
11	4.	3. +	5.5	5.	5.	5.	9.5++	7.5	4.5	5.4	4.5	5.4	4.5	5.4	4.5	5.4	4.5	5.4	4.5	5.4	1.9	4.7		
12	4.5	3. +	5.5	5.5	5.	13.5++	7.5	5.5	5.5	6.1	5.5	6.1	5.5	6.1	5.5	6.1	5.5	6.1	5.5	6.1	3.0	4.9		
13	6.5	2.5+	7.	6.	5.	14.5++	7.5	5.5	5.5	6.6	5.5	6.6	5.5	6.6	5.5	6.6	5.5	6.6	5.5	6.6	3.3	5.3		
14	6.	3. +	7.	7.	5.	6.5	17. ++	7.	4.5	7.0	4.5	7.0	4.5	7.0	4.5	7.0	4.5	7.0	4.5	7.0	4.0	5.5		
15	7.	3.5+	6.5	6.5	6.	6.	16.5++	5.5	4.5	6.9	4.5	6.9	4.5	6.9	4.5	6.9	4.5	6.9	4.5	6.9	3.8	5.4		
16	5.5	4.5+	6.5	7.	6.	7.5	9.5++	7.	5.5	6.6	5.5	6.6	5.5	6.6	5.5	6.6	5.5	6.6	5.5	6.6	1.5	6.0		
17	5.5	5. +	6.5	6.5	6.5	8.	11.5++	7.5	5.5	6.9	5.5	6.9	5.5	6.9	5.5	6.9	5.5	6.9	5.5	6.9	2.0	6.1		
18	4.5+	5.	6.5	7.5	7.	8.	15. ++	7.5	5.5	7.4	5.5	7.4	5.5	7.4	5.5	7.4	5.5	7.4	5.5	7.4	3.1	6.2		
19	4.5+	5.5	5.5	7.	5.	7.	13.5++	7.	5.5	6.7	5.5	6.7	5.5	6.7	5.5	6.7	5.5	6.7	5.5	6.7	2.7	5.7		
20	5. +	6.	5.5	6.5	5.5	8.	15. ++	7.	9.	7.5	9.	7.5	9.	7.5	9.	7.5	9.	7.5	9.	7.5	3.1	6.3		
21	5.5+	7.	6.5	7.5	5.5	9.	16.5++	7.5	10.	8.3	10.	8.3	10.	8.3	10.	8.3	10.	8.3	10.	8.3	3.4	7.0		
22	7.	7.5	6.5+	8.5	8.	9.	11.5++	8.5	10.	8.5	10.	8.5	10.	8.5	10.	8.5	10.	8.5	10.	8.5	1.5	7.9		
23	6.5	7.5	6. +	8.5	8.5	9.5	9.5	7.	10.5++	8.1	10.5++	8.1	10.5++	8.1	10.5++	8.1	10.5++	8.1	10.5++	8.1	1.5	7.5		
24	6.	7.5	5.5+	7.	8.5	8.	7.5	7.	10. ++	7.4	10. ++	7.4	10. ++	7.4	10. ++	7.4	10. ++	7.4	10. ++	7.4	1.3	6.9		
25	6. +	6.	7.	8.5	9.5	10.5	7.5	8.5	10.5	8.2	10.5	8.2	10.5	8.2	10.5	8.2	10.5	8.2	10.5	8.2	1.7	7.5		
26	5. +	6.5	7.5	9.5	9.	14. ++	6.	10.5	10.	8.7	10.5	8.7	10.5	8.7	10.5	8.7	10.5	8.7	10.5	8.7	2.8	7.6		
27	5. +	7.5	8.	9.5	9.5	15. ++	6.	11.5	9.	9.0	11.5	9.0	11.5	9.0	11.5	9.0	11.5	9.0	11.5	9.0	3.0	7.8		
28	5. +	7.	8.	10.5	10.	14. ++	5.	11.5	12.	9.2	11.5	9.2	11.5	9.2	11.5	9.2	11.5	9.2	11.5	9.2	3.2	8.0		
29	5.	9.5	6.	12.5	16.5++	11.5	4.5+	12.5	12.	10.0	12.5	10.0	12.5	10.0	12.5	10.0	12.5	10.0	12.5	10.0	4.1	8.4		
30	4.5	11.	4.5	13.5	18. ++	13.	4.5+	12.5	10.5	10.2	12.5	10.2	12.5	10.2	12.5	10.2	12.5	10.2	12.5	10.2	4.8	8.4		

Note: + Denotes minimum blowcount at this depth
 ++ Denotes maximum blowcount at this depth
 * Denotes that this blowcount was not counted in the averaging

TABLE 4: SUMMARY OF EQUIVALENT SPT BLOWCOUNTS FROM BECKER SOUNDINGS ALONG DOWNSTREAM FLAT OF MORMON ISLAND AUXILIARY DAM - STATION 445 AND 455 (continued)

DEPTH (ft.)	BCC 86-7		BCC 86-8		BCC 86-9		BCC 86-10		BCC 86-11		BCC 86-12		BCC 86-13		BDT-1		BDT-2		MEAN		Standard Dev.		35th Percentile	
	N ₆₀	N ₆₀	N ₆₀	N ₆₀	N ₆₀	N ₆₀	N ₆₀	N ₆₀	N ₆₀	N ₆₀	N ₆₀	N ₆₀	N ₆₀	N ₆₀	N ₆₀	N ₆₀	N ₆₀	N ₆₀	N ₆₀	N ₆₀	N ₆₀	N ₆₀	N ₆₀	N ₆₀
31	4.5	12.	3.5+	12.	16.5++	13.5	5.	11.5	10.	9.8	4.5	8.1												
32	4.5	10.5	4.5	12.5	15. ++	12.5	4. +	12.	10.5	9.6	4.1	8.0												
33	4.5	8.5	4.5	11.	13.	13.5++	3.5+	11.5	10.5	8.9	3.9	7.4												
34	6.5	9.	6.	12.5	12.5++	13.5++	3.5+	10.5	9.	9.2	3.4	7.9												
35	4.5	10.	6.	12.5	11.5	12.5++	4.5+	10.5	9.	9.0	3.2	7.8												
36	5.5	9.	6.	13.	10.5	13. ++	5. +	10.5	11.5	9.3	3.1	8.1												
37	6.5+	9.	7.	13.5++	11.	12.	7.	10.5	11.5	9.8	2.5	8.8												
38	6.5	9.5	8.5	11.5	11.	13. ++	5.5+	11.5	11.5	9.8	3.5	8.8												
39	8.	8.5	11.5	10.5	14.	14.	4.5+	16.5++	10.	10.4	3.5	9.1												
40	5.5	8.5	12.	11.	10.	14. ++	5. +	12.5	9.	9.7	3.1	8.5												
41	4. +	9.5	11.5	10.5	11.5	13.5++	4.5	10.5	8.5	9.3	3.2	8.1												
42	4. +	9.5	10.5	11.	10.5	12. ++	4.5	12.	7.5	9.1	3.1	7.9												
43	5. +	9.	11.	8.5	7.	11.5	6.5	16.5++	7.5	9.2	3.5	7.9												
44	5.5+	8.	12.5	12.	6.	12.5	18.5*	15. ++	7.5	9.9	3.5	8.6												
45	6. +	8.	13.5	16. ++	6.5	11.5	39. *	9.	8.5	9.9	3.5	8.6												
46	6.5+	7.	9.	14. ++	10.5	12.	60.5*	10.5	9.	9.8	2.5	8.5												
47	6. +	7.5	6.5	14.5++	13.	11.	83. *	10.5	9.	9.8	3.1	8.6												
48	7.5	9.5	5.5+	11.	14.5++	10.5	125. *	10.	9.	9.7	2.6	8.7												
49	8.	7.5	6. +	11.	10.	11.		12. ++	8.5	9.3	2.1	8.5												
50	7.5	8.	6.5+	8.5	11.	11.5++		10.	11.5	9.3	1.9	8.6												
51	7.5	8.5	5.5+	8.5	7.5	16.5++		9.	14.5	9.7	3.8	8.2												
52	6.	5.5	5.5+	8.	6.	13.5++		8.5	8.5	7.7	2.7	6.6												
53	8.	5. +	6.	9.	5.5	11. ++		9.	8.5	7.8	2.1	7.0												
54	6.5	6.	6.5	11.	5.5+	14.5++		8.5	8.5	8.4	3.1	7.2												
55	11.	6.5	6.5+	17.++	8.	10.5		9.	10.	9.8	3.4	8.5												
56	22.5*	6. +	7.5	13.++	12.	8.		11.5	10.5	9.8	2.6	8.8												
57	>130. *	11.	10.5	11.	12.5++	9.5+		11.5	10.5	10.9	0.9	10.6												
58		12.5	>64. *	11.	12.5++	10. +		10.5	10.5	11.2	1.1	10.8												
59		> 85. *	15.	29. ++	10. +			10.5	10.5	16.3	8.8	12.9												
60			>94. *	26. ++	9.5+			10.5	10.5	14.1	7.9	11.1												

Note: + Denotes minimum blowcount at this depth
 ++ Denotes maximum blowcount at this depth
 * Denotes that this blowcount was not counted in the averaging

blowcount values used in the averaging process together with the results. Figure 45 presents minimum, maximum, mean, and 35th percentile values for this set of data. In general, the 35th percentile blowcount was 1 to 2 blows less than the mean value. Figure 46 shows that both the mean and the 35th percentile values represent $(N_1)_{60}$ values generally between 6 and 8 blows per foot.

For soundings performed along the midpoint of the downstream slope between Stations 445 and 455, the same averaging process was performed. Table 5 details the blowcount values used in the averaging process together with the results. Figure 47 presents minimum, maximum, mean, and 35th percentile values for this set of data. In general, the 35th percentile blowcount for both embankment shell and tailings data was 3 to 5 blows less than the mean value. Figure 48 shows that both the mean and the 35th percentile values within the embankment shell represent $(N_1)_{60}$ values generally between 20 and 30 blows per foot. Figure 49 shows that both the mean and the 35th percentile values in the dredge tailings beneath the slope represent $(N_1)_{60}$ values generally between 10 and 20 blows per foot.

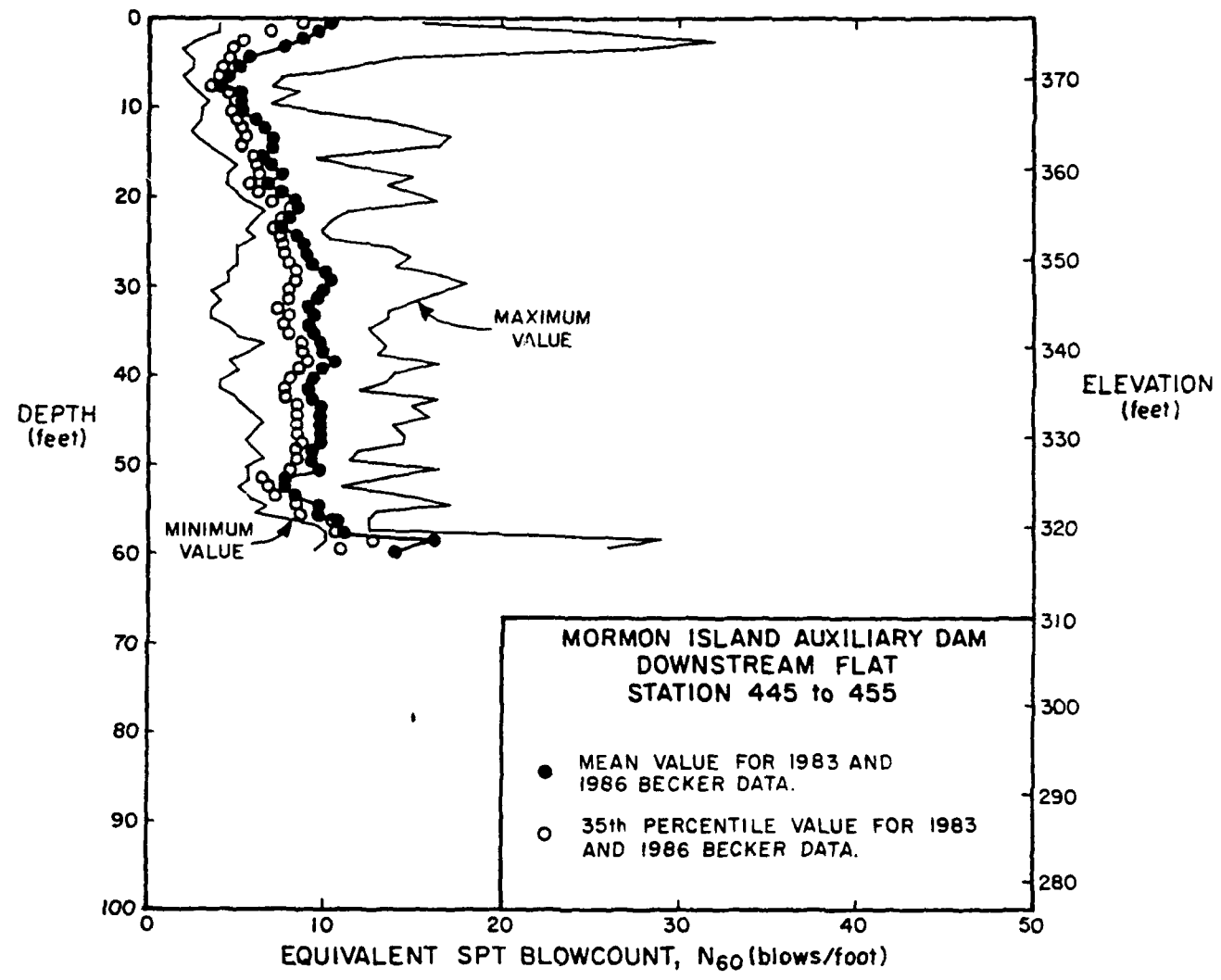


FIGURE 45: RANGE OF EQUIVALENT SPT BLOWCOUNTS OBTAINED FROM BECKER SOUNDINGS PERFORMED IN DOWNSTREAM FLAT OF MORMON ISLAND AUXILIARY DAM BETWEEN STATIONS 445 AND 455

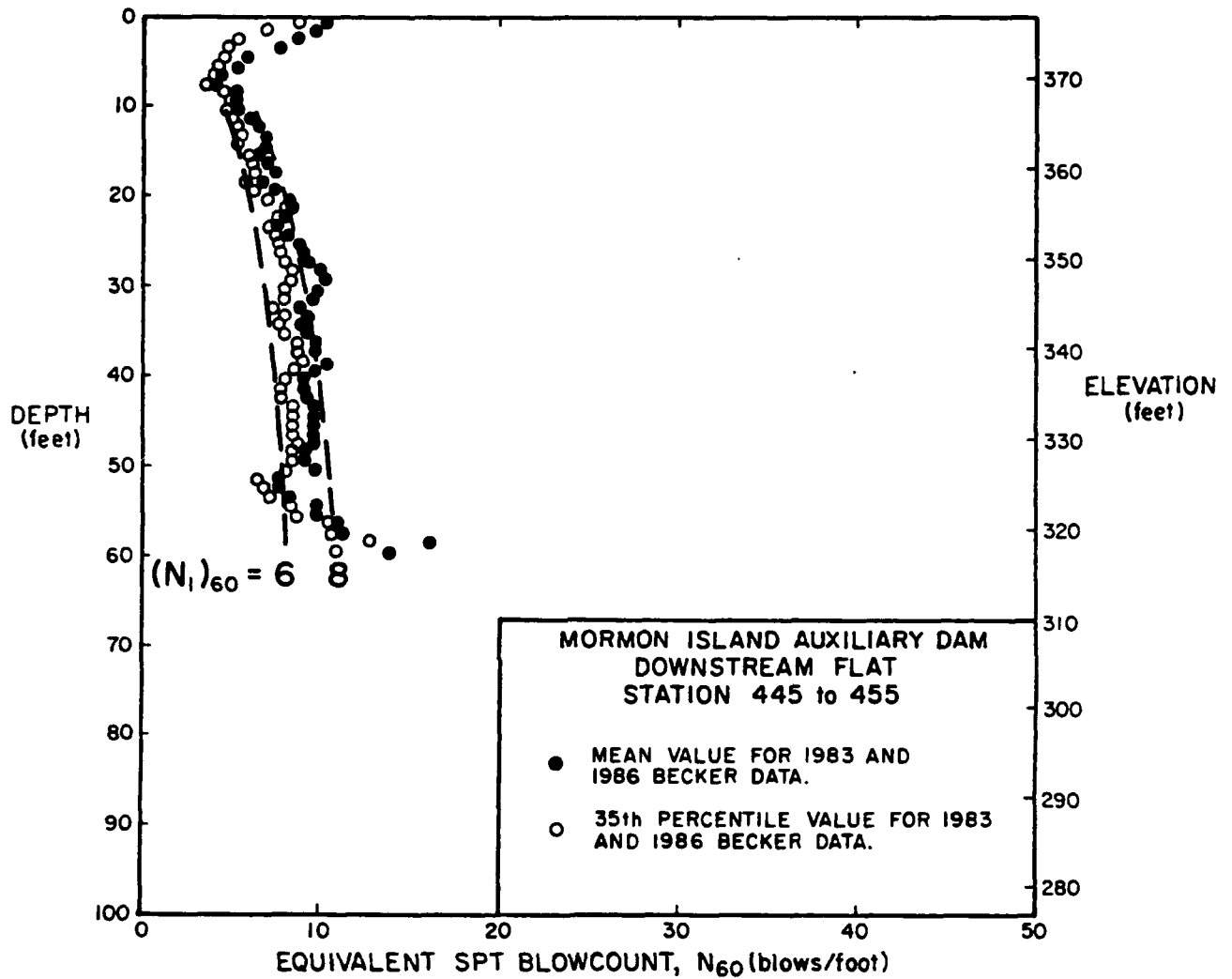


FIGURE 46: MEAN AND 35TH PERCENTILE EQUIVALENT SPT BLOWCOUNTS OBTAINED FROM BECKER SOUNDINGS PERFORMED IN DOWNSTREAM FLAT OF MORMON ISLAND AUXILIARY DAM BETWEEN STATIONS 445 AND 455

TABLE 5: SUMMARY OF EQUIVALENT SPT BLOWCOUNTS FROM BECKER SOUNDINGS ALONG MIDPOINT OF DOWNSTREAM SLOPE OF MORMON ISLAND AUXILIARY DAM -- STATIONS 445 TO 455

DEPTH (ft)	BCC 86-21	BCC 86-20	BCC 86-19	BCC 86-18	BCC 86-17	BCC 86-16	BCC 86-15	MEAN	Standard Dev.	35th Percentile
	N ₆₀	N ₆₀	N ₆₀	N ₆₀	N ₆₀	N ₆₀	N ₆₀	N ₆₀	N ₆₀	N ₆₀
1	7.	7.5	7.	8.	15.5 +	14.	5.5 +	9.2	3.9	7.7
2	10.	14.	8.5 +	8.5	15.5	19.	12.5	12.6	3.9	11.1
3	11.5	25.5	15.	8.5 +	15.5	26.	14.5	16.6	6.7	14.0
4	15.	20.5	16.	9.5 +	15.	28.5 ++	15.5	17.1	5.9	14.8
5	14.	13.5	20.5	12.5 +	17.5	29.	12.5	17.1	6.0	14.8
6	18.5	13.	20.5	18.5	21.	23.5 ++	10.5	17.9	4.6	16.1
7	23.5	9.5 +	26.5 ++	18.5	23.5	20.5	14.	19.4	6.0	17.1
8	25.	8.5 +	25.	22.	25.	19.	13.	19.6	6.6	17.1
9	33.5	12.5 +	33.5 ++	31.	26.	21.5	15.	24.7	8.7	21.3
10	31.5 ++	15.	25.	30.5	23.5	20.	13.	22.6	7.1	19.9
11	26.	21.5	25.5	33.	27.5	21.5	14.5 +	24.2	5.8	22.0
12	31.5	23.5	32.5	50.5 ++	-	25.	19.	30.3	11.1	26.0
13	32.5	30.5	36.5	78.	20.	29.5	27.5	36.4	19.1	29.0
14	35.	26.	35.	60.5 ++	24.5 ++	24.5	27.5	33.3	12.8	28.4
15	27.5	18.5 +	25.5	45.	57.5 ++	26.	27.5	32.5	13.7	27.2
16	25.	14.	22.	36.5	57.	48.5	40.5	34.8	15.3	28.9
17	23.	17.	22.	31.	38.5	41.5 ++	36.5	29.9	9.4	26.3
18	23.5	17.5 +	23.	25.5	32.5	33.5 ++	31.	26.6	5.9	24.3
19	24.5	18.5	19.	19.	31.	31.5 ++	16.5 +	22.9	6.2	20.5
20	28.	21.	21.	24.5	29.	29.	18.5 +	24.4	4.3	22.7
21	26.	25.5	20.5	24.5	31.	27.5 ++	19.	24.9	4.1	23.3
22	29.	40.5 ++	31.	28.	35.	32.5	18.5 +	30.6	6.8	28.0
23	24.5	29.	34.5	29.5	65.	26.	19.5 +	32.6	15.0	26.8
24	24.5	41.	27.5	26.	57.	23.	27.	32.3	12.4	27.5
25	31.	39.	24.5	21.5 +	54.	22.	29.5	31.6	11.6	27.1
26	33.	76.	29.	16.5 +	47.	23.	34.5	37.0	19.7	29.4
27	40.5	79.	37.	16.	33.	23.	35.	37.6	20.1	29.9
28	39.	61.	33.	20.5 +	32.5	28.	27.5	34.5	13.0	29.5
29	30.5	48.	34.5	11.5 +	31.	33.5	27.	30.9	10.8	26.7
30	28.	51.	45.	22.	41.	36.	28.	35.9	10.5	31.9

Note: + Denotes minimum blowcount at this depth
 ++ Denotes maximum blowcount at this depth
 * Denotes that this blowcount was not counted in the averaging

TABLE 5: SUMMARY OF EQUIVALENT SPT BLOWCOUNTS FROM BECKER SOUNDINGS ALONG MIDPOINT OF DOWNSTREAM SLOPE OF MORMON ISLAND AUXILIARY DAM - STATIONS 445 TO 455 (continued)

DEPTH (ft)	BCC 86-21	BCC 86-20	BCC 86-19	BCC 86-18	BCC 86-17	BCC 86-16	BCC 86-15	MEAN	Standard Dev.	35th Percentile
	M ₆₀	M ₆₀	M ₆₀	M ₆₀	M ₆₀	M ₆₀	M ₆₀	M ₆₀	M ₆₀	M ₆₀
31	25.5 +	48.5	54.	34.5	64. ++	30.5	27.	40.6	15.0	34.8
32	25. +	49.	62.5 ++	47.5	53.	31.	31.	42.7	13.8	37.4
33	24.5 +	42.5	51.5 ++	42.5	36.5	33.5	33.	37.7	8.7	34.3
34	28.	40.5	50. ++	36.5	36.5	41.5	26. +	37.0	8.2	33.8
35	33.5	31.	50.5 ++	34.5	36.	26. +	27.5	34.1	8.1	31.0
36	27.5	36.5	49. ++	29.5	31.5	23. +	23.5	31.5	9.0	28.0
37	25.5	29.5	58. ++	29.	26.	19. +	27.	30.6	12.6	25.7
38	21.5 +	31.5	47. ++	27.5	23.5	31.5	33.5	30.9	8.4	27.7
39	23.5 +	31.5	45.5 ++	31.5	28.	33.	29.	31.7	6.8	29.1
40	29.5	34.5	60. ++	45.5	37.	29.	26. +	37.4	11.9	32.8
41	28.	33.	51. ++	41.	37.	31.	28.	35.6	8.3	32.4
42	29.5 +	30.5	53. ++	40.5	38.5	36.	30.5	36.9	8.3	33.7
43	27.5 +	29.5	46. ++	40.5	33.5	37.	33.	35.3	6.4	32.8
44	29.5	29. +	41.5 ++	38.5	34.5	38.	38.5	35.6	4.8	33.8
45	29. +	36.5	31.	36.5	35.	45.5 +	38.5	36.3	5.4	34.2
46	29.5	36.	29. +	34.5	29.5	39.	42.5 ++	34.3	5.3	32.3
47	27.5	35.	27.	23.	25.5	39.	40.5 ++	31.1	7.0	28.4
48	27.	25.5	25.	18.5	25.5	38.5 +	46. *	26.7	6.5	24.2
49	27.	20.5	26.	16.	26.	29. +	33.5 *	24.1	4.9	22.2
50	27.5	19.	23.	16.5	30.5 ++	28.	40. *	24.1	5.5	22.0
51	27.	19.5	22.	16.	30.5 ++	28.	41. *	23.8	5.0	21.9
52	29.	19.5	21.5	16.	26.	32.5 ++	44. *	24.1	6.2	21.7
53	27.5	21.	25.	14.5	22.5	33. ++	42.5 *	23.9	6.3	21.5
54	29.	23.5	25.5	16.5	19.5	29. ++	26. *	23.8	5.1	21.8
55	27.5 ++	16. +	22.	23.	17.5	25.5	27.5 *	21.9	4.5	20.2
56	34.5 ++	22.5	22.	20.	20.	26.	29. *	24.2	5.5	22.1
57	34.5 ++	23.5	23.	18.5	20.5	27.	40.5 *	24.5	5.7	22.3
58	29.5	23.	26.	20.5	20. +	31. ++	35. *	25.0	4.6	23.2
59	22.5	23.	27.5	24.5	18.5 +	36. ++	45. *	25.3	6.0	23.0
60	24.5	25. ++	18.5 +	23.	22.	24.5	37. *	22.9	2.4	22.0

Note: + Denotes minimum blowcount at this depth

++ Denotes maximum blowcount at this depth

* Denotes that this blowcount was not counted in the averaging

TABLE 5: SUMMARY OF EQUIVALENT SPT BLOWCOUNTS FROM BECKER SOUNDINGS ALONG MIDPOINT OF DOWNSTREAM SLOPE OF MORMON ISLAND AUXILIARY DAM - STATIONS 445 TO 455 (continued)

DEPTH (ft)	BCC 86-21	BCC 86-20	BCC 86-19	BCC 86-18	BCC 86-17	BCC 86-16	BCC 86-15	MEAN	Standard Dev.	35th Percentile
	N ₆₀	N ₆₀	N ₆₀	N ₆₀	N ₆₀	N ₆₀	N ₆₀	N ₆₀	N ₆₀	N ₆₀
61	21.	25. ++	19. +	20.	22.	19.5	43.5 *	21.1	2.2	20.3
62	23.5	23.5 ++	20.5	20.5	22.5	18.5 +	46. *	21.5	2.0	20.7
63	20.	23.5	20.5	19.	24.5 ++	14.5 +	45.5 *	20.3	3.6	18.9
64	26. ++	16. +	21.5	19.5	25.	17.	51.5 *	20.8	4.1	19.2
65	58. *	19.	22.	20.	22.5 ++	16. +	35. *	19.9	2.6	18.9
66	68. *	19.5 +	23.	19.5	31. ++	20.	49. *	22.6	4.9	20.7
67	77. *	19.	25.	16.5 +	27. ++	18.	51.5 *	21.1	4.6	19.3
68	72. *	-	26. ++	14. +	25.	20.	47.5 *	21.3	5.5	19.2
69	91. *	15.	31.5 ++	13. +	18.5	22.5	50.5 *	20.1	7.3	17.3
70	85. *	16.	32.5 ++	11.5 +	20.	20.	41.5 *	20.0	7.8	17.0
71	108. *	18.5	31.5 ++	15. +	22.5	23.	53.5 *	22.1	6.2	19.7
72	101. *	18.	47. ++	14. +	26.	25.	47. *	26.0	12.7	21.1
73	97. *	20.5	45.5 ++	18.5 +	38.	25.	51. *	29.5	11.7	25.0
74	87. *	20.5	45.5 ++	19.5 +	41.	28.	58. *	30.9	11.9	26.3
75	101. *	24.5	55. ++	18.5 +	46.	25.	64. *	33.8	15.8	27.7
76	122. *	25.5	63. ++	17. +	49.	21.5	60. *	35.2	19.9	27.5
77		34.5	56.5 ++	19.5 +	51.5	21.	72. *	36.6	17.0	30.0
78		32.5	54.5 ++	20. +	51.5	21.	>90. *	35.9	16.4	29.6
79		31.5	48.5	25.	51. ++	20.5 +		35.3	13.8	30.0
80		29.	43.5	25.5	53. ++	24.5 +		35.1	12.6	30.2
81		24.5 +	47.	25.5	48. ++	26.		34.2	12.2	29.5
82		26. +	50.5	26.	50.5 ++	32.5		37.1	12.5	32.3
83		27.5 +	42.5	27.5	45.5 ++	33.		35.2	8.4	32.0
84		27.5	30.5	27.5	40.5 ++	19.5 +		29.1	7.6	26.2
85		27.5	33.	27.	41.5 ++	17. +		29.2	9.0	25.7
86		36. ++	33.	31.5	34.	17. +		30.4	7.7	27.4
87		32.5	34.5 ++	25.5	27.	24.5 +		28.8	4.4	27.1
88		4.	40. ++	27.5	25. +	33.5		30.4	6.3	28.0
89		4.	38. ++	26.	25. +	31.		30.6	5.3	28.6
90		4.	29.5	25.5	21.5 +	27.		28.5	6.5	26.0

Note: + Denotes minimum blowcount at this depth

++ Denotes maximum blowcount at this depth

* Denotes that this blowcount was not counted in the averaging

TABLE 5: SUMMARY OF EQUIVALENT SPT BLOWCOUNTS FROM BECKER SOUNDINGS ALONG MIDPOINT OF DOWNSTREAM SLOPE OF MORMON ISLAND AUXILIARY DAM - STATIONS 445 TO 455 (continued)

DEPTH (ft)	BCC 86-21	BCC 86-20	BCC 86-19	BCC 86-18	BCC 86-17	BCC 86-16	BCC 86-15	MEAN	Standard Dev.	35th Percentile
	N ₆₀	N ₆₀	N ₆₀	N ₆₀	N ₆₀	N ₆₀	N ₆₀			
91		28.	43.5 ++	27.5	18.5 +	25.		28.5	9.2	25.0
92		32.5	34.5 ++	29.5	21.5 +	24.5		28.5	5.4	26.4
93		30.5	37. ++	32.5	22. +	29.		30.2	5.5	28.1
94		24.5	44. ++	36.5	22. +	36.		32.6	9.2	29.1
95		30.5	41.	42.5 ++	22. +	29.5		33.1	8.6	29.8
96		37.	42.5 ++	33.	23.5 +	25.		32.2	8.0	29.1
97		40.5	48.5 ++	37.	23.5	21. +		34.1	11.6	29.6
98		43.5	51.5 ++	23.	21.	19.5 +		31.7	14.8	26.0
99		47.5 ++	98. *	22.5	20.5	20. +		27.6	13.3	22.5
100		63. *	80. *	27.	23.5	22. +		24.2	2.6	23.2
101		64. *	104. *	30.5	23.5 +	33.5 +		29.2	5.1	27.2
102		76. *	31. ++	31. ++	23. +	28.		27.3	4.0	25.8
103		97. *		40. ++	40.5	19. +		29.5	14.9	23.8
104				37. ++	>116. *	17.5 +		27.3	13.8	22.0
105				32.5 ++		17. +		24.8	11.0	20.6
106				28. ++		18.5 +		23.3	6.7	20.7
107				27.5 ++		18. +		22.8	6.7	20.2
108				28. ++		22. +		25.0	4.2	23.4
109				31.5 ++		15. +		23.3	11.7	18.8
100				31.5 ++		>94. *				
111				45. *						
112				>84. *						

Note: + Denotes minimum blowcount at this depth

++ Denotes maximum blowcount at this depth

* Denotes that this blowcount was not counted in the averaging

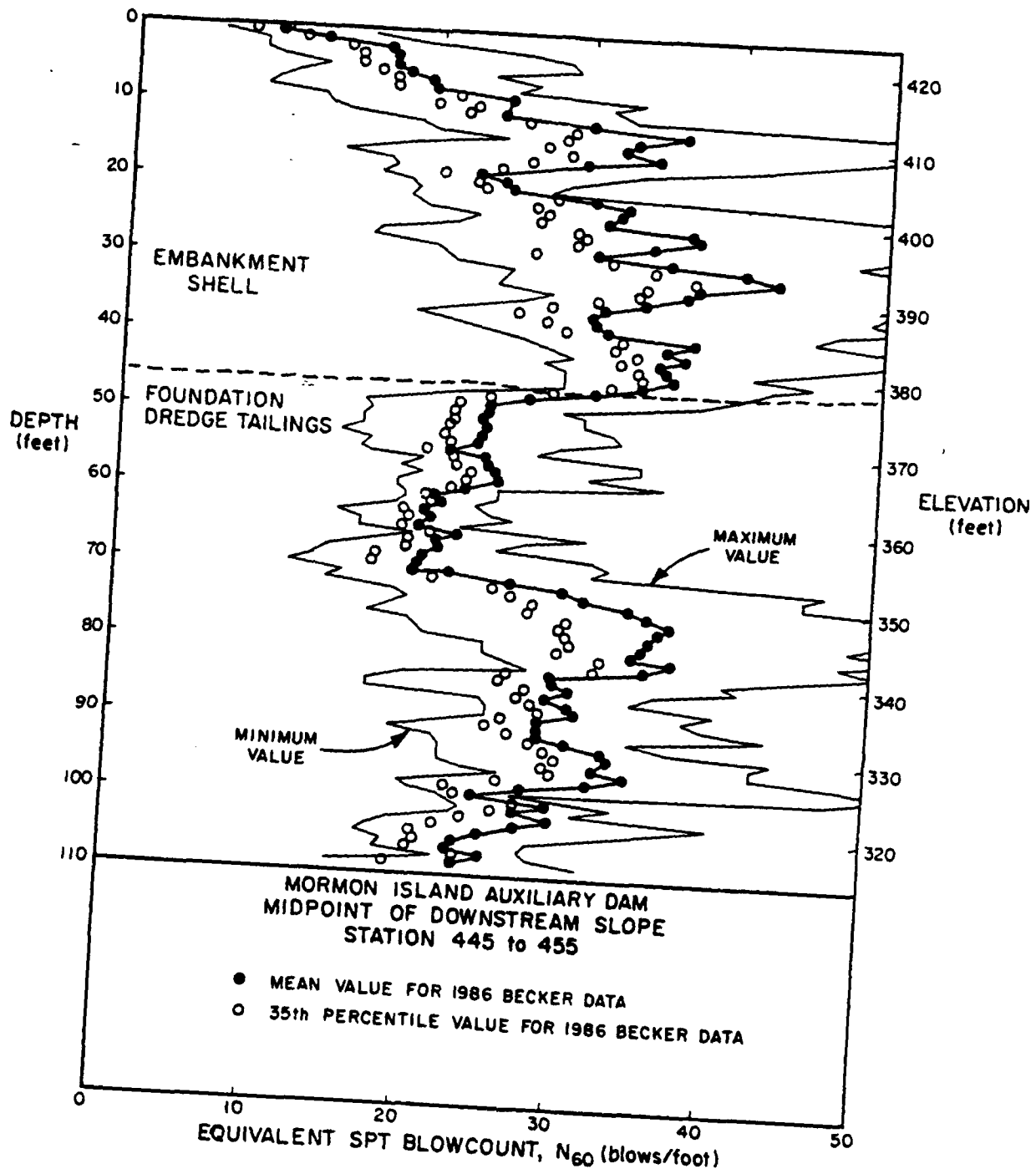


FIGURE 47: RANGE OF EQUIVALENT SPT BLOWCOUNTS OBTAINED FROM BECKER SOUNDINGS PERFORMED AT MIDPOINT OF DOWNSTREAM SLOPE OF MORMON ISLAND AUXILIARY DAM BETWEEN STATIONS 445 AND 455

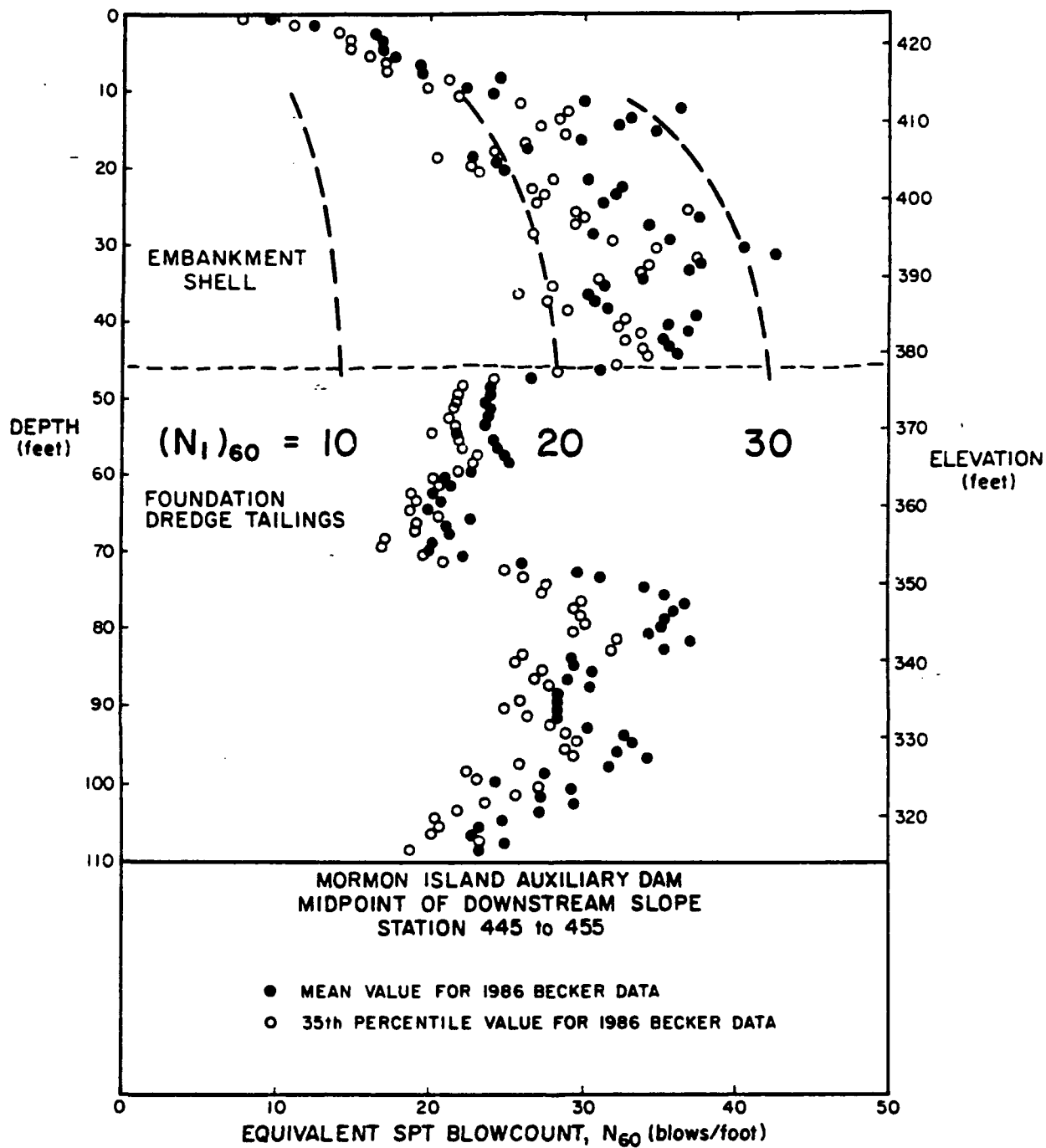


FIGURE 48: MEAN AND 35TH PERCENTILE EQUIVALENT SPT BLOWCOUNTS IN EMBANKMENT SHELL OBTAINED FROM BECKER SOUNDINGS PERFORMED AT MIDPOINT OF DOWNSTREAM SLOPE OF MORMON ISLAND AUXILIARY DAM BETWEEN STATIONS 445 AND 455

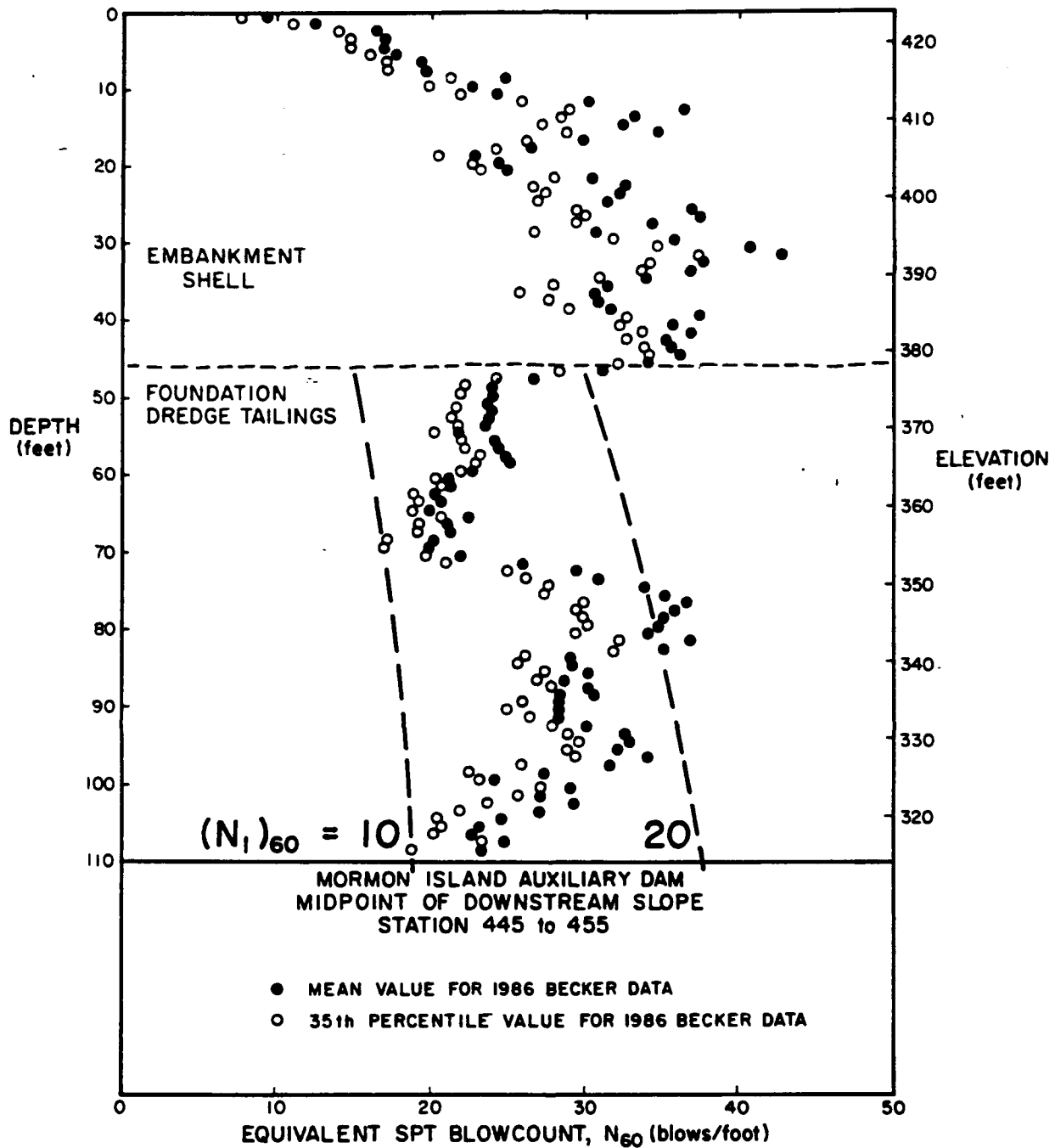


FIGURE 49: MEAN AND 35TH PERCENTILE EQUIVALENT SPT BLOWCOUNTS IN DREDGE TAILINGS OBTAINED FROM BECKER SOUNDINGS PERFORMED AT MIDPOINT OF DOWNSTREAM SLOPE OF MORMON ISLAND AUXILIARY DAM BETWEEN STATIONS 445 AND 455

5. SUMMARY OF FINDINGS

1. The 1986 Becker soundings generally confirmed the results of the 1983 Becker explorations regarding the natures of both the embankment shell material and the foundation dredge tailings. Beyond the downstream toe, the dredge tailings exist in a very loose state. Beneath the midpoint of the downstream slope, the tailings appear to be somewhat denser, but remain moderately loose. The embankment shell material exhibits penetration resistance corresponding to a medium dense soil.
2. Except in the upper 10 feet, Becker soundings performed along the downstream toe in the Blue Ravine Alluvium and in slope wash soils exhibit very high resistance. In the upper 10 feet in these areas, there is a very low blowcount layer, which although resembles the penetration resistance of the dredge tailings, appears to have a significantly higher percentage of clayey fines. It is unclear whether this layer exists in the Blue Ravine Alluvium in areas beneath the embankment. A sounding performed through the embankment overlying slope wash soils did not encounter the low blowcount layer.
3. Soundings performed through the downstream half of the downstream slope indicate that a larger amount of dredge tailings was incorporated into the downstream slope than was previously thought.

4. The equivalent SPT $(N_1)_{60}$ blowcounts for the gravelly soils in the foundation and embankment shell which should be used for seismic safety evaluations are as follows:

DREDGE TAILINGS (D/S Flat):	6 - 8	blows/foot
DREDGE TAILINGS (Midpoint of D/S Slope):	11 - 18	blows/foot
EMBANKMENT SHELL (Midpoint of D/S Slope):	22 - 25	blows/foot

6. REFERENCES

1. Harder, Jr., Leslie F. (1986) "Evaluation of Becker Penetration Tests Performed at Mormon Island Auxiliary Dam," Report prepared for the Waterways Experiment Station, U. S. Army Corps of Engineers, October, 1986.
2. Harder, Jr., Leslie F. and Seed, H. Bolton (1986) "Determination of Penetration Resistance for Coarse-Grained Soils Using the Becker Penetration Test," University of California, Berkeley, EERC Report No. UCB/EERC-86-06, May, 1986.
3. Hynes-Griffin, Mary Ellen (1986), Geotechnical Laboratory, Waterways Experiment Station, U.S. Army Corps of Engineers, personal communication.
4. Koester, Joe (1987), Plots, Charts, and Tables Containing Data Relating to the 1986 Becker Explorations Conducted at Mormon Island Auxiliary Dam, Geotechnical Laboratory, Waterways Experiment Station, U. S. Army Corps of Engineers, personal communication.
5. LAYNE-WESTERN CO., INC. (1987) personal communication.
6. Marcuson, W. F., III and Bieganousky, W. A. (1977a) "Laboratory Standard Penetration Tests on Fine Sands," Journal of the Geotechnical Engineering Division, American Society of Civil Engineers, Vol 103, No. GT6, June, 1977.
7. Marcuson, W. F., III and Bieganousky, W. A. (1977b) "SPT and Relative Density in Coarse Sands," Journal of the Geotechnical Engineering Division, American Society of Civil Engineers, Vol 103, No. GT11, November, 1977.
8. Seed, H. Bolton, Idriss, I. M. and Arango, Ignacio (1983) "Evaluation of Liquefaction Potential Using Field Performance Data," Journal of the Geotechnical Engineering Division, ASCE, Vol. 109, No. 3, March, 1983.
9. Seed, H. Bolton, Mori, Kenji, and Chan, Clarence K. (1975) "Influence of Seismic History on the Liquefaction Characteristics of Sands," University of California, Berkeley, Report No. EERC 75-5, August, 1975.
10. Seed, H. Bolton, Tokimatsu, K., Harder, L.F., and Chung, Riley M. (1984) "Influence of SPT Procedures in Soil Liquefaction Resistance Evaluations," Journal of the Geotechnical Engineering Division, ASCE, Vol. 111, No. 12, December, 1985.
11. U.S. Army Corps of Engineers, Sacramento District (1984) "Preliminary Evaluation of Liquefaction Potential at Mormon Island Auxiliary Dam", Draft Report.

6. REFERENCES (continued)

12. Vaid, Y. P. and Chern, J. C. (1983) "Effect of Static Shear Stress on Resistance to Liquefaction," Soils and Foundations, Vol. 23(1).
13. Wahl, Ron (1986), Results of Finite Element Static Stress Analysis (Program FEADAM) of Mormon Island Auxiliary Dam, Geotechnical Laboratory, Waterways Experiment Station, U.S. Army Corps of Engineers, personal communication, 1986.

APPENDIX A:

COMPUTATION TABLES FOR DETERMINING EQUIVALENT SPT BLOWCOUNTS FROM
1986 PLUGGED-BIT BECKER SOUNDINGS PERFORMED AT MORMON ISLAND AUXILIARY DAM

BCC -

BCC-2

DEPTH (ft)	BCC -				BCC-2			
	N _B	BP (psig)	N _{BC}	SPT N ₆₀	N _B	BP (psig)	N _{BC}	SPT N ₆₀
10	11	11	6½	6½ 49	18	18	16½	16½ 12A
15	12	12	7½	7½ 56	33	19	27	24½ 18A
10	10	10	6	6 45	22	17	17	17 12B
12	13	13	8	8 6	18	12	9	9 6B
10	14	14	8½	8½ 64	9	8	5	5 3B
12	14	14	9	9 68	8	7	4	4 3
15	15	15	11½	11½ 86	6	10	5	5 3B
14	15	15	11	11 83	8	10	5½	5½ 41
11	14	14	8½	8½	6	7	3½	3½
12	14	14	9	9	7	9	4½	4½
11	14	14	8½	8½	7	10	5	5
10	15	15	9	9	8	10	5½	5½
14	15	15	11	11	7	11	5½	5½
15	16	16	12½	12½	19	18	17	16½
17	18	18	16	16	25	17	18½	18
20	18	18	17½	17	30	20	27	24½
26	20	20	24	22	42	22	39	32½
25	21	21	24½	22½	53	24	52	41
36	22	22	37	29	46	24	46	37
46	25	25	48	38½	47	25	49	39
88	27	27	89	63½	60	25	60	46
80	29	29	89	63½	70	27	74	54½
81	29	29	90	64	131	29	137	92
86	30	30	98	69	150+	31	170+	113+
200+	31	31	200+	130+				

BCC-3

BCC-4

DEPTH (ft)	N _B	BP (psia)	N _{BC}	SPT N ₆₀	N _B	BP (psia)	N _{BC}	SPT N ₆₀	DEPTH (ft)
1	35	20	30	26 ^{19.5}	29	20	26	23½ ^{17.6}	1
2	42	20	35	29½ ^{22.1}	47	19	35	29½ ^{22.1}	2
3	46	21	40	33 ^{24.8}	30	17	20	19 ^{14.3}	3
4	36	19	28	25 ^{19.8}	23	15	14½	14½ ^{10.9}	4
5	20	15	13½	13½ ^{10.1}	14	12	8	8 ^{6.0}	5
6	12	15	10	10 ^{7.5}	10	10	6	6 ^{4.5}	6
7	10	11	6½	6½ ^{4.9}	8	8	4½	4½ ^{3.4}	7
8	9	9	5	5 ^{3.8}	6	8	4	4 ^{3.0}	8
9	10	7	4½	4½	3	7	2½	2½	9
10	9	8	5	5	5	4	2½	2½	10
11	6	12	5½	5½	7	10	5	5	11
12	15	18	14½	14½	42	23	41	33½	12
13	28	19	23½	22	49	20	39	32½	13
14	35	21	32	27½	57	23	53	41½	14
15	63	25	62	47½	69	24	60	46	15
16	66	25	65	49	76	26	76	56	16
17	63	27	68	51	58	27	63	48	17
18	92	28	97	68	72	28	78	57	18
19	103	28	106	73	84	26	83	60	19
20	106	28	110	76	89	28	89	63½	20
21	99	29	107	74	86	28	91	65	21
22	125	30	137	92	88	25	82	59½	22
23					81	27	83	60	23
24					82	28	87	62½	24
25					138	30	148	93	25
26					157	30	167	104	26
27					185	30	193	127	27
28					215	30	220	130+	28
29									29
30									30
31									31
32									32
33									33
34									34
35									35
36									36
37									37
38									38
39									39
40									40

BCC-5

BCC-6

DEPTH (FE)	BCC-5				BCC-6				DEPTH (FE)
	N _B	BP (PSIG)	N _{BC}	SPT N ₆₀	N _B	BP (PSIG)	N _{BC}	SPT N ₆₀	
1	32	18	24	22 ^{16 1/2}	54	22	47	38 ^{28.5}	1
2	28	16	18	17 1/2 ^{14.1}	60	23	54	42 1/2 ^{31.9}	2
3	18	13	10	10 ^{7.5}	35	17	23	21 1/2 ^{16.1}	3
4	14	12	8	8 ^{6.0}	26	15	15 1/2	15 1/2 ^{11.4}	4
5	7	8	4 1/2	4 1/2 ^{3.4}	10	14	8 1/2	8 1/2 ^{6.4}	5
6	5	6	3	3 ^{2.3}	15	13	9	9 ^{6.8}	6
7	3	6	2 1/2	2 1/2 ^{1.9}	25	17	18 1/2	18 ^{13.5}	7
8	2	4	2	2 ^{1.5}	45	18	31	27 ^{20.3}	8
9	2	4	2	2	76	20	53	41 1/2	9
10	5	15	6 1/2	6 1/2	50	21	42	34 1/2	10
11	19	17	15 1/2	15 1/2	38	23	37	31	11
12	35	18	26	23 1/2	17	23	21	20	12
13	48	20	38	31 1/2	43	25	45	36 1/2	13
14	46	21	40	33	56	26	59	45 1/2	14
15	42	20	35	29 1/2	52	26	56	43 1/2	15
16	51	22	45	36 1/2	57	25	57	44	16
17	67	25	65	49	77	26	76	56	17
18	63	26	65	49	62	26	64	48 1/2	18
19	84	26	83	60 1/2	68	27	72	53 1/2	19
20	91	26	87	62 1/2	60	27	65	49	20
21	88	27	89	63 1/2	85	27	86	62	21
22	109	27	107	74	88	29	96	67 1/2	22
23	139	29	144	97	96	29	104	73	23
24	108	30	120	82	102	29	110	76	24
25	140	30	150	100	107	29	114	79	25
26	188	30	195	128	106	29	113	78	26
27	200+	30	207+	135+	94	28	99	69 1/2	27
28					96	27	96	67 1/2	28
29					69	25	67	50 1/2	29
30					63	29	73	54	30
31					122	30	131	88	31
32					127	30	140	94	32
33					105	30	115	79	33
34					198	30	203	132	34
35					183	29	183	121	35
36					143	29	148	98	36
37					169	29	172	114	37
38					170	29	172	114	38
39					234	30	236	140+	39
40					228	30	230	140+	40

BCC-7

BCC-8

COLUMN FEET	BCC-7				BCC-8				DEPTH (ft)
	N _B	BP (psig)	N _{BC}	SPT N ₆₀	N _B	BP (psig)	N _{BC}	SPT N ₆₀	
1	33	12	12½	12½ ^{9.4}	9	10	5½	5½ ^{4.1}	1
2	14	8	5½	5½ ^{4.1}	10	11	6½	6½ ^{4.9}	2
3	3	8	3	3 ^{2.3}	7	12	6	6 ^{4.5}	3
4	3	5	2½	2½ ^{1.9}	7	10	5	5 ^{3.8}	4
5	4	6	3	3 ^{2.3}	5	10	4½	4½ ^{2.4}	5
6	5	5	3	3 ^{2.3}	7	10	5	5 ^{3.8}	6
7	4	5	2½	2½ ^{1.9}	10	8	5	5 ^{3.8}	7
8	5	6	3	3 ^{2.3}	7	8	4½	4½ ^{3.4}	8
9	7	11	5½	5½	6	5	3	3	9
10	6	11	5	5	7	5	3½	3½	10
11	6	8	4	4	5	5	3	3	11
12	8	8	4½	4½	6	5	3	3	12
13	14	10	6½	6½	4	5	2½	2½	13
14	10	10	6	6	6	5	3	3	14
15	16	10	7	7	8	5	3½	3½	15
16	11	9	5½	5½	8	8	4½	4½	16
17	6	12	5½	5½	6	10	5	5	17
18	6	9	4½	4½	6	11	5	5	18
19	7	8	4½	4½	8	10	5½	5½	19
20	10	8	5	5	7	12	6	6	20
21	10	9	5½	5½	8	13	7	7	21
22	13	11	7	7	10	13	7½	7½	22
23	8	12	6½	6½	9	13	7½	7½	23
24	6	13	6	6	9	13	7½	7½	24
25	6	13	6	6	10	10	6	6	25
26	7	10	5	5	10	11	6½	6½	26
27	10	8	5	5	9	13	7½	7½	27
28	5	11	5	5	7	14	7	7	28
29	6	10	5	5	11	15	9½	9½	29
30	7	9	4½	4½	12	16	11	11	30
31	5	10	4½	4½	14	16	12	12	31
32	5	10	4½	4½	13	15	10½	10½	32
33	6	9	4½	4½	10	14	8½	8½	33
34	11	11	6½	6½	15	13	9	9	34
35	5	10	4½	4½	18	13	10	10	35
36	4	13	5½	5½	14	13	9	9	36
37	8	12	6½	6½	15	13	9	9	37
38	6	14	6½	6½	14	14	9½	9½	38
39	9	14	8	8	11	14	8½	8½	39
40	8	10	5½	5½	13	13	8½	8½	40

BCC-7

BCC-8

	N _B	BP (psig)	N _{BC}	SPT N ₆₀	N _B	BP (psig)	N _{BC}	SPT N ₆₀	DEPTH (ft)
41	5	9	4	4	14	14	9½	9½	
42	4	10	4	4	14	14	9½	9½	
43	4	12	5	5	12	14	9	9	
44	5	13	5½	5½	11	13	8	8	
45	6	13	6	6	13	12	8	8	
46	6	14	6½	6½	10	12	7	7	
47	10	10	6	6	10	13	7½	7½	
48	9	13	7½	7½	13	14	9½	9½	
49	8	15	8	8	8	14	7½	7½	
50	7	15	7½	7½	8	15	8	8	50
51	7	15	7½	7½	11	14	8½	8½	
52	6	13	6	6	6	12	5½	5½	
53	9	14	8	8	6	11	5	5	
54	7	13	6½	6½	8	11	6	6	
55	9	18	11	11	9	12	6½	6½	
56	25	21	24½	22½	7	12	6	6	
57	200+			130+	14	15	11	11	
58					18	15	12½	12½	
59					150+	25	125+	85+	60
60									
61									
62									
63									
64									
65									
66									
67									
68									
69									
70									70
71									
72									
73									
74									
75									
76									
77									
78									
79									
80									80

BCC-9

BCC-10

COLUMN - DATE	BCC-9				BCC-10			
	N _B	BP (psig)	N _{BC}	SPT N ₆₀	N _B	BP (psig)	N _{BC}	SPT N ₆₀
1	35	17	23	2 1/2 16.1	17	13	7 1/2	4 1/2 7.1
2	21	15	13 1/2	1 3/2 10.1	10	12	7	7 5.3
3	17	13	9 1/2	9 1/2 7.1	8	10	5 1/2	5 1/2 4.1
4	10	12	7	7 5.3	6	10	5	5 3.8
5	10	11	6 1/2	6 1/2 4.9	9	11	6	6 4.5
6	11	10	6	6 4.5	9	10	5 1/2	5 1/2 4.1
7	11	11	6 1/2	6 1/2 4.9	9	10	5 1/2	5 1/2 4.1
8	10	11	6 1/2	6 1/2 4.9	10	10	6	6 4.5
9	8	12	6 1/2	6 1/2	7	11	5 1/2	5 1/2
10	6	12	5 1/2	5 1/2	7	11	5 1/2	5 1/2
11	6	12	5 1/2	5 1/2	7	10	5	5
12	7	11	5 1/2	5 1/2	7	11	5 1/2	5 1/2
13	8	13	7	7	9	11	6	6
14	8	13	7	7	10	12	7	7
15	9	12	6 1/2	6 1/2	10	11	6 1/2	6 1/2
16	8	12	6 1/2	6 1/2	10	12	7	7
17	8	12	6 1/2	6 1/2	9	12	6 1/2	6 1/2
18	8	12	6 1/2	6 1/2	10	13	7 1/2	7 1/2
19	6	12	5 1/2	5 1/2	10	12	7	7
20	6	12	5 1/2	5 1/2	9	12	6 1/2	6 1/2
21	8	12	6 1/2	6 1/2	9	13	7 1/2	7 1/2
22	8	12	6 1/2	6 1/2	10	14	8 1/2	8 1/2
23	7	12	6	6	11	14	8 1/2	8 1/2
24	6	12	5 1/2	5 1/2	8	13	7	7
25	8	13	7	7	11	14	8 1/2	8 1/2
26	10	13	7 1/2	7 1/2	11	15	9 1/2	9 1/2
27	11	13	8	8	11	15	9 1/2	9 1/2
28	11	13	8	8	13	15	10 1/2	10 1/2
29	7	12	6	6	15	16	12 1/2	12 1/2
30	6	8	4 1/2	4 1/2	15	17	13 1/2	13 1/2
31	5	6	3 1/2	3 1/2	14	16	12	12
32	5	8	4 1/2	4 1/2	13	17	12 1/2	12 1/2
33	5	10	4 1/2	4 1/2	12	16	11	11
34	7	12	6	6	13	17	12 1/2	12 1/2
35	6	13	6	6	13	17	12 1/2	12 1/2
36	5	14	6	6	14	17	13	13
37	6	15	7	7	15	17	13 1/2	13 1/2
38	9	15	8 1/2	8 1/2	13	16	11 1/2	11 1/2
39	11	17	11 1/2	11 1/2	11	16	10 1/2	10 1/2
40	14	16	12	12	12	16	11	11

BCC-9

BCC-10

DEPTH

	N ₆₀	BP (PSI)	N ₆₀	SPT N ₆₀	N ₁₅	BP (PSI)	N ₆₀	SPT N ₆₀	
41	13	16	11½	11½	11	16	10½	10½	41
42	13	15	10½	10½	12	16	11	11	
43	14	15	11	11	9	15	8½	8½	
44	15	16	12½	12½	11	18	12	12	
45	15	17	13½	13½	17	18	16	16	
46	12	17	9	9	14	18	14	14	
47	8	12	6½	6½	15	18	14½	14½	
48	8	10	5½	5½	12	16	11	11	
49	6	13	6	6	12	16	11	11	
50	7	13	6½	6½	9	15	8½	8½	50
51	5	13	5½	5½	9	15	8½	8½	
52	6	12	5½	5½	8	15	8	8	
53	7	12	6	6	8	16	9	9	
54	8	12	6½	6½	10	17	11	11	
55	7	13	6½	6½	18	19	17½	17	
56	7	15	7½	7½	14	17	13	13	
57	7	20	10½	10½	9	18	11	11	
58	100+	25	90+	64+	9	18	11	11	
59					13	20	15	15	
60					150+	27	140+	94+	60
61									
62									
63									
64									
65									
66									
67									
68									
69									
70									70
71									
72									
73									
74									
75									
76									
77									
78									
79									
80									80

BCC-11

BCC-12

DEPTH (FE)	BCC-11				BCC-12				DEPTH (FE)
	N _B	BP (PSI)	N _{BC}	SPT N ₆₀	N _B	BP (PSI)	N _{BC}	SPT N ₆₀	
1	22	17	17	16 ^{12.4}	25	19	21 ^{1/2}	20 ^{15.4}	1
2	19	15	13	13 ^{9.8}	54	20	42	34 ^{25.9}	2
3	13	13	8 ^{1/2}	8 ^{6.4}	60	23	54	42 ^{31.9}	3
4	9	12	6 ^{1/2}	6 ^{4.9}	52	21	44	36 ^{27.0}	4
5	8	11	6	6 ^{4.5}	24	18	19 ^{1/2}	18 ^{13.9}	5
6	6	10	5	5 ^{3.8}	18	16	14	14 ^{10.5}	6
7	7	10	5	5 ^{3.8}	15	14	10	10 ^{7.5}	7
8	7	10	5	5 ^{3.8}	13	14	9 ^{1/2}	9 ^{7.1}	8
9	7	10	5	5	13	13	8 ^{1/2}	8 ^{1/2}	9
10	6	10	5	5	12	10	6 ^{1/2}	6 ^{1/2}	10
11	6	10	5	5	9	9	5	5	11
12	6	10	5	5	10	8	5	5	12
13	7	10	5	5	13	6	4 ^{1/2}	4 ^{1/2}	13
14	6	10	5	5	8	12	6 ^{1/2}	6 ^{1/2}	14
15	7	12	6	6	11	10	6	6	15
16	6	13	6	6	14	11	7 ^{1/2}	7 ^{1/2}	16
17	7	13	6 ^{1/2}	6 ^{1/2}	12	13	8	8	17
18	7	14	7	7	12	13	8	8	18
19	7	10	5	5	10	12	7	7	19
20	9	10	5 ^{1/2}	5 ^{1/2}	11	13	8	8	20
21	8	10	5 ^{1/2}	5 ^{1/2}	12	14	9	9	21
22	12	13	8	8	12	14	9	9	22
23	10	14	8 ^{1/2}	8 ^{1/2}	13	14	9 ^{1/2}	9 ^{1/2}	23
24	10	14	8 ^{1/2}	8 ^{1/2}	11	13	8	8	24
25	11	15	9 ^{1/2}	9 ^{1/2}	13	15	10 ^{1/2}	10 ^{1/2}	25
26	10	15	9	9	16	17	14	14	26
27	11	15	9 ^{1/2}	9 ^{1/2}	18	17	15	15	27
28	12	15	10	10	18	16	14	14	28
29	18	18	16 ^{1/2}	16 ^{1/2}	13	16	11 ^{1/2}	11 ^{1/2}	29
30	22	18	18 ^{1/2}	18	16	16	13	13	30
31	21	17	16 ^{1/2}	16 ^{1/2}	15	17	13 ^{1/2}	13 ^{1/2}	31
32	20	16	15	15	15	16	12 ^{1/2}	12 ^{1/2}	32
33	16	16	13	13	15	17	13 ^{1/2}	13 ^{1/2}	33
34	15	16	12 ^{1/2}	12 ^{1/2}	15	17	13 ^{1/2}	13 ^{1/2}	34
35	15	15	11 ^{1/2}	11 ^{1/2}	13	17	12 ^{1/2}	12 ^{1/2}	35
36	13	15	10 ^{1/2}	10 ^{1/2}	14	17	13	13	36
37	14	15	11	11	12	17	12	12	37
38	14	15	11	11	14	17	13	13	38
39	13	15	10 ^{1/2}	10 ^{1/2}	16	17	14	14	39
40	10	16	10	10	16	17	14	14	40

BCC 11

BCC-12

	N _B	BP (psia)	N _{BC}	SPT N ₆₀	N _B	BP (psia)	N _{BC}	SPT N ₆₀	
41	11	17	11½	11½	15	17	13½	13½	41
42	11	16	10½	10½	14	16	12	12	
43	7	14	7	7	13	16	11½	11½	
44	7	12	6	6	13	17	12½	12½	
45	7	13	6½	6½	13	16	11½	11½	
46	13	15	10½	10½	14	16	12	12	
47	14	17	13	13	12	16	11	11	
48	17	17	14½	14½	13	15	10½	10½	
49	9	17	10	10	10	17	11	11	
50	10	17	11	11	10	18	11½	11½	50
51	7	15	7½	7½	18	18	16½	16½	
52	7	12	6	6	15	17	13½	13½	
53	7	11	5½	5½	12	16	11	11	
54	7	11	5½	5½	15	18	14½	14½	
55	8	15	8	8	11	16	10½	10½	
56	14	16	12	12	8	15	8	8	
57	15	16	12½	12½	9	16	9½	9½	
58	12	18	12½	12½	10	16	10	10	
59	36	22	34	29	10	16	10	10	
60	32	21	30	26	11	15	9½	9½	60
61	150+	27	140+	94+	10	15	9	9	
62					10	16	10	10	
63					11	20	13½	13½	
64					20	22	22	20½	
65					26	22	27	24½	
66					15	21	17½	17	
67					16	20	17	16½	
68					16	22	19	18½	
69					150+	25	125+	85+	70
70									
71									
72									
73									
74									
75									
76									
77									
78									
79									
80									80

BCC-13

BCC-14

COLUMN NO.	BCC-13				BCC-14				DEPTH (ft)
	N _B	BP (psig)	N _{BC}	SPT N ₆₀	N _B	BP (psig)	N _{BC}	SPT N ₆₀	
1	17	15	12	12 ^{7.0}	10	14	8½	8½ ^{6.2}	1
2	25	16	16½	16½ ^{12.4}	12	11	7	7 ^{5.3}	2
3	22	15	14	14 ^{10.5}	12	10	6½	6½ ^{4.9}	3
4	18	15	12½	12½ ^{9.4}	9	10	5½	5½ ^{4.1}	4
5	19	13	10	10 ^{7.5}	10	10	6	6 ^{4.5}	5
6	15	12	8	8 ^{6.0}	12	10	6½	6½ ^{4.9}	6
7	11	10	6	6 ^{4.5}	13	10	6½	6½ ^{4.9}	7
8	9	8	4	4 ^{3.0}	12	11	7	7 ^{5.3}	8
9	4	8	3½	3½	16	12	8½	8½	9
10	8	10	5½	5½	12	14	9	9	10
11	20	12	9½	9½	44	20	36	30½	11
12	21	15	13½	13½	65	20	48	38½	12
13	23	15	14½	14½	56	20	44	36	13
14	27	16	17½	17	53	21	44	36	14
15	26	16	17	16½	52	21	44	36	15
16	11	15	9½	9½	50	22	45	36½	16
17	15	15	11½	11½	54	22	48	38½	17
18	24	15	15	15	48	21	41	33½	18
19	21	15	13½	13½	70	24	65	49	19
20	25	15	15	15	115	27	112	77	20
21	30	15	16½	16½	125	28	126	86	21
22	15	15	11½	11½	135	26	121	83	22
23	12	14	9	9	94	26	90	64	23
24	10	13	7½	7½	55	26	58	45	24
25	10	13	7½	7½	65	26	67	50½	25
26	10	10	6	6	80	27	83	60	26
27	10	10	6	6	85	26	84	60½	27
28	10	8	5	5	93	27	94	66½	28
29	7	8	4½	4½	70	26	71	53	29
30	7	8	4½	4½	65	26	67	50½	30
31	9	8	5	5	60	26	62	47½	31
32	7	7	4	4	65	27	70	52	32
33	6	7	3½	3½	67	27	71	53	33
34	5	8	3½	3½	77	28	83	60	34
35	7	8	4½	4½	74	29	83	60	35
36	7	10	5	5	95	29	104	73	36
37	12	11	7	7	105	30	115	79	37
38	11	9	5½	5½	87	30	91	69½	38
39	7	8	4½	4½	110	30	121	83	39
40	9	8	5	5	87	29	96	77	40

BCC-13

BCC-14

DEPTH (ft)	N _B	BP (psig)	N _{BC}	SPT N ₆₀	N _B	BP (psig)	N _{BC}	SPT N ₆₀	DEPTH (ft)
41	7	8	4½	4½	103	29	110	76	41
42	8	8	4½	4½	110	29	117	80	42
43	10	11	6½	6½	107	30	117	80	43
44	19	20	19½	18½	112	29	119	81	44
45	50	24	49	39	125	30	137	92	45
46	91	25	84	60½	150	30	160	107	46
47	118	28	121	83	200	30	207	135	47
48	200+	28	190+	125+	200+	30	207+	135+	48
49									49
50									50
11									
12									
13									
14									
15									
16									
17									
18									
19									
20									
21									
22									
23									
24									
25									
26									
27									
28									
29									
30									
31									
32									
33									
34									
35									
36									
37									
38									
39									
40									

BCC-15

BCC-16

COLUMN WRITE	BCC-15				BCC-16				DEPTH (ft)
	N _B	BP (psig)	N _{BC}	SPT N ₆₀	N _B	BP (psig)	N _{BC}	SPT N ₆₀	
1	21	10	7½	7½ 5.6	19	20	19½	18½ 13.9	1
2	30	15	16½	16½ 12.4	33	20	29	25½ 19.1	2
3	36	16	20½	19½ 14.6	45	22	42	34½ 25.9	3
4	40	16	22	20½ 15.4	50	23	47	38 28.5	4
5	30	15	16½	16½ 12.4	49	24	48	38½ 28.9	5
6	22	15	14	14 10.5	41	22	38	31½ 23.6	6
7	31	16	19	18½ 13.9	38	20	32	27½ 20.6	7
8	27	16	17½	17 12.8	32	20	28	25 18.9	8
9	21	16	15	15	27	19	23	21½	9
10	16	16	13	13	25	19	21½	20	10
11	19	16	14½	14½	27	19	23	21½	11
12	25	13	20	19	29	21	28	25	12
13	35	21	32	27½	42	20	35	29½	13
14	33	22	32	27½	30	20	27	24½	14
15	33	22	32	27½	27	24	30	26	15
16	52	24	51	40½	62	26	64	48½	16
17	45	24	45	36½	52	25	53	41½	17
18	39	22	37	31	40	24	41	33½	18
19	30	15	16½	16½	39	23	38	31½	19
20	28	17	19½	19½	36	22	34	29	20
21	30	17	20	19	33	22	32	27½	21
22	27	17	19	18½	42	22	34	32½	22
23	26	18	20½	19½	32	21	30	26	23
24	39	19	31	27	28	20	25	23	24
25	43	20	35	29½	26	20	24	22	25
26	50	21	42	34½	28	20	25	23	26
27	55	20	43	35	26	21	25	23	27
28	41	19	32	27½	30	24	33	28	28
29	40	19	31	27	40	24	41	33½	29
30	40	20	33	28	43	24	44	36	30
31	34	21	31	27	36	23	36	30½	31
32	38	23	37	31	38	23	37	31	32
33	43	22	40	33	40	24	41	33½	33
34	33	21	30	26	58	23	53	41½	34
35	35	21	32	27½	30	22	30	26	35
36	21	20	26	23½	30	19	25	23	36
37	32	22	31	27	20	20	20	19	37
38	42	23	41	33½	36	24	38	31½	38
39	35	22	34	29	38	24	40	33	39
40	30	22	30	26	35	22	34	29	40

BCC-15

BCC-16

	N _B	BP (psig)	N _{BC}	SPT N ₆₀	N _B	BP (psig)	N _{BC}	SPT N ₆₀	DEPTH (ft)
41	32	23	33	28	38	23	37	31	41
42	36	23	36	30½	46	23	44	36	42
43	39	24	40	33	46	24	46	37	43
44	46	25	48	38½	50	23	47	33	44
45	46	25	48	38½	59	25	59	45½	45
46	53	25	54	42½	50	24	49	39	46
47	50	25	51	40½	50	24	49	39	47
48	60	25	60	46	48	24	48	38½	48
49	38	25	41	33½	38	21	34	29	49
50	58	22	50	40	40	20	33	28	50
51	56	23	52	41	57	21	33	28	51
52	60	24	57	44	42	22	39	32½	52
53	60	23	54	42½	43	22	40	33	53
54	35	20	30	26	41	20	34	29	54
55	33	22	32	27½	31	21	29	25½	55
56	33	23	34	29	31	22	30	26	56
57	55	23	51	40½	34	21	31	27	57
58	45	23	43	35	45	20	37	31	58
59	58	25	58	45	86	17	44	36	59
60	43	23	46	37	34	19	27	24½	60
61	58	24	56	43½	23	19	20½	19½	61
62	64	24	60	46	24	18	19½	18½	62
63	35	23	59	45½	15	18	14½	14½	63
64	75	24	69	51½	20	18	17½	17	64
65	45	23	43	35	16	19	16	16	65
66	70	24	65	49	18	22	21	20	66
67	75	24	69	51½	18	20	18½	18	67
68	66	24	62	47½	20	21	21	20	68
69	73	24	67	50½	25	21	24½	22½	69
70	52	25	53	41½	22	20	21	20	70
71	63	27	72	53½	26	21	25	23	71
72	65	24	61	47	30	21	28½	25	72
73	70	25	68	51	28	22	28	25	73
74	42	24	80	58	36	21	33	23	74
75	45	26	90	64	30	21	28½	25	75
76	24	26	83	60	25	20	23	21½	76
77	112	26	103	72	24	20	22½	21	77
78	150+	26	132+	40+	24	20	22½	21	78
79					23	20	22	20½	79
80					28	21	27	24½	80

BCC-15

BCC-16

DEPTH (ft)	BCC-15				BCC-16				
	N _B	BP (psig)	N _{bc}	SPT N ₆₀	N _B	BP (psig)	N _{bc}	SPT N ₆₀	
81					30	22	30	26	81
82					42	22	39	32½	82
83					50	20	40	33	83
84					21	20	20½	19½	84
85					18	19	17½	17	85
86					18	19	17½	17	86
87					26	22	27	24½	87
88					42	23	41	33½	88
89					37	23	37	31	89
90					34	21	31	27	90
91					32	20	28	25	91
92					28	21	27	24½	92
93					38	21	34	29	93
94					52	21	44	36	94
95					37	22	35	29½	95
96					32	20	28	25	96
97					24	20	22½	21	97
98					21	20	20½	17½	98
99					22	20	21	20	99
100					26	20	24	22	100
101					44	22	41	33½	101
102					50	18	33	28	102
103					29	17	20	19	103
104					28	16	18	17½	104
105					27	16	17½	17	105
106					31	16	19	18½	106
107					30	16	18½	18	107
108					86	13	24	22	108
109					96	10	15	15	109
110					150+	27	140+	94+	110
111									111
112									112
113									113
114									114
115									115
116									116
117									117
118									118
119									119
120									120

BCC - 17

BCC - 18

COLUMN WRITE	BCC - 17				BCC - 18				DEPTH (FE)
	N _B	BP (psig)	N _{bc}	SPT N ₆₀	N _B	BP (psig)	N _{bc}	SPT N ₆₀	
1	29	18	22	20½ 15.4	13	15	10½	10½ 7.9	1
2	33	17	22	20½ 15.4	16	15	11½	11½ 8.6	2
3	30	18	22	20½ 15.4	15	15	11½	11½ 8.6	3
4	27	18	21	20 15	15	16	12½	12½ 9.4	4
5	34	18	25	23 17.3	16	20	17	16½ 12.4	5
6	40	20	33	28 21	30	20	27	24½ 18.4	6
7	43	21	38	31½ 23.6	26	22	27	24½ 18.4	7
8	50	20	40	33 24.8	35	22	34	29 21.8	8
9	35	20	30	26	42	21	37	31	9
10	31	19	26	23½	41	21	36	30½	10
11	33	22	32	27½	43	22	40	33	11
12		23			69	25	67	50½	12
13	28	18	21½	20	125	26	113	78	13
14	23	24	27	24½	100	24	84	60½	14
15	75	27	79	57½	64	23	58	45	15
16	79	26	78	57	47	23	45	36½	16
17	51	23	48	38½	42	21	37	31	17
18	42	22	39	32½	31	21	29	25½	18
19	42	21	37	31	20	20	20	19	19
20	35	22	34	29	28	21	27	24½	20
21	37	23	37	31	28	21	27	24½	21
22	40	25	43	35	32	23	33	28	22
23	56	28	91	65	37	22	35	29½	23
24	84	25	78	57	33	21	30	26	24
25	83	24	73	54	27	19	23	21½	25
26	62	25	61	47	19	18	17	16½	26
27	38	24	40	33	17	18	16	16	27
28	37	24	39	32½	23	20	22	20½	28
29	35	24	37	31	16	15	11½	11½	29
30	51	25	52	41	32	18	24	22	30
31	85	28	90	64	50	21	42	34½	31
32	74	25	71	53	77	22	62	47½	32
33	45	24	45	36½	70	21	54	42½	33
34	41	26	45	36½	60	20	45	36½	34
35	42	25	44	36	54	20	42	34½	35
36	36	24	38	31½	43	20	35	27½	36
37	31	22	30	26	41	20	34	29	37
38	27	21	26	23½	37	20	32	27½	38
39	32	23	33	28	41	22	38	31½	39
40	49	23	46	37	62	24	59	45½	40

BCC - 17

BCC - 18

	N _B	BP (psig)	N _{BC}	SPT N ₆₀	N _B	BP (psig)	N _{BC}	SPT N ₆₀	DEPTH (FE)
41	48	23	46	37	56	23	52	41	41
42	48	24	48	38½	55	23	51	40½	42
43	42	23	41	33½	55	23	51	40½	43
44	41	24	42	34½	55	22	48	38½	44
45	40	25	43	35	50	22	45	36½	45
46	35	23	35	29½	45	22	42	34½	46
47	29	22	29	25½	30	19	25	23	47
48	29	22	29	25½	22	19	19½	18½	48
49	30	22	30	26	16	19	16	16	49
50	36	23	36	30½	19	18	17	16½	50
51	34	24	36	30½	17	18	16	16	51
52	30	22	30	26	17	18	16	16	52
53	25	21	24½	22½	15	18	14½	14½	53
54	21	20	20½	19½	19	18	17	16½	54
55	19	19	18	17½	28	20	25	23	55
56	22	20	21	20	24	19	21	20	56
57	23	20	22	20½	21	19	19	18½	57
58	22	20	21	20	26	19	22	20½	58
59	19	20	19½	18½	34	19	27	24½	59
60	23	21	23½	22	30	19	25	23	60
61	24	21	24	22	24	19	21	20	61
62	25	21	24½	22½	26	19	22	20½	62
63	27	22	27½	24½	25	18	20	19	63
64	30	21	28½	25	23	19	20½	19½	64
65	25	21	24½	22½	25	19	21½	20	65
66	37	23	37	31	23	19	20½	19½	66
67	32	22	31	27	19	18	17	16½	67
68	28	22	28	25	16	17	14	14	68
69	21	19	19	18½	14	17	13	13	69
70	22	20	21	20	11	17	11½	11½	70
71	27	20	24½	22½	14	19	15	15	71
72	32	21	30	26	16	17	14	14	72
73	45	25	47	38	23	18	19	18½	73
74	51	25	52	41	26	18	20½	19½	74
75	4	24	60	46	23	18	19	18½	75
76	70	24	65	49	20	18	17½	17	76
77	64	27	69	51½	21	20	20½	19½	77
78	65	26	69	51½	22	20	21	20	78
79	80	23	68	51	29	21	28	25	79
80	77	24	71	53	34	20	29½	25½	80

BCC - 17

BCC - 18

COLUMN NO. (ft)	BCC - 17				BCC - 18				DEPTH (ft)
	N _B	BP (psig)	N _{BC}	SPT N ₆₀	N _B	BP (psig)	N _{BC}	SPT N ₆₀	
81	68	24	63	48	33	20	29	25½	81
2	73	24	67	50½	35	20	30	26	82
3	66	23	59	45½	35	21	32	27½	83
4	59	22	51	40½	35	21	32	27½	84
5	57	23	53	41½	34	21	31	27	85
6	46	22	42	34½	40	22	38	31½	86
7	34	21	31	27	33	20	29	25½	87
8	30	21	28½	25	35	21	32	27½	88
9	29	21	28	25	33	21	30	26	89
90	25	20	23	21½	33	20	29	25½	90
11	19	20	19½	18½	37	20	32	27½	91
12	25	20	23	21½	39	21	35	29½	92
13	24	21	24	22	45	21	39	32½	93
14	23	21	23½	22	59	20	45	36½	94
15	23	21	23½	22	76	20	54	42½	95
16	27	21	26	23½	50	20	40	33	96
17	27	21	26	23½	62	20	46	37	97
18	22	21	22½	21	28	20	25	23	98
19	21	21	22	20½	27	20	24½	22½	99
100	27	21	26	23½	36	20	31	27	100
21	29	20	26	23½	44	20	36	30½	101
22	28	20	25	23	46	20	37	31	102
23	50	25	51	40½	63	21	50	40	103
24	200+	28	175+	116+	57	21	46	37	104
25					49	20	39	32½	105
26					37	21	33	28	106
27					35	21	32	27½	107
28					34	22	33	28	108
29					40	22	38	31½	109
110					41	22	38	31½	110
31					61	24	58	45	111
32					160+	24	122+	84+	112
33									113
34									114
35									115
36									116
37									117
38									118
39									119
120									120

BCC-19

BCC-20

COLUMN NO.	BCC-19				BCC-20				DEPTH (ft)
	N _B	BP (psig)	N _{BC}	SPT N ₆₀	N _B	BP (psig)	N _{BC}	SPT N ₆₀	
1	10	15	9	9 6.8	12	15	10	10 7.5	1
2	14	15	11	11 8.3	28	17	14 1/2	18 1/2 13.1	2
3	27	18	21	20 15	53	19	41 1/2	34 25.5	3
4	35	17	23	21 1/2 16.1	46	18	32	27 1/2 20.6	4
5	46	18	31	27 20.3	30	16	18 1/2	18 13.5	5
6	47	18	32	27 1/2 20.6	27	16	17 1/2	17 12.2	6
7	55	20	43	35 26.3	18	15	12 1/2	12 1/2 9.4	7
8	52	20	41	33 1/2 25.1	20	14	11 1/2	11 1/2 8.6	8
9	65	18	41	33 1/2	15	16	12 1/2	12 1/2	9
10	40	18	28 1/2	25	14	19	15	15	10
11	33	20	29	25 1/2	27	19	23	21 1/2	11
12	40	23	39	32 1/2	29	20	26	23 1/2	12
13	43	25	45	36 1/2	41	21	36	30 1/2	13
14	45	23	43	35	35	20	30	26	14
15	31	21	29	25 1/2	23	18	19	18 1/2	15
16	26	20	24	22	16	17	14	14	16
17	24	21	24	22	20	18	17 1/2	17	17
18	28	20	25	23	21	18	18	17 1/2	18
19	20	20	20	19	21	19	19	18 1/2	19
20	24	20	22 1/2	21	19	20 23	22 1/2	21	20
21	21	21	22	20 1/2	27	23	29	25 1/2	21
22	38	23	37	31	55	23	51	40 1/2	22
23	44	23	42	34 1/2	31	24	34	29	23
24	35	21	32	27 1/2	53	24	52	41	24
25	31	20	27 1/2	24 1/2	50	24	49	39	25
26	35	22	34	29	106	28	110	76	26
27	48	23	46	37	108	29	114	79	27
28	38	24	40	33	94	25	85	61	28
29	41	24	42	34 1/2	61	26	63	48	29
30	58	25	58	45	70	25	68	51	30
31	72	26	73	54	65	25	64	48 1/2	31
32	85	27	87	62 1/2	67	25	65	49	32
33	64	27	69	51 1/2	70	21	54	42 1/2	33
34	64	26	66	50	64	21	51	40 1/2	34
35	66	26	67	50 1/2	45	20	37	31	35
36	66	25	65	49	60	20	45	36 1/2	36
37	81	26	80	58	43	20	35	29 1/2	37
38	62	25	61	47	47	20	38	31 1/2	38
39	56	26	59	45 1/2	34	25	38	31 1/2	39
40	84	26	83	60	39	25	42	31 1/2	40

BCC-19

BCC-20

	N _B	BP (psig)	N _{BC}	SPT N ₆₀	N _B	BP (psig)	N _{BC}	SPT N ₆₀	DEPTH (ft)
41	67	26	68	51	38	24	40	53	41
2	74	25	71	53	36	23	36	30½	
3	60	25	60	46	32	24	35	29½	
4	54	24	53	41½	41	20	34	29	
5	38	23	37	31	46	25	48	38½	
6	36	22	34	29	42	25	44	36	
7	34	21	31	27	40	25	43	35	
8	30	21	28½	25	24	25	29	25½	
9	33	21	30	26	23	20	22	20½	
50	26	21	25	23	20	20	20	19	50
11	23	21	23½	22	21	20	20½	19½	
12	25	20	23	21½	21	20	20½	19½	
13	32	20	28	25	24	20	22½	21	
14	33	20	29	25½	29	20	26	23½	
15	26	20	24	22	20	17	16	16	
16	24	21	24	22	20	24	24½	22½	
17	26	21	25	23	21	25	26	23½	
18	32	21	30	26	20	25	25	23	
19	38	20	32	27½	20	25	25	23	
60	19	20	19½	18½	20	28	28	25	60
21	20	20	20	19	20	28	28	25	
22	21	21	22	20½	21	25	26	23½	
23	23	20	22	20½	21	25	26	23½	
24	25	20	23	21½	24	16	16½	16	
25	26	20	24	22	25	18	20	19	
26	28	20	25	23	26	18	20	19½	
27	29	21	28	25	25	18	20	19	
28	31	22	30	26	24	10?	5	8?	
29	40	22	38	31½	24	15?	15	15	
70	40	23	39	32½	20	17	16	16	70
31	41	22	38	31½	28	17	17½	18½	
32	70	23	61	47	26	17	18½	18	
33	66	23	59	45½	29	18	22	20½	
34	65	23	59	45½	26	17	22	20½	
35	86	24	75	55	22	25	27	24½	
36	98	25	88	63	34	20	29½	25½	
37	81	25	77	56½	50	21	42	34½	
38	78	25	74	54½	45	21	39	32½	
39	69	24	64	48½	44	21	38	31½	
80	62	23	56	43½	26	22	34	24	80

BCC-19

BCC-20

COLUMN NUMBER	BCC-19				BCC-20				DEPTH (ft)
	N _B	BP (psia)	N _{BC}	SPT N ₆₀	N _B	BP (psia)	N _{BC}	SPT N ₆₀	
81	62	25	61	47	27	22	27½	24½	81
2	69	25	67	50½	27	24	30	26	2
3	60	23	54	42½	29	24	32	27½	3
4	36	23	36	30½	27	25	32	27½	4
5	39	24	40	33	27	25	32	27½	5
6	38	24	40	33	39	26	44	36	6
7	39	25	42	34½	34	26	39	32½	7
8	48	25	50	40	33	21	30	26	8
9	50	23	47	38	51	20	40	33	9
90	53	23	49	39	43	20	35	29½	90
11	62	23	56	43½	36	21	33	28	11
12	45	22	42	34½	45	21	34	32½	12
13	48	23	46	37	41	21	36	30½	13
14	56	25	57	44	30	20	27	24½	14
15	56	23	52	41	44	20	36	30½	15
16	60	23	54	42½	68	19	46	37	16
17	69	24	64	48½	90	18	51	40½	17
18	75	24	69	51½	108	18	56	43½	18
19	187	25	148	98	160	17	62	47½	19
100	140	25	118	80	164	20	88	63	100
21	200	25	156	104	170	20	70	64	21
22					138	24	110	76	22
23					240	24	145	77	23
24									24
25									25
26									26
27									27
28									28
29									29
110									110
31									31
32									32
33									33
34									34
35									35
36									36
37									37
38									38
39									39
40									40

BCC-21

BCC-22

COLUMN WRITE	BCC-21				BCC-22				DEPTH (ft)
	N _B	BP (PSIG)	N _{BC}	SPT N ₆₀	N _B	BP (PSIG)	N _{BC}	SPT N ₆₀	
1	3	14	9½	9½ 7.1	9	11	6	6 4.5	1
2	17	16	13½	13½ 10.1	11	12	7½	7½ 5.6	2
3	21	16	15	15 11.3	12	12	7½	7½ 5.6	3
4	25	19	21½	20 15	12	12	7½	7½ 5.6	4
5	22	19	19½	18½ 13.9	12	13	8	8 6	5
6	31	20	27½	24½ 18.4	12	13	8	8 6	6
7	44	21	38	31½ 23.6	13	14	9½	9½ 7.1	7
8	51	20	40	33 24.8	10	12	7	7 5.3	8
9	44	22	41	33½	11	9	5½	5½	9
10	44	21	38	31½	7	8	4½	4½	10
11	33	21	30	26	7	9	4½	4½	11
12	40	22	38	31½	8	8	4½	4½	12
13	40	23	39	32½	8	7	4	4	13
14	47	22	43	35	10	10	6	6	14
15	37	20	32	27½	11	12	7½	7½	15
16	28	22	28	25	11	11	6½	6½	16
17	26	21	25	23	11	12	7½	7½	17
18	29	20	26	23½	12	13	8	8	18
19	31	20	27½	24½	13	14	9½	9½	19
20	36	21	33	28	10	14	8½	8½	20
21	30	22	30	26	10	14	8½	8½	21
22	36	22	34	29	9	14	8	8	22
23	31	20	27½	24½	10	13	7½	7½	23
24	28	21	27	24½	8	13	7	7	24
25	35	24	37	31	11	14	8½	8½	25
26	37	25	40	33	11	13	7½	7½	26
27	49	25	51	40½	11	14	8½	8½	27
28	47	25	49	39	10	13	7½	7½	28
29	38	22	36	30½	10	13	7½	7	29
30	34	22	33	28	12	14	9	9	30
31	29	22	29	25½	10	14	8½	8½	31
32	28	22	28	25	10	14	8½	8½	32
33	26	22	27	24½	12	14	9	9	33
34	30	24	33	28	13	15	10½	10½	34
35	40	24	41	33½	12	15	10	10	35
36	31	23	32	27½	11	14	8½	8½	36
37	29	22	29	25½	10	14	8½	8½	37
38	25	20	23	21½	12	13	8	8	38
39	22	24	26	23½	13	15	10½	10½	39
40	31	25	35	29½	10	15	9	9	40

BCC-21

BCC-22

	BCC-21				BCC-22				DEPTH (ft)
	N _B	BP (psig)	N _{BC}	SPT N ₆₀	N _B	BP (psig)	N _{BC}	SPT N ₆₀	
41	30	24	33	28	10	15	9	9	41
	33	24	35	29½	11	15	9½	9½	42
3	29	24	32	27½	11	16	10½	10½	43
4	32	24	35	29½	12	16	11	11	44
5	34	23	34	29	13	16	11½	11½	45
6	32	24	35	29½	11	16	10½	10½	46
7	31	23	32	27½	15	16	12½	12½	47
8	29	23	31	27	17	17	14½	14½	48
9	29	23	31	27	16	15	11½	11½	49
50	31	23	32	27½	11	15	9½	9½	50
11	30	23	31	27	11	15	9½	9½	51
12	34	23	34	29	10	17	11	11	52
13	31	23	32	27½	17	19	17	16½	53
14	33	23	34	29	20	19	18½	18	54
15	31	23	32	27½	17	19	17	16½	55
16	43	23	42	34½	17	19	17	16½	56
17	43	23	42	34½	16	18	15½	15½	57
18	35	23	35	29½	13	17	12½	12½	58
19	25	21	24½	22½	12	17	12	12	59
60	28	21	27	24½	11	17	11½	11½	60
21	22	21	22½	21	14	18	14	14	61
22	25	22	26	23½	14	18	14	14	62
23	22	20	21	20	19	19	18	17½	63
24	27	24	30	26	24	20	22½	21	64
25	76	27	80	58	33	20	29	25½	65
26	92	28	97	68	36	20	31	27	66
27	104	29	111	77	29	21	28	25	67
28	100	28	103	72	29	20	26	23½	68
29	134	28	134	91	24	19	21	20	69
70	125	28	126	85	23	19	20½	19½	70
31	158	29	161	108	23	19	20½	19½	71
32	147	29	152	101	23	19	20½	19½	72
33	146	28	144	97	25	19	21½	20	73
34	136	27	129	87	24	19	21	20	74
35	156	28	152	101	23	19	20½	19½	75
36	200	28	185	122	25	19	21½	20	76
37					24	18	19½	18½	77
38					36	20	31	27	78
39					42	21	37	31	79
80					33	20	29	25½	80

BCC-21

BCC-22

	N _B	BP (psig)	N _{BC}	SPT N ₆₀	N _B	BP (psig)	N _{BC}	SPT N ₆₀	DEPTH (ft)
81					24	20		22 1/2	81
82					27	19		23	82
83					21	22		23	83
84					42	22		39	84
85					54	22		47	85
86					200+	25		156+	86
87									87
88									88
89									89
90									90
11									11
12									12
13									13
14									14
15									15
16									16
17									17
18									18
19									19
20									20
21									21
22									22
23									23
24									24
25									25
26									26
27									27
28									28
29									29
30									30
31									31
32									32
33									33
34									34
35									35
36									36
37									37
38									38
39									39
40									40

BCC-23

BCC-24

	N _B	BP (psig)	N _{BC}	SPT N ₆₀		N _B	BP (psig)	N _{BC}	SPT N ₆₀	DEPTH (ft)
1	6	4	3	3 2.3		11	9	5½	5½ 4.1	1
2	6	6	3	3 2.3		10	9	5½	5½ 4.1	2
3	8	7	4	4 3		11	8	5	5 3.8	3
4	7	7	4	4 3		13	8	5½	5½ 4.1	4
5	9	8	5	5 3.8		13	8	5½	5½ 4.1	5
6	9	10	5½	5½ 4.1		12	7	5	5 3.8	6
7	8	10	5½	5½ 4.1		8	8	4½	4½ 3.4	7
8	9	10	5½	5½ 4.1		6	6	3	3 2.3	8
9	7	12	6	6		8	4	3	3	9
10	8	12	6½	6½		6	4	3	3	10
11	9	12	6½	6½		8	4	3	3	11
12	9	12	6½	6½		8	6	4	4	12
13	7	12	6	6		6	6	3	3	13
14	9	11	6	6		7	10	5	5	14
16	8	12	6½	6½		8	9	5	5	15
16	8	11	6	6		6	11	5	5	16
17	9	11	6	6		7	8	4½	4½	17
18	9	11	6	6		12	9	6	6	18
19	9	12	6½	6½		11	9	5½	5½	19
20	9	12	6½	6½		16	10	7	7	20
21	9	13	7½	7½		15	11	7½	7½	21
22	10	13	7½	7½		14	11	7½	7½	22
23	8	13	7	7		14	11	7½	7½	23
24	8	13	7	7		14	11	7½	7½	24
25	9	13	7½	7½		13	11	7	7	25
26	8	13	7	7		13	12	8	8	26
27	10	13	7½	7½		14	12	8	8	27
28	10	14	8½	8½		17	13	9½	9½	28
29	8	14	7½	7½		12	14	9	9	29
30	9	14	8	8		13	14	9½	9½	30
31	8	14	7½	7½		14	14	9½	9½	31
32	11	15	9½	9½		15	13	9	9	32
33	10	15	9	9		14	13	9	9	33
34	12	15	10	10		11	14	8½	8½	34
35	12	16	11	11		13	15	10½	10½	35
36	14	17	13	13		17	16	13½	13½	36
37	12	16	11	11		17	15	12	12	37
38	14	16	12	12		19	15	13	13	38
39	12	16	11	11		15	15	11½	11½	39
40	13	16	11½	11½		14	13	14	14	40

BCC-23

BCC-24

	N _B	BP (psig)	N _{bc}	SPT N ₆₀	N _B	BP (psig)	N _{bc}	SPT N ₆₀	DEPTH (ft)
41	14	15	11	11	13	18	13½	13½	41
42	10	15	9	9	13	18	13½	13½	42
43	11	15	9½	9½	12	17	12	12	43
44	9	16	9½	9½	17	18	16	16	44
45	13	16	11½	11½	18	18	16½	16½	45
46	12	16	11	11	16	17	14	14	46
47	12	16	11	11	11	15	9½	9½	47
48	12	16	11	11	12	15	10	10	48
49	13	16	11½	11½	9	14	8	8	49
50	13	17	12½	12½	10	15	9	9	50
51	19	19	18	17½	9	15	8½	8½	51
52	21	19	19	18½	14	16	12	12	52
53	17	18	16	16	14	16	12	12	53
54	17	18	16	16	17	16	13½	13½	54
55	15	18	14½	14½	21	20	20½	19½	55
56	16	18	15½	15½	33	19	27	24½	56
57	23	19	20½	19½	23	17	17½	17	57
58	19	19	18	17½	16	17	14	14	58
59	27	20	24½	22½	14	17	13	13	59
60	30	22	30	26	16	19	16	16	60
61	25	21	24½	22½	18	21	19½	18½	61
62	24	21	24	22	34	24	36	30½	62
63	24	21	24	22	121	25	104	73	63
64	21	20	20½	19½	200	24	147	98	64
65	20	20	20	19					65
66	19	21	20½	19½					66
67	20	20	20	19					67
68	21	20	20½	19½					68
69	21	21	22	20½					69
70	24	21	24	22					70
71	25	20	23	21½					71
72	25	21	24½	22½					72
73	28	21	27	24½					73
74	27	20	24½	22½					74
75	29	22	29	25½					75
76	36	22	34	29					76
77	29	22	29	25½					77
78	30	20	27	24½					78
79	44	24	45	36½					79
80	200	27	178	17					80

BCC - 25

BCC - 26

	N _B	BP (psig)	N _{8c}	SPT N ₆₀	N _B	BP (psig)	N _{8c}	SPT N ₆₀	DEPTH ft.
1	10	11	6½	6½ 4.9	-	12			1
2	10	16	10	10 7.5	-	12			2
3	13	17	15	15 11.3	22	12	7½	9½ 7.1	3
4	12	17	12	12 9	28	12	11	11 8.3	4
5	14	17	13	13 9.8	27	12	10½	10½ 7.9	5
6	24	18	18	17½ 13.1	24	12	10	10 7.5	6
7	22	17	17	16½ 12.4	28	13	12½	12½ 9.4	7
8	28	19	23½	22 16.5	24	15	15	15 11.3	8
9	32	19	26	23½	23	15	14½	14½	9
10	30	20	27	24½	27	15	16½	16½	10
11	29	20	26	23½	28	16	18	17½	11
12	31	20	27½	24½	34	17	22½	21	12
13	30	20	27	24½	30	16	18½	18	13
14	39	21	35	29½	22	17	17	16½	14
15	32	20	28	25	19	18	17	16½	15
16	31	20	27½	24½	40	18	28½	25	16
17	34	21	31	27	91	18	51	40½	17
18	34	21	31	27	84	18	49	39	18
19	35	21	32	27½	81	18	47	38	19
20	27	20	24½	22½	54	19	39	32½	20
21	30	21	28½	25	48	20	38	31½	21
22	36	21	33	28	41	20	34	29	22
23	33	21	30	26	38	20	32	27½	23
24	33	21	30	26	62	18	40	33	24
25	37	22	35	29½	60	20	45	36½	25
26	40	22	38	31½	45	20	37	31	26
27	44	22	41	33½	36	20	31	27	27
28	40	23	39	32½	45	20	37	31	28
29	41	22	38	31½	68	20	50	40	29
30	44	22	41	33½	40	20	33	28	30
31	60	22	52	41	32	18	24	22	31
32	98	22	73	54	30	18	22	20½	32
33	85	22	66	50	32	19	26	23½	33
34	72	21	55	43	43	20	35	29½	34
35	69	22	57	44	150	20	82	59½	35
36	92	22	70	52	105	20	66	50	36
37	111	22	80	58	86	20	58	45	37
38	81	22	64	48½	66	14	45	36½	38
39	65	22	55	43	62	14	43	35	39
40	50	21	42	34½	35	20	30	26	40

BCC-25

BCC-26

	N _B	BP (psig)	N _{BC}	SPT N ₆₀	N _B	BP (psig)	N _{BC}	SPT N ₆₀	DEPTH (ft)
41	62	21	50	46	37	20	32	27½	41
2	46	21	40	33	35	20	30	26	42
3	64	22	54	42½	36	20	31	27	43
4	74	23	64	48½	40	20	33	28	44
5	116	23	88	63	40	20	33	28	45
6	86	22	67	50½	35	21	30	26	46
7	78	23	66	50	38	21	32	27½	47
8	93	22	71	53	47	21	40	33	48
9	91	22	70	52	40	21	36	30½	49
50	120	23	93	66	53	20	42	34½	50
11	130	23	125	85	67	20	49	39	51
12	148	23	106	73	77	20	54	42½	52
13	156	23	110	76	64	20	47	38	53
14	158	23	111	77	68	20	50	40	54
15	120	23	93	66	98	21	68	51	55
16	79	23	67	50½	90	21	64	48½	56
17	76	23	65	49	64	21	51	40½	57
18	124	23	92	65½	50	21	42	34½	58
19	94	23	76	56	51	21	43	35	59
60	75	23	64	48½	57	21	46	37	60
21	78	23	78	57	48	21	41	33½	61
22	129	23	95	67	35	21	32	27½	62
23	165	23	115	79	36	21	33	28	63
24	155	23	110	76	53	21	44	36	64
25	190	23	126	85	50	21	42	34½	65
26	154	23	109	75	38	21	34	29	66
27	112	23	85	61	39	20	33	28	67
28	130	23	96	67½	37	20	32	27½	68
29	144	23	104	73	34	20	29½	25½	69
70	100	22	74	54½	27	20	24½	22½	70
31	96	22	72	53½	28	21	27	24½	71
32	134	22	90	64	43	21	38	31½	72
33	124	23	92	65½	40	21	36	30½	73
34	146	23	105	73	36	21	33	28	74
35	180	23	123	84	31	21	29	25½	75
36	220	23	142	96	29	21	28	25	76
37	204	23	135	91	29	21	28	25	77
38	140	23	101	71	27	21	26	23½	78
39	112	23	85	61	26	21	25	23	79
80	98	21	68	51	34	20	29½	25½	80

BCC-25

BCC-26

	N _B	BP (psig)	N _{BC}	SPT N ₆₀	N _B	BP (psig)	N _{BC}	SPT N ₆₀	DEPTH (ft)
81	110	21	74	54½	38	20	32	27½	81
2	125	21	80	58	38	18	28	25	82
3	137	22	92	65½	24	18	19½	18½	83
4	170	22	110	76	43	18	30	26	84
5	126	23	94	66½	60	21	45	36½	85
6	125	24	100	70	54	21	42	34½	86
7	138	23	101	71	43	20	35	29½	87
8	76	23	65	49	70	21	54	42½	88
9	92	24	80	58	130	21	82	59½	89
90	95	22	72	53½	110	21	74	54½	90
11	88	22	68	51	76	21	57	44	91
12	82	23	69	51½	56	21	46	37	92
13	94	23	76	56	50	21	42	34½	93
14	82	23	69	51½	38	21	32	27½	94
15	86	23	72	53½	36	21	31	27	95
16	83	23	70	52	47	21	40	33	96
17	102	23	80	58	34	21	31	27	97
18	96	23	77	56½	33	21	30	26	98
19	91	23	75	55	28	21	27	24½	99
100	90	22	69	51½	23	20	22	20½	100
21	110	21	74	54½	24	20	22½	21	101
22	130	20	76	56	23	20	22	20½	102
23	112	20	70	52	26	20	24	22	103
24	120	20	72	53½	30	20	27	24½	104
25	156	19	76	56	32	20	28	25	105
26	140	23	101	71	35	20	30	26	106
27	98	23	78	57	36	20	31	27	107
28	96	23	77	56½	34	20	29½	25½	108
29	108	23	84	60½	35	20	30	26	109
110	75	23	69	48½	38	21	34	29	110
31	80	23	68	51	35	20	30	26	111
32	101	23	80	58	28	20	25	23	112
33	99	23	79	57½	32	20	28	25	113
34	77	23	66	50	38	20	32	27½	114
35	54	23	50	40	37	20	32	27½	115
36	47	23	45	36½	36	20	31	27	116
37	46	23	44	36	55	21	45	36½	117
38	45	23	43	35	43	21	33	31½	118
39	52	23	44	39	39	21	35	29½	119
120	71	22	58	45	38	21	34	29	120

BCC-25

BCC-26

	N _B	BP (psig)	N _{8c}	SPT N ₆₀	N _B	BP (psig)	N _{8c}	SPT N ₆₀	DEPTH (ft)
21	61	22	52	41	44	21	39	31½	121
2	83	22	65	49	43	21	38	31½	122
3	70	23	61	47	40	21	36	30½	123
4	56	23	52	41	45	21	39	32½	124
5	71	23	62	47½	54	21	45	36½	125
6	86	24	75	55	47	21	40	33	126
7	102	24	85	61	48	21	41	33½	127
8	90	24	78	57	101	22	75	55	128
9	88	24	77	56½	151	22	100	70	129
30	120	23	90	64	80	21	59	45½	130
11	141	23	102	71	300+		180+	120+	131
12	106	23	83	60					132
13	94	23	76	56					133
14	90	23	74	54½					134
15	97	23	78	57					135
16	106	23	83	60					136
17	80	23	68	51					137
18	47	23	45	36½					138
19	42	23	41	33½					139
40	82	20	56	43½					140
21	150	22	100	70					141
22	201	22	123	84					142
23	250	23	160	107					143
24									144
25									145
26									146
27									147
28									148
29									149
50									150
31									151
32									152
33									153
34									154
35									155
36									156
37									157
38									158
39									159
40									160

APPENDIX B:

**CLASSIFICATION DATA FOR SAMPLES OBTAINED FROM 1986 OPEN-BIT
BECKER SOUNDINGS PERFORMED AT MORMON ISLAND AUXILIARY DAM**

U.S. ARMY ENGINEER DIVISION LABORATORY -- SOUTH PACIFIC DIVISION

SOIL TEST RESULT SUMMARY

PROJECT Folsom Laboratory Program

DATE February 1987

Division Serial No.	Hole No.	Field Sample No.	Depth Or Elevation	Laboratory Descriptive Classification	Mechanical Analysis - % Finer										Liquid Limit	Plasticity Index	Field Moisture %		
					Gravel					Sand									
					1 1/2	3/4	1/2	3/8	#4	#10	#40	#60	#100	#200					
98133	1		0 - 2	Gravelly Clayey Sand(SC) ✓	100	93	85	80	76	68	62	50	45	39	32	34	12	6.6	
98134	"		2 - 4	Gravelly Clayey Sand(SC) ✓	100	92	85	80	76	67	60	49	45	40	34	35	15	6.8	
98135	"		4 - 6	Gravelly Silty Sand (SM) SC	100	97	86	82	79	70	63	49	44	40	34	32	9	3.0	
98136	"		6 - 8	Sandy Clayey Gravel(GC) SC	100	92	86	84	82	76	71	56	50	43	36	35	14	3.4	
98137	"		8 - 10	Clayey Sandy Gravel(GC) ✓	100	91	84	80	74	70	62	57	46	40	35	29	33	11	3.4
98138	"		10 - 12	Gravelly Sandy Clay (CL) ✓	100	93	87	86	84	79	75	69	65	61	54	31	10	2.1	
98139	"		12 - 14	Sandy Clay (CL) ✓	100	99	98	97	96	94	90	84	81	77	70	29	10	2.7	
98140	"		14 - 16	Sandy Gravelly Clay (CL) ✓	100	99	87	82	78	73	68	63	60	58	52	47	25	4.9	
98141	"		16 - 18	Sandy Clayey Gravel(GC) ✓	100	98	81	74	68	59	53	48	46	44	40	43	20	4.8	
98142	"		18 - 20	Sandy Clayey Gravel(GC) ✓	100	94	79	72	65	54	49	45	43	42	38	40	17	4.3	
98143	"		20 - 22	Sandy Clayey Gravel(GC) GM	100	96	79	69	61	55	47	39	37	34	31	38	13	3.8	
98144	"		22 - 24	Gravelly Clayey Sand(SC) ✓	100	99	93	89	86	83	77	66	61	56	47	31	13	2.6	
98145	"		24 - 25	Clayey Sandy Gravel(GC) ✓	100	87	64	55	50	37	27	16	15	13	12	34	14	1.3	

804

SPD Form 66A
1 May 83

U.S. ARMY ENGINEER DIVISION LABORATORY -- SOUTH PACIFIC DIVISION

SOIL TEST RESULT SUMMARY

Division Serial No.	Hole No.	Field Sample No.	Depth Or Elevation		Laboratory Descriptive	Mechanical Analysis - % Finer												Fines #200	Liquid Limit %	Plasticity Index	Field Moisture %
			From	To		Gravel															
			Sand																		
98146	2		0	3	Clayey Gravelly Sand SM	100	95	92	86	79	76	66	59	46	40	35	27	31	8	1.9	
98147	"		2	4	Clayey Sandy Gravel (GC) ✓	100	78	67	62	55	52	46	41	33	29	26	23	38	17	2.6	
98148	"		4	6	*Clayey Gravelly Sand (SP-SC) ✓	100	78	67	62	55	52	46	41	33	29	26	23	38	17	2.6	
98149	"		6	8	*Gravelly Sandy Clay (CL) ✓	100	95	92	86	79	76	66	59	46	40	35	27	31	8	1.9	
98150	"		8	10	*Clay (CL) ✓	100	95	92	86	79	76	66	59	46	40	35	27	31	8	1.9	
98151	"		10	12	Gravelly Sandy Clay (CL) ✓	100	95	92	86	79	76	66	59	46	40	35	27	31	8	1.9	
98152	"		12	14	Sandy Silt (ML) ✓	100	71	68	66	64	64	62	61	52	45	39	32	26	5	1.9	
98153	"		14	16	Sandy Clayey Gravel (GC-GM) ✓	100	97	99	99	97	95	92	87	80	76	70	59	33	8	2.7	
98154	"		16	18	Clayey Sand (SC-SM) SM	100	97	99	99	97	95	92	87	80	76	70	59	33	8	2.7	
98155	"		16	18	Clayey Gravelly Sand (SP-SG) ✓	100	97	99	99	97	95	92	87	80	76	70	59	33	8	2.7	
98156	"		20	30	Clayey Gravelly Sand (SP-SG) ✓	100	97	99	99	97	95	92	87	80	76	70	59	33	8	2.7	
98157	"		34	36	Clayey Sandy Gravel (GP-GC) ✓	100	83	72	60	48	39	26	19	13	12	10	8	24	5	1.4	
					*Visual Classification																

B.O.F.

U.S. ARMY ENGINEER DIVISION LABORATORY -- SOUTH PACIFIC DIVISION

SOIL TEST RESULT SUMMARY

PROJECT Folsom - Laboratory Program

DATE February 1987

Division Serial No.	Hole No.	Field Sample No.	Depth Or Elevation		Laboratory Descriptive	Mechanical Analysis - % Finer											Liquid Limit (%)	Plasticity Index (%)			
			From	To		Gravel			Sand					Fines							
						1 1/2	3/4	1/2	3/8	#4	#10	#40	#60	#100	#200						
98158	3		0	2	Silty Gravelly Sand(SH) ✓	100	99	96	89	84	75	62	37	30	24	19	34	10	8.9		
98159	"		2	4	Clayey Sandy Gravel(GC) ✓	100	58	47	45	41	39	35	24	21	18	13	28	8	1.7		
98160	"		4	6	*Sandy Clayey Gravel(GC) ✓	pale brown damp, plastic fines, 15% light brownish gray, dry angular #4 gravel	52	med to hard angular gravel, 10% med													
98161	"		6	8	*Sand(SP) ✓																
98162	"		8	10	*Insufficient material for classification																
98163	"		10	12	*Insufficient material for classification																
98164	"		12	14	Sandy Silty Gravel(GM) ✓	100	89	84	73	69	67	65	62	59	53	50	46	39	35	10	2.9
98165	"		14	16	Sandy Silt(ML) ✓				100	98	94	92	86	80	71	55	31	6	3.2		
98166	"		16	18	Sandy Silt(ML) ✓						100	99	95	89	81	67	31	4	2.9		
98167	"		18	20	Silty Sand(SM) ✓			100	99	98	92	82	71	65	58	47	31	5	2.7		
98168	"		20	22	Silty Sand(SM) ✓			100	99	97	89	85	73	66	57	46	32	6	2.9		

- BOH.

SPD Form 66A
1 May 83

U.S. ARMY ENGINEER DIVISION LABORATORY -- SOUTH PACIFIC DIVISION

SOIL TEST RESULT SUMMARY

Division Serial No.	Hole No.	Field Sample No.	Depth Or Elevation		Laboratory Descriptive Classification	Mechanical Analysis - % Piner										Li-Quid Limit %	Plasticity Index %	Field Moisture %	
			From	To		Gravel					Sand								Pines #200
						1 1/2	3/4	1/2	3/8	3/4	10	40	60	100	200				
98169	4	1	0	2	Gravelly Sandy Clay (SC) ✓	100	97	90	81	74	61	51	34	29	23	18	66	15	1.9
98170	"		2	4	Sandy Gravelly Clay (SC) GC ✓	100	86	78	71	68	62	55	43	38	33	26	31	11	2/2
98171	4	1	4	6	Clayey Gravelly Sand (SC) ✓		100	97	85	81	70	61	49	43	36	29	31	12	2.0
98172	"		6	8	Clayey Gravelly Sand (SC) ✓		100	99	90	86	69	58	38	33	29	24	32	14	1.9
98173	"		8	10	Clayey Sandy Gravel (GC) ✓	100	81	66	62	60	54	52	44	41	38	32	31	15	2.4
98174	"		10	12	Clayey Sandy Gravel (GC) ✓	100	94	86	77	74	64	57	45	40	35	29	46	24	5.5
98175	"		12	14	Silty Gravelly Sand (SH) ✓	100	95	94	89	85	77	69	51	44	37	29	37	10	5.0
98176	"		14	16	Clayey Sandy Gravel (GC) ✓	100	78	66	60	56	48	43	33	30	27	22	39	16	4.2
98177	"		16	18	Clayey Gravelly Sand (SC) GC ✓	100	97	85	78	72	61	53	37	32	28	22	37	18	3.1
98178	"		18	20	Clayey Sandy Gravel (GC) ✓	100	83	68	60	53	44	39	27	23	20	16	41	21	3.0
98179	"		20	22	Clayey Sandy Gravel (GC) ✓		94	74	64	58	46	37	23	19	16	13	40	20	2.5
98180	"		22	24	Clayey Gravelly Sand (SM-SC) GC ✓	100	90	78	59	52	42	35	19	14	12	10	44	20	2.0
98181	"		24	26	Gravelly Silty Sand (SM) ✓		100	87	82	78	70	65	55	50	44	37	31	7	2.8
98182	"		26	28	Sandy Silt (ML) ✓						100	99	95	92	86	73	33	7	3.1

Box

U.S. ARMY ENGINEER DIVISION LABORATORY -- SOUTH PACIFIC DIVISION

SOIL TEST RESULT SUMMARY

Division Serial No.	Hole No.	Field Sam- ple No.	Depth Or Elevation		Laboratory Descriptive	Mechanical Analysis-% Finer										Plas- ticity Index	Field Moist %			
			From	To		Gravel					Sand							Fines #200		
						3/8	1/2	3/4	1	5/16	1/4	3/8	1/2	3/4	1				5/16	1/4
98183	5		0	2	Clayey Gravelly Sand (SC) ✓	100	89	85	83	80	77	69	59	42	36	32	26	35	14	1.9
98184	"		2	4	Clayey Sandy Gravel (GC) ✓		100	86	81	75	71	59	49	37	32	29	24	34	14	2.2
98185	"		4	6	Clayey Sandy Gravel (GC) ✓		100	89	81	73	62	53	37	33	29	25	20	36	14	2.6
98186	"		6	8	Clayey Gravelly Sand (SP-SC) ✓	Yellowish angular to silty	100	94	89	88	87	83	76	47	36	26	19	31	10	5.1
98187	"		8	10	Gravelly Clayey Sand (SC) ✓		100	94	89	88	87	83	76	47	36	26	19	31	10	5.1
98188	"		10	12	Silty Sandy Gravel (GH) ✓		100	83	63	60	58	54	48	35	31	26	21	33	9	1.1
98189	"		12	14	Clayey Sandy Gravel (GC) ✓		100	79	71	64	59	53	49	38	32	28	23	40	16	3.5
98190	"		14	16	Clayey Sandy Gravel (GC) ✓		100	86	74	65	59	54	49	36	31	27	22	41	18	3.2
98191	"		16	18	Clayey Sandy Gravel (GC) ✓		100	84	70	65	59	47	42	31	26	22	18	38	16	1.2
98192	"		18	20	Clayey Sandy Gravel (GP-GC) ✓		100	78	62	43	36	30	29	24	19	16	12	34	14	2.2
98193	"		20	22	Clayey Sandy Gravel (GH-GC) ✓		100	77	47	42	38	34	31	21	17	13	11	38	16	1.7
98194	"		22	24	Clayey Sandy Gravel (GP-GC) ✓		100	81	64	51	42	38	34	32	24	17	13	32	12	1.3
98195	"		24	26	Clayey Sandy Gravel (GP-GC) ✓		100	69	49	41	36	33	30	29	24	20	16	31	11	1.8
98196	"		26	28	Clayey Sandy Gravel (GP-GC) ✓		100	89	62	52	43	38	30	26	19	16	12	24	3	1.1

SPD Form 66A
1 May 83

U.S. ARMY ENGINEER DIVISION LABORATORY -- SOUTH PACIFIC DIVISION

SOIL TEST RESULT SUMMARY

PROJECT		FOLSOM LABORATORY PROGRAM										DATE		March 1987				
Division Serial No.	Hole No.	Field Sample No.	Depth Or Elevation		Laboratory Descriptive Classification	Mechanical Analysis - % Finer								LL - Liquid Limit	Plasticity Index			
			From	To		Gravel				Sand								
			6	3	2 1/4	1 3/4	1/2	3/8	#4	#10	#40	#60	#100	#200				
98210	6		24	26	* Inadequate Material													
98211	"		26	28	Clayey Sandy Gravel (GP-GC)	100	90	67	60	50	44	25	19	15	12	30	10	14
98212	"		28	30	* Clayey Gravel (GP-GC)													
98213	"		30	32	Clayey Sandy Gravel (GP-GC)	100	75	58	51	46	36	21	16	10	6	36	15	1.7
98214	"		32	34	Clayey Sandy Gravel (GW-GC)	100	80	62	53	46	34	24	11	9	5	31	11	1.5
98215	"		34	36	Clayey Sandy Gravel (GP-GC)	100	67	58	42	37	29	21	10	8	5	32	13	1.7
98216	"		36	38	Clayey Sandy Gravel (GW-GC)	100	87	66	53	48	39	32	16	13	8	37	18	1.6
98217	"		38	40	Clayey Sandy Gravel (GC)	100	79	57	49	46	42	36	22	19	13	45	25	1.9
98218	"		40	42	Clayey Sandy Gravel (GW-GC)	100	90	65	50	46	38	32	16	13	9	34	14	1.4
98219	"		42	44	Clayey Sandy Gravel (GW-GC)	100	75	58	42	38	30	24	13	10	7	29	10	1.4
98220	"		44	46	Clayey Sandy Gravel (GW-GC)	100	85	72	54	49	40	34	22	18	9	26	6	1.1
98221	"		46	48	Sandy Gravel (GP)	100	89	71	33	29	22	19	9	6	4	45	25	1.6
98222	"		48	50	Clayey Sandy Gravel (GP-GC)	100	93	68	44	40	30	24	14	12	8	33	13	1.6

BQH

SPD Form 66A
1 May 83

U.S. ARMY ENGINEER DIVISION LABORATORY -- SOUTH PACIFIC DIVISION

SOIL TEST RESULT SUMMARY

PROJECT Folsom Laboratory Program

DATE March 1987

Division Serial No.	Hole No.	Field Sample No.	Depth Or Elevation		Laboratory Descriptive Classification	Mechanical Analysis - % Finer										Plasticity Index	Field Moisture Content %		
			From	To		Gravel					Sand							Fines #200	
						1 1/2"	3/4"	1/2"	3/8"	#4	#10	#40	#60	#100	#200				
98223	7		0	2	Clayey Sand(SC)	100	98	95	94	90	72	43	33	27	22	37	16	25	
98224	"		2	4	*Clayey Gravelly Sand(SP-SC) ✓														
98225	"		4	6	*Clay (CL) ✓														
98226	"		6	8	*Sandy Clay(CL) ✓														
98227	"		8	10	Silty Sandy Gravel(GP-GC) ✓	100	46												
98228	"		10	12	*Clayey Sand(SC) ✓	59	41	40	39	38	28	14	11	9	7	25	4	25	4
98229	"		12	14	*Clayey Sand(SC) ✓														
98230	"		14	16	*Clayey Sand(SC) ✓														
98231	"		16	18	Clayey Sandy Gravel(SC) ✓	100	97	97	93	91	80	75	57	48	37	26	34	14	14
98232	"		18	20	Clayey Gravelly Sand(SH-SC) ✓	100	92	88	79	73	70	42	28	18	10	41	20	20	20
98233	"		20	22	Gravelly Clayey Sand(SC) ✓														
98234	"		22	24	*Insufficient Material														
98235	"		24	26	*Insufficient Material														

SPD Form 66A
1 May 83

U.S. ARMY ENGINEER DIVISION LABORATORY -- SOUTH PACIFIC DIVISION

SOIL TEST RESULT SUMMARY

Division Serial No.	Hole No.	Field Sample No.	Depth Or Elevation		Laboratory Descriptive Classification	Mechanical Analysis - % Finer										Plasticity Index	Field Moisture %
			From	To		Gravel					Sand						
						1 1/2"	3/4"	1/2"	3/8"	#4	#10	#40	#60	#100	#200		
98236	7		24	30	** Sand(SP)	Grayish brown #4 gravel, trace fines											
98237	"		54	56	Clayey Gravel (GP-GC)	100 61	52 41	34 27	22 22	15	14	11	10	8	6		?
98238	8		0	2	Clayey Sandy Gravel(GC)	100 90	83 73	67 67	52	42	31	28	25	21			?
98239	"		2	4	Gravel(GP)	Pale brown, 5% coarse graded sand, 95% med. subangular to subrounded plastic fines.											
98240	"		4	6	**Clayey Gravel (GP-GC)	Pale brown, slightly damp, gravel to 1 1/2", 5% coarse graded sand, 90% med. subangular to subrounded plastic fines.											
98241	"		6	8	**Clayey Sandy Gravel(GP-GC)	Pale brown, slightly damp, 15% coarse graded sand, 80% med. subangular to subrounded plastic fines.											
98242	"		8	10	**Clayey Gravel (GP-GC)	Pale brown, slightly damp, gravel to 1 1/2", coarse graded sand, 90% med. subangular to subrounded plastic fines.											
98243	"		10	12	*Clayey Sandy Gravel(GP-GC)	Pale brown, slightly damp, gravel to 1 1/2", 15% med. subangular to subrounded plastic fines.											
98244	"		12	14	Clayey Sand(SC)	Pale brown, slightly damp, plastic fines, 10% med. subangular gravel to 3/8"											
98245	"		14	16	*Clayey Sand (SP-SC)	Pale brown, slightly damp, #4 gravel, 5% med. subangular gravel to 3/8"											
98246	"		16	18	Sand(SP)	Pale brown, slightly damp, gravel to 3/8", trace fines.											
98247	"		18	20	*Insufficient Material												
98248	"		20	22	**Clayey Sandy Gravel(GP-GC)	Pale brown, slightly damp, 50% med. subangular to subrounded plastic fines.											

SPD Form 66A
1 May 83

80H.

U.S. ARMY ENGINEER DIVISION LABORATORY -- SOUTH PACIFIC DIVISION

SOIL TEST RESULT SUMMARY

PROJECT Folsom Laboratory Program

DATE March 1987

Division Serial No.	Hole No.	Field Sample No.	Depth Or Elevation		Laboratory Descriptive Classification	Mechanical Analysis-% Finer				Li-Plas Liquid Limit Index	Field Moisture %	
			From	To		Gravel	Sand	#4	#10			#40
98249	8		22	24	**Clayey Gravelly Sand (SP) SC	pale brown, slightly damp, subangular #4 gravel, 15% med. plastic fines.						30% med.
98250	"		26	28	** Gravelly Sand (SP) ✓	pale brown, slightly damp, subangular gravel to 3/4".						20% med.
98251	"		28	30	** Gravel (GP)							
98252	"		30	32	**Clayey Sandy Gravel (GP-GC) ✓	pale brown, slightly damp, 10% med. plastic fines.						
98253	"		32	34	*Clayey Sand (SC) ✓	pale brown, slightly damp, 5% med. subangular #4 gravel.						30% med.
98254	"		34	36	**Insufficient	Material						
98255	"		36	28	** Sand (SP) ✓	light grayish brown, slightly damp, graded sand w/ gravel.						
98256	"		38	40	** Gravel (GP)	two 3" cobbles trace minus 4.						
98257	"		40	42	*Gravelly Clayey Sand (SC) ✓	pale brown, slightly damp, 15% med. subangular #4 gravel.						
98258	"		42	44	* Insufficient	Material						
98259	"		44	46	** Sandy Clay (CL) ✓	pale brown, slightly damp, 10% med. subangular sand.						35% fine
98260	"		46	48	*Clayey Gravelly Sand (SC) ✓	pale brown, slightly damp, 15% med. plastic fines.						
98261	"		48	50	** Clayey Sand (SC) ✓	pale brown, slightly damp, 60% fine sand fines.						40% med plastic

SPD Form 66A
1 May 83

U.S. ARMY ENGINEER DIVISION LABORATORY -- SOUTH PACIFIC DIVISION

SOIL TEST RESULT SUMMARY

Division Serial No.	Hole No.	Field Sample No.	Depth Or Elevation	Laboratory Descriptive	Mechanical Analysis - % Finer											LI-Plas-Field Liquid Limit, %	Plasticity Index, %	Moisture Content, %	
					Gravel					Sand									Fines #200
					3/4	1/2	3/8	#4	#10	#40	#60	#100	#200						
98262	8		From 50 To 52	*Clayey Gravelly Sand(SC) ✓	2	1 1/2	3/4	1/2	3/8	3/8	60% fine sand, slightly damp, 20% med. subangular gravel to 1/2"	60% fine sand, 20% med. subangular fines.	20% med. subangular						
98263	"		52 54	*Clayey Sand(SC) ✓							60% fine sand, slightly damp, 30% med. plastic fines, 10% med. subangular gravel.	30% med. plastic							
98264	"		54 56	*Insufficient Material															
98265	"		56 58	*Clayey Gravelly Sand(SP-SC) ✓							80% graded sand, slightly damp, 5% med. subangular gravel to 1/2"	5% med. subangular							
98266	"		58 60	Clayey Sandy Gravel(GC) ✓	100	95	87	76	63	56	43	34	26	22	19	14	28	8	1.5
98275	9		0 2	Clayey Gravelly Sand(SC) ✓	100														
98276	"		2 4	Clayey Sandy Gravel(GC-GM) ✓															
98277	"		4 6	Sandy Gravel(GM) ✓	100	80	57	40	29	17	11	6	5	4	3	28	10	1.4	
98278	"		6 8	*Clayey Gravelly Sand(SP-SC) ✓							60% graded sand, slightly damp, 5% med. plastic fines.	60% graded sand, 35% med. sub-							
98279	"		8 10	*Gravelly Clayey Sand(SC) ✓							45% graded sand, 30% med. plastic fines, 25% med. subangular gravel to 1/2"	30% med. plastic							
98280	"		10 12	Gravel(GP) ✓							95% med. subangular to 1", 5% graded sand, trace med. pl. fines.	95% med. subangular to subang. gravel							
98281	"		12 14	Gravel(GP) ✓							60% graded sand, slightly damp, trace - 4.	60% graded sand, slightly damp, trace - 4.							
98282	"		14 16	**Insufficient Material															

B.O.H

SPD Form 66A
1 May 83

U.S. ARMY ENGINEER DIVISION LABORATORY -- SOUTH PACIFIC DIVISION

SOIL TEST RESULT SUMMARY

PROJECT Folsom Laboratory Program

DATE March 1987

Division Serial No.	Hole No.	Field Sample No.	Depth Or Elevation	Laboratory Descriptive Classification	Mechanical Analysis-% Finer										Li-Plas liquidity Index	Field Moisture %			
					Gravel					Sand									
					1 1/2	3/4	1/2	3/8	#4	#10	#40	#60	#100	#200					
98296	10		0 to 2	Clayey Sandy Gravel (GC) ✓	100	80	74	62	55	44	37	25	22	19	15	31	10	1.9	
98297	"		2 to 4	*Clayey Gravelly Sand (SP-SC) ✓	40% med. subang.	Light grayish brown, slightly subang. to subround. to 1"													
98298	"		4 to 6	*Clayey Gravel (GP-GC) ✓	Light grayish gravel to 1/2"	Light grayish brown, slightly fine to med. sand, 5% med. pl. fines.													
98299	"		6 to 8	**Clayey Sandy Gravel (GP-GC) ✓	Light grayish gravel to 1"	Light grayish brown, slightly graded sand, 10% pl. fines.													
98300	"		8 to 10	**Gravel (GP) ✓	Yellowish brown, slightly gravel to 3" trace sand, trace fines.														
98301	"		10 to 12	**Clayey Gravelly Sand (SP-SC) ✓	Light grayish subang. to subround #4	Light grayish brown, slightly damp, 10% med. pl. fines													
98302	"		12 to 14	**Clayey Sandy Gravel (GC) ✓	Light grayish 3/8, 30% med. sand, 25% med. pl. fines.														
98303	"		14 to 16	*Clayey Gravelly Sand (SP-SC) ✓	Light grayish subang. gravel to 3/8"	Light grayish brown, slightly damp, 5% med. pl. fines.													
98304	"		16 to 18	*Clayey Gravelly Sand (SP-SC) ✓	Pale brown, #4 gravel, 5% med. pl. fines.														
98305	"		18 to 20	*Insufficient Material															
98306	"		20 to 22	*Gravelly Clayey Sand (SC) ✓	Pale brown, plastic fine, 15% med. subang. gravel to 1/2"														
98307	"		22 to 24	*Clayey Gravelly Sand (SP-SC) ✓	Pale brown, gravel to 1/2"	Light grayish brown, slightly damp, 10% med. pl. fines.													
98308	"		24 to 26	**Clayey Gravelly Sand (SP-SC) ✓	Yellowish med. subang. gravel to 1/2"	Yellowish brown, slightly damp, 5% graded sand, 40% med. pl. fines.													

SPD Form 66A
1 May 83

U.S. ARMY ENGINEER DIVISION LABORATORY -- SOUTH PACIFIC DIVISION

SOIL TEST RESULT SUMMARY

Division Serial No.	Hole No.	Field Sample No.	Depth Or Elevation		Laboratory Descriptive Classification	Mechanical Analysis - % Finer										LI - Plasticity Index	Field Moisture %		
			From	To		Gravel					Sand							Fines #200	
						1 1/2"	3/4"	1/2"	3/8"	#4	#10	#40	#60	#100	#200				
98309	10		26	28	*Sand(SP) ✓	3	1 1/2"	3/4"	1/2"	3/8"	#4	#10	#40	#60	#100	#200			
98310	"		28	30	*Sandy Clay(CL) ✓		Light grayish brown, subang. #4 gravel												
98311	"		30	38	*Insufficient Material														
98312	"		38	46	*Insufficient Material														
98313	"		46	48	*Clayey Gravelly Sand(SC) ✓		Yellowish brown, wet, to 1/2" 20% med. pl. fines.												
98314	"		48	56	*Insufficient Material														
98315	"		56	58	**Clayey Sandy Gravel(GP-GC) ✓		Yellowish brown, sand, 5% med. pl. fines.												
98316	"		58	60	**Sandy Clay(SC) ✓		Yellowish brown, med. subangular #4 gravel.												
98317	"		60	62	**Clayey Sand(SC) ✓		Yellowish brown, trace #4 gravel.												
98318	11		0	2	Clayey Sandy Gravel(GP-GC) ✓		80	69	50	41	27	20	15	13	11	9	34	12	22
98319	"		2	4	Clayey Sandy Gravel(GC) ✓		100	80	61	48	36	32	26	23	21	18	32	10	19
98320	"		4	6	Clayey Sandy Gravel(GC) ✓		100	71	63	43	35	32	23	21	19	16	32	10	18
98321	"		6	8	Sand(SP) ✓		100	73	45	38	35	32	23	21	19	16	32	10	18
										100	90	70	14	6	4	3			NP

SPD Form 66A
1 May 83



-B.2-

U.S. ARMY ENGINEER DIVISION LABORATORY -- SOUTH PACIFIC DIVISION

SOIL TEST RESULT SUMMARY

PROJECT Folsom Laboratory Program										DATE March 1987									
Division Serial No.	Hole No.	Field Sample No.	Depth Or Elevation		Laboratory Descriptive Classification	Mechanical Analysis - % Finer								Plasticity Index	Field Moisture %				
			From	To		Gravel				Sand									
						3/8	1/2	3/4	1 1/2	#4	#10	#40	#60	#100	#200				
98322	11		8	10	Clayey Gravelly Sand (SW-SC)	100	98	98	97	96	83	58	20	14	12	10	27	8	
98323	"		10	12	Silty Gravelly Sand (SW-SM) ✓	100	97	97	95	71	32	10	8	6	5			NP	
98324	"		12	14	Gravelly Sand (SW) ✓		100		98	75	35	4	3	3	2			NP	
98325	"		14	16	Clayey Sand (SC)				100	94	82	35	27	23	19	28	8	1(4)	
98326	"		16	18	Silty Clayey Sand (SC) ✓				100	90	66	27	21	18	14	35	11	1.3	
98327	"		18	20	Gravelly Sand (SP) ✓	100	99	99	98	79	50	10	7	5	4			NP	
98328	"		20	22	Gravelly Sand (SP)				100	99	84	53	8	4	3			NP	
98329	"		22	24	Gravelly Sand (SP)			99	99	85	65	11	6	5	4			NP	
98330	"		24	26	Gravelly Sand (SP) ✓				100	97	78	57	10	6	4			NP	
98331	"		26	28	*Clayey Gravelly Sand (SP-SC)					Pale brown, slightly damp, 65% graded sand, 10% med. subangular to angular gravel to 1" max. fines.									
98332	"		28	32	*Insufficient Material														
98333	"		32	34	*Clayey Sand (SC)					Yellowish brown, wet, 85% graded sand, 15% med. fines, trace gravel to 1/2".									
98334	"		34	36	Sandy Clayey Gravel (GC) ✓	100	74	64	58	51	46	36	32	26	24	21	18	36	
																		14	

SPD Form 66A
1 May 83

U.S. ARMY ENGINEER DIVISION LABORATORY -- SOUTH PACIFIC DIVISION

SOIL TEST RESULT SUMMARY

Division Serial No.	Hole No.	Field Sample No.	Depth Or Elevation		Laboratory Descriptive Classification	Mechanical Analysis - % Finer										Plasticity Index	Field Moisture %		
			From	To		Gravel					Sand							Fines #200	
						3/8	1/2	3/4	1/4	3/8	#4	#10	#40	#60	#100				
98335	11		36	38	Sandy Clayey Gravel(GC) ✓	100	65	58	50	48	42	37	32	31	30	28	52	28	3.7
98336	"		38	40	Sandy Clayey Gravel(GC) ✓	100	81	75	74	64	57	49	47	46	43	50	26	3.6	
98337	"		40	42	Sandy Clayey Gravel(GC) ✓	100	85	72	54	50	42	37	31	30	29	27	47	23	3.2
98338	"		42	44	Clayey Gravel (GC) ✓	100	87	64	64	54	29	21	17	16	16	15	47	23	3.0
98339	"		44	46	Silty Clayey Gravel(GP-GC) ✓	100	85	51	34	27	17	13	10	10	9	8	44	20	2.8
98340	"		46	48	Gravelly Clayey Sand(SC) ✓	100	96	86	83	77	69	60	58	56	50	40	17	3.1	
98341	"		48	50	* Gravelly Sand(SP) ✓	Dark grayish brown angular gravel to 1/2"	100	86	86	80	77	69	60	58	56	50	40	17	3.1
98342	"		50	52	Clayey Sandy Gravel(GP-GC) ✓	100	73	55	45	34	25	17	16	14	12	34	12	2.7	
98342A	"		52	54	Clayey Sandy Gravel(GC) ✓	100	80	57	49	44	33	26	19	18	17	15	45	23	2.1
98343	"		54	56	Sandy Silty Clay(CL) ✓	100	99	98	98	95	91	76	71	64	54	33	11	2.5	
98344	"		56	58	Silty Gravelly Sand(SP-SM) ✓	100	79	65	63	59	53	20	13	9	7	NP	1.5		
98345	"		58	60	Clayey Sandy Gravel(GP-GC) ✓	100	91	77	58	52	37	24	13	11	9	7	33	10	1.5

SPD Form 66A
1 May 83

-B-

U.S. ARMY ENGINEER DIVISION LABORATORY -- SOUTH PACIFIC DIVISION

SOIL TEST RESULT SUMMARY

Division Serial No.	Hole No.	Field Sample No.	Depth Or Elevation		Laboratory Descriptive Classification	Mechanical Analysis - % Finer										Li-Plas-Field Liquid Limit Index	Field Moist. %		
			From	To		Gravel					Sand								
						#2	#4	#10	#40	#60	#100	#200							
98347	12		2	4	Clayey Sandy	100	84	70	61	55	44	37	25	21	17	13	30	11	1.7
98348	"		4	6	Clayey Gravelly Sand (SP-SC)	100	75	70	61	55	44	37	25	21	17	13	30	11	1.7
98349	"		6	8	Clayey Sandy Gravel (GP-GC)	100	91	84	73	68	56	43	25	20	16	12	29	8	1.4
98350	"		8	10	Gravelly Clayey Sand (SC)	100	91	84	73	68	56	43	25	20	16	12	29	8	1.4
98351	"		10	12	Gravelly Clayey Sand (SC)	100	91	84	73	68	56	43	25	20	16	12	29	8	1.4
98352	"		12	14	Clayey Gravelly Sand (SP-SC)	100	91	84	73	68	56	43	25	20	16	12	29	8	1.4
98353	"		14	16	Clayey Gravelly Sand (SP-SC)	100	91	84	73	68	56	43	25	20	16	12	29	8	1.4
98354	"		16	18	Clayey Sand (SP-SC)	100	91	84	73	68	56	43	25	20	16	12	29	8	1.4
98355	"		18	20	Sandy Clay (CL)	100	91	84	73	68	56	43	25	20	16	12	29	8	1.4
98356	"		20	22	Clayey Sand (SC)	100	91	84	73	68	56	43	25	20	16	12	29	8	1.4
98357	"		22	24	Clayey Sand (SC)	100	91	84	73	68	56	43	25	20	16	12	29	8	1.4
98358	"		24	26	Clayey Sand (SC)	100	91	84	73	68	56	43	25	20	16	12	29	8	1.4
98359	"		26	28	Clayey Sand (SP-SC)	100	91	84	73	68	56	43	25	20	16	12	29	8	1.4

PROJECT FOLSOM LAB PROGRAM

DATE May 1987

SPD Form 001
1 May 83

U.S. ARMY ENGINEER DIVISION LABORATORY -- SOUTH PACIFIC DIVISION

SOIL TEST RESULT SUMMARY

Division Serial No.	Hole No.	Field Sam- ple No.	Depth Or Elevation		Laboratory Descriptive Classification	Mechanical Analysis-% Finer										Liquidity Index	Field Moist %		
			From	To		Gravel			Sand				Fines						
						#4	#10	#40	#60	#100	#200	MP	MP	MP					
98360	12		28	30	*Gravelly Clayey Sand(SC)	100	89	86	83	77	34	19	10	9	7	6	31	10	1.3
98361	"		30	32	*Clayey Sand(SC)	100	84	65	58	45	38	33	24	20	17	13	35	12	2.3
98362	"		32	34	*Clayey Sand(SC)	100	84	65	58	45	38	33	24	20	17	13	35	12	2.3
98363	"		34	36	*Clayey Sand(SC)	100	84	65	58	45	38	33	24	20	17	13	35	12	2.3
98364	"		36	38	*Clayey Sand(SC)	100	84	65	58	45	38	33	24	20	17	13	35	12	2.3
98365	"		38	40	*Clayey Sand(SC)	100	84	65	58	45	38	33	24	20	17	13	35	12	2.3
98366	"		40	44	*Clayey Sand(SC)	100	84	65	58	45	38	33	24	20	17	13	35	12	2.3
98367	"		44	48	Clayey Sandy ✓	100	92	88	83	77	34	19	10	9	7	6	31	10	1.3
98368	"		48	50	Gravel(GP-GC)	100	89	86	83	77	34	19	10	9	7	6	31	10	1.3
98369	"		50	52	Clayey Sandy ✓	100	84	65	58	45	38	33	24	20	17	13	35	12	2.3
98370	"		52	54	Gravel(GC) ✓	100	84	65	58	45	38	33	24	20	17	13	35	12	2.3
98371	"		54	56	Clayey Sandy ✓	100	84	65	58	45	38	33	24	20	17	13	35	12	2.3
98372	"		56	58	Gravel(GC) ✓	100	84	65	58	45	38	33	24	20	17	13	35	12	2.3

SPD Form 66A
1 May 83

U.S. ARMY ENGINEER DIVISION LABORATORY -- SOUTH PACIFIC DIVISION

SOIL TEST RESULT SUMMARY

PROJECT FOLSOM LAB PROGRAM		DATE May 1987													
Division Serial No.	Hole No.	Field Sample No.	Depth Or Elevation		Laboratory Descriptive Classification	Mechanical Analysis-% Finer							Plasticity Index	Liquid Limit %	
			From	To		1/2	3/8	Sand				Plasticity Index			
						1/2	3/8	#4	#10	#40	#60	#100	#200		
98373	12		58	60	Gravelly Clayey Sand(SC) ✓	100	87	85	99	99	77	66	55	42	34
98374	"		60	62	Silty Clayey Sand(SC)	100	99	99	99	95	77	66	55	42	34
98375	"		62	64	Silty Clayey Sand(SC)				100	98	95	80	68	57	43
98376	"		64	66	Clayey Gravelly Sand(SC)	100	78	74	73	69	65	51	42	34	26
98377	"		66	68	Gravelly Clayey Sand(SC) ✓	100	88								
98378	"		68	70	Clayey Gravelly Sand(SC) ✓	88	86	85	85	83	81	71	63	54	38
						91	87	80	75	66	56	42	37	33	26
98379	13		0	2	Clayey Sandy Gravel(GC) ✓	91	80	74	70	58	50	35	30	26	20
98380	"		2	4	Clayey Sandy Gravel(GC) ✓	100	80	71	65	55	43	28	25	22	18
98381	"		4	6	Clayey Sand(SC)	100	95	93	92	90	84	71	64	58	50
98382	"		6	8	Clayey Sandy Gravel(GC) ✓	100	50	45	42	38	34	27	25	22	18
98383	"		8	10	Sandy Clayey Gravel(GC) ✓	100	60	55	52	48	44	37	33	30	25
98384	"		10	12	Clayey Gravel (GP-GC) ✓	100	33								
98385	"		12	14	Clayey Sandy Gravel(CC)	50	27	24	23	22	21	18	16	14	12
						88	74	60	52	38	28	19	17	15	13
						100	82								

SPD Form 66A
1 May 83

U.S. ARMY ENGINEER DIVISION LABORATORY -- SOUTH PACIFIC DIVISION

SOIL TEST RESULT SUMMARY

PROJECT	FOLSOM LAB PROGRAM				MECHANICAL ANALYSIS-% FINER										DATE	May 1987			
	Division Serial No.	Hole No.	Depth Or Elevation		Laboratory Descriptive Classification	Gravel					Sand						Fines #200	Li-Plas-Field Liquid Limit Index %	
			From	To		#4	#10	#40	#60	#100	#200	#4	#10	#40					#60
98399	13		40	42	*Clayey Sand(SC)	Pale brown, trace #4 gravel.	3/4	1/2	3/8	#4	#10	#40	#60	#100	#200	10% MP fines,			
98400	"		42	44	*Clayey Sand(SC)	Pale brown, slightly damp, 5% med. subangular #4 gravel.										30% MP fines,			
98401	"		44	46	*Clayey Sand(SC)	Pale brown, 10% med. subangular gravel to #4.										30% MP fines,			
98402	"		46	48	*Clayey Sand(SC)	Pale brown, slightly damp, trace #4 gravel.										30% MP fines,			
98403	"		48	50	*Sandy Clay(CL)	Pale brown, slightly damp, med. sand, trace #4 gravel.										45% fine to			
98404	"		50	52	*Clayey Sand(SC)	Yellowish-brwn, damp #4 gravel.										40% MP fines, trace			
98405	"		52	54	*Clayey Sand(SC)	Pale brown, slightly damp, trace #4 gravel.										35% MP fines,			
98406	"		54	56	*Gravelly Clayey Sand(SC)	Light grayish-brown, med. subangular gravel to #4.										60% graded sand, 10%			
98407	"		56	58	*Clayey Sand(SC)	Pale brown, slightly damp, 5% med. subangular gravel to #4.										70% graded sand, 20% MP fines,			
98408	"		58	60	*Clayey Sand(SC)	Yellowish-brwn, damp 5% med. subangular gravel to #4.										40% MP fines,			
98409	"		60	62	*Clayey Sand(SC)	Yellowish-brwn, slightly damp, 10% med. subangular gravel to #4.										55% graded sand, 35% MP fines,			
98410	"		62	64	Clayey Sandy Gravel(GC)	87	100	85	75	70	65	54	47	36	31	26	21	2.0	

SPD Form 66A
1 May 83

U.S. ARMY ENGINEER DIVISION LABORATORY -- SOUTH PACIFIC DIVISION

SOIL TEST RESULT SUMMARY

Division Serial No.	Hole No.	Field Sample No.	Depth Or Elevation		Laboratory Descriptive	Mechanical Analysis - % Finer										Liquid Limit	Plasticity Index	Field Moisture %	
			From	To		Gravel			Sand				Fines						
						3/4	1/2	3/8	#4	#10	#40	#60	#100	#200					
98411	14		0	2	Clayey Sandy Gravel (GC)	100	60	47	41	39	36	30	20	18	16	13	2.1		
98412	"		2	4	Clayey Gravelly Sand (SC)	100	96	86	80	77	72	67	57	53	45	35	16	3.5	
98413	"		4	6	Silty Clayey Sand (SC)	100	100	98	97	97	96	94	91	87	72	50	9	3.6	
98414	"		6	8	Sandy Clay (CL)	100	100	99	99	98	97	94	88	83	72	56	13	1.3	
98415	"		8	10	Sandy Clay (CL)	100	100	100	99	99	98	95	89	85	80	69	18	3.2	
98416	"		10	12	Sandy Clay (CL)	100	100	100	100	100	100	95	89	86	75	59	19	5.0	
98417	"		12	14	Sandy Clay (CL)	100	100	100	100	100	100	99	97	91	72	52	19	4.8	
98418	"		14	16	Clayey Silty Sand (SM) SC	100	100	100	100	100	100	97	91	75	46	29	35	11	4.2
98419	"		16	18	Sandy Silt (ML)	100	100	100	100	100	100	96	90	84	69	51	32	6	3.5
98420	"		18	20	Clayey Sandy Gravel (GC)	100	96	77	66	60	50	44	34	29	23	16	32	10	2.4
98421	"		20	22	Clayey Sandy Gravel (GC)	100	88	75	67	61	52	44	30	25	20	14	32	10	2.3
98422	"		22	24	Clayey Sandy Gravel (GC)	100	100	100	83	68	58	41	35	24	18	14	34	13	2.1
98423	"		24	26	Clayey Sandy Gravel (GC)	100	99	78	66	59	46	38	24	20	17	13	38	17	2.6
98424	"		26	28	Clayey Sandy Gravel (GC)	93	100	83	73	67	56	48	26	22	18	15	37	16	2.3

SPD Form 66A
1 May 83

PROJECT FOLSON LAB PROGRAM

DATE: May 1987

U.S. ARMY ENGINEER DIVISION LABORATORY -- SOUTH PACIFIC DIVISION

SOIL TEST RESULT SUMMARY

Division Serial No.	Hole No.	Field Sample No.	Depth Or Elevation		Laboratory Descriptive Classification	Mechanical Analysis - % Finer										Li-liquid Limit	Plasticity Index	Field Moist %				
			From	To		Gravel			Sand				Fines									
						3/4	1/2	3/8	#4	#10	#40	#60	#100	#200								
98425	14		28	30	Clayey Gravelly Sand(SC)	100	89	81	78	74	68	38	29	25	20	35	14	2.0				
98426	"		30	32	Clayey Sand (SP-SC)			98	96	92	86	20	10	9	8	32	11	0.9				
98427	"		32	34	Silty Clayey Sand(SC)				98	94	91	88	58	48	36	39	16	2.8				
98428	"		34	38	Clayey Gravelly Sand(SC)				86	75	68	63	45	37	26	40	17	2.5				
98429	"		36	38	Clayey Sandy Gravel(GP-GC)				100	88	62	45	39	31	25	18	15	13	11	37	15	2.3
98430	"		38	40	Clayey Sandy Gravel(GP-GC)				100	83	55	48	36	18	15	13	11	36	13	1.7		
98431	"		40	42	Clayey Sandy Gravel(GP-GC)				100	75	64	55	48	38	29	18	16	14	12	39	16	2.1
98432	"		42	44	Silty Sandy Gravel(GP-GC)				100	65	51	45	34	25	14	12	10	8	39	14	1.6	
98433	"		44	46	Clayey Sandy Gravel(GP-GC)				93	78	58	52	40	27	15	13	11	10	39	17	1.7	
98434	"		46	48	Clayey Sandy Gravel(GC)				93	80	66	60	50	41	26	22	19	15	38	17	1.8	
98435	"		48	48	Gravelly Clayey Sand(SC)				100	90	88	82	77	74	63	57	50	45	41	18	2.5	
98436	15		0	2	Silty Clayey Sand(SC)					100	98	97	94	90	71	62	53	43	38	15	2.8	
98437	"		2	4	Clayey Sandy Gravel(GP-GC)				60	52	43	39	31	26	18	15	13	11	29	8	1.6	

SPD Form 66AV
1 May 83

U.S. ARMY ENGINEER DIVISION LABORATORY -- SOUTH PACIFIC DIVISION

SOIL TEST RESULT SUMMARY

Division Serial No.	Hole No.	Field Sample No.	Depth Or Elevation		Laboratory Descriptive Classification	Mechanical Analysis - % Finer										LL- Liquid Limit %	Plasticity Index %	
			From	To		Gravel					Sand							Fines #200
						3/4	1/2	3/8	#4	#10	#40	#60	#100	#200				
98438	15		4	6	Clayey Silty Gravel (SC) GC	100	86	75	67	55	45	32	28	23	18	27	8	1.6
98439	"		6	8	Clayey Silty Gravel (SC) GC	86	70	58	50	38	31	21	18	15	12	28	8	1.8
98440	"		8	10	Gravel (GP-GC)	100	91	54	45	33	26	17	14	11	10	28	9	1.5
98441	"		10	12	Clayey Silty Gravel (GP-GM)	100	76	65	58	47	38	25	21	17	13	24	5	1.4
98442	"		12	14	Clayey Silty Gravel (GP-GC)	100	73	55	41	32	25	17	14	12	10	26	7	1.5
98443	"		14	16	Clayey Silty Gravel (GP-GC)	100	55	47	37	30	18	14	10	8	7	26	7	1.3
98444	"		16	18	Clayey Silty Gravel (GP-GC)	100	96	71	58	51	37	28	18	15	13	25	7	1.4
98445	"		18	20	Clayey Silty Gravel (GP-GC)	100	89	71	58	50	36	27	18	13	10	26	7	1.3
98446	"		20	22	Silty Silty Gravel (GP-GC)	100	80	58	47	40	29	22	14	12	10	25	6	1.5
98447	"		22	24	Silty Silty Gravel (GP-GC)	100	75	61	52	45	34	27	18	15	13	29	10	1.2
98448	"		24	26	Clayey Silty Gravel (GP-GC)	100	92	69	59	51	37	30	19	16	14	24	5	1.2
98449	"		26	28	Silty Silty Gravel (GP-GC)	100	97	73	58	49	36	28	18	15	12	24	6	1.6
98450	"		28	30	Silty Silty Gravel (GP-GC)	100	82	64	55	47	36	30	21	18	15	27	8	1.6

SPD Form 66A
1 May 83

U.S. ARMY ENGINEER DIVISION LABORATORY -- SOUTH PACIFIC DIVISION

SOIL TEST RESULT SUMMARY

Division Serial No.	Hole No.	Field Sam- ple No.	Depth Or Elevation		Laboratory Descriptive	Mechanical Analysis - % Finer												Li- quid Limit % Plasticity Index	Field Moisture % Index		
			From	To		Gravel						Sand								#100	#200
						#3/4	1/2	3/8	#4	#10	#40	#60	#100	#200							
98451	15		30	32	Clayey Sandy Gravel (GP-GC) ✓	100	67	53	46	42	35	28	20	17	15	12	30	10	1.7		
98452	"		32	34	Clayey Sandy Gravel (GP-GC) ✓	100	82	73	60	50	37	27	16	14	11	9	30	10	1.7		
98453	"		34	36	Clayey Sandy Gravel (GP-GC) ✓	100	60	42	34	30	23	19	14	12	10	8	31	11	2.0		
98454	"		36	38	Clayey Sandy Gravel (GC) ✓	100	94	76	63	55	41	33	22	19	16	15	30	11	1.6		
98455	"		38	40	Clayey Sandy Gravel (GP-GC) ✓	100	80	67	55	49	37	29	20	17	14	11	26	6	1.3		
98456	"		40	42	Clayey Sandy Gravel (GP-GC) ✓	100	83	64	54	46	35	29	20	17	14	12	27	7	1.4		
98457	"		42	44	Clayey Sandy Gravel (GP-GC) ✓	100	84	66	58	52	41	33	22	19	16	13	25	6	1.3		
98458	"		44	46	Clayey Sandy Gravel (GC) ✓	100	92	76	64	56	42	31	21	18	15	14	26	8	1.4		
98459	"		46	48	Clayey Sandy Gravel (GP-GC) ✓	100	83	67	57	50	38	34	20	16	13	10	26	6	1.2		
98460	"		48	50	Clayey Sandy Gravel (GP-GC) ✓	100	92	76	64	56	42	31	19	16	14	12	27	7	1.4		
98461	"		50	52	Clayey Sandy Gravel (GP-GC) ✓	100	88	68	57	50	37	28	19	16	13	10	27	6	1.3		
98462	"		52	54	Clayey Sandy Gravel (GP-GC) ✓	100	81	63	53	48	39	29	19	16	14	12	32	14	1.9		
98463	"		54	56	Clayey Sandy Gravel (GC) ✓	100	95	78	70	65	54	45	29	25	21	17	35	15	1.5		

PROJECT FOLSOM LAB PROGRAM DATE May 1987

SPD Form 66A
1 May 83

U.S. ARMY ENGINEER DIVISION LABORATORY -- SOUTH PACIFIC DIVISION

SOIL TEST RESULT SUMMARY

PROJECT		FOILSOM LAB PROGRAM		DATE June 1987													
Division Serial No.	Hole No.	Field Sample No.	Depth Or Elevation		Laboratory Descriptive Classification	Mechanical Analysis - % Finer										Plasticity Index	Liquid Limit %
			From	To		Gravel			Sand				Fines				
						3/4"	1/2"	3/8"	#4	#10	#40	#60	#100	#200			
98464	15		56	58	Clayey Sandy Gravel (G-C)	94	78	69	63	54	45	20	16	14	12	41	20
98465	"		58	60	Clayey Sandy Gravel (G-C) ✓	100	81	73	67	57	46	24	19	17	15	40	20
98466	"		60	62	Clayey Gravelly Sand (SC)	98	84	78	75	68	61	39	32	28	23	39	19
98467	"		62	64	Clayey Sandy Gravel (G-C) ✓	100	69	60	54	44	36	19	16	14	13	37	17
98468	"		64	66	Clayey Sandy Gravel (G-C)	95	72	57	50	39	30	17	14	12	10	40	19
98469	"		66	68	Clayey Sandy Gravel (G-C)	100	71	59	51	51	40	24	21	18	17	39	18
98470	"		68	70	Clayey Sandy Gravel (G-C)	96	80	68	61	51	44	24	21	18	15	40	18
98471	"		70	72	Clayey Sandy Gravel (G-C)	100	68	60	55	47	37	21	18	16	14	37	16
98472	"		72	74	Clayey Sandy Gravel (G-C)	100	76	65	59	47	38	22	18	15	14	40	19
98473	"		74	76	Clayey Sandy Gravel (G-C) ✓	96	68	58	50	39	29	17	14	12	11	36	16
98474	"		76	78	Clayey Sandy Gravel (G-C)	100	79	71	66	55	47	34	31	28	24	38	17
98475	"		78	80	Clayey Sandy Gravel (G-C) ✓	100	89	81	76	63	45	31	26	23	18	32	12
98476	"		80	82	Clayey Sandy Gravel (G-C) ✓	94	82	74	69	60	54	38	33	28	22	32	13
					Gravel (G-C)	100											

SPD Form 66A
1 May 83

U.S. ARMY ENGINEER DIVISION LABORATORY -- SOUTH PACIFIC DIVISION

SOIL TEST RESULT SUMMARY

PROJECT FOLSOM LAB PROGRAM

DATE JUNE 1987

Division Serial No.	Hole No.	Field Sample No.	Depth Or Elevation		Laboratory Descriptive Classification	Mechanical Analysis - % Finer										Liquidity Index	Plasticity Moisture %		
			From	To		Gravel					Sand							Pines #200	
						3/4	3/8	3/4	1/2	3/8	#4	#10	#40	#60	#100				
98477	15		82	84	Gravel (GM)	100	70	45	32	24	9	8	5	4	4	3	33	14	2.0
98478	16		0	2	Clayey Sandy Gravel (GC) ✓	94	87	82	76	72	68	62	52	48	44	37	38	18	3.0
98479	"		2	4	Clayey Sandy Gravel (GP-GC) ✓	90	74	66	56	49	37	29	20	17	13	9	22	5	1.4
98480	"		4	6	Clayey Sandy Gravel (GC) ✓	100	83	64	55	49	39	34	25	22	19	15	29	10	1.9
98481	"		6	8	Gravel (GP) ✓	100	21	18	16	14	12	9	5	5	4	4	26	7	1.2
98482	"		8	10	Clayey Gravelly Sand (SP-SM) ✓	100	99	96	91	84	73	62	42	35	29	22	23	6	1.4
98483	"		10	12	Clayey Sandy Gravel (GC-GM) ✓	100	83	76	69	64	52	42	30	26	22	16	21	4	1.1
98484	"		12	14	Clayey Sandy Gravel (GC-GM) ✓	100	88	78	67	60	48	38	26	22	19	14	22	5	1.3
98485	"		14	16	Clayey Sandy Gravel (GP-GC) ✓	100	53	39	35	30	25	20	13	11	9	7	24	5	1.1
98486	"		16	18	Silty Sandy Gravel (GM-GM) ✓	100	80	71	62	55	43	32	18	15	12	9	20	2	1.0
98487	"		18	20	Silty Sandy Gravel (GP-GM) ✓	100	85	66	54	46	31	23	14	12	10	7	20	2	0.9
98488	"		20	22	Silty Sandy Gravel (GP-GM) ✓	100	70	63	50	42	30	21	12	10	8	5		NP	0.9
98489	"		22	24	Silty Gravel (GP-GM) ✓	100	47	21	13	10	6	4	2	2	1	1		NP	0.8

SPD Form 66A
1 May 83

U.S. ARMY ENGINEER DIVISION LABORATORY -- SOUTH PACIFIC DIVISION

SOIL TEST RESULT SUMMARY

PROJECT	FOLSOM LAB PROGRAM		DATE												June 1987						
	Division Serial No.	Hole No.	Field Sample No.	Depth Or Elevation	Laboratory Descriptive Classification	Mechanical Analysis - %						Finer				Liquid Limit	Plasticity Index	Field Moisture %			
						Gravel			Sand			#100	#200	#40					#60	#100	
From	To	1 1/2	3/8	#4	#10	#40	#60	#100	#200												
98503	16			50	52	Could not be found															
98504	"			52	54																
98505	"			54	56	Silty Sandy Gravel (GP-GM)	100	71	61	48	40	26	18	14	12	10	7	18	1	0.5	
98506	"			56	58	Gravelly Sandy (SP)	100	85	78	71	57	42	9	6	4	2				NP	0.7
98507	"			58	60	Clayey Sandy Gravel (GM-GC)	100	78	73	63	56	44	36	24	20	16	11	24	4	1.1	
98508	"			60	62	Silty Sandy Gravel (GM-GM)	100	63	57	47	41	29	21	13	11	8	6	21	3	1.0	
98509	"			62	64	Clayey Sandy Gravel (GP-GC)	100	80	57	47	39	28	20	12	10	9	7	23	6	1.2	
98510	"			64	66	Gravelly Clayey Sand (SC)	100	95	94	93	91	83	69	40	32	26	21	27	9	1.4	
98511	"			66	68	Clayey Sandy Gravel (GM-GC)	100	89	78	64	55	42	34	21	17	15	11	26	8	1.4	
98512	"			68	70	Clayey Sandy Gravel (GP-GC)	100	75	69	55	46	32	24	15	12	10	8	28	9	1.6	
98513	"			70	72	Clayey Sandy Gravel (GP-GC)	100	75	69	62	49	39	25	19	12	10	9	7	28	9	1.2
98514	"			72	74	Clayey Sandy Gravel (GP-GC)	100	53	48	39	35	27	21	11	9	8	6	25	7	1.2	
98515	"			74	76	Clayey Sandy Gravel (GP-GC)	100	85	65	53	47	33	25	14	12	10	7	26	8	1.4	

From this point forward I will not note Ca, Cu to check part vs. wet position. 5c

SPD Form 66A
1 May 83

U.S. ARMY ENGINEER DIVISION LABORATORY - SOUTH PACIFIC DIVISION
SOIL TEST RESULT SUMMARY

PROJECT: FOLSOM LAB PROGRAM

DATE: JUNE 1987

Division Number	Note Number	Field Sample No.	Depth or Elevation From Top	Laboratory Descriptive Classification	Mechanical Analysis - % Finer										Liquid Limit	Plasticity Index	Field Moist. %		
					3	2	1.5	3/4	1/2	3/8	#4	#10	#40	#60				#100	#200
98516	16		76	Clayey Gravel (GP-GC)	100	57	51	30	25	22	17	14	10	9	7	6	27	0	1.7
98517	16		78	Clayey Sandy Gravel (GP-GC)	100	64	55	45	40	37	31	27	18	15	13	11	28	9	1.3
98518	16		80	Clayey Sandy Gravel (GP-GC)	100	68	68	61	51	43	32	24	14	12	10	0	26	7	1.2
98519	16		82	Clayey Sandy Gravel (GP-GC)	100	59	61	56	43	37	28	21	14	12	10	0	26	6	0.9
98520	16		86	Sandy Gravelly Clay (CL)	100	94	94	83	79	76	74	72	69	68	65	57	40	17	3.2
98521	16		88	Sandy Silty Clay (CL)	100	95	95	100	99	95	84	65	32	9	2.7				
98522	16		90	Clayey Sandy Gravel (GP-GC)	100	93	82	65	55	51	45	42	38	33	28	22	20	7	2.1
98523	16		92	Clayey Gravel (GP-GC)	100	89	67	53	37	30	20	15	11	10	0	6	30	0	1.6
98524	16		92	Clayey Gravel (GP-GC)	100	83	83	48	32	28	20	15	11	10	0	7	30	0	1.6
98525	16		94	Gravelly Clayey Sand (SP) GP	100	96	96	15	14	13	11	10	0	7	6	4	30	0	1.7
98526	16		96	Clayey Gravelly Sand (SC-SM)	100	97	100	85	79	77	72	67	45	36	28	21	26	7	1.5
98527	16		98	Sandy Silty Clay (CL)	100	94	94	94	94	94	94	93	87	78	67	52	29	0	2.3
98528	16		100	Gravelly Clayey Sand (SC)	100	89	89	80	76	74	70	60	63	60	53	35	32	9	2.5

-B.O.H

U.S. ARMY ENGINEER DIVISION LABORATORY -- SOUTH PACIFIC DIVISION												
SOIL TEST RESULT SUMMARY												
PROJECT: FOLSOM LAB PROGRAM												
DATE: JULY 1967												
Division Number	Mo Number	Field Sample No.	Depth or Elevation From To	Laboratory Descriptive Classification	3	1.5	Gravel	Mechanical Analysis - % Finer Sand	Fines	Liquid Limit	Plasticity Index	Field Moist.
					2	1	3/4 1/2 3/8	#4 #10 #40 #60 #100 #200				%
98529	16		102 104		Sample could not be found.							
98530	16		104 106		Sample could not be found.							
98531	16		106 108		Sample could not be found.							
98532	16		108 110		Sample could not be found.							
98533	16		110 111		Sample could not be found.							
98534	17		0 2	Gravelly Clayey Sand (SC)	100	98	96 88 84	76 70 62 58 51 41	30	9	2.1	
98535	17		2 4	Clayey Sandy Gravel (GC)	100	86	76 71 68	61 56 49 46 42 35	29	0	2.0	
98536	17		4 6	Clayey Sandy Gravel (GP-GC)	100	62	55 46 41	31 23 17 15 13 11	26	0	1.5	
98537	17		6 8	Clayey Sandy Gravel (GP-GC)	100	81	61 51 45	34 28 19 16 14 12	27	9	1.4	
98538	17		8 10	Clayey Sandy Gravel (GC)	100	87	78 66 58	43 33 24 21 18 14	27	0	0.6	
98539	17		10 12	Clayey Gravel (GC)	100	45	35 30 28	24 21 19 18 16 13	27	0	1.0	
98540	17		12 14	Insufficient Material for Atterberg.	100	71	70 59 54	40 29 16 14 11 8				
98541	17		14 16	Silty Sandy Gravel (GP-GH)	100	58	52 45 40	31 23 16 14 12 9			NP	

Sample was classified as NP because it could not be rolled out with any degree of accuracy even though it contained some LP fines.

CPH FROM KKT

U.S. ARMY ENGINEER DIVISION LABORATORY - SOUTH PACIFIC DIVISION

SOIL TEST RESULT SUMMARY

PROJECT: FOLSOM LAB PROGRAM

DATE: JUNE 1967

Division Number	Hole Number	Field Sample No.	Depth or Elevation From	Laboratory Descriptive Classification	Mechanical Analysis - % Finer										Fines #200	Liquid Limit	Plasticity Index	Field Moist. %		
					3	2	1.5	3/4	3/8	3/16	#4	#10	#60	#100					#400	
98542	17	18	16	Silty Sandy Gravel (GP-GH)	100	78	74	67	57	40	36	27	16	13	11	0	19	2		
98543	17	20	10		Sample inadvertently discarded before Sieve Analysis and Atterberg could be determined.															
98544	17	22	20		100	100	100	100	100	100	100	100	100	100	100	100	100	100	100	100
98545	17	24	22	Silty Sandy Gravel (GP-GH) ✓	100	82	68	60	50	44	34	27	19	16	13	9		MP	0.8	
98546	17	26	24	Silty Sandy Gravel (GP-GH) ✓	100	88	75	64	54	46	34	27	18	16	14	10	21	3	1.1	
98547	17	28	26	Sandy Silty Gravel (GP-GH) ✓	100	71	59	52	45	41	33	26	16	14	12	8		MP	0.6	
98548	17	30	28	Sandy Silty Gravel (GP-GH) ✓	100	96	88	76	62	56	38	27	18	16	13	10	21	3	0.7	
98549	17	32	30	Clayey Sandy Gravel (GP-GC) ✓	100	78	70	50	48	41	31	25	17	15	13	10	23	6	1.2	
98550	17	34	32	Clayey Gravel (GP-GC) ✓	100	86	73	64	52	44	32	25	17	14	12	0	20	2	1.1	
98551	17	36	34	Clayey Sandy Gravel (GP-GC) ✓	100	89	87	74	61	51	35	27	17	15	13	10	23	5	1.2	
98552	17	38	36	Silty Sandy Gravel (GP-GH) ✓	100	71	59	53	45	39	29	21	13	10	9	6	20	3	1.1	
98553	17	40	38	Clayey Sandy Gravel (GP-GC) ✓	100	89	79	67	56	40	30	22	19	16	12	26	6	1.7		
98554	17	42	40	Clayey Sandy Gravel (GC) ✓	100	74	62	55	48	43	34	28	21	18	16	13	25	8	1.0	
					Barrelly plastic-Accuracy of rolled out.															

U.S. ARMY ENGINEER DIVISION LABORATORY -- SOUTH PACIFIC DIVISION

SOIL TEST RESULT SUMMARY

PROJECT: FOLSOM LAB PROGRAM DATE: JUNE 1987

Division Number	Mole Number	Field Sample No.	Depth or Elevation From	Laboratory Descriptive Classification	Mechanical Analysis - % Finer Sand										Liquid Limit	Plasticity Index	Field Moist. %		
					3	1.5	3/4	1/2	Gravel	3/8	3/4	#4	#10	#40				#60	#100
98555	17		42	44 Clayey Sandy Gravel (GP-GC) ✓	100	89	75	66	55	47	33	23	14	12	10	8	23	5	1.5
98556	17		44	46 Clayey Sandy Gravel (GP-GC) ✓	100	89	77	62	47	39	25	18	11	10	8	6	27	6	1.7
98557	17		46	48 Silty Sandy Gravel (GP-GM) ✓	100	69	63	57	47	41	31	24	15	13	11	8	28	3	1
98558	17		48	50 Clayey Sandy Gravel (GP-GC) ✓	100	75	62	57	47	42	32	25	17	15	13	10	24	5	1.2
98559	17		50	52 Clayey Sandy Gravel (GP-GC) ✓	100	82	66	55	45	37	26	18	12	10	8	6	25	7	1.3
98560	17		52	54 Silty Sandy Gravel (GP-GM) ✓	100	92	82	75	64	55	41	31	20	17	14	11	22	4	1.2
98561	17		54	56 Clayey Sandy Gravel (GP-GC) ✓	100	62	49	45	37	32	24	19	13	12	10	8	26	7	1.4
98562	17		56	58 Clayey Sandy Gravel (GP-GC) ✓	100	97	76	69	61	56	48	42	24	17	12	9	23	6	1.1
98563	17		58	60 Silty Sand (SP-SM) ✓				100	99	99	98	94	30	13	9	6		MP	0.0
98564	17		60	62 Sand (SP) ✓						100	96	75	9	4	3	3		MP	0.0
98565	17		62	64 Silty Gravelly Sand (SM-SH) ✓					100	99	73	34	12	10	9	7		MP	0.0
98566	17		64	66 Sandy Gravel (GW) ✓		100	97	92	80	73	49	27	4	2	2	1	27	8	1
98567	17		66	68 Clayey Sandy Gravel (GP-GC) ✓	100	71	62	55	46	40	30	22	14	11	10	8	26	7	1.4

SPU FORM 66A

U.S. ARMY ENGINEER DIVISION LABORATORY - SOUTH PACIFIC DIVISION

SOIL TEST RESULT SUMMARY

PROJECT: FOLSOM LAB PROGRAM

DATE: JUNE 1967

Division Number	Hole Number	Field Sample No.	Depth or Elevation From To	Laboratory Descriptive Classification	6.3	1.5	Mechanical Analysis - % Finer						Liquid Limit	Plasticity Index	Field Moist. %				
							2	1	3/4	1/2	3/0	84				110	40	60	100
98568	17		68	70 Clayey Sandy Gravel (GP-GC)	100	89	75	64	52	45	32	24	15	12	10	8	26	7	1.3
98569	17		70	72 Clayey Sandy Gravel (GP-GC)	100	91	81	72	56	46	32	22	13	10	9	7	27	8	1.4
98570	17		72	74 Silty Sandy Gravel (GP-GC)	100	75	61	54	46	43	36	30	22	19	17	14	28	0	1.1
98571	17		74	76 Silty Sandy Gravel (GP-GC)	100	84	76	66	54	47	36	29	21	19	17	14	32	11	2
98572	17		76	78 Silty Gravel (GP-GC)	100	80	60	45	33	26	15	9	8	7	6	5	30	9	1.0
98573	17		78	80 Silty Sandy Gravel (GP-GC)	100	75	69	65	57	53	46	38	22	16	11	6			0.8
98574	17		80	82 Gravel (GW)	100	69	56	42	29	20	9	5	3	3	2	2			0.9
98575	17		82	84 Gravel (GP)	100	17	15	12	9	7	6	5	3	3	2	2			1.1
98576	17		84	86		100	76	64	43	33	18	10	7	2	6	5			1.1
98577	17		86	88 Gravel (GP)	100	86	69	55	33	25	15	10	7	6	5	4	27	7	1.3
98578	17		88	90 Sandy Gravel (GP)	100	76	63	60	46	34	20	13	8	7	5	4	30	7	1.3
98579	17		90	92 Sandy Silty Clay (GP-GC)	100.63	38	31	28	25	22	19	17	12	10	8	6	25	6	1.4
98580	17		92	94 Clayey Gravel (GP-GC)	100	83	64	51	33	26	19	16	13	12	11	10	45	25	2.0
					Insufficient material for Atterberg														



SPD FORM 65A

U.S. ARMY ENGINEER DIVISION LABORATORY - - SOUTH PACIFIC DIVISION

SOIL TEST RESULT SUMMARY

PROJECT: FOLSOM LAB PROGRAM DATE: JUNE 1987

Division Number	Hole Number	Field Sample No.	Depth or Elevation From	Laboratory Descriptive Classification	Mechanical Analysis - % Finer										Liquid Limit	Plasticity Index	Field Moist. %	
					3	1.5	3/4	1/2	3/8	#4	#10	#40	#60	#100				#200
98581	17		94	Sandy Clayey Gravel (GC)	100	81	68	65	62	54	48	40	37	34	30	44	23	2.5
98582	17		96	Sandy Clayey Gravel (GC)	100	76	61	55	53	48	44	37	34	31	27	38	16	2.9
98583	17		98		100	100	91	79	71	62	54	43	39	35	20			2.6
98584	17		100	Clayey Sand (SC)		100	99	95	94	86	78	63	57	50	43	33	12	2.2
98585	17		102	Gravelly Clayey Sand (SC)		100	97	89	86	72	65	57	54	50	44	33	10	2.4
98586	17		104	Clayey Sandy Gravel (GC)		100	94	89	83	70	61	51	49	46	41	32	10	2.9
98587	17		106	Clayey Sandy Gravel (GC)	100	87	79	73	67	56	47	39	36	32	27	33	10	2.3
98588	18		0	Clayey Gravel (GC)	100	88	65	52	42	32	29	26	24	22	19	33	10	2.1
98589	18		2	Clayey Gravel (GP-GC)	100	68	44	34	27	19	16	12	10	9	7	31	9	2
98590	18		4	Sandy Clayey Gravel (GC)		100	89	83	73	67	53	43	37	29	26	32	11	1.9
98591	18		6	Sandy Clayey Gravel (GP-GC)	100	68	55	44	36	24	17	11	9	8	7	30	10	1.8
98592	18		8	Clayey Sandy Gravel (GP-GC)	100	91	71	59	50	35	26	17	14	12	9	28	9	1.4
98593	18		10	Clayey Sandy Gravel (GC)	100	89	75	69	61	51	44	34	30	25	19	26	8	1.4

-B.D.H.

U.S. ARMY ENGINEER DIVISION LABORATORY - - SOUTH PACIFIC DIVISION

SOIL TEST RESULT SUMMARY

PROJECT: FOLSOM LAB PROGRAM

DATE: JUNE 1967

Division Number	Hole Number	Field Sample No.	Depth or Elevation From To	Laboratory Descriptive Classification	Mechanical Analysis - % Finer										Liquidity Index	Plasticity Index	Field Moist. %			
					3	1.5	1	3/4	3/8	3/16	#4	#10	#20	#40				#60	#100	Fines #200
98594	18		12	14	Clayey Sandy Gravel (GP-GC)	100	86	69	57	46	40	30	25	20	10	15	11	27	0	1.6
98595	18		14	16	Clayey Sandy Gravel (GW-GC)	100	68	61	58	49	44	36	30	22	19	16	11	23	5	1.8
98596	18		16	18	Silty Sandy Gravel (GP-GH)	100	90	67	59	48	41	29	23	16	13	10	7	19	2	1.2
98597	18		18	20	Sandy Clayey Gravel (GC)	100	100	Not enough material for Att. Plasticity visualized MP.	54	47	41	39	37	33	30	27	23			2.2
98598	18		20	22	Clayey Gravel (GC)	100	42	Not enough material for - 4 MA. Atterberg visualized MP.	17	11	8	7	4							1.3
98599	18		28	30	Clayey Gravelly Sand (SC-SH)	100	100	Not enough material for Att. No visual plasticity.	92	84	78	69	62	50	45	38	27			1.6
98600	18		30	32	Clayey Gravelly Sand (SC-SH)	100	100	91	82	74	64	55	41	37	31	23	25	4	1.3	
98601	18		32	34	Clayey Sandy Gravel (GW-GC)	100	93	86	76	66	60	49	37	25	21	17	13	24	6	1.8
98602	18		34	36	Clayey Sandy Gravel (GW-GC)	100	66	63	61	56	52	41	33	23	19	16	12	26	7	1.9
98603	18		36	38	Clayey Sandy Gravel (GP-GC)	100	83	75	68	58	51	38	28	18	15	13	10	26	7	1.5
98604	18		38	40	Clayey Sandy Gravel (GP-GC)	100	100	93	85	74	65	50	37	24	21	17	13	23	6	1.3
98605	18		40	42	Clayey Sandy Gravel (GW-GC)	100	75	66	60	51	45	34	26	16	13	10	8	25	7	1.3
98606	18		42	44	Clayey Sandy Gravel (GP-GC)	100	78	62	51	42	36	29	24	15	12	10	7	25	7	1.6

SPU TURN 66M

U.S. ARMY ENGINEER DIVISION LABORATORY - SOUTH PACIFIC DIVISION
SOIL TEST RESULT SUMMARY

PROJECT: FOLSON LAB PROGRAM

DATE: JUNE 1987

Division Number	Hole Number	Field Sample No.	Depth or Elevation From To	Laboratory Descriptive Classification	G	M	Mechanical Analysis - % Finer										Liquid Limit	Plasticity Index	Field Moist. %
							3	1.5	2	3/4	1	Gravel	3/8	3/16	1/4	3/20			
98607	18	46	44	Silty Sandy Gravel (GP-GM) GC	100	93	73	62	49	42	29	21	13	11	8	6	24	4	1.3
98608	16	48	46	Silty Sandy Gravel (GP-GM)	100	80	58	52	40	32	18	15	11	9	8	6		MP	1.5
98609	18	50	48	Silty Sandy Gravel (GP-GM)	100	93	89	83	68	56	38	29	19	16	13	9	23	3	1.6
98610	18	52	50	Clayey Sandy Gravel (GP-GC)	100	89	67	58	45	37	24	17	10	8	7	5	25	5	1.2
98611	18	54	52	Gravel (GP)	100	63	36	27	19	16	12	10	8	8	6	4		MP	1.2
98612	18	56	54	Silty Sandy Gravel (GP-GM) GC	100	69	62	52	45	31	23	17	13	11	8	8	25	4	1.4
98613	18	58	56	Clayey Gravelly Sand (SC-SM)	100	96	91	85	78	62	49	29	24	20	15	15	24	5	1.2
98614	18	70	68	Silty Sandy Gravel (GP-GM)	100	96	84	67	52	31	21	14	12	10	9	9	37	5	1.7
98615	18	72	70	Silty Sandy Gravel (GP-GM)	100	81	45	32	27	24	21	19	16	14	12	9	35	8	2.4
98616	18	74	72	Gravelly Silty Sand (SM)	100	87	87	83	82	75	66	52	42	35	27	27	33	9	2.1
98617	18	76	74	Silty Clayey Sand (SM) SM	100	96	96	95	94	92	86	50	35	28	21	21	30	7	1.7
98618	18	78	76	Clayey Gravelly Sand (SC)	100	87	81	78	75	74	72	70	49	36	28	22	27	6	1.8
98619	18	80	78	Clayey Gravelly Sand (SM) SC-SM	100	96	93	83	79	72	66	49	37	30	23	27	7	1.1	

Notes: Samples were classified as MP because they could not be rolled out with any degree of accuracy even though they contained some LP fines.

U.S. ARMY ENGINEER DIVISION LABORATORY - SOUTH PACIFIC DIVISION
SOIL TEST RESULT SUMMARY

PROJECT: FOLSOM LAB PROGRAM DATE: JULY 1987

Division Number	Hole Number	Field Sample No.	Depth or Elevation From To	Laboratory Descriptive Classification	3	1.5	Mechanical Analysis - %							Fines #200	Liquid Limit	Plasticity Index	Field Moist. %	
							2	1	3/4	1/2	3/8	3/16	1/8					10
98620	18		80 82	Clayey Gravel (GP-GC)	100	87	59	39	29	22	20	16	13	11	0	28	7	2.0
98621	18		82 84	Clayey Sandy Gravel (GC-GH)	100	81	70	59	51	42	36	28	22	18	14	28	7	1.8
98622	18		84 86	Silty Gravel (GP-GH)	100	77	61	35	28	21	18	14	11	9	7	31	0	1.8
98623	18		86 88	Clayey Sandy Gravel (GC)	100	96	74	60	55	48	45	39	34	29	24	33	11	2.6
98624	18		88 90	Silty Sandy Gravel (GH) SC	100	89	73	58	47	37	34	29	24	21	18	32	9	2.7
98625	18		90 92	Silty Gravel (GH)	100	100	82	63	46	30	27	23	20	18	16	35	0	2.2
98626	18		98 100	Clayey Gravel (GP-GC)	100	29	23	21	19	14	12	9	8	6	5	32	9	2.1
98627	18		100 102	Gravelly Clayey Sand (SC) SC-SM	100	99	98	92	86	73	62	49	41	35	28	29	7	2.0
98628	18		102 104	Clayey Gravelly Sand (SC)	100	94	88	83	79	67	52	38	32	28	23	32	10	1.9
98629	19		0 2	Clayey Sandy Gravel (GC-GH)	100	97	82	70	63	49	38	27	23	19	14	26	7	1.6
98630	19		2 4	Clayey Sandy Gravel (GC-GH)	100	79	66	55	50	42	35	24	21	17	14	25	6	1.6
98631	19		4 6	Clayey Sandy Gravel (GP-GC)	100	78	61	51	46	36	29	19	16	13	10	25	7	1.7
98632	19		6 8	Clayey Sandy Gravel (GP-GC)	100	83	69	57	50	38	31	20	17	15	12	26	6	1.7

U.S. ARMY ENGINEER DIVISION LABORATORY -- SOUTH PACIFIC DIVISION
SOIL TEST RESULT SUMMARY

PROJECT: FOLSOM LAB PROGRAM DATE: JULY 1987

Division Number	Hole Number	Field Sample No.	Depth or Elevation From To	Laboratory Descriptive Classification	Mechanical Analysis - %							Fines #200	Liquid Limit	Plasticity Index	Field Moist.				
					3	1.5	1	3/4	3/8	3/16	1/8					1/40	1/20		
98633	19		8 10	Clayey Sandy Gravel (GP-GC-GM)	100	97	87	79	62	55	44	35	23	20	17	13	23	5	1.3
98634	19		10 12	Clayey Sandy Gravel (GP-GC)	100	87	80	69	52	45	35	28	19	16	14	10	24	6	1.3
98635	19		12 14	Clayey Sandy Gravel (GP-GC)	100	100	89	78	58	50	37	27	17	14	11	8	22	5	1.2
98636	19		14 16	Clayey Sandy Gravel (GP-GC)	100	81	78	59	51	46	36	29	20	17	14	11	22	4	1.3
98637	19		16 18	Clayey Sandy Gravel (GP-GC)	100	93	93	77	55	47	35	28	18	15	13	10	25	6	1.4
98638	19		18 20	Clayey Sandy Gravel (GP-GC)	100	72	67	61	47	41	31	25	17	14	12	9	25	7	1.4
98639	19		20 22	Clayey Sandy Gravel (GP-GC)	100	70	74	53	45	38	29	22	15	12	10	8	26	7	1.4
98640	19		22 24	Silty Sandy Gravel (GP-GC-GM)	100	84	79	57	50	44	33	26	18	15	13	9	22	4	1.3
98641	19		24 26	Clayey Sandy Gravel (GC-GM)	100	82	82	73	67	61	51	42	30	27	23	18	24	5	1.3
98642	19		26 28	Clayey Gravel (GP-GC)	100	43	36	22	20	20	19	17	11	9	8	7	25	6	1.5
98643	19		28 30	Insufficient material for Atterberg.	100	100	53	53	52	50	47	44	40	39	36	28			1.9
98644	19		30 32	Clayey Sandy Gravel (GC-GM)	100	100	93	78	59	52	45	38	28	25	21	16	24	6	1.6
98645	19		32 34	Clayey Sandy Gravel (GC-GM)	100	92	88	70	62	55	44	35	25	22	19	15	24	5	1.4

SPU FORM 66A

U.S. ARMY ENGINEER DIVISION LABORATORY -- SOUTH PACIFIC DIVISION

SOIL TEST RESULT SUMMARY

Division Serial No.	Hole No.	Field Sample No.	Depth Or Elevation		Laboratory Descriptive Classification	Mechanical Analysis - % Finer										Plasticity Limit Index	Field Moisture %	
			From	To		Gravel					Sand							Fines #200
						3/4	2	40	60	100	4	10	40	60	100			
92646	19		34	36	GRAVEL (GW-GC)	100	81	72	63	54	41	33	21	18	15	11	23	95
92647			36	38	MISSING													92.19
92648			38	40	GRAVEL (GW-GM)	100	83	73	64	54	41	32	21	18	15	11	23	95
92649			40	42	GRAVEL (GP-GC)	100	87	67	56	44	28	22	15	13	11	9	24	95
92650			42	44	GRAVEL (GP-GC)	100	76	57	49	42	33	25	18	15	13	11	25	95
92651			44	46	GRAVEL (GP-GC)	100	84	76	66	56	41	31	21	18	15	11	22	95
92652			46	48	GRAVEL (GP-GC)	100	75	58	48	41	31	24	15	13	11	8	24	95
92653			48	50	GRAVEL (GP-GC)	100	85	64	57	52	43	35	26	22	18	14	24	95
92654			50	52	GRAVEL (GC)	100	75	60	54	49	43	38	29	26	21	17	28	95
92655			52	54	GRAVEL (GW-GC)	100	77	64	63	60	51	39	20	16	14	11	24	95
92656			54	56	HEAVY GRAVELLY SAND (SW-SM)			100	97	81	61	19	12	9	7			92.19
92657			56	58	GRAVELLY SAND (SP)			100	97	78	51	5	2	2	2			95
92658			58	60	GRAVELLY SAND (SP)			100	96	76	54	8	4	3	3			95

Notes #19 8.0.4. @ 103'

U.S. ARMY ENGINEER DIVISION LABORATORY -- SOUTH PACIFIC DIVISION

SOIL TEST RESULT SUMMARY

Division Serial No.	Hole No.	Field Sample No.	Depth Or Elevation		Laboratory Descriptive Classification	Mechanical Analysis - % Finer										Plasticity Index	Field Moisture %			
			From	To		Gravel		Sand						Fines						
						#20	#40	#60	#100	#200	#4	#10	#40	#60	#100			#200		
78672	19		88	-	CLAYEY SAND (SP-SC)	100	98	98	93	72	74	63	41	22	19	16	12	30	9	P
78673			88	-	CLAYEY SAND (SW-SC)	100	97	91	83	75	83	57	40	20	17	14	11	31	10	W
78674			90	-	CLAYEY SAND	100	97	89	77	69	84	57	49	36	32	27	21	30	8	2.79
78675			92	-	GRAVEL (GC)	100	93	73	66	60	83	45	33	19	17	15	12	31	10	P
78676			94	-	SILT CLAYEY SAND (SC)	100	99	99	99	98	99	96	90	75	67	59	47	30	8	2.80
78677			96	-	GRAVEL (SC)	100	93	91	89	89	93	81	75	61	58	50	40	30	9	
78678			98	-	CLAYEY SAND	100	77	68	58	52	77	44	40	32	28	24	19	29	8	
78679			100	101	CLAYEY SAND	100	91	87	76	68	91	76	68	47	38	31	23	29	8	
78680	20		0	2	CLAYEY SAND (SC)	100	96	70	85	79	96	79	75	63	56	48	37	29	9	2.79
78681			2	4	CLAYEY SAND	100	80	69	55	47	87	39	34	27	24	20	16	29	9	
78682			4	6	CLAYEY SAND	100	73	54	46	34	73	34	26	15	13	10	8	27	9	P
78683			6	8	GRAVEL (GP-GC)	100	44	32	27	24	66	20	17	11	9	7	5	26	8	2.77
78684			8	10	CLAYEY SAND	100	74	62	55	45	84	45	36	23	19	16	13	27	8	

SPD Form 66A

* NOT REPORTED MATERIAL

U.S. ARMY ENGINEER DIVISION LABORATORY -- SOUTH PACIFIC DIVISION

SOIL TEST RESULT SUMMARY

PROJECT FOLJOM LAG PROGRAM

DATE

Division Serial No.	Hole No.	Field Sample No.	Depth Or Elevation		Laboratory Descriptive Classification	Mechanical Analysis - %										Liquid Limit %	Plasticity Index	Field Moisture %		
			From	To		Gravel			Sand				Fines							
						7/2	3/4	1/2	#4	#10	#40	#60	#100	#200						
98685	20		10	12	CLAYEY SANDY GRAVEL (GC)	100	74	60	49	44	37	32	24	21	18	14	27	9	62	
98686			12	14	CLAYEY SANDY GRAVEL (G.P.G.C.)	100	74	61	53	46	36	29	18	15	13	10	26	8	2.81	
98687			14	16		7	7	6	6	6	5	5	5	5	5	5	5	5		
98688			16	18		100	71	59	41	21	21	21	16	14	13	10	27	7	2.84	
98689			18	20	CLAYEY GRAVEL (G.P.G.C.)	100	57	33	30	27	23	21	16	14	13	10	27	7	2.84	
98690			20	22	CLAYEY GRAVEL (G.P.G.C.)	100	61	42	34	29	22	19	15	13	12	9	25	7		
98691			22	24	CLAYEY GRAVEL (G.P.G.C.)	100	72	53	35	30	22	19	15	13	12	9	27	8		
98692			24	26	CLAYEY SANDY GRAVEL (GC)	100	100	76	55	45	34	29	23	21	19	15	27	9	2.84	
98693			26	28	CLAYEY SANDY GRAVEL (GC)	100	88	65	73	66	55	48	36	35	31	25	27	9		
98694			28	30	MISSING															
98695			30	32	CLAYEY GRAVEL (G.P.G.C.)	100	79	56	35	27	18	14	10	9	8	7	26	8	2.84	
98696			32	34	CLAYEY GRAVEL (G.P.G.C.)	100	79	51	34	26	18	13	10	8	8	6	25	8		
98697			34	36	MISSING															

SPD Form 66A

U.S. ARMY ENGINEER DIVISION LABORATORY -- SOUTH PACIFIC DIVISION

SOIL TEST RESULT SUMMARY

Division Serial No.	Hole No.	Field Sample No.	Depth Or Elevation		Laboratory Descriptive Classification	Mechanical Analysis - % Finer										Liquid Limit %	Plasticity Index	Field Moisture %
			From	To		Gravel			Sand				Fines					
						3/4	1/2	3/8	#4	#10	#40	#60	#100	#200				
9F698	20		36	38	CLAYEY SANDY GRAVEL (SP-GC)	100	93				39	16	9	8	6	26	7	P284
9F699			38	40	CLAYEY SANDY GRAVEL (SP-GC)	100	78	54	55	45	21	13	11	8		24	6	P
9F700			40	42	CLAYEY SANDY GRAVEL (GC)	100	83	72	60	50	33	24	22	18		28	10	P285
9F701			42	44	GRAVEL (GP)	52	37	23	18	8	5	4	3			25	8	
9F702			44	46		100	89	66	56	42	29	14	9	7				
9F703			46	48		100	87	71	62	49	21	15	12	8				
9F704			48	50	CLAYEY SANDY GRAVEL (SP-GC)	100	84	64	53	45	27	18	15	13		25	8	P288
9F705			50	52	CLAYEY SANDY GRAVEL (SP-GC)	100	73	65	53	44	23	15	10	8		24	6	P
9F706			52	54	SANDY GRAVEL (GW)	100	94	79	65	39	14	8	6	4		24	6	P
9F707			54	56	CLAYEY SANDY GRAVEL (SP-GC)	100	77	69	56	45	28	18	10	8		24	6	P288
9F708			56	58	CLAYEY SANDY GRAVEL (SP-GC)	100	85	73	55	43	27	18	9	7		26	7	P
9F709			58	60	CLAYEY SANDY GRAVEL (SP-GC)	100	92	60	51	40	24	15	10	8		24	6	P
9F710			60	62	CLAYEY SANDY GRAVEL (SP-GC)	100	80	69	55	40	23	15	11	9		26	7	P284

SPD Form 66A

* NOT EMPLOYED FOR ATT

U.S. ARMY ENGINEER DIVISION LABORATORY -- SOUTH PACIFIC DIVISION

SOIL TEST RESULT SUMMARY

PROJECT: *Folsom Lab P.*

DATE

Division Serial No.	Hole No.	Field Sample No.	Depth Or Elevation		Laboratory Classification	Mechanical Analysis - % Finer										Li-liquid Limit Index	Plasticity Index	Field Moist %		
			From	To		Gravel					Sand								Fines #200	
						3/8	1/2	3/4	100	#4	#10	#40	#60	#100						
98724	20		98	100	SAND (SC)			100	97	96	94	89	25	62	45	40	31	25	9	64
98725			100	102	SAND (SC)			100	97	94	86	76	70	52	44	37	29	30	10	2.81
98726			102	104	GRAVEL (GP-GC)			100	86	72	60	37	30	21	18	15	16	29	10	P BDN
98727	21		0	2	GRAVEL (GP-GC)			100	50	71	59	51	40	31	20	16	13	10	29	P
98728			2	1	GRAVEL (GP-GC)			100	85	62	49	41	31	26	19	16	14	11	25	8
98729			4	6	GRAVEL (GP-GC)			100	82	64	51	46	34	18	15	13	12	10	25	8
98730			6	8	GRAVEL (GP-GC)			100	89	70	60	49	35	28	19	16	14	11	27	9
98731			8	10	SAND (SC) SM			100	96	87	80	74	65	57	43	36	29	22	24	7
98732			10	12	SAND (SC) SM			100	57	75	26	21	12	10	7	6	5	4	23	6
98733			12	14	GRAVEL (GP-GC)			100	58	56	49	46	40	36	31	28	24	18	23	6
98734			14	16	GRAVEL (GP-GC)			100	90	78	71	64	52	45	33	29	25	20	24	7
98735			16	18	GRAVEL (GP-GC)			100	86	75	65	56	42	33	22	18	15	11	24	7
98736			18	20	GRAVEL (GP-GC)			100	88	65	58	51	42	35	32	29	23	26	7	

SPD Form 66A

U.S. ARMY ENGINEER DIVISION LABORATORY -- SOUTH PACIFIC DIVISION

SOIL TEST RESULT SUMMARY

Division Serial No.	Hole No.	Field Sam- ple No.	Depth Or Elevation		Laboratory Descriptive Classification	Mechanical Analysis-% Finer										Plas- ticity Index	Field Moist % G _s	
			From	To		Gravel			Sand				Fines					
						3/4	3/8	2/4	#10	#40	#60	#100	#200	Li- quid Limit				
98737	21		20	22	CLAY SANDY SANDS (G.P.G.C.)	100	94	79	61	54	40	30	19	16	14	10	24	7
98738			22	21	CLAY SANDY SANDS (G.P.G.C.)	100	74	60	47	40	30	23	15	13	11	9	24	7
98739			24	26		100	85	69	54	48	39	30	20	18	15	11		
98740			26	28		100	77	66	51	50	40	31	21	18	15	12		
98741			28	30						100	99	96	91	88	83	72		
98742			30	32		100	77	55	50	46	40	35	27	24	20	16		
98743			32	34			100	74	65	60	48	38	25	20	16	11		
98744			34	36				100	93	85	71	60	40	33	26	18		
98745			36	38				100	92	85	72	57	30	21	15	10		
98746			38	40			100	85	67	60	47	36	25	22	19	14		
98747			40	42			96	86	72	66	54	44	30	25	22	16		
98748			42	44			100	91	86	72	65	51	41	29	25	21		
98749			44	46			97	84	74	68	54	45	31	27	24	18		

SPD Form 66A

U.S. ARMY ENGINEER DIVISION LABORATORY -- SOUTH PACIFIC DIVISION

SOIL TEST RESULT SUMMARY

Division Serial No.	Hole No.	Field Sample No.	Depth Or Elevation		Laboratory Descriptive Classification	Mechanical Analysis-%										Li-liquid Limit	Plasticity Index	Field Moist %
			From	To		Gravel			Sand				Fines					
						3/16	3/8	1/2	#4	#10	#40	#60	#100	#200				
98750	21		46	48		100	87	67	51	46	35	28	18	16	13	10		2.84
98751			48	50		100	91	83	67	60	45	37	26	22	19	14		2.83
98752			50	52		100	69	55	48	43	33	27	19	17	14	11		2.85
98753			52	54		100	86	65	52	44	32	24	15	12	10	8		2.83
98754			54	56		100	81	69	58	53	41	32	21	18	15	12		2.83
98755			56	58		100	77	64	53	46	34	26	16	14	12	10		2.85
98756			58	60			100	86	66	59	45	35	23	20	17	13		2.85
98757			60	62		100	91	77	68	50	36	25	16	14	12	10		2.85
98758			62	64		100	95	77	63	56	43	36	25	22	19	16		2.85
98759			64	66		100	96	80	68	62	52	45	30	26	23	19		2.85
98760			66	68		100	92	83	73	69	60	50	33	29	26	22		2.84
98761			68	70		100	89	78	64	59	51	44	28	25	22	19		2.84
98762			70	72		100	90	88	78	64	54	46	38	25	22	16		2.84

U.S. ARMY ENGINEER DIVISION LABORATORY -- SOUTH PACIFIC DIVISION

SOIL TEST RESULT SUMMARY

PROJECT	FO.	SOM	AB	PJ	DATE	Laboratory Descriptive Classification	Mechanical Analysis - % Finer											Li-Plas-Field Liquid Limit Index %	Plasticity Index %			
							Gravel			Sand					Fines							
							3/16	1/2	3/8	#4	#10	#40	#60	#100	#200	#200	#100			#60	#40	
78763	21						100	82	77	68	62	58	50	43	29	26	23	18			61	
78764							100	92	89	77	68	63	52	42	28	24	21	17				2.84
98765							100	86	86	69	60	54	44	35	22	19	17	14				2.84
98766							100	94	93	78	67	60	45	34	22	19	17	14				2.84
98767							100	90	84	72	65	61	52	44	30	27	23	19				2.84
98768	22						100	86	86	75	68	61	49	40	31	28	26	22				2.83
98769							100	71	71	65	47	39	28	22	15	13	10	8				2.82
98770							100	72	72	68	51	42	31	23	14	11	9	6				2.82
98771							100	63	63	63	53	48	40	35	21	16	13	9				2.82
98772							100	100	100	46	36	27	15	9	8	7	7	5				2.87
98773							100	100	100	87	76	58	47	28	20	19	14	8				2.87
98774							100	91	77	60	51	33	21	12	11	9	7					2.87
98775							100	78	71	54	45	28	17	10	9	7	6					2.87

SPD Form 66A

U.S. ARMY ENGINEER DIVISION LABORATORY -- SOUTH PACIFIC DIVISION

SOIL TEST RESULT SUMMARY

Division Serial No.	Hole No.	Field Sample No.	Depth Or Elevation		Laboratory Descriptive Classification	Mechanical Analysis - % Finer										Li- quid Limit %	Plas- ticity Index	Field Moist %
			From	To		Gravel			Sand				Fines					
						3/8	1/2	3/4	#4	#10	#40	#60	#100	#200				
98776	22		22	24		100	100	57	24	14	8	4	3	2			2.85	
98777			24	26		100	100	52	36	26	18	11	9	8	6			2.85
98778			26	28					100	97	97	49	26	14	10			
98779			38	46					100	89	39	6	3	2	1			
98780			46	48					100	98	96	90	76	67	60			2.82
98781			48	58					100	96	90	79	52	45	38			
98782			68	78					100	93	88	70	51	39	36			
98783			84	87					100	85	63	40	26	21	18			2.86
98784	23		0	4					100	85	78	61	53	40	37			
98785			4	6					100	89	52	37	25	20	13			
98786			6	8					100	83	57	43	28	21	12			2.84
98787			8	18					100	86	74	66	54	46	32			
98788			28	34					100	83	62	40	22	17	9			

SPD Form 66A

U.S. ARMY ENGINEER DIVISION LABORATORY -- SOUTH PACIFIC DIVISION

SOIL TEST RESULT SUMMARY

Division Serial No.	Hole No.	Field Sample No.	Depth Or Elevation		Laboratory Descriptive Classification	Mechanical Analysis - % Finer										Li-Plasticity Index	Field Moist %
			From	To		Gravel			Sand				Fines				
						3/16	1/4	3/8	#4	#10	#40	#60	#100	#200			
98789	23		34	36		100	86	69	55	50	40	30	20	18	15	12	2.82
98790			36	38		100	95	55	44	36	25	20	11	9	8	6	2.84
98791			38	44		100	67	54	47	42	33	26	18	16	13	10	2.81
98792			44	48		100	76	64	60	57	51	46	33	28	24	18	2.79
98793			48	50		100	91	66	48	41	32	26	16	13	11	9	2.83
98794			50	52		100	95	66	40	33	23	16	8	6	5	4	2.81
98795			52	58		100	81	61	78	73	58	46	25	19	16	13	2.79
98796			58	68					100	96	91	80	46	35	26	18	2.83
98797			68	78						100	87	78	62	55	45	33	2.79
98798			78	80					100	99	96	94	84	73	65	55	2.83
98799	24		0	2		100	92	82	74	58	47	35	32	29	26		
98800			2	4		100	87	74	69	53	42	29	25	22	18		
98801			4	6		100	95	87	75	60	40	27	16	14	12	9	

SPD Form 66A

U.S. ARMY ENGINEER DIVISION LABORATORY -- SOUTH PACIFIC DIVISION

SOIL TEST RESULT SUMMARY

Division Serial No.	Hole No.	Field Sample No.	Depth Or Elevation		Laboratory Descriptive Classification	Mechanical Analysis - % Finer										Li-Plas-Field Liquid Limit Index %	Plasticity Index %
			From	To		Gravel			Sand				Pines				
						2 1/2	1/4	3/8	#4	#10	#40	#60	#100	#200			
98802	24		6	8		100	91	71	57	34	20	10	8	7	5	67	2.87
98803			8	18		100	79	55	43	25	21	15	13	11	8		
98804			18	28		100	79	52	38	21	15	10	9	7	6		
98805			28	38			100	77	99	77	73	46	19	15	13		2.84
98806			38	40		100	78	70	67	65	50	40	23	18	14		
98807			48	58		100	75	52	39	31	19	14	8	7	5		
98808			58	60		100	74	55	43	35	20	14	9	8	7		2.85
98809			60	62		100	88	78	68	61	47	35	26	23	20		
98810			62	64			100	77	65	58	43	31	20	17	14		-80N
98811	25		0	2			100	73	63	52	36	28	24	21	18		2.79
98812			2	4		100	78	72	59	49	36	28	19	16	14		
98813			4	6		100	80	80	60	51	35	30	21	19	16		
98814			6	8		100	89	89	76	64	44	29	16	14	13		2.88

SPD Form 66A

U.S. ARMY ENGINEER DIVISION LABORATORY -- SOUTH PACIFIC DIVISION

SOIL TEST RESULT SUMMARY

PROJECT: FOLSOM LAB P.1

DATE

Division Serial No.	Hole No.	Field Sample No.	Depth Or Elevation		Laboratory Descriptive Classification	Mechanical Analysis - % Finer										Li-Plasticity Index	Field Moist %		
			From	To		Gravel			Sand				Fines						
						3/8	1/2	3/4	#4	#10	#40	#60	#100	#200					
98815	25		8	10		100	41	19	13	7	5	3	2	1	1	1	1	NP	
98816			10	12		100	100	93	82	75	56	42	27	23	20	15			
98817			12	14		100	61	50	42	33	28	20	13	8	7	6	5		2.85
98818			14	16		100	100	71	43	36	7	6	4	4	3	2			
98819			16	18	GRAVEL (GP)	100	12	7	7	5	3	1	1	0	0	0			
98820					NO SUCH SAMPLE														
98821			18	20		100	78	78	78	78	56	14	7	3	3	3			2.79
98822			20	22	GRAVEL (GP)	100	7	7	7	7	4	3	3	3	3	2			
98823			22	24		100	86	74	57	49	36	24	15	12	10	7			
98824			24	26		100	100	80	58	50	33	23	12	10	8	5			2.84
98825			26	28		100	89	80	55	47	31	20	11	8	7	5			
98826			28	30		100	64	55	40	38	32	25	15	14	12	8			
98827			30	32		100	85	67	51	44	31	22	13	10	8	6			2.82

SPD Form 66A

U.S. ARMY ENGINEER DIVISION LABORATORY -- SOUTH PACIFIC DIVISION

SOIL TEST RESULT SUMMARY

Division Serial No.	Hole No.	Field Sam- ple No.	Depth Or Elevation		Laboratory Descriptive Classification	Mechanical Analysis - % Finer											Li- quid Limit % Plasticity Index	Field Moist % Index
			From	To		Gravel			#4	Sand			#100	#200				
						3/8	1/2	3/4		#10	#40	#60						
98828			32	34		100	89	73	54	15	33	25	16	13	11	8	65	
98829			34	36		100	95	80	55	17	33	24	14	12	10	8	2.83	
98830			36	38		100	93	76	60	53	38	29	18	15	13	10	2.83	
98831			38	40			100	76	42	26	14	12	7	6	5	4		
98832			40	42		100	94	77	57	50	36	26	16	14	11	8	2.82	
98833			42	44		100	97	77	56	49	34	23	13	11	9	7	2.82	
98834			44	46		100	95	79	59	51	38	28	17	15	13	11		
98835			46	48		100	95	78	66	57	40	28	17	14	12	10	2.83	
98836			48	50		100	93	76	53	45	32	27	19	16	14	10		
98837			50	52		100	92	75	53	45	33	26	16	14	12	10		
98838			52	54		100	86	70	55	50	38	28	17	14	12	8		
98839			54	56		100	98	84	63	55	40	30	20	17	15	11	2.84	
98840			56	58		100	91	76	60	53	40	31	19	16	14	11		

SPD Form 66A

U.S. ARMY ENGINEER DIVISION LABORATORY -- SOUTH PACIFIC DIVISION

SOIL TEST RESULT SUMMARY

PROJECT **FU-SOM LAB P.**

DATE

Division Serial No.	Hole No.	Field Sam- ple No.	Depth Or Elevation		Laboratory Descriptive Classification	Mechanical Analysis - % Finer										Li- quid Limit %	Plas- ticity Index	Field Moist %	
			From	To		Gravel			Sand				Fines						
						#2	#10	#40	#60	#100	#200								
98841			58	60		100	79	34	72	38	23	17	11	9	8	6	61		
98842			60	62			100	74	49	39	33	23	17	11	9	8	6	2.84	
98843			62	64		100	92	78	63	56	41	32	19	16	13	10		2.84	
98844			64	66		100	87	71	59	53	40	31	18	15	12	8		2.83	
98845			66	68		100	84	63	48	42	31	24	15	13	10	7		2.83	
98846			68	70		100	73	53	31	27	19	14	10	9	9	7		2.84	
98847			70	72		100	81	67	53	47	36	26	15	12	10	7		2.84	
98848			72	74			100	89	71	61	45	34	20	20	14	10		2.84	
98849			74	76		100	88	69	52	46	35	25	14	11	8	6		2.83	
98850			76	78		100	74	60	46	41	29	20	13	11	9	7		2.83	
98851			78	80		100	87	61	48	39	28	21	15	13	11	8		2.83	
98852			80	82			100	85	72	64	46	34	19	16	13	10		2.87	
98853			82	84			100	91	77	70	58	44	22	19	16	11		2.87	

SPD Form 66A

U.S. ARMY ENGINEER DIVISION LABORATORY -- SOUTH PACIFIC DIVISION

SOIL TEST RESULT SUMMARY

PROJECT	Division Serial No.	Hole No.	Field Sample No.	Depth Or Elevation		Laboratory Descriptive Classification	Mechanical Analysis - % Finer										Li- quid Limit %	Plas- ticity Index %	Field Moist %				
				DATE			Gravel			Sand				Fines									
				From	To		3	3 1/2	3/4	1/2	3/8	#4	#10	#40	#60	#100				#200			
	92267			124	126		100	87	77	74	52	43	29	18	6	5	4	3				61	
	92268			126	128		100	91	83	63	55	45	31	20	11	9	8	6					284
	92269			128	130		100	95	77	60	47	40	27	18	8	7	6	5					284
	92270			130	132		100	76	70	60	50	43	30	20	11	9	8	6					284
	92271			132	134		100	67	67	52	46	41	30	20	10	8	6	5					284
	92272			134	136		100	96	88	63	56	51	42	33	15	10	8	6					284
	92273			136	138		100	95	73	75	68	62	51	39	18	12	7	3					284
	92274			138	140		100	81	70	57	46	42	34	28	16	12	7	3					280
	92275			140	142		100	81	75	64	39	31	7	6	5	4	3	3					280
	92276			142	144		100	78	25	60	54	48	41	34	24	20	17	13					280
	92277			144	145		100	90	86	76	69	65	57	36	17	13	10	7					80H
	92278	21		145	145		100	90	88	81	77	75	70	67	58	49	39	29					285
	92279			4	6		100	88	88	66	54	47	34	25	14	11	8	5					285

SPD Form 66A

U.S. ARMY ENGINEER DIVISION LABORATORY -- SOUTH PACIFIC DIVISION

SOIL TEST RESULT SUMMARY

PROJECT	FOLSOM LAB P.	Division Serial No.	Hole No.	Field Sample No.	Depth Or Elevation		Laboratory Descriptive Classification	Mechanical Analysis - % Finer										Li- quid Limit %	Plas- ticity Index %	Field Moist. %
					From	To		Gravel			Sand				Fines					
								#2	#10	#20	#4	#10	#40	#60	#100	#200				
98860		26			6	8		100	68	51	33	23	16	9	7	6	4	61		
98871					8	14		100	16	11	6	4	3	2	1	1	1			2.77
98882					14	16		100	68	51	37	31	27	18	14	11	8			
98893					16	18		100	25	28	17	13	7	4	2	2	1			
98894					18	22		100	68	51	38	22	17	10	8	6	5			2.64
98895					22	28		100	61	39	28	19	13	10	5	3	2			2.15
98896					28	31	MISSING													
98897					34	38		100	64	51	38	26	26	26	26	25	20			2.87
98898					38	42		100	75	61	45	39	27	18	8	6	4			
98899					42	48		100	48	37	31	23	16	11	5	3	2			
98900					48	52		100	81	59	44	33	23	14	12	10	7			2.83
98901					52	58		100	91	64	43	29	20	10	8	6	4			
98902					58	60		100	72	60	36	22	16	10	8	6	5			

SPD Form 66A

U.S. ARMY ENGINEER DIVISION LABORATORY -- SOUTH PACIFIC DIVISION

SOIL TEST RESULT SUMMARY

PROJECT FOLSOM LAB P.1

DATE

Division Serial No.	Hole No.	Field Sam- ple No.	Depth Or Elevation		Laboratory Descriptive Classification	Mechanical Analysis - % Finer										Li- quid Limit % Plas- ticity Index	Field Moist % 2.85	
			From	To		Gravel					Sand							Fines #200
						#2	#10	#20	#40	#60	#100	#200	#4	#10	#20			
92893	26		60	62		100	87	34	58	48	33	22	12	10	8	6		2.85
92894			62	64		100	89	63	52	45	34	25	15	12	9	7		2.85
92895			64	66		100	73	62	51	44	38	26	18	9	7	5		2.83
92896			66	68		100	91	61	50	43	28	19	9	7	6	4		2.83
92897			68	70		100	78	63	57	46	38	24	16	8	7	6		2.85
92898			70	72		100	66	51	42	36	31	23	18	11	8	6		2.85
92899			72	74		100	82	70	64	56	47	31	21	10	8	6		2.85
92900			74	76		100	73	61	53	47	39	27	20	13	11	8		2.85
92901			76	78		100	92	71	62	50	41	29	19	6	3	2		2.85
92902			78	82		100	53	44	39	33	28	20	16	9	7	4		2.85
92903			82	84		100	88	65	58	47	39	26	18	9	7	6		2.85
92904			84	86		100	87	75	68	55	46	32	23	12	9	7		2.85
92905			86	88		100	94	72	75	60	53	38	23	8	6	4		2.85

SPD Form 66A

APPENDIX B
DATA ACQUIRED FROM BECKER HAMMER DRILL PENETRATION
TESTS FOR PHASE II FIELD INVESTIGATIONS

1. Figures B1 through B26 contain data acquired from each of the 26 open- and closed-bit Becker soundings performed during the Phase II field investigations in 1986. Each figure contains plots of equivalent Standard Penetration Test blowcount N_{60} , equivalent overburden corrected SPT blowcount $(N_1)_{60}$, percentage of fines of Becker samples divided by 2, liquid limit, and the plasticity index versus depth. N_{60} was converted into $(N_1)_{60}$ using the blowcounts from the closed bit soundings. The raw Becker blowcounts N_B were converted into the equivalent SPT N_{60} blowcounts in Appendix A by Dr. Leslie F. Harder, Jr. The N_{60} values were in turn corrected for overburden using the procedures and charts discussed in Part III of the report. The fines content of the gradations of the Becker samples retrieved from the open-bit soundings was divided by a factor of two to account for their tendency to overestimate the fines content of in situ gradations of the materials present in the field. The liquid and plastic limit index tests were performed by the South Pacific Division Laboratories.

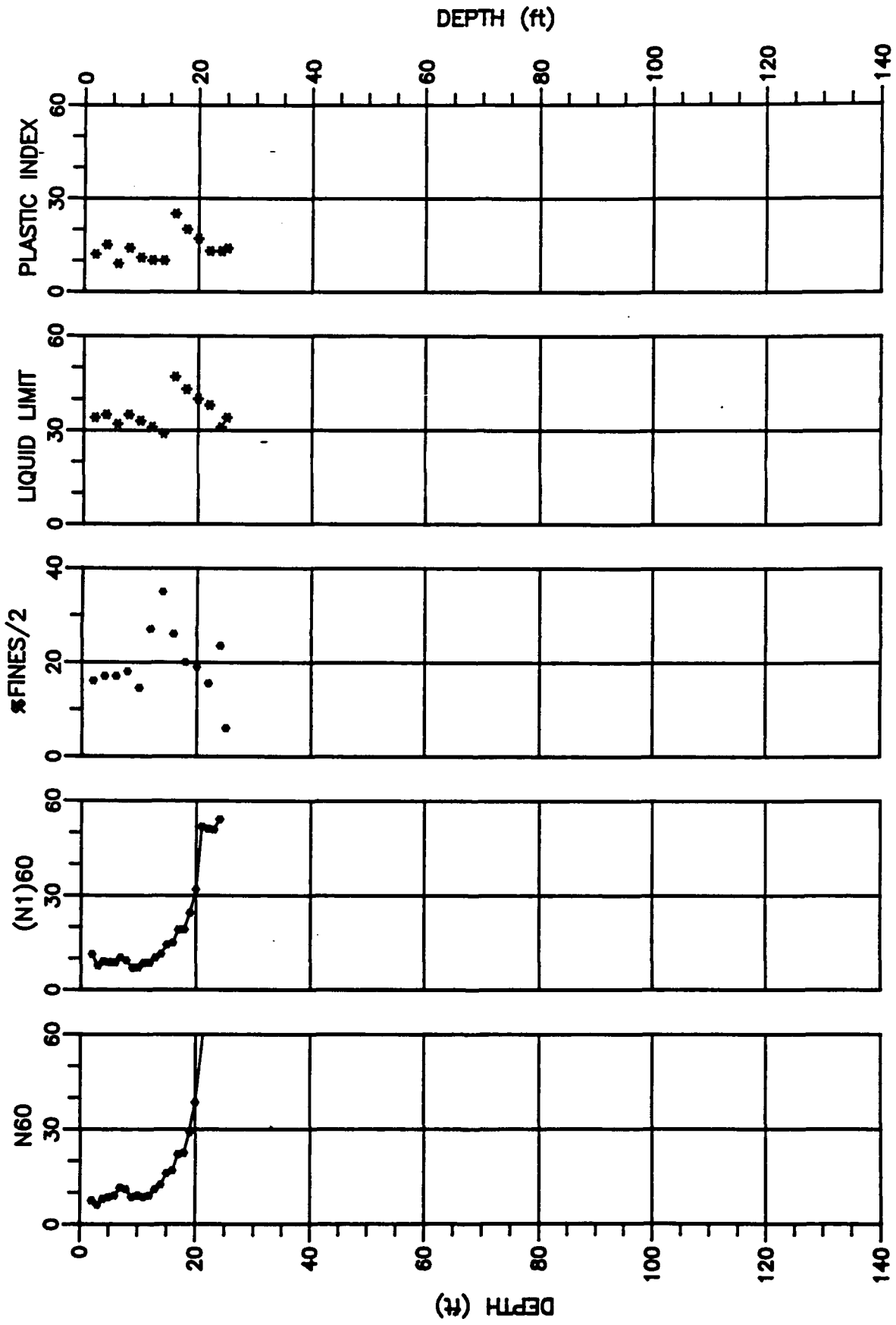


Figure B1. Data acquired from Becker Penetration Sounding BH1

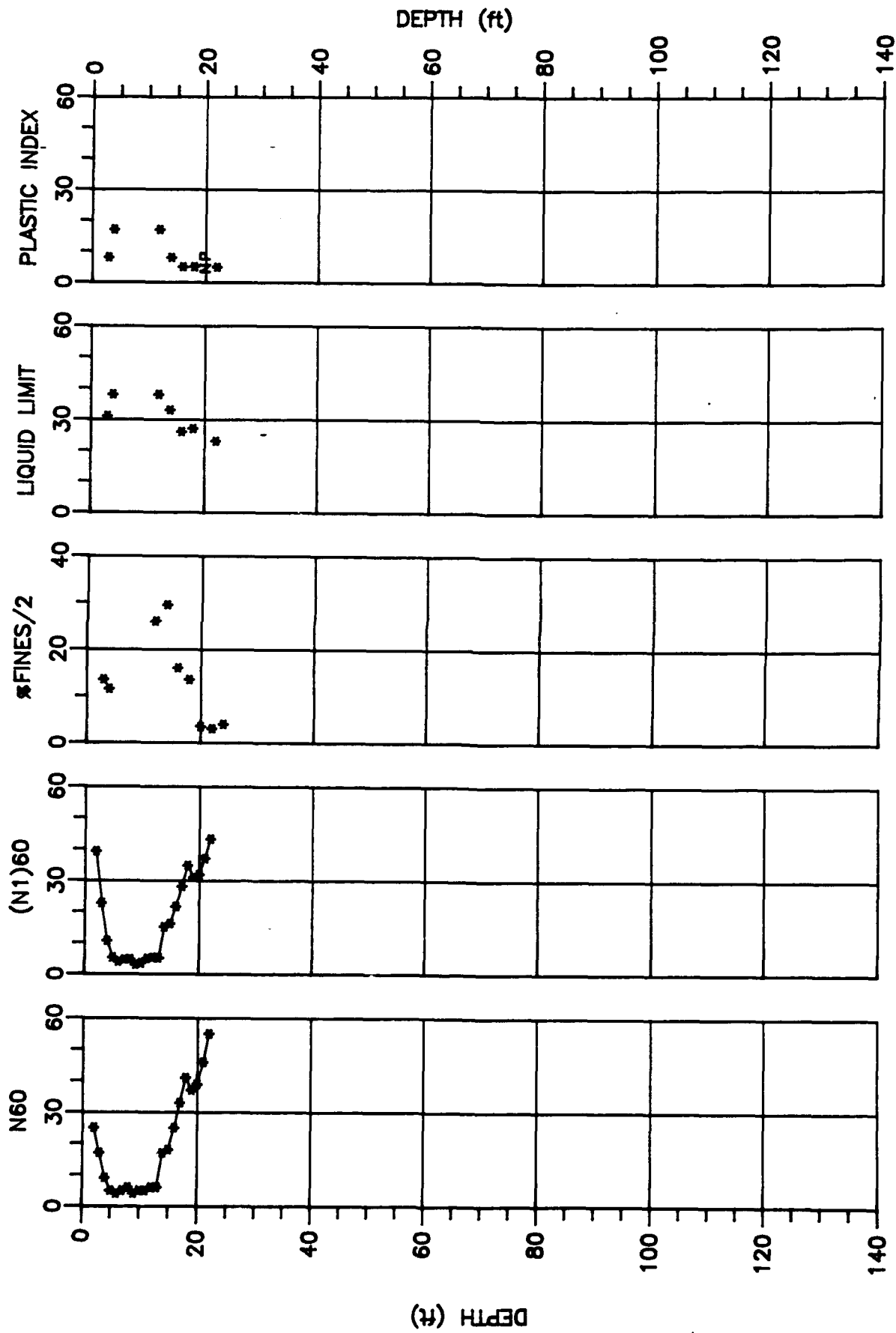


Figure B2. Data acquired from Becker Penetration Sounding BH2

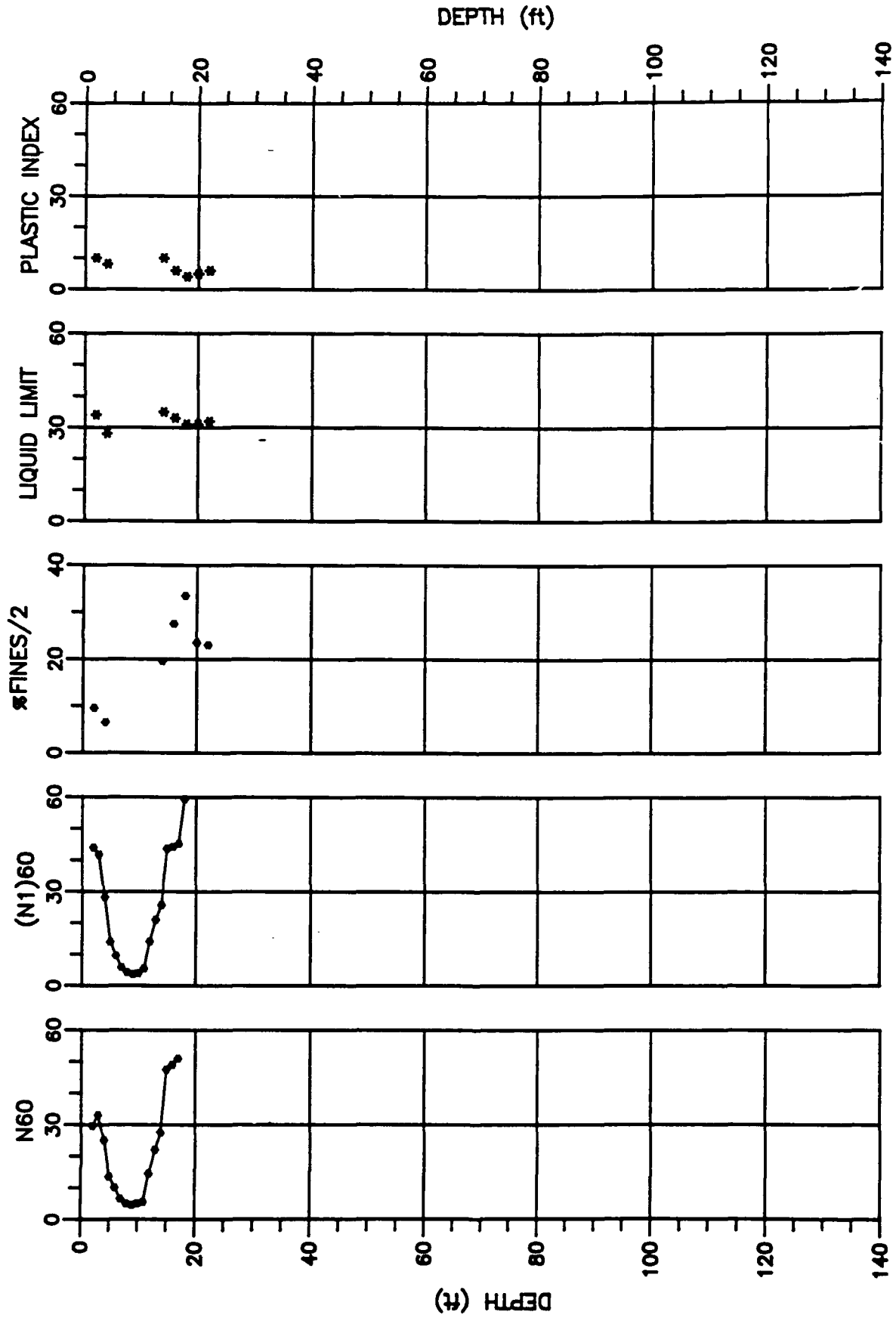


Figure B3. Data acquired from Becker Penetration Sounding BH3

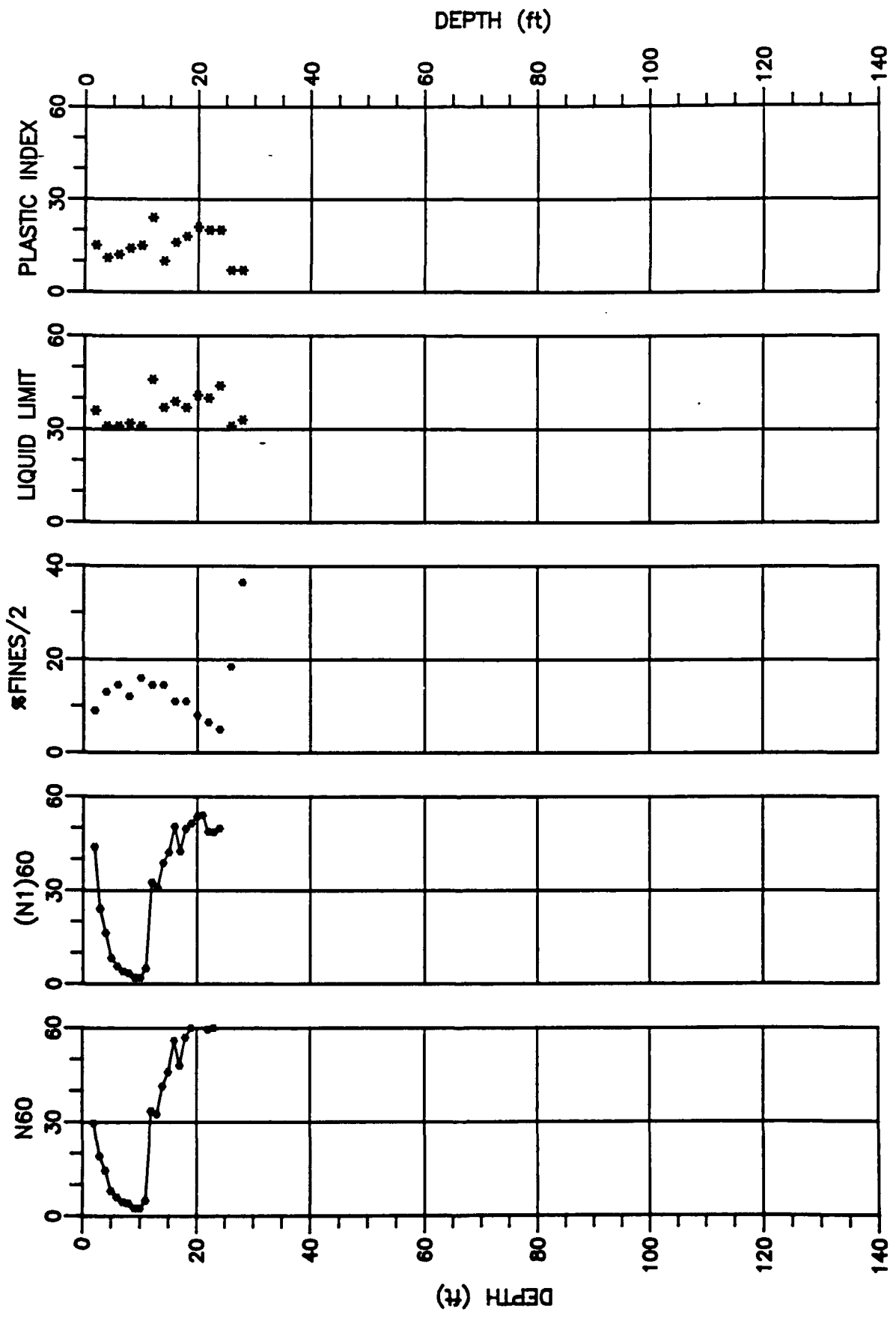


Figure B4. Data acquired from Becker Penetration Sounding BH4

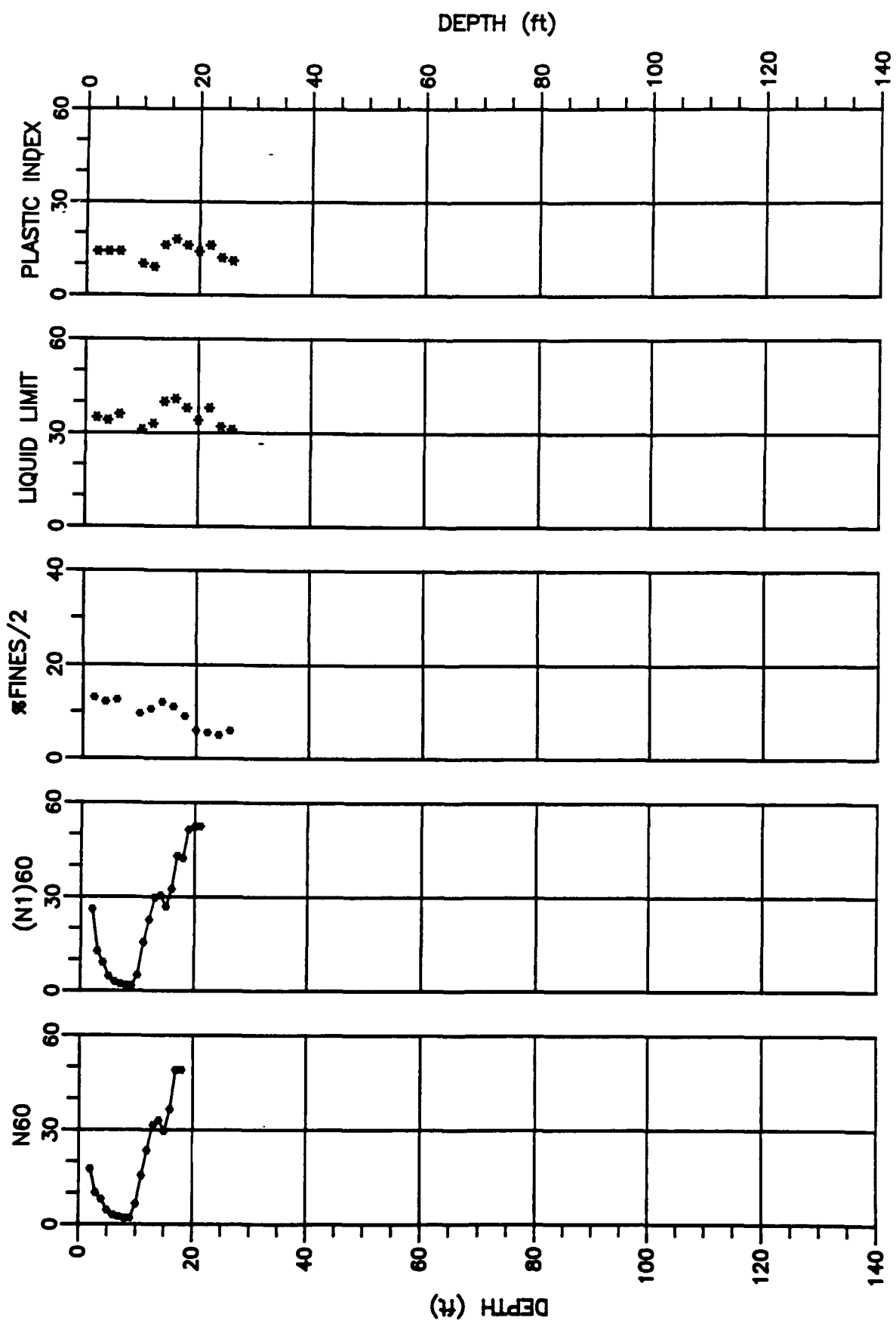


Figure B5. Data acquired from Becker Penetration Sounding BH5

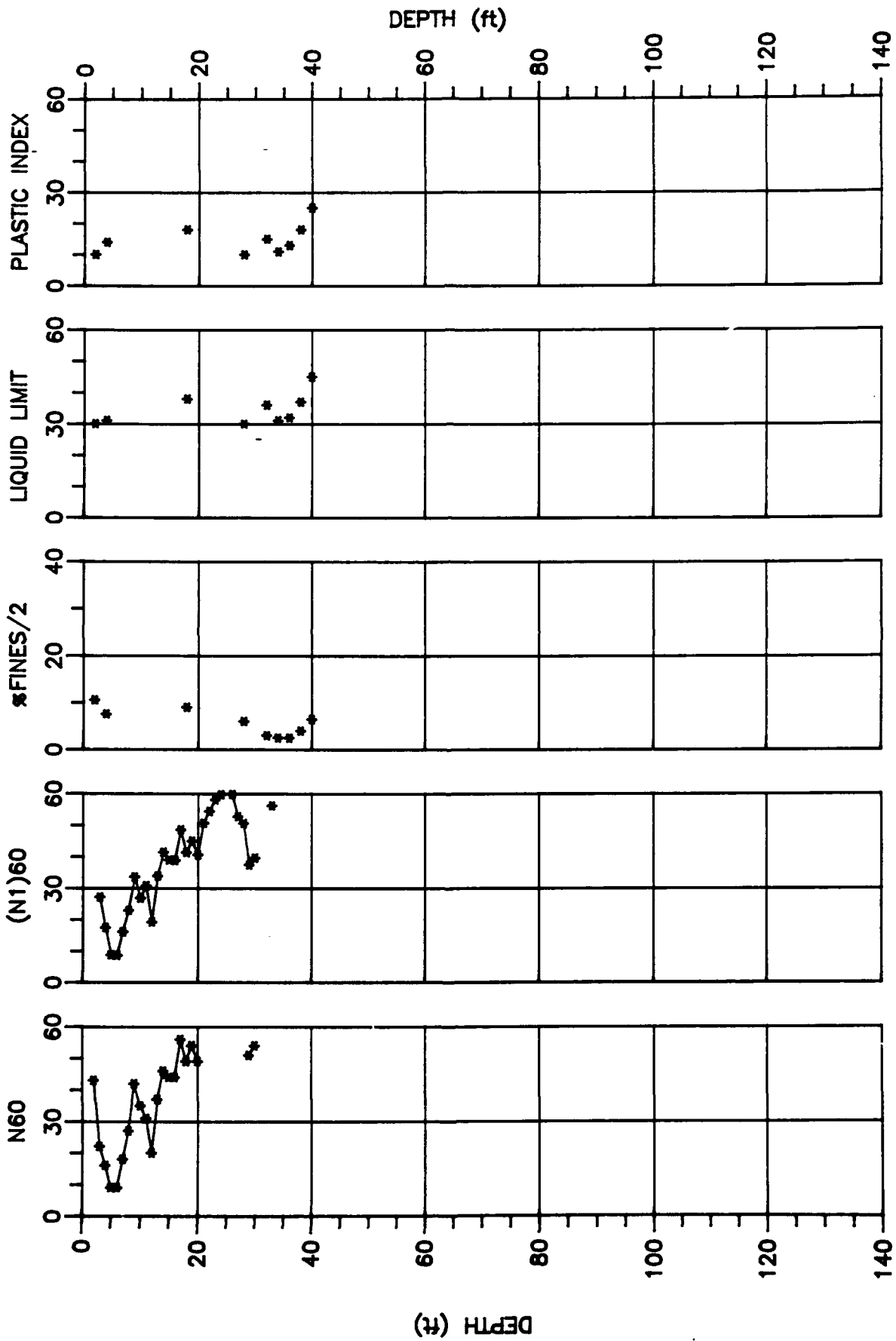


Figure B6. Data acquired from Becker Penetration Sounding BH6

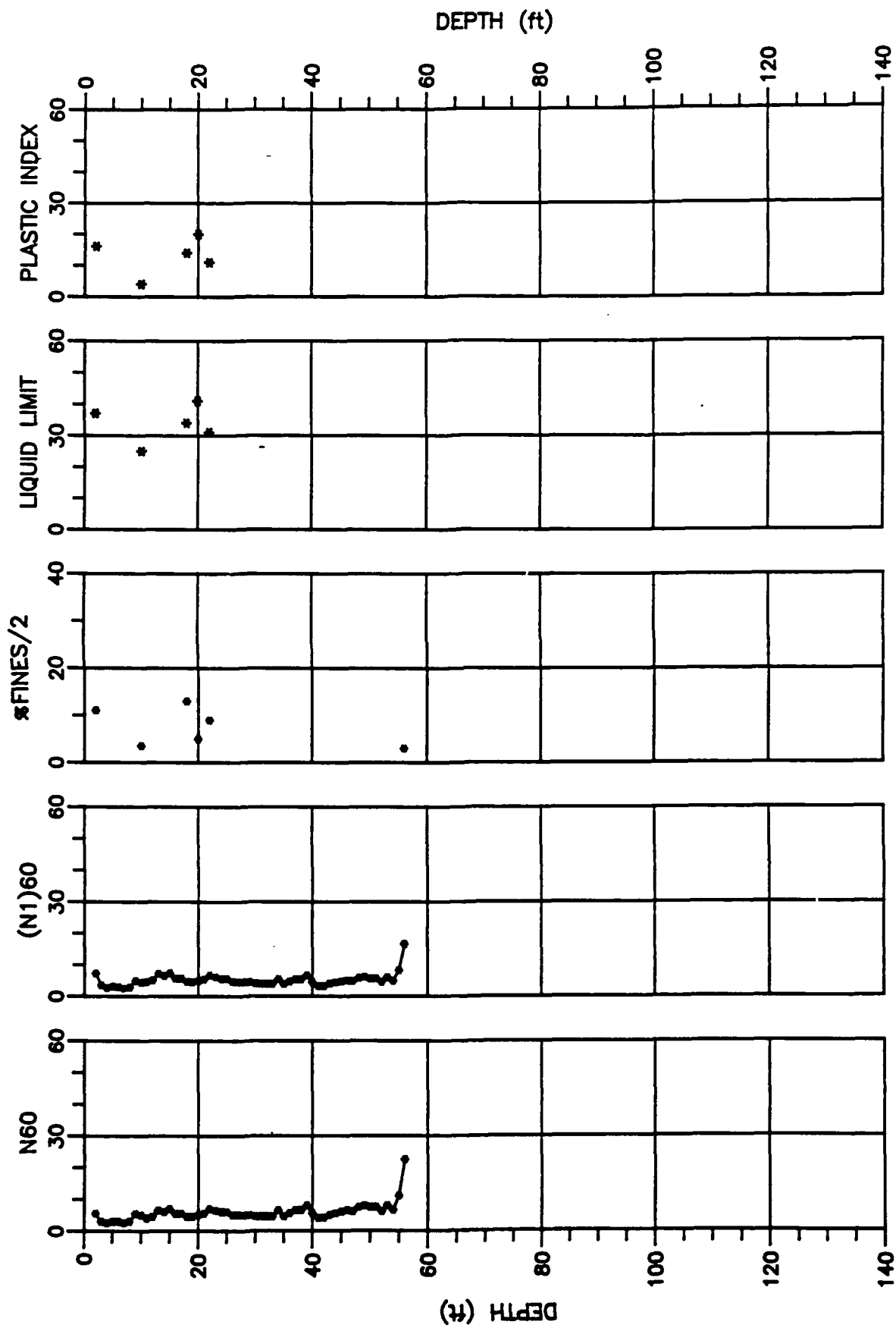


Figure B7. Data acquired from Becker Penetration Sounding BH7

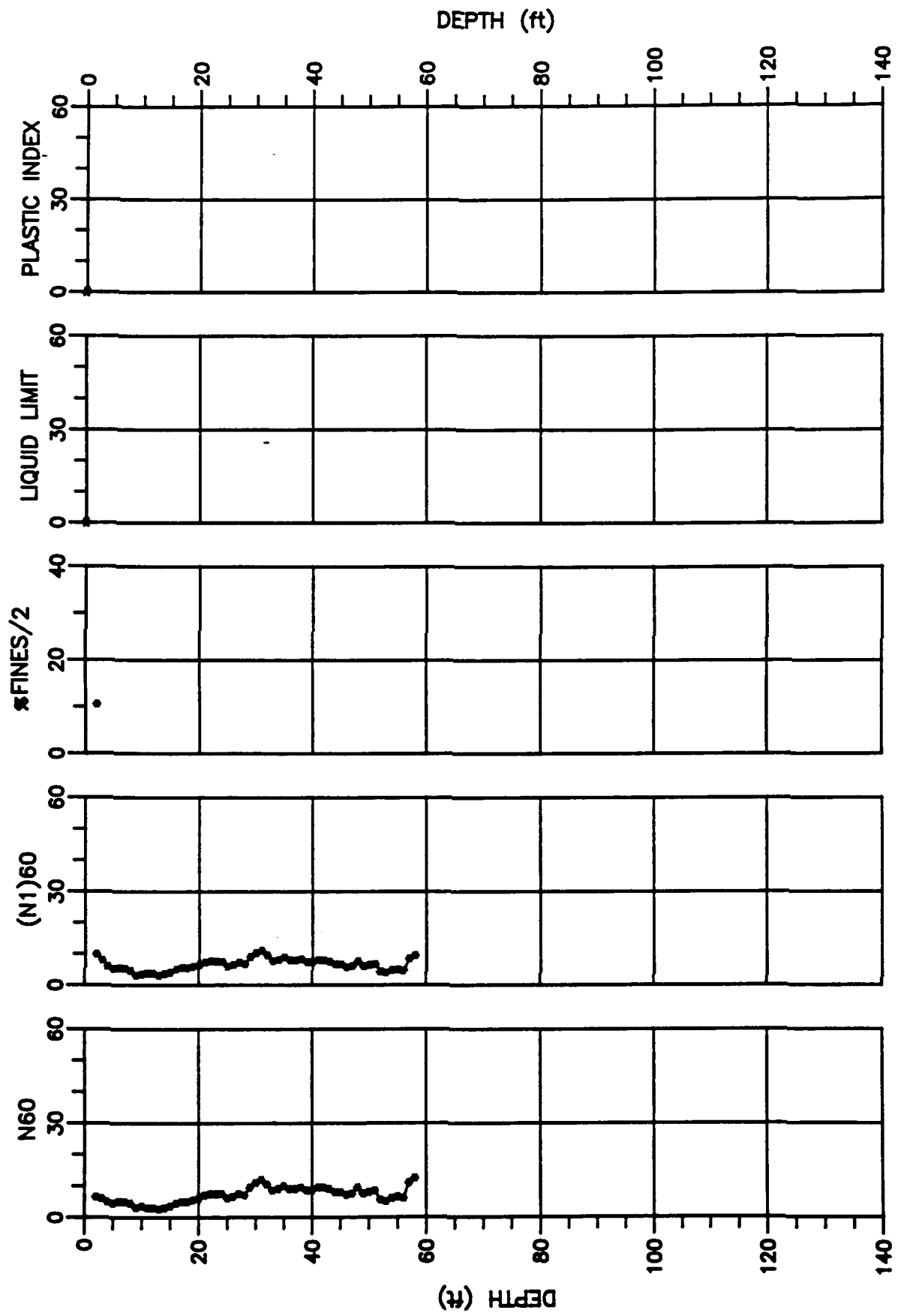


Figure B8. Data acquired from Becker Penetration Sounding BH8

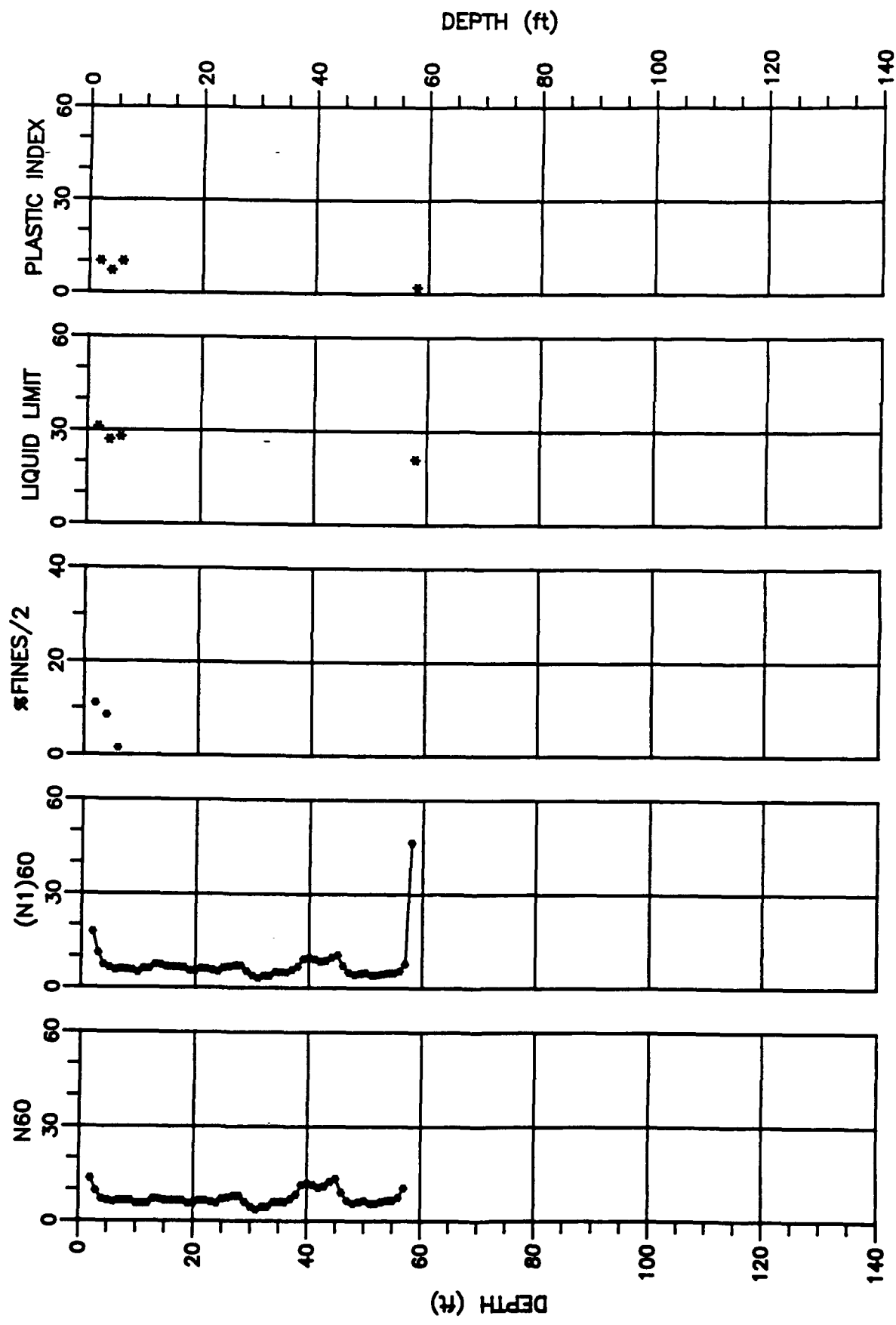


Figure B9. Data acquired from Becker Penetration Sounding BH9

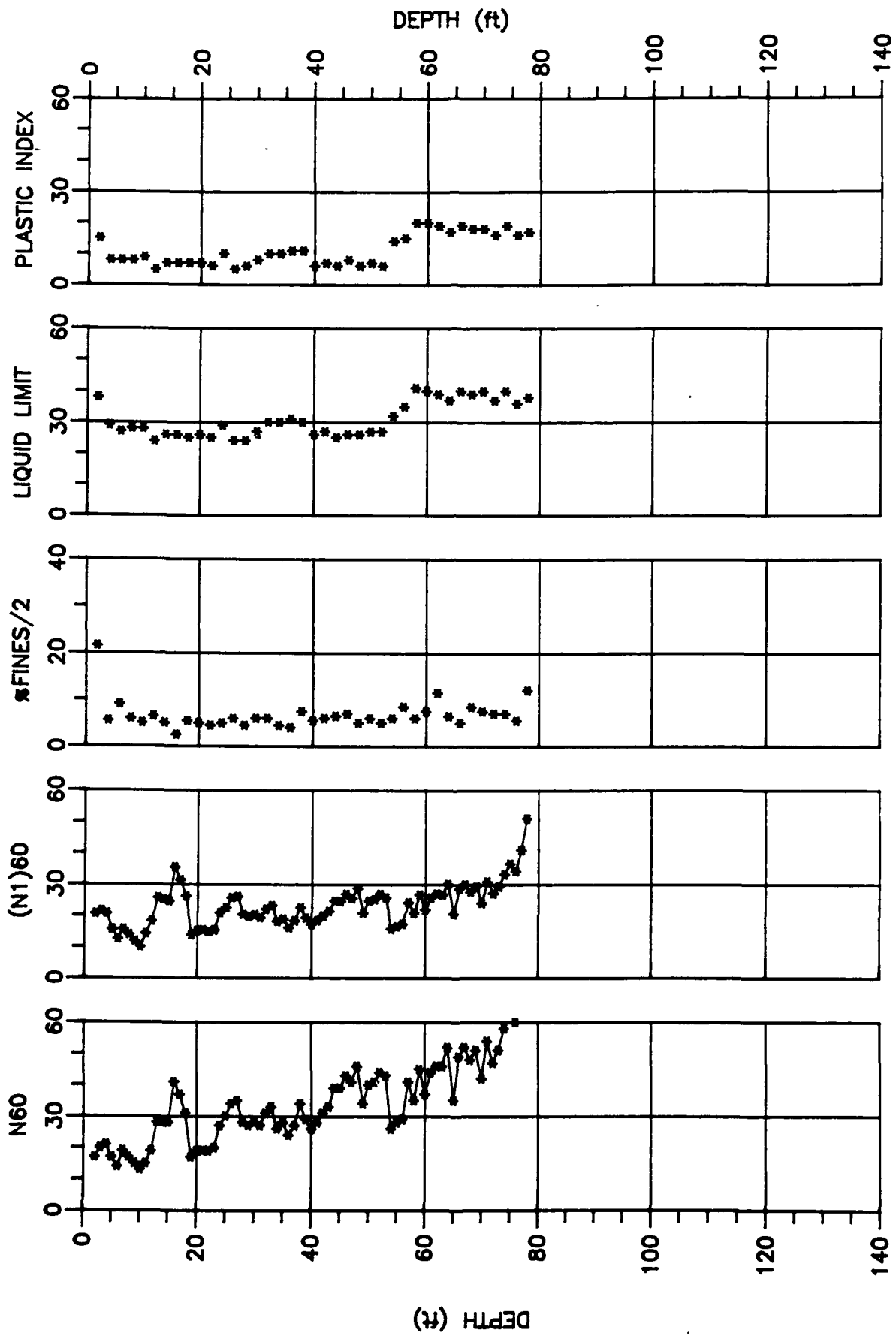


Figure B10. Data acquired from Becker Penetration Sounding BH10

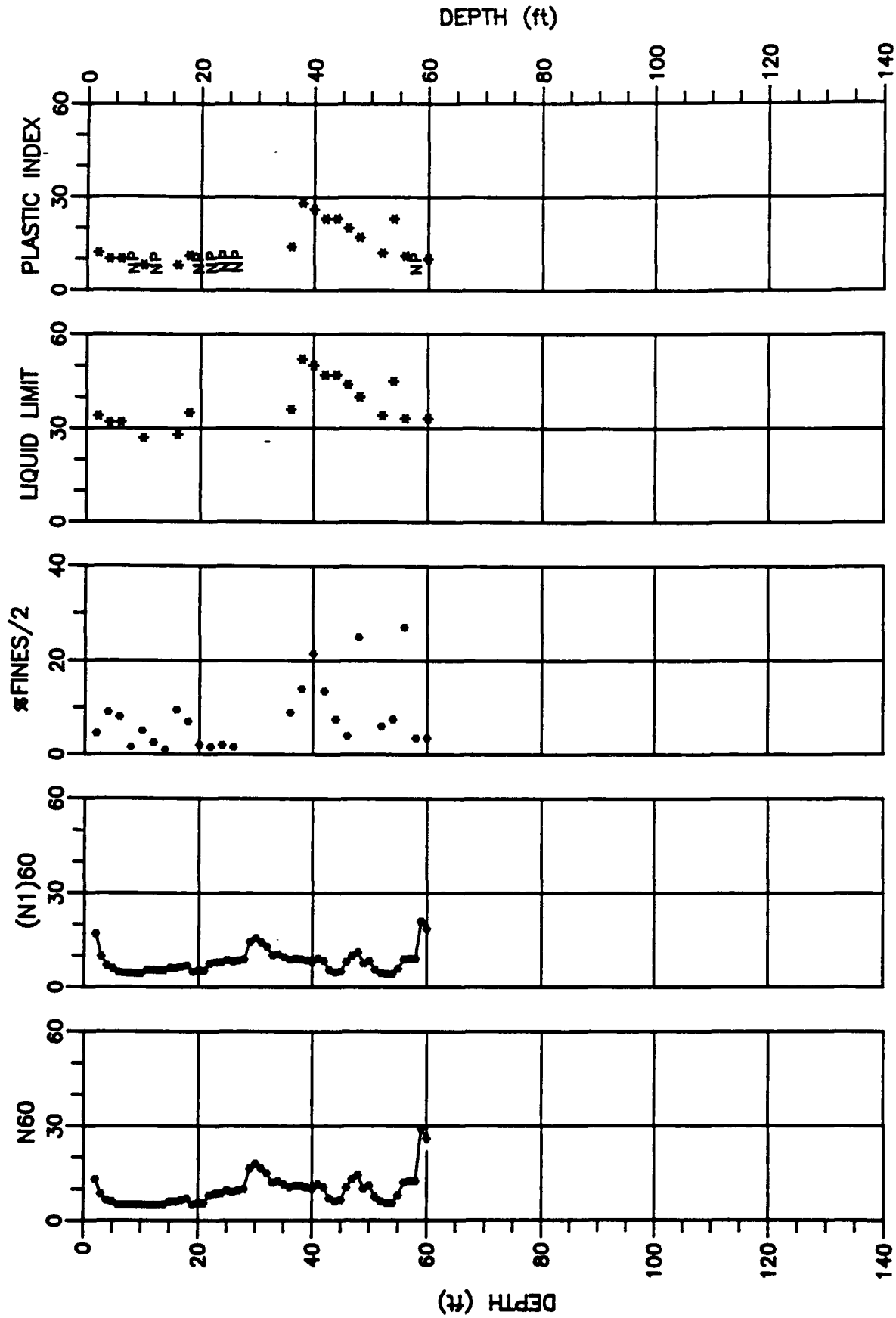


Figure B11. Data acquired from Becker Penetration Sounding BH11

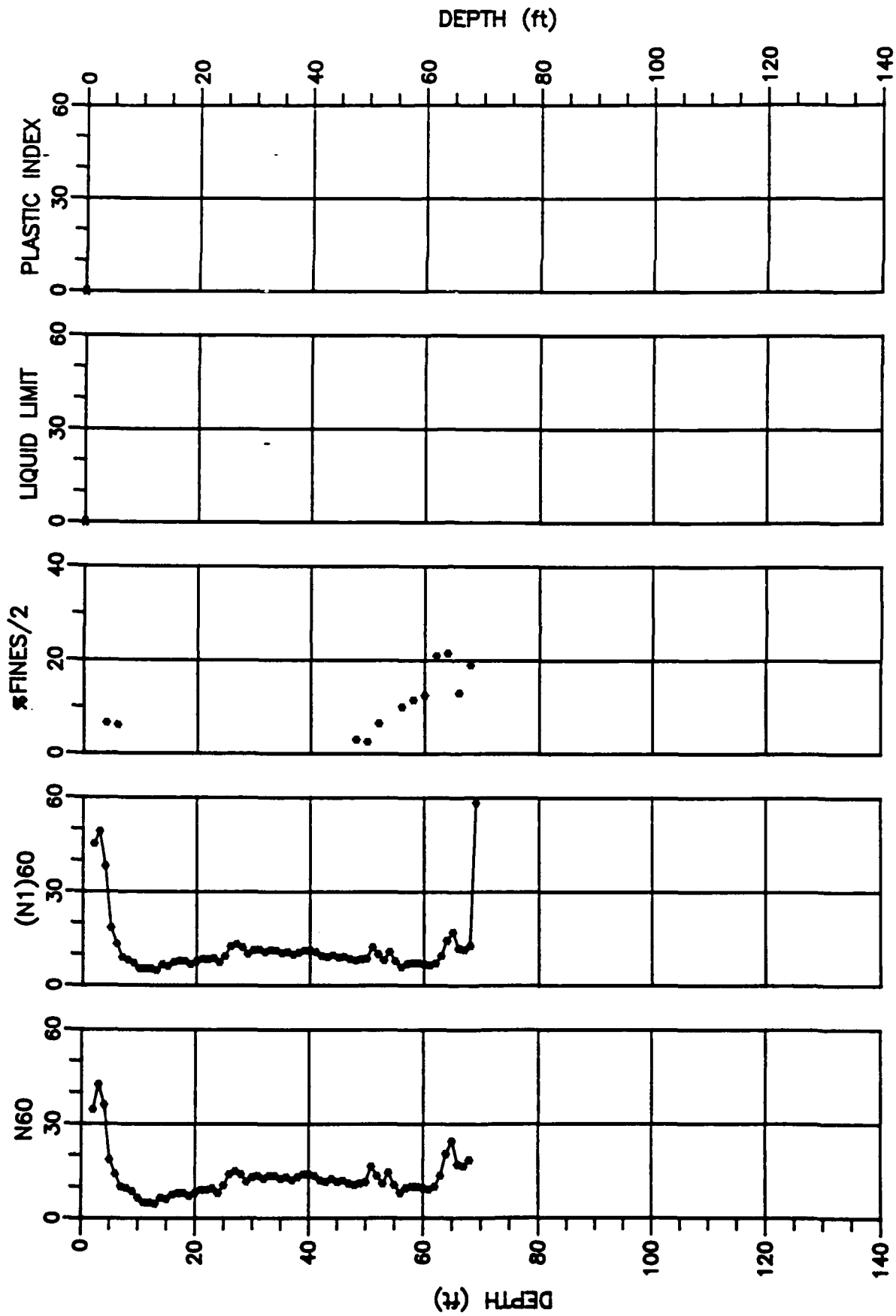


Figure B12. Data acquired from Becker Penetration Sounding BH12

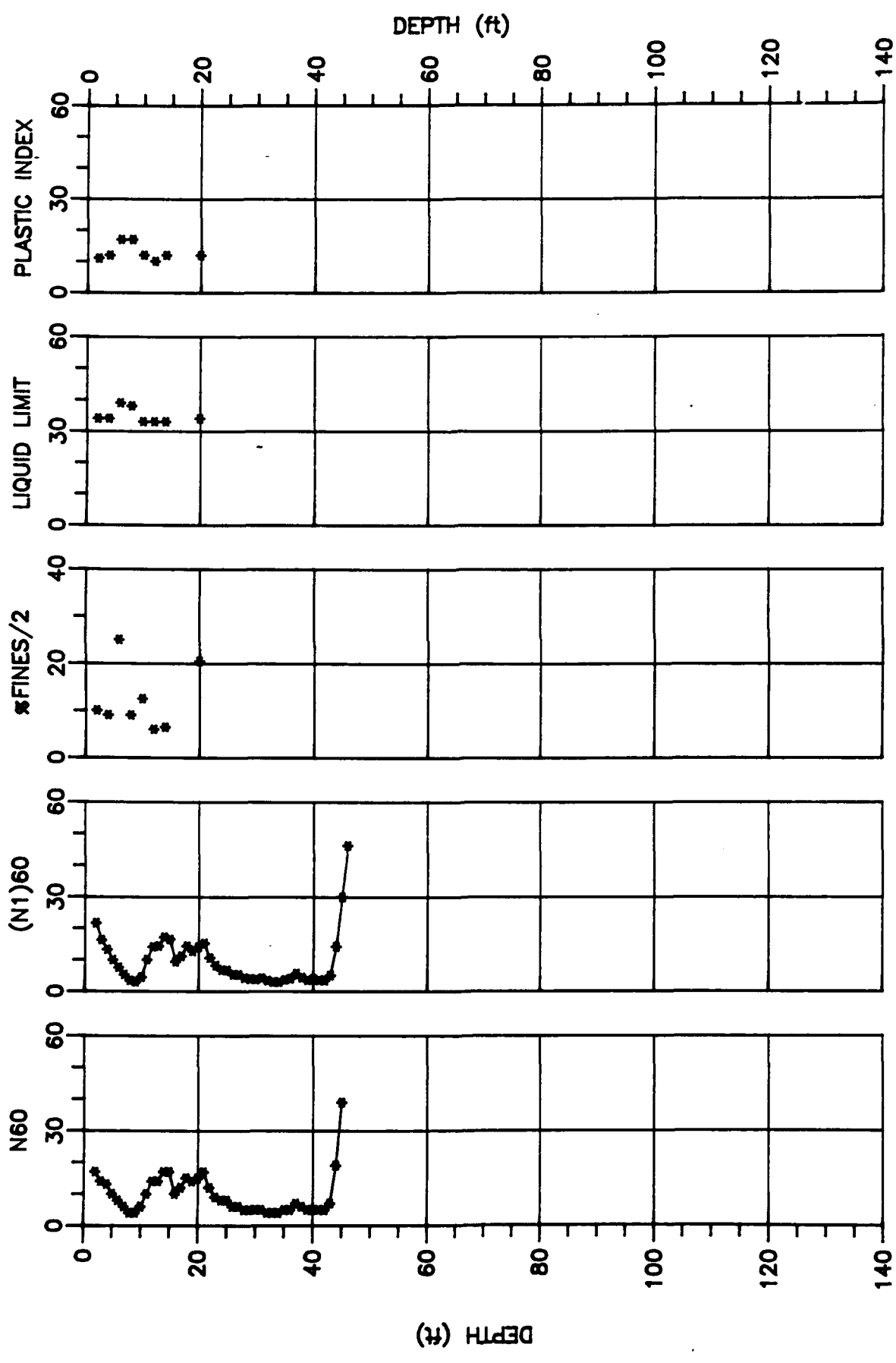


Figure B13. Data acquired from Becker Penetration Sounding BH13

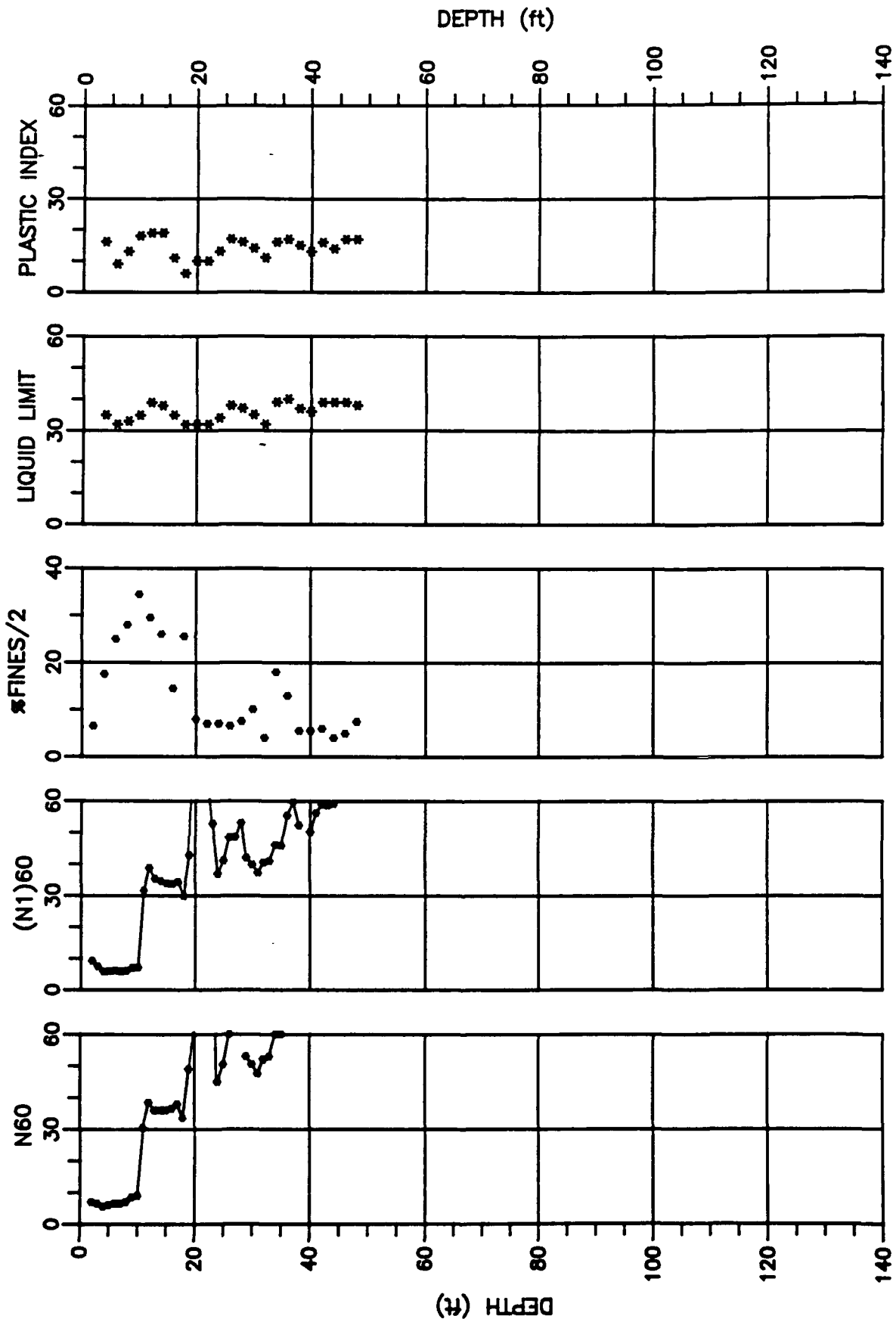


Figure B14. Data acquired from Becker Penetration Sounding BH14

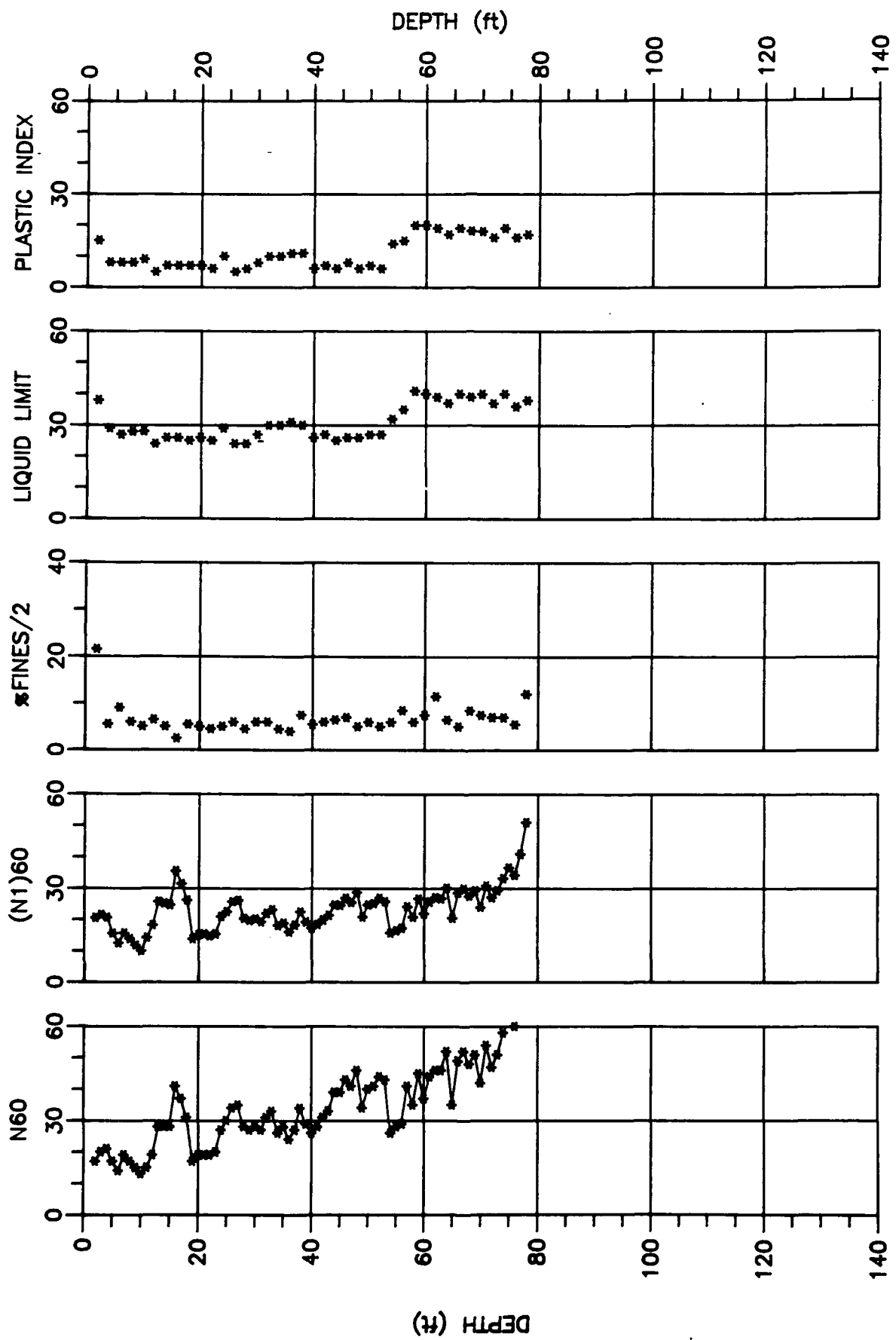


Figure B15. Data acquired from Becker Penetration Sounding BH15

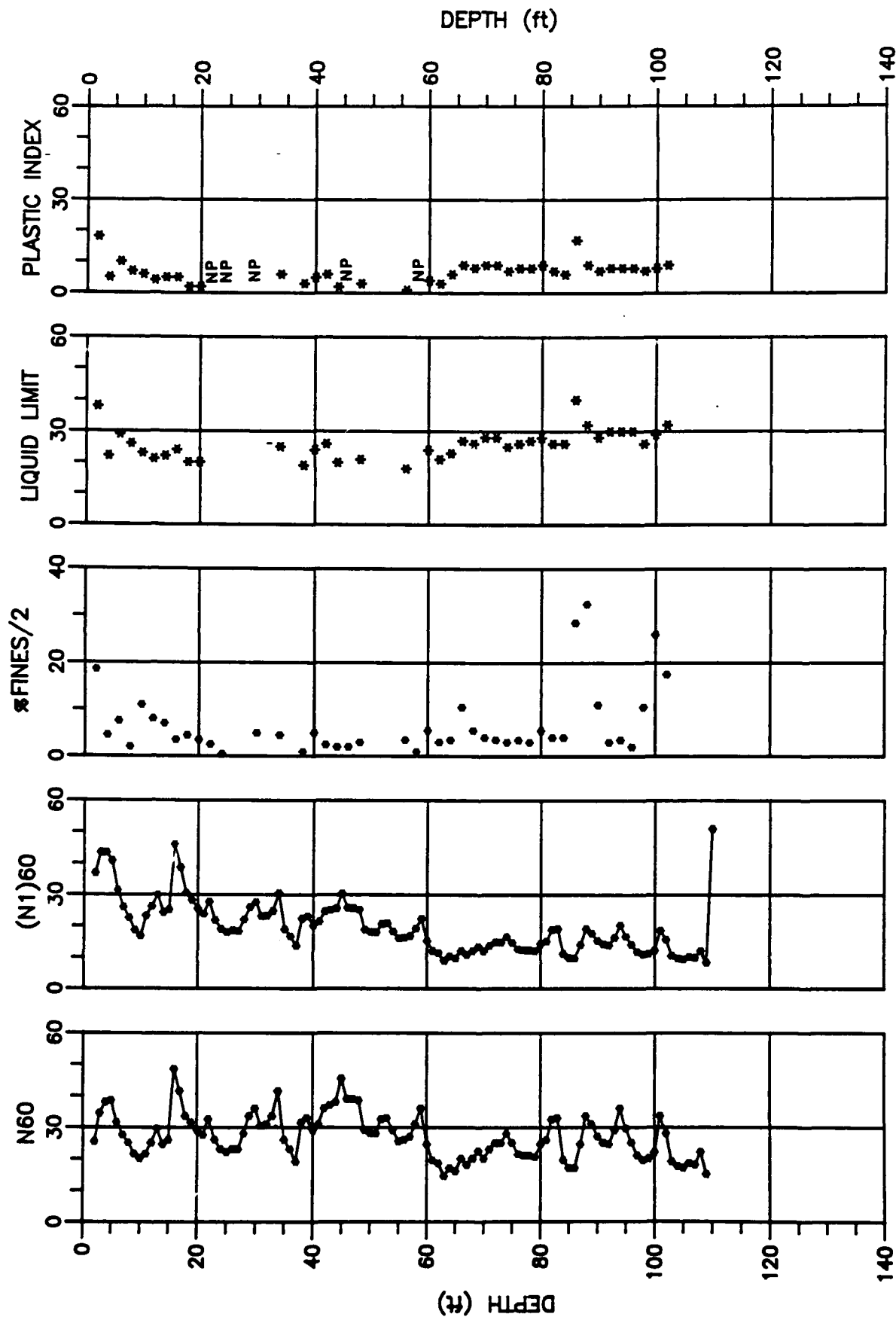


Figure B16. Data acquired from Becker Penetration Sounding BH16

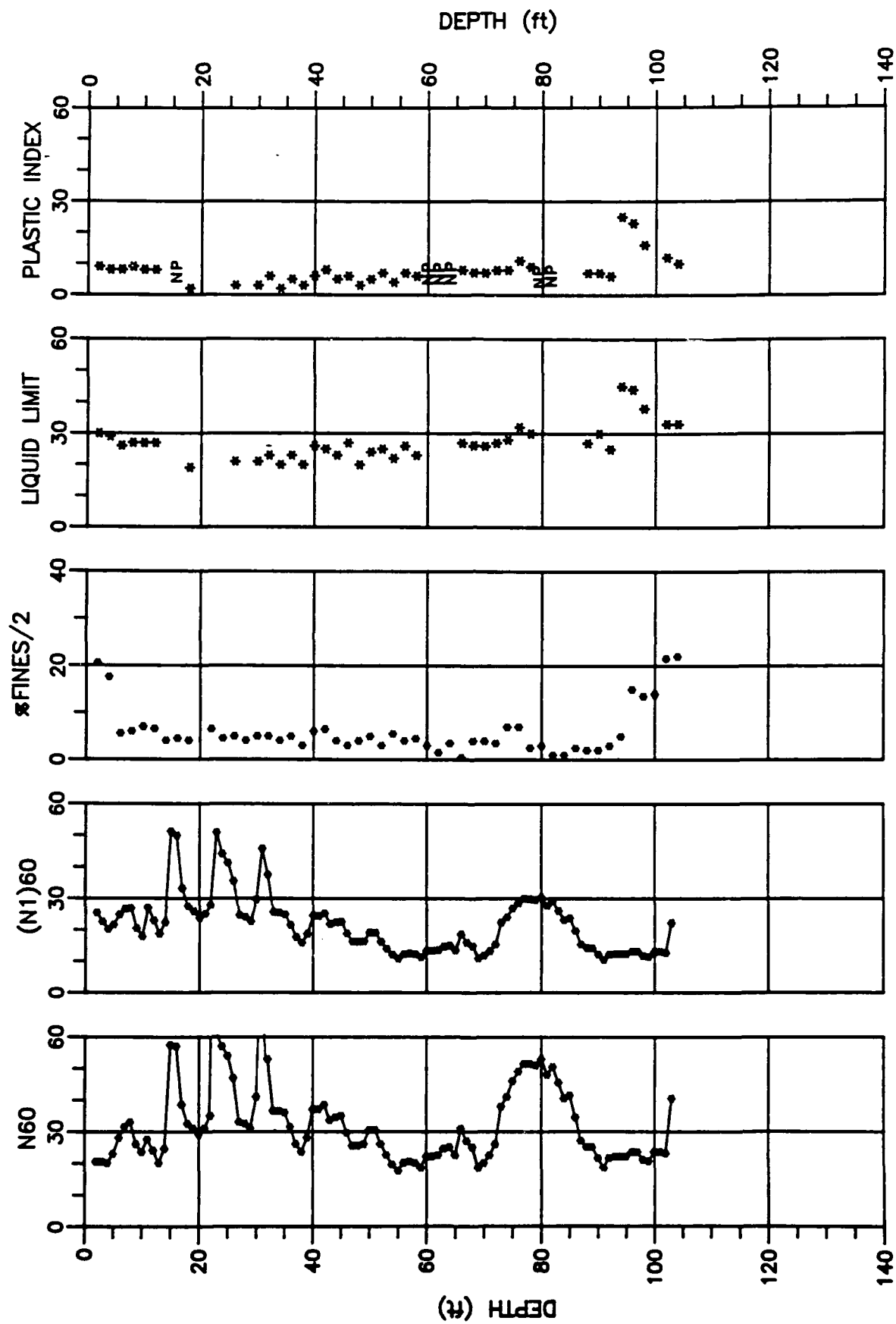


Figure B17. Data acquired from Becker Penetration Sounding BH17

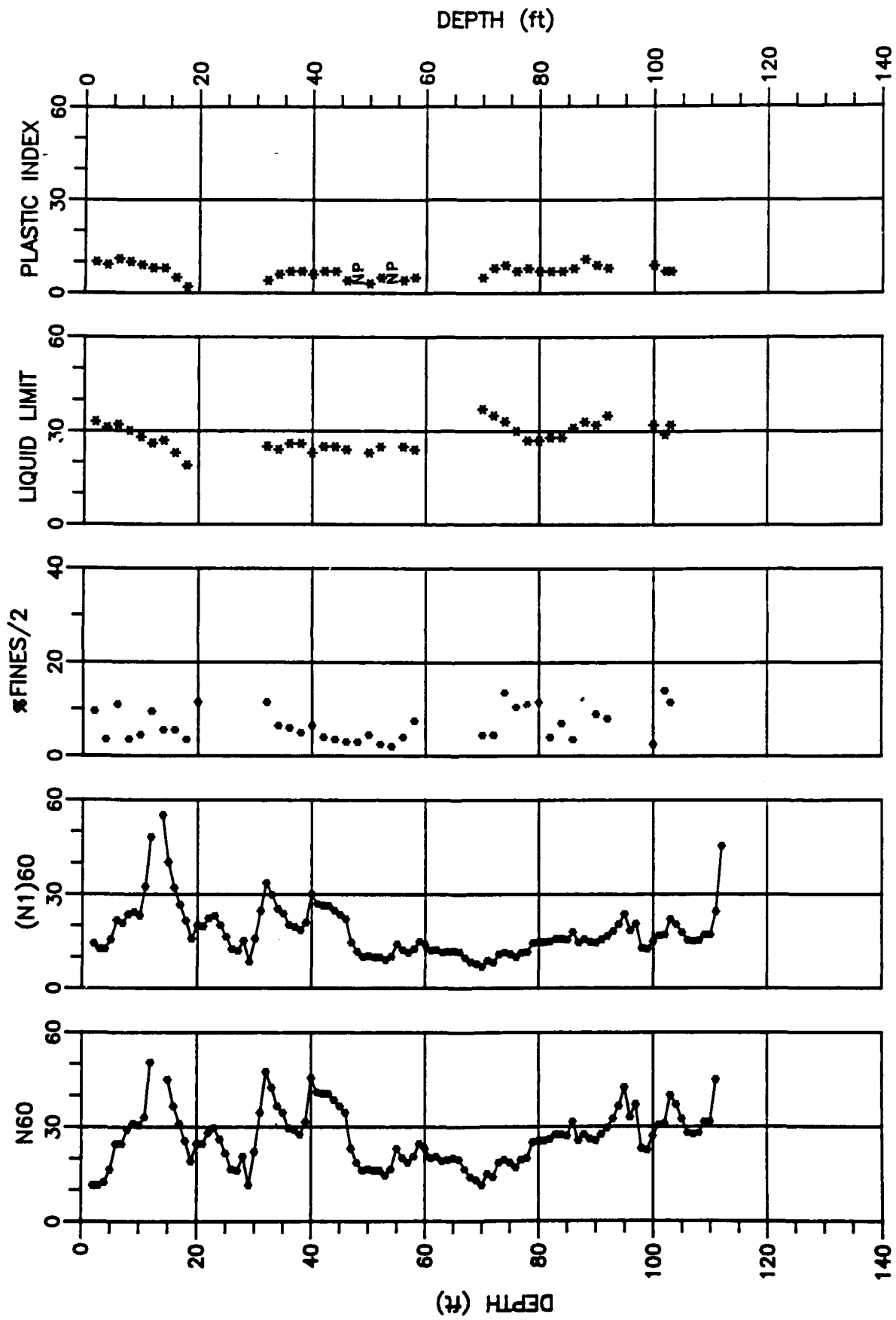


Figure B18. Data acquired from Becker Penetration Sounding BH18

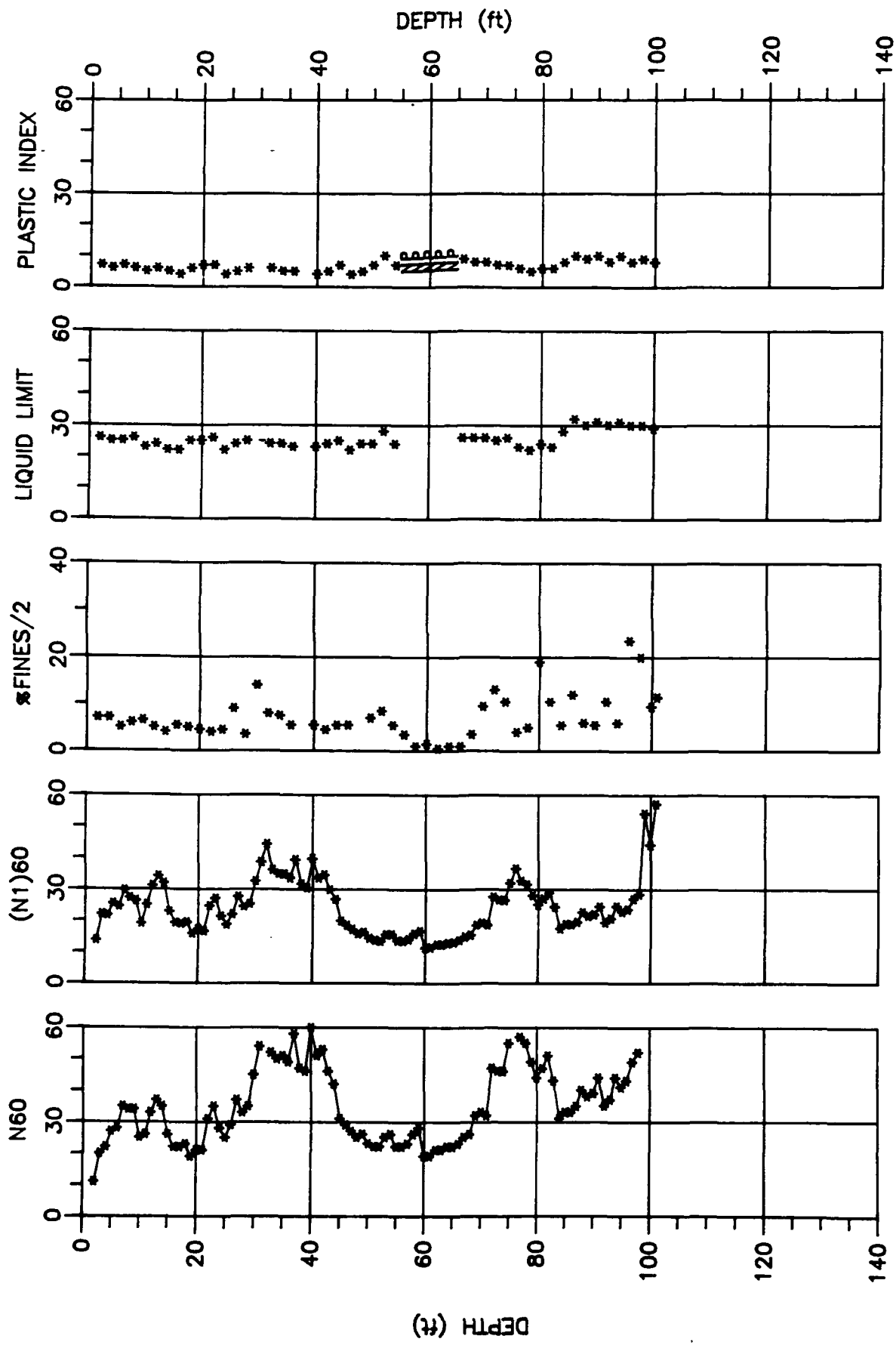


Figure B19. Data acquired from Becker Penetration Sounding BH19

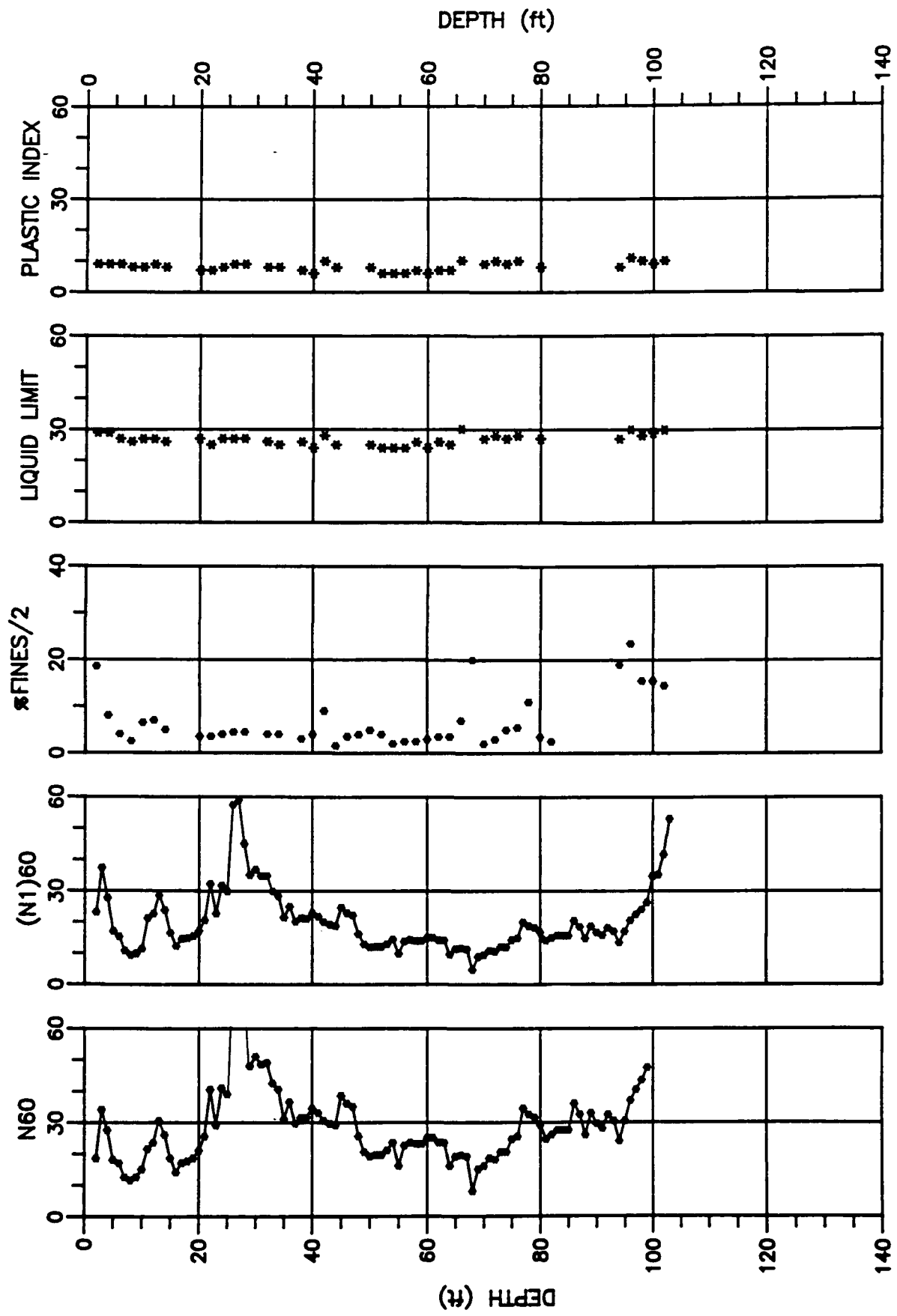


Figure B20. Data acquired from Becker Penetration Sounding BH20

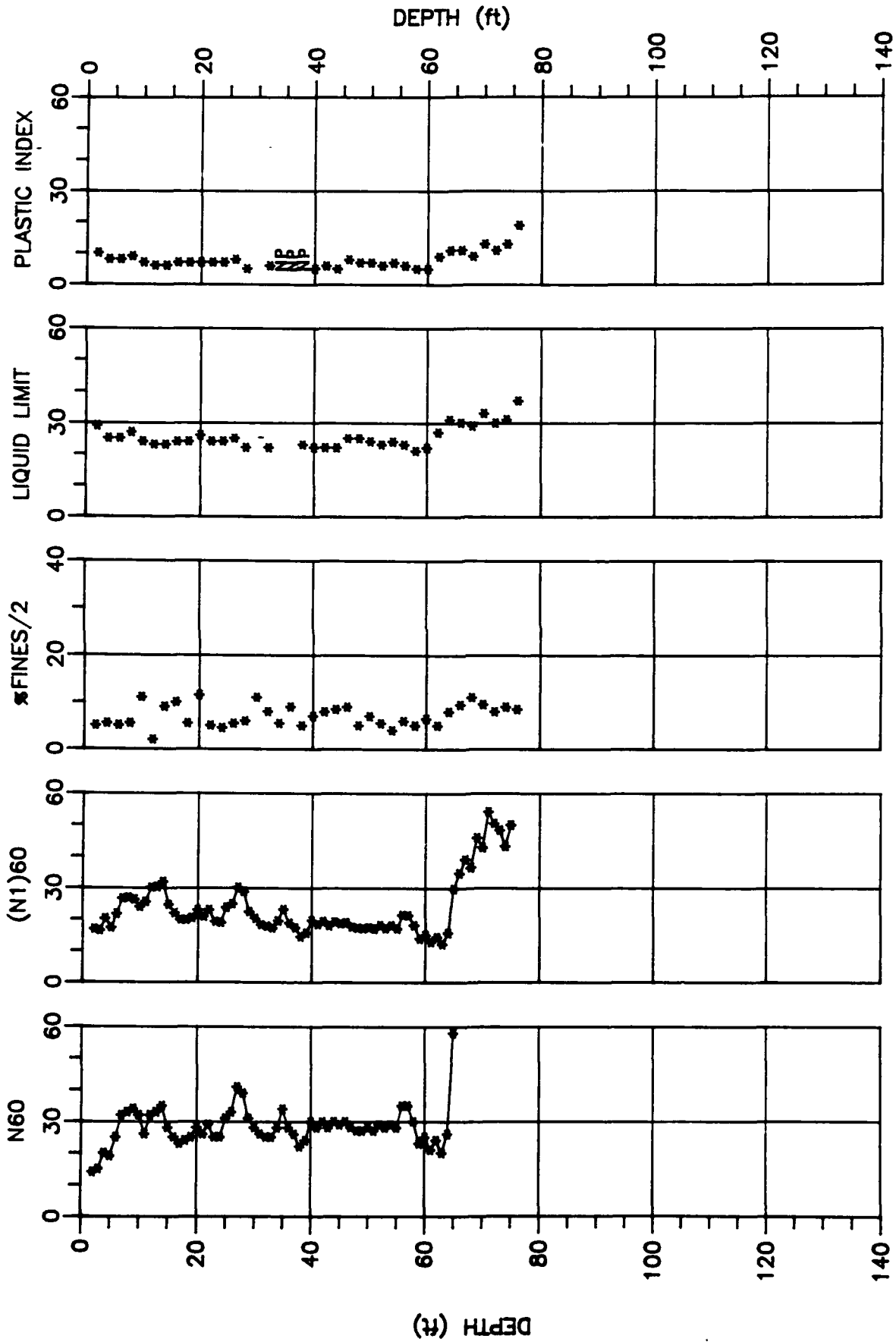


Figure B21. Data acquired from Becker Penetration Sounding BH21.

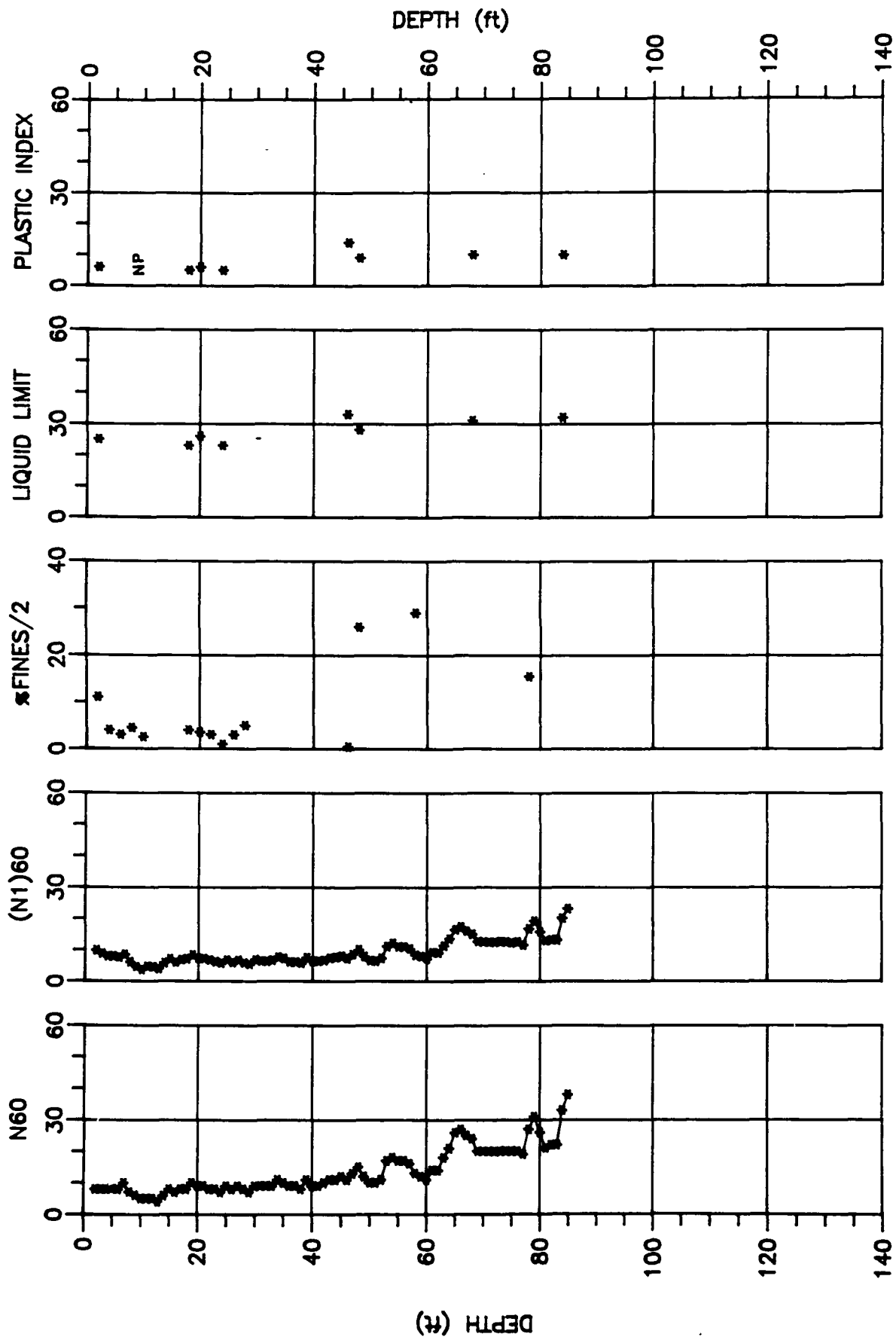


Figure B22. Data acquired from Becker Penetration Sounding BH22

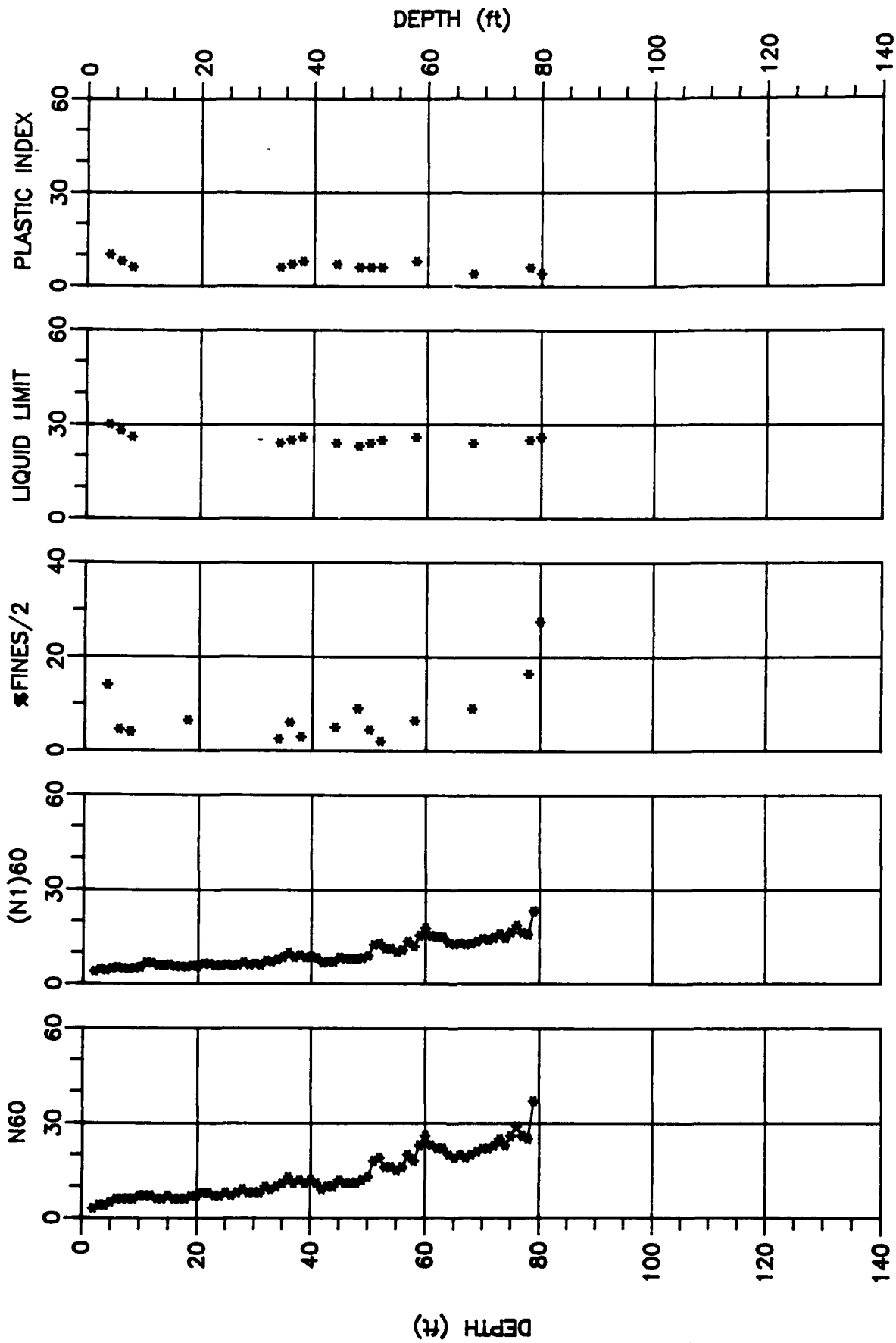


Figure B23. Data acquired from Becker Penetration Sounding BH23

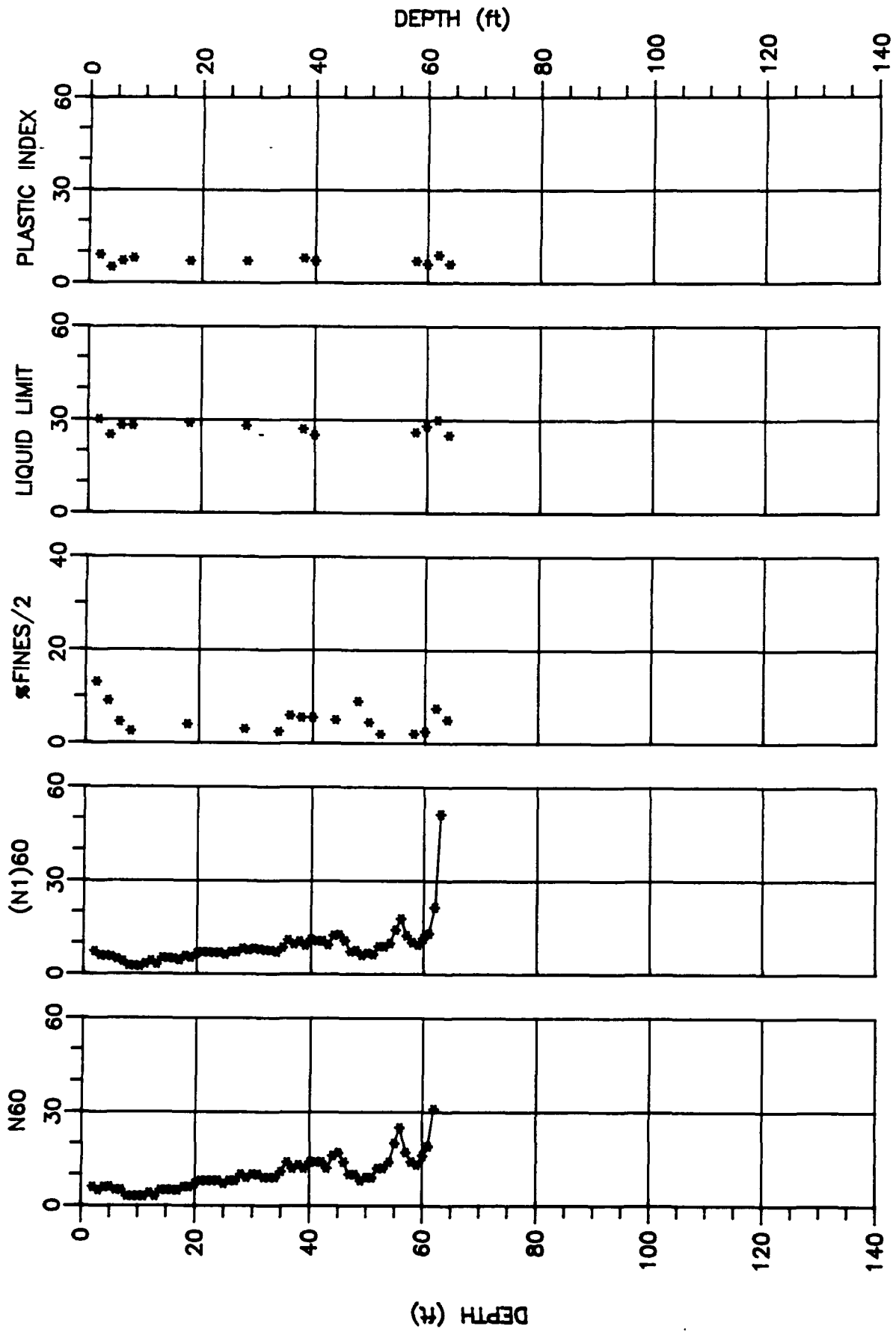


Figure B24. Data acquired from Becker Penetration Sounding BH24

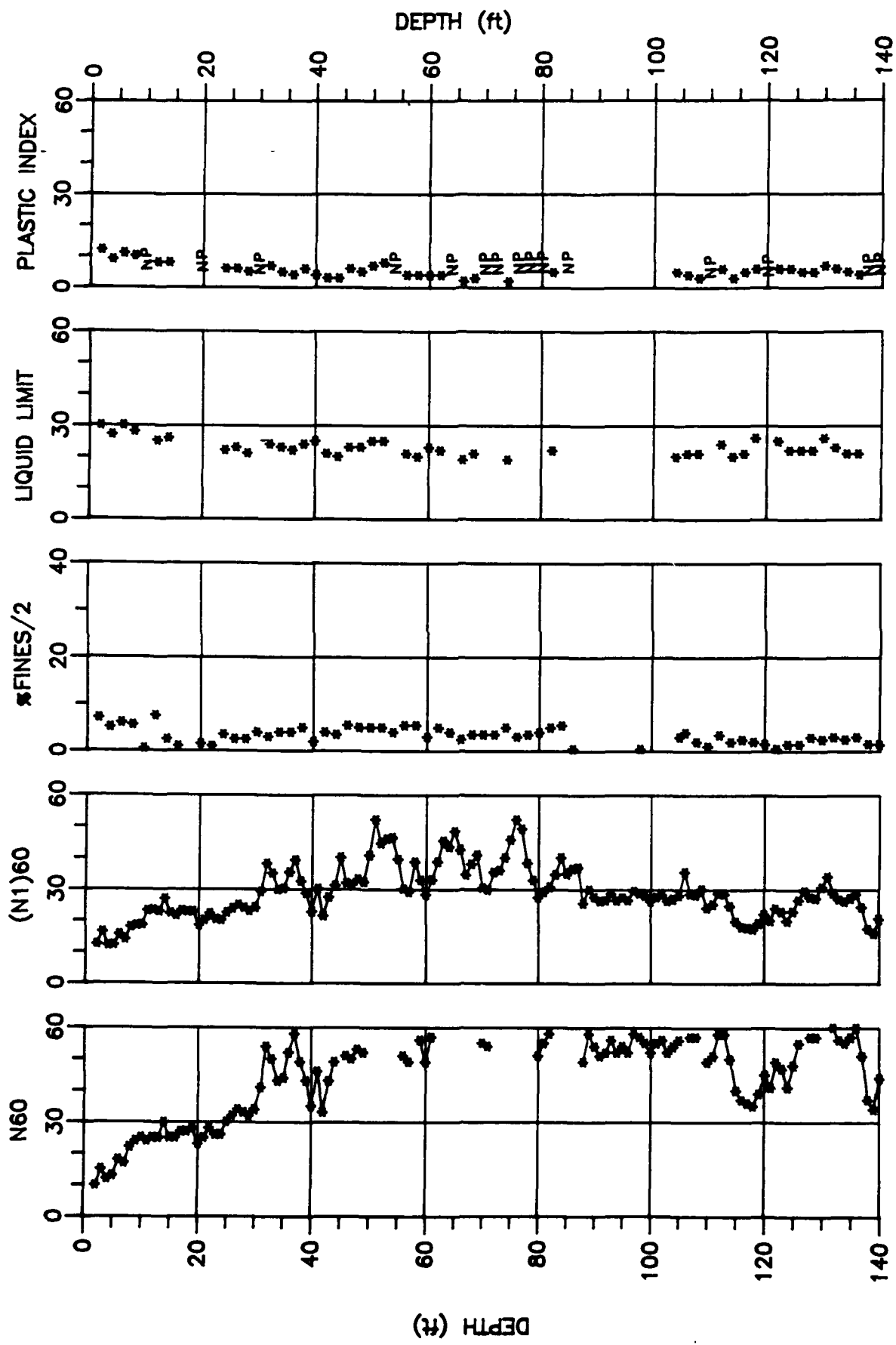


Figure B25. Data acquired from Becker Penetration Sounding BH25.

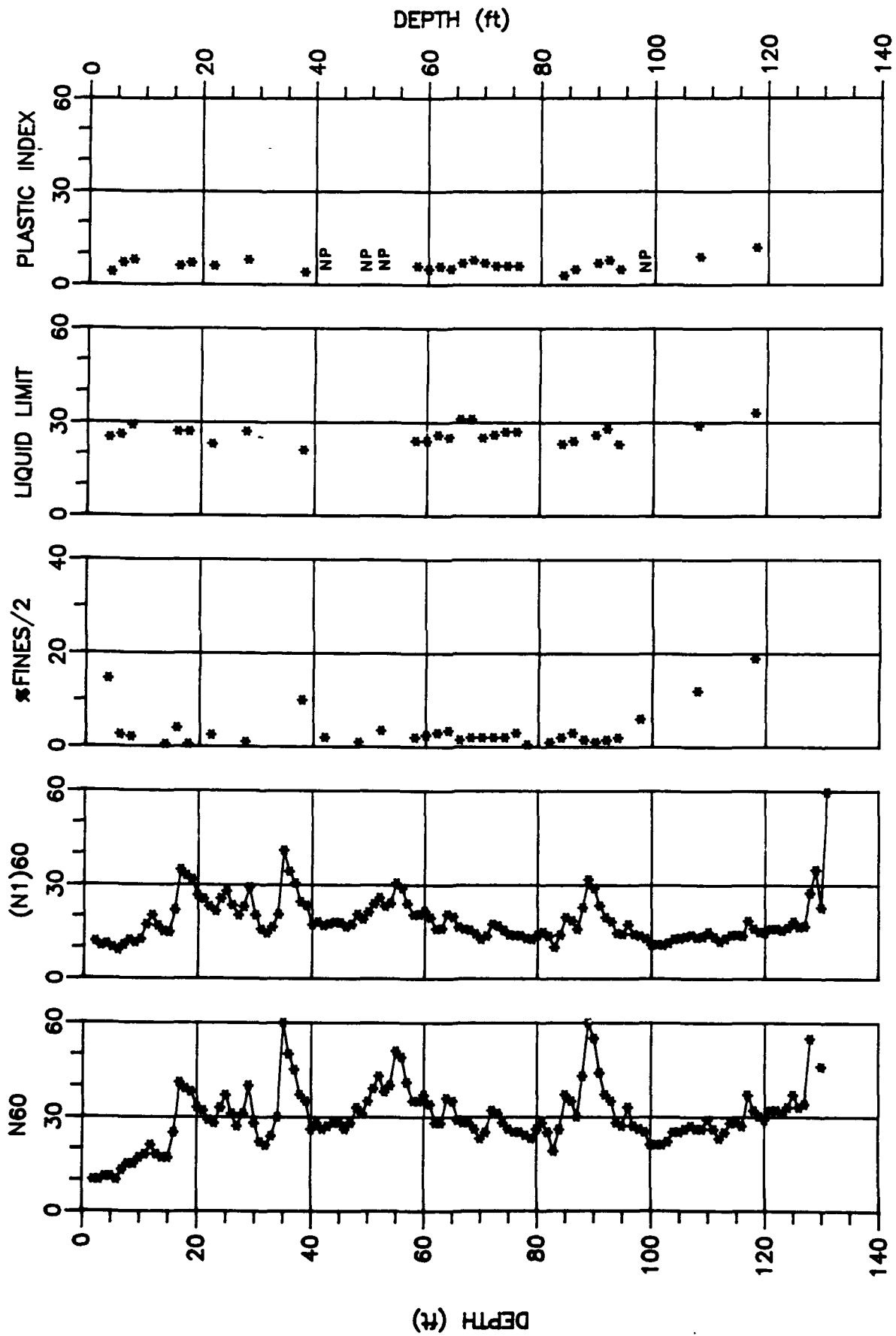


Figure B26. Data acquired from Becker Penetration Sounding BH26

Waterways Experiment Station Cataloging-in-Publication Data

Wahl, R. E.

Stability evaluation of Folsom Dam and Reservoir Project. Report 8, Mormon Island Auxiliary Dam - Phase II / by R.E. Wahl ... [et al.]; prepared for US Army Engineer District, Sacramento.

410 p. : ill. ; 28 cm. — (Technical report ; GL-87-14 rept. 8)

Includes bibliographical references.

1. Dams — California — Earthquake effects. 2. Structural stability — Evaluation. 3. Folsom Dam (Calif.) 4. Finite element method. I. Wahl, Ronald E. II. United States. Army. Corps of Engineers. Sacramento District. III. U.S. Army Engineer Waterways Experiment Station. IV. Title: Mormon Island Auxiliary Dam - Phase II. V. Series: Technical report (U.S. Army Engineer Waterways Experiment Station) ; GL-87-14 rept. 8. TA7 W34 no.GL-87-14 rept.8